AD NUMBER

AD217822

NEW LIMITATION CHANGE

TO

Approved for public release, distribution unlimited

FROM

Distribution authorized to U.S. Gov't. agencies and their contractors; Administrative/Operational Use; 19 Mar 1959. Other requests shall be referred to the Office of Naval Research, 800 North Quincy Street, Arlington, VA 22217-5660.

AUTHORITY

ONR ltr, 6 Sep 1973

AD

217822

"NOTICE: When Government or other drawings, specifications or other data are used for any purpose other than in connection with a definitely related Government procurement operation, the U.S. Government thereby incurs no responsibility, nor any obligation whatsoever; and the fact that the Government may have formulated, furnished, or in any way supplied the said drawings, specifications or other data is not to be regarded by implication or otherwise as in any manner licensing the holder or any other person or corporation, or conveying any rights or permission to manufacture, use or sell any patented invention that may in any way be related thereto."

A symposium

MATERIALS RESEARCH IN THE NAVY

Office of Naval Research
Department of the Navy
Washington, D.C.

ONR-5
Volume I

A symposium

MATERIALS RESEARCH IN THE NAVY

A Symposium sponsored by
THE OFFICE OF NAVAL RESEARCH

March 17, 18, and 19, 1959
The Benjamin Franklin Hotel
Philadelphia, Pennsylvania

Office of Naval Research
Department of the Navy
Washington, D.C.

PREFACE

More than in any previous period, advances in engineering design and weapons development are frequently limited by the lack of suitable materials. In spite of this situation, materials research and development as such is not yet receiving the attention it merits. As a result, any step which will increase the effectiveness of materials research in the Navy is of great importance. It is expected that this symposium will contribute to the improvement of the materials capabilities of the Navy by providing a forum for the rapid exchange of already existing information, and even more so, by bringing to the attention of a broad group of experts the pressing problems which have to be solved in order to take full advantage of new ideas for the design of equipments and weapons.

R. Bennett

R. BENNETT
Rear Admiral, USN
Chief of Naval Research

Members of the Symposium Program Committee

Office of Naval Material	Mr. W. D. Barlow
Bureau of Aeronautics	Mr. N. E. Promisel Mr. R. F. Speaker Mr. F. S. Williams (NAMC, Philadelphia)
Bureau of Medicine and Surgery	Dr. H. T. Karsner
Bureau of Ordnance	Dr. E. S. Lamar Dr. R. H. Lyddane (NPG, Dahlgren)
Bureau of Naval Personnel	Cdr. E. G. Fitzpatrick, USN
Bureau of Ships	Mr. G. Sorkin Mr. E. J. Jehle (Mat. Lab, N.Y.)
Marine Corps	Dr. C. E. Wise, Jr.
Office of Naval Research	Capt. G. F. Gell, USN Dr. J. H. Shenk Mr. J. J. Harwood Dr. J. S. Smart Dr. P. King (NRL) Dr. I. Estermann, Chairman

VOLUME 1
CONTENTS

Remarks by

Dr. I. Estermann
Symposium Chairman
Office of Naval Research

This year's symposium will concentrate on material research, a subject which has recently received a tremendous amount of attention. But, to paraphrase Mark Twain, "Everybody talks about it, but far too little is being done about it". I hope that this symposium will, at least in part, correct the situation.

Holding this symposium in Philadelphia is no accident. This city has a tradition of basic and applied research as exemplified by the large number of scientific and educational institutions within its borders. In particular, holding it at this hotel is even more meaningful because the hotel bears the name of one of the foremost applied scientists in the United States, Benjamin Franklin. Moreover, the Navy has had associations with Philadelphia for a very long time and is operating a large number of research and development establishments in this area. Unfortunately, these establishments are much less known than they deserve, even within internal Navy circles. This may be due to the fact that Philadelphia is so close to New York on one hand and Washington on the other hand that most of us don't ever bother to stop here. I, personally, have been through Philadelphia at least a hundred times, but I think this is the third time that I have ever gotten off the plane or off the train. I must confess that many of the Navy Research and Development Activities in this area are still unknown to me. A symposium here will give us an opportunity to become more familiar with the excellent work that is being done by the Navy in this area.

Remarks by

Rear Admiral J. N. Murphy, USN
Commander
U. S. Naval Air Research and Development
Activities Command

The Naval Air Research and Development Activities Command, until very recently known as the Naval Air Development and Material Center, is greatly honored and is most appreciative of the fact that one of its activities, the Naval Air Material Center, has been selected by the Office of Naval Research to serve as your host for the Third Navy Science Symposium.

The Naval Air Research and Development Activities Command (or NARDAC) has on board today just under seven thousand capable and dedicated people. Our mission covers practically every aspect of research, development, test, and evaluation of naval aviation equipment other than complete weapon systems.

Almost every component and sub-system that is used in our Naval aircraft and associated guided missile weapon systems, as well as all equipment used to launch and arrest aircraft on board our carriers, is of vital interest to the various activities of our command.

Concentrated in the Delaware valley area, NARDAC is composed of five subordinate activities. These are: The Naval Air Development Center, Johnsville, Pennsylvania; The Naval Air Turbine Test Station, Trenton, New Jersey; The Naval Air Test Facility (Ship Installations), Lakehurst, New Jersey; The Naval Air Technical Services Facility, Philadelphia; and last, but the oldest and largest, The Naval Air Material Center, Philadelphia - your host activity.

The work of these activities covers every possible application of materials. Because of the great diversity of our work, we can certainly see and appreciate the vital importance that materials research

plays in our complex technology today.

To the public, the discovery of a new alloy, or a new lubricant, or perhaps a new fabrication technique is not as glamorous as a rocket soaring into space, or a super-sonic airplane going through its trails. But we can gain everlasting satisfaction from the knowledge that, without materials research these rockets and super-sonic aircraft would have been impractical. Every day we see examples of ideas that are scientifically feasible but which are technically impracticable because we do not have materials with which to convert such ideas to hardware.

I hope that through this symposium, we may gain knowledge, and exchange ideas which will provide new materials, and new applications of materials, so that our technological progress will be outstanding in the years ahead.

REMARKS

Rear Admiral R. Bennett, USN
Chief of Naval Research
Washington, D. C.

I am very happy indeed to welcome you to this Third Navy Science Symposium. I think we all appreciate the problems that the Navy faces in the materials area. Moreover, I think we all appreciate the importance of the factors of reliability and availability in meeting our material needs. However, I do not think that generally--although I would exempt most of those here--there is enough appreciation of the bottlenecking that is occurring because we do not have enough investigation of materials and components. I would say that there is hardly a development project on the books in Washington today which will not have to be compromised or, at best, delayed for lack of proper materials.

It is trite to remind you that the Navy is now involved in all possible environments from the latest proposed submarine depths of 1000 feet to outer space. Each of these areas of operation has its own requirements. One thing I must continually stress is reliability, particularly as we prepare for the space age in which the Navy will definitely play an important part.

Without regard to whether the Air Force, the Army, or the Navy puts a man in space or not, the Navy is bound to have some vehicles in space since such vehicles would be of paramount importance in carrying out that part of our mission which involves observing and controlling the seas of the world. And yet when one considers the degree of reliability that must be achieved in such vehicles, one can really get cold feet.

We have already had a taste of this in the very interesting Navy Vanguard project. The original engineering predictions were

that it would require the launching of six vehicles to place one full-scale satellite in orbit during the 18-month IGY, which ended December 31, 1958. We are pleased that Vanguard has performed exactly according to these predictions, barring a six weeks delay beyond the Navy's control. This was the postponement of the firing of the sixth vehicle from December to February by the National Aeronautics and Space Administration in reviewing the project.

Actually, we received a bonus in the form of the first or baby satellite. To place that or the more recent one into orbit, not only did the 300,000 odd parts of this three-stage vehicle have to hold together but more than 10,000 of them had to function in proper order. If this were not enough, the satellite itself had to function perfectly. The success we have had is a tribute to the fact that some of you gentlemen and others have been doing your homework.

What was achieved in the case of the first Vanguard satellite was an orbit that is at present so stable that my mathematical friends refuse to say how many thousands of years it will endure for fear they will be laughed at. Actually, the estimate of 200 years in orbit is probably a gross understatement. What is most interesting of all to you people is the fact that as of today the transmitter in that satellite powered by solar cells will have been operating for more than 9000 hours continuously without any measurable change in signal strength.

Now I would like to close with the unnecessary reminder that our laboratories play an extremely important part in the development of components and materials. To my way of thinking, the emphasis of this role is why this sort of symposium is a must. I wish you all the best of luck and success in obtaining the greatest increase of information in the course of your meeting. I especially recommend that in talking to your colleagues from other laboratories, you make a special point of finding out what they did that did not work. This is sometimes a most important piece of research information, and it is almost never published. Thank you.

MATERIALS RESEARCH IN THE NAVY

Keynote Address by
VADM E. W. Clexton, USN, Chief of Naval Material
Before the Third Navy Science Symposium

Good Morning Dr. Estermann, ADM Murphy, ADM Bennett, CAPT Arnold, Ladies and Gentlemen:

I am very pleased to have the opportunity to address this group, particularly here in Philadelphia. The holding of the Third Navy Science Symposium at this site is most propitious, for it is here that we see the shadow of one of America's men of science everywhere that we look. As far back as 1727 Benjamin Franklin organized a group of men who were interested in keeping themselves informed of the developments in literature, art and science. This group was the forerunner of the American Philosophical Society, which was founded in 1743, the oldest scientific society on the American continent. Today we still have this society in Philadelphia. In addition, we have other famous organizations in this city that are contributing materially to the fields of science: the Franklin Institute, which is devoted to the study and promotion of mechanical and applied science, the University of Pennsylvania and Temple University. These are but a few organizations who are making an outstanding contribution to the sciences. The list of the outstanding companies working in this area is too long for me to list.

For nearly forty (40) years my life has been the Navy. All devoted Navy men have one goal: To see to it that the United States has the finest Navy in the world. Today, more than ever before, this is a task which is dependent upon obtaining better tools than any hostile forces can get. To attain this goal, the

Navy is dependent upon you, our scientists, and later on our engineers and production people.

The fact that you are aware of the importance of the Navy to the nation is evidenced by your presence here today. So I am not going to talk Navy with you. I am going to talk on the importance of a coordinated materials research program, because I personally feel that if we are to make significant advances in materials technology, it will only be done through a properly coordinated program.

Engineering design has outstripped materials research. The design engineer in translating military requirements into a blueprint, searches, all too often, for a material that he cannot find. Like Mother Hubbard, seeking a bone for her dog, he goes to the cupboard, only to find it bare. Unlike Mother Hubbard, however, he is looking for an item whose supply is not merely depleted but something he suspects does not exist. How, then, does he obtain it? We all know the answer -- "A crash program" is initiated. The crash program eventually solves the problem at hand, and, although it is very expensive in scientific talent and effort, it contributes little to the over-all understanding so necessary for significant advances in materials technology. To make matters worse, unless the maximum dissemination of this "hard to come by" knowledge is made, a similar problem may be the cause of a further crash program that dissipates additional research effort. Such symposia as this will, it is our sincerest belief, help the Navy, and eventually the whole Defense Department, realize the greatest return for its investment. We must continue working on a program of coordinated basic materials research and then disseminate the scientific knowledge obtained.

To solve some of these problems is not going to be easy. Indeed, it is going to be made more difficult because every time our potential enemies have made a breakthrough in a given area, we seem to have to resort to the crash program approach so that we too can show that we have made equal or greater advances. Whatever we do in our approach to solving our many problems in this area I feel that we must think along these lines--

The time available to us;
The use of every available individual; and finally,
The cost.

Navy procurement and production must be increasingly concerned with the materials developed by industry for use in its weapons and equipment. Our requirements have imposed demands on

materials of a magnitude never before conceived of. The list of new products which the Navy is seeking is too great for me to enumerate here. Let it suffice to say that supersonic aircraft and engines, miniaturization, automation, high reliability, exact navigation systems, fire control, communications, anti-submarine detection identification and destruction devices, and guidance systems are only a few of the haunting unanswered problems. Answers to these problems are being sought from you ladies and gentlemen. Problems that perhaps none of us have considered at all may be but a moment away. For one of the most significant changes in our national life is that no longer can we be sure that time is working in our favor. Indeed, there is every evidence that it is not working in our favor, and that we must seek new avenues and new approaches to solving our problems which will offset this former reliance on time.

At the turn of the present century the U. S. Navy had a new coal burning fleet. The dreadnought, an all big gun ship, was on the drawing boards. Today we have attack aircraft carriers, super high pressure steam, nuclear power, and our big guns are now missiles. In 1900, the Wrights first flight was three years away. Today the exploration of outer space and the depths of the sea are upon us. In the fields of humanity, new diseases are being conquered year by year; and new improvements for our comfort, for our entertainment, and for our happiness, surround us.

But in the annals of history, what a short period of time this is! And how little we have learned about controlling these inventions that they may be used for peaceful purposes! The Russo-Japanese War, World Wars I and II, Korea and the continuing threat of nuclear holocaust are all mute evidence that we have failed. But we must try and try again to seek an answer to this most compelling problem of all.

The pressure is on our research institutions--private and public-- to give us more and more technical superiority in our military endeavor. This must be a rapid and continuing development. The users of your scientific achievements are impatient for your dreams of tomorrow. Advances in technology required to modernize military equipment come either directly or indirectly from basic research. Consequently, research in the basic physical sciences is the principal source of technological innovations affecting the concepts and techniques of warfare.

If we accept this theory of the criticalness of time we are forced to look at compensating means. This means the testing of

every idea, the use of all existing resources, and the coordination of effort. Can you really think of any more staggering problem?

It means digesting, synthesizing the experiments of basic research and broadcasting the efforts and results to the nation's scientists so that like effort is not expended by them once a development has become successful; or, that the pattern of failure may be made known to them and to solicit their help for another attempt. It means the discoveries of one individual or group on which to build for future developments. How very nice and what a comfortable feeling it might be to assign to one certain group of research laboratories a specific field and limit them to that area. At least the spectrum we seek would be reduced. But you will note that I said <u>might</u>. For competition is still the best stimulus to new breakthroughs.

I know of no simple way for coordinating the efforts of a materials research program except the patient review by qualified scientific personnel followed by firm decisions. The Department of Defense, as you have probably heard, has several competing components. Within bounds, I believe that this is good for the country. Certainly our Army, Navy, Air Force competitive research programs should be coordinated by the Director of Research and Engineering of the Office of the Secretary of Defense who has been given the broadest latitude by the Congress to channel all defense research efforts. This office also works with other national agencies of like purpose. Within the Navy, RADM Bennett, from whom you have just heard, heads our Office of Naval Research, whose mission is to coordinate the Navy's research efforts. This has been well done. It provides a pattern which could be used by higher echelons.

But I feel, in fact I know, that we have many untapped resources. These must also be explored and pulled together to save time and effort.

Finally, I would like to pursue further this saving of money. Most of you here today are scientists. But, Gentlemen, I work on the other side. My efforts are concerned with using what you invent and develop. It must be good. And this is going to be costly. On the other hand, we cannot afford either time, manpower or money to duplicate the effort which must be put into this project, and I might add we cannot afford to refine a product to such a degree that we are driving a Cadillac when a Rambler will get us there.

So, Ladies and Gentlemen, I would like to leave these few thoughts with you as you enter upon your extensive and excellent

program. You need a strong Navy, including the Marine Corps, and you also need a strong Army and Air Force. The country expects each to be ready and expert in its field. These Services cost a great deal of money, but they provide, with our Allies, the only known shield today for our western way of life. A strong Navy is dependent upon the most improved technical systems continually flowing from our research laboratories.

Time is priceless, since we do not know what the scientists in Moscow have just presented to the Soviet Minister of Defense. To gain this time, we must capture and disseminate every idea, breakthrough, discovery, and development to insure that we have what we need and we get the most for our efforts.

This whole problem is one to which the Government and industry has given a great deal of thought. As I stated earlier, I am sure that there is no easy answer. But there is an answer. We must continue--both industry and the military--to seek an optimum answer in this area of materials research planning and programing to insure a broad base of materials research knowledge in lieu of the narrow channels of crash program results. The price always seems high. I know that we cannot afford to dissipate our time, our scientific manpower and our money. These efforts must be channeled properly, and it is to you, Ladies and Gentlemen, that we look for our answers as to how best we can do this.

Research and Materials

Dr. A. B. Kinzel
Vice President - Research
Union Carbide Corporation

Mr. Chairman, fellow citizens of the United States of America. It is really a particular pleasure to be here with you today, not only because of my associations with the Navy, but also because of my associations with the city of Philadelphia. My first association with the Navy actually had to do with the Naval Shipyard here, where Mac Kennedy was and is the Metallurgist. He would bring his problems to Temple University. Mac and I ran the Laboratory at Temple University where we gave the laboratory course, in connection with a series of lectures that I gave in Advanced Metallurgy. I, too, have been through Philadelphia more than a hundred times but once I stayed here for a few years. It is also a rare pleasure to be here because one of my pet avocations is the International Benjamin Franklin Association of which I am a member of the Board of Trustees. So putting it all together, you see why I am happy to be here with you.

In introducing a symposium on materials of this kind, it seems to me worthwhilefirst to put the subject in its historic perspective. I could do this by statistics, of course, but I am very leary of statistics, you can draw so many conclusions from them. My pet illustration on that subject has to do with the life insurance tables. The companies put out tables showing the proper weight and height relationship for people of various ages. If you look at these and then take the data on most Americans, there is only one obvious conclusion, and that is that most Americans are two inches too short. So I will take the illustrative approach.

Instead of starting with materials themselves and their development over the centuries, I am going to take the speed of man as a first illustration. For hundreds of thousands of years, man could

go no faster than his feet would carry him. One mile in slightly more than four minutes. In the last few years man has done it in slightly less than four minutes. But that is unimportant. And he could go no faster than that from time immemorial until about 4000 years ago, when he got on the back of a horse. And when he got on the back of a horse he doubled his speed. A mile in two minutes, roughly. That was 4000 ago. Then from 4000 years ago until the first third of the last century he went no faster. Then we had the steam engine and the railroad tracks. It wasn't long before he was doing a mile in one minute. Well, he did essentially no better than that until the first half of this century. Then came the airplane. With the conventional airplane, we covered a mile in twelve seconds. And with the jet, twenty odd years later, a mile in two seconds. And now within the next 10 years we will have a man in orbit, with a speed of a mile in one fifth of a second.

This makes a very imposing, rising, accelerating curve even if you plot it on log-log paper and with it, of course, have come new material problems. Let's see what happened to materials while this was going on. Man used stone and wood originally and then discovered those elements that occur in their native state - gold and copper. Somehow or other he discovered how to handle the easily reduceable ores that were available. He had silver and lead, zinc, tin and iron and this was pretty much the list during the age when he was travelling as fast as a horse would carry him. Then we come into the nineteenth century. Just before that time, Watt had discovered the steam engine and with it came a demand for stronger and better materials and then, with the railroad, this demand increased further. Chemistry changed from a black art to a science and the science of Chemistry was applied to materials and so, in the nineteenth century, we could add to our list of known metals most of those materials that are common today - maybe not in quantity, maybe not with todays economic possibility, but they had been made, they were there, they were recognized and they were used - tungsten, columbium and so on. Now, what else was happening to Chemistry in this time? Among chemical materials, salt has been available from time immemorial; sulphur exsisted in elemental form in the earth and man discovered it and put it to use pretty early; as soon as he had enough Chemistry to do something with it. That was just about it until Chemistry really went to work at the end of the nineteenth century. At the beginning of this century, we find new chemicals and new materials based on Chemistry, non-metallic in character, coming into the picture in a big way and then what happened? During World War I and shortly thereafter, Bragg, in England, following up on the work of the French and the Germans in X-Rays, learned how to locate atoms in matter. He learned that a crystal comprised a regular arrangement of atoms. This was the beginning of the application of physics to the science of

materials, and with this combination of the application of chemistry and the application of physics to the science of materials we come to the present. Today we truly have a science of materials. We can begin to think in theoretical terms of producing materials to a truly tailor-made specification, and to apply that theory and really do it.

Now I want to go off on another track, partly historical, partly psychological. You've heard from my predecessors here on the platform this morning that now, as never before, we've needed new materials and that materials are the greatest limitation in engineering. I submit that there's nothing new about that at all. Materials have always been the limiting factor on engineering design. But there is a difference. I'm not contradicting what they said but I am trying to point out that this is not a new phenomenon. It is new in degree, but not in kind. What happened all through the last century? We built ships, we built telephone lines, we built machinery and what did the engineers do? They had the concepts and they accepted the limitations of the materials at hand because there was no great hope of getting anything else within a reasonable time. They cried for better materials and this cry was heard and we did get better materials later. Materials were improved. The two hundred thousand pound per square inch landing gear steel of World War II was an impossibility in World War I and so on. We could give many illustrations. We all know the story. Materials were vastly improved because of the cry of the engineer, but the engineer didn't wait for them and didn't count on them. He still doesn't. This is where the psychological change has come into the picture. With this very rapid increase in scientific knowledge, and with the rapid increase in the application of that knowledge to our engineering structures, military and otherwise, we have gotten to a stage where a good many of the newer things dreamed up by the scientists are being put into development and to to use so fast that the engineer hardly gets a look at them. They're engineered by the physicists and the scientists in large measure. Now these people have a different tradition. These people know that the science of materials has potentialities. These people not only cry for new materials, they say this is what we want to do, we know we can't do it without the new materials, we are not going to do anything less - so roll up your sleeves in the laboratories and get the new materials for us, not later but now! This is a very different psychological approach than we had twenty-five years ago, and it is different than what we get from engineers today because most engineers take the position that reliability is still the most important factor as Rawson Bennett said. By virtue of their training and upbringing, engineers feel that the only way to guarantee reliability is by experience. Now the physicist and the scientist feel otherwise. They feel that they can guarantee reliability by having a device that is theoretically correct. There is something to be said for both points of view, but it explains why we now have this terrific cry and urge for new materials.

What are we doing about it, and where does industry come into the picture? Here, we come to the question of motivation. The defense forces, including the Navy, are motivated by a need to meet a requirement without the same kind of an economic limitation that motivates industry to meet a requirement. Now I do not mean by that that there are no economics in the defense picture. There are! The titanium story is a case in point. The Air Corps said they could use titanium - at $20.00 a pound. The Navy said they couldn't use it until it was under $6,00 a pound, if I remember my numbers correctly, and the Army said they couldn't use it until it was under $3.00 a pound. I submit that no matter what you're talking about, the economic factor does come in. We heard about a new battery that is going to last forever powered by one of the radio-isotopes. The newspaper accounts were glorious, and the battery will do everything that the newspapers said it will do. What they failed to state was that it took about $425,000 worth of this particular radio-isotope to make one small battery! This, you see, brings in the economic factor again. So, even in the military problem we have the economic factor, but it is there to a lesser degree. Often, the two motivations can jibe; that is, the material needed for a military (Navy) requirement is also needed for a civilian requirement, and can be made cheaply enough if we are smart enough to do the right kind of research in industry, so that it meets industry's profit motive. When this happens, it is wonderful. But, take a thing like scandium for example, it is pretty hard to figure out how any industry is going to satisfy the profit motive by producing, developing and getting into the market with scandium, and so we need a slightly different approach. Now, if somewhere in industry you have the skills to do this but industry does not want to do it, but the Navy or the Military do want to do it, we have the possibility of getting together by virtue of financial support to industry for this particular kind of work from the defense departments, and I say that this is completely in order. Admiral Clexton bemoaned the fact that industry had not solved some of the problems that he is interested in out there on the West Coast, and I join him in bemoaning this fact. On the other hand, I say, if you really want them solved, you must take a look at the incentives to solve them, and see that the incentives are properly set forth. The matter of what you do in industry on materials is tied up directly with these incentives.

We do a great deal of basic research in industry. The enlightened progressive growth companies are all devoting a large part of their research programs to basic research in about the same degree. This has not come about by collusion or even by swapping notes; it has just happened as a result of the best judgment of the people that are directing these programs. Today, in these companies, about thirty-five per cent of the research, and I distinguish research

from development now, is basic. When you do basic research, you don't know what you're going to come up with, and you frequently come up with something that may not have economic interest to your particular company or to any other company. However, it may have great interest and be able to stand on its own feet within the economical limitation put on by the Military or the Navy. When this happens, it behooves industry and the Defense Departments to get together and to get together fast. How can this be promulgated? How can we speed up this process and better this process? Well, one way to do it is to do basic research in the Defense Departments; and you may say: What's that got to do with it? It is very simple. I submit that you cannot appreciate, much less project into an exploitable area, basic research findings by reading a paper, by looking over a guy's shoulder or by having people whose business it is to just walk around and find out what is happening. They will not get the result because they cannot appreciate the findings. These findings are only appreciated and spotted by men who are actually doing work in the same broad area, and I submit that one of the major reasons why the Navy should continue its present research program, and expand it in large measure, is what we call "coupling effect". Without it, the Navy is going to lose a good many of the findings that are appearing in other laboratories, be they industrial laboratories or in the academic world.

No one institution can do more than a very few per cent of all the work in the field. The Navy research in the basic area that they are working in, as I figured it out casually, is of the order of magnitude of less than one per cent of the nation's total research activity in these areas. Sure, they may stumble on something; they may have good luck and hit the jackpot. But if that one per cent figure is anywhere near right, there are ninety nine other people competing research wise. Therefore, there are ninety nine other chances to hit a jackpot. This number is large and you've got to couple to it and the only way to couple to it is to be doing basic research in that field. Now, you can couple in this way - simply by having people that know; you can also couple by letting your requirements be known. These requirements have to known not only to the chief salesman of a company but to the men down at the working level in research and development. If a material doesn't exist yet, and you need it, these are the fellows that have to know. They'll keep their eyes open for it. We are able today, between Physics and Chemistry in our science of materials, to do many things that we were never able to do before. We can make new metals and new alloys for this vast area that the Navy has to cover-everything from materials for atomic reactors to aircraft structural frames and fuels. We not only can make such new materials, but we can make others. In the field of medicine for example, today, there is real hope with respect

to the chemotherapy approach to cancer. The purines certainly destroy cancer cells. There is no question about this at all, it has been very well established. The only trouble is that they are apt to destroy about everything else around, including the normal cells. They are somewhat preferential. As the physicists and the chemists look at them, they begin to see what it is in the structure, in the electronic, polar bonding, or coordinate bonding, that makes them do more damage to a cancer cell than a normal cell. We actually have taken certain of these purines and said they would be much less toxic to living cells if it were not for a particular bonded radical. So let us make a modification of it in which we eliminate that or tack something else on to it or shift its location. The modified flurourosils are one outcome of this approach and there are more coming. I cite this simply to tell you that in the science of materials today, knowing how to handle dislocations and spot them in metals, knowing how to place bonds and atoms in organics, knowing how to polymerize plastics, we have a tool, a concept that we have never had before. But let us not hit everything with a crash program. Let us remember that all you are doing in a crash program is using up the assets that you have stored up in your past basic research. Let us have some crash programs - sure, we need them - but at the same time let us keep building up this whole reservoir of knowledge and know-how.

I want to give you one final illustration of coupling effect and this is absolutely true. Just before World War II, Imperial Chemicals in England figured out how to make a new kind of insulating material called polyethylene in the laboratory. The process that they had for making it was such that with all the effort in the world, you could not make more than a few pounds. It was a laboratory curiosity, a little more than that, but essentially that. Our Navy had need for insulation of just such properties in connection with some of their radar and they took this stuff to industry. They came to Carbide as well as to many others, and in Carbide, and I know the same thing happened in many of the other first class chemical companies, the Chemical Engineers took a look at it and they threw up their hands. There is no way to take this process and make this stuff in quantities without getting into the class of $425,000 a pound stuff that I was telling about. But it so happened that at Carbide, not in our chemicals company at all, but in another laboratory devoted primarily to very high pressure phenomena and very low temperature phenomena, we had a man working for years trying to make synthetic diamonds. He never succeeded. But, one of our chemical engineers happened to mention to him the problem in connection with the production of poly-ethylene. He stated that this technique he had been using was adaptable to that problem. He tried it. In one week, he turned out more polyethylene than had been turned out in the previous

six months by everybody. In three weeks, we were in pilot plant production and three months latter, we were taking care of the Navy's needs for polyethylene. This was war time, we were motivated by nothing but the desire to help the defense effort. We have a very nice by-product in that business today, we are one of the dominant factors in the polyethylene business. (That means squeeze the bottle to you who don't recognize polyethylene as such.) It's a business that runs up into the high, high millions of dollars. We got the lead just as described. I submit that this is not necessarily an isolated case; that if we have more basic research going on in the Navy, more people that understand what it is that they are trying to, that if we increase their communications with the men at the bench in industry, we shall have many more cases such as this to the great glory and effectiveness of the defense forces and profit to industry.

Remarks by

Captain H. C. Ferguson, USN
Executive Officer
Naval Air Material Center

Dr. Estermann, Admirals, Conferees, Ladies, Gentlemen and Friends. Before I start I would like to introduce to you Rear Admiral Lyman, the new Commandant of the Fourth Naval District, and Commander of the Naval Base, Philadelphia. Admiral Lyman.

Captain Arnold, Commanding Officer of the Naval Air Material Center, your host activity, regrets very much that he cannot be here personally to greet you. In his behalf and for all of us at NAMC, we welcome you to Ben Franklin's home town, the Cradle of Liberty, Declaration of Independence, Continental Congress and City of Brotherly Love. As hosts, and with the cooperation of the Ben Franklin Hotel management, we believe your conference stay will be a pleasant and profitable experience.

It is quite appropriate that this all-Navy Symposium be held in Philadelphia. The Philadelphia Navy Shipyard was the Navy's first primary shipbuilding yard. The Navy, being farsighted and economy minded, bought a thousand acres from Philadelphia in 1868 for one dollar. The shipyard has progressed and developed through four wars and three or four campaigns to its present status. The Naval Air Material Center is the site of what used to be the old Naval Aircraft Factory which dates back to 1917. It is closely related to Naval Aviation progress throughout the years. During World War I we designed, developed and built approximately two hundred seaplanes and patrol planes. If you know your early aviation history, you read of the old F5L Patrol Plane. After the war the mission of the NAF was changed to development and manufacture of experimental aircraft and aircraft accessories of a nature requiring confidential development. During

this period we built the Shenandoah, the first of our dirigibles. We developed and built the famous PN-9 airplane, which established six world records. One of its world records was climbing to an altitude of 19,593 feet. Another was the first trans Pacific flight. Its design still is basically the same for today's seaplanes. During this period, in addition to seaplanes we designed and manufactured Navy fighters, scouts, torpedo and bombing planes. In the 1930's, we started building parachutes and, for many years, built all of the Navy's parachutes.

In 1934, under the terms of a Congressional Act, 10% of all government aircraft and aircraft engines had to be constructed and/or manufactured in government aircraft factories. NAF, as the government's only aircraft factory, designed and developed the famous Yellow Peril (N3N) training plane - still used at Annapolis. The planes were powered by engines designed and built at NAF. One thousand were built prior to World War II. During the war years, the NAF produced fourteen airplanes of various types, thirteen hundred aircraft engines, thirty-thousand parachutes, three hundred thousand tow target sleeves.

In addition to aircraft and aircraft engines, the NAF has been the center of catapult and arresting gear development since 1919 when it was authorized to design the catapult for the USS LANGLEY. From that time to the present, we have designed and developed the catapults for the U. S. Fleet; likewise, we have had the primary responsibility for the design and development of the arresting gear for all carriers -99- thru World War II.

Following World War II we again reorganized from our war time endeavor to an experimental and development activity.

The Naval Air Material Center now is a major research and development activity, with four laboratories and the Naval Air Engineering Facility (Ship Installations) - a sixty million dollar plant and fifty million annual expenditures.

Materials is our most important research in each of our laboratories. We seem to have reached a point where progress toward our technical goals is limited by the capabilities of our structural and functional materials. Structural design criteria and materials previously used are no longer adequate and we rapidly are developing engineering requirements far beyond the state of the arts involved. Therefore, I feel it highly desirable and worthwhile for those engaged in the field of materials research to hold a conference such as this, where the participants can get a perspective on their own endeavors - where they can find out what the other fellow is thinking

and why - and where an attempt will be made to more clearly define the problems, the solutions to which control the rate and direction of technical advance.

Now I would like to quote our yearbook of thirty years ago:

"Our work consists of the assembly and repair of all types of aircraft, from the swift, breathtaking fighting planes to the massive, powerful patrol ships. Engines, controls, guns, bomb mechanisms, navigating instruments, communication devices and safety devices must operate smoothly and perfectly. The finished ship must be a perfect machine, capable of carrying out the exacting wishes of the Navy's magnificent pilots. Eternal vigilance is the price of safety and safety is the priceless ingredient of all aircraft. In our assembly, this attribute has reached its highest peak; perfect planes. Our perfect planes mean adequate defense; defense is the safety of your home and life."

It appears we are still trying to reach these goals. When this was written thirty years ago, a young Lieutenant Junior Grade was the assistant officer-in-charge of this work. His only laboratory was two small rooms. He must have been a pretty good Junior Grade for now he's a Vice Admiral. His name - CLEXTON - with us today as Chief of Naval Material.

We certainly are pleased and gratified at the response to this Third Navy Science Symposium. 500 of you distinguished representatives are attending. Tomorrow, we have a very interesting tour and exhibits scheduled for you at Johnsville and Philadelphia. We are at your service to assist you in any way we can during the conference. I hope your attendance here will have a valuable and stimulating effect. Have a good meeting. Thank you.

ACCEPTANCE OF
CAPTAIN ROBERT DEXTER CONRAD AWARD

by

Robert M. Page
Director of Research
Naval Research Laboratory

The Office of Naval Research, as we all know, is characterized by a philosophy of management of its research activities which was unique in the Department of Defense 12 years ago and is still unique in the Department of Defense today. That Capt. Robert Dexter Conrad was instrumental in getting the Office of Naval Research established in this philosophy makes the award that is graced by his name especially prized by the Naval scientist. It is therefore with warmth of pleasure and gratitude that I accept this award tonight.

In this particular instance, however, I like to think that this recognition is given not to an individual, but to an organization. For 36 years the Naval Research Laboratory has been in operation for the sole purpose of generating and conducting a program of scientific research in support of the defense of this country under the sponsorship of the U. S. Navy. Every person on the staff, every part of the Laboratory, is there primarily for one, and only one purpose: to support the program of scientific research. The achievements which justify this award were not only made possible, they were in substantial part accomplished by — my scientific colleagues, of course, but equally importantly by the craftsmen, the people of the shops, of public works, the clerical support, the administrative support — all the components of the Laboratory working together in a common cause.

If it may seem that my personal efforts have contributed to these achievements, it is my pleasure to acknowledge publicly here tonight, that all the credit, all the honor, and all the glory belong to God my creator, my inspiration and my strength.

Note: The Captain Robert Dexter Conrad Award was presented to Dr. Page by Rear Admiral Rawson Bennett at the Symposium banquet on March 17, 1959.

TOXICOLOGY IN RELATION TO NAVY MATERIAL PROBLEMS

Cdr. J. Siegel, MSC, USN
U. S. Navy Toxicology Unit
National Naval Medical Center
Bethesda, Maryland

The rapid development of new materials and military chemicals and the concurrent development of nuclear-powered submarines and space vehicles, has necessitated the search for a new body of toxicity data and a new frame of reference. Captain Richard B. Laning, former skipper of the record-breaking Seawolf, stated on 13 February, 1959 that the atomic submarines could operate on a war patrol for four (4) months without surfacing. Under these conditions or continuous exposure over a period of months, the body of toxicity data developed for industrial applications during an 8-hour day, 40-hour week does not apply. Closely related to the submarine problem, is the problem of space travel. The success of manned-space will be dependent in a large measure on our ability to provide the capsule with a habitable atmosphere free of toxic materials.

It may be worthwhile at the outset of this conference, therefore, to devote a little time to the subject of potential toxicity of materials as this may be the critical limiting factor in the ultimate utilization of the materials by the fleet.

Every time a new weapon system is developed in which a military chemical is contained, two major questions are asked, or should be asked:

1. Does it meet performance objectives, and

2. Is it potentially toxic?

DEFINITION OF SUBJECT

For the purpose of this presentation, only that portion of the Navy's toxicology program pertaining to military chemicals will be discussed. Many of these chemicals and related materials are new; others are well known substances being used in a new way. Some are exotic in nature like the high energy fuels; others are run-of-the-mill compounds like carbon tetrachloride and freon. They all have a common denominator in that toxicity is an unwanted property.

Several examples may be useful at this point to indicate the range of our interest as follows:

	MATERIALS	USE
1.	Triaryl phosphate hydraulic fluids	To replace petroleum based hydraulic fluids
2.	Waterless hand cleaners	Conservation of water in submarines
3.	Exotic fuels	Missile propellants
4.	Red fuming nitric acid	Oxidizers for propellants
5.	Rocket and missile decomposition products	Weapons systems
6.	Freons	Refrigerants
7.	Fire extinguishment agents	For use in polar regions
8.	Rubber-based paints	Navy wide
9.	"Teflon" (plastics)	Coatings, gaskets

These illustrations will serve to indicate the diversity of materials on which we are called upon to make toxicological evaluations. At the present time, we are involved in evaluating approximately 150 materials, over 100 of which are tied in with the fleet ballistic missile submarine problem. Please note that none of these examples include drugs or medicinals used in the treatment of disease, nor do they include chemical warfare agents or war gases.

BACKGROUND

As a result of the Leyte and Bennington disasters in 1953 and 1954, an intensive search was started by the Bureau of Ships for substitute non-flammable hydraulic fluids which would meet performance requirements. Many compounds were screened and in June 1954, one material, a triaryl phosphate compound (T.A.P.) appeared to show promise from an engineering point of view. One major question had to be resolved first, and that was the question of toxicity. The Bureau of Medicine and Surgery was requested to come up with a fast answer to the following question: Could this new hydraulic fluid be used without limit aboard carriers from the toxicity point of view? The predicament we were in is shown in figure #1. Not only did we not know the composition of this material, the manufacturer did not know it either! Only extremely meager information was available on the oral toxicity of these types of compounds, but nothing was known about inhalation toxicity or skin absorption toxicity----- our main interests. No methods were available for detecting and measuring the minute ---- yet physiologically significant ------- quantities of material which might be generated into the atmosphere, and even if the concentrations would have been measured, no standards had been developed or proposed.

It is not the intent of this paper to delve into the complicated mode of action by which the organo-phosporous compounds act on the body. Suffice it to say, there was enough "smoke" to indicate that exposure of personnel to an unknown mixture of organic phosphate compounds might be extremely risky.

This hydraulic fluid problem pointed up our weakness in the field of toxicology. The mechanisms which were available were too slow and cumbersome; they were not conductive to the development of the rapid advice needed by the various bureaus and offices. I do not wish to minimize the value of the mechanisms which did exist, particularly the committee on toxicology of the national research council. This committee has always been of great assistance to BuMed, and they came through the hydraulic fluid problem within the limitation of their operations. Another mechanism which contributed significantly, and at great sacrifice to their assigned mission, was the performance of crash projects by the Naval Medical Research Institute, Bethesda. However, because of lack of over-all adequate mechanisms it was two years before we were finished with the aircraft carrier hydraulic fluid problem.

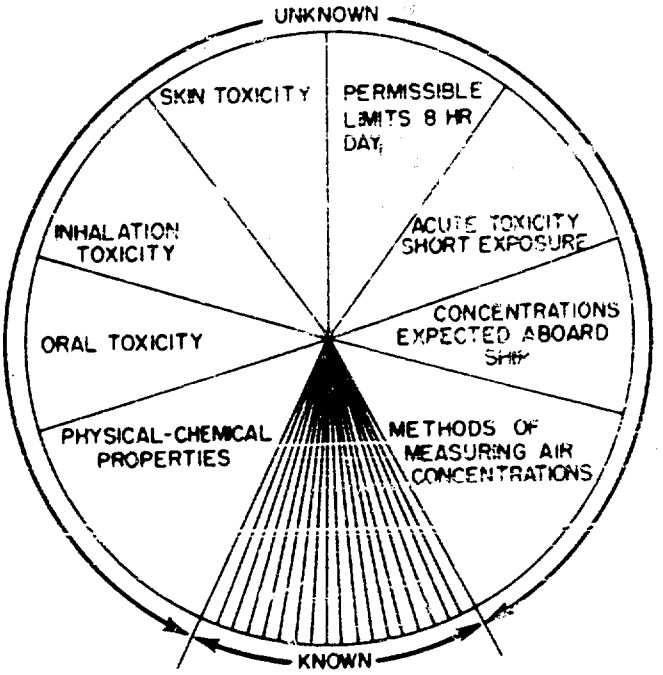

1. TYPE OF COMPOUNDS IN MIXTURE
2. ORAL TOXICITY OF TRI-O-CRESYL PHOSPHATE.
3. INHALATION OF INSECTICIDES OF THIS TYPE ARE CONSIDERABLY TOXIC.

Figure 1 - Nonflammable hydraulic fluids

The need for better mechanisms was obvious, for it just didn't make sense to arrive at critical decisions affecting the health of personnel, and costing a considerable amount of money, without basic data. Nor did it make sense to begin to develop the needed toxicity data only after the material was placed into service-wide usage.

Five (5) major steps were taken by the Bureau of Medicine and Surgery in an effort to remedy this situation:

STEPS TAKEN TO PROVIDE INFORMATION
ON POTENTIALLY TOXIC MATERIALS

1. SECNAVINST 6260.2 - Nov 1955 - Potentially Toxic Materials.

2. SECNAVINST 6260.4 - May 1957 - Establishment of Toxicological Information Center - N.R.C.

3. Establishment of liaison with each bureau and office

4. Establishment of U. S. Navy Toxicology Unit - Jan 1959

5. Development of a philosophy on toxicology

SECNAV Instruction 6260.2, entitled "Potentially Toxic Materials", sets up an orderly mechanism for obtaining the toxicological information needed by bureaus and offices in conjunction with their research and development program. It sets out step by step the responsibilities and actions required of the various bureaus and offices involved. When a toxicity problem is submitted to BuMed, the following machinery is set in motion, figure #2.

1. If sufficient information is available, BuMed may come up with a quick, final, answer. This would be unusual because toxicity data on most of the materials submitted are non-existent.

2. If insufficient information is available, (a) BuMed sends back a tentative evaluation with tentative precautionary measures via The Office of Naval Research, and (b) The problem is referred to the Toxicological Information Center and/or the Committee on Toxicology of the National Research Council.

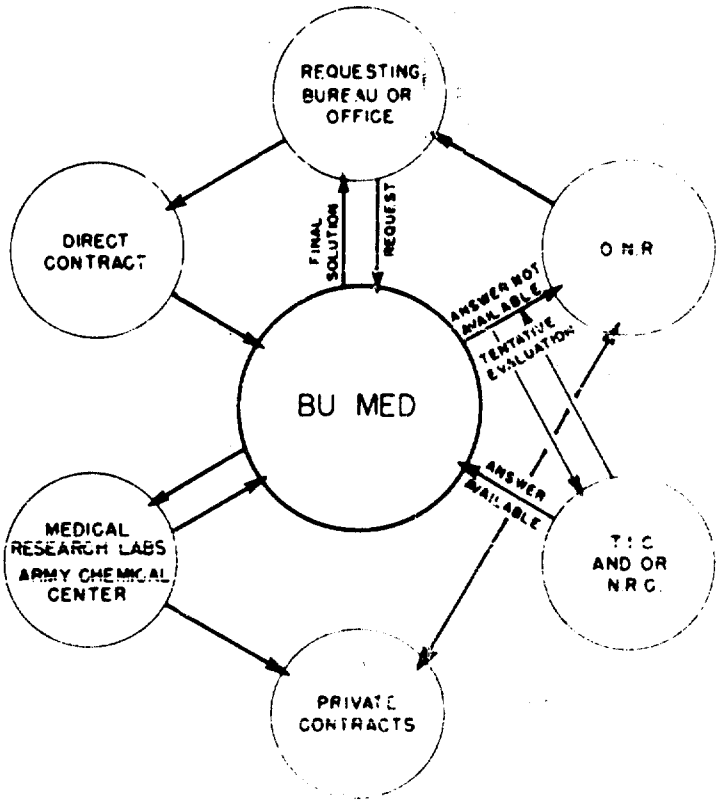

Figure 2 - Procedure for toxicity evaluation

3. If on the basis of advice from BuMed, the requesting bureau decides to sponsor toxicity work then BuMed assists in setting up an adequate toxicity protocol. This is usually done in conjunction with the Office of Naval Research if a contract is to be let.

4. If the project is urgent, BuMed may set up a crash project at one of its medical research laboratories.

5. Finally, BuMed re-evaluates the toxicity of the material in light of the additional information developed by contract and/or in-service studies and sends back to the requestor a complete estimate of the health hazards involved together with recommended precautionary measures.

TOXICOLOGICAL INFORMATION CENTER

The second major step taken by BuMed was the spearheading of the establishment of a toxicological information center as part of the National Research Council. This center is currently funded by the three military services and the Atomic Energy Commission. The center's mission is outlined in SECNAV Instruction 6260.4 of 2 May 1957. Its major function, as the name implies, is to provide a central source of toxicological information and advice on military chemicals.

The center got underway in February 1957, just two years ago. During this period it has worked up 20 toxicity reports for the Navy alone. The speed-up in obtaining answers has been amazing. Instead of the previous average of 1 to 3 years, we are now obtaining answers in 1 to 3 months. This is a tribute to the Director of the center, Dr. Harry W. Hays, and his dedicated staff.

To keep the center from being flooded with requests from all over the Navy, the Bureau of Medicine and Surgery was designated as The Navy Liaison Office to the Toxicological Information Center. All bureaus and offices were asked to refer their problems to BuMed through designated liaisons established at bureaus and offices.

U.S. NAVY TOXICOLOGY UNIT

The Toxicological Information Center is essentially advisory in nature and is intended to supplement rather than supplant current toxicological activities in the Navy. It is a paper organization

and performs no research, animal testing, or laboratory work. The Navy Toxicology Unit was established to provide this missing link. Efforts to obtain needed laboratory and field data through established mechanisms have proven unsuccessful. The type of data needed was inhalation toxicity data over prolonged periods of explosure for 30, 60, 90, or more days. We were unable to interest contractors in these types of studies for it apparently introduced extremely complicated administrative problems involving round-the-clock operations.

The Navy Toxicology Unit was established by the Secretary of the Navy on 1 January 1959 as an activity under the management control of BuMed. It will occupy 3600 square feet at the National Naval Medical Center, Bethesda, and will be staffed by 4 officers, 10 enlisted and 5 civil service personnel. The initial funding is being provided primarily by BuShips and by BuOrd's special project office for the Polaris Missile; personnel and space are being provided by BuMed.

The mission of the unit is to provide rapid, practical answers to toxicity problems. The animal toxicity tests will be of a "crash" nature and all problems will be handled on an urgent basis. The philosophy will be such as to stop the work as soon as sufficient data are developed for design purposes and operational needs. Although adequate for operational purposes, the data developed will not have the completeness or finesse required of basic research. This type of data should nevertheless enable the various bureaus and offices to proceed intelligently with their procurement plans, and the design of new weapon systems. The two major spheres of operation of the Navy Toxicology unit will be:

1. Field testing during actual operations, and

2. Animal and Laboratory studies.

in addition to the usual toxicological methods, emphasis will be placed on inhalation toxicity studies. To this end we will have a battery of ten (10) exposure chambers, designed for continuous inhalation studies.

It is our hope that this new toxicology unit, by being continually in a ready state, will be in an excellent position to provide rapid toxicity answers to urgent problems so that lead time in weapons development can be reduced to a minimum.

BuMED"S PHILOSOPHY ON POTENTIALLY TOXIC MATERIALS

The Bureau of Medicine and Surgery is charged by Navy regulations with maintaining the health and safety of Naval Personnel. To achieve this end it sets health standards and prescribes preventive precautionary measures whenever health is threatened. This applies to all facets of occupational health and preventive medicine. Protection against toxic materials is but one area in this over-all health program.

It is our belief at BuMed that almost every material ------ regardless of its toxicity ------ can be handled without hazard to health. It should be noted that BuMed does not forbid or prohibit the use of materials. It advises on the health measures that should be instituted if the material is to be used without ill effect to personnel. These health measures include limits on the amount of contaminants which can be tolerated in the air. In view of the paucity of toxicity information needed today, we have been forced to make "guess-estimates" based on the best information available. This "guess-estimate" includes suggested standards and health precautionary measures, and is subject to change as soon as additional information becomes available. These tentative values are used to help set parameters for design and operations. The chances are good that our estimate will be in the right ball park, if not plumb center. It is our belief, not original with us, that "a preliminary analysis based on incomplete data may often be much more valuable than a more thorough study using adequate data, simply because the crucial decisions cannot wait on the slower study but must be based on the preliminary analysis"*

I have attempted to outline the five steps undertaken by BuMed in order to resolve problems in toxicology. It is hoped that through these 5 mechanisms we will be able to provide you with fast, practical answers in the field of toxicology.

The active mechanisms presently available are shown in the following table:

* Methods of Operations Research, by Philip M. Morse and George E. Kimball. John Wiley and Sons, First Edition, 1950.

TOXICOLOGY MECHANISMS AVAILABLE

	PAST 1954	PRESENT 1958	FUTURE 1959
COMMITTEE ON TOXICOLOGY N.R.C.	X	X	X
ARMY CHEMICAL CENTER (LIMITED)	X	X	X
O.N.R. CONTRACTS (PRIVATE LABS)	X	X	X
MEDICAL RESEARCH INSTITUTE (LIMITED)	X	X	X
SECNAVINSTR 6260.2	-	X	X
TOXICOLOGICAL INFORMATION CENTER (NRC)	-	X	X
NAVY TOXICOLOGY UNIT	-	-	X

You could assist us greatly by contacting BuMed as soon as you get involved with any material which is suspected of having a toxic potential. It takes time to run animal work. We would like to keep parallel with your requirements so that health precautionary measures adequate to protect the health of personnel will be available to the fleet concurrent with the completion of your materials research.

RELIABILITY AS APPLIED TO MATERIALS RESEARCH AND SELECTION

E. J. Nucci
Office of Electronics
Office of the Director of Defense Research and Engineering
Washington, D. C.

When asked to participate in this symposium I was very gratified for it offers me an excellent opportunity to present my thoughts on the urgent need for accelerating research on new materials to improve present-day military electronics--materials for the component parts to meet the tremendously advanced electronic requirements of the space age into which we have entered.

In the past decade, electronics in my opinion has not received its deserved share of military-sponsored fundamental and applied research; and this is particularly true in the area of materials. The military have sponsored a good deal of research to provide lightweight, superstrong, heat-resistant materials for use in supersonic and hypersonic aircraft and to meet the structural and propulsion requirements of missiles. But far less emphasis--indeed, far too little--has been placed on research to provide the materials needed to make electronic equipment that can be produced in an economically practical domain and will operate satisfactorily in these new vehicles and environments.

It is sometimes argued that we are overemphasizing this deficiency in fundamental techniques and electronic components, which to my way of thinking is a serious one. We are asked to face reality; it is pointed out that we now have complex electronic devices in new aircraft and missiles, even in satellites, that are operating quite satisfactorily and with a fair degree of reliability. I can only say that persons advancing this argument are misinformed or, perhaps, are taking too narrow a viewpoint, for the facts do not bear out this conclusion.

I suggest that an analysis be made to determine what costs of development and production are attributable to component derating, circuit redundancy and other special design techniques—perhaps better labeled "design dodges"—which are necessary to obtain even partially acceptable reliability. Similarly, we need to determine the costs of critical mechanical design and construction techniques that are needed to crowd all the required components into the ever-shrinking space available in high-performance aircraft and missiles and to reduce the internal environmental levels, such as temperature, shock and vibration, to a level commensurate with the capabilities of available components. Do we realize how much money, manpower and facilities are used annually in testing available component parts to determine their maximum stress levels so that designers can get the most out of them? I also suggest that we take an honest and realistic look at the service reliability of some of our so-called "modern" electronic systems and compute their logistics supply and maintenance costs.

When all these factors are objectively considered, there are certain unavoidable conclusions. It costs a fantastic sum to produce and maintain today's complex electronic devices using yesterday's electronic components. I am thinking of a new interceptor fire-control system whose development cost the government approximately one hundred million dollars. This amount would buy more than 200,000 home television receivers of high quality. Of course, we can't be sure how much the costs would be reduced by an adequately supported program of research in materials and electronic components, but I am confident that such a program would save us many millions of dollars every year, perhaps more than one hundred million.

In FY 1958, the combined expenditure of the three military departments for supporting research in the area of electron tubes and component parts amounted to roughly $30 million. This is only 3/4 of 1 percent of the approximately four billion dollars spent on developing and producing military electronic equipment and systems. This imbalance is more glaring when we consider the annual expenditure for maintenance, which for fiscal year (FY) 1960 is estimated at $8.5 billion and about 25 percent of this will be charged to electronics systems maintenance.

Now let's look at some problems of operational weapons requirements, for both today and the future, and try to correlate the role of electronic parts and materials research with the whole. In what respect are these requirements so demanding? (1) There is a continual demand for more electronic functions with better

performance, and all within the same size envelope as before, or even a smaller one; (2) aircraft space travel and satellite operations are establishing requirements for much longer missions (in time) that, for some period to come, will demand unattended, failure-free operation. On the other hand, ground equipment for surveillance, air defense, guidance and weapon control, as well as communications systems, will have to be much more reliable than ever before, in view of the time compression resulting from new weapon capabilities. (3) In many cases, the operational environments of the future will be much more severe, for instance, with respect to temperature, nuclear radiation, acceleration, vibration, etc. Furthermore, some pieces of the environment picture are still unknown, or not known very well.

Now the first of these problems is, "How critical is the situation?" Based on its present orbit, the most recent Vanguard weather satellite is expected to stay up there for a period of 10 to 100 years. Yet how long will the electronic equipment perform satisfactorily? Next, what are the considerations for a moon vehicle? Since a one-way trip to the moon is roughly $2\frac{1}{2}$ days, the over-all system requirement for a 95-percent assurance of reaching the moon is of the order of 50 days mean time between failure (MTBF); if we want a 99-percent probability of success, in view of the tremendous cost of this type of operation, the MTBF design requirement would be something like 250 days. When we consider a 250-day, one-way trip to Mars, with a 99-percent probability of completing the trip with no equipment failure, the MTBF requirement for the system becomes fantastic--about 25,000 days, or roughly seven years!

What will the environmental problems be? With high-performance aircraft and missiles, again for penetration of deep space, we face the need for equipments fabricated from parts and materials that are resistant to the effects of high temperature, nuclear radiation, vibration, acceleration and pressure. Whereas up to now we were striving for reliable operation at 85°C to 125°C and are now interested in the range from 350°C to 500°C, we are looking forward to future requirements for prolonged exposure at temperatures on the order of 1200°F to 2500°F.

Electronic equipment for power control of nuclear-propulsion systems will be built in close proximity to the reactor to avoid the extra weight required by shielding. At the associated speeds, extreme vibration and acoustical noise are generated. I could mention still other environmental factors that must be taken into account in designing electronic equipment for advanced systems.

And, to complicate matters further, our materials and component parts must not only be able to withstand these individual factors but combinations of several, which in most cases will change the mode, pattern and stress levels of failure.

This leads me to a very important aspect of this problem--the expectation that we will encounter new and unknown environments and the need for anticipating the consequent requirements. In reaching for new capabilities (such as higher power outputs and higher missile and aircraft speeds for probing outer space), we are continually meeting new environmental conditions. We attempt to estimate the environments that may be met, based on knowledge obtained from previous research and from instrumentation data on development probe vehicles. In my opinion, the problem of the unknown environmental aspects, aggravated by the mixture of these unknown factors, is perhaps tougher than the problem of developing parts and materials to very high known levels.

Coming down to the practical needs of the moment, can we meet some of our new requirements with present-day parts, materials and fabrication techniques? The answer is that we can, to a limited degree, by designing around present technical capabilities. When we must use components that are designed for operation at 125°C, we can cool the units or compartments to achieve a degree of success. However, there is a penalty--and quite a substantial one--in terms of the weight and space taken up by the oversized parts, blower motors, refrigeration units and blocks of heat-sink material, plus added power for cooling and oversized propulsion plant to compensate for the additional weight. We can also shield nuclear reactors and put the electronic controls outside the shield, but again we pay! Incidentally, I understand that in some of our present space probe vehicles, every pound of instrumentation or payload increase results in an increase in power plant weight in the order of 300 to 1. The obvious inference is that the use of parts and materials specifically designed and developed for these extreme environments will result in a smaller package and, for the same propulsion plant, greater vehicle performance and payload capacity with lower costs of system design and production. Through the important area of materials research, we can derive high-temperature materials for nose cones, high-temperature lubricants and perhaps new solder, and new electronic parts and materials suitable for all the previously mentioned environments.

Please note that in this paper my examples are mainly in the temperature area. We may find later that temperature may not be the toughest environment. Prolonged exposure to cosmic radiation may be the "killer"--perhaps a combination of several may become

our principle concern.

In the field of component reliability, again, new mission requirements and demands for higher performance leading to increased complexity are causing our people in component-parts work to think in terms of failure rates on the order of 0.001 percent per 1,000 hours for future designs, as compared to present figures of 0.2 percent to 10 percent per 1,000 hours. In the past, we tried to meet our systems requirements mainly by using available parts and materials and designing around deficiencies. Thermal design, redundancy techniques and derating to a permissible failure-rate level have helped us thus far; but--let's face it!-- equipment and systems employing parts and materials now at hand have just about reached their ultimate application.

The only hope for fulfilling new requirements, which will surely demand greater reliability by at least an order of magnitude, lies in carrying out research on basic properties of materials and new design concepts based upon total functional systems requirements. It is not enough to gain marginal improvements through rigid engineering discipline applied to available circuit elements. Only by achieving major breakthroughs can we succeed. We have seen this principle demonstrated before, perhaps to a lesser degree than is needful today. The styrenes, the glass capacitor, teflon and ferrite cores are examples of a few areas in which vitally needed breakthroughs occurred. For eight to ten years we conducted a frontal attack on the receiving-tube problem, which resulted in the development of the reliable lines of miniature receiving tubes and subminiature tubes for missile applications.

It is interesting to note that according to recent calculations by ARINC Research Corporation comparing the removal rates of receiving tubes in 1954 to the presently used higher quality line, there has been an 11-to-1 improvement for aircraft applications and a 12-to-1 improvement for shipboard uses. This was accomplished through the use of the highest quality materials and under very stringent control of all materials processing and assembly. The transistor, a major breakthrough in the use of physical properties of materials, is increasingly coming into play in the tube sphere of influence. Looking at this advance from the materials viewpoint, the first transistors were germanium types; in a short time, silicon units were developed for higher temperature and higher power uses.

In the parts area, there are only a few examples of efforts to significantly extend the life of an item, although several capacitor manufacturers have established high reliability lines.

Actually, the situation about eight years ago was such that attention was focused on tubes, for all reliability surveys indicated that 70 to 80 percent of electronic failures were due to tubes. As a consequence of the tube improvements I mentioned and with the advent of semiconductor diodes and transistors in their electronic roles, the failure distribution of electronic parts has changed. Despite these over-all improvements, however, we are fortunate if we can meet even present requirements.

A few weeks ago I attended a briefing and progress report on the Signal Corps Micro-Module Program. Those of you familiar with this effort know that the first objective is to develop micro-modules utilizing available techniques and materials, then to improve the module capability to meet requirements for higher temperature, greater reliability, etc. It is interesting to me that 21 sub-contractors are materials suppliers offering advanced materials. It is also noteworthy that the research and development program proposed by the Signal Corps, which is necessary to provide the back-up to the present effort and to prepare for future requirements. This projected effort consists mainly of materials research.

We know that current research projects are uncovering amazing capabilities in new materials, as well as in some that are in use today. Studies of ceramics, metallurgy, and the molecular structure and chemistry of materials have recently opened new avenues that hold great promise of breakthroughs in the near future. Closely allied to these efforts are development and research efforts on fabrication techniques, which may prove to be as important as the materials research itself.

Today, an extremely important phase of electronics is solid-state physics, for this may completely change the electronics art and industry within the next ten years. Research studies in microcircuitry are in progress. We are thinking in terms of thin films and solid circuits employing molecular elements for redundancy and greater reliability. We are working out techniques of crystal growing and materials integration, with the aim of creating solid equivalent circuits and eliminating the present-day standard component. This simplification of circuitry—eliminating failure-prone components and the numerous connections needed--promises to make possible further miniaturization and improved reliability. Only through these efforts will we achieve objectives such as obtaining microscopic sized filters of virtually infinite "Q" (limited only by dielectric loss) or a 3-inch-cube, solid-circuit computer with a storage capacity of a billion bits. Following present trends, the future technology will employ the basic electrical nature of matter

to perform electronic functions.

I do not wish to give you the impression that I feel all is fine, so let's relax. Present research and development efforts are very encouraging, but there is still much to be done. Once the feasibility of an item is established, we must then conduct follow-up development to improve these new devices so that they will withstand the prevailing environments and attain the necessary reliability levels. Furthermore once these items are developed, test techniques and equipment must be developed to measure these new capabilities. This phase can be most important. In new developments such as cryogenics, we must consider the size and weight of the associated refrigeration equipment; in solid-circuit computers, the input and output techniques and the required power supply.

Recognizing the importance of supporting research programs in the electronics parts, tubes and materials area, the Deputy Secretary of Defense some months ago approved emergency funding to supplement the normal budget for long range supporting research programs in electronic tubes and parts. His instructions were to continue the new level of effort through FY 1960.

I have said that our present research programs in materials promise great things for the future. So that materials research will proceed as fast as possible, the users of the research products--the equipment and systems designers--must define their requirements in terms of the functions and environmental stresses to be anticipated. Here, a good example is the categorization of environments established by the Advisory Group on Electronic Parts. This publication is called the Environmental Requirements Guide for Electronic Component Parts. Moreover, all research groups, as well as designers, should make it their business to know what programs are being conducted in their fields of interest, what techniques are being developed and the status of these activities.

Now, to ensure full use of new developments and to speed up systems programs, it is most important that details of new applications be quickly disseminated to the hardware designers. We simply haven't the time, money or manpower to repeat investigations, tests and design efforts that have already been accomplished satisfactorily. Information exchange on research and development can make possible the earlier attainment of higher performance capabilities and can secure for us greater numbers of electronic functions with the required level of reliability. This speed-up could achieve from two to ten times the rate of normal progress.

The Advisory Group on Electronic Parts recently issued a report entitled "A Capsule Summary of the AGEP Program in the Area of Electronic Parts and Materials." Copies of this report as well as detailed information on specific projects can be obtained from the Secretariat of the Advisory Group.

In this matter of dissemination of information I understand that the Air Force has recently reviewed its reports distribution lists to insure that all interested groups receive copies of the ASTIA printed Air Force reports. Additionally, the Air Force is arranging to provide the Aircraft Industries Association and the Electronic Industries Association with lists of new reports on file at ASTIA.

Yes, I am aware that there are stubborn problems in the exchange and dissemination of information on new design techniques and application data. Nevertheless, I am asking management groups to recognize the importance and urgency of this operation in the light of our national military posture, our economic welfare and our position at the table of international negotiation.

I'd like to leave two thoughts with you. First, our ability to meet future requirements for electronic systems will depend significantly upon new developments in materials, process control and fabrication techniques. Second, the speed with which new principles, techniques and materials are used will be a function of the time required to make known the availability of the new application data and associated design techniques.

DEVELOPMENT OF URETHANE PLASTIC FOAMS AND INORGANIC CERAMIC FOAMS FOR PRECISION RADOMES

Dr. Howard R. Moore
U. S. Naval Air Development Center
Johnsville, Pennsylvania

Radomes (radar domes) are aerodynamic housings to protect the antenna and associated electronic equipment from the air stream, so designed as to transmit maximum radar energy with minimum pattern distortion and deflection of the beam radiated by the antenna. Ideally, radomes should have the same transmission as free space and at the same time meet mechanical strength and aerodynamic requirements.

Radomes may be classified broadly as "search" or "precision" types according to their mission in piloted aircraft and missiles. Patrol planes are usually fitted with both types of radomes; for example, Cadillac search radomes and precision nose radomes are installed in the Navy's P2V bomber and WV-2 Super Constellation. Search radomes approximate the ideal hemispherical structure shown in Figure 1 since these configurations are characterized by minimum pattern distortion, phase delay, and refraction of the radiated beam. In this sense, hemispherical domes may be considered broadly as precision radomes, although they are seldom used for this purpose because of their poor resistance to aerodynamic loading.

The attainment of 90 to 95 percent transmission over wide variations in antenna scan poses no problem with search domes based on plastic glass reinforced honeycomb cores and skins; however, this objective becomes considerably more difficult for the ogive and conical designs shown in Figure 1. These shapes, predicated by aerodynamic requirements for tracking, intercept, and terminal guidance radar installations in high speed aircraft and missiles, exact much higher standards in the uniformity of dielectric constant and wall thickness over the design range of scan angles than the search types.

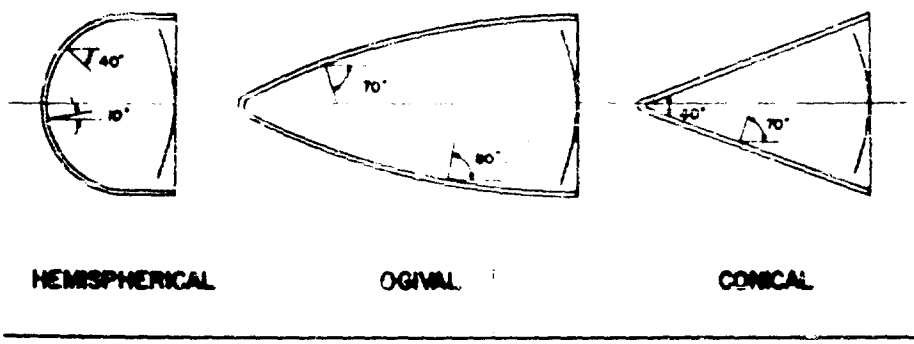

Figure 1 - Schematic designs of three precision foamed radomes

Figure 2 - Tooling used in foaming Lark ogival radomes

As may be expected, the difficulty of compensating adequately for variations in reflection, absorption, refraction, and phase delay of rays incident on the radome wall to secure high microwave transmission for accurate location of distant targets increases greatly with the "fineness ratios" of precision domes, expressed in terms of the ratios of their altitudes to base diameters. Fineness ratios for the ogive and conical shapes shown in Figure 1 are 2.210 and 1.375, respectively. Ogive shapes are more versatile than conical types in this respect, since their continually varying radii of curvature permit the transmission of radiation at slightly higher angles of incidence than their average angles of scan.

Although it has been demonstrated that both ogive and conical domes can be designed to give 90 percent and even higher power transmission at design microwave incidence angles of 70 to 85 degrees, corresponding to progressive increases in fineness ratios and aerodynamic efficiency, this approach soon reaches a point of diminishing returns because of abrupt reductions in power transmission at angles of incidence ranging from zero to 60 degrees. These unfavorable results can be mitigated by sharp reductions in wall thickness, and by increasing the dielectric constant of the materials used in fabricating "half wave" walls from 4 to 9, or even higher. Unfortunately, these methods weaken the wall and decreases thickness tolerance from ±0.01-in. to ±0.005-in. However, still tighter fabrication tolerances of ±0.002-in. are required in the thickness of the facings for precision sandwich structure conical and/or ogival domes designed for optimum transmission at design angles of 60 to 70 degrees.

The foregoing conclusions on the electrical and dimensional criteria for precision radomes were derived from a consideration of transmission curves and numerical data published by this Center for both half wave and sandwich structure radomes (1). A weighed analysis of these data has indicated that the half wave concept of radome design permits more accurate tracking of the target than sandwich designs. This favorable result was believed due to better control of variations in phase delay of emergent rays within limits consistent with maximum boresight shift requirements over the operating range of angles of incidence, as well as to transmission efficiencies exceeding 90 percent for the maximum angles of incidence for which the domes were designed. Moreover, the design thickness, d_1, of half wave domes is independent of the power loss (loss tangent) in the dielectric, and may be readily calculated from the equation

$$d_1 = \frac{\lambda_o}{2\sqrt{\epsilon_1 - \sin^2\theta}} \qquad (1)$$

where the free space wavelength, λ_o is 1.26 inches for X band frequency 9375 mc; ϵ_1, the dielectric constant of the radome wall; and θ, the design angle of incidence.

Despite the greater theoretical and practical justification for half wave versus sandwich structure radome designs, the nose radomes of the Navy's F4H interceptor and F11F fighter are presently based on plastic sandwich structures with glass reinforced honeycomb cores and facings. The greater weight penalty in using solid half wave structures was undoubtedly a factor in the adoption of sandwich designs. For example, a radome wall of this type 0.33-in. thick weighs 2.92 lb/ft^2, as contrasted to 0.88 lb/ft^2 for a plastic sandwich construction based on honeycomb of 9.9 lb/cft density and glass reinforced facings 0.03-in. thick. Nevertheless, there was no alternative to the use of rigid urethane foamed-in-place (FIP) foams in the nose sections of all categories of precision radomes of this type, because of the impracticality of machining plastic honeycomb to sharp radii of curvature. This circumstance emphasizes the need of increasing the strength of FIP cores to the level required to justify their substitution for honeycomb for the entire sandwich structure.

Several years ago, the Emerson Electric Company demonstrated the reduced boresight error obtained by substituting rigid urethane foams of 10 to 12 lb/cft density for honeycomb cores in sandwich structure domes (2). At this time, Behrens called attention to the advantages of producing urethane foamed cores with a graduated thickness, or taper, with the aid of matched dies to secure still further reductions in boresight error (3). Raytheon Manufacturing Company subsequently confirmed Behrens' calculations in the design of the now obsolete Lark surface-to-air ogive domes 22-in. high and 15-in. base diameter. This Center made the necessary tooling, Figure 2, to produce these domes in quantity for a training course in the repair of FIP radomes (4), and for verifying the efficiency of the recommended wall taper of only 0.11-in. from the nose to the attachment section in securing hitherto unsurpassed reductions in boresight error.

The superior electrical characteristics and more liberal manufacturing tolerances of half wave radome designs were the main factors in this Center's decision to establish programs for making improved light weight urethane and ceramic foams. In developing

these structures, it was recognized that suitable additives could be incorporated in both plastic and ceramic formulations to raise the dielectric constants of the foams to any desired level, within the range 4 to 10, to match the dielectric constants of the sandwich facings within the same range. The envisioned sandwich structures should then possess the advantages of light weight and high strength/weight ratios, and function electrically in the same way as presently used solid wall half wave structures.

Part I is a review of the present status of materials and processes investigations conducted by this Center on improved urethane plastic foams. Part II is likewise a brief summary of contract studies on ceramic foams carried out by Professor A. J. Metzger and his assistants in the Department of Ceramic Engineering, Virginia Polytechnic Institute, from 1950 to the present time.

Part I

Urethane Plastic Foams

This research relates to the development, first, of low temperature-viscosity cycling processing techniques to increase the degree of cross linking of unesterified hydroxyl and carboxyl groups in foam resin compositions; and secondly, the synthesis and evaluation of four classes of foaming resins based on widely different functionality patterns of interacting poly- and monofunctional reactants.

Analysis of the state-of-the-art that prevailed at the time this work was planned indicated that the quality of rigid urethane foams based on the condensation of organic diisocyanates, such as toluene diisocyanate (TDI), with partially esterified alkyd resins, was dependent mainly on two factors:

1. The process used in converting the resins to foam.
2. The composition and properties of the resins themselves.

As a result of investigating many facets of urethane foam technology under Air Force contracts from 1946 to 1952, Goodyear Aircraft Corporation developed a constant temperature process by which the preferred resin, Alkyd 100, later offered to industry as Selectron 5922 by Pittsburgh Plate Glass Company, was reacted at temperatures of 80-85°F for 32-35 minutes until decarboxylation was firmly established, at which point 4.2% acetone-Aerosol OT on the weight of the batch was added to obtain a suitably low pour point viscosity (5).

This process was well adapted to the manufacture of radomes since the increased induction time to foaming allowed removal of air bubbles and accurate placement of matched dies before pouring. Nevertheless, a study of the Goodyear reports indicated that considerable improvements were needed in upgrading the cross linking efficiency of free carboxyl groups in the resin before the newly expanded foams were immobilized by gelation. Thus it was found that foamed radomes based on recommended materials and processes specifications (5) were subject to spontaneous blistering and delamination in service and on prolonged storage (6). This effect could be produced at will by subjecting foamed radomes to a second post-curing operation (7).

Similar evidence of incomplete cross linking was obtained by this Center in foaming several Lark radomes with the Lockfoam A-210 quick-mix formulation for a training course on foam repair methods (4). Thus it was found necessary to cure foamed-in-place (FIP) patches for 3 hrs. at 175°F, considerably below the recommended cure temperature of 225-250°F, to prevent immediate post-curing blistering and delamination effects.

In seeking the reasons for the post-curing evolution of CO_2, Goodyear Aircraft Corporation concluded that the foams contained substantial amount of partially cross linked polymers of the type

$$OCN - R' - NHC(=O) - R(OH) - OC(=O) - N(H) - R' - N(H) - C(=O) - OR(OH) - COOH$$

This conclusion was based on the following observations:

1. Immersion of cured foam caused a secondary expansion of 40% and a 40°F rise in heat distortion temperatures.

2. Boiling water hydrolysis of powdered foams produced measurable quantities of CO_2 gas.

These experiments proved the existence of free NCO and COOH groups in cured foams. Since primary urethane and amide linkages are resistant to hydrolysis, the relatively high water vapor absorption of the foams at 160°F could be readily attributed to the presence of free hydrophilic OH groups in the cured specimens.

The first object of this research was then to devise processing techniques capable of minimizing the occlusion of partially cross linked low molecular polymers in the cured foam. In devising these techniques, it appeared desirable to stabilize the viscosity of the condensate for as long a time as possible in consideration of Hebermehl's findings (8) that the rate of viscosity increase in such systems is so rapid that not all free groups can possibly react due to steric hindrance effects caused by the rapid increase in molecular size.

In achieving this objective, due consideration was given the need of somehow compensating for the higher TDI reactivity of residual water of esterification in the resin and unesterified hydroxyl groups, as expressed by Bayer's reactivity series

$$HN \cdot H > HO \cdot H > RO \cdot H > RCOO \cdot H > C_6H_5O \cdot H > HC \cdot H$$

In this respect, it was concluded that neither Bayer nor American investigators (9) had optimized the selection of polyfunctional reactants, starting OH/COOH functional group ratios, and the degree of esterification of these groups in synthesizing resins. A desirable balance of these factors presumably might reduce the steric hindrance of adjacent free OH groups in branched polymers, and point up the advantages of controlling the degree of branching to reduce the competition of these groups for TDI in the production of foams.

Goodyear's success in obtaining a 100% improvement in the tensile strengths of foams based on Selectron 5922 provided further incentive for a resin development program. This resin was made merely by reducing the starting OH/COOH functional group ratio of the same reactants used by Bayer from 2.0 to 1.9, and by discontinuing the esterification at an acid number of 44 instead of 35 as recommended by Bayer for Desmophen 800S (5). However, Selectron 5922 still contains an undesirably high OH/COOH free group ratio of 11:1, as computed from analytical determinations of 475 and 44 for the hydroxyl and acid numbers.

As a result of this survey, a research proposal was drafted for the synthesis of 100 partially esterified alkyds of widely different functionality patterns depending on the numbers of active groups present in polyfunctional alcohol and acid branching reactants, and corresponding di- and mono-functional branching reducers.

After securing Bureau of Aeronautics approval for the proposed research, it was decided that the Naval Ordnance Laboratory (NOL), White Oak, Md. would prepare the resins in accordance with

the principles delineated by the proposal. The National Bureau of Standards (NBS), in turn, would determine the physical properties of resulting foams in accordance with improved processing techniques developed by this Center.

Process Development

The main goal in process studies was to develop long time mixing cycles capable of generating a sufficiently low pour point viscosity to offset the need of adding solvents, such as acetone-Aerosol OT, which reduce the adhesion of the foam to plastic glass reinforced facings (5), and conceivably might contribute to blistering and reduced heat stability if significant amounts are retained in the unicellular foam structure after cure. Secondly, to obtain improved cross linking efficiency, the new techniques should be effective in suppressing the reactivity of free hydroxyl groups in the resin to provide an opportunity for more complete decarboxylation of the condensate, while still mobile, before gelation of the expanded foam.

Both of these objectives have been realized by various low temperature processing cycles, wherein pulverized Dry-Ice served as a refrigerant to conserve a sufficient fraction of the total potential exothermic heat of the system, in early stages of the condensation, to activate more complete decarboxylation on cessation of cooling, as illustrated by the reaction

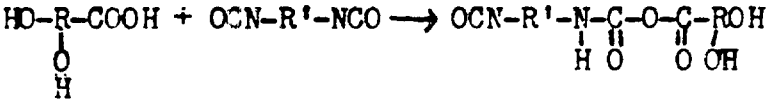

(intermediate unstable acid amide anhydride)

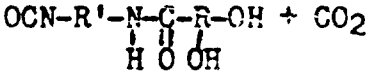

(polyamide)

In this connection, it is pointed out that the CO_2 gas liberated by the sublimation of dry ice solid CO_2 does not contribute to the expansion of the foam; the gas is promptly expelled from the batch, thereby insulating the reactants from ambient air of varying moisture content.

Carbon dioxide snow obtained by sudden release of CO_2 gas from inverted cylinders and pulverized Dry-Ice from 50 lb blocks may be used optionally in these processes if precautions are taken to

(Q)

store the material in a vented dessicator or Dewar flask to prevent the ingress of moist air. Moisture added in this way supplements the quantity of linear polyureas formed, due to residual water of esterification in the resin, in accordance with the TDI hydrolysis reaction

$$2\ OCN\text{-}R\text{-}NCO + H_2O \longrightarrow OCN\text{-}R\text{-}\underset{\displaystyle H}{\overset{\displaystyle |}{N}}\text{-}\overset{\displaystyle O}{\overset{\displaystyle ||}{C}}\text{-}\underset{\displaystyle H}{\overset{\displaystyle |}{N}}\text{-}R\text{-}NCO$$

(polyureas with terminal isocyanate groups)

Obviously, the concentration of linear polyureas should be held to a minimum because of their plasticizing action on derived foams.

While it is true that equivalent results, in terms of foam product properties, were obtained by intermittent outside ice-water cooling of small batches of condensates based on normal reacting resins similar to Selectron 5922; early experiments proved that there was no alternative to the use of solid CO_2 in removing exotherm from highly reactive NOL resins. On this basis it was decided to evaluate the effect of varying intensities of internal cooling on the performance properties of foams derived from Selectron 5922, with the expectation that these schedules could be adapted to NOL resins of unknown, but varying TDI reactivity.

Table I is a resume of the two prior art methods and four of the ten experimental low temperature-viscosity cycling processing schedules used in converting 45 of the 75 NOL resins to foams, as well as Selectron 5922 adopted as the comparison standard.

Complete details on the remaining six mixing schedules investigated for Selectron 5922 are given in a detailed report on both the theoretical and practical aspects of viscosity cycling methods (10).

At the outset, due emphasis should be given the fact that the mixing schedules cited by Table I were predetermined by the relatively high solidification temperature, 69.8°F, of the meta (2,4-) isomer of TDI, the only isomer commercially available at the time these experiments were performed. More recently, the 80/20 and 65/35 blends of 2,4-2,6- isomers with melting points of 48.2 to 53.6°F and 35 to 41°F, respectively, have been offered. Theoretically, these isomer blends are better adapted to the low temperature processing of all categories of resins, since TDI compatibility can be established at lower temperature levels. The proportionately higher conservation of reaction exotherm in forming labile, secondary

(C)

TABLE I

IDENTIFICATION OF PROCESSING SCHEDULES FOR CONDENSING 2,4-TDI WITH FOAMING RESINS

Process Designation	Description	Process Code
X	Prior art, fast mix, no temperature control	Exo/viscRwo
Y	Prior art, external constant temperature control to threshold of white opacity followed by solvent	Cm83/Pkvisc1500wo(83)/ solv4.2
1 exp.	Internal temperature control only to compatibility end point at 83°F	Cm83/exo/viscRwo
1A exp.	Internal temperature control only to compatibility end point at 71°F	Cm71/exo/viscRwo
2 exp.	Internal temperature control for 10-11 minutes at 60-65°F	PC60-65/exo/viscRwo
3 exp.	Prolonged internal temperature control at 71°F to abrupt viscosity increase	Cm71/PKvisc800-1600/ exo/viscRwo

Legends

Exo - Liberation of exothermic heat
ViscRwo - Viscosity regain at white opacity
PKvisc - Designated peak viscosity in poises

Cm - Attainment of compatibility at designated temperature
PC - Preliminary cooling at designated temperatures
Solv4.2 - Addition of 4.2% acetone-Aerosol

valence low viscosity urethane linkages with the following Nos. I and II hypothetical configurations:

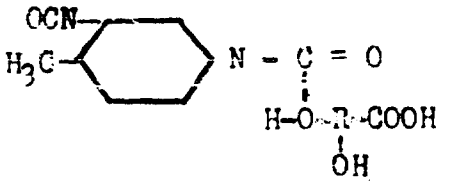

(I)

(Labile urethane linkage from 2,4- isomer)

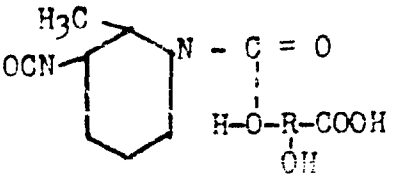

(II)

(Labile urethane linkage from 2,6- isomer)

should then develop higher temperatures on cessation of cooling with resultant more complete foaming (decarboxylation) reactions.

The lot of Selectron 5922 used in determining the effect of different mixing schedules required 0.87 grams of TDI per gram of resin, as calculated from the equation

$$\frac{\text{gms TDI}}{\text{gms resin}} = 1/2\left[\frac{n+h}{56{,}100} + \frac{W_p}{18 \times 100}\right]174, \qquad (2)$$

where n and h represent the acid and hydroxyl numbers, 44 and 475 as determined analytically, and W_p the weight percentage residual water of esterification, 1.5% as obtained by the Dean-Stark method.

In further reference to Table I, Method 1 exp. was developed originally as a screening test to classify NOL resins into three groups of "normal", "fast", and "very fast" TDI reactivity relative to Selectron 5922 adopted as standard. The procedure in this case was to maintain temperatures of 80-85°F until the end point of TDI compatibility, as indicated by the initial formation of a one phase system in spatula smear tests. At this stage, cooling was stopped and mixing continued until decarboxylation was firmly established subsequent to reaching a viscosity minimum considerably below the compatibility viscosity.

Method 1A exp. was identical with the above procedure, except that precooling temperatures of 70-72°F, slightly above the crystallization temperature of 2,4-TDI, were maintained to the end point of compatibility before allowing the reaction to proceed on its own exotherm.

Method 2 exp. was similar to the prior art constant temperature method "Y" in failing to develop a viscosity minimum. This method, ostensibly developed to convert very fast reacting NOL resins to foams, was carried out by precooling the resin to temperatures 5 to 10°F below the 2,4-TDI crystallization temperature of 69.8°F,

and maintaining these temperatures for 10 to 11 minutes before discontinuing solid CO_2 additions. Subsequent slow melting of the TDI crystals slowed up the reaction speed, but the terminal incipient foaming viscosity was too high to yield foams of acceptable texture and physical properties.

These results emphasized the potential unsefulness of the lower melting 2,4- 2,6-TDI isomer blends, cited above, in achieving true compatibility at a lower temperature range.

Method 3 exp. was carried out by continued additions of solid CO_2 for 17-18 minutes beyond the end point of compatibility temperatures of 70-72°F. At this stage an abrupt increase in viscosity took place, conceivably due to the transition of secondary labile urethane linkages to primary types. Thereafter, on cessation of cooling, mixing was continued until foaming occurred subsequent to the attainment of a viscosity minimum of about 300 poises.

Characteristically, each of the solvent-free methods of Table I developed minimum viscosities before the condensates gradually changed in appearance from transparent amber to a white opaque color due to the evolution of CO_2 bubbles throughout the mass. The occurrence of viscosity minima was evidently due to the action of exothermic heat in reducing the viscosity of the condensates at a more rapid rate than the increase normally attending cross linking reactions. This phenomenon is advantageous since it permits the preparation of condensates with low pour points, not exceeding 400 poises, to obtain rigid solvent-free foams of improved physical properties.

Incidentally, the prior art method "X" of no temperature control is also a viscosity cycling process in consideration of the recorded minimum of 35 ps prior to attainment of the foaming threshold at 90 ps. However, the mixing time, 10 minutes, was so short that a major fraction of the total exothermic heat of reaction was trapped in the expanded foam. The resulting high internal temperatures frequently caused cracking and incipient carbonization of thick reactions of the foam. Users of this process (11) have recommended multiple pours to eliminate this difficulty and counteract the effect of short induction times.

Figure 3 shows the Brabender Plastograph used interchangeably with the Hobart Planetary Mixer, Figure 5, in obtaining the trend of condensate viscosities and temperatures from the instant of adding TDI to the precooled resin to the time of pouring.

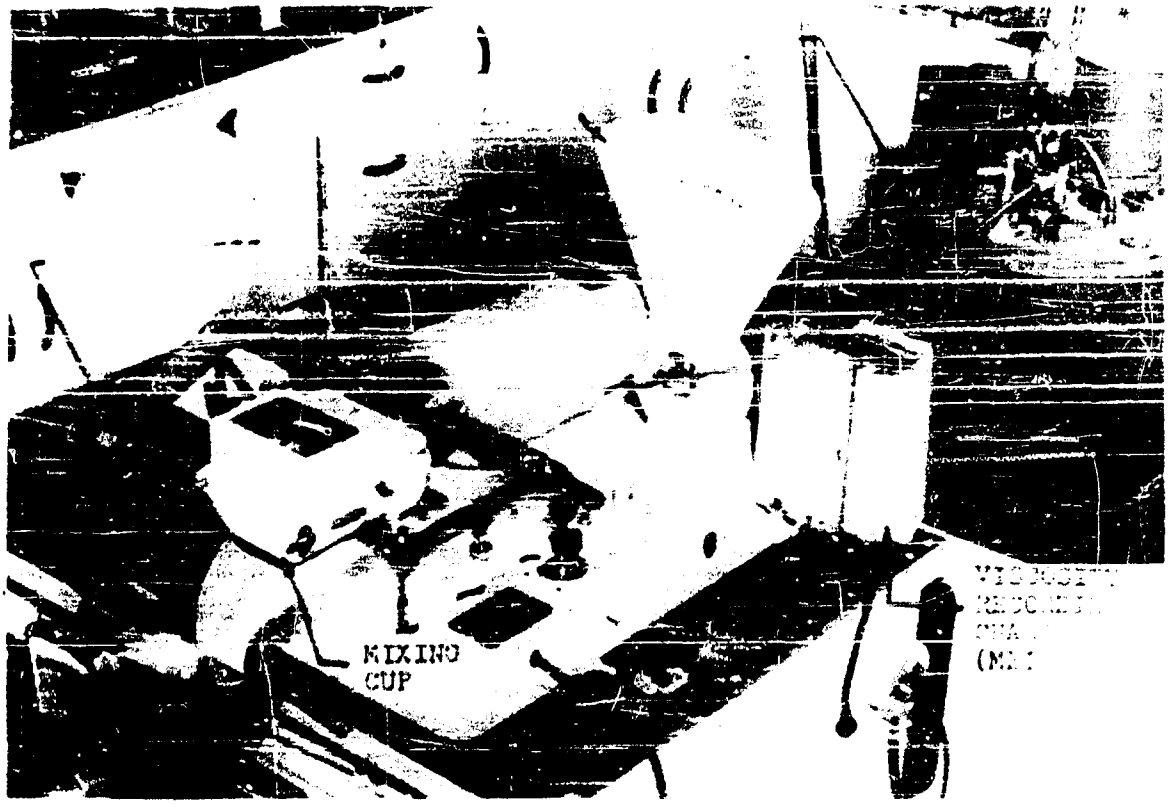

Figure 3 - Plastograph used in mixing alkyd-TDI condensates by the dry-ice method

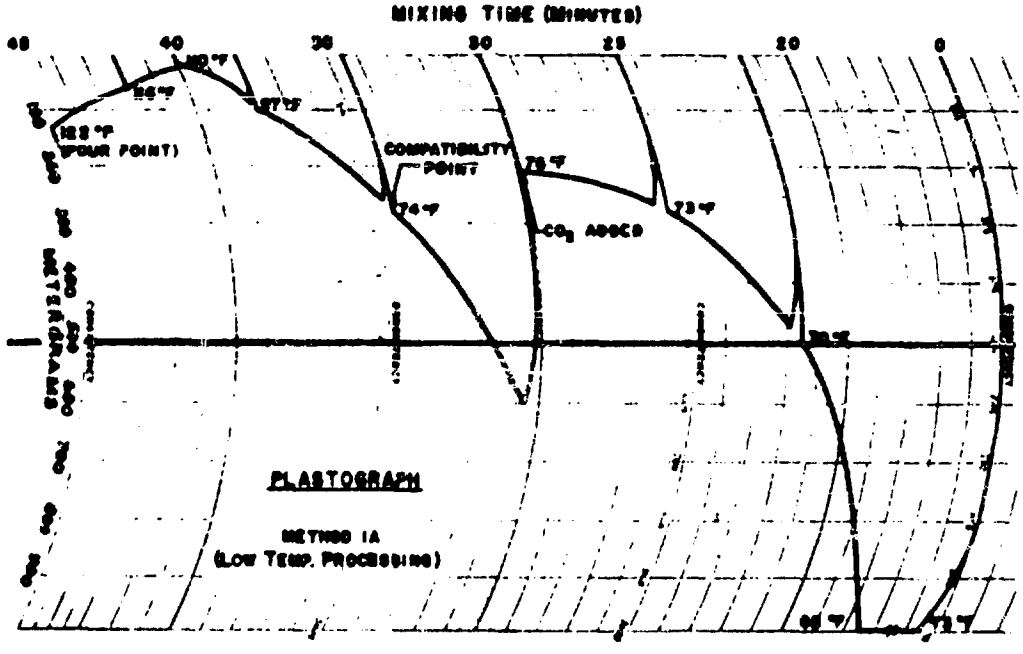

Figure 4 - Typical plastograph recording of condensate viscosity to the pour point

Figure 4 is a typical Plastograph chart recording of condensate viscosities and temperatures as a function of time for a slow reacting NOL resin prepared by Method 1A. This chart illustrates a gradual decrease of condensate viscosity from a maximum of 280 metergrams at the end point of compatibility to a minimum of 35 metergrams, followed by an increase to 125 metergrams where decarboxylation was noted. Metergram values were converted to poises with the aid of a calibration chart (not shown), based on independent determinations of the metergram readings of NOL resins whose viscosities varied from 50 to 8,000 poises over temperatures ranging from 70 to 150°F.

The automatic viscosity recording feature renders the Plastograph ideally suited for determining process criteria; however, the 525 gram limitation in batch size and 7000 poises upper limit in viscosity comprised restrictions not shared by Hobart Planetary Mixers. The main disadvantage of these machines was the necessity of interrupting the mixing for Brookfield viscosity determinations, but this is no longer a drawback after viscosity variations for a given resin have been established in preliminary tests.

Figure 5 depicts the 1/8 H.P. laboratory size Hobart Mixer used in procuring all intermediate and final pour point criteria. Much stronger 1/3 to 1 H.P. mixers were required in variations of the extended compatibility procedure, Method 3 exp., developed by Raytheon Manufacturing Co. in an early sandwich design for Sparrow III radomes.

In general, all viscosity cycling methods, whether carried out by the release of exothermic heat at the compatibility end point, or after reaching an abrupt "peak viscosity" following a viscosity plateau of considerable duration, were characterized by a pronounced drop in viscosity followed by a slow increase to the foaming threshold. Figure 6 illustrates this property for cessation of cooling at the compatibility end point (Methods 1 exp. and 1A exp.) and an earlier version of Method 2 exp. wherein solid CO_2 additions were reduced in quantity until a minimum was attained at 500 ps.

The extended compatibility procedure generated considerably higher minima, 300 ps, for Method 3 exp., and 750 to 850 ps for the long time (75-90 minutes) modifications of this process adopted by Raytheon Manufacturing Co.

Table II gives the terminal pour point criteria for 525 gram batches of condensates processed by each of six different methods, 357 grams of which was poured into demountable aluminum

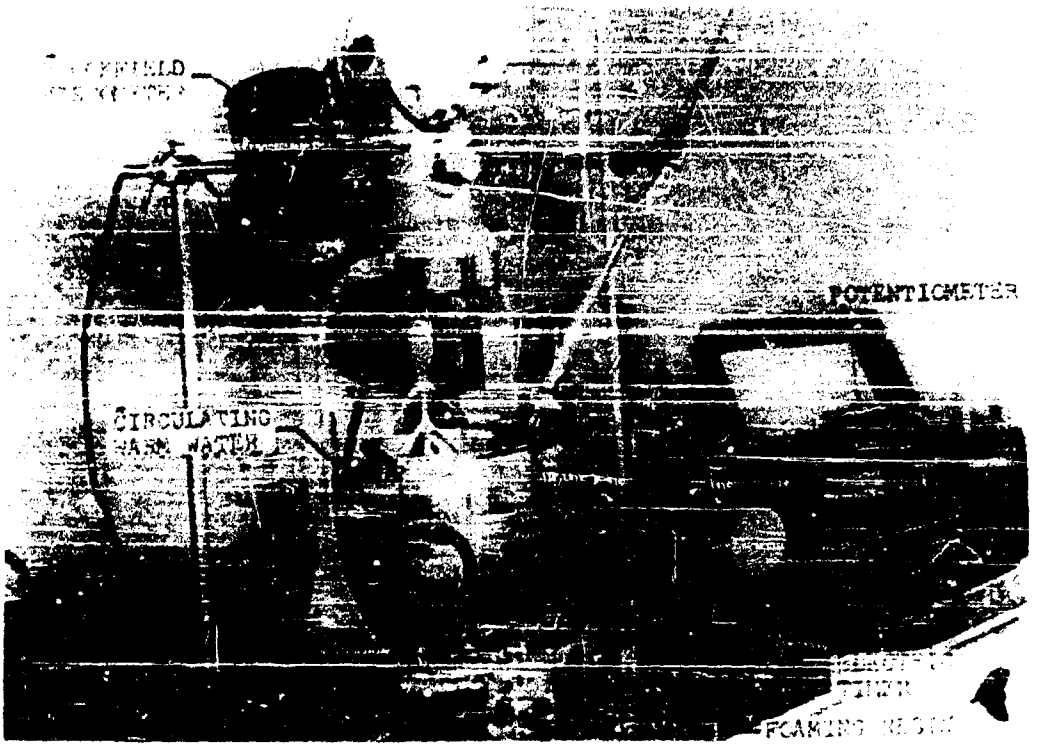

Figure 5 - Planetary mixer used in preparing condensates by internal or external cooling

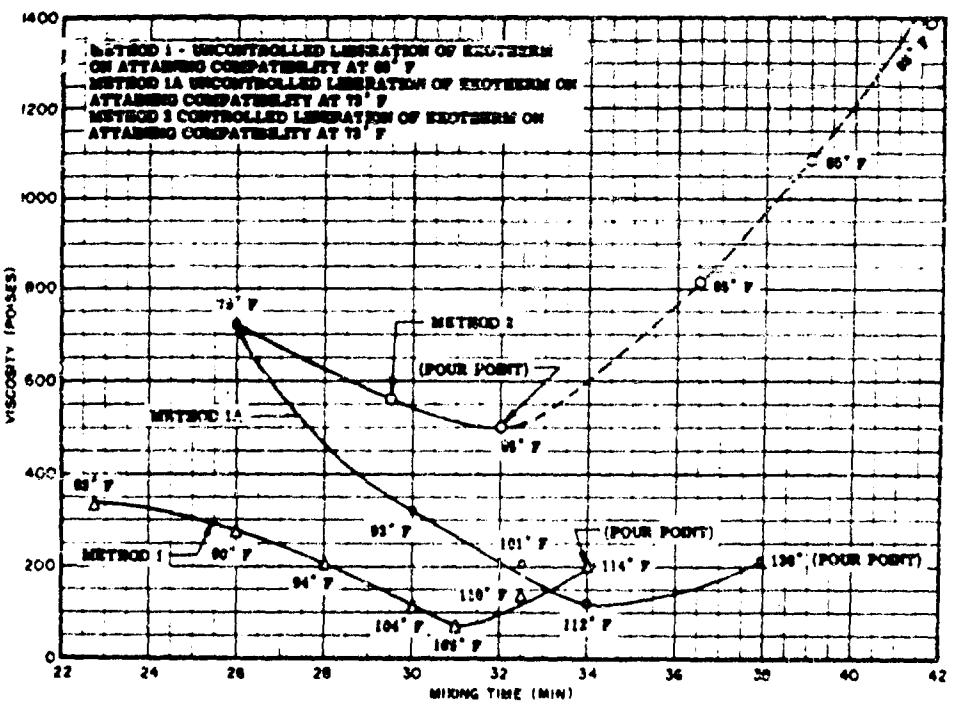

Figure 6- Typical process curves obtained by hand and machine mixing

molds with internal dimensions of 9 x 10 x 1-1/2 in. to produce restricted foams of about 10 lb/cft density. Prior to pouring, the molds were preheated to 150°F to avoid sudden chilling of the batch. Freshly poured condensates were then transferred to an air circulating oven pre-set to 150°F to complete expansion and gelation of the foams within 1/2 hour before raising the temperature to 275° for post-gelation cure cycles of 3 hours.

Half size batches of condensates were made in separate experiments to ascertain the ranges in expansion temperatures, viscosities, and gelation times of 100 gram quantities poured into quart-size paper cups. The purpose here was to determine whether increased duration of mixing was accompanied by increased mobility and higher gelation viscosities of expanding condensates. In general, these data support a direct correlation between pre-pour and post-pour criteria on the one hand, and foam performance properties on the other.

Table II product data show that Methods 1 exp. and 1A exp. were equal, within experimental data, to Process "Y", and that Method 2 exp. was inferior. However, all four viscosity cycling methods were superior to "X" and "Y" control procedures if allowance is made for their effectiveness in improving the resistance to compressive heat distortion of resulting foams, as obtained by the NBS with the aid of a Williams Plastometer. Percentage decreases in thickness of specimens subjected to a 1 hour heat-soak at 266°F in a thermostatically controlled oven were found to be 15, 20, 4.5, 2.5, 6.3 and 1.7 for each of the six processes in the order given by Table II. Poor cross linking was undoubtedly responsible for Process "X" results, while entrapment of an appreciable quantity of acetone-Aerosol OT solvent in "Y" processed foams could easily account for their still higher heat deflection.

As stated above, Table II results could be reproduced by external cooling of small batches not exceeding 525 grams. Considerable difficulty, however, was encountered in maintaining reaction temperatures within stated limits by outside cold water circulation through jacketed Hobart and Brabender reaction vessels. Intermittent cooling with a removable cold water source was usually required. Further difficulties were encountered in the solidification of resin condensate on the walls of the container. The solid CO_2 method of viscosity-cycling bypasses these difficulties. Cornell Aeronautical Laboratory, for example, has adopted preferred versions of the solid CO_2 procedure in preparing 75 lb batches of condensate in foaming KDM-1 drone wings, and for converting newly developed terpolymer unsaturated alkyds to heat resistant foams (12). At the present time,

TABLE II

EFFECT OF PROCESS SCHEDULES ON THE PROPERTIES OF RIGID 10 LB/CFT FOAMS BASED ON SELECTRON 5922

Process	Process Criteria							Product Criteria			
	Pour Point Expansion						Induct Time min	Comprs psi	Shear psi	Tensile psi	Water Vapor Abs %
	Temp °F	Visc ps	Time min	Temp Av °F	Visc Av ps	Time mins					
X	137	90	10	160	850	0.5	0.5	240	140	150	5.5
Y	85	400	35	110	1600	3	3	270	160	181	3.4
1 exp	125	200	21	140	1100	2	2	272	171	176	2.2
1A exp	135	350	27	150	1500	3	3	275	179	180	2.1
2 exp	105	600	35	130	2500	5	4	250	150	160	2.5
3 exp	88	450	45	130	4000	6	6	300	195	210	2.1

the same technique is being used by CAL in foaming modular units for building and housing construction (13).

Confirmatory evidence on the improved cross linking efficiency of Method 3 exp. relative to Method "Y" was obtained by prolonged (200 hour) extractions of 25 gm samples of pulverized foams placed in Soxhlet extractions containing 250 ml butyl acetate. Analysis of the amber colored resin extracts, in amount equal to 7.5% and 4.5% by weight of foam given by Methods "Y" and 3 exp. schedules, revealed a decrease in nitrogen content of 9.7%, acid numbers 0.7 unit, and hydroxyl numbers 137 units for Method 3 exp. This degree of reduction in the content of low molecular cross linked polymers with free NCO, COOH and OH groups, while significant, was considerably below the level sought for improved foams. Evidently, improved processing techniques cannot in themselves compensate for defects inherent in the composition of the resin itself.

Resin Development

In order to obtain data on the effects of variations in the chemical structure of poly- and monofunctional reactants, starting functional group ratio, and degree of esterification in controlling the number of free hydroxyl and carboxyl groups and the molecular weights of resulting polymers, NOL made 75 foaming alkyds classified as follows with respect to the condensation functionality of interacting materials:

	Functionality Patterns	Number of Resins
Class I (Unmodified Desmophen Types)	3:2,2 3:2,2,2 4:2,2	28
Class II (Diol or dibasic acid modified types)	3-2:2,2 3-2:2,2,2 3-2,2,2:2,2 3-2:2,2,2 4-2:2,2* 4-2:2* 3,3-2:2* 2,2:3-2,2*	33
Class III (Monobasic acid modified types)	3-1:2,2 4-1:2,2* 2-1:3*	10

	Functionality Patterns	Number of Resins
Class IV (Diol and monobasic acid Modified types)	3-2-1:2,2 3-2:3-2,2*	4

*Note: 30 formulations based on functionality patterns designated by asterisks were rejected because of excess TDI reactivity.

The functionality patterns of all reactants used in making the resins are herein defined in terms of the number of OH equivalents present in the branching alcohols followed by a minus sign and the integers 2 or 1 if diols or monobasic branching reducers are present; these are succeeded by a colon and another integer, or integers, separated by commas designating the functionality of the acids or combinations of organic acids used in making the resins. In this connection, it is pointed out that monobasic acids, such as caprylic and lauric, are considered branching reducers since their first action in the cooking cycle is production of the mono-esters of branching and dihydric alcohols in proportions corresponding to the molar quantities of these reactants initially present.

Complete information on the starting formulations and properties of all 75 NOL alkyds is given in a forthcoming report (14), which interprets the physical properties of resulting foams in terms of an extension of Flory's theory of branching to partially esterified alkyds based on starting functional group ratios in excess of the minima required to produce polymers free from surplus branching monomers and branching controllers (15).

Unfortunately, due to their high TDI reactivity, 30 of the 75 resins could not be converted to foams because of their rapid gelation tendencies when processed by Method 2 exp. considered most effective of the four experimental processes cited by Table I in retarding the rate of 2,4-TDI cross linking reactions. However, it is likely that satisfactory foams would have been obtained if the 80/20 and 65/35 2,4-2,6-TDI had been available when these experiments were performed.

Table III lists the molar proportions of the reactants used in making four typical Class I resins and four Class II types with functionality patterns of 3:2,2 and 3-2:2,2, respectively.

Column 9 tabulates the percentages of starting carboxyl equivalents attributed to short chain aliphatic and aromatic dibasic

TABLE III

STARTING MATERIALS USED IN MAKING FOAM RESIN COMPOSITIONS

Resin Number	Branching Reactant		Branching Reducer		Branching Reduction Ratio, % $1-\rho$	Dibasic Acids		% COOH Equivs, Types 1&2	OH/COOH Equiv. Ratio, r
	Symbol	Moles	Symbol	Moles		Symbol	Moles		
1,1-D*	Glyc	3.8				AdA PAA	2.5 0.5	16.7	1.90
2,2-D	Glyc	3.8				AdA PAA	2.25 0.75	25.0	1.90
3,3-D	Glyc	3.8				AdA PAA MAA	2.0 0.5 0.5	33.3	1.90
4,4-D	Glyc	4.0				PAA SebA	1.5 1.5	50.0	2.00
5	Glyc	3.15	DEG	1.0	17.5	FA AdA PAA	1.5 1.0 1.0	71.4	1.63
6	TMP	2.8	EtG	1.5	26.4	Suc-AA PAA	2.5 0.5	100.0	1.90
7	TMP	2.8	1,4 Bu-ol	1.5	26.4	Suc-AA PAA	2.5 0.5	100.0	1.90
8	Glyc	3.0	1,3 Bu-ol	2.0	30.8	AdA 4Cl-PAA	1.5 1.5	50.0	2.06

* 1-D - Same formulation as Selectron 5922

Alcohols - Glycerine (Glyc), Trimethylpropane (TMP), Butane diol (1,3 or 1,4 Bu-ol), Ethylene glycol (EtG), Diethylene glycol (DEG)

Acids - Types 1 and 2 Short Chain Aliphatic and Aromatic: Maleic, Succinic, phthalic, and tetrachlorophthalic anhydrides (MAA, Suc-AA, PAA, 4Cl-PAA), and fumaric acid (FA)
Type 3 Long Chain Aliphatic: Adipic and sebacic acids (AdA, SebA)

acids in these formulations. These data were utilized in interpreting the behavior of resulting foams. Types 1 and 2 acids were required to counteract the plasticity induced by increased chain lengths between branch points, due to the use of sebacic acid in resin formulations 4 and 4-D and increasing proportions of diols in Resins Nos. 5-8 inclusive.

The OH/COOH starting equivalent ratios, r, tabulated in Col. 10 were obtained from the ratios $\frac{N_A}{N_B}$, where N_A and N_B are the products of the functionality of the alcohol and acid reactants and the numbers of corresponding molar equivalents initially present.

Table IV shows that the duplicate "D" resins are low acid number counterparts of Resins 1-4, inclusive, whose acid numbers varied from 60 to 66. Resin 1-D is essentially a match for Selectron 5922.

Acid and hydroxyl numbers of the resins were determined by the usual methods of alkaline titration and acetylation with a 7/1 blend of pyridine and acetic anhydride. The extents of reaction of carboxyl group equivalents were calculated from the equation

$$P_B = \frac{\frac{N_B(45,000)}{W_i} - AN(0.802)}{\frac{N_B(45,000)}{W_i}} \qquad (3)$$

where N_B is the number of carboxyl equivalents in the original formulations; 45,000, the equivalent weight of the carboxyl group in milligrams; AN, the observed acid number; 0.802, the COOH/KOH conversion factor; and Wi, the weight of the initial charge in grams equal to the sum of the products of the molecular weights and number of moles of each reactant.

Equation 3 was based on the assumption that the observed acid numbers represent the total free carboxyl content present in the resinous products. In thus neglecting the possible effect of steric hindrance, due to coiling of the molecule, in reducing observed acid numbers below their real values, it is evident that the reaction extent of COOH equivalents is given by the quotient of the number of esterified equivalents to the total number of COOH equivalents in the starting formulation. The number of esterified equivalents, in turn, is equal to the difference between the number originally present per gram of charge and the number remaining per gram of product as calculated from acid number determinations.

TABLE IV

ANALYTICAL PROPERTIES, DEGREE OF ESTERIFICATION AND BRANCHING COEFFICIENTS OF FOAM RESIN COMPOSITIONS

Resin No.	Visc. ps 75°F	Water Content %	Acid No.	Hydroxyl No. Obsd	Hydroxyl No. Calcd	Total Free Groups,%	Free OH/COOH Ratio	PBx100, %	Branching Coeff, α
Selectron 5922	550	1.5	44.0	465	488	18.3	4.3	89.7	0.43
1	320	2.0	65.0	490	498	20.4	2.9	86.5	0.39
1-D*	660	1.7	46.2	463	485	18.5	4.0	89.3	0.42
2	1640	1.7	66.0	438	510	20.6	2.9	84.5	0.38
2-D	2650	1.1	46.1	427	488	18.4	4.0	89.2	0.42
3	2570	2.4	60.0	426	577	22.3	3.6	87.7	0.40
3-D	4950	1.7	34.2	414	550	19.3	6.1	93.0	0.45
4	2300	2.7	65.0	475	492	20.1	2.9	82.8	0.34
4-D	4950	0.9	45.5	461	473	18.0	3.9	88.0	0.39
5	6150	0.2	26.0	371	365	13.2	5.3	94.3	0.50
6	3400	1.3	29.6	440	471	15.7	6.0	93.0	0.38
7	1700	1.6	31.2	411	447	16.1	5.4	92.3	0.37
8	560	0.8	50.8	437	443	17.5	3.3	83.3	0.25

* NOL match for Selectron 5922

Column 6 data on the theoretical hydroxyl numbers, h, of the resin compositions were obtained from the formula

$$h = \frac{N_A' \times 17{,}000 \times 3.3}{W_f}, \qquad (4)$$

where N_A' is the number of unreacted hydroxyl equivalents; 17,000, the equivalent weight of the OH group in milligrams; 3.3, the KOH/OH conversion factor; and W_f the final weight, or yield, of the resin in grams.

Equation 4 was derived from a consideration of the identity

$$P_A N_A \equiv P_B N_B \qquad (5)$$

wherein P_A designates the extent of reaction of all hydroxyl group equivalents, N_A, initially present. But since the number of unreacted OH equivalents is the difference between the number originally present and the number that have reacted,

$$N_A' = N_A - P_B N_B \qquad (6)$$

Further, it is obvious that the theoretical yield of resin may be calculated from the equation

$$W_f = W_i - W_d \qquad (7)$$

where the theoretical weight of aqueous distillate, W_d, is $P_B N_B \times 18$ since one molecule of water is evolved for each esterified carboxyl group. Hence, product yield is given by

$$W_f = W_i - P_B N_B \times 18 \qquad (8)$$

Hydroxyl numbers were readily calculated by substituting equations 6 and 8 data for N_A' and W_f in equation 4.

Calculated values of W_f were always slightly higher than experimental values obtained by measuring the volume of aqueous condensate expelled by the reactants during the esterification process. Measured values of W_d were always somewhat less than theoretical values predicted by the product $P_B N_B \times 18$. However, the order of agreement was sufficiently good to preclude the possibility

of higher than theoretical quantities of water due to etherification reactions.

Table IV shows that the calculated hydroxyl numbers were always higher than the observed values. Much better agreement was obtained for the Class II types, as expected by the effectiveness of diol modifications in reducing the steric hindrance of adjacent hydroxyl groups in the resin polymers.

Total free group percentages and free OH/COOH group ratios, also tabulated in Table IV, were computed from the equivalent weight percentages ratios for carboxyl and hydroxyl groups; namely,

$$\frac{n(obsd) \times 0.802}{1000} \times 100 \text{ and } \frac{h(calcd) \times 0.303}{1000} \times 100,$$

where 0.802 and 0.303 represent the COOH/KOH and OH/KOH conversion factors.

Total free group concentration is a measure of the potential cross linking density of the resins, and free OH/COOH ratios their foaming capacity. The total free group content of Resins 1-4 was appreciably higher than their 1D-4D counterparts, while their free group ratios were appreciably lower. These conditions presage a high density of TDI cross linking reactions and reduced competition of hydroxyl for carboxyl groups in converting to foams. However, the total free group concentration in Resins 5-8 was considerably lower than the Class I types. This circumstance may contribute to their greater freedom from steric hindrance and capability for undergoing more complete cross linking reactions.

Lastly, Table IV data on the branching coefficients, α, of the reference standard, Selectron 5922, and the eight Class I resins were calculated from the formula

$$\alpha = \frac{P_B^2}{r} \qquad (9)$$

derived by Flory for unmodified branched polymers with short growth chains. The expression

$$\alpha = \frac{P_B^2}{\left[r - P_B^2(1-\rho)\right]}, \qquad (10)$$

also developed by Flory (16), was used to calculate the branching coefficients of the remaining four Class II resins with elongated growth chains.

The factor ρ in equation 10 is defined by the ratio

$$\rho = \frac{N_{A(b)}}{N_{A(b)} + N_{A(d)}} \qquad (11)$$

where $N_{A(b)}$ and $N_{A(d)}$ designate the number of OH groups originating from branching alcohols and diol branching reducers. From this it follows that the branching reduction factor, $1-\rho$, is given by the inverse ratio

$$1-\rho = \frac{N_{A(d)}}{N_{A(b)} + N_{A(d)}} \qquad (12)$$

Table III records the $1-\rho$ values for four of the 33 Class II resins made in this research whose branching reduction ratios varied over the range 8.8 to 67.8 percent.

The branching coefficient, α as defined by Flory, is the probability that a hydroxyl group emanating from a tri- or higher functionality alcohol is connected via a linear growth chain to another hydroxyl group originating from a branching alcohol rather than to a chain terminated by an unreacted hydroxyl or carboxyl group.

Since it was assumed that hydroxyl and carboxyl groups have equal reactivity, the probability of formation of branched polymers with short growth chains is the product of separate OH and COOH reaction probabilities, hence

$$\alpha = P_A P_B \qquad (13)$$

for Class I polymers. But if diols are present, as in Class II polymers, the branching probability becomes

$$\alpha = \frac{P_A P_B \rho}{1 - P_A P_B (1-\rho)} \qquad (14)$$

Proceeding on the assumption that the reaction probabilities, P_A and P_B, can be identified with tangible experimental

criteria, namely the extents of reaction of the hydroxyl and carboxyl groups as determined analytically, Flory derived equations 9 and 10 by substituting P_B/r for P_A in equations 12 and 13.

Incidentally, P_A measurements should be avoided wherever possible, since analytical determinations of hydroxyl number are subject to the magnitude of the steric factor and to variations in the concentration of acetic anhydride in the pyridine acetylating reagent.

Numerical values of the branching coefficients, as such, provide no information on the molecular weights or numbers of branch points present in the polymer fractions of the resins; however, high values of α for Class I resins correspond to high molecular weights of the branched polymers. The opposite is true for the Class II types; in this case, for fixed values of P_B and r, the branching coefficient decreases with increased values of the branching reduction ratio, $1-\rho$. Hence low values of α for Class II resins indicate high molecular weights of their polymer components. Linear molecules, for example, with zero values for α, can attain molecular weights of 25,000 or more (16), considerably higher than recent estimates of the molecular weights of different classes of partially esterified branched polymers (15).

Figure 7 shows the NOL reaction train used for preparing each of the 75 resins in a three necked flask of 3-liters capacity. The temperature of the charge at various stages of the condensation was controlled with the aid of a Glas-Col electrically heated mantle connected to a Variac. Provisions were made for aspirating nitrogen continuously through the charge during the reaction cycle, removing samples for acid number determinations at desired intervals, collecting and measuring the water of esterification, and finally removing, from selected resins, all but the last traces of water by vacuum distillation at reduced temperatures. Water vapor evolved during the condensation process was first passed through a Friedrichs steam condenser to expedite its removal before passage through a West condenser and collection in the Bogert distillation receiver.

Table V shows a definite relation between the numerical values of α for the Class I resins and their foam product properties. The high acid number version of these resins, with branching coefficients of 0.34 to 0.40, gave decidedly stronger foams at normal and elevated temperature than their "D" more highly esterified counterparts whose branching coefficients varied from 0.39 to 0.45. As explained in the forthcoming report on resin formulations (14), Methods 1 exp., 1A exp., and 2 exp. were used in converting these

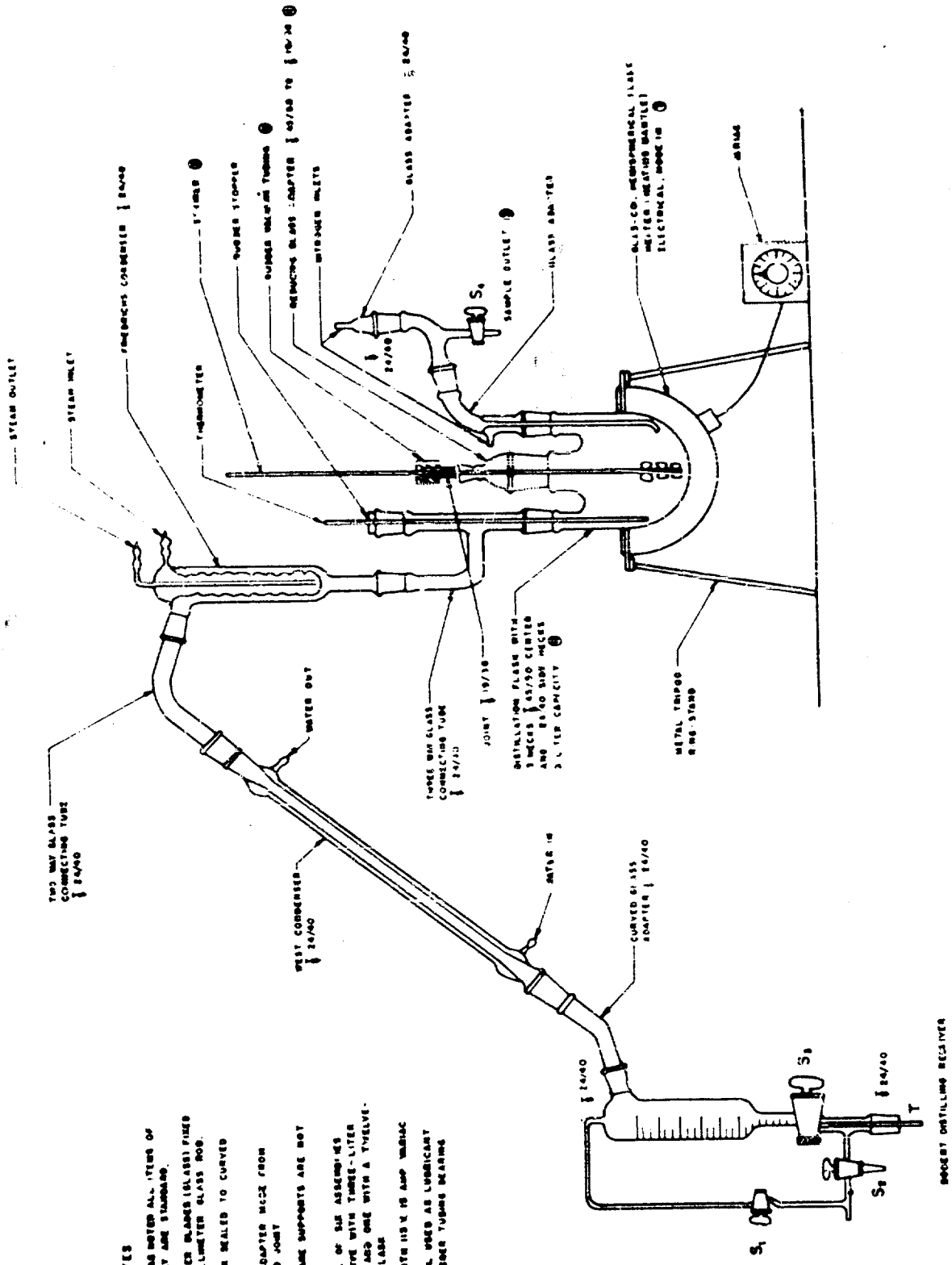

Figure 7 - Apparatus used in synthesis of foam resin compositions

TABLE V

FOAM PROCESSING CRITERIA AND PHYSICAL PROPERTIES OF RESULTING 10 LB/CU.FT. FOAMS

Resin Number	TDI/ Resin	Process	Pour Point Temp °F	Pour Point Visc Ps	Pour Point Time min	Water Vapor Abs %	Heat Defl'n % 230°F	Heat Defl'n % 266°F	Mech. Strength, psi Compr	Mech. Strength, psi Shear	Mech. Strength, psi Tensile	Rating
Selectron	1.03	1	125	200	21	2.2	2.2	1.9	272	171	176	6
5922	1.03	1A	135	350	27	2.1	2.0	1.7	275	179	180	5
1	1.16	1	118	100	22	1.3	1.8	1.5	298	186	195	4
1-D*	1.04	1	118	120	20	1.5	1.2	1.7	271	123	165	8
2	1.03	1	125	120	15	1.3	1.8	1.6	307	184	189	4
2-D	0.89	1	117	100	19	1.9	2.5	2.0	232	163	154	8
3	1.10	1	122	220	23	1.9	1.2	1.0	317	187	188	3
3-D	0.70	1	129	300	15	1.8	3.8	20.0	244	160	167	9
4	0.98	1A	110	180	16	1.7	1.9	2.1	290	220	232	2
4-D	0.85	1A	104	150	14	1.5	1.3	1.5	316	232	242	1
5	1.03	1	118	100	26	1.6	0.7	1.4	309	192	195	3
6	1.05	1	124	150	11	1.6	1.8	1.5	291	225	261	1
7	0.91	1	122	160	12	1.8	1.8	1.6	289	220	257	2
8	0.76	2	102	115	15	1.5	1.6	6.3	267	212	314	2

* Offset for Selectron 5922

resins to foams rather than the preferred method of extended compatibility, Method 3 exp., since these methods are similar and permitted conclusions to be drawn on the role of resin constitution in determining foam properties rather than processing technique. However, it was concluded that most of the resins were undermixed, in consideration of their low pour point viscosities, which should have approached 400 poises to yield stronger foams in accordance with the proved advantages (10) of prolonging mobility of the 2,4-TDI condensates for as long a time as possible before pouring.

Despite this failure to optimize mixing schedules, Table V shows that the high acid number Class I resins, Nos. 1-4, and all of the four Class II resins gave improvements of the order of 10 to 15 percent in compression, 15 to 30 percent in shear, and 20 to 75 percent in tensile over the control, Selectron 5922, processed by Method 1A exp. Significant improvements also were recorded in reduced water vapor absorption at 160°F and compressive heat distortion at 230 and 266°F.

The data recorded in Tables III, IV and V indicate a general correlation between the kinds of polyfunctional reactants, their starting functional group ratios, degrees of esterification, and resultant foam performance characteristics. Further work should be done to optimize these variables for Resins 4, 4-D, 6, 7 and 8 which gave superior results in these preliminary tests. For example, it is conceivable that the replacement of succinic anhydride and adipic acid by phthalic anhydride and/or tetrachlorophthalic anhydride in Resins 6, 7 and 8 would improve the compression strengths of derived foams at both normal and elevated temperatures. It is also likely that more favorable results would have been obtained if low temperature-long time cooking cycles had been adopted for all resin formulations. In this work, cooking times varied from 3.2 to 15 hr and esterification temperatures from 150 to 250°C. Several years ago, Bruntzinger and co-workers found that low condensation temperatures and long cooking times should be adopted whenever possible to forestall rapid viscosity build-up of polyesters for the same degree of esterification(17).

Polymer Structure

Flory's equations for branching coefficients immediately suggest methods of controlling the degree of branching of foam resin polymers by judicious manipulation of the variables r, P_B, and ρ . These equations take on a new meaning if interpreted in the light of the schematic branched structures (a) and (b) shown in Figure 8.

(a) Class I - Polymer Component Based on r = 1.500

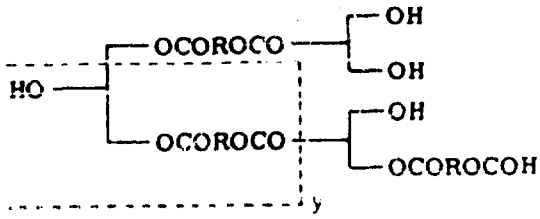

(b) Class II - Polymer Component Based on r = 1.375

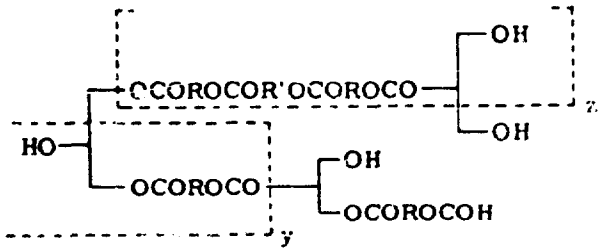

(c) Segment of Cross Linked Alkyd Gel Based on r = 1.000

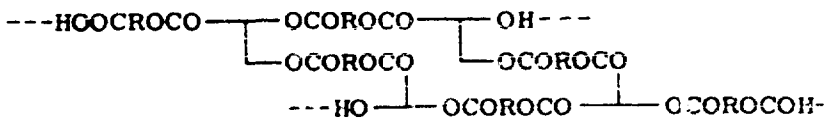

Figure 8 - Branched structures of alkyd foam polymers and gel based on decreasing starting functional group ratios

10:

These concepts of polymer structure are useful in explaining the phenomenon of steric hindrance of unesterified functional groups. Flory has interpreted steric hindrance in terms of the coiling tendencies of branched molecules (18). Highly branched molecules of low acid number are more subject to coiling than low molecular species of relatively high acid numbers. Short growth chains in Class I polymers may increase the steric factor because of the proximity of free hydroxyl groups. The introduction of esterified diols in the chain structure of Class II polymers reduces the magnitude of this effect to a considerable extent; consequently, it was expected that TDI cross linking reactions would proceed to a higher degree of completion with polymers of this type.

Dostal (19), and Dostal and Mark (20) have proposed equations for determining the magnitude of the steric factor for partially cross linked polymers of varying molecular weight. Normally, the terminal carboxyl groups in such polymers are sterically unhindered, but adjacent OH gps in condensation polymers are subject to varying degrees of steric hindrance depending on chain lengths between branch points and the degree of branching of the molecule as a whole.

Bawn has pointed out that the total number of growth and terminal chains in branched molecules may be computed from the formula

$$N_t + N_g = 2(y + z) + 1 \qquad (15)$$

where y and z represent the number of branch points attributed to short and elongated growth chains (21). Structures (a) and (b) of Figure 8 each possess three branch points, two growth chains, and five terminal groups, one of which is carboxyl. Obviously, z is zero for structure (b). Structure (b) has a higher molecular weight than (a); further, it can be shown that for equal molecular weights Class II polymers possess fewer branch points than Class I types. Likewise, it is evident that as the number of branch points increase with higher degrees of esterification the number of free OH groups also increase, although the weight percentages of these groups, expressed in terms of hydroxyl numbers or free group percentages, become progressively less. The data recorded in Columns 6 and 7 for the Class I resins in Table IV bear out this point.

The symbol R in structures (a) and (b) of Figure 8 represents a single partially esterified dibasic acid in these polymers and several completely esterified residues depending on the number of -OCOROCO- growth chains, y, in the molecule. R' represents a

a single completely esterified diol residue in the elongated growth chain z of structure (b). The maximum starting functional group ratios, r, required to produce these polymers free from monomer are 1.5 and 1.375. These ratios are constant, independent of the number of branch points in the molecule.

Although equations 9 and 10 presumably are valid for all values of α, the early work on branched polymers was limited to alkyds based on starting functional group ratios of unity, corresponding to equimolecular proportions of branching alcohols with dibasic acids (22) (23). This circumstance, more than any other, has delayed the application of branching theory in the design of resins with reduced monomer content. Theoretically, the coexistence of low molecular polyurethanes derived from these polyfunctional alcohol monomers will degrade the properties of the foams in proportion to their concentration.

Branched molecules based on equivalent functional group ratios undergo rapid cross linking reactions of the type illustrated by structure (c) of Figure 8, resulting in gelation when only 63 to 79.5 percent of the reactants are esterified. It has been estimated that branched molecules of this type become extremely large, eventually attaining molecular weights of 10^{22} or more before gelling.

The incidence of gelation at relatively low extents of reaction has been interpreted by Flory in the light of his concept of the existence of a critical, or gelation threshold value of the branching coefficient, α_c, as defined by the equation

$$\alpha_c = \frac{1}{f - 1} \qquad (16)$$

where f is 3 for reactions based on trihydric alcohols and equimolecular proportions of OH and COOH groups. In this case, the critical extent of reaction, p_c, is equal to α_c, since P_A and P_B are equal. While it is conceivable that foams made by interrupting the condensation at lower P_A and P_B values than correspond to gelation, such foams would be unusable because of their high monomer content and the need of a high surplus of OH groups to impart rigidity by urethane cross linking reactions.

The supplementary report on foaming resins (15) gives full details on the theoretical background, calculations, and experimental evidence in support of Figure 8 structures (a) and (b) for polymers containing one free carboxyl group, as contrasted to alternate structures of considerably higher molecular weight bearing two or

more such groups. Clearly, insufficient quantities of dibasic acids were used in Class I formulations, and still lesser quantities in Class II types, to tie in all the polyfunctional alcohols into a single polymeric complex. Selectron 5922, for example, was based on the reaction of 2.5 moles adipic acid and 0.5 moles phthalic anhydride with 3.8 moles of glycerine. Since only two of the three OH groups are esterified in the production of branched polymers, only 3.0 moles of glycerine, or integral multiples of 3.0 moles, can be condensed with 3.0 moles or integral multiples of 3.0 moles of dibasic acids. Therefore the excess, 0.8 moles of glycerine, or integral multiples of 0.8 moles, depending on the degree of esterification of the resin, must remain admixed with the polymer components whose number average molecular weight satisfies the equation

$$AN_p = \frac{W_f\ (AN_c)}{W_p}\ , \qquad (17)$$

where AN_p is the average acid number of the polymers; AN_c, the observed acid number of the resin composition; W_f, the resin yield; and W_p the weight percent polymer in the product as obtained from the equation

$$\%\ W_p = \frac{W_f - W_m}{W_f} \times 100 \qquad (18)$$

W_m is the weight percent free triol monomer in excess of the quantity required to produce branched polymers with one or more free COOH terminal groups.

It is shown, further, that the supposition of two or three free COOH groups can only be satisfied by starting functional group ratios of 1.350 and 1.312, considerably lower than the 1.5 ratio required for the production of Class I polymers with one free COOH group.

Since 1.9 to 2.0 functional group ratios were used in the production of Class I polymers, the probability of formation of branched structures with two or more free COOH groups is very small. However, the calculated AN_p value of 49.4 for Selectron 5922 can be satisfied by the assumption of 5 to 6 branch points for polymers with one free carboxyl group, and 9 and 14 branch points for polymers with two and three carboxyl groups. Corresponding number average molecular weights for these polymers are 1133, 2629, and 4223, respectively.

These calculations indicated the desirability of extracting the unreacted glycerine monomer to obtain polymer samples for molecular weight determinations. Alternately, quantitative analysis of the monomer extract was expected to throw light on the structure of the polymer since resinous compositions based on polymer components with one, two or three free COOH groups should contain 10.6, 14.6, and 15.6 weight percent free glycerine.

Since facilities were not immediately available for molecular weight determinations of the polymer fractions, the content of free glycerine in Selectron 5922 was determined after first making a boiling water extract of the resin preheated to 350°F. After cooling, the supernatant aqueous extract was evaporated to dryness in an inert atmosphere. Aliquot samples of the dry extract, comprising 15 percent of the initial weight of resin were re-dissolved in water and analyzed for glycerine by the periodate method (24). This method utilizes sulfuric acid to liberate periodic acid from sodium meta-periodate, which oxidizes glycerine in accordance with the equation

$$C_3H_5(CH)_3 + 2H_5IO_6 \longrightarrow 2CH_2O + CH_2O_2 + 2HIO_3 + 5H_2O$$

Alkaline titration of the formic acid liberated by the reaction corresponded to a glycerine content of 8.5 percent, appreciably less than 10.6 percent predicted on the hypothesis of only one terminal COOH group in the polymer fractions of the resin. Control tests carried out with ethyl acetate solutions of the water insoluble fraction, comprising 85 percent by weight of the resin, revealed no formic acid or iodic acid whatsoever.

The accuracy of the periodate titrations undoubtedly would be improved if a solvent of high selectivity could be found to remove small quantities of low molecular weight emulsified polymers from the aqueous extract. Nevertheless, the order of agreement was sufficiently good to preclude the existence of substantial quantities of high molecular polymers bearing two or more carboxyl groups. As explained in the supplementary report, the formation of such polymers would yield much higher percentages of unreacted glycerine.

Figure 8 structures of the resin polymers has received added support from calculations of the hydroxyl number contributions of the polymer and monomer fractions of the resins. Hydroxyl numbers for the polymer and monomer fractions are given by equations 19 and 20

$$h_p = \frac{N_A' \times 17{,}000 \times 3.3}{W_f \times \% W_p} \qquad (19)$$

$$h_m = \frac{\% \text{ OH in monomer} \times 3.3 \times 1000 \times W_m}{100} \qquad (20)$$

For Selectron 5922, h_p and h_m are 294 and 194. Their sum, 488, agrees exactly with the calculated value recorded in Table V for this resin.

This proof of the existence of free monomers, as predicted from branching theory, highlights the need of preparing resins with little or no unreacted monomers. The limiting factor in such a project is the anticipated high viscosity of partially esterified polymers not containing free monomers which exercise a plasticizing effect. However, it is felt that this difficulty may be overcome by carefully selecting polyfunctional alcohols and acids capable of undergoing condensation reactions by long time-low temperature procedures.

Part II

Inorganic Ceramic Foams

Dense unexpanded ceramics have long been considered desirable radome materials because of their good dimensional, electrical and chemical stability over a wide temperature range, and their low water absorption and resistance to rain erosion. Hence, it is not surprising that the Office of Naval Research awarded a contract to Rutgers University in 1952 to investigate the adaptability of these materials to radome manufacture (25).

Despite notable success in the fabrication of prototype steatite solid wall ogival radomes of moderate size, the Rutgers team soon recognized the potential difficulties of machining still larger domes ranging in height from 4 to 9 feet and base diameters of 2 to 5 feet, presently based on symmetrical sandwich and half wave wall plastics constructions. The need of fundamental research to increase the tensile strength and impact resistance of these dense bodies also was recognized.

Even if these limitations are surmounted, their high weight penalty will always remain a deterrent to the use of solid ceramics

in the manufacture of precision radomes. Anticipating the advantages of dielectric sandwich structures in overcoming this drawback, the Air Force sponsored contract studies with Stupakoff Ceramic and Manufacturing Company to investigate the efficacy of the "burn out" process for levigating solid ceramic formulations (26). When it was demonstrated that foamed radomes based on this process had non uniform electrical properties due to lack of homogeneity in their pore structure, this Center approved a contract proposal submitted by Professor A. J. Metzger of Virginia Polytechnic Institute to investigate porous bodies made by the aeration of aqueous suspensions of inorganic materials.

Initially, Metzger's studies were directed to the development of porous ceramics of dielectric constants ranging from 1.4 to 1.8 for "A" type symmetrical sandwich structure radomes. Some 20 monthly and quarterly reports covering this phase of the work, have been summarized by two final reports published in 1952 and 1955 (27) (28). A third report summarizing progress in the development of alkaline earth titanate bodies was published in 1957 (29). Recent studies describe high alumina levigated bodies of low dielectric constants and exceptionally high flexural strengths (30). While presently suited only for "A" type sandwich constructions with impervious ceramic coatings of dielectric constants 4 to 8, it is expected that the controlled addition of small amounts of inorganic materials to these formulations will increase their dielectric constants to the levels required for half wave domes of variable fineness ratios without undue sacrifice in their resistance to thermal shock.

Formulations

Table VI lists the starting materials and resulting foam body compositions of two typical low dielectric constant ceramic foams (B-77 and B-109) and four calcium titanate formulations (CT-3, CT-8, CT-15 and CT-16) whose dielectric constants varied from 4 to 12. Pioneer Georgia Kaolin was used in B-77 and Ball Clay in B-109 formulas.

Each of the components listed by Table VI was functional in contributing to desirable properties of the aerated slips and the end product properties of the resulting foams. Plaster of Paris, for example, served as a binder and stabilizer for the lime-alumina-silica systems B-1 through B-81, and as a source of calcium oxide for the CT- series of foams. Initially, CT-3 was based on the starting formulation $CaTiO_3$,39/TiO_2,5/Kaolin,25/alumina,9/plaster,22

TABLE VI

SOLID COMPONENTS OF AERATED SLIPS AND RESULTING COMPOSITIONS OF CERAMIC FOAMS

	Starting Components						Foam Body Compositions			
Formulation	Plaster	Clay	SiO_2	CaO	$CaTiO_3$	Al_2O_3	CaO	Al_2O_3	SiO_2	$CaTiO_3$
B-77*	21	34				45	10	71	19	
B-109*		8				92	2	95	3	
CT-3*			14	6	57	23		26	17	57
CT-8			7	6	62	25		28	7	65
CT-15			5	2	78	15		16	4	80
CT-16*			4		70	26		26	4	70

* Preferred Compositions

until it was found that calcium aluminate formed by metathesis reactions during firing accomplished the same result. Pioneer Georgia Kaolin likewise was functional in these and other formulas by acting as a plasticizer in easing the flow of aerated mixes, increasing the green strengths of dried forms, and in providing aluminum silicate fluxes for accelerating solid state reactions during firing.

Phase rule three dimensional equilibrium diagrams prepared by the Geophysical Laboratory were utilized in selecting desirable proportions of lime, alumina, and silica for the B- series porous ceramic foams with dielectric constants varying from 1.4 to 2.2. The isoliquidus boundary lines of these diagrams also were helpful in predicting the maturing heats, firing range, quantities of glass (SiO_2 phase), and the kinds and amounts of different crystalline compounds formed.

Unfortunately, no phase equilibrium diagrams were available for the CT- series of foams; hence there was no alternative to the use of empirical methods in ascertaining their optimum body compositions.

Prediction of Dielectric Constants

The successful use of all categories of foams, whether plastic or ceramic, is predicated on mathematical relationships between dielectric constants and densities. Several years ago, scientists affiliated with the MIT Radiation Laboratory (31) and the Telecommunications Research Establishment in England (32) found that the dielectric constants of organic plastics foams could be predicted reliably by the equation

$$\log \epsilon_r = \rho/\rho_s \log \frac{\epsilon_s}{\epsilon_o} \qquad (1)$$

where ϵ_r is the dielectric constant of the foam relative to air ($\epsilon_o = 1.0008$), ρ and ρ_s the densities of the foams and unexpanded plastics of the same composition, and ϵ_s/ϵ_o the relative dielectric constants of the unexpanded plastic component of the foam.

In early studies of the B- series low dielectric constant foams, Metzger found that equation 1 gave much lower values of than experimental values. The linear equation

$$\epsilon_r = 1 + k\rho \ , \qquad (2)$$

in contrast, gave much better agreement with experimental values when k was set equal to 0.02. However, equation 2 gave unreasonably high calculated values of ϵ_f for calcium and/or strontium titanate foams whose measured values were 4 to 25. Proceeding on the assumption that the Gladstone-Dale Index for glasses was valid for porous ceramics of comparatively high dielectric constants, Metzger derived the equation

$$\epsilon_f = (1 + k \times \rho)^2 \qquad (3)$$

for predicting relative foam dielectric constants from density determinations. The constant k in this equation was computed from the expression

$$k = \frac{\sqrt{\epsilon_s} - 1}{\rho_s} \qquad (4)$$

which is analogous to the Gladstone-Dale Index, k, for glasses

$$k = \frac{\sqrt{n^2} - 1}{\rho_s}$$

since $\epsilon_s = n^2$ by electromagnetic theory. The numerical value of k in equation 4 was found to be 3.4528 with a standard deviation of ±0.1462.

Figure 9 shows that several measured values of the dielectric constants of calcium and strontium titanate foams coincided with predicted values given by Curve B plot of equation 3. In this regard, the application of equations 3 and 4 to foams of known density has indicated that fairly wide variations in the dielectric constants of corresponding solid CT- ceramics gave substantially the same calculated values of ϵ_f for the levigated bodies. For example, ϵ_s can vary from 44 to 53 and from 63 to 76 to obtain half wave core dielectrics of 4.0 and 5.0, respectively.

Curve A of Figure 9 likewise shows good agreement with equation 2 calculated values in the low range (1.3 to 2.4) of dielectric constants. This curve has been extended upwards to emphasize wide differences between the values of ϵ_f given by equations 1 and 3. Curve C plot of equation 1 has been included to illustrate the marked discrepancies between the dielectric constants and densities of plastic and ceramic foams.

Processing Methods

Metzger's 1952 and 1955 summation reports for the B- series foams (27) (28), and the 1957 report for the CT- series (29), give full details on the progressive stages of processing, comprising: (1) preparation of aerated slips, (2) forming procedures, (3) firing schedules, and (4) application of sealant and impervious glazed coatings. Meticulous observance of these instructions is required to secure light weight bodies meeting the stiuplated performance characteristics.

1. Preparation of Aerated Slips - A three speed Hobart Planetary Mixer provided with a 12-qt. bowl was used to prepare 5 to 10 lb. batches of aqueous suspensions. Dry mixes of the various ingredients were first blended with Style B flat beater before adding 43 to 52 parts by weight of water containing 0.5 percent Aresket 240 (Monsanto's monobutyl biphenyl sodium monosulfonate). The B- series formulations required 49 to 52 percent liquid and the CT- series 43 to 49 percent relative to the total weights of aqueous suspensions. Aeration was accomplished by replacing Style B beater with a wire loop blade, and by operating the mixer on high speed until the volume and viscosity of the batch simultaneously increased to predetermined levels corresponding to desired porosities in the final products.

Prior to casting the slip into molds for preparation of the green foams, one or more deflocculents similar or equal to sodium or ammonium alginate and carboxymethylcellulose (CMC) was added, and the pH adjusted to 7.35-7.45 with dilute amonium hydroxide. Armac 12D or Armac CD cationic surfactants in amount equal to 0.1 percent on the weight of the water were substituted advantageously for the anionic surfactant, Aresket 240, in several of the CT- formulations to obtain finer pore structure, but these substitutions were usually accompanied by higher green form firing shrinkages.

2. Forming Procedures - Rectangular specimens were made by casting the slips into wooden frames placed on glass plates covered with wax paper. The material was allowed to dry for 16-24 hrs. under controlled temperatures and relative humidities until no further shrinkage was noted. Conical shapes were made by pouring the slip into sheet galvanized molds of 30 and 40 degrees cone angle. Male galvanized molds of the same cone angle were then lowered into the mix to produce forms approximately 7/8-in. thick. After the material has set, the inner cone was removed and replaced by a conical copper screen to permit rapid evaporation of water. Several hours later, the outer cone was taken off and the piece allowed to dry thoroughly.

The largest green conical form made in this way had a base diameter of 26-in. and altitude of 30-in. The linear shrinkages of B- series green forms obtained by this technique were 24-26 percent, but the CT- series developed appreciably higher shrinkages of 30-32 percent.

3. Firing Schedules - The preferred firing schedule for most of the 81 Series B- lime/alumina/silica foams was a preliminary 12 hr. heat soak at 2200°F to remove the last traces of sulfur trioxide liberated by thermal decomposition of the plaster of paris ingredient. Thereafter, the temperature of the kiln was brought up rapidly to 2552°F where it was held for 3 hr. before the specimens were allowed to cool. Conical forms were supported in an octagon shaped refractory cone and fired with the apex of the cone placed downward.

The B107-B115, inclusive, high alumina bodies (3) were fired at much higher temperatures of 2700-2800°F to realize optimum strength. The CT- bodies, in contrast, were fired at a considerably lower temperature range of 2200-2350°F. The upper limit of this range was very critical, and must be held within ±25°F of the optimum temperature.

The firing shrinkage of the B- series foams was 27 to 29 percent. Still higher shrinkages of 32 to 34 percent were recorded for the CT- series foams. Clearly, in producing radomes of specified core thickness, the thickness of newly cast slips must be estimated with great accuracy to forestall excessive machining of inner and outer surfaces of the conical shapes and the outer surfaces of specimens prepared for physical property evaluation.

4. Application of Sealant and Ceramic Glaze - Because of their high porosity, light weight bodies made by the aeration process first must be treated with appropriate sealants to prevent penetration of the glaze into the foam cores. Preliminary experiments conducted with B-77 bar stock of 35 lb/cft density showed that a non-aerated slip of the same composition could be applied to provide an impervious sealant 0.025-in. thick. The firing temperature of this unexpanded coating was 2200°F. Thereafter, two applications of a high lime-boric acid glaze were made in separate steps. Maturing temperature of the glaze was 2030°F.

The sealant and glaze coatings gave flexural strength increments of the foamed core consistent with sandwich theory. The B-77 bar stock had a flexural strength of 372 psi. A single application of sealant raised this to 478 psi, and the first and second applications of glaze increased the strength to 1222 and 1455 psi.

Figure 10 shows a B-77 foamed cone 11-in. high and 8-in. base diameter sealed and glazed by this procedure. Eventually stress cracks developed in the core due to inequalities in the thermal conductivities of the glazed coating and core. New ceramic finishes and novel methods of application are being investigated at the present time to equalize the coefficients of thermal expansion of the impervious coating and the foamed core.

Physical Properties of Porous Ceramics

Tabulated in Table VII are numerical data on the mechanical, thermal, and electrical properties of two each B- and CT- light weight ceramics at arbitrary densities given in parentheses.

The flexural strengths of these bodies were obtained by single point loading of 6 x 1/2 x 1/4-in. thick specimens mounted on a jig with a 4-in. span. The tensile machine used in these tests was adjusted to a loading rate of 0.25-in. per minute. Moduli of elasticity in flexure were calculated from the slopes of the load-deflection curves before attaining the proportional limit.

Compressive strength data were based on 3/4-in. deformations of 2 x 2 x 1-in. thick specimens subjected to the same loading speed of 0.25-in. per minute. These tests were discontinued when a review of the data showed that the crushing strengths were 2.5 to 4 times as high as ultimate strengths in flexure.

Linear coefficients of thermal expansion and porosities were determined in accordance with ASTM Designations C210-46 and C20-46. The method and apparatus described by Watts and King (33) was used in measuring thermal conductivities.

Resistance to thermal shock was determined by furnace tests for slow rates of heating, but when rapid rates of heating were required to simulate high burn-out speeds of radar guided missiles the induction heating version of carrying out the electrothermal test developed by Moore (34) was used.

Dielectric constants and loss tangents at X-band microwave frequencies were determined by the widely used shunted waveguide method (35).

Table VII data show that the CT-3 and CT-16 bodies have limited usefulness because of their poor resistance to thermal shock. In other respects, these foams were satisfactory. The two CT- foams not listed, CT-8 and CT-15, had flexural strengths of 1057 and 818

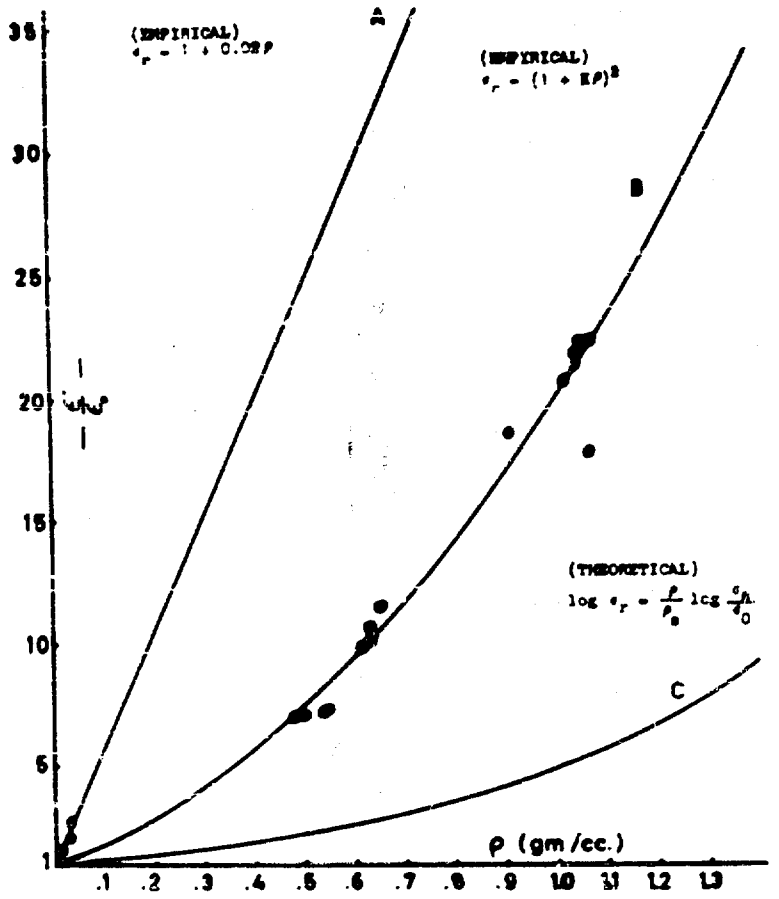

Figure 9 - Validity of empirical equations in predicting densities of foamed ceramics of arbitrary dielectric constants

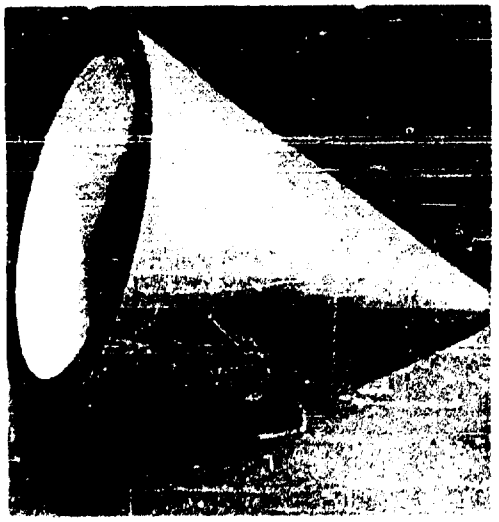

Figure 10 - Glazed ceramic foamed cone, included angle 40° and base diameter 8 inches

TABLE VII

PHYSICAL AND ELECTRICAL PROPERTIES OF CERAMIC FOAMS AT STATED DENSITIES

	B-77	B-109	CT-3	CT-16
Density Range, lb/cft	20-60	20-80	30-80	30-80
Flexural Strength, psi	95(20 lb) 1600(60 lb)	556(32 lb) 2920(82 lb)	360(35 lb) 1025(56 lb)	1105(57 lb)
Modulus of Elasticity, psi x 10^6	0.4×10^6			
Compression Strength, psi	916(35 lb)			
Specific Heat, BTU/lb/^oF	0.27	0.24	0.20	0.20
Thermal Conductivity, BTU/ft^2. hr.^oF/in.	0.90(500^oF) 1.20(1000^oF) 1.50(1500^oF)			
Coeff.of Expansion, in/in./^oF	8×10^{-6}	10×10^{-6}		9.7×10^{-6}
Porosity, percent	92(20 lb) 75(60 lb)	92(20 lb) 64(80 lb)	88(30 lb) 68(80 lb)	90(30 lb) 70(80 lb)

TABLE VII (cont'd)

	B-77	B-109	CT-3	CT-16
Softening Temperature	2552°F	2800°F	2400°F	2400°F
Maximum Operating Temperature	2425°F	2600°F	2250°F	2250°F
Thermal Shock Resistance	To 1200°F in 3 sec.		To 500-600°F in 10 sec.	To 500-600°F in 10 sec.
Dielectric Constant, X-band	1.4(20 lb) 2.2(60 lb)	1.35(20 lb) 1.79(80 lb)	4.65(40 lb) 3.01(65 lb)	10.2(57 lb)
Loss Tangent, X-band	0.002(35 lb)	< 0.005(50 lb)	< 0.005(45 lb)	< 0.003(32 lb)

psi, dielectric constants of 6.6 and 11.3, and loss tangents less than 0.005 at density levels of 57 and 52 lb/cft, respectively.

Smyth has pointed out that the resistance to thermal shock of porous ceramics is a composite function of their mechanical strengths, moduli of elasticity, thermal conductivities, and thermal coefficients of expansion (36). Sandwich structure ceramic dielectrics offer a better prognosis for radome installations on supersonic aircraft and missiles than solid wall types, since their coefficients of thermal expansion and elastic constants are significantly lower and their thermal conductivities are not appreciably higher than values recorded for solid ceramics.

LITERATURE CITATIONS

1. NADEVCEN Reports Nos. NADC-EL-52195, Vol I, 11 Feb 1954 and Vol II, 7 Oct 1954 by S. Wolin; NADC-EL-52188, 22 Oct 1953 by S. Wolin; NADC-EL-5313, 1 Jul 1953 and 16 June 1954 by J. A. di Toro

2. Emerson Electric Company, Report No. 123, 14 Sep 1958 by E. C. Branson

3. F. H. Behrens, WADC, Cado Digest (Astia), 1948

4. NADVCEN Report No. NADC-EL-54151 of 8 Feb 1955 by H. R. Moore and R. A. Coen; Training Course and Instructions for Foaming-In-Place and Thermal Forming of Foamed Structures

5. Goodyear Aircraft Corporation Final Engineering Reports on Foaming-In-Place of Alkyd Resins for Sandwich Radomes, GER 4097 of 22 Dec 1959 (PB 110,497), GER 2423 of 15 Oct 1950 (PB 110, 498s), GER 4097 of 29 Feb 1952 (PB 111,417); USAF Contract W33-038ac-15228

6. Goodyear Aircraft Corporation Interim Engineering Reports on Radome Materials Research and Fabrication Development Service, Appendix 44, 29 Jun 1951; USAF Contract W33-038ac-15228(16528)

7. Goodyear Interim Report, Appendix 42, 12 Sep 1950

8. R. Hebermehl, Farbe, Lacke, Anstrichstoffe 2, 123-8 (1948)

9. U.S. Patents Nos. 2,577,279, -280, -281; Eli Simon and Frank W. Thomas, assignors to Lockheed Aircraft Corporation

10. NADEVCEN Report No. NADC-EL-5556 of 30 Jan 1956 (PB 131,123) by H. R. Moore; Low Temperature Condensation Process for Producing More Highly Cross Linked Alkyd Diisocyanate Foams

11. "Nopco Lockfoam", Nopco Chemical Co., Harrison, N. J., and "Stayfoam", American Latex Products Co., Hawthorne, Calif.; 1953 Brochures

12. WADC Technical Report 54-249 of Mar 1954 (PB 111,692) by Phillip J. Campagna, Harold M. Preston and Norman E. Wahl, Cornell Aeronautical Laboratory, Inc.

13. "Perspective", Cornell Aeronautical Laboratory, Inc., Sep-Oct 1958 issue

14. Forthcoming NADEVCEN Report No. NADC-EL-5942, entitled Controlled Branching of Foam Resin Polymers Synthesized for Precision Radomes

15. Supplementary Forthcoming NADEVCEN Report No. NADC-EL- , entitled Polymer Structure, Number Average Molecular Weight, and Monomer Content of Foam Resin Compositions

16. Paul J. Flory, Principles of Polymer Chemistry, Cornell University Press, Ithaca, N. Y., 1953; p. 42 and pp 348-356

17. E. Bruntzinger, K. H. Lochner, and H. Noeske, Farbe, Lacke, Anstrichstoffe 3, 249-259 (1949)

18. Paul J. Flory, Chemical Reviews 39, 154 (1946)

19. H. Dostal, Monatschefte f. Chemie, 67,63 (1935); 70, 324, 469 (1937)

20. H. Dostal and H. Mark, Z. Physik Chem. (B), 299 (1935); (A), 50, 348 (1933)

21. C. E. H. Bawn, The Chemistry of High Polymers. Interscience Publishers, Inc., New York, 1948; pp 38-39 and pp 22-35

22. R. H. Kienle, P. A. Van der Meulen, and F. E. Petke, J. Am. Chem. Soc. 61,2258, 2268 (1939); Kienle and Petke, ibid, 62, 1053 (1940); 63, 481 (1941)

23. W. H. Stockmayer and L. L. Weil, Advancing Fronts in Chemistry, edited by S. B. Twiss, Reinhold Publishing Corp., New York, 1945

24. Organic Analysis, Volume I, edited by John Mitchell, Jr., I. M. Kolthoff, E. S. Proskauer, and A. Weissberger, Interscience Publishers, New York, 1953; pp 41-43

25. Technical Reports Nos. 1, 2, and 3 of 15 Jun 1953, 1954, and 1955, Project NONR 40403, Rutgers University

26. Stupakoff Ceramic and Manufacturing Company, Final Engineering Report No. U-12224-28 on Research and Development, Five Radomes, and Data of 10 Dec 1951 under USAF Contract No. W-33-038ac-21307 (20345) for the Period 27 Sep 1958 to 1 Dec 1951

27. Summation Report VPI-128-24 of Sep 1952 on Navy Contract No. N383s-31915 by A. J. Metzger, Virginia Engineering Experiment Station, Virginia Polytechnic Institute, Blacksburg, Va.

28. Summation Report of Feb 1955 on Project 195 by A. J. Metzger, Navy Contract No. N383s-95917, Virginia Polytechnic Institute

29. Summation Report VPI-278-4 of May 1957 by A. J. Metzger, Navy Contract N383(62269)23378A, Virginia Polytechnic Institute

30. Interim Reports Nos. VPI-278-22 and VPI-278-23 of May and Sep 1958 by A. J. Metzger, Navy Contract No. N62269-258, Virginia Polytechnic Institute

31. Radiation Laboratory Series, Vol. 26, pp 409-413, Radar Scanners and Radomes by Cady, Karelitz, and Turner; McGraw Hill Book Co., 1948

32. J. B. Birks, Expanded Dielectrics, TRE Report No. T-1812, Feb 1945

33. A. S. Watts and R. M. King, Bulletin No. 64, 1931, Relative Heat Transfer Through Refractories, Ohio State University Engineering Experiment Station

34. Howard R. Moore, U.S. Patent No. 2,551,624 of 8 May 1951; Apparatus for Determining Thermal Stability of Materials

35. Von Hippel and Westphal, NRDC Report of Apr 1943; The Measurement of Dielectric Constant and Loss Tangent with Standing Waves in Coaxial Wave Guides

36. WADC Conf Technical Report 57-67 of Sep 1957, ASTIA Document No. AD 142001, Techniques for Airborne Radome Design, Chapter 9 Inorganic Materials and Radome Construction, Unclassified, by H. T. Smyth

REINFORCED PLASTICS FOR ROCKET MOTORS AND RE-ENTRY HEAT SHIELDS

H. A. Perry
I. Silver
F. A. Mihalow
H. C. Anderson
U. S. Naval Ordnance Laboratory
White Oak, Silver Spring, Maryland

INTRODUCTION

Reinforced plastics are currently under intensive development for use in the construction of rocket motors and re-entry heat shields. This work is underway because of the outstanding thermal insulating properties of reinforced plastics, their low density and their great resistance to erosion during exposure to hot, moving gases. Because of these properties, reinforced plastics have been found to provide such excellent temporary, lightweight protection for heat-sensitive structures, and to ablate or erode away so slowly, that it becomes practical to employ them as liners for rocket motors and rocket nozzles and as protective overlays on re-entry bodies.

In 1943, the Naval Ordnance Laboratory undertook the development of reinforced plastics cartridge cases and reinforced plastics rocket motor casings with the goal of eliminating excess weight from these ordnance components. At that time it was observed that reinforced plastics are very resistant to decomposition by flames, provided that the time of exposure is short. It was also observed that these materials provide good thermal insulation and that the weight of structures required to survive temporary exposure to hot gases is much less than the weight required by similar structures constructed of steel, brass or aluminum. As a result of this investigation, reinforced plastics cartridge cases were developed for 5", 6" and 8" Naval guns which performed satisfactorily and weighed less than the corresponding brass cases. Also, as

a result of this work, a satisfactory reinforced plastic motor casing was developed for a small-caliber solid-propellant rocket which was lighter than the equivalent aluminum casing. Further, under a task assignment from the Office of Chief of Ordnance, a reinforced plastic cartridge case was developed for the 105 mm Howitzer which performs satisfactorily under all service conditions and weighs much less than the corresponding brass or steel case. Many similar applications have been found for reinforced plastics in JATO units and in larger air-air and ground-air rockets.

In all these applications the reinforced plastics not only present an erosion-resistant surface, but also function structurally. Because of their self-insulating properties the materials protect themselves against gross deterioration and mechanical weakening during short periods of exposure of flames.

With the inception of major programs for the development of large-caliber solid-propellant rockets such as POLARIS and MINUTEMAN the engineering problems involved in the exploitation of the favorable properties of reinforced plastics to resist contact with moving flames has increased greatly in severity. It became imperative to increase the chamber pressures, the combustion temperatures and the burning times in order that the total impulse of the rocket could be made to meet operational requirements. In attaining higher specific impulses it became necessary to employ novel solid-propellants, some of which discharge abrasive materials in their exhaust. For the same reasons it is also imperative that dimensional changes, although permitted, be kept at a minimum and that structural weight also be kept at a minimum. The reinforced plastics which were adequate in the older rockets are now deemed inadequate for use in these advanced rocket systems.

With the advent of the ballistic missile re-entry body and the concept of a space-flight recovery vehicle it was a rather obvious step to consider the use of reinforced plastics in the construction of heat shields for these devices. The total heat-pulse to be endured by a heat shield in some cases may not exceed the heat-pulse to be endured by a rocket motor lining. However, the heat-source temperatures in an aerodynamic boundary layer may greatly exceed any known flame temperature and the gas in contact with the surface contains an excess of oxygen, which latter condition is in contrast with the conditions in a flame, most of which contain less than a stoichiometric amount of oxygen. A comparison of the various conditions to which a reinforced plastic may be exposed is present in Figure 1. A reinforced plastic which is adequate for use in a rocket may not be suited for atmospheric re-entry.

Since the survival of a man, or a weapon, will depend on the vehicle during acceleration and re-entry, it is imperative that the performance of the rocket and heat shield, and the materials of which they may be constructed, be known with a high degree of confidence.

Methods for testing materials for their resistance to contact with very hot gases have been found to be very costly, particularly when it becomes necessary to provide close simulation of actual flight conditions. Figure 2 presents curves showing the variation of temperature of air at the stagnation point of a flight vehicle and shows the positions occupied by various types of test facilities in the field of temperature and Mach Number. In general, the devices to the left are relatively inexpensive to build and operate whereas the devices to the right become increasingly expensive, and an arc-heated tunnel capable of simulating the aerothermodynamic conditions at higher Mach Numbers will consume enormous amounts of electric power. Another limitation not covered in Figure 2 is the Reynolds Number which must also be simulated if true shear stresses and heat-transfer coefficients are also to be of the right order of magnitude.

Reinforced plastics constitute a broad class of composite materials consisting of a thermoplastic or thermosetting resin matrix containing fibrous reinforcements, which fibers may be either polymeric or ceramic in chemical composition. Typical combinations include: Phenolic-fiberglass laminates, Teflon-fibersilica laminates and Phenolic-nylon cloth laminates. In some combinations of resin matrix and fiber it has been found advantageous to add a third component in the form of a powdered filler, the function of which is to absorb thermal energy, or to convert the other components into a more heat-resistant substance, or both. These newer forms of reinforced plastics show greatly improved resistance to hot, moving gases and offer considerable promise for the solution of current problems in the construction of large-caliber rockets and re-entry heat shields.

Considering the very great number of possible combinations of resins, fiber and fillers, and considering the tremendous expense and lead-time involved in screening, testing and obtaining reliable engineering data on these possible combinations, it becomes very important that means be found for reducing the amount of testing required for intelligent research and development in this field. One way to facilitate the work would be to develop theories linking the chemical and physical properties of the materials with their behavior in contact with hot gases. The purpose of this paper is to discuss the current status of ablation theory, to discuss a mathematical theory for pyrolytic ablation and to discuss new test methods for obtaining the data required for the calculation of ablation rates and temperature profiles in ablating materials.

Status of Ablation Theory

Ablation in this context may be defined as the loss or removal of matter from a solid surface, due in part to the action of heat. The physical and chemical effects involved in ablation are shown in Figure 3. The theory of melting ablation is now under development covering the behavior of surface consisting entirely of a fusible substance such as glass or ceramic. Sutton (1) obtained numerical solutions for pyrex and was restricted to the case of no vaporization. He pointed out the important influence of viscosity on the surface temperature. The higher the viscosity the higher the surface temperature. Bethe and Adams (2) extended the theory to include partial vaporization of the molten surface. They showed that the viscosity has an equally important effect on the energy absorbed by vaporization, namely as the viscosity is increased so is the fraction of ablated material which vaporizes.

The instability of molten layers on ablating bodies and their tendency to move by wave action has been investigated by Feldman (3).

The effect of gas injection by a surface into an aerodynamic boundary layer has been described by Low (4) who considered a homogeneous layer and illustrated that both the stress and the heat-transfer at the surface are decreased simultaneously. A considerable amount of attention has been focused on this effect and the field of mass-transfer cooling is being explored extensively (5). Also, means have been developed for coupling a molten vaporizing surface to an aerodynamics boundary layer in the mathematical theory of ablation (3), (5).

The other physical effects of spalling, sloughing and mechanical erosion are described extensively elsewhere in the literature and are not of particular interest here.

The ablation of a reinforced plastic surface involves the melting of ceramic fibers, if any, the vaporization of molten ceramics, if any, the pyrolysis of the resins in the matrix and, in some cases, the melting and pyrolysis of polymeric fibers. Since the gases evolved will disrupt any molten layers when they emerge from the ablating surface, and since the gases evolved will have an effect on the heat transfer characteristics of an aerodynamic boundary layer, and since polymers will absorb substantial quantities of thermal energy during the chemical reactions and phase changes involved in their pyrolysis, it is of interest to consider the energy-transfer and mass-transfer balances which may be established in an ablating

surface and to develop mathematical means for including pyrolytic effects in the foregoing theories of ablation.

General Chemical Behavior during Ablation

Up to this point, the paper has discussed the physical aspects of ablation. Another aspect of the problem is the relationship between the chemical composition and molecular structure of a resin and its ablation resistance. From available information on the thermal degradation of resins and the conversion of organic matter to carbon residues, certain general concepts regarding these relationships can be postulated.

The thermal flux attained in re-entry and rocket exhausts is generally sufficient to decompose all organic matter. However, within the relatively short periods of exposure to intense heat, large differences in ablation rates are found to occur with various resin systems. Although these differences, in part, are attributable to the presence of reinforcement and filler, the chemistry of the resin is believed to play a major role in affecting the ablation rate.

The subject of thermal degradation of resins has been treated by several investigators (6), (7), (8). Much of what has been found can be used as a basis for understanding the pyrolytic behavior of resins in ablation. In ablation, the specimen is subjected to high heating rates on the outside surface. At any one time, the specimen is undergoing varying degrees of decomposition depending on the rate of heating, time of exposure and distance from the surface. Under these conditions, it would be difficult, within the present state of knowledge, to prescribe a definitive mechanism to cover the multitude of possible reactions. In addition to the expenditure of energy in dissociation of the resin, oxidation effects at the surface complicate the energy balance by the exotherm of the combustion process.

It has been shown that thermoplastics vary in their thermal behavior depending upon their particular chemical composition and their tendency to cross-linking on heating. Certain resins, such as polymethylmethacrylate, decompose in vacuo wholly to volatiles comprised essentially of the monomer with scission occurring at the ends of the molecular chain. At the other extreme, polyethylene decomposes to volatiles, of which only about 3% is monomer and the rest fragments with an average molecular weight of 700. Scission appears to be a random process here. Polystyrene and polyisobutylene yield intermediate amounts of monomer indicating degradation by both random and chain-end scission (9). Vinyl chloride resins behave differently depending on the number of chlorines present in the

structure. Polyvinyl chloride, heated to above 400°C, returns only 15% of the original carbon in the original sample: polyvinylidene chloride, on the other hand, converts quantitatively to carbon (6).

The high dissociation energy of the C-F bond (107 K-cal/mol) makes fluorinated resins attractive for their thermal resistance. Under ablating conditions, it is doubtful that the endothermic potentialities of this class of resins are fully realized. Since the C-C bond is (62 K-cal/mol) is weaker than the C-F bond, degradation in Teflon occurs at the C-C bond with the formation of the tetrafluoroethylene monomer in a molecular chain-end type of scission. Very little of the C-F dissociation may actually occur if the volatile products are swept away by the gas stream to cooler areas. If the C-F bond could be contained at or near the heated surface, Teflon as an ablating material would be more effective. Polyvinylidene fluoride, containing two fluorines to Teflon's four, yields a coke deposit close to 100% of the original carbon content. By a process of dehydrohalogenation, six membered carbon cyclic adducts are formed by a Diels-Alder addition across double bonds. Further dehydrohalogenation-condensation sequences lead to bridged hexagon carbon ring systems.

The ease of forming carbon residues can be controlled to a considerable extent by the cross-linking properties of the resin (7). It has been shown that by introducing divinyl and trivinyl benzene into polystyrene, that the added cross-linking retards depolymerization, produces dark colored polymer residues of increased thermal stability and gives up to about a 6% carbonaceous residue (6). By preoxidizing the cross-linked styrenes (8), conversion to carbon is sharply increased to over 50% of the original carbon content. The degradation mechanism involves the oxidation and splitting off of aliphatic segments on the structure and the condensation at the reactive sites to form additional cyclic compounds. On further heating, by a process of dehydrogenation and loss of carbon oxides, a structure of highly cross-linked polyphenyl results, which is the basis for the hexagonal graphitic crystallites in carbon residues.

It is thus apparent that not only the chemical composition but the structural characteristics of the resin are important aspects of the problem. If the presence of an aromatic structure, oxygen and high cross-linking density are characteristics of a high carbon residue formation, then one would expect phenolic resins to be high carbon formers. Laboratory data show that some resins heated in air give residues close to 100% of theoretical. On the basis that high carbon formers are desirable materials for ablation applications, then one would expect phenolics to show a high degree of ablation

resistance. Laboratory and rocket motor tests confirm this expectation (10).

Phenolic resins vary in structure with type of phenol, phenol-to-formaldehyde-ratio , catalyst, and curing conditions. Long chain compounds with little cross-linking occur where certain phenols are sterically hindered, preventing substitution in all three active positions (11). In such cases, one would expect these long chain segments to break-off with the formation of volatiles. It would be desirable to eliminate such chain formations and attain the maximum degree of cross-linking. For example, it has been shown that the coke-like residues from phenolic resins can be increased in yield by employing higher concentrations of formaldehyde (11).

In practice, phenolic resins are generally compounded with fillers. These fillers can conceivably have catalytic effects on the thermal stability of the resin. Evidence is available to show that the addition of small concentrations (1%) of various inorganic chemicals to sugar resulted in close to theoretical yield of carbon residue (7). Similar effects probably will occur in other resin systems, particularly in those oxygenated resins in which the elimination of water can increase the effective cross-linking density.

Although the cooling effect of volatiles or gases emanating from the resin may be useful in minimizing the effects of ablation, in practice, the generation of such gases under certain conditions may have disastrous effects. At some point behind the surface of the resin, the sudden temperature rise may cause the destructive distillation of volatiles. If generated in force, these volatiles can be forcibly ejected with the formation of voids and sudden loss of surface materials. For this reason, molecular structures which minimize the formations of volatiles and favor a high degree of cross-linking with attendant high carbon formation appear to be more desirable.

As previously stated, the higher thermal fluxes generally result in a decreasing ablation rate per heat input. At the extreme conditions in which gas temperatures of over 5000°K are attained, dissociation of gases into atomic and ionic species can occur with the absorption of considerable amounts of energy. Such a condition would prevail if the heating rate was sufficiently fast and temperatures sufficiently high so that dissociation occurred at the surface or in the boundary layers before the decomposition products from the resin escaped into the gas stream. Grundfest and Shenker (11) have shown that an all-organic resin system, such as nylon fiber reinforced phenolic capable of generating relatively higher amounts of N_2 and

H_2, actually outperform the glass reinforced phenolic at the higher temperature regimes.

Certain general degradation effects can be anticipated in resins at different temperatures (13). Below 600°C, molecular reactions occur in which are liberated volatiles consisting of water, hydrocarbons, oxygenated compounds and hydrogen, and in the case of nitrogenous resins NH_3 and N_2. The solid residue remaining is essentially a carbon skeleton to which are bound H_2, O_2 and N_2. Above 600°C, chemical rearrangements occur in the solid residue with the elimination of additional gases, non-condensable in nature such as CO, H_2 and N_2. For example, (14), melamine formaldehyde resin heated to 500°C forms a product which contains about 42% nitrogen. Heated to 1000°C, the nitrogen content is reduced to 0.4%. At temperatures above 1000°C, changes continue to occur in the carbon structure which form the basis of a graphitic or amorphous residue. Hydrogen continues to be evolved at temperatures greatly in excess of 1000°C.

For ablation purposes, the physical characteristics of the carbon residue are expected to have important effects. Carbon residues, which are structurally weak and contain high internal stresses, may, particularly on rapid heating, disintegrate into a powder (8) and be carried away in the gas stream. The carbon must be capable of serving as a refractory matrix for the fiber reinforcement and other endothermic fillers and, in addition, absorb large amounts of heat by virtue of its high sublimation temperature (about 3500°C) and heat of sublimation (170 K-cal/g. atom) (15).

In order to understand those factors which determine the physical structure of carbon, it would be advantageous to review the results of investigations of coke and graphitic materials. Graphite is a crystalline material with a weakly cross-linked hexagonal carbon structure which is formed synthetically by the thermal treatment of cokes. In this treatment, chemical and physical reactions occur which permit the suitable development of the crystalline structure. Under very fast rates of heating, the development of the graphitic crystalline structure does not appear to occur easily. In addition, non-graphitic carbons are also formed from organic materials having comparatively little hydrogen or much oxygen. On heating, there develops, at relatively low temperatures, a high cross-linked network which essentially immobilizes the structure. Isolated graphitic-like crystallites are formed, but they are held apart and in random orientation by the cross-links. These carbons are characterized by a fine-structured porosity varying from 20 to 50% and having diameters in the order of tens of Angstroms and are extremely hard and strong in

contrast to graphite. Further heat treatment up to 3000°C does not effectively change this structure. Organic materials having a high fraction of hydrogen, such as pitch or petroleum coke, produce crystalline nuclei which remain relatively mobile. On further heating, these crystallites are favorably oriented and a graphitic carbon is formed with maximum density and a small number of pores.

From the above, resins such as phenolic or epoxy can be expected to give amorphous carbon residues. What is not known is how the pertinent characteristics of these residues vary with resin composition and their effect on the ablation rate.

It is apparent, however, that ablating resins should be highly cross-linked, capable of conversion to high carbon residues with the minimum formation of volatiles and composed of chemical bonds having high heats of dissociation. At the extreme thermal fluxes and temperatures, resin systems capable of yielding relatively higher portions of N_2 and H_2 with their subsequent dissociation into atomic and ionic species would appear to be more advantageous.

Heat-Transfer in a Pyrolyzing Surface

The process of ablation of a decomposable surface under heat, wind and accelerations passes through three phases: an initiation phase, a terminal phase, and, in some cases, a steady-state phase.

The conditions for steady-state ablation are as follows: a constant heat input to the surface over a period of time, which is large with respect to the response time in the initiation phase; a relatively homogeneous material; a thickness of material large with respect to the thickness of the ablation zone at the ablation rate involved; and a one-dimensional heat-flux.

Under steady-state conditions the surface recedes at a constant velocity when the velocity is measured in the coordinate system of the structure. This coordinate system is important for engineering purposes, say for the design and prediction of performance of a rocket nozzle or of a re-entry body, since by integration of the ablation rate the progressive dimensional changes of the device can be calculated as a function of time. However, the use of this coordinate system in the analysis of ablation phenomena presents a number of formidable difficulties. Instead, it is convenient to fix the coordinates on the ablating surface $(x, y, z)_A$ where in the ablation rate ($\dot{x}$) now appears as the velocity of material toward $x = 0$.

In ablation coordinates $(x, y, z)_A$ under steady-state:

a. The rate of mass-transfer toward $x = 0$ is a constant throughout the semi-infinite body in compliance with the law of conservation of matter.

b. The energy entering any given zone in the surface is equal to the energy leaving that zone in compliance with the law of conservation of energy.

The following phenomena are invariant with time: heat-flux, temperatures, material properties, reaction rates, gas velocities, and pressures.

These phenomena may be variable in (x), the distance from the ablating surface in the body, and also in terms of $(\dot{x})$, the mass-transfer velocity.

Let us consider a cubical element (dx, dy, dz) at depth (x) in the ablating zone, as shown in Figure 3. In accordance with the law of conservation of matter, the rate of mass-transfer through the element (dx, dy, dz) is a constant under steady state.

$$\frac{d\dot{M}}{dx} = 0 \qquad (1)$$

where (M) is the weight of matter and

$$\dot{M} = \frac{dM}{dt} = \rho \dot{x}$$

and (ρ) is the original density of the laminate.
In accordance with the law of conservation of energy, the sum of the energies in all forms entering and leaving the element (dx, dy, dz) must also be equal to zero. Thus:

$$q_{in} + E_{i,in} + J(E_f + E_k + E_p)_{in} = q_{out} + E_{i_{out}} + J(E_f + E_k + E_p)_{out} \qquad (2)$$

where

q = heat energy (calories or British thermal units).

E_i = internal energy of matter including vibrational energies and energies of formation of molecules (cal. or BTU).

E_f = flow-work energy (PV).

E_k = kinetic energy ($1/2\ mv^2$).

E_p = potential mechanical energy (energy stored by virtue of the relative vertical elevation above a horizontal reference plane).

J = Joule's mechanical equivalent of heat.

However, in the distance (dx):

$$q_{in} - q_{out} = dq/dx$$
$$E_{in} - E_{out} = dE/dx$$

Therefore:

$$\frac{dq}{dx} + \frac{dE_i}{dx} + J\left(\frac{dE_f}{dx} + \frac{dE_k}{dx} + \frac{dE_p}{dx}\right) = 0 \qquad (3)$$

To render this equation compatible with aerodynamic heat-transfer theory and with Equation (1), it is necessary and proper to differentiate Equation (3) with respect to time. Then

$$\frac{d\dot{q}}{dx} + \frac{d\dot{E}_i}{dx} + J\left(\frac{d\dot{E}_f}{dx} + \frac{d\dot{E}_k}{dx} + \frac{d\dot{E}_p}{dx}\right) = 0 \qquad (4)$$

where ($\dot{q}$) and the terms $J\dot{E}$ have the dimensions of power (one BTU/sec = 778 ft-lbs/sec = 1.06 kilowatts = 1.06×10^6 ergs/second = 1.41 horsepower), Equation (4) states that the sum of the rates of change of power with respect to (x) equals zero. Since none of these derivatives are measurable directly, it is necessary to expand the terms using measurable quantities.

$\dot{q}$ - Heat-Transfer Rate. The rate of heat conduction through a solid, liquid or gas is equal to the thermal conductivity (K) of the material times the temperature gradient (dT/dx) in the material:

$$\dot{q}_x = K_x \left(\frac{dT}{dx}\right)_x - \sum_1^k \Delta H_j \dot{n}$$

Since the thermal conductivity (k) can be a variable in (x), and differentiating with respect to (x):

$$\frac{d\dot{q}}{dx} = K_x \frac{d^2T}{dx^2} + \frac{dT}{dx}\frac{dK}{dx} - \sum_1^k \Delta H_j \frac{d\dot{n}}{dx} \quad (5)$$

$\dot{E}$ - Internal Energy Transfer Rate. The rate of transfer of energy as internal energy of matter is equal to the sum of the rates of transfer via sensible heat and via the heats of formation of the molecules:

$$\dot{E}_{i_x} = \dot{m}_s c_s T_x + \sum_1^k E_j \dot{m}_j$$

where

$\dot{m}_s$ = mass-transfer rate of solids.

$\dot{m}_i$ = mass-transfer rate of the jth molecular species.

c_s = specific heat of solids.

E_i = heat of formation of the jth molecular species.

T_x = temperature of the solids.

The sensible heat of the gases is not included in this term, but it is taken account in the (PV) flow-work term. Differentiating with respect to (x)

$$\frac{d\dot{E}_i}{dx} = \dot{m}_s c_s T_x \left(\frac{1}{\dot{m}_s}\frac{d\dot{m}_s}{dx} + \frac{1}{c_s}\frac{dc_s}{dx} + \frac{1}{T_x}\frac{dT}{dx}\right) + \sum_1^k E_j \frac{d\dot{m}_j}{dx} \quad (6)$$

This term will show significant changes in zones of thermal decomposition, melting and vaporization.

$\dot{E}_p$ - Potential Energy Transfer Rate. Since the differences in elevation within an ablation zone are small, it is assumed that:

$$\dot{E}_p = 0 \quad (7)$$

$\dot{E}_f$ = Flow-Work Rate. The net work done by a unit mass of gas on the surroundings in expanding from P_1 to P_2 is given by $E_f = P_2V_2 - P_1V_1$. The work done in expanding along a path with length (dx) is $dE_f/dx = d(PV)/dx$. For a non-ideal gas, $PV = CnRT$ where (C) is a compressibility factor varying about unity depending weakly on pressure, and (n) is the number of moles occupying volume (V). Considering one mole, (n = 1), PV = CRT. Then the work performed in expanding (n) moles per second past (dx) is

$$\frac{d\dot{E}_f}{dx} = \frac{d(\dot{n}CRT)}{dx} = CR\frac{d(\dot{n}T)}{dx}$$

or

$$\frac{d\dot{E}_f}{dx} = CR\left(\dot{n}\frac{dT}{dx} + T_x\frac{d\dot{n}}{dx}\right) \qquad (8)$$

Here

$$\dot{n} = \frac{\dot{m}_g}{(\text{mol. wt})_{av.}} \quad \text{and} \quad \dot{m}_g = \dot{M} - \dot{m}_s$$

$\dot{E}_k$ - Kinetic Mechanical Energy Transfer Rate. The kinetic energy involved in the transfer of matter through (dx) is equal to the sum of the kinetic energy of the moving solids and the kinetic energy of the moving gases. Since the solids are moving very slowly, it is reasonable to ignore this factor. The moving gases with velocity (U_g) have the following kinetic energy:

$$\dot{E}_k = \dot{m}_g\frac{U_g}{2G}, \quad \frac{d\dot{E}_k}{dx} = \frac{1}{2G}\frac{d(\dot{m}_g U^2)}{dx}$$

and

$$\frac{d\dot{E}_k}{dx} = \frac{\dot{m}_g}{G}U_g\frac{dU_g}{dx} + \frac{U_g^2}{2G}\frac{d\dot{m}_g}{dx} \qquad (9)$$

where G = the acceleration due to gravity.

U_g - Velocity of Gases. The average velocity of gases in an ablating plastic is:

$$U_{g_x} = \left(\frac{\dot{m}_g}{\rho_g A_p}\right)_x$$

where (ρ_g) is the density of the gas mixture and (A_p) is the fractional cross-section area of the pores.

The fractional pore area is equal to the void fraction at (x). Assuming that the density of the solids remaining in the

plastic is essentially unchanged in the process of ablation,

$$A_p = \frac{\dot{m}_g}{\dot{M}_i} \quad \text{and} \quad U_g = \frac{\dot{M}}{\rho_g}$$

The density of a gas mixture at standard conditions is equal to the average molecular weight divided by the standard molal volume. Corrected for temperature and pressure at (x),

$$\rho_{g_x} = \frac{\text{mol. Wt.}}{\text{mol. volume}} \frac{T_s}{P_s} \frac{P_x}{T_x}$$

Since we would like to eliminate pressure as a variable in Equation (4), one can look for other relationships. Darcy's law (17) states that the volume of fluid (V) crossing unit area of a porous medium per unit time under pressure gradient (dP/dx) is related empirically:

$$k' \frac{dP}{dx} = V$$

where k' is a constant dependent on both the fluid and the porous medium. Further, $k' = k/\mu$ where (μ) is the coefficient of shear viscosity of the fluid and (k) is the permeability of the medium. Kozeny's Equation (17) gives a good approximation of the permeability of porous media having a minimum of blind pores. This equation is:

$$k = \frac{1}{20\pi}\left(\frac{A_p^2}{1 - A_p^2}\right) = \frac{1}{20\pi}\left(\frac{\dot{m}_g^2}{\dot{M}^2 - \dot{m}_g^2}\right)$$

and

$$V = \frac{1}{20\pi\mu_x}\left(\frac{\dot{m}_g^2}{\dot{M} - \dot{m}_g^2}\right)\frac{dP}{dx}$$

but

$$V = \frac{\dot{m}_g}{\rho_g}$$

so

$$P_x\, dP = 20\pi\mu T_x \frac{\text{mol. wt}}{\text{mol. vol.}} \frac{T_s}{P_s}\left(\frac{\dot{M}^2 - \dot{m}_g^2}{\dot{m}_g^2}\right) dx$$

Integrating from $P_w \rightarrow P_x$, (P_w) being the pressure at the wall,

$$P_x = P_w + \sqrt{\left(\frac{\dot{M}^2 - \dot{m}_g^2}{\dot{m}_g^2}\right)\left(\frac{\text{mol. Wt.}}{\text{mol. Vol.}}\right)\left(\frac{T_s}{P_s}\right) 40\pi\mu_x T_x}$$

and

$$U_{g_x} = \dot{M}\left(\frac{\text{mol. wt.}}{\text{mol. Vol.}}\right)\left(\frac{P_s}{T_s}\right)\left(\frac{T_x}{P_x}\right)$$

Thus, it appears that the velocity term becomes small at very high pressures, as in a rocket. As a result, the kinetic energy term

becomes very small, since (P_w^2) becomes very large. Therefore, the kinetic energy term can be neglected in internal ballistic problems. However, it may be included in high-altitude problems where (P_w^2) is relatively small.

Substituting in Equation (9),

$$\frac{d\dot{E}_k}{dx} = \frac{\dot{M}^2}{G}\left(\frac{\text{mol. vol.}}{\text{mol. wt.}}\ \frac{T_s}{P_s}\right)^2 + \dot{m}_g\left(\frac{1}{P_x}\frac{dP}{dx} + \frac{1}{T_x}\frac{dT}{dx}\right) + \left(\frac{T_x}{P_x}\right)^2 \frac{d\dot{m}_g}{dx} \quad (10)$$

$\dot{m}_g$ - Mass-Transfer Rate of Gas. The amount of gas passing a point (x) in the body is equal to the amount of gas generated deeper in the body. In this coordinate system, with temperature gradients which are invariant with time, and with a constant supply of matter, it can be expected that the types and rates of chemical reactions at any given point in the body will also be invariant with time. As a generalization, the chemical theory of rate processes (7) states that the jth reaction proceeds at the rate:

$$\dot{n} = c^*_x \frac{k^*}{h^*} T_x e^{-\frac{\Delta H^*}{RT}} e^{+\frac{\Delta S^*}{R}} \quad (11)$$

where

c^* = a constant determined by the nature of the reactants

k^* = Boltzmann constant

h^* = Plank's constant

H^* = a heat of activation for the reaction

S^* = an entropy of activation for the reaction.

If the rate $(\dot{n})$ is defined as the number of moles of gas generated per second, then the weight of gas being generated per second at point (x) is equal to the product of the mole rate and the molecular weight of the gas evolved (MW_i). Summing up for all reactions from first to the kth and integrating forward to (x),

$$\dot{m}_g = \int_{\infty}^{x} \sum_{1}^{k} (MW)_j \, C_j^* \frac{k^*}{h^*} T_x \, e^{-\frac{\Delta H_j^*}{RT} + \frac{\Delta S_j^*}{R}} \, dx \qquad (12)$$

The unknowns in this equation are (C_j^*), (ΔH_j^*) and (ΔS_j^*). In those instances when these data are available on all of the reactions in the body, then the mass-transfer rates of gases and solids could be calculated by computer techniques. In the absence of these data, it will be sufficient to develop techniques for determining the rate of evolution of gas from the solids at given rates of heating, to sample and analyze the gases evolved, and to assign values to the average molecular weight and the apparent specific heat of the gas (MW) and (C_g).

Assembly of Terms. Referring to Figure 1, the flow of heat is to the right and the mass transfer is to the left. Therefore, Equation (4) can be written:

$$\frac{d\dot{q}}{dx} = \frac{d\dot{E}_i}{dx} + J\left(\frac{d\dot{E}_r}{dx} + \frac{d\dot{E}_k}{dx}\right)$$

where

$$\frac{d\dot{E}_r}{dx} \equiv 0$$

Substituting Equations (5), (6), (8) and (10) in Equation (4),

$$K\frac{d^2T}{dx^2} + \frac{dT}{dx}\frac{dK}{dx} = (\dot{M} - \dot{m}_g) c_s T_x \left(\frac{1}{c_s}\frac{dc_s}{dx} + \frac{1}{T_x}\frac{dT}{dx} - \frac{1}{\dot{M}-\dot{m}_g}\frac{d\dot{m}_g}{dx}\right)$$

$$+ \sum_{1}^{k} E_j \frac{d\dot{m}_j}{dx} + \frac{JCR}{mol.wt.}\left(\dot{m}_g \frac{dT}{dx} + T_x \frac{d\dot{m}_g}{dx}\right)$$

$$+ \frac{J\dot{M}}{G}\left(\frac{mol.vol.}{mol.wt.}\frac{P_s}{T_s}\frac{T_x}{P_x}\right)^2 \left(\frac{\dot{M}}{2}\frac{d\dot{m}_g}{dx} - \frac{\dot{m}_g}{P_x}\frac{dP}{dx} + \frac{\dot{m}_g}{T_x}\frac{dT}{dx}\right).$$

$$+ \sum_{1}^{k} \Delta H_j \frac{d\dot{m}_j}{dx} . \qquad (13)$$

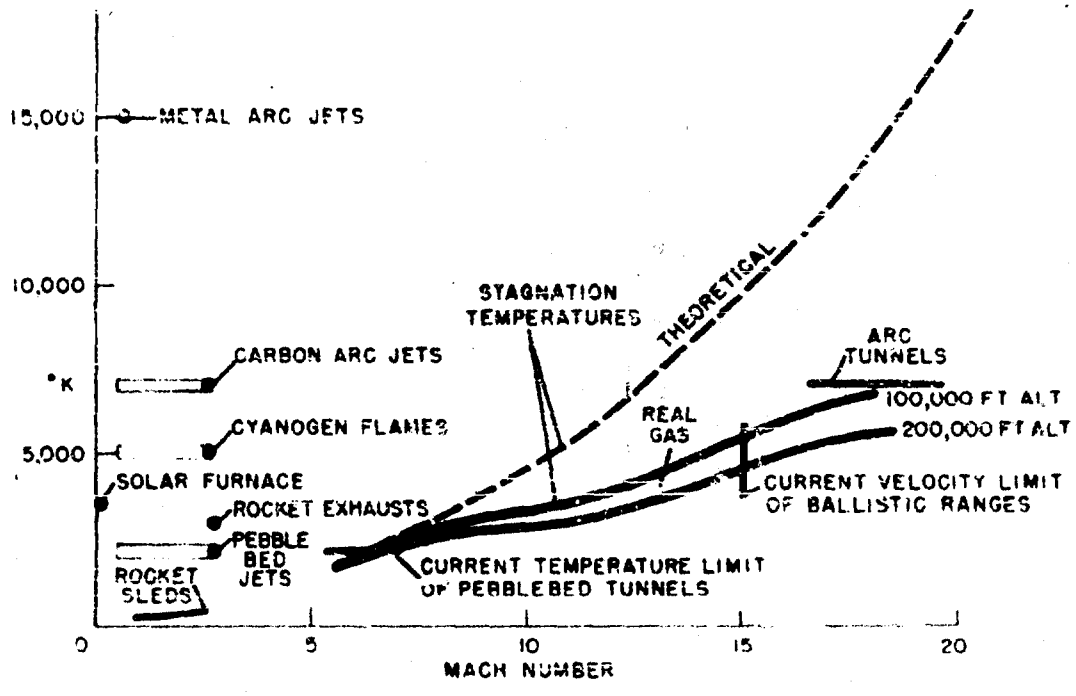

Figure 1 - Flight conditions and current facilities for testing materials

ITEM	ROCKET PARTS	GUN CHAMBERS	AERODYNAMIC HEAT SHIELDS
GAS TEMPERATURE	3000°C	3000°C	7000
PRESSURE	2500 PSI	50,000 PSI	500
EXPOSURE TIME	100 SEC	0.01 SEC	30
INPUT RADIATION SPECTRA	CONTINUOUS		LINE
GASES	CO, CO_2, H_2O, N_2		O_2, N_2
ENTRAINED MATTER	UNBURNT FUEL METALLIC OXIDES ABLATION PRODUCTS		DUST WATER DROPLETS ABLATION PRODUCTS

Figure 2 - Range of ablation conditions

Collecting derivatives,

$$K\frac{d^2T}{dx^2} + \frac{dT}{dx}\left(\frac{dK}{dx} - (\dot{M}-\dot{m}_g)c_s - JCR\frac{\dot{m}_a}{mol.wt} - \frac{J\dot{M}\dot{m}_g}{G}V^2\right)$$

$$= \frac{dc_s}{dx}(\dot{M}-\dot{m}_g)T_x + \frac{d\dot{m}_a}{dx}\left(\frac{JCRT_x}{mol.wt.} + \frac{J\dot{M}^2}{2G}V^2\right) \qquad (14)$$

$$- \frac{dr}{dx}\left(\frac{J\dot{M}\dot{m}_g}{G\ P_x}V^2\right) + \sum_1^k E_j\frac{d\dot{m}_j}{dx} - \sum_1^k \Delta H_j\frac{d\dot{n}_j}{dx}$$

and $$\frac{d\dot{M}}{dx} \equiv 0 \qquad (15)$$

where $$\dot{n} = c_x^* \frac{k^*}{h^*} T_x e^{-\frac{\Delta H^*}{RT} + \frac{\Delta S^*}{R}}$$

$$\dot{m}_g = \int_\infty^x \sum_1^k (MW)_j\, \dot{n}_j\, dx$$

$$V = \frac{\text{Mol. Volume}}{\text{Mol. Weight}}\frac{P_s}{T_s}\frac{T_x}{P_x}$$

$$P_x = P_w + \sqrt{\left(\frac{\dot{M}^2-\dot{m}_q^2}{\dot{m}_q^2}\right)\left(\frac{mol\,wt}{mol.vol.}\frac{T_s}{P_s}\right)40\pi\mu T_x}$$

$$\frac{dP}{dx} = \frac{1}{P_x}\left(\frac{\dot{M}^2-\dot{m}_q}{\dot{m}_q}\right)\left(\frac{mol.wt.}{mol.Vol.}\frac{T_s}{P_s}\right)20\pi\mu T_x$$

and μ = viscosity of gas at (x).

Boundary Conditions

Assuming an original temperature of the laminate (T_o), the temperature at $X=\infty$ is $T_x = T_o$. Also assuming an original flow of gas through the laminate ($\dot{m}_{g_o}$), the gas transfer rate at $x=\infty$ is $\dot{m}_{g_x} = \dot{m}_{g_o}$. The original gas transfer rate ($\dot{m}_{g_o}$) may not equal zero if the laminate is decomposing at (T_o). This situation might prevail if the laminate had been subjected to heating at an earlier time.

Equation (13) holds only for one-dimensional heat and mass flow. Therefore, a boundary condition for Equation (13) at x = 0 is

$$T_{x_0} = T_{melt}$$

$$(\dot{M})_{y,z} = 0$$

$$(\dot{q})_{y,z} = 0$$

$$(\dot{q})_{x=0} = K_{melt}\left(\frac{dT}{dx}\right)_{melt}$$

$$(P)_{x=0} = P_{melt}$$

At the melt-gas interface,

$$K_{melt}\left(\frac{dT}{dx}\right)_{melt} = h_c(T_R - T_{melt}) + \sigma\epsilon_{melt}(\epsilon_g T_R^4 - T_{melt}^4)$$

$$\mu_{melt}\frac{dU_{melt}}{dx} = \mu_{gas}\frac{dU_{gas}}{dx}$$

$$P_{melt} = P_{gas}$$

Using these boundary equations, it would be possible to program the ablation and melting zone equations with a set of equations for the aerodynamic boundary layer for computations on a digital computer.

Properties of Materials

Equations (1) and (13) are simultaneous differential equations in the mass-transfer rate ($\dot{M}$), the temperature (T) and coordinate (x). Equation (13) also contains properties of materials which must be known as functions of temperature (T), together with a term for the gas mass-transfer rate $(\dot{m}_g)_x$ which depends on rates of reactions in the material. Equations (22) and (25) also contain certain properties of melted materials which must be known as functions of temperature (T).

The properties required consist of:

$(K)_T$ = the thermal conductivity of the solids at temperature (T).

$(c_s)_T$ = the specific heat of the solids at temperature (T).

$(\mu_g)_T$ = the viscosity of the gas at temperature (T).

$(\mu_M)_T$ = the viscosity of the molten material at temperature (T),

$(MW)_{av.}$ = the average molecular weight of the gas.

(E_i) = the heat of formation of the jth species in the matter being transferred, solid, liquid and gaseous.

The chemico-kinetic data needed are:

(ΔH_j) = heat of reaction of jth reaction
$(\Delta H_j^{\ddagger})$ = heat of activation of the jth reaction.
$(\Delta S_j^{\ddagger})$ = entropy of activation of the jth reaction.
(C_j^{*}) = concentration factor for the jth reaction.

The reactions taking place during pyrolysis of some resins can be quite involved. For example, after fifty years of common use the phenolics are poorly understood and their exact structure remains unknown. On the other hand, polymers such as polymethylmethacrylate decompose thermally to yield a large percentage of monomer fragments, the further degradation of which can be studied quite readily. Other materials, such as nylon, polytetrafluoroethylene and polyethylene, may also yield useful data when their degradation mechanisms are

studied further. In the latter material, polyethylene being a relatively pure hydrocarbon, it is likely that a survey of the knowledge accumulated by the petroleum refining industry on the thermodynamics of cracking processes will yield data which will be applicable in these calculations.

Approximate Energy Balance at a Pyrolyzing Surface

The foregoing second-order partial differential equations offer promise for the calculation of many important factors in the pyrolytic ablation of polymeric materials and for the prediction of ablation rates and temperature profiles under steady-state ablation. However, Equations (14) and (15) are not readily amenable to solution by analytical means. Further, the relative importance of the many materials properties in the phenomenon of ablation cannot be estimated readily by inspection of these equations. A simpler relationship between ablation rate and materials properties would be useful for some purposes, even at some loss of accuracy.

Referring again to Equations (1) and (2) we may consider the energy balance at the pyrolyzing surface, $x = 0$. Under steady-state conditions the heat-flux ($\dot{q}$) into the surface must just equal the heat-flux out of the surface. The heat-flux out must take the form of sensible heat-energy, intrinsic energy and kinetic energy. Again, it is assumed that the potential energy term is negligible. On this basis:

$$\dot{q} = J\sum_{1}^{k} \dot{n}_j R T_w + \frac{J \dot{m}_g}{2g} U_g^2 + \sum_{1}^{k} \dot{n}_j \Delta H_j \qquad (16)$$

where ($\dot{n}_j$) is the number of moles of the jth species of gas passing through the surface, (ΔH_j) is the heat of formation per mole of the jth species, (T_w) is the wall temperature and (U) is the velocity of the gases passing through the surface. But,

$$U_g = \sum_{1}^{k} \dot{n}_j \,(\text{mole/volume})\left(\frac{P_s}{T_s}\right)\left(\frac{T_w}{P_w}\right)$$

When the exact composition of the gases emitted are not known, it may be assumed that

$$\sum_{1}^{k} \dot{n} \simeq \frac{\dot{m}_g}{(MW)_{est.}}$$

and

$$\sum_{1}^{k} \dot{n}_j \Delta H_j \simeq \frac{\dot{m}_g}{(MW)_{est}} \Delta H_p$$

Also, in the case of complete volatilization,

$$\dot{m}_g = \dot{M} = \rho \dot{X}$$

where (ρ) is the original density of the polymer, (ΔH_p) is the heat of pyrolysis as determined by experiment and ($MW_{est.}$) is the estimated molecular weight of the gases of pyrolysis.

Substituting and rearranging, Equation (16) becomes

$$\dot{X} = \frac{(MW)_{act.}}{\rho\left[\Delta H_p + J\left(RT_w + \frac{\beta^2}{2G}\frac{\rho^2 u^2}{(MW)_{est.}}\frac{T_\infty^2}{P_w^2}\right)\right]}\dot{q} \qquad (17)$$

where $\beta = (\text{molal volume})(P_s/T_s)$; (P_s) is the pressure at one atmosphere and (T_s) is the standard temperature.

This relationship supports the generally accepted philosophy concerning the desired characteristics of an ablation-resistant plastic, namely that the ablation rate is approximately proportional to the molecular weight of the gases evolved and inversely proportional to the heat of pyrolysis. However, Equation (17) also indicates the role of temperature and pressure in the process. As the wall temperature is increased and the wall pressure is reduced the fraction of energy going into mechanical forms is increased. Considering that in some circumstances the incoming energy may consist almost entirely of radiant energy and that the process may take place in a near vacuum, it is conceivable that substantial portions of the incoming energy will be taken up in accelerating the gases evolved. The addition of ceramic materials to the plastic composition which would accumulate on the surface and attain a higher temperature, or the formation of coke which could also sustain a higher temperature would also tend to increase the energy going into mechanical forms.

Temperature Profiles in the Ablation Zone

In certain design problems it is of value to be able to forecast the thickness of the ablation zone and the associated temperature profiles in the slab, particularly when the reinforced plastic serves both as a sacrificial layer and as a thermal insulation for temperature-sensitive devices or structures. The thickness of the ablation zone and the temperature gradients in the reinforced plastic during steady-state ablation can be determined by solving Equation (13), provided that data are available. This equation takes into account the variable properties in the material.

If, however, it can be assumed with a reasonable degree of accuracy that the thermal diffusivity of the material is a constant,

or if an average value is assumed, then an estimate can be made of the thickness of the ablation zone by the use of the well known equation for heat-transfer in solids:

$$\frac{dT}{dt} = \frac{K}{\rho c} \frac{d^2T}{dx^2} \tag{18}$$

With coordinates moving with velocity

$$\dot{x} = \frac{dx}{dt}$$

The above equation is transformed (8) as follows:

$$\frac{dT}{dt} = \frac{K}{\rho c} \frac{d^2T}{dx^2} - \dot{x}\frac{dT}{dx} \tag{19}$$

Under steady-state ablation with velocity ($\dot{x}$) the term

$$\frac{dT}{dt} = 0$$

and

$$\frac{K}{\rho c} \frac{d^2T}{dx^2} = \dot{x}\frac{dT}{dx} \tag{20}$$

A solution of the above equation when ($\dot{x}$) is greater than zero, is of the form

$$\frac{T_x}{T_w} = c' e^{+\frac{\rho c}{K} x \dot{x}} + c''$$

If $x = 0$, $T_x = T_w$; if $x = \infty$, $T_x/T_w = 0$, then

$$\frac{T_x}{T_e} = e^{+\frac{\rho c}{K} x \dot{x}} \tag{21}$$

If ($\dot{x}$) is constant and (x_e) is that depth at which $T = \frac{T_w}{e}$, $\frac{K}{\rho c} = \alpha$, then $x_e = \alpha / \dot{x}$.

This is the depth in the material at which the temperature (T_x) is 0.368 T_{wall}. At twice this depth, the temperature (T_x) is $0.1355T_w$. At three times this depth, the temperature (T_x) is $0.0498T_w$. In general, one can conclude that a high thermal diffusivity leads to deep penetration of heat into the material. Also, in general, it can

be concluded that the thickness of the ablation zone in any given material is inversely proportional to the ablation rate.

Experiments

Equation (14) and its boundary conditions indicate, as may be expected, that the thermal conductivity of the ablating material has a marked influence on the amount of heat entering the reinforced plastic to deteriorate it. It, therefore, becomes of considerable interest, as a first step in the process of unraveling the mysteries of pyrolytic ablation, to determine the thermal conductivity of the ablating material as a function of (x), or of $(T)_x$.

If $(K/\rho c)$ is a variable in (T), it can be shown (20)

$$\left(\frac{K}{\rho c}\right)_{T,\dot{x}} = \dot{x}^2 \frac{T_x}{\left(\frac{dT}{dt}\right)_x} \qquad (23)$$

where (dT/dt) is the slope of a time-temperature curve at point (x) in the ablating solid. Since the ablation rate $(\dot{x})$, the temperature (T_x) and the time derivative of the temperature (dT/dt) are all measurable quantities, it becomes possible to determine the effective diffusivity $(K/\rho c)_{eff}$, as a function of temperature and ablation rate. However, (K) cannot be separated from (ρc).

Measurement of Effective Diffusivity

The design of an experiment for determining the effective thermal diffusivity $(K/\rho c)_{T,\dot{x}}$ of an ablating material as a function of temperature and ablation rate requires that the conditions for steady-state ablation be maintained, and further, that the flow of heat into the ablating surface be one-dimensional. It is further necessary that means be provided for the measurement of temperature at a point in the ablating material as a function of time. Accordingly, it was suggested by Mr. Kendall of this Laboratory, that a thermocouple be imbedded in a semi-infinite slab and that the surface of the semi-infinite slab be ablated toward the thermocouple at a constant rate of ablation; that the temperature be recorded as a function of time; that the temperature-time derivative be calculated at each point (x); that the ablation rate $(\dot{x})$ be measured; that these data be substituted in Equation (21); and that the effective diffusivity be plotted as a function of temperature for each measured ablation rate, or, with enough repeated tests, as a function of ablation rate for typical temperatures in the ablating material.

A criterion for a one-dimensional heat flow was taken to be the maintenance of a flat surface during ablation since any inequality or nonlinearity of flow could be expected to cause unequal ablation and a curved surface. It was then possible to experiment with various ratios of thermocouple depth to specimen width and to observe the flatness of the ablated surface in the region of the thermocouple. It was also thought that a guard ring around the sides of a specimen would assist in maintaining a flat surface during ablation, particularly on small samples of experimental materials for which large specimens could not be constructed for lack of sufficient material.

To maintain the required condition of a homogeneous body of effectively infinite extent in the direction of heat flow, it was decided to mold the thermocouple into the specimen, or failing that, to bond it in place with an adhesive whose properties closely matched those of the laminating resin. Further, it was decided that the thermocouple was to be backed-up using identical laminate, or in the absence of sufficient material, to back it up using a laminate whose properties might come as close as possible to that of the sample. Finally, it was decided to employ the thinnest possible thermocouple wires in order that the heat capacity of the wires might influence the heat flux past the wires to the least possible extent.

The experimental set-up, as shown in Figure 4, consists of a guarded cylindrical specimen containing a thermocouple and exposed endwise to the flame. The guard ring was successful in maintaining a flat frontal surface on the specimen and in preventing ablation of the sides of the specimen.

A typical time-temperature curve for a phenolic glass cloth laminate is presented in Figure 5. Having transformed the curve to T/x coordinates and having determined the time-temperature derivative at each point (x) in the body a curve of the effective thermal diffusivity versus temperatures was calculated and plotted. By letting

$$t = \frac{x}{\dot{x}} \qquad (24)$$

the curve was transformed to temperature-depth and diffusivity-depth coordinates, as shown in Figure 6. This curve shows that significant changes take place in the effective thermal diffusivity of this laminate in the ablation zone.

Measurement of Volumetric Heat Capacity During Pyrolysis

Equation (13) calls for data on the conductivity of the material as a function of depth. It is, therefore, not possible to

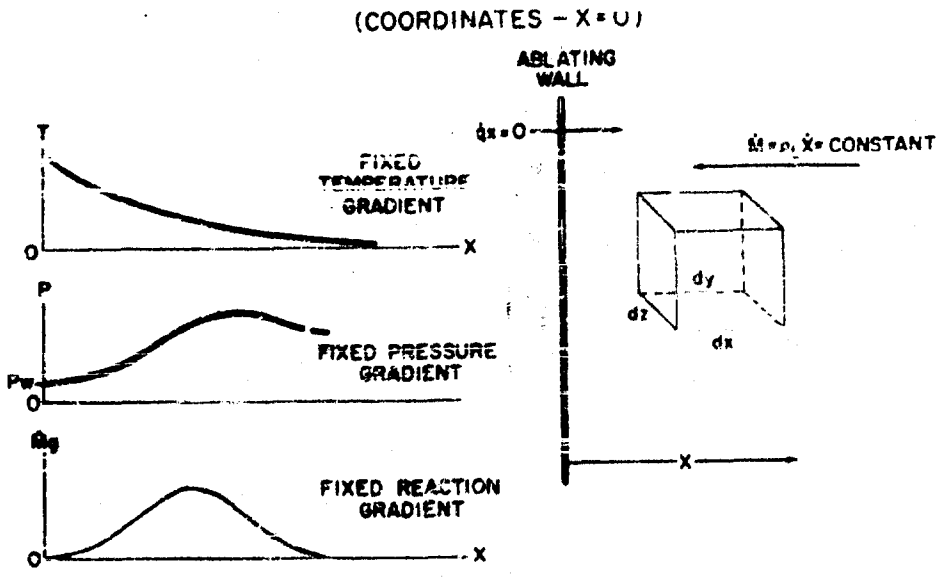

Figure 3 - Steady-state ablation

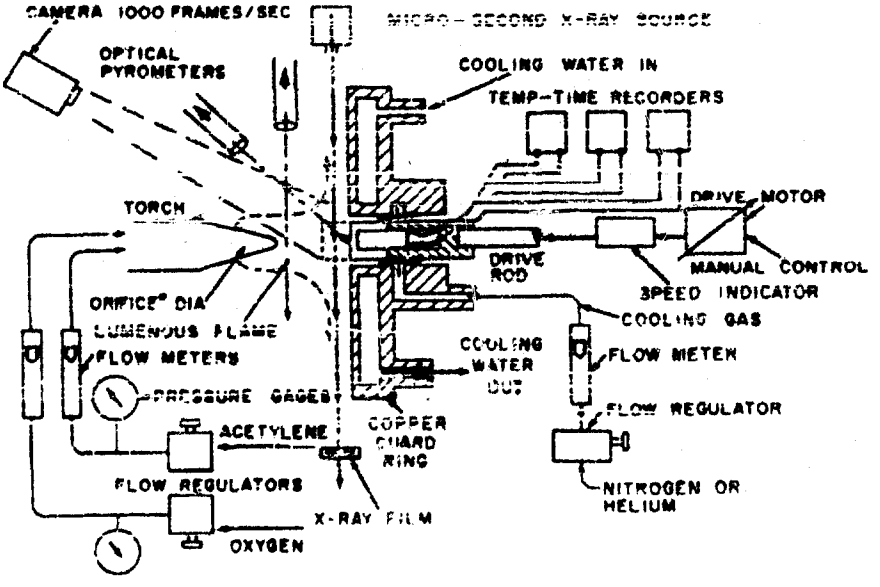

Figure 4 - Guard ring ablation test

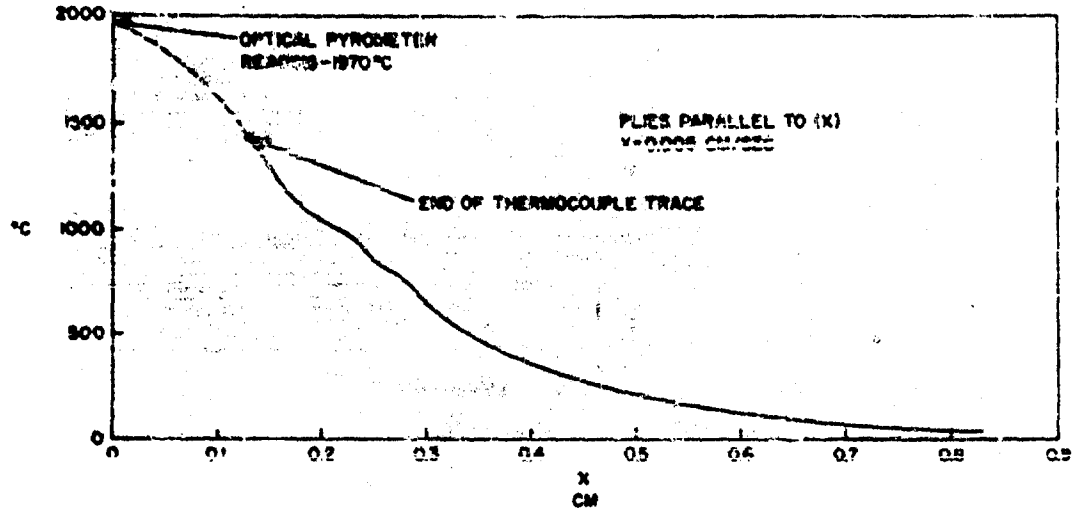

Figure 5 - Steady-state ablation temperature profile in a phenolic glass-cloth laminate

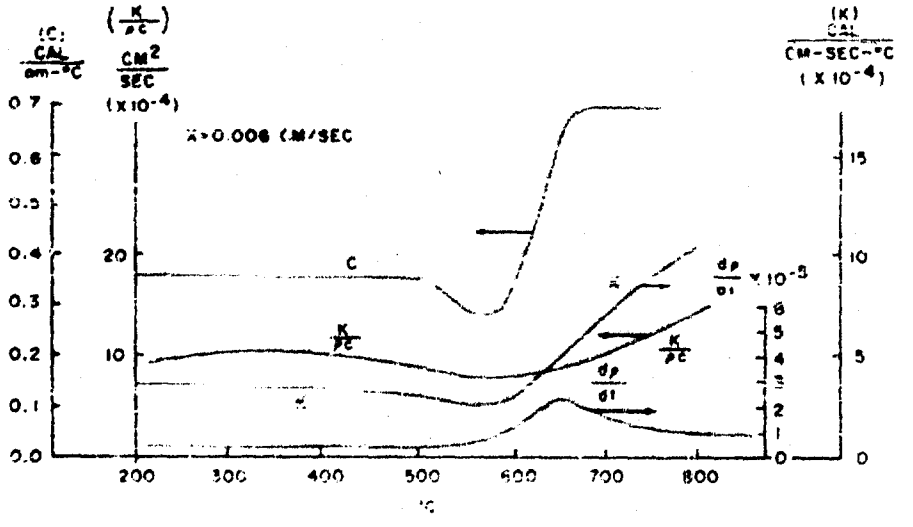

Figure 6

employ directly the diffusivity-depth data of the type presented in Figure 6. Accordingly, means were sought for determining the value of (ρC) under equivalent conditions so that $(K)_{\sim}$ and its derivatives could be calculated. This required that the heat input to raise a unit volume of material a degree of temperature be measured; the measurements being made at the temperatures and heating rates of ablation.

Two methods suggested themselves: the Differential Thermal Analyzer (DTA) (21), and a Hot-Sandwich Method suggested by Kendall (20).

It should be noted that the temperature rise observed in the specimen ablating in the torch is about 150°/second, a very rapid rise, indeed. At higher heat fluxes this rise could be much higher. By contrast, the Differential Thermal Analyzer proceeds at a rate of about 0.167°/second, or about one thousand times slower. Remembering the chemico-kinetic term for $(\dot{m}_g)$ in Equation (13), it was thought that the DTA would yield valuable data under essentially equilibrium conditions, but that a faster method would be required to evaluate the materials at progressively higher heating rates, in expectation that the population fractions of the decomposition products will differ from those generated at very slow temperature rises. The Hot-Sandwich Method seemed to offer promise of attaining this goal.

DTA Estimation of Heats of Pyrolysis

Differential Thermal Analysis (21) is a dynamic technique which consists essentially of heating simultaneously, at a constant rate, a reference material (e. g., aluminum oxide) and the substance being studied. The temperature difference developed between the reference and sample is recorded as a continuous function of time and/or temperature. Any thermal processes (melting, boiling, sublimation, oxidation, polymerization or depolymerization, decomposition, etc.) occurring in the samples will appear on the DTA record as endothermic or exothermic peaks.

The overall heat of decomposition of the samples can be obtained from the area under the thermal peak and the following equation:

$$\Delta H_p = \frac{K'(c_s W_s + c_r W_r + c_g W_g)\int \Delta T\, dt}{W_s\, \Delta t} \qquad (25)$$

Where (ΔH) is the lumped heat of reaction, (C_s), (C_r) and (C_g) are specific heats of the plastic samples, filler, and glass, respectively, (W_s), (W_r) and (W_g) are the respective weights, and (Δt) represents the time interval over which the integral is evaluated. The integral represents the area under the exothermic or endothermic peak. (K) is a constant for the apparatus used and may be evaluated by calibrating with substances of known thermodynamic properties.

The DTA experimental arrangement is described in reference (21). It is a modification of that used by Gordon and Campbell (22). It consists mainly of the following: an X, Y recorder, with a built-in time marker, for recording the differential temperature versus temperature of the sample and time; a program controller for maintaining a constant heating rate in the furnaces; a Brown recorder for monitoring the furnace temperature; and a metal heating block for holding the Pyrex sample cells in the furnace.

The apparatus was calibrated with benzoic acid and silver nitrate. All of the samples were pulverized to pass a 100 mesh sieve. A typical DTA curve is shown in Figure 7. The estimated (ΔH) values for the various materials are given in Figure 8.

Some of the factors which may contribute to the inaccuracy of the (ΔH) value are: (a) shifting of the base line due to unsymmetrical location of the differential thermocouples or due to dissimilar thermal parameters (specific heat, heat conductivity, etc.), of the sample and reference; (b) inability to position accurately a base line from which the area under the curve may be delimited. This is due to a gradual rather than sharp departure of the DTA curve from the base line; and (c), changing specific heats due to the decomposition.

Estimation of Effective Volumetric Heat Capacity and Gas Evolution Rates as Functions of Temperature by "Hot-Sandwich Method"

Under adiabatic conditions,

$$(\rho C)^*_{T,\dot{T}} = \frac{1}{V}\dot{q} \qquad (26)$$

where $(\rho C)^*_{T,\dot{T}}$ is the effective volumetric heat capacity as a function of temperature (T) and heating rate ($\dot{T} = dT/dt$) and where (q) is the heat flux into sample of Volume (V). Also,

$$(\rho)_{T,\dot{T}} = \frac{(W)_{T,\dot{T}}}{V} \qquad (27)$$

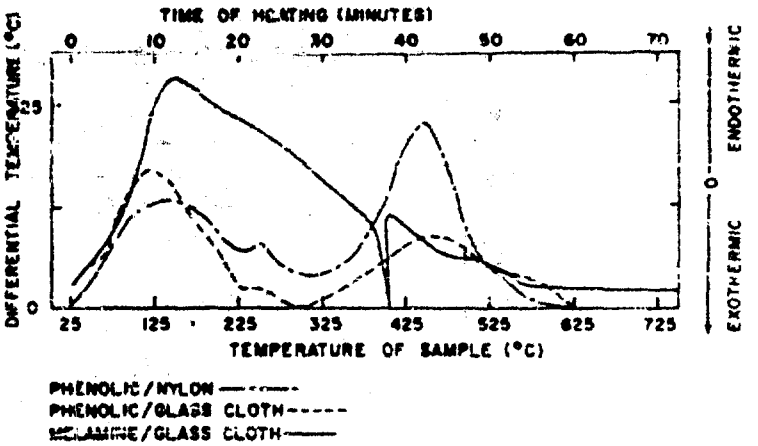

Figure 7 - Typical DTA thermograms

TYPE OF REINFORCED PLASTIC		LOCATIONS OF MAXIMUM (°C)	ΔH (CAL/GRAM)	PERCENT WEIGHT LOSS (720° C)
RESIN	REINFORCEMENT			
PHENOLIC	GLASS CLOTH	122 450	−11.1*	11.2
MELAMINE	GLASS CLOTH	147	−12.8	35.2
PHENOLIC	NYLON CLOTH	134 434	−85.0	82

*A NEGATIVE SIGN INDICATES AN ENDOTHERMIC REACTION. NOTE: $\frac{dT}{dt}$ = 10°C/min.

Figure 8 - Apparent heats of reaction and weight losses during thermal decomposition of reinforced plastics

where $(\rho)_{T,\dot{T}}$ is the density as a function of temperature (T) and heating rate ($\dot{T}$) and $(W)_{T,\dot{T}}$ is the weight of sample of Volume (V) as a function of temperature (T) and heating rate ($\dot{T}$). Then,

$$(c^*)_{T,\dot{T}} = \frac{1}{(W)_{T,\dot{T}}} \dot{q} \qquad (28)$$

where $(c^*)_{T,\dot{T}}$ is the effective specific heat.

Based on this theory sandwiches were assembled of alternate plies of laminate and heating wires, with thermocouples imbedded in one of the plies of laminate, one at the center of the block of sandwich and another offset toward the edge of the block. The assembly is shown in Figure 9, and was instrumented as shown in Figure 10.

The specimen was suspended from the sensing element of an Instron load cell, the output of which was recorded versus time on the Instron load-time recorder using the 100 gram scale. The thermocouples were connected to milliammeters which had been calibrated with the thermocouples using a standard voltage cell. In a later setup, it is proposed to record the thermocouple outputs automatically. The heating wires were connected in series to a stepdown transformer with a wattage measuring device. The power input into the transformer was controlled by a Variac. The specimen was suspended in a ventilated hood.

In running the test the power was turned on and maintained at a constant level by constant manual adjustment of the Variac. Figure 11 shows a typical temperature-time curve and a typical weight-curve for a glass cloth phenolic laminate with density of 1.6 grams per cc. It is to be noted that the center of the block sandwich was essentially adiabatic, since the two thermocouples followed together within fifty degrees. The weight-time recording was smooth. The cental thermocouple circuit opened for unknown causes at the end of five minutes of heating. By that time the temperature had reached 1600°F (870°C).

During the course of the heating cycle the slope of the temperature-time curve remained constant up to 480°C. Beyond 680°C the temperature-time curve took a lesser slope. At about 260°C an offset occurred in the curve. It has not yet been determined whether this was an instrumental error or whether this represented a rather temporary endothermic reaction. This offset has been temporarily ignored in interpreting the results. At 510°C a marked change in slope occurred which has been interpreted as being real.

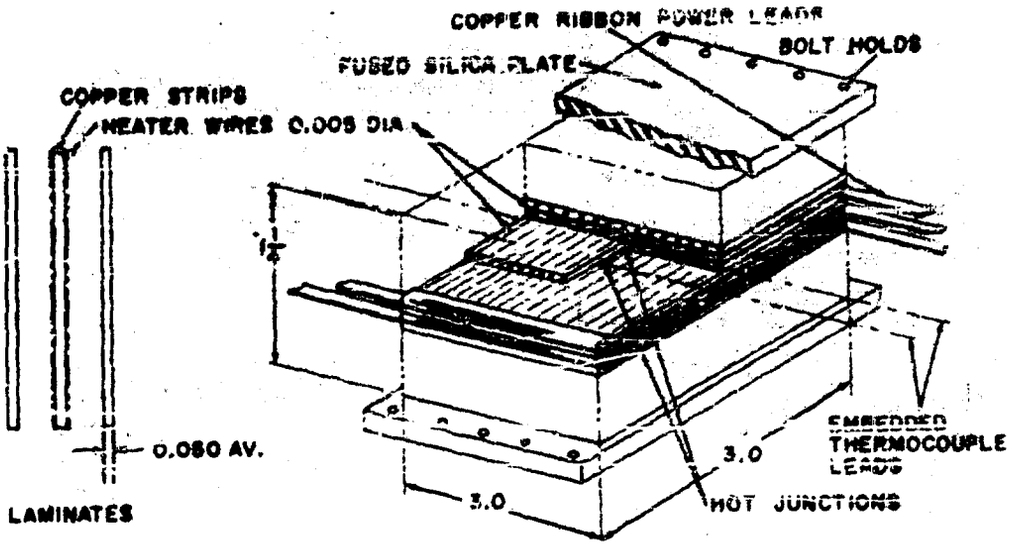

Figure 9 - Hot-sandwich (cut-away view)

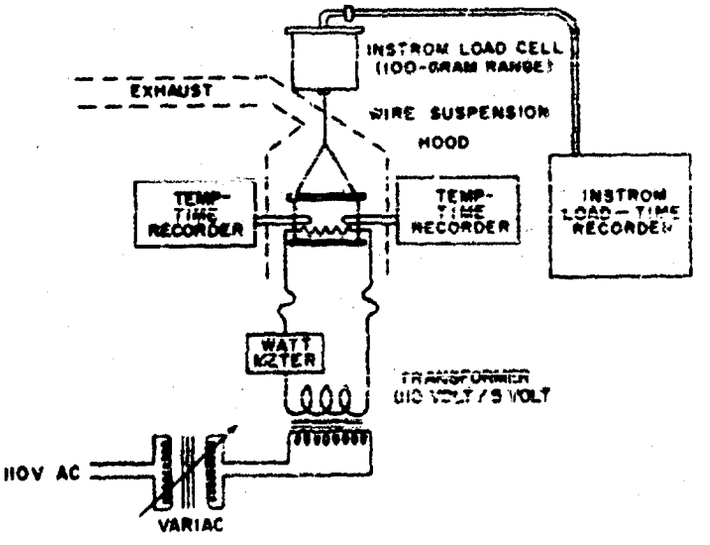

Figure 10 - Hot-sandwich test for ρc and ρ

The slopes of the important portion of the curve were determined by graphical means. These were measured to be:

30 - 480°C - 6.3°/second

510°C - 7.7°/second

630°C up - 3.45°/second

The above data were inserted in Equations (22), (23) and (24). The results are plotted in Figure 6.

Figure 6 also shows plots of (c) and ($d\rho/dt$). The plots indicate that the specific heat $(c)_{eff}$ remains constant in this material as the temperature rises until a transition takes place at about 480°C, at which temperature $(c)_{eff}$ dips and then rises to a new level which was maintained constant up to 840°C. The ($d\rho/dt$) indicates a gradual increase in the rate of weight change, which reached a peak at the time that the transition occurred in the volumetric heat capacity of the material. The peak in ($d\rho/dt$) occurred at the instant when the observed amount of smoke gushing from the specimen was at a peak. At that instant, the weight loss in the laminate was about 4%. Later, the heating cycle having been continued long after the thermocouple had burned out, the weight loss reached a level of 13%, beyond which it did not pass even though the whole block sandwich assembly became incandescent. On disassembly, the glass cloth residue was found to be cemented together and located with a black deposit, presumably a graphitic form of carbon.

This test proceeded at a heating rate of 6.3°C, or about thirty-eight times faster than the Differential Thermal Analyzer could proceed. It would appear that useful information can be obtained by this method. Steps are being taken to reduce the size of the block specimen and to pack the heating wires in close contact within the specimen. With a block of one-ninth the volume and with twice the power input it is hoped to reach a heating rate of 150°/second. It is hoped that the data obtained by this faster means will be directly applicable to the determination of the thermal conductivity of the material as a function of temperature when used in the formula:

$$(\alpha)^{*}_{torch}(\rho c)^{*}_{T,\dot{T}} = (K)_{T,\dot{T}} \qquad (29)$$

Since the $(\rho c)^*$ test can be conducted at variable power levels and hence at variable heating rates it is expected that the method will provide rough estimates of the reaction rates as a function of the temperature and the rate of heating in the ablating laminate.

Recognizing that a $(\rho c)^*$ heating rate of 6-7°C per second is not directly comparable with an ablation rate of 150°C per second, the thermal conductivity was calculated as a matter of curiosity. This questionable result is shown also in Figure 6. This curve indicates that the thermal conductivity may be reduced at first as the material enters the ablation zone, and then increase as pyrolysis becomes more advanced. This is possible in view of the carbonization of the organic residues and of the increase of conductivity of glass by ionization at higher temperatures.

Heating Rates versus Reaction Rates

In comparing the curves obtained on the phenolic glass-cloth laminate in the Differential Thermal Analyzer at 1/6°C/second, the $(\rho c)^*$ test at 6-7°C/second and the ablation test at 150°C/second, it becomes apparent that the DTA shows the effects of a reaction at low temperatures which is not apparent in the higher speed tests. Also, the temperature of the second peak in the DTA test does not correlate with the temperature at which the big changes occurred in the faster tests. Therefore, these preliminary measurements indicate that the chemical reactions are rate sensitive.

High Speed Photography of Ablating Laminate

There is considerable speculation on the behavior of the molten glass in the ablation of a glass-fiber reinforced phenolic plastic. Accordingly, it was of interest to take moving pictures of the ablating surface. This was done at a speed of 750 frames a second.

Figure 12 shows two frames selected from the motion picture. The unguarded ablating surface was being maintained in a relatively flat condition. The ablation rate in this test was about 0.01 cm/sec. Beads of molten glass clung to the shoulder of the right circular cylindrical specimen. The frontal surface of the specimen appeared to be lumpy. It is questionable whether these represent isolated droplets of glass or alternately a film of glass containing gas pockets or bubbles. The second frame shows a streak of incandescent matter moving in the gas stream away from the frontal surface. The streak may represent a filament of molten material or alternatively droplet of molten material moving at a very high

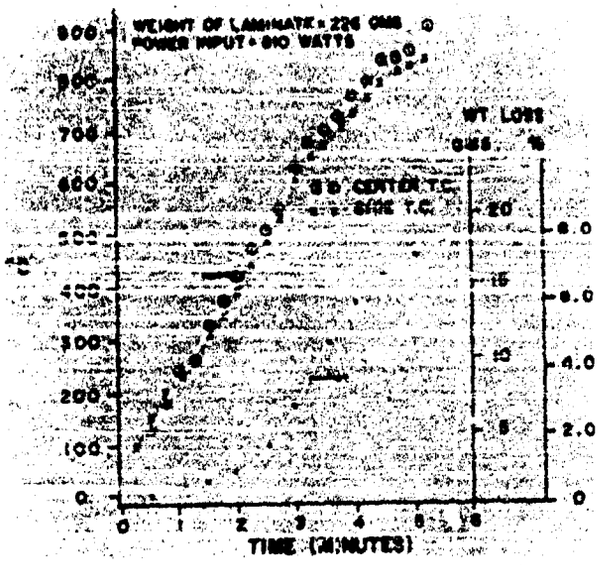

Figure 11 - Mass-transfer and power balance during steady-state ablation

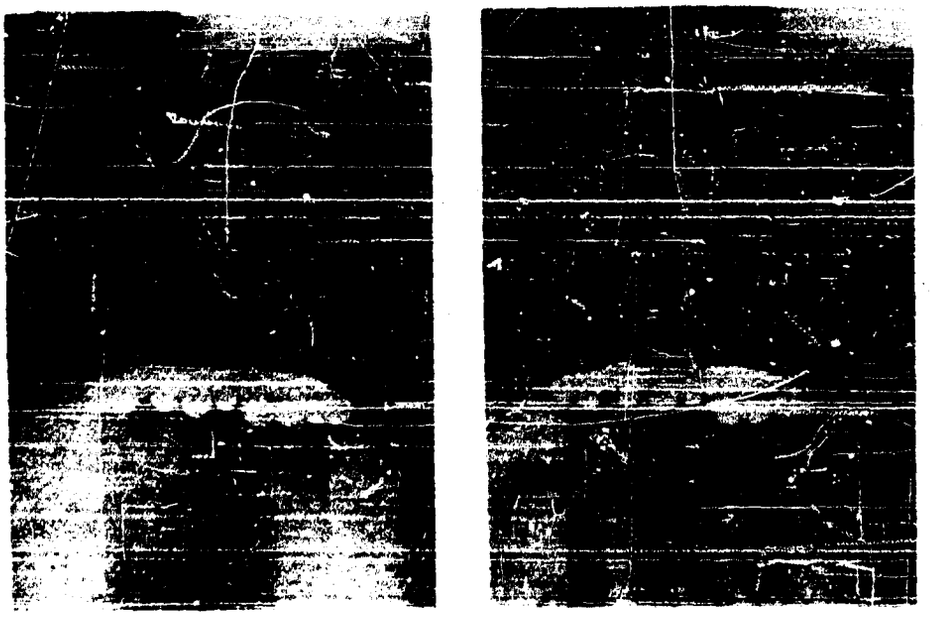

Figure 12 - Phenolic glass-cloth laminate in oxyacetylene flame

velocity so that the 700 frame/second camera did not stop it. These streaks were found at frequent intervals in the film, occupying one frame only.

Figures 13, 14 and 15 show six consecutive frames of the film in which a droplet at the shoulder of the specimen is breaking away. The droplet has left a dark spot at the spot it had occupied, which may be taken to indicate that the droplets are hollow. This is supported by the observation that hollow droplets of frozen glass were found around the test equipment. The formation of such droplets is not impossible in view of the considerable surface tension which must exist in the glass at this temperature as will be discussed later.

The droplet is still attached to the site by a filament of molten glass. In very rapid succession the filament elongates, develops two distinct nodes between the big droplet and the site, and in the next frame is converted to two small droplets. This conversion of a filament with nodes to two droplets was completed in 1/700 of a second. It would seem, therefore, that the surface tension in the glass at this temperature (about 1800°C) is very strong. The little droplets then accelerated faster than the large droplet and won the race off the screen. The diameter of the specimen was 3/4 inches. The large droplet appears to be about 0.08 inches in diameter. The small droplets appear to be about 0.02 inches in diameter.

In view of some of the questions raised by these photographs, it is intended to investigate these phenomena at higher film speeds. Some modifications of the theories of melting ablation (1), (2), (3), may be required to adapt them to the conditions encountered in pyrolytic ablation.

Possible Future Experiments

The phenolics and other highly cross-linked thermosetting laminating resins represent an important and interesting class of resins in connection with applications wherein the reinforced plastic is in contact with hot gases. Further investigation of the mechanisms of degradation at high heating rates of these resins seems to be indicated. In view of the complicated and somewhat mysterious structure of these resins, and remembering the ever-present possibility of interactions with fillers and fibers, it would seem to be in order to undertake an investigation of the fragments emitted by the materials as a function of time, temperature and composition. The use of gas sampling techniques together with mass-spectrometry, infra-red analysis, chromatography, X-ray diffraction and chemical

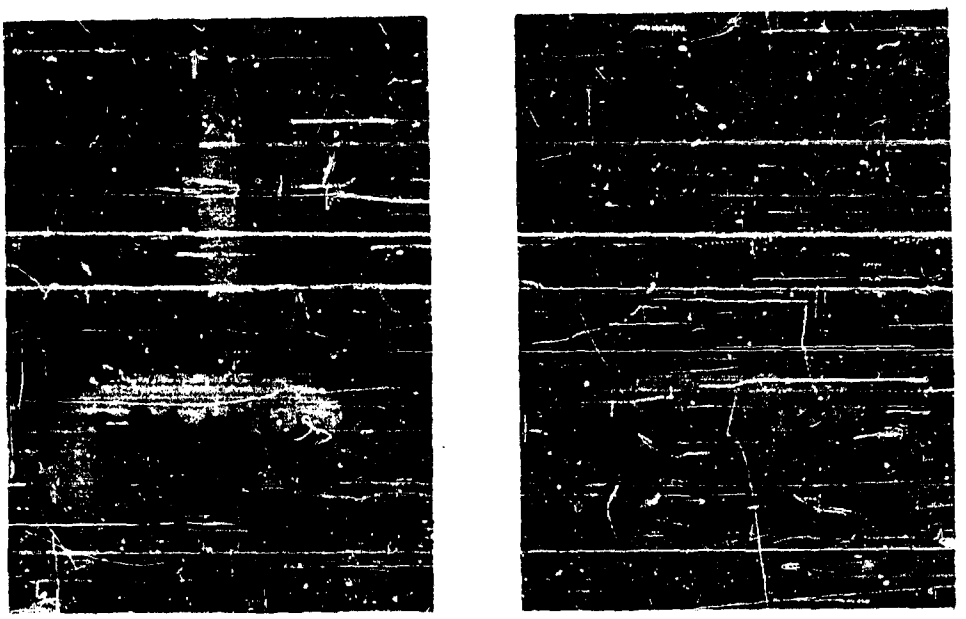

Figure 13 - Droplet formation during ablation of a phenolic glass-cloth laminate

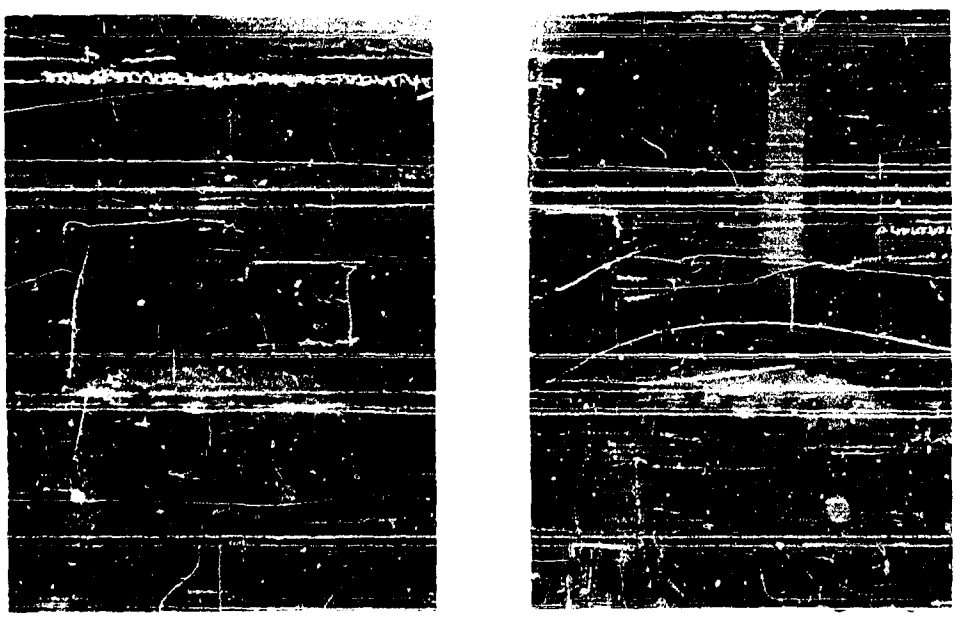

Figure 14 - Droplet formation during ablation of a phenolic glass-cloth laminate

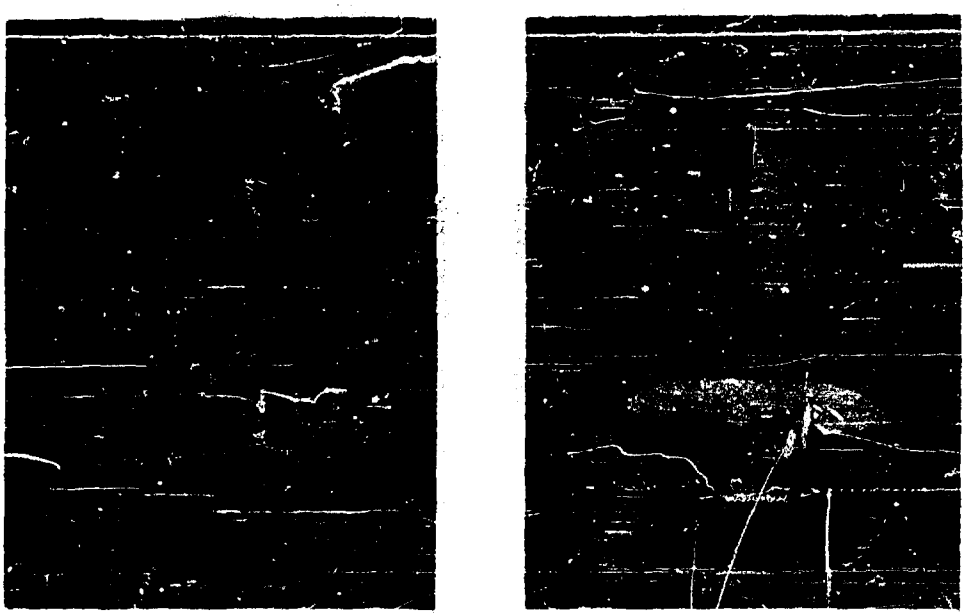

Figure 15 - Droplet formation during ablation of a phenolic glass-cloth laminate

analysis of fractions should give a clearer insight into the original structure, mode of fragmentation and residues of the structure under heat.

Having identified the species of degradation products and having estimated their proportions as a function of (T) and (T), we should then be closer to being able to predict the behavior of these materials in contact with molten glass layers, exhaust flames and aerodynamic boundary layers.

With reference to the motion of molten layers and their effect on the heat-transfer rate, it is to be noted that the guard-ring ablation tests so far have employed chemical flames. Much higher temperatures and a variety of gas compositions can be generated in high-intensity arc plasmas. Future work should include the substitution of a jet of hot gas mixture, or of hot air, for the chemical flame employed in these tests.

It is also to be noted that the flame is subsonic. For this reason the shear stress to which the surface is subjected is not high. The guard-ring ablation test should be extended to apply high wind-shear stresses to the surface.

It is further to be noted that the body forces in this test are limited to one gravity. From the high speed photographs and the condition of the specimens after a test there is no evidence that this weak body force had any appreciable effect on the motion of the molten layers. The full simulation of conjoint wind-shear and body stresses under a large heat flux can of course be accomplished employing large whirling-arm devices. Perhaps a simpler beginning in this direction could be undertaken if the right-circular cylindrical specimen were to be spun on its axis within the guard-ring.

Finally, it is to be noted that the ambient pressure in the hot gases on the test surface in the present test are about one atmosphere. As noted in connection with the theory of pyrolytic ablation, (P_w) can have a significant effect on the chemical kinetics and gas dynamics within the ablating zone. It was also noted in Figure 2 that the ambient pressure on an ablating surface can range from 0.01 atmospheres at 100,000 ft. altitude to 100.0 atmospheres, or higher, in a rocket motor casing. Perhaps the simulation of these conditions during ablation could be accomplished by the enclosure of the test specimen and heat source in a pressurized chamber.

BIBLIOGRAPHY

(1) Journal of Aero. Sci., Jan. 1958, pp. 29-32, "The Hydrodynamics and Heat Conduction of a Melting Surface," Sutton, George W.

(2) AVCO Research Laboratory Research Report 38, November, 1958, "A Theory for the Ablation of Glassy Materials," Bethe, Hans A.

(3) AVCO Research Laboratory Research Report 34, August, 1958, "On the Instability Theory of the Soft or Melted Surface of an Ablating Body when Entering the Atmosphere," Feldman, Saul.

(4) NACA Tech. Note 3404, March, 1955, "The Compressible Boundary Layer with Fluid Injection," Low, G. M.

(5) Mass-Transfer Cooling Symposium, Rand Corp., June, 1957, including unclassified papers by Baron, J. R., Eckert, E. R. G., Sziklas, E. A., Rubesin, M. W., Leadon, B. M., and van Driest, E. R.

(6) Proceedings of the First and Second Conferences on Carbon, p. 93, 1956, Winslow, F. H., Baker, W. O., Yager, W. A.

(7) J. Polymer Science, 23, 315, 1956, Winslow, F. H., and Matieyek, W.

(8) J. Polymer Science, 16, 101, 1955, Winslow, F. H., Baker, W. O., Paper, N. K., and Matieyek, W.

(9) J. Polymer Science, 9, 133, 1952, Madorsky, S. L.

(10) Modern Plastics, June, 1958, Grund Fest, I. J., Shenker, L. H.

(11) Trans. Faraday Soc., 32, 336-345, 1936, Megson, N. J. L.

(12) J. Chemical Soc., 125, 192, 1924, Lessing and Banks

(13) Science Prog. 37, 657, 1949, Kipling, J. J.

(14) Nature, 180, 1190, 1957, Watt, J. D., and Franklin, R. E.

(15) Thermodynamic Properties of the Elements, A. C. S., 1956, Stull and Sinke

(16) Proc. Roy. Soc. London, A209, 196, 1951, Franklin, R. E.

(17) American Institute of Physics Handbook, 1957.

(18) McGraw Hill Book Co., "Theory of Rate Processes," Glasstone, Laidler and Eyring.

(19) "Conduction of Heat in Solids", Oxford Press, 1948, Carslaw and Jaeger.

(20) Unpublished work by J. M. Kendall of the Naval Ordnance Laboratory.

(21) NAVORD Report 6210, "The thermal Decomposition of Polymers, Part I - Thermal Differential Analysis as a Tool," Anderson, Hugh C.

(22) Anal. Chem. 27, 1102, 1955, Gordon, S., and Campbell, C.

DEVELOPMENTS IN REINFORCED PLASTICS AT THE NAVAL ORDNANCE LABORATORY

I. Silver
P. W. Erickson
F. R. Barnet
H. A. Perry
U. S. Naval Ordnance Laboratory
White Oak, Silver Spring, Maryland

INTRODUCTION

For many years now glass reinforced plastics have been finding wide use as primary plastics structures in naval ordnance and other military applications. This wide acceptance by material design engineers is due in part to the inherent high strengths in glass reinforced plastics and confidence in the quality and reproducibility of this class of materials.

This situation did not prevail ten years ago and the deficiencies in glass reinforced plastics were such as to cast doubt on their acceptance in critical structural naval ordnance applications. At the Naval Ordnance Laboratory, it was realized that considerably more work was necessary to upgrade the strength, to improve the heat and moisture resistance of glass reinforced plastics, and to advance the status of assembly techniques, quality control, and test methods, as well as to accumulate an adequate body of engineering performance data.

Considerable progress towards these goals has been made by both industrial and military laboratories. This paper describes in summary form the results of the experimental work carried out at the Naval Ordnance Laboratory in the following areas of interest:

A. The upgrading of the strength and moisture resistance properties of glass reinforced plastics through the development and application of universal type glass fiber finishes.

B. The development of a test method to characterize the properties of glass roving for use in filament wound structures.

C. The study of the engineering properties of external pressure vessels as a basis for the design of such vessels as housings in underwater applications.

A. Chemical Finishes for Glass Fibers

There are potentially many applications in naval ordnance where reinforced plastics are the ideal materials of construction. This is, however, conditioned on their ability to retain for relatively long periods of time a substantial fraction of their inherent strength properties in a moist environment. The problem of wet strength retention in reinforced plastics is known to be dependent on the adhesive bond between the cured resin and the glass fiber surface. At the start of this investigation, the use of fiberglass reinforced plastics in structural items for naval ordnance was severely limited in applications requiring long time immersion in sea water. This limitation still exists but to a lesser degree.

The main objective of this research was the development of glass fiber reinforced plastics with improved strengths, both dry and after prolonged exposure to moisture. The approach to the problem was to devise novel treatments (finishes) for the glass fiber which would lead to improved bonding between the fibers and the cured resin.

A total of 38 organo-chlorosilanes, most of which were synthesized at this Laboratory, were applied to glass fabric and evaluated for their effect on the dry and wet strength properties of laminates made with several commonly used thermosetting resins. These finishes were selected on the premise that appropriate chemical functional groups firmly fixed to the glass surface could partake in the curing reaction of the resin and in this manner bridge the glass-resin interface with chemical bonds. Many of the finishes were designed to contain more than one type of functional group so that the finish could be effective with a variety of thermosetting resin types.

The mechanism by which chemical finishes for glass fibers lead to better strength properties is not too well understood, but there is much evidence that appropriate chemical functional groups in the finish are essential in securing laminates with superior strength properties. The reason for selecting chlorosilanes as a vehicle to place chemical functional groups on the glass was that these were known to react with trace amounts of absorbed water, which

is ever present on glass surfaces. Chlorosilanes react with this absorbed water with the evolution of hydrogen chloride and in the process become attached in a manner suggesting chemical bonding, since they can be removed only by strong hot alkali or abrasion. Thus, the problem of the bonding of the finish to the glass was simplified by selecting chlorosilanes as the vehicle for introducing different functional groups into these finishes.

The new finish reagents, which are sensitive to moisture, were dissolved in dry xylene at a concentration of about 1-2%. The treatment consisted of immersing glass fabric in these solutions for varying periods of time and temperature. The various finishes and their methods of application have been the subject of several reports (1. 2, 3, 4, 5 and 6).

The finish designated NOL-24, which is the product from the reaction of allyltrichlorosilane and resorcinol, was selected for further study and development. This finish was found to be universal in character, since it was effective with many resin systems. Polyester, epoxy, phenolic and melamine laminates made with NOL-24 treated cloth give not only improved dry flexural strength properties but superior wet strength retention, in some cases up to 100%.

As a result of the good laminate strength data obtained in the laboratory phase of this study, a commercial finisher became interested in the NOL-24 treatment. With the cooperation of NOL, this processor carried out several treatments on a pilot scale. Treated fabric became available in 100 yard quantities, some of which was evaluated at this Laboratory. Table I shows ultimate flexural strength data from laminates made with fabric from the first four pilot treatments. Included for comparison are strength values from laminates with other commercial finishes.

The laminates in Table I were made in a similar manner and had resin contents in the range 29 to 34% (4). The averages shown with NOL-24 laminates with polyester, epoxy and phenolic resins are based on 27, 24 and 21 laminates, respectively, and include up to four different pilot treatments. Ultimate flexural strength averages of over 100,000 were obtained for all three resin systems under dry conditions. Averages of 80,000, 98,000 and 100,000 psi were obtained after a two-hour boiling water conditioning with polyester, epoxy and phenolic resins, respectively. These data show that NOL-24 yielded higher flexural strengths than the best commercial finish, both dry and wet, respectively, of 20% and 11% with the polyester resin, 16% and 22% with the epoxy resin, and 24% and 28% with the phenolic resin.

TABLE I

ULTIMATE FLEXURAL STRENGTH FROM LAMINATES USING 181 STYLE GLASS FABRIC WITH VARIOUS FINISHES

	Paraplex P-43		Epon 828 with CL		BV 17085	
Finish	Dry	Wet	Dry	Wet	Dry	Wet
112	73,000	39,000	88,000	73,000	52,000	30,000
Garan	66,000	74,000	49,000	51,000	45,000	47,000
136	69,000	73,000	49,000	53,000	36,000	28,000
Volan	86,000	72,000	93,000	80,000	84,000	78,000
NOL-24	103,000	80,000	108,000	98,000	104,000	100,000

TABLE II

VARIATION OF COLLAPSING PRESSURE RESISTANCE AND EFFECTIVE MODULUS WITH INCREASING TUBE DIAMETER

Tube I. D. inches	Collapsing Pressure psi	Effective Modulus psi
3.06	355	3.90×10^6
6.02	350	3.85×10^6
9.86	350	3.81×10^6

Each value is an average of three tests.

$L/D = 2.90$ $t/D = 0.025$

Tubes reinforced with 181-Volan glass fabric and bonded with a general purpose polyester resin mixture of 80% rigid resin, 15% flexible resin and 5% styrene.

A more recent evaluation was carried out at this Laboratory in connection with a survey to determine whether the present specification for strength properties of reinforced plastic laminates was realistic in terms of what could be achieved with the new improved fabric finishes. Another object of this evaluation was to determine the effect of resin content over the range 35 ± 5% on various strength properties of the laminate. This study was carried out with 181 style fabric having A-1100, A-172 (Silicones Div., Union Carbide Co.) and NOL-24 finishes and using polyester, epoxy, phenolic and melamine resins. The reason for selecting A-1100 and A-172 finishes for this study was that these were more recently developed finishes which were showing promise in a rather widespread evaluation by industry and the military agencies. Ultimate flexural strengths were obtained, as well as a limited amount of tensile and compressive strength data (6).

The ultimate flexural strength data are shown in Figures 1 through 4. The laminate strength data in Fig. 1 were obtained with an epoxy resin cured with metaphenylenediamine (CL). The results show that flexural strength is not particularly dependent upon resin content in the range 31.1 to 39.6% and that the NOL-24 laminate data are about 15% above those from the A-1100 laminates.

Laminate flexural strength data for polyester laminates made from fabric with A-172 and NOL-24 finishes are shown in Fig. 2. The results show that with the A-172 finish the strength properties are not affected over the range of resin content 31.1 to 38.8%. Resin content had a slight effect on the dry strength with the NOL-24 finish but none on the wet strength. The NOL-24 laminate dry strengths were 12 to 15% higher than those from the A-172 laminates. The NOL-24 laminate wet strengths were about the same as for the A-172 laminates.

Similar data for phenolic laminates made with A-1100 and NOL-24 finished fabrics are shown in Fig. 3. Resin content seems to be unimportant over the range 26.6 to 37.1% with the A-1100 finish. Best strengths are obtained with the NOL-24 laminates in the 29 to 35% range. With both finishes, 100% (or better) wet strength retention is obtained in 9 out of 12 cases. The present specification requires values of 50,000 and 45,000 psi dry and wet, respectively.

Flexural strengths from melamine laminates made with A-1100 and NOL-24 finished fabric are shown in Fig. 4. Resin content, as this relates to laminate strength, appears to be unimportant over the range 29.1 to 39.0%. The dry and wet strengths from the

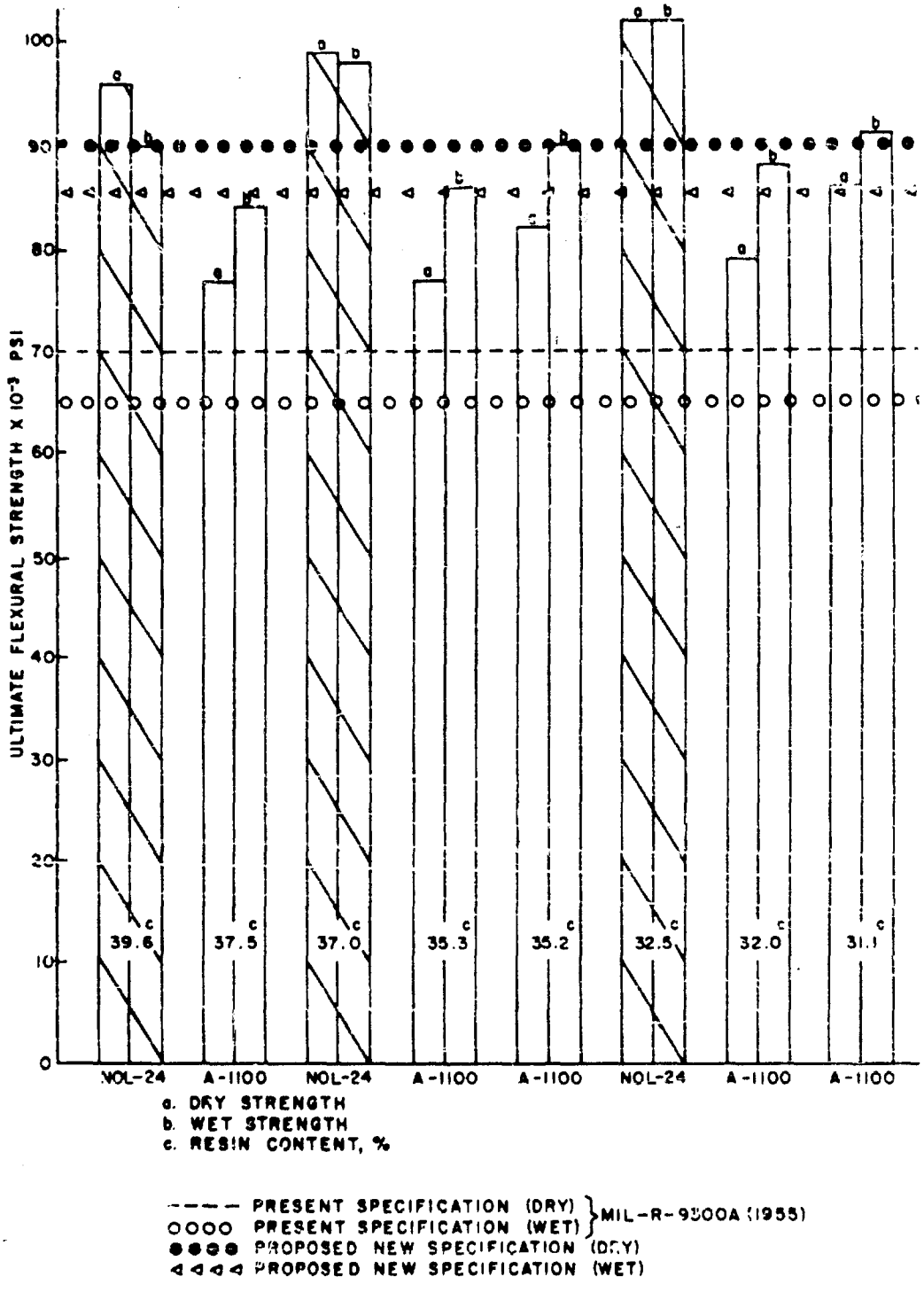

Figure 1 - Ultimate flexural strength for laminates with A-1100 and NOL-24 finishes using Epon 828 and CL

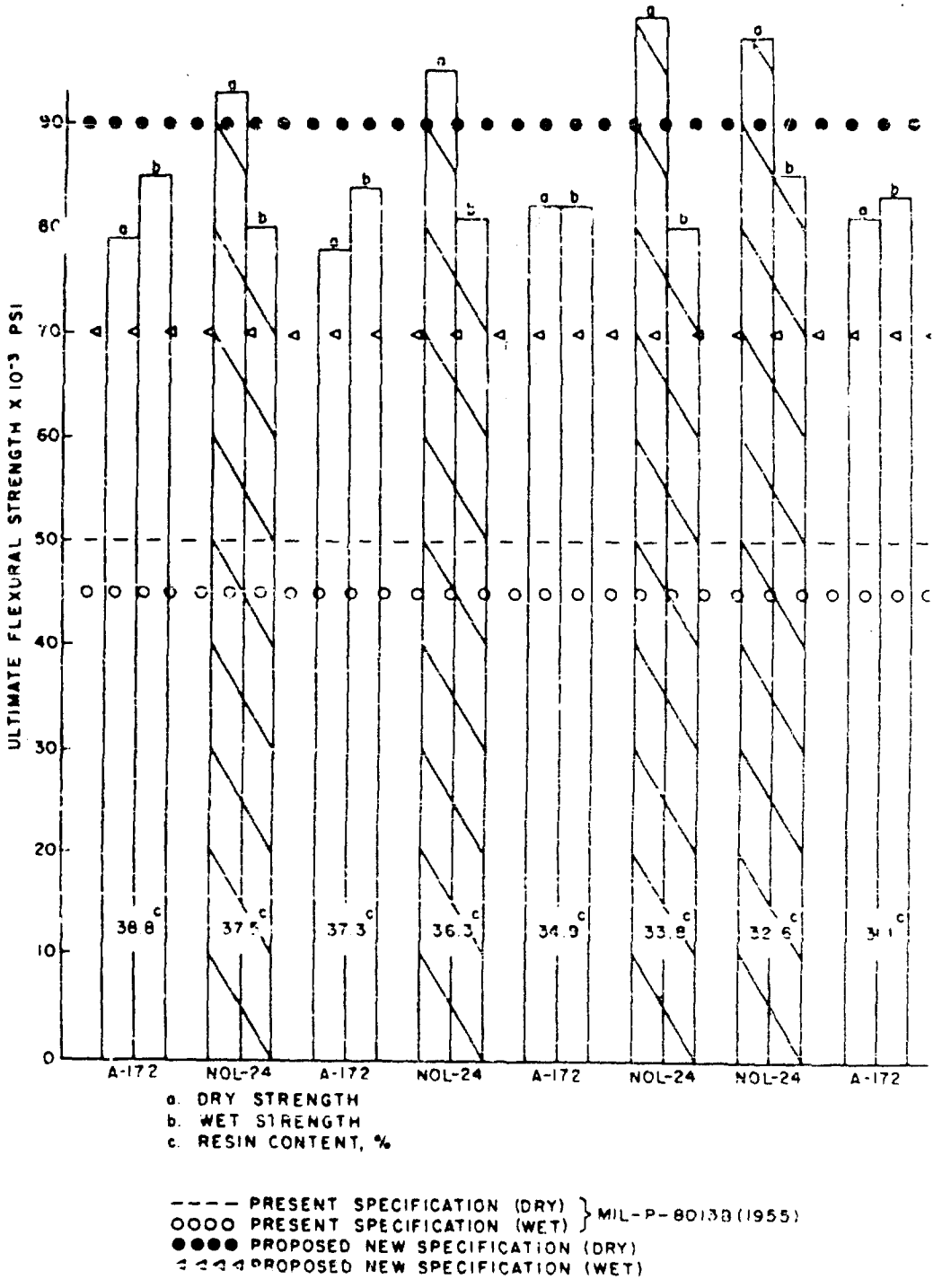

Figure 2 - Ultimate flexural strength for laminates with A-172 and NOL-24 finishes using Paraplex P-43 polyester resin

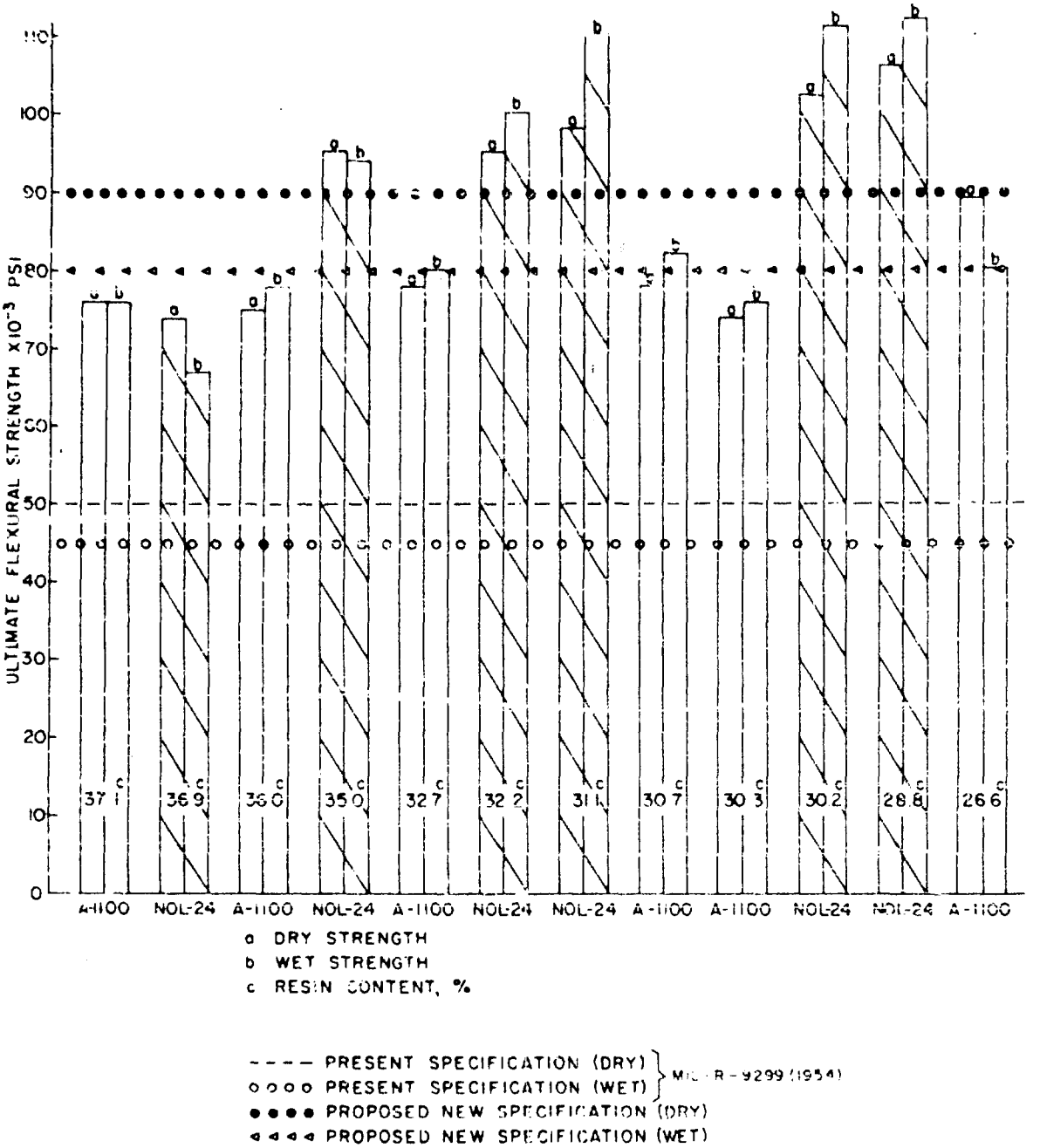

Figure 3 - Ultimate flexural strength for laminates with A-1100 and NOL-24 finishes using BLL 3085 phenolic resin

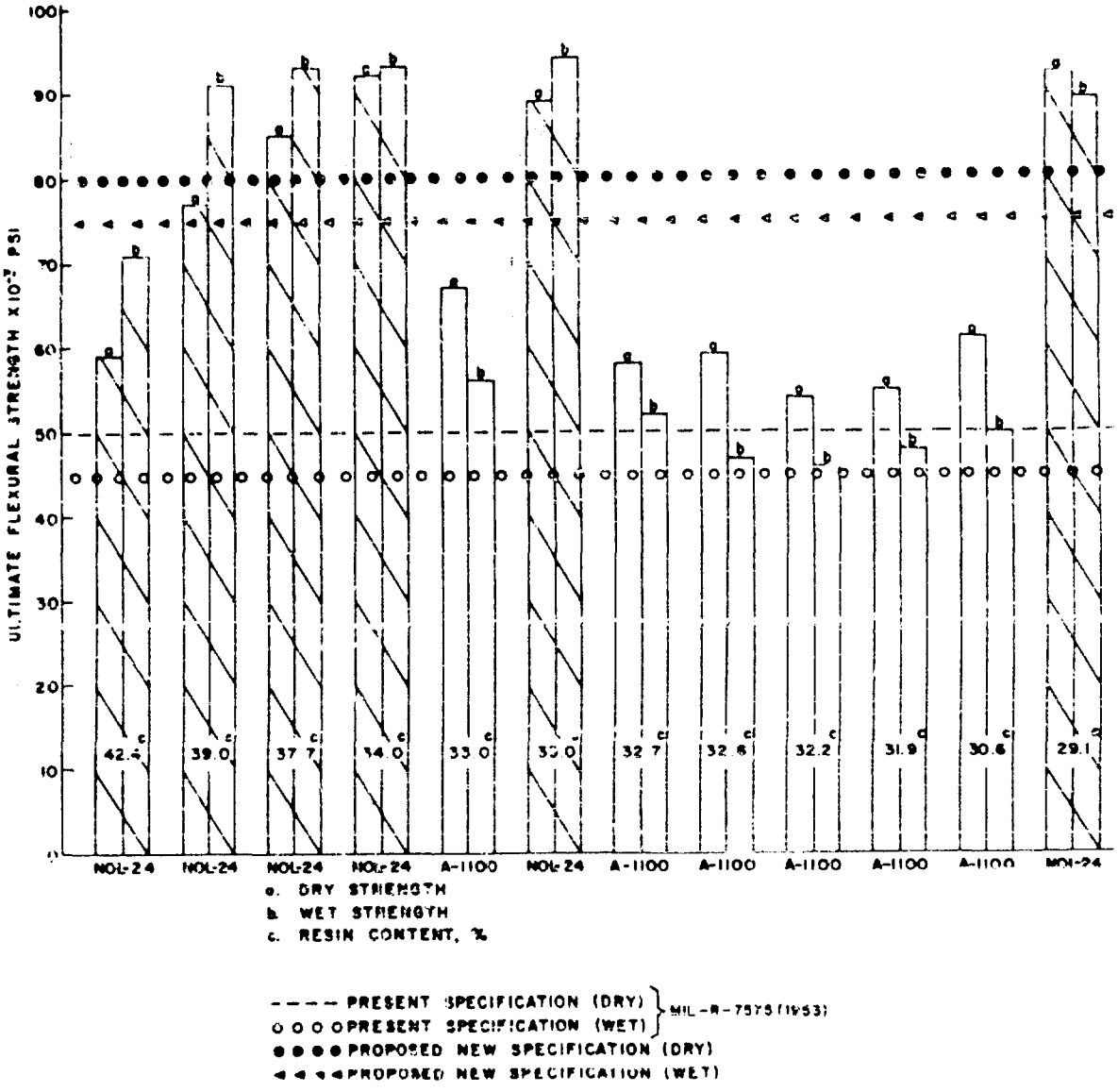

Figure 4 - Ultimate flexural strength for laminates with A-1100 and NOL-24 finishes using cymel 405 melamine resin

NOL-24 laminates are at least 50% higher than those from the A-1100 laminates. Wet strength retention with the NOL-24 finish is 100% or better in five out of six cases.

It is apparent from these data that NOL-24, A-1100 and A-172 produce laminates with substantially higher strengths than the requirements set forth in current specifications for the several types of laminating resins discussed here. In most cases, NOL-24 gave strengths over a range of resin contents higher than those obtained with the other two finishes. In view of this, it is proposed in Fig. 1-4 that the specification limits be raised to provide for a new class of quality finished cloth to reflect the higher dry and wet strengths possible with the new commercial and experimental finishes. The proposed values are tentative and are only offered as a basis for discussion leading to the revision of present specifications so that the full potential of these new and better material combinations can become available to the design engineer.

This study at NOL of chemical treatments for glass fibers not only resulted in the development of the universal type chemical finish, NOL-24, but it also stimulated this type of work in industry. As a result, considerable work in this area has been done by at least three large industrial concerns. While the work at NOL has not proved that the resin becomes chemically bonded to the finish, much indirect evidence has been accumulated in favor of the chemical theory of finishes.

It is believed that finishes to be effective must not only fulfill the chemical requirements with respect to functional groups but must also be capable of performing several other functions. The finish should provide a polymeric sheath to protect the fiber against strength degradation by self-abrasion and moisture attack; it should result in better wetting of the fiber with the elimination of voids and consequent improvement in moisture resistance; and it should act as a deformable layer capable of accommodating local stresses along the fiber which are set up in curing and in temperature cycling.

Further work on finishes is needed to understand more fully the mechanism by which certain finishes lead to better dry and wet strength laminate properties. More needs to be known about the effects of thickness and physical characteristics of the finish. Finishes in the past have been designed largely for improvement of laminate wet strength properties. Perhaps it is time to begin the planning of new finishes designed to resist the effects of high temperature on laminates. A better knowledge of the mechanism of bonding is urgently needed in the design of the finishes of the future.

B. The NOL Ring Test Method for the Evaluation of Chemical Finishes on Glass Roving

The subject of glass roving reinforced plastics is currently of growing interest to both industry and several of the defense agencies. Much effort is being expended with these materials in developing means of economical machine fabrication of cylindrical and spherical structures and the evaluation of the performance characteristics of these products.

In the area of reinforced plastics, glass roving will undoubtedly become steadily more important as a reinforcement material. One reason for this is cost, as compared with that of woven glass fabric. In addition, glass fiber in roving form offers the reinforced plastics engineer a means of controlling directional strength properties, which is not possible in designing with glass fabric or mat.

A major obstacle in the development of this class of structural material has been the problem of testing the strength properties. The design data usually needed, such as flexural, compressive, shear and tensile strengths, based on standard tests, have not been available to the engineer. As a result, test specimens in many cases have been the actual prototypes which are usually expensive to fabricate and, perhaps, give information which is pertinent only to a single end use. This also often leads to over-design, thereby losing much of the possible weight saving advantage which is critical in many applications, such as those involving missiles.

As an extension of the work with glass fabric finishes, a study of the effect of various chemical finishes on glass roving, as this related to the strength properties of the reinforced plastic, was undertaken. It soon became apparent that test methods were very inadequate, as compared to those for fabric reinforced plastics. A literature survey on the subject of test methods for glass roving reinforced plastics was made (7). It was concluded from this survey that very little progress in this area had been made. The main difficulty with all the test methods tried had been the problem of fabrication of uniform and reproducible test specimens. In order, therefore, to evaluate roving treatments, the Laboratory undertook the additional problem of developing more reliable test methods for determining various strength properties of parallel fiber reinforced plastics.

The NOL Ring Test Method is built around a ring which can be easily and inexpensively made with a high degree of uniformity and reproducibility. This ring has an outside diameter of 6" and is

1/4" wide and 1/8" thick. It is fabricated by drawing 8-end roving through a resin bath onto a split circular mold under controlled conditions of temperature, tension, and angle of wind. Liquid epoxy and polyester resins are used with equal ease. Up to six rings can be consecutively made with a single catalyzed batch of these resins using only 250 grams of resin. Resin content can be varied from 15 to 30%. In addition, this type of specimen has the advantage that it is more closely related geometrically to shapes that are most likely in practice to be fabricated, such as tubes and spheres.

Figure 5 is a schematic diagram of the functioning parts. The entire apparatus consists of three parts; the tensioning device, the resin impregnation bath, and the mechanism for drawing and placing in a uniform fashion the impregnated roving into the mold. The details of the fabrication of a ring are discussed in references 7 and 8.

All the important strength properties for design purposes may be obtained from the ring or segments of it. Ultimate flexural strength is obtained from segments of the ring, which are 3" long. Horizontal shear strength is obtained from segments measuring 0.6" to 0.8" long. Tensile strength can be obtained on the entire ring, which is hydraulically pressurized internally between parallel plates to failure. Compressive strength could be similarly obtained by pressurizing the ring externally to failure. Flexural test specimens are shown in Fig. 6, item 1, and horizontal shear test specimens are shown in item 2 of the same figure. A typical horizontal shear failure is shown in Fig. 7.

This Laboratory was primarily interested in developing the test method for use in the evaluation of chemical finishes (and sizes) on roving as these relate to the various strength properties of the reinforced plastic. The tests have now been brought to the point that this has been accomplished. The ultimate flexural strength test and the horizontal shear strength test can both be used for this purpose.

Ultimate flexural strength data are shown in Fig. 8 for rings with various roving surface treatments, which were made with an epoxy resin cured with metaphenylenediamine. It should be noted that testing under standard (dry) condition does not clearly differentiate between treatments. It was found with this resin system that boiling the specimens up to 12 hours before testing was necessary to bring out the differences shown. Horizontal shear strength data from duplicate rings of those shown in Fig. 8 are shown in Fig. 9. Again it is seen that the specimens have to be severely boil conditioned

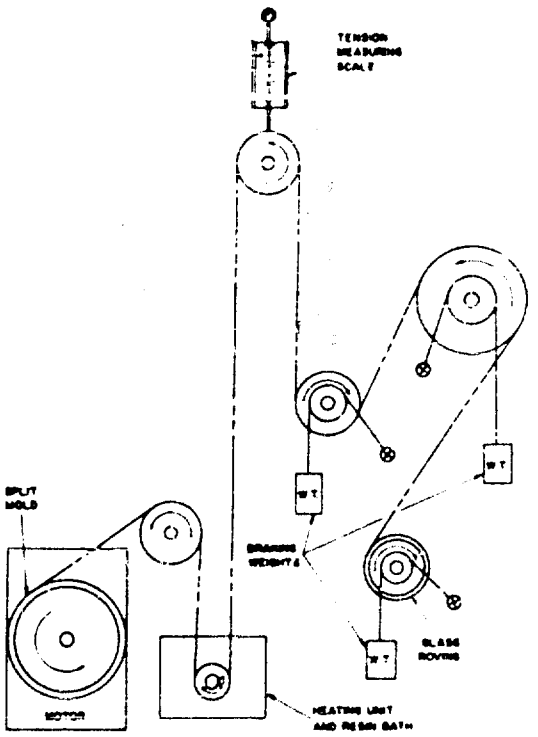

Figure 5 - Schematic diagram of functioning parts of winder

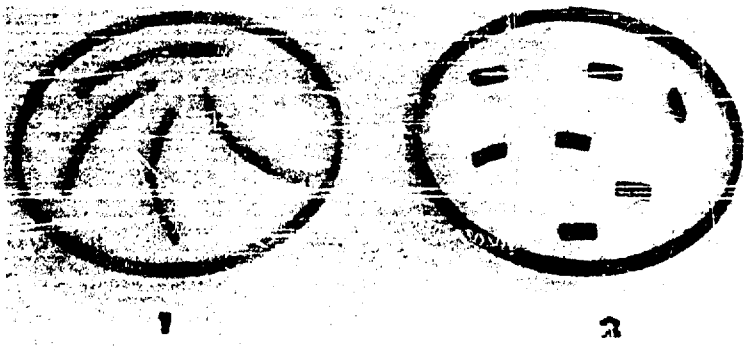

Figure 6 - Flexural and horizontal shear test specimens

Figure 7 - Typical horizontal shear failure; end view

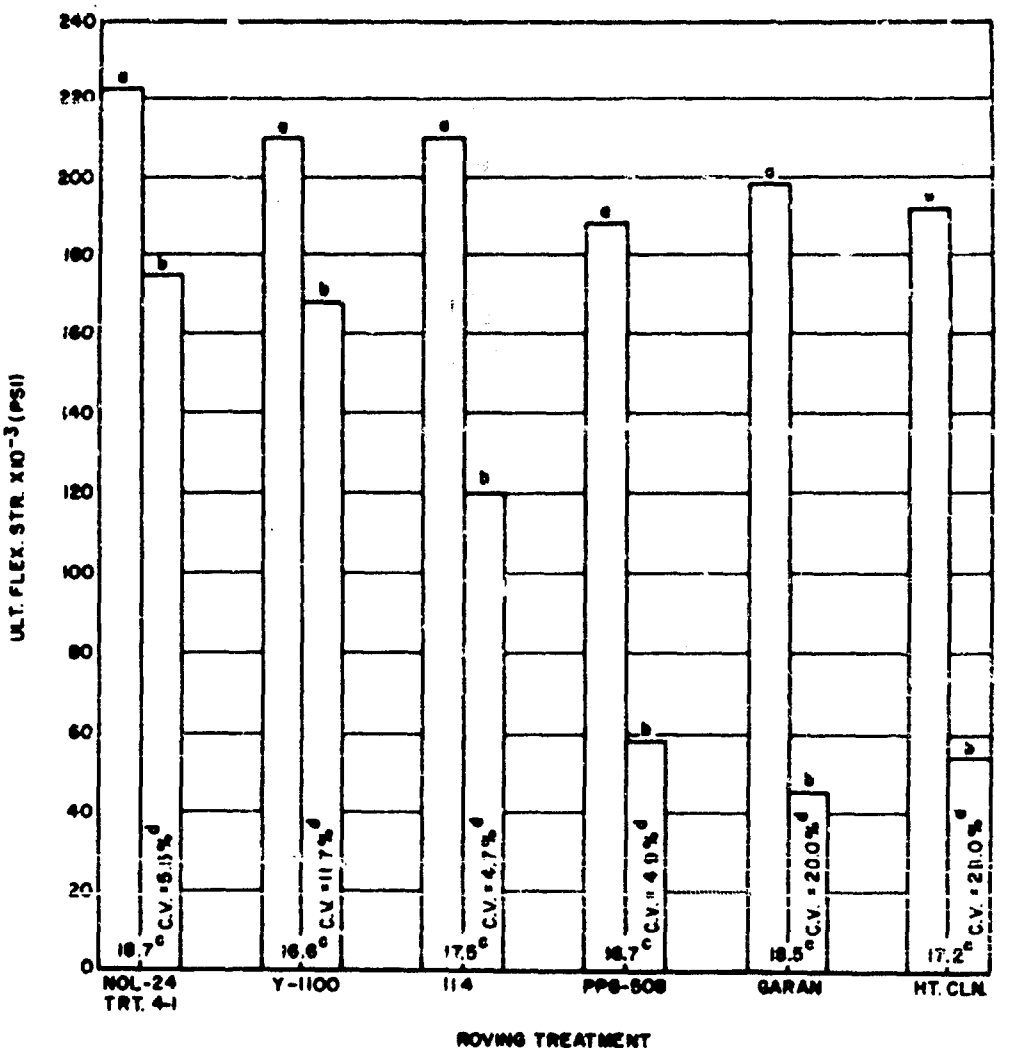

a. Dry strength; average of 4 specimens from 2 rings

b. Strength after 12 hours in boiling water; average of 6 specimens from same 2 rings

c. Resin content, %

d. C.V. = coefficient of variation

Figure 8 - Flexural strength from rings with m-phenylenediamine-cured Epon 828 resin using various roving treatments

to bring out differences due to finishes. It should be noted that no wet shear values are reported for several of the roving treatments in Fig. 9. Serious degradations occur in these specimens on boiling and failure by shear does not result. The coefficients of variation shown indicate that both methods have fair to good reliability. The coefficients of variation tend to increase when the values get low.

Ultimate flexural strength data with a polyester resin are shown in Fig. 10. A two-hour boiling water conditioning is sufficient here to differentiate between roving treatments. The relative order of values is what would have been expected from fabric laminates. Horizontal shear strength data on duplicate rings for those shown in Fig. 10 are shown in Fig. 11. Again it is seen that the specimens having inferior roving surface treatments fail to shear. The coefficients of variation indicate that both methods have sufficient reliability to be useful.

This Laboratory has designed a test fixture to obtain tensile data on the entire ring. It is expected that these data will also be available in the near future. There are at the moment no plans to design a similar fixture to get compressive strength data, but this would be highly desirable, since many end items of interest are external pressure vessels.

The NOL Ring Test Method is being proposed tentatively as a standard test method for specifications use. Perhaps more work needs to be done on the method of making rings and the manner of testing. At this time, however, it is possible to make rings uniformly and reproducibly, and for this Laboratory's purpose it has been able to differentiate very clearly between glass roving surface treatments.

C. Reinforced Plastics in the Construction of External Pressure Vessels

Reinforced plastics are structural materials which are suitable for the fabrication of mine cases and other underwater housings. They are non-magnetic with high electrical resistivities and are corrosion resistant, lightweight and utilize non-critical materials. When they were first considered for this use, their creep and fatigue characteristics under long-term pressure conditions were unknown. Therefore, it was necessary to develop basic data on the selection of materials and on the design of pressure vessels prior to their acceptance for the fabrication of mine cases.

A half-scale model program was initiated to provide these data with emphasis on the submarine launched mine case Mk 57 (9).

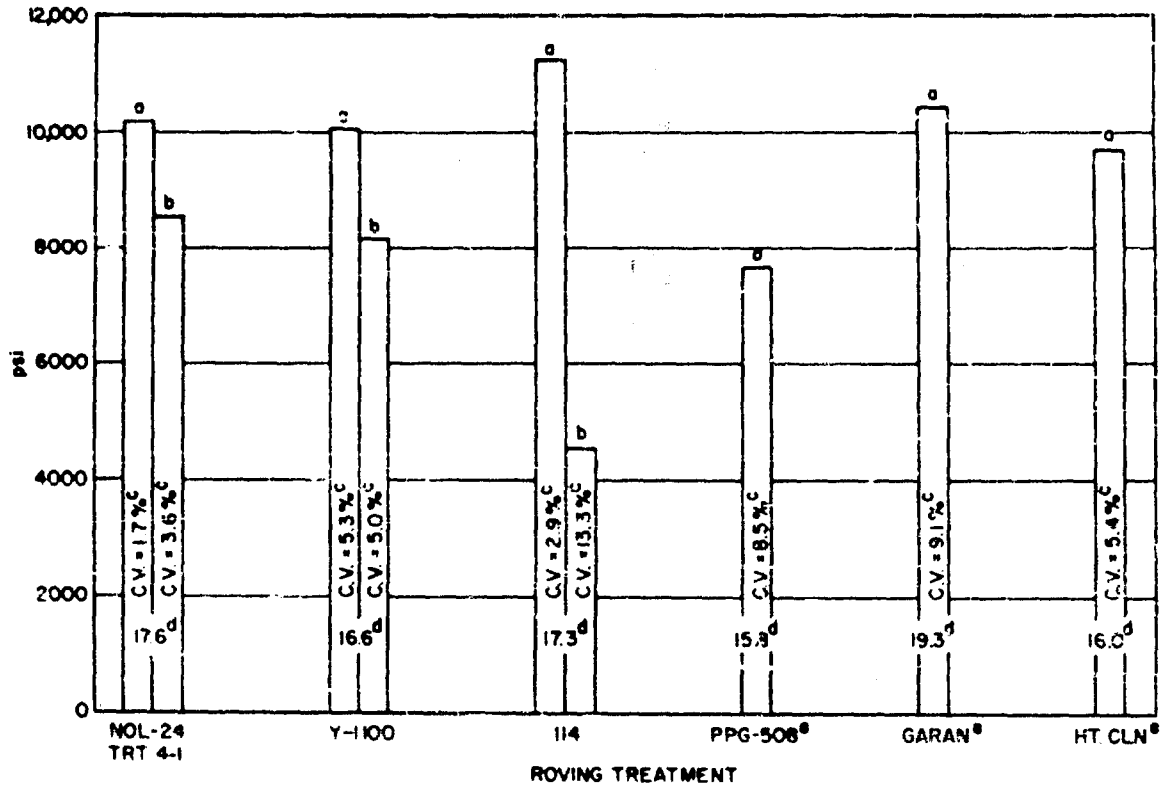

a. Dry strength, average of 8 specimens

b. Strength after 6 hours boiling water conditioning; average of 8 specimens

c. C.V. = coefficient of variation

d. Resin content, %

e. Specimens failed to shear after boiling water conditioning

Figure 9 - Horizontal shear strength from rings with m-phenylenediamine-cured Epon 828 resin using various roving treatments

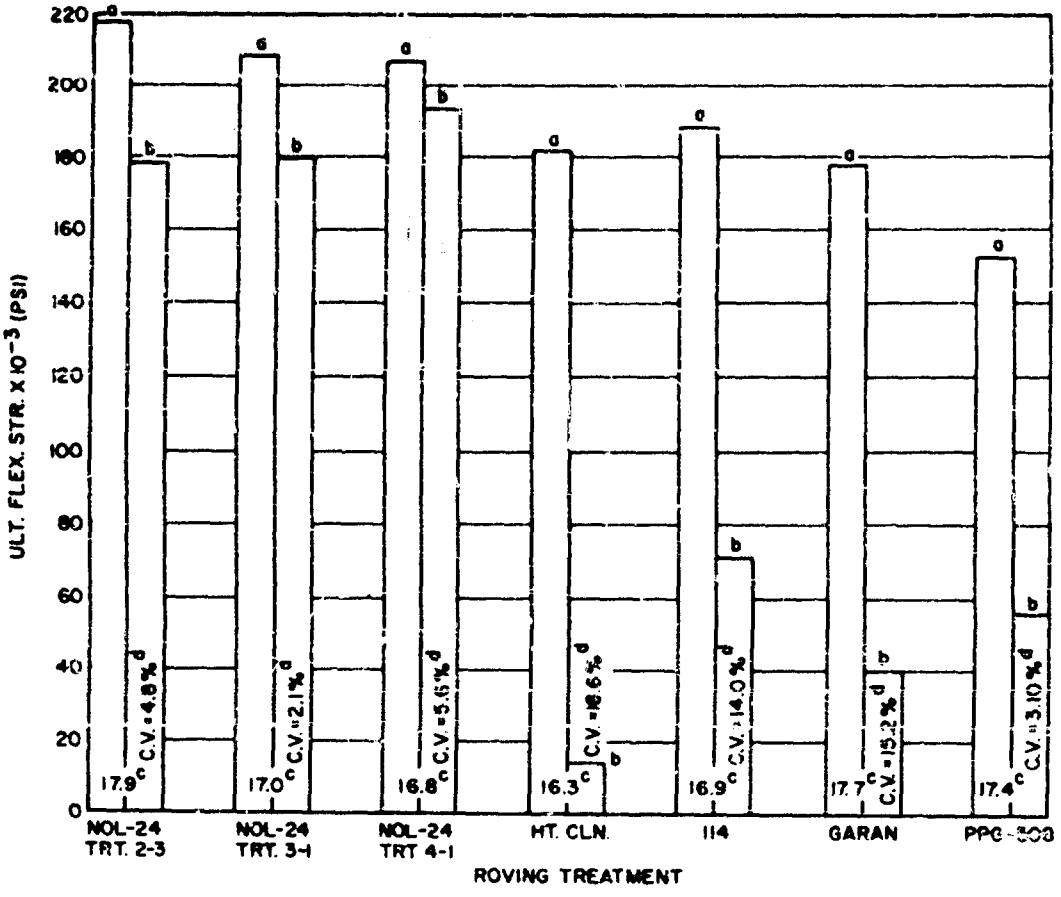

a. Dry strength; average of 4 specimens from 2 rings

b. Strength after 2 hours in boiling water; average of 6 specimens from 2 rings

c. Average resin content, %

d. C.V. = coefficient of variation

Figure 10 - Ultimate flexural strength from rings with paraplex P-43 resin using three experimental NOL-24 treatments

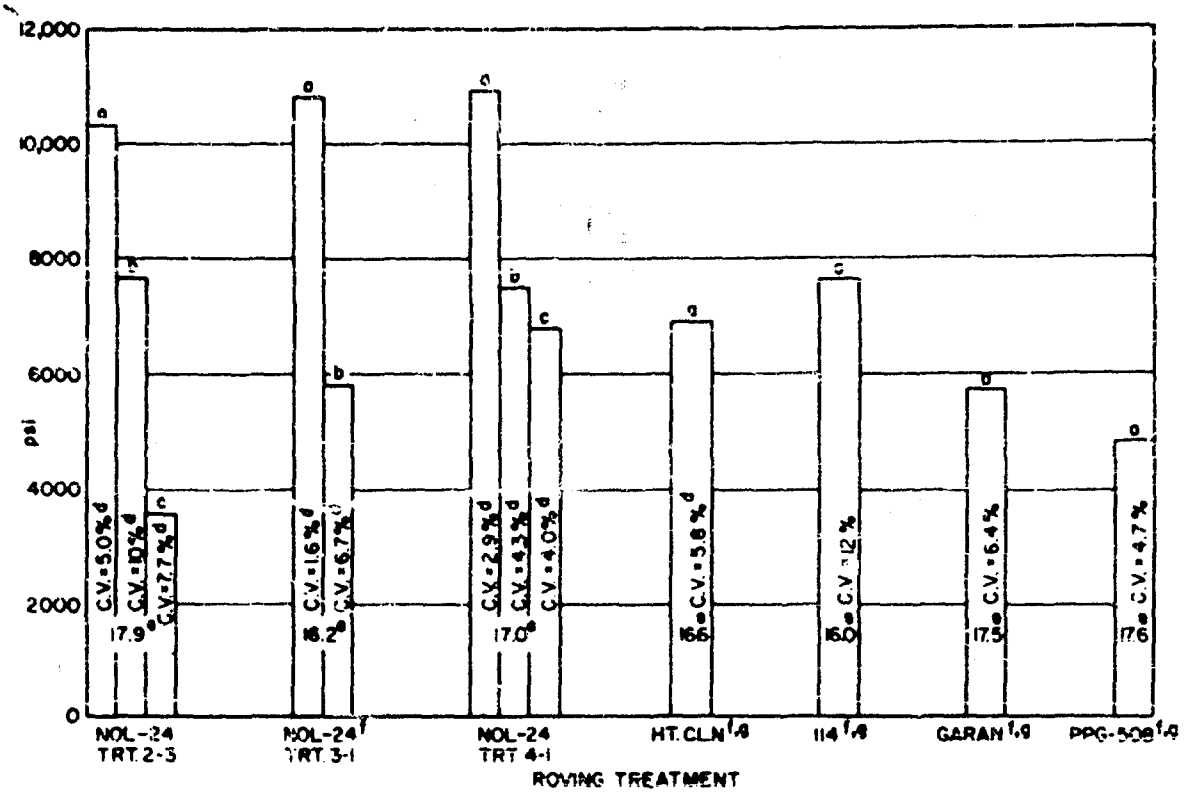

a. Dry strength; average of 8 specimens

b. Strength after 1 hour boiling water conditioning

c. Strength after 2 hour boiling water conditioning

d. C.V. = coefficient of variation

e. Resin content, %

f. All 8 specimens failed to shear after 1 hour in boiling water

g. All 8 specimens failed to shear after 2 hours in boiling water

Figure 11 - Horizontal shear strength from rings with paraplex P-43 resin using three experimental NOL-24 treatments and other commercial treatments

Small tubes were used to establish the variation of collapsing pressure with length-diameter ratios, thickness-diameter ratios, and reinforcement strength characteristics. Large tubes and models were investigated with respect to the degree to which ribbing would reinforce a tube and increase its collapsing pressure resistance. Long-term hydrostatic loading of models was carried out to determine the time-to-failure of promising designs and fabrications.

A formula for calculating the collapsing pressure (Pc) of reinforced plastics vessels was taken from one used for metal structures. For short cylinders (L = 6D maximum) under uniform external radial and axial pressures the Trilling-Windenburg formula was used:

$$Pc = \frac{2.42\ E}{(1-\mu^2)^{3/2}} \quad \frac{(t/D)^{5/2}}{\left[\frac{L}{D} - 0.45\ (t/D)^{1/2}\right]}$$

Where t/D is the wall thickness-to-diameter ratio and L/D is the length-to-diameter ratio. Poisson's ratio (μ) had been determined as equal to 0.3 and was used as a constant in the equation. The formula gives good results when the failures are of the instability type where excessive deformations give rise to highly stressed areas. When the failure is by yield without appreciable deformation, the formula is not strictly applicable. Nevertheless, it was used empirically to permit calculations of experimental vessels of known dimensions. This required the collapsing of cylinders of varying L/D and t/D ratios and the calculation of E (Effective Young's Modulus) to demonstrate its characteristic variations.

The initial series of experiments was with small diameter, convolutely wound cylindrical pressure vessels. Fig. 12 shows data for style 181 glass fabric reinforced polyester tubes. It is readily seen that Pc increases with a decrease in the L/D ratio and with an increase in the t/D ratio. Here then are two ways by which the strength may be controlled. It should also be noted that the slopes of these curves change markedly in the range of L/D ratios from one to two. At L/D ratios above this range, failure in the specimen is of a typical instability nature, while below the failure is typically yield. At extremely low L/D ratios, the axial compression strength of the cylinder appeared to be the yield mechanism of importance.

Once Pc was determined on a series of tubes of known t/D and L/D ratios, E was calculated. A plot of E against L/D for various t/D's, such as in Fig. 13, allowed the estimation of Pc for experimental cylinders. The drop in E at low L/D ratios again

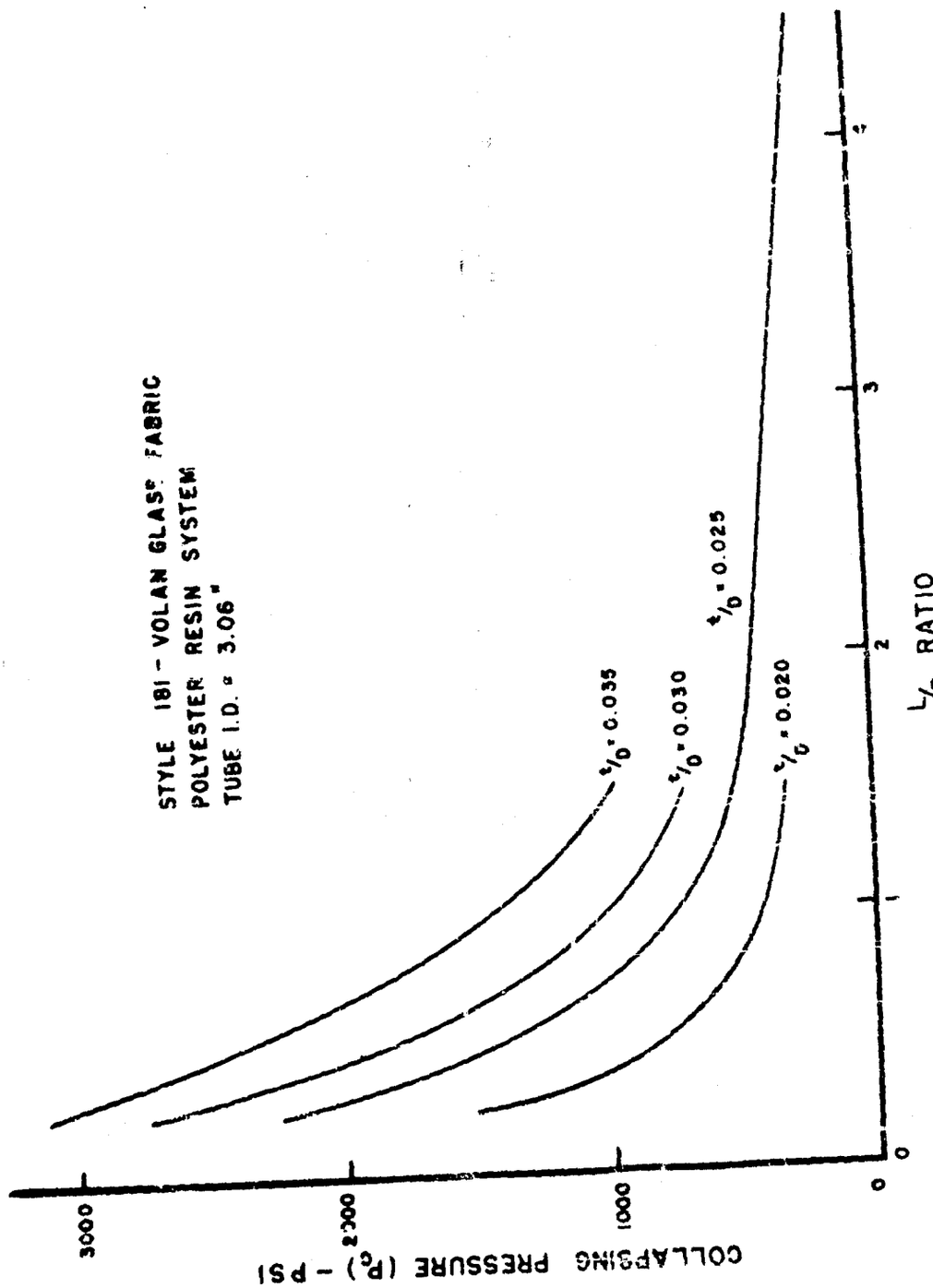

Figure 12 - Collapsing pressure of reinforced plastic tubes

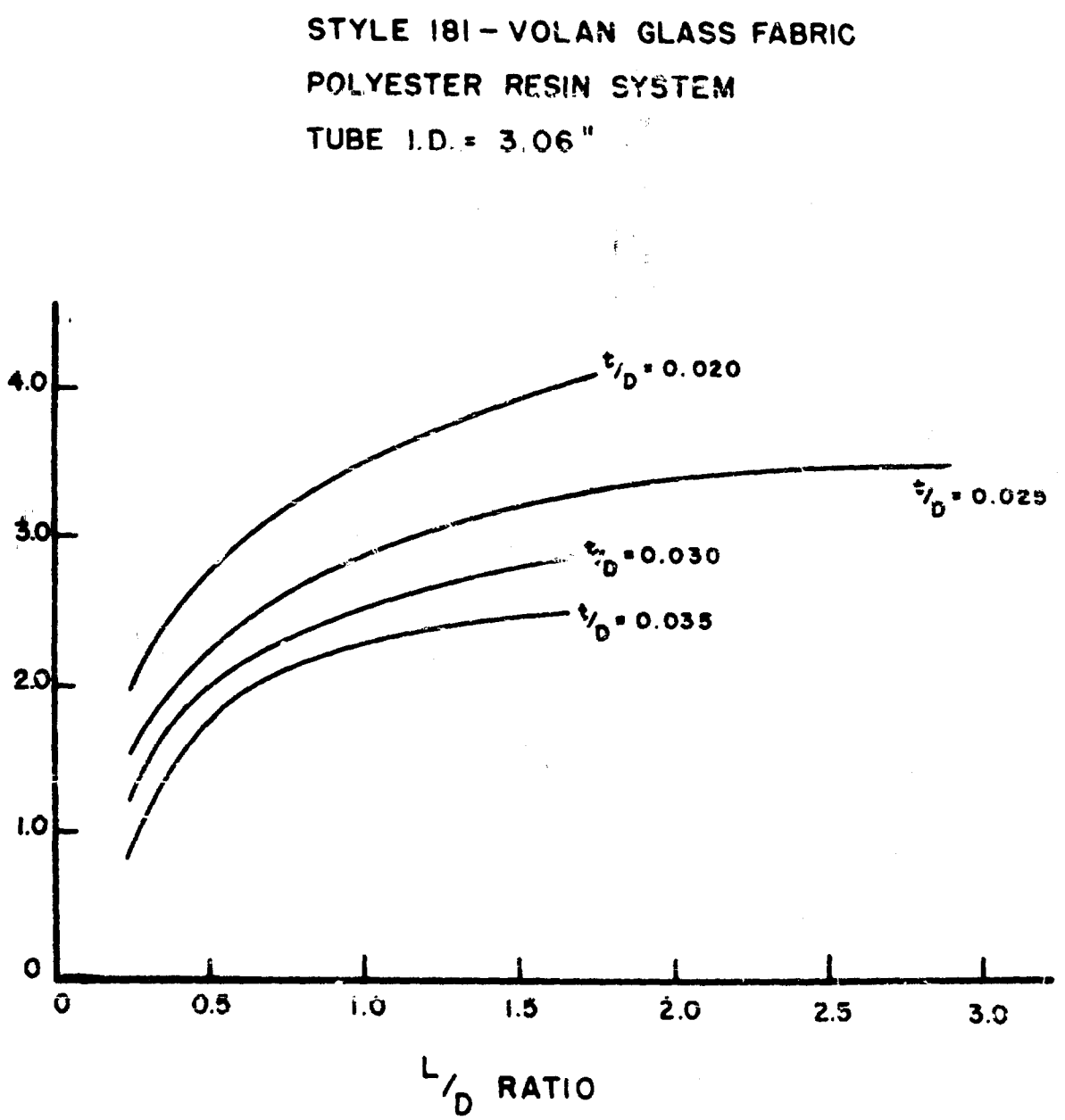

Figure 13 - Effective modulus variation of reinforced plastic tubes

illustrates the limited applicability of the formula to failures of a yield nature. It can, however, be used empirically by introducing an estimated E consistent with the specific t/D and L/D ratio of the proposed vessel.

Glass rovings were also used in a helical pattern to reinforce a cylindrical structure. Excellent results were obtained, as indicated by the variations of Pc and E versus the helix angle of wind, as shown in Fig. 14. Similarly, as with fabric reinforced tubes, it was noted that as the hoop strength of the tube is increased pressure resistance and stiffness increased. In contrast to the helical distribution of glass, the rovings were also placed so that they lay only in the axial and hoop directions (C-90° wind). With this technique, the axial hoop strength ratio can be controlled as with helical windings. The effect of these variations is shown by the points 2:1 and 4:1 (representing the hoop-to-axial ratio) over the 90° helix line in Fig. 14. Certain theoretical advantages accrue by using the 0° - 90° wind technique, as the glass is put more nearly in direct line with the applied stresses than when wound helically. It is, therefore, to be expected that these structures would have better stress resisting characteristics under both short-term and long-term loading conditions. Also, at the higher collapsing pressures, the maximum axial strengths for the application can be more readily maintained. The 0° - 90° wound tubes have axial compression strengths of 23,000 psi for a 2:1 axial-to-hoop strength ratio, as compared to 18,000 psi and 15,000 psi for a 60° and 80° helix wind, respectively.

Scale factor is an important consideration in the use of the foregoing data. A series of data in Table II show that the scale factor is effectively 1:1, as would be predicted from the Trilling-Windenburg formula. Since any increase in the radii of a tube approaches the ideal conditions of a flat sheet, it is expected that the 1:1 scale factor ratio will hold true at diameters larger than those tested to date.

In practical applications, a cylinder will generally have a specified length, yet its collapsing pressure requirement may demand a much lower effective L/D ratio than that of the basic tube. The use of ribs represents a means by which the effective L/D ratio can be reduced. Fig. 15 shows that Pc was controlled in the instability failure region by this method. In the yield region, however, these same ribs failed to give sufficient support to obtain Pc values as great as the ones on the theoretical Pc-L/D curve. The units failed in instability. Although the theoretical curve was not followed, the collapsing resistance was increased three-fold without a major weight increase. Further increases in collapsing pressure

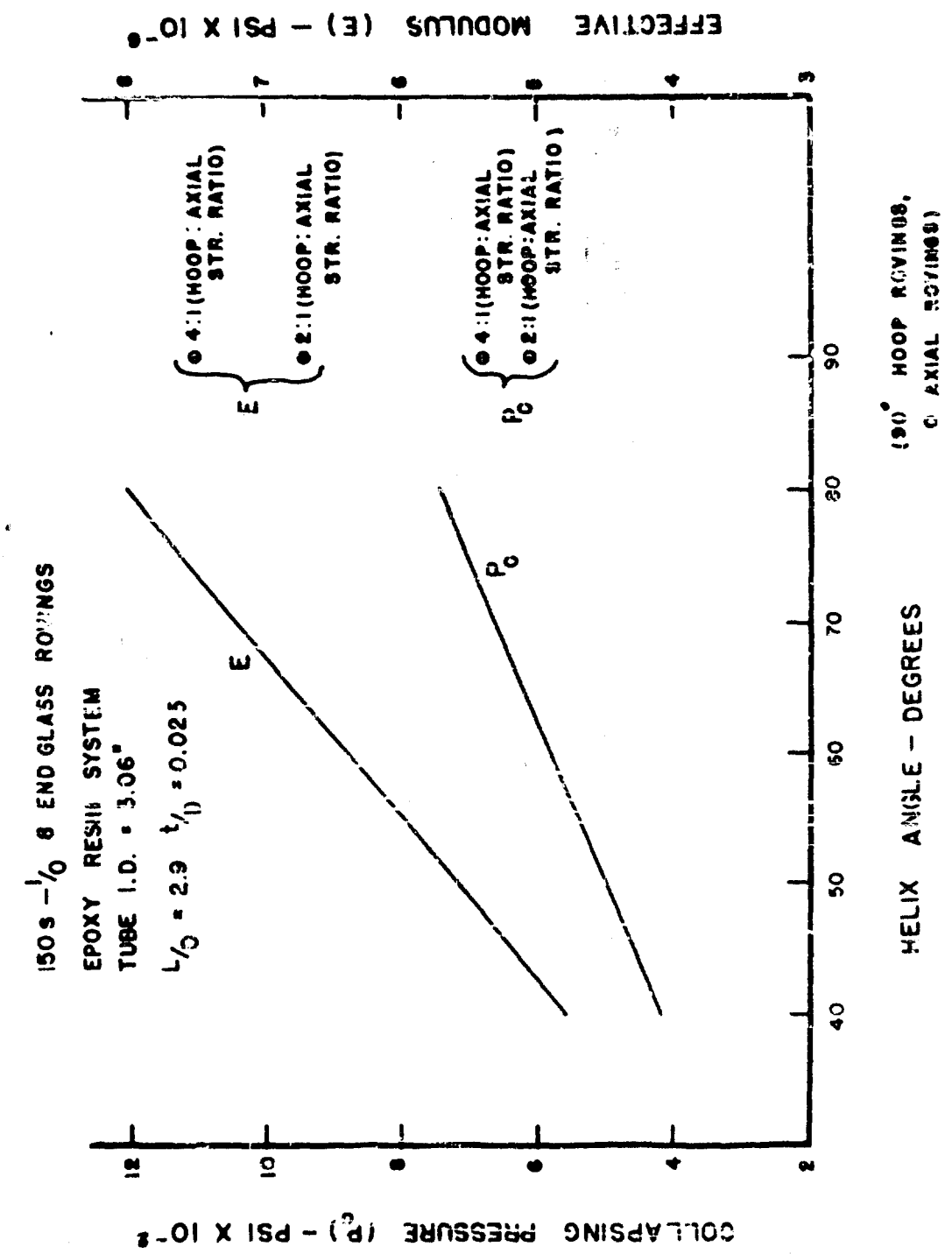

Figure 14 - Collapsing pressure characteristics of glass roving reinforced plastics tubing

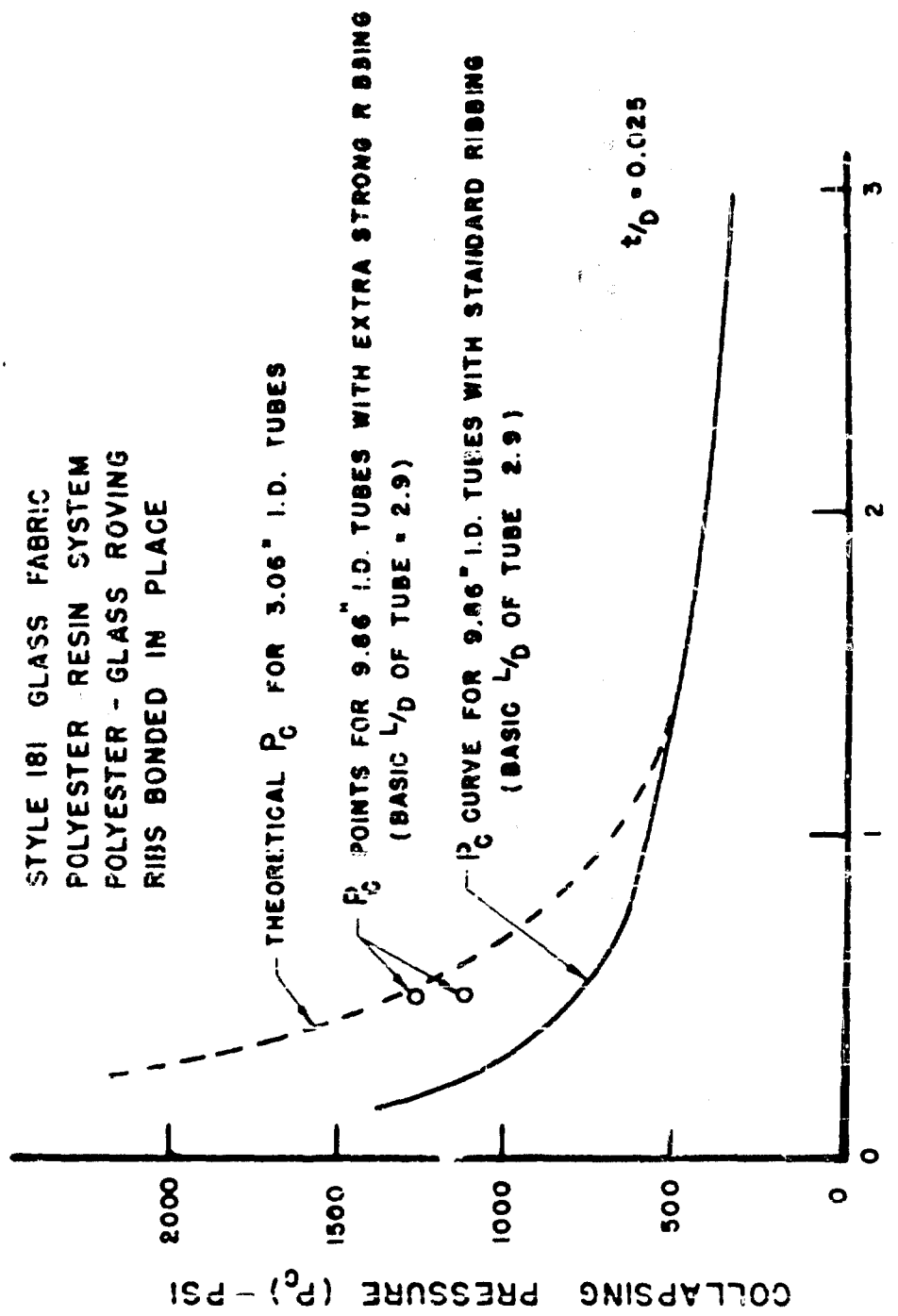

Figure 15 - Efficiency of ribbed reinforced plastic tubes

were obtained by increasing the rib cross-section or the number of ribs but at the expense of an increase in weight as well. Increasing the rib size resulted in a yield failure.

Not only must a reinforced plastics pressure vessel have a high resistance to short-term external pressure, but it must be able to resist a high proportion of this pressure for an extended period of time. Results of long-term exposure to external pressure in Fig. 16 showed that convolutely wound cloth vessels loaded to 80% of their short-term strengths did not withstand continuous pressure for any great length of time. At 60%, these vessels lasted about 300 days. It was shown that with a load of not over 50% of the short-term strength, the vessel lasted well in excess of one year. Vessels loaded at 40% of their ultimate strength were found to maintain their full short-term strength even after one year's long-term loading. Glass roving helically wound tubes, although having initially higher collapsing pressures, were found to fall off more rapidly on exposure than cloth wound tubes and maximum allowable pressure for long-term use was below that of the cloth wound tubes.

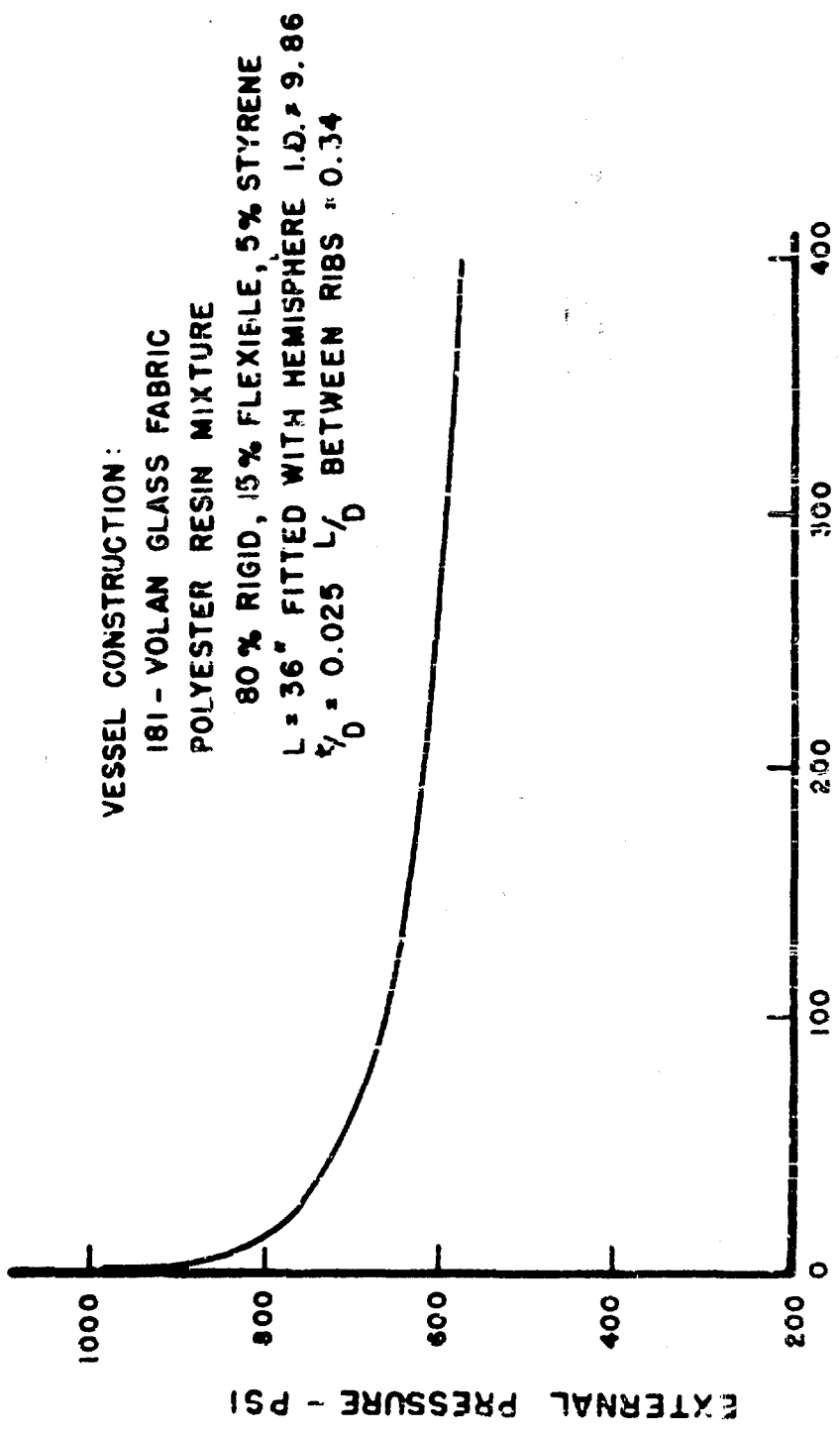

Figure 16 - Time-to-failure of reinforced plastics structures under external hydrostatic pressure

BIBLIOGRAPHY

1. NavOrd Report 2802, Chemical Finishes for Glass Fiber.

2. NavOrd Report 3811, Universal Type Chemical Finishes for Glass Fibers Used in Reinforced Plastics.

3. NavOrd Report 3889, Improved Reinforced Plastics with the Universal Type Chemical Finish NOL-24.

4. NavOrd Report 4461, Summary Report on NOL-24 Finish on Glass Cloth.

5. NavOrd 5742, A Comparison of the NOL-24 Finish with Y-1100 and A-172 Finishes as These Relate to Plastic Laminate Strength Properties.

6. NavOrd Report 6133, Proposed New Specification Requirements for 181 Style Glass Fabric Reinforced Plastics.

7. NavOrd Report 5680, Proposed NOL Ring Test Method for Parallel Glass Roving Reinforced Plastics; Evaluation of Chemical Finishes.

8. NavOrd Report 6153, Improved NOL Ring Test Method for Parallel Glass Roving Reinforced Plastics: Evaluation of Chemical Finishes.

9. NavOrd Report 4109, The Design of Reinforced Plastics Structures to Resist External Hydrostatic Pressures.

THE PHOSPHINIC NITRIDES - POTENTIAL HIGH TEMPERATURE POLYMERIC DIELECTRICS

A. J. Bilbo
U. S. Naval Ordnance Laboratory
Corona, California

During the past ten years, the demand for polymeric dielectric materials which can withstand temperatures in the region of 500 to 1,000°C has become increasingly insistent. Since most of the conventional organic polymer systems fail long before the required temperatures are reached, a solution in the field of inorganic polymer chemistry is being sought with increasing vigor by research laboratories.

Of the several areas studied by the group at NOL Corona, the most promising inorganic system is that known as phosphinic nitrides (also commonly referred to as phosphonitriles). The system is made up of alternate phosphorus and nitrogen atoms forming a conjugated, unsaturated polymer chain.

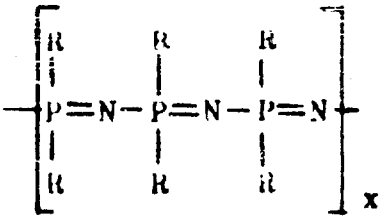

Figure 1

In this type of molecule, the phosphorus is pentavalent and wide variation in mechanical, physical and chemical properties can be obtained by varying the side chain substituents on the phosphorus atom.

The various phosphinic nitride compounds with which our Laboratory has been working are shown on the next page.

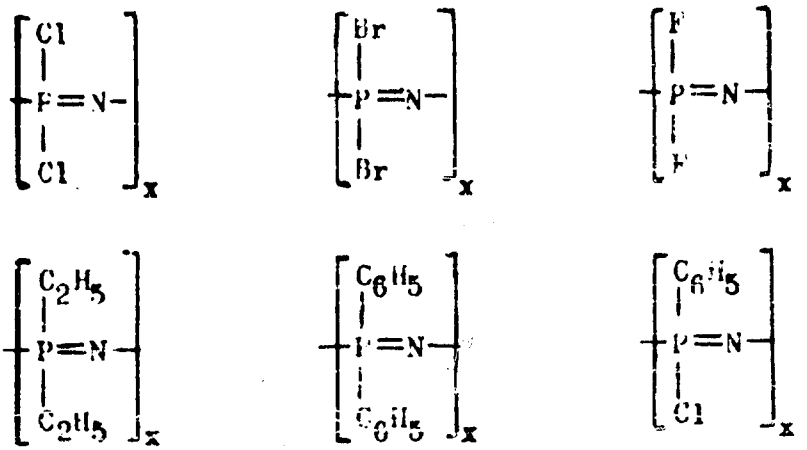

Figure 2

Historically, the parent materials in this family are the dichlorophosphinic nitridee, first made in 1834 by Liebig.[1] The lowest molecular weight members of that system are the trimer and tetramer.

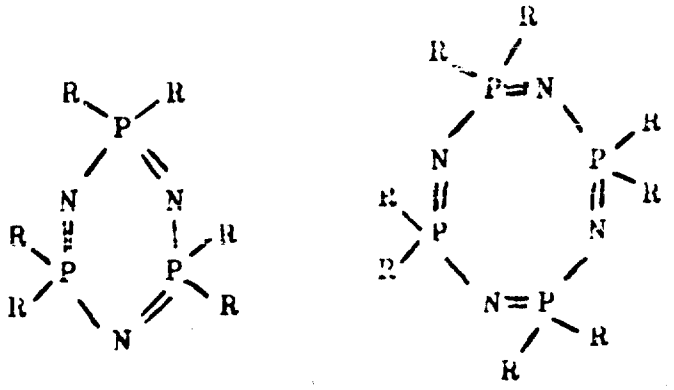

$(PNCl_2)_3$ $(PNCl_2)_4$

Figure 3

Studies of the electron diffraction pattern,[2] infrared and Raman spectra,[3],[4] and crystal structure[5] have established the cyclic structure of both trimer and tetramer. The trimer ring is planar, but the tetramer has a puckered ring configuration.

When $(PNCl_2)_{3 \text{ or } 4}$ is heated in a sealed tube at 270°C,[6] the ring is ruptured and the products shown below are obtained (the yields of each depend on the length of heating).

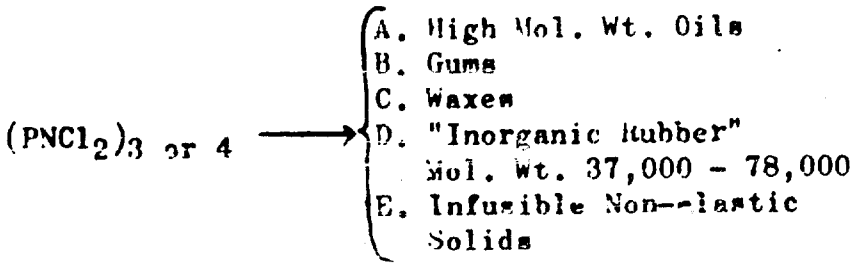

Figure 4

At 350°C, conversion to the "inorganic rubber" occurs within an hour. The "inorganic rubber" bears a remarkable resemblance to a good grade of slightly vulcanized natural rubber. Its elastic quality is as good, or better than natural rubber. It is colorless when made from pure trimer or tetramer, and is insoluble in ordinary solvents, but swells in benzene. The elastomer is stable toward acids and bases, but is decomposed by long boiling with water. A loss of elasticity occurs when the material is exposed to air for a period of weeks and it eventually becomes quite brittle. Slow heating of the elastomer to red heat converts it to a porous horny mass.

Let us now consider the methods by which the members of the phosphinic nitride system can be made.

$(PNCl_2)_{3 \text{ and } 4}$ can be obtained[7] in satisfactory quantities by the reaction of PCl_5 with NH_4Cl in an inert solvent.

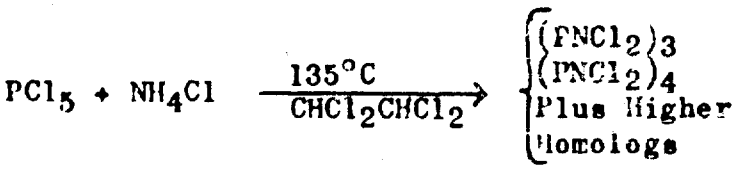

Figure 5

The mixture of products is separated by benzene extraction, fractional distillation, and slow sublimation.

$(PNBr_2)_{3 \text{ and } 4}$[8] are obtained in an analogous reaction between NH_4Br and PBr_5.

Mixed phenylchlorophosphinic nitrides can be obtained by the reaction of $C_6H_5PCl_4$ with NH_4Cl.[9]

Fully substituted phenylphosphinic nitrides can be prepared by the reaction of diphenylphosphorus trichloride with NH_4Cl in an inert solvent.

$$(C_6H_5)_2PCl_3 + NH_3 \xrightarrow{-40^\circ} \xrightarrow[NH_4Cl]{135^\circ} [(C_6H_5)_2PN]_x$$

Figure 6

The use of liquid ammonia instead of NH_4Cl[10] gives a more convenient reaction technique. Ammonia is not used in the reaction with PCl_5 in the formation of $(PNCl_2)_n$ because over-ammonolysis will occur. The initial products obtained from the liquid ammonia reaction with $(C_6H_5)_2PCl_3$ are water-sensitive, chlorine-containing compounds which must be heated to about 275°C in order to convert them to the cyclic diphenylphosphinic nitrides. It is noteworthy that the cyclic tetramer is formed almost exclusively.

$[(C_6H_5)_2PN]_4$ forms a higher polymer only when heated to temperatures above 400°C. When it is heated in a sealed tube at 540°C for short intervals, a brittle, amber glass is formed, together with a quantity of benzene equivalent to the loss of two phenyl groups per tetramer molecule. The glassy substance is insoluble in all solvents and resists molding even at 400-500°C. This evidence strongly suggests that extensive cross-linking must occur. Heating at 400°C for one hour in the air leads to less than 5% loss in weight, but prolonged heating in air leads to its conversion into a tarry mass.

The preparation of the diethylphosphinic nitrides[11] follows a similar path to that outlined for the diphenyl derivatives. Again the moisture-sensitive intermediates are converted to the cyclic compounds by heating at elevated temperatures (180-200°C).

The cyclic dialkylphosphinic nitrides are unique in that they are water soluble, and can be recovered unchanged from a cold water solution. When $[(C_2H_5)_2PN]_3$ is heated to 340°C for 16 hours in an evacuated tube, a dark, brittle, resinous material is formed, together with a quantity of ethane gas equivalent to the loss of 2 ethyl groups per trimeric molecule. The polymer begins to decompose when heated above 350°C.

Dimethylphosphinic nitride, recently prepared by Searle,[12] was found to have properties similar to those of the diethyl derivative.

Another method of obtaining substituted phosphinic nitrides involves the replacement of the chlorine atoms on the already formed

$(PNCl_2)_3$.

When $(PNCl_2)_3$ or 4 is treated with C_6H_5MgBr, partial or complete replacement of Cl occurs. However, the yields are not satisfactory due to the tendency of the Grignard reagent to cleave the $(PNCl_2)_3$ ring and thus form unidentifiable tars.

A more satisfactory Cl replacement reaction occurs when $(PNCl_2)_3$ and 4 are treated with KSO_2F.[14],[15]

$$(PNCl_2)_{3 \text{ and } 4} + 2\ KSO_2F \xrightarrow{125^\circ C} (PNF_2)_{3 \text{ and } 4} + 2\ KCl + 2\ SO_2$$

Figure 7

Here the conversion to $(PNF_2)_3$ and 4 is better than 75%. Heating $(PNF_2)_3$ and 4 in an evacuated tube at 350°C for 16 hours yields a clear, colorless elastomer which is thermally stable up to 450°C. The hydrolytic stability, however, is very poor, since overnight exposure to the atmosphere converts the material to a white, sticky mass having little or no elasticity.

The reaction between sodium azide and halophosphines[16] provides an interesting and potentially important method of preparing phosphinic nitrides.

$$R_2PCl + NaN_3 \xrightarrow{\text{heat}} \left[R_2P{-}N_3\right] + NaCl$$
$$\downarrow$$
$$(R_2PN)_x + N_2$$

R = C_6H_5, Cl, Br

Figure 8

The reaction occurs when the azide is added dropwise to the heated halophosphine. Nitrogen is evolved as the intermediate phosphorus azide decomposes to yield a mixture of polymeric phosphinic nitrides. If the reaction temperature is too low, the phosphorus azide may accumulate and explode violently, as happened in the reaction of $(CF_3)_2PI$ with NaN_3. PCl_3 with NaN_3 also yields an explosive compound. $(PNCl_2)_3$ yields the diazidophosphinic nitride, $\left[PN(N_3)_2\right]_3$,[17] when treated with NaN_3.

Appreciable yields of $[(C_6H_5)_2PN]_4$ are obtained by this method when the polymerized material, obtained from the azide, is heated to 275°C.

$C_6H_5PCl_2$ and NaN_3 react to give a soluble polymeric, fibrous material of molecular weight in excess of 5,000.

$(PNBr_2)_x$ elastomer is obtained directly by this method.

In addition to the synthetic phase of the inorganic polymer program at NOL Corona, a kinetic study(18) of the polymerization of the dichlorophosphinic nitrides is also in progress. The uncatalyzed thermal polymerization of $(PNCl_2)_{3 \text{ or } 4}$ is difficult to study because results could not be reproduced despite strenuous efforts to control all reaction variables. These difficulties were alleviated when it was discovered that a large number of organic compounds and some metals catalyze the reaction to a pronounced degree, bringing about an extensive polymerization in 24 hours at 210°C. Among the catalytically active materials are ethers, ketones, alcohols, and organic acids, zinc, tin, and sodium.

Bulk polymerization data typical of $(PNCl_2)_3$ are shown below:

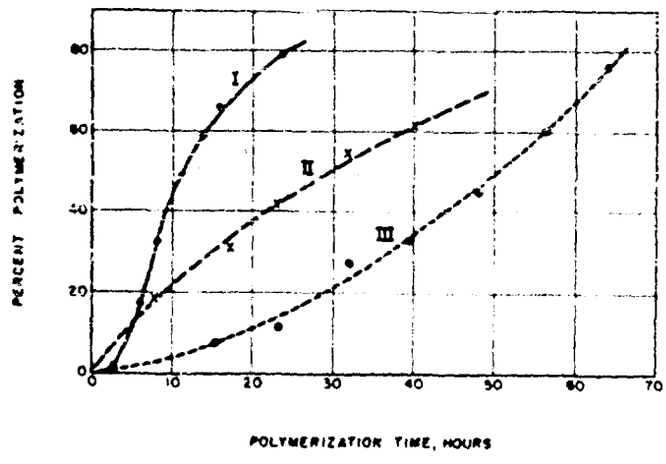

Figure 9

Curve I is the reaction catalyzed by 8.4 mg of ether per gram trimer; Curve II, 2.6 mg of ethyl alcohol per gram trimer; and Curve III, by 20 mg of tin per gram of trimer.

At the temperature at which our investigations were carried out, namely 210°C, the increasing amount of polymer being formed causes the reaction medium to be quite viscous, thus the data from the bulk polymerizations only lend themselves to mathematical analysis during the early stages of polymerization. In order to obtain results more amenable to kinetic interpretation, the polymerization was carried out in solution.

Figure 10 shows the polymerization data using benzene solutions containing 22% by weight of $(PNCl_2)_3$ and different concentrations of benzoic acid as catalyst.

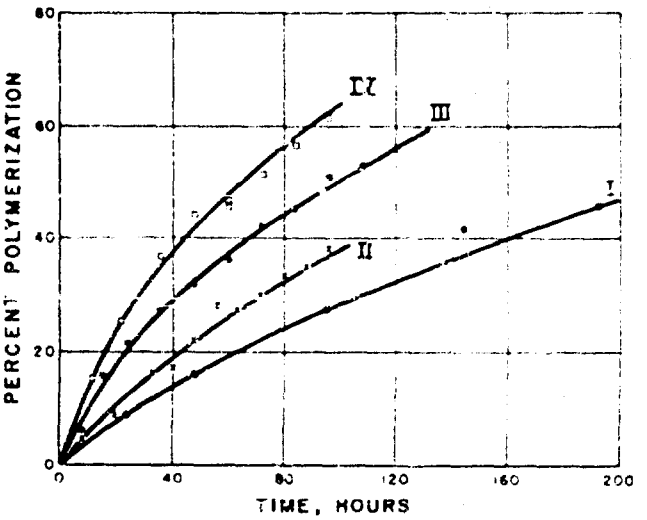

Figure 10

Curve I was obtained when 2.89 mg of benzoic acid per gram of benzene was used; Curve II, 5.70 mg; Curve III, 9.80 mg; and Curve IV, 13.7 mg of benzoic acid.

Figure 11 gives the first order plot of the same data, as seen on the next page.

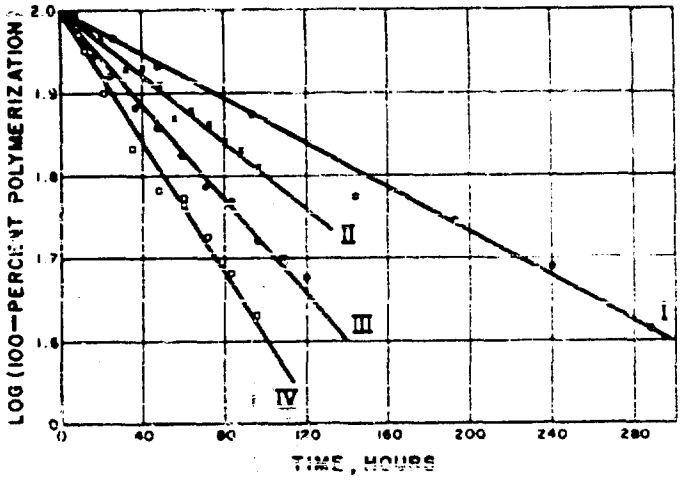

Figure 11

All curves appear to satisfy an equation for a first order reaction with respect to catalyst concentration.

The values of the first order rate constants, calculated from the first order relationships shown in Figure 11 are plotted as functions of benzoic acid concentration in Figure 12.

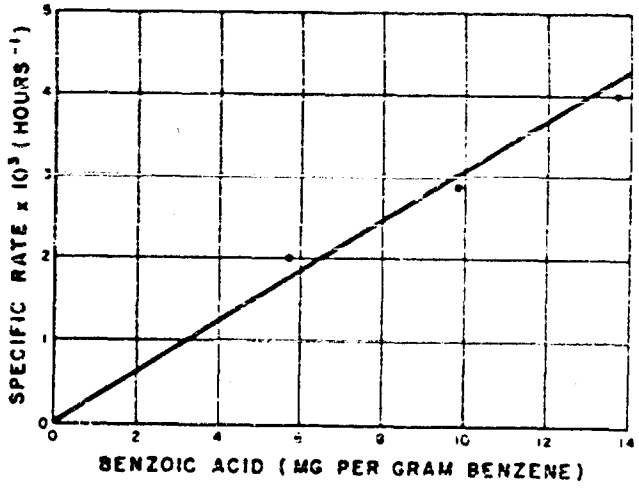

Figure 12

The rates are seen to be directly proportional to the concentration of the catalyst. The high value of the rate at the lowest concentration of benzoic acid is attributed to the uncatalyzed solution polymerization of the trimer. Since data for the uncatalyzed solution are as poorly reproducible as those for the bulk polymerization, a reliable correction cannot be made; however, values as high as 6%

polymerization in 100 hours have been observed, and rates of this magnitude would account for the observed elevation.

The comparable effectiveness of the very different types of catalysts makes it obvious that their action is not specific. The catalysis by metals and the formation of hydrogen chloride from the organic compounds suggest that the important step in the initiation is the removal of a chlorine atom from the phosphorus. This reaction must occur in an environment where the chlorine cannot be replaced by another stable group, for water and ammonia had only a small effect on the polymerization, although they react readily with $(PNCl_2)_3$. In view of these considerations, it appears that upon removal of a chlorine atom from phosphorus, an activated species such as $P_3N_3Cl_5$* is formed. The propagation of the polymerization proceeds when this active species react further with other trimer molecules. The termination step could possibly occur upon combination of two long chain reactive specie.

References

1. Liebig, J., Ann. 11, 139 (1834)
2. Brockway and Bright, JACS 65, 1551 (1943)
3. Daasch, L. W., JACS 76, 3403 (1954)
4. de Ficquelmont, A. M.; Magat, M. and Ocha, L., Compt. rend. 208, 1900 (1939)
5. Ketelaar, J. A. A. and de Vries, T. A., Rec. Trav. Chim. 58, 1081 (1939)
6. Audrieth, L. F.; Steinanan, R. and Toy, A. D. F., Chem. Rev. 32, 119 (1943)
7. Schenk, R. and Romer, G., Ber. 57B, 1343 (1924)
8. Bode, H., Z. Anorg. Chem. 252, 113 (1943)
9. Shaw, R. A. and Stratton, C., Chem. and Ind. 52 (1959)
10. Haber, C. P.; Herring, D. L. and Lawton, E. A., JACS 80, 2116 (1958)
11. Bilbo, A. J., Navord Report 5925, 15 (1958)
12. Searle, H. T., Proc. Chem. Soc. 7 (1959)
13. Bode, H. and Thamer, K., Ber. 76B, 121 (1943)
14. Seel, F. and Langer, J., Angew. Chem. 68, 461 (1956)
15. Haber, C. P. and Uemishi, R. K., Chem. and Eng. Data 3, 323 (1958)
16. Herring, D. L., Navord Report 5920, 38 (1958)
17. Grundman and Ratz, Z. Naturforch 10b, 116 (1955)
18. Konecny, J. O. and Douglas, C. M., J. Polymer Chem., in press.

EFFECTS OF ELEVATED TEMPERATURE ON ELECTRICAL PROPERTIES OF THERMOSETTING PLASTICS

W. Hand
Naval Material Laboratory
New York Naval Shipyard
Brooklyn, New York

In recent years, the evaluation of heat resistance of electrical insulation has become a subject of growing interest and importance among research and design engineers. Increased interest is being generated by the widespread and continuing trend toward miniaturization of electrical and electronic equipment, necessitating the functioning of insulation at ever higher temperatures. Furthermore the rapid development of printed circuits, growing Naval electronic applications, and space flight technology have also served to create a demand by the Navy and other Military agencies for higher temperature dielectrics and for specific engineering information regarding the behavior of insulating materials at anticipated temperatures. Difficulties in solving these problems arise from the wide variety of environmental conditions encountered in applications, the demand on the part of development and design engineers for concise, yet scientifically sound, heat resistance classifications of insulating materials and the disagreement of researchers on methods of obtaining and interpreting the required data.

Recognizing the future need for specific information on elevated temperature properties of insulating materials for shipboard applications the Naval Material Laboratory, under the sponsorship of the Bureau of Ships undertook a program of investigations to obtain a comprehensive view of the heat resistance of dielectrics. It was also intended that this program would promote the development of research methods, procedures and instrumentation for the evaluation of dielectric materials at elevated temperatures as well as supplying specific information useful for design purposes.

METHOD

The test program included the development of apparatus and procedures for conducting elevated temperature measurements of electrical properties such as dielectric strength, dielectric constant, dissipation factor, volume and surface resistance. In addition, the electrical program was paralleled by a similar elevated temperature investigation of mechanical properties, described in reference (1).

In contrast to the prevalent practice of conducting measurements of properties of insulating materials at room temperature after heat aging, and often not considering the duration of the heat aging period, the Laboratory's evaluations were conducted by performing measurements at elevated temperatures and as functions of time of exposure at these temperatures. In addition, special attention was devoted to investigating very short term exposure effects because of unusual behavior observed on initial heating of some materials.

In accomplishing these investigations, special equipment or modifications of conventional equipment were devised. These included the construction of test chambers for conducting measurements at elevated temperature, the development of high temperature electrode systems, and the use of silver paint and spray metal electrodes. For example, the chamber illustrated in Figure 1 was constructed to conduct dielectric strength measurements in the direction parallel to forming pressure of the material under test. This apparatus consists essentially of a thermally and electrically insulated enclosure containing a 3/4 inch diameter electrode system and thermostatically controlled electric heaters. Spring loaded, 3/4 inch electrode assemblies are installed in clearance holes through the center of two large ceramic insulators. The upper insulator is fastened to the reenforced roof of the chamber and its electrode, protruding through a hole in the roof, is connected to the high tension side of the test voltage source. The lower insulator, containing the grounded electrode is mounted concentrically on an insulated stand fastened through a hole in the floor of the chamber to a hydraulic jack. The opposing faces of the insulators are covered with 1/8 inch thick sheet silicone rubber with 1 inch center holes provided for protrusion of the electrodes. In a test, the specimen is placed centrally between electrodes and the lower electrode assembly hydraulically raised to compress the specimen against the upper electrode assembly. Thus, "flashover" across the surfaces of the specimens is inhibited when voltage is applied. Although the specimen is subjected to a pressure of 25 to 50 psi. when tested, the area of the specimen under the electrodes experiences only negligible spring pressure. The equipment is capable of withstanding voltages up to 60 kilovolts and operating at temperatures as high as 250C. To minimize statistical

Fig. 1 - Dielectric Strength Measuring Apparatus - Front Wall Removed

variability, data was taken as the average of at least 3 measurements for each test point on randomly selected specimens.

MATERIALS

The materials investigated were commercially available, and commonly used laminated and molded thermosetting plastics. The laminates were cut into 3 inch squares from 1/8 inch thick sheets and included electrical grades of the following types: phenolic-paper

(PBE), phenolic-fabric (PBG), melamine-glass cloth (GMG), and silicone-glass cloth (GSG). Molded materials were phenolic-asbestos (MFT-20), phenolic-cellulose (CFG), melamine-glass fiber (MMI-5), alkyd-glass fiber (MAI-60), and silicone-glass fiber (MSI-30); molded into 1/8 inch thick, 4 inch diameter discs.

RESULTS

Dielectric strength, measured in the chamber described, was investigated using a 500 volts per second linear rate of voltage rise. Measurements were conducted at 50C temperature increments at temperature levels of from 50 to 250C. Dielectric strength was computed as the ratio of breakdown voltage to specimen thickness in volts per mil (vpm).

The results of dielectric strength, short time temperature exposure tests (measurements made during the first four hours of heat aging) are considered first. These may be separated into three groups. In the first catagory are materials such as silicone-glass laminate, which show little change in properties during this initial heating period. The second group includes phenolic materials as typically illustrated in Figure 2 by the curves obtained for phenolic-fabric laminate. With these materials a reduction in dielectric strength starts almost as soon as the specimen is inserted in the preheated test chamber and the decline continues for five minutes to four hours or more, depending on material and exposure temperature. This is immediately followed by rather rapid recovery, often beyond initial strength. In the material shown, a drop from a room temperature value of 254 to 32 vpm was observed within five minutes of insertion of the specimen and exposing it to a constant temperature of 150C. Paper base phenolic, at this temperature and exposure interval, dropped from an initial value of 510 to 63 vpm; retaining only 12% of its original dielectric strength. At moderate elevated temperatures, such as

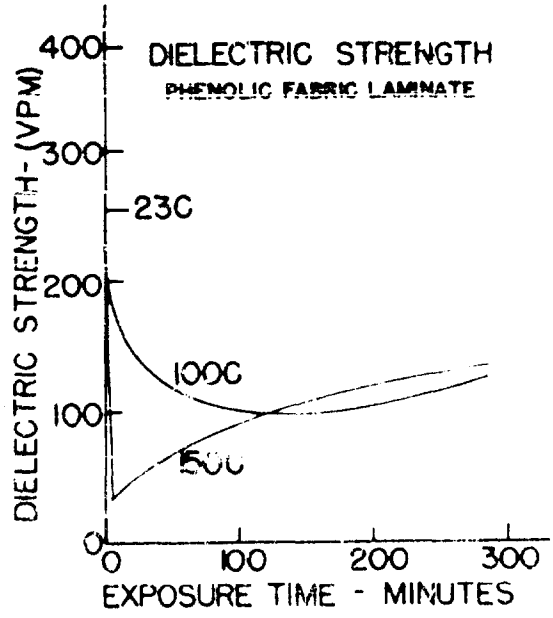

Fig. 2 - Short-term Elevated Temperature Dielectric Strength of Phenolic-fabric Laminate

50 and 100C, the loss of dielectric strength was not as great as exhibited at higher temperatures, however longer time was required to reach minimum values. At temperatures of 200 and 250C, initial drops were often so rapid that minimum strengths could not be measured with certainty. After reaching minimum dielectric strengths, somewhat slower recovery followed. Improvement, often beyond initial dielectric strength values, was still continuing after 1,000 hours of heating at the milder temperatures, but the trend was again reversed downward within 24 hours for 250C exposures.

The third group of short interval heat aging results are represented by molded and laminated melamine-glass and molded alkyd-glass. The behavior these materials are typically illustrated by the curves obtained with the melamine-glass molded material of Figure 3. Here, as in the second group, a very sharp drop in dielectric strength was observed as soon as the material was exposed to heat, but contrary to the previous group, recovery on continued heating was small so that dielectric strength remained substantially at a low level. Typical data show a drop from 385 to 60 vpm in 15 minutes of exposure at 150C; a retention of only 16% of initial dielectric strength. The maximum subsequent recovery to 148 vpm, indicated a net loss of 62% of initial dielectric strength.

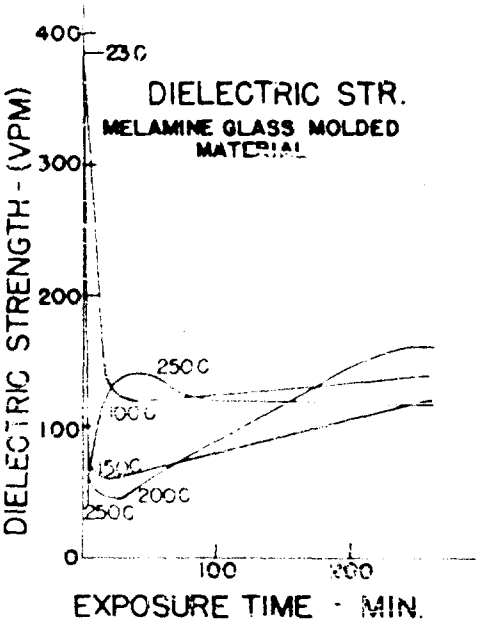

Fig. 3 - Short-term Elevated Temperature Dielectric Strength of Melamine-glass Molded Material

The results of dielectric strength measurements during long term heat aging indicated the following:

Elevated temperature exposures for durations beyond the initial transient range eventually produced progressive dielectric strength deterioration, determined by temperature level and duration of exposure. Many of the materials, however, did not follow a linear pattern of dielectric strength reduction with heat aging time, particularly at higher temperatures. Under these conditions, it was found that deterioration progressed slowly for several hundred hours and then in a relatively short period dropped to a considerably lower level, after which slow deterioration was resumed. For example, in

Figure 4, the long term heat aging curves of molded silicone-glass show rapid loss of dielectric strength at 200 and 250C; each of these drops occurring between intervals of slow decline. On the other hand, lower temperature exposures showed no sudden drops in dielectric

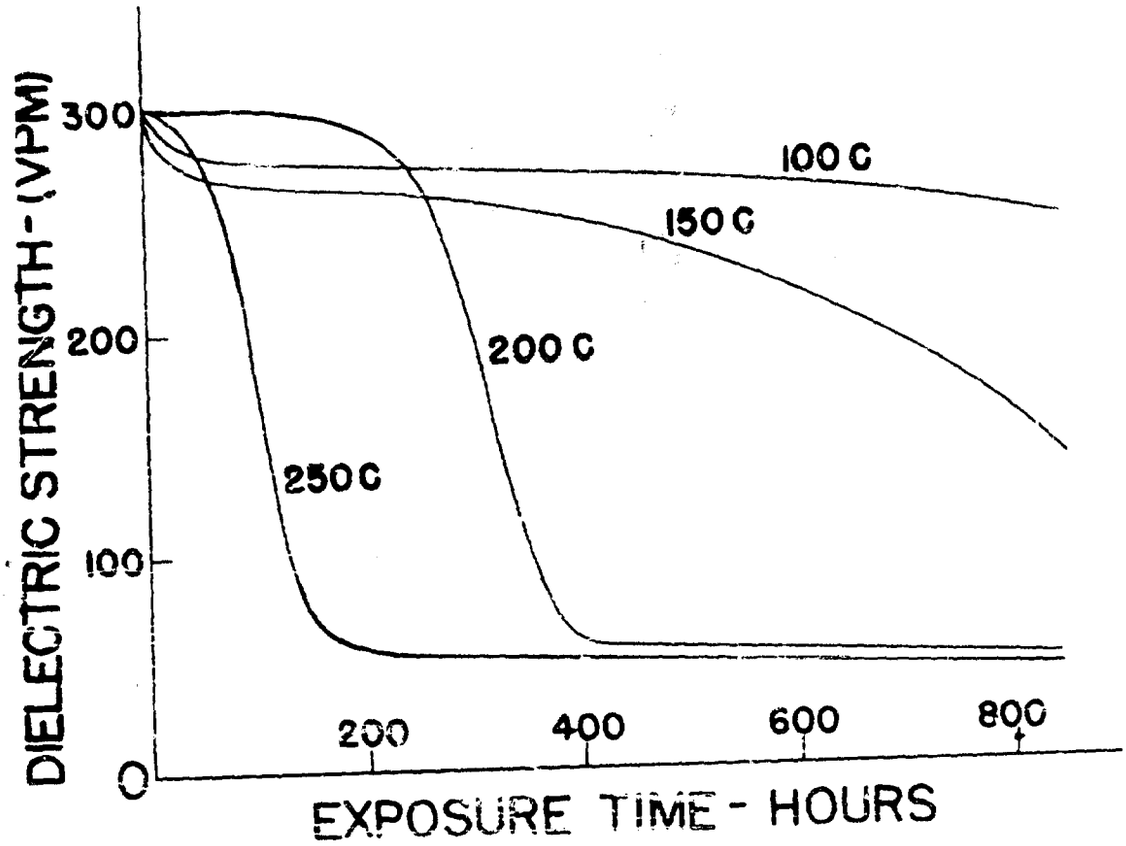

Fig. 4 - Long-term Elevated Temperature Dielectric Strength of Silicone-glass Molded Material

strength, although it is conceivable that they could occur beyond 1,500 hours, the maximum aging period investigated. In many cases long term heat aging failed to produce the extremely low values observed during initial heating. The salient aspects of these dielectric strength measurements are shown in Table I.

Many of the initial effects noted in dielectric strength measurements had their counterparts in measurements of other properties under similar circumstances. This was observed in such diverse measurements as flexural strength (1), dielectric constant, dissipation factor, volume resistance and surface resistance. Thus, Figure 5, illustrating volume resistivity of four laminate materials at

TABLE I

Salient Results of Dielectric Strength Elevated Temperature Investigations

Dielectric Strength (D.S.)-Volts per Mil (VPM)

Mat'l and Group	Temp. °C	Initial vpm	Transient Minimum vpm	Time to reach Minimum	Recovery Maximum vpm	Time to reach max. hrs.	D.S. at 768 hrs. vpm	D.S. at 1500 hrs. vpm
PBE	100	510	152	4 hrs.	>600	>1000	>600	-
2	150	"	63	5 min.	550	1000	550	-
	200	"	40	<3 min.	Blistered		Blistered	
PBG	100	255	100	2 hrs.	420	300 hrs.	420	-
2	150	"	30	5 min.	361	96 hrs.	278	-
	200	"	20	<3 min.	Blistered		Blistered	
GMG	50	480	320	24 hrs.	355	48 hrs.	308	-
3	100	"	185	4 hrs.	215	24 hrs.	120	-
	150	"	85	5 min.	230	3 hrs.	85	-
	200	"	Not obtained [1]		224	1 hr.	79	-
	250	"	"	"	208	5 min.	60	-
GSG	100	372	No Transient		375	1 hr.	350	-
1	150	"	Instability		400	3 hrs.	393	-
	200	"	Observed		471	48 hrs.	308	-
	250	"			428	5 min.	226	-
MMI-5	100	385	120	30 min.	234	24 hrs.	151	149
3	150	"	60	15 min.	148	192 hrs.	145	144
	200	"	47	15 min.	169	4 hrs.	106	94
	250	"	Not obtained [1]		143	30 min.	59	52

TABLE I (Cont'd)

Salient Results of Dielectric Strength
Elevated Temperature Investigations

Dielectric Strength (D.S.)-Volts per Mil (VPM)

Mat'l and Group	Temp. °C	Initial vpm	Transient Minimum vpm	Time to reach Minimum	Recovery Maximum vpm	Time to reach max. hrs.	D.S. at 768 hrs. vpm	D.S. at 1500 hrs. vpm
MAI-60 3	100	405	315	5 min.	373	30 min.	323	340
	150	"	200	30 min.	371	1 hr.	285	266
	200	"	244	15 min.	268	4 hrs.	42	35
	250	"	157	5 min.	202	4 hrs.	43	41
MSI-30 1	100	304	No Transient Instability Observed		308	192 hrs.	247	239
	150	"			279	24 hrs.	165	123
	200	"			367	30 min.	59	58
	250	"			346	30 min.	64	56
MFI-20 2	100	59	35	15 min.	103	192 hrs.	89	107
	150	"	19	15 min.	111	192 hrs.	108	122
	200	"	17	15 min.	89	24 hrs.	35	27
	250	"	18	5 min.	66	4 hrs.	31	23

Notes: 1. Not measureable by method used. Minimum value occurs in less than 5 minutes.

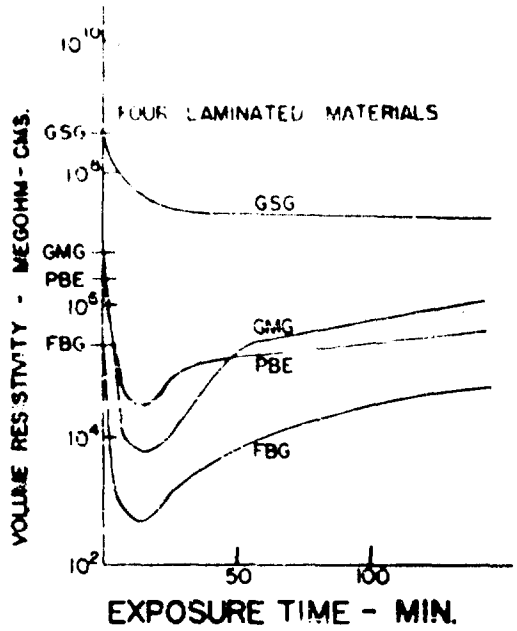

Fig. 5 - Volume Resistance at 150C of Four Laminated Materials

150C, shows that 3 of the 4 materials exhibit characteristic initial transient effects, consisting of rapid temporary loss of resistance during the first minutes of heating, followed by slower recovery on continued heating. Silicone-glass laminate, relatively stable during short interval elevated temperature dielectric strength measurements, also exhibited similar stability with respect to volume resistance and other electrical properties.

To determine whether the initial instability effects observed were attributable to under curing and therefore subject to improvement by further heating, measurements were conducted to determine the effect of cyclic periods of heat aging. Thermal cycles at 100 and 150C, consisting of 6 hours at elevated temperature and 18 hours at room temperature were repeated three times on the sensitive phenolic cellulose (CFG) molded material. Measurements of dielectric constant and dissipation factor at one kilocycle were taken almost continuously during the six hour heating periods. Figure 6 shows the effect of 100C thermal cycles on dissipation factor. Similar characteristic were found for dielectric constant and for the measurements at 150C. It is evident from these curves that substantial improvement is achieved after the first cycle, resulting in reduction of the initial peak by half. Subsequent cycles produced minor further improvement, illustrating that inadequate cure may be responsible for only part of the initial thermal instability.

CONCLUSIONS

As a result of these investigations it is believed that insulation failure or malfunction of electrical apparatus at elevated temperatures can be caused by a form of transient instability occurring within a few minutes of elevated temperature exposure. The possibility of this form of early failure is inherent in specific types of insulating materials, and, in apparatus utilizing these materials, the danger of failure is greatest where temperature rises are both substantial and rapid. Examples of such situations might be

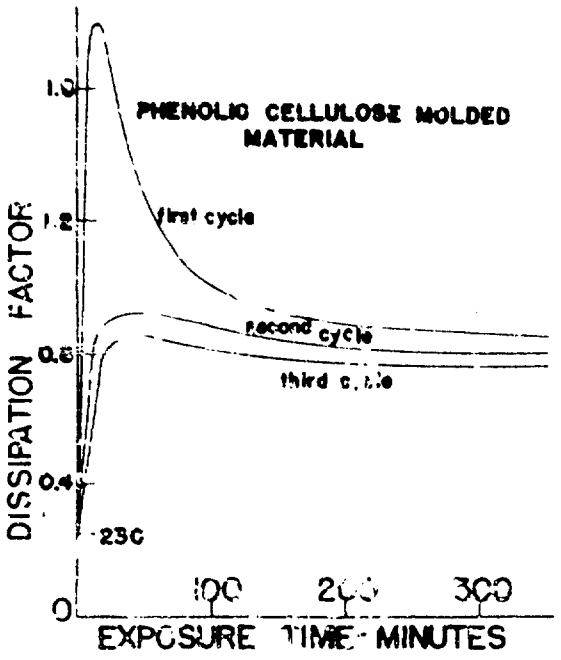

Fig. 6 - Effect of Thermal Cycling at 100C on Dissipation Factor of CFG Material

found in the electrical equipment of guided missiles, jet aircraft, proximity fuses and shipboard and airborne radar. Awareness of the possibility of this form of failure is needed to take precautions against it. The condition is somewhat alleviated by the fact that most applications of insulating materials do not involve the rapid temperatures rises employed in the Laboratory tests described. In ordinary applications this may be sufficient to carry the material beyond the critical initial heating period.

The results of the investigations also indicate that the task of classifying insulating materials into temperature ratings of heat resistance on a scientifically sound basis will be more difficult than first anticipated. The various forms of initial thermal behavior of materials and the non-uniformity of their long term characteristics do not lend themselves to the generalizations required for simple thermal classification of materials or the prediction of life expectancy under specified conditions. For the immediate future it appears that the selection of dielectric materials will continue to require extended testing as dictated by the specific environmental requirements of each new application.

REFERENCES

1. N. Fried, R.R. Winans and L.E. Siefert "Effects of Elevated Temperatures on Strength of Thermosetting Plastic Laminates", Proceedings Am. Soc. Testing Matls. Vol 50 p. 1383 (1950)

2. R.R. Winans, and W. Hand "Electrical Properties of Thermosetting Plastics at Elevated Temperatures", Am. Soc. Testing Matls. Special Technical Publication No. 160 p. 59-77 (1954)

3. W.W. Staley and E.B. Burstein "How Temperature, Humidity, & Cleanliness Affect Electrical Properties of Printed Circuit Laminates" Insulation, Feb 1959 p. 10

4. L.J. Berberich and T.W. Dakin "Guiding Principles in the Thermal Evaluation of Electrical Insulation" A.I.E.E. Transactions paper No. 56-248 (1956)

5. W.B. Kouwenhoven, C.C. Knickerbocker, K. Wechsler "Thermal Stability of Laminated Thermosetting Plastics" A.I.E.E. Conference Paper CP-57-141 (1957)

6. J.J. Chapman, L.F. Blickley, E.A. Szymkowiak, "Surface and Volume Dielectric Losses" A.I.E.E. Transactions Paper No. 55-81 (1955)

7. G.E. Power, "Appraisal of the High Temperature Behavior of Laminates with Time" A.I.E.E. Conference Paper CP 55-234 (1955)

LAMINATED FABRICS
STRUCTURAL MATERIAL OF AIRSHIP ENVELOPES

W. T. Kelly
Naval Air Material Center
Aeronautical Materials Laboratory
Philadelphia 12, Pa.

Aviation pioneers used laminated fabrics to manufacture nonrigid airships for first steered air flight. Since the airship keeps its shape by pressure of the lifting gas, these pioneers had considerable difficulty with change of shape after inflation that could only be corrected by tailoring. In addition, and more important, stresses applied by the rudder when turning could bend the airship and nullify the effect of the rudder. To solve these problems, studies of weave design and biaxial loading effects, the first scientific analysis of a textile material, were performed in the period of 1910 to 1915.(1)* From these studies developed high strength balloon cloths woven in plain and basket weaves, diagonal lamination to control elongation, and use of left and right bias laminations in alternate panels. These improvements in fabric design eliminated elongation problems. However, as larger airships could then be more readily designed in the rigid type, there was little development work on nonrigid type airships until World War II. The laminated fabrics used in nonrigid airships of 1940 to 1950 were similar to the earlier materials except that neoprene was used in place of natural rubber.

The development of electronic means of submarine detection and use of airships as mobile radar in the early warning network necessitated the development of larger airships. These airships are required to be on patrol duty for longer continuous periods; hence, on a yearly basis, the fabric is subjected to more weathering. The large size of these airships results in a considerable loss of helium as the laminated cotton fabric has a

*Numbers refer to literature cited

gas loss of 1/8 cubic foot per square yard per 24 hours. The high strength fabric requirement for these airships has been met by use of two layer cotton laminated fabrics. A 6 ounce per square yard cotton cloth is used for both plies of the fabric for ZPG-2W early warning airships of 1,000,000 cubic foot volume while 7.5 and 8.0 ounce per square yard cloths are used for ZPG-3W airships of 1,500,000 cubic foot capacity. The heavier cotton yarns in these cloths produce a rough surface so that with amounts of coatings previously used, the permeability and weather resistance have not been entirely satisfactory. To avoid use of increased coating, work was directed to the selection of high strength synthetic textile materials of a smoother nature.

The number of synthetic textile fibers has increased in the last few years. However, on a basis of strength and commercial availability, consideration is limited to use of continuous filament nylon, Dacron, Fortisan and glass fibers. The strongest fiber is nylon, whose strength is slightly more than twice that of cotton.

The strengths of glass, Dacron, and Fortisan are approximately equal, 6 to 7 grams per denier, when considered on a strength-weight basis and are only slightly lower in strength than nylon yarns.(2) Strengthwise, laminated fabrics from any of these synthetics should be suitable and in fact several airship envelopes have been made of Fortisan cloths. Moreover, the strength of textile materials is affected by atmospheric conditions. Moisture has an appreciable effect as nylon loses 10 percent and Fortisan and glass lose 15 percent of their dry strength by being wet.(2) The strength of Dacron is not changed by moisture while cotton has a 10-30 percent high strength when wet. The high temperature which result from absorption of radiant energy, such as the wing of an aircraft reaching 193°F in Tucson, Arizona (3) are below that reported (2) to effect the strength of these fibers. The effect of temperature, however, is important when evaluating the laminated fabric because softening of the fiber or loss of adhesion can reduce strength at high temperatures. Laminated fabrics of Fortisan were found to have a 40 percent loss in strength and a 50 percent loss in adhesion when tested at 140°F. On the other hand, strength and adhesion performed at room temperature on this Fortisan fabric after exposure at 158°F for 6 days gave results equal to initial test values.

Another basic property for an airship fabric is low elongation. Cotton, Fortisan, and glass fibers have approximately 7 percent elongation at ultimate strength. The elongation of nylon and Dacron fibers depend upon the degree of orientation received during manufacture. The high tenacity type of Dacron has approximately 13 percent elongation while elongation of high tenacity nylon is 18-23 percent at ultimate strength. The stress-strain curve for Dacron, however, shows that the major part of the elongation occurs after 85 percent of the ultimate load has been applied.(4) Thus, under operating load conditions in an airship, the elongation of Dacron cloths would be less that that of cotton cloths. The fiber elongation also affects flex and crease resistant properties. Bending yarns of low elongation fibers will stress the fibers on the outside of the bend beyond its rupture point. This effect is severe on glass fiber yarns and to a lesser extent on Fortisan yarns. Since the large envelope size will result in considerable creasing and folding during manufacture and erection, glass and Fortisan cloths were not considered for this application.

The cloth properties are governed by the strength necessary to conform to airship design requirements. Since envelope weight subtracts from the available lift, the envelope cannot be subjected to a high weight disadvantage resulting from high factors of safety. The maximum operating pressure in an envelope is designed to set fabric stress at 25 percent of the fabric's ultimate strength. This strength is determined on cylinders 8 inches in diameter and 15 inches long, tested under rapid loading of 5 to 10 seconds. Time load studies based on 1 x 6 inch specimens have indicated that application of the maximum designed load for 8 to 10 years would cause failure.(5) However, maximum loads are only applied for short periods (1 minute) and specimens removed from airships have not shown strength losses that could be attributed to sustained loads.

The airship for which an improved fabric was initially desired was the ZSG-1 design. This envelope has a total length of 282 feet, a maximum diameter of 67 feet, and a volume of 650,000 cubic feet. The fabric stress is at a maximum during ascent when the gas pressure is at 3.5 inches of water. The fabric stress under these conditions is 66 pounds per inch in warp and 58 pounds per inch in filling. Therefore, the nominal strength requirement in the directions of the inner (straight) cloth is 265 pounds per inch in warp and 220 pounds per inch in filling. This is equivalent to loads of 12,000 to 15,000 psi. The cotton cloth previously used for both plies in the laminated fabric weighed five ounces per square yard and was woven in a 4 x 1 twill weave.

The nominal weight of this laminated fabric was 18.8 ounces per square yard of which 6 ounces per square yard consisted of neoprene between the plies.

The properties of a cloth are affected by its weave as it governs the surface characteristics and yarn interaction. Thus cloth permeability, adhesion of the coating, weather resistance, and breaking resistance strength and elongation are modified by the weave. The type of yarn and degree of twist also affect surface characteristics. Thus, selection of cloth details must be based on a combination of factors and no one construction can be said to be the optimum.

The desired cloth construction from a manufacturing aspect is one that would permit its use in both plies. The unavailability of yarns of suitable strengths and deniers to obtain desired strength and optimum surface conditions prevented this type of construction. Thus, a heavier cloth for the straight direction was developed. This cloth weighed 4.35 ounces per square yard and was woven in 2 x 2 basket weave from type 51 Dacron. The nominal breaking strength by the strip method was 205 pounds per inch in warp and filling directions. A cloth weighing 3.35 ounces per square yard and woven in a 3 x 2 twill weave from type 55 Dacron was developed for the outer ply. This cloth had a strength of 110 pounds in the warp and 100 pounds in the filling. The strength of the outer bias cloth is proportionately lower than that of the inner cloth since high strength type 51 Dacron yarns of the necessary denier were not available. The smooth surface of continuous filament yarns produce a flatter fabric. Thus, less coating is necessary on Dacron cloths for permeability and weathering resistance. In order to improve weather resistance of this Dacron fabric, the outer surfaces were coated more heavily than is customary with cotton airship fabrics. In addition, the aluminized coating layer was compounded of chlorosulfonated polyethylene known commercially as Hypalon. This coating has good ozone resistance and should provide good weather resistance.

This laminated fabric of Dacron has a slightly higher cylinder bursting strength, half the permeability, and weighs approximately 3.0 ounces per square yard less than the comparable cotton laminated fabric. This weight reduction results in a weight saving of slightly over 800 pounds for a ZS2G-1 envelope. The weight reductions on larger airships will be greater as high tenacity yarns will be used in both plies. Studies are now in progress to determine the minimum coating weight for permeability and weathering properties.

The permeability of the laminated fabric can be affected by the shearing stresses applied during service. Some fabrics developed for airship envelopes, have shown a considerable increase in permeability when tested under tension. When the tension is removed the fabric rapidly returns to a low permeability state. The tensions in this test are applied in the warp and filling direction of the inner cloth. Thus the shear stresses on the inner coating layer are small. To increase coating shear stresses, a test axis of 30° to the filling of the inner cloth was selected for a cyclic application of load. This direction is used as elongation of the fabric is higher since the load is carried by filling yarns of both plies. The specimen is cut in a "dumbbell" shape 6 inches wide at the 4 inches long central portion and flaring out to a 10-inch width at the ends. A load equal to 25 percent of the breaking load of an identical specimen is applied at 30 cycles a minute. A total of 10,000 cycles are applied with the specimen at 140°F. The permeability of fabrics subjected to this cyclic test has shown good correlation with permeability of similar constructed fabrics removed from airships.

The evaluation procedures performed on the Dacron laminated fabric are based on conditions occurring during airship service. However, in service these various conditions usually occur simultaneously and are not duplicated by various combinations of laboratory tests. Thus, exposure in service is necessary for a complete evaluation. The ZS2G-1 airship of laminated Dacron fabric has been in service less than a year so that only limited information is available. The helium records, however, indicate that the loss of helium is considerably less than that experienced with cotton laminated airship fabric. Development of Dacron laminated fabrics for the larger airships is continuing and it is expected that all near future airships will be of Dacron.

LITERATURE CITED

(1) Haas, Rudolf, Dr. Eng. "The Stretching of the Fabric and the Shape of the Envelope", Third Annual Report of National Advisory Committee for Aeronautics, Gov't. Printing Office 1918.

(2) 1957 Man-Made Fiber Table, Textile World, Sep 1957.

(3) Brooks, C. E. P., "Climate in Everyday Life," New York, Philosophical Library, 1951.

(4) Dacron Technical Manual, E. I. du Pont de Nemours and Co., Inc., Wilmington 98, Del.

(5) Goodyear Aircraft Corporation Report Number R-45-53 "Breaking Strength of Ballon Fabric vs. Time for Failure to Occur" undated.

FOREIGN WOODS OF INTEREST TO THE NAVY FOR SHIPBUILDING APPLICATIONS

J. M. Richolson
D. H. Kallas
A. W. Cizek, Jr.
Naval Material Laboratory
New York Naval Shipyard
Brooklyn, New York

INTRODUCTION

It would seem that wooden vessels have all but disappeared from the modern navy, and wood, itself, appears to be an anachronism in a navy of super-carriers, fleet ballistic missiles and atomic-powered submarines.

This, however, is far from true. Wood played, and still plays, a vital role as a basic raw material in our Navy as well as in other branches of the Defense Department. During World War II wood was first in volume and second in tonnage of raw materials needed for all types of Naval construction afloat and ashore.

But with the compelling exigencies of World War II drastic changes were wrought in the use of wood as an engineering material in Naval construction. The historical craft methods of fabricating wooden members and fashioning them into ships and boats were seriously modified or abandoned completely. New concepts in vessel design, embodying unconventional, but, nevertheless, sound engineering practices, resulted in mass-production techniques which enabled the Navy to build over 40,000 wooden boats and ships during that period. This was made possible through comprehensive research and development programs leading to improvements in laminating and gluing; preservation against decay, fire and marine organisms; fastening systems and bending of wood to form.

The outbreak of the Korean hostilities gave renewed impetus to the concept of wood as an engineering material. Utilizing the structural capabilities of wood, an entirely new class of minesweepers was conceived and constructed in which wood was the principal material.

Today teak is still the best wood for decking on certain classes of submarines. Teak laminated to Douglas fir, or Douglas fir alone, compose the major portion of the flight deck of the Essex class carriers. White oak is the prime structural wood for the frames and keels of minesweepers. Mahogany, cypress and Alaskan cedar may be found as planking in the hulls of the smaller wooden boats. White pine makes an excellent templet wood for laying out steel ship components. The ease of working and dimensional stability favor mahogany and white pine for pattern making while creosoted southern yellow pine, white oak and greenheart are in use as piling or as the heavy structural timbers of piers, wharves and drydocks.

In addition to these specialized uses, millions of board feet of lumber are consumed annually by the Navy in a myriad of industrial operations.

The diminishing supply of the present Navy woods in the quality and dimensions required for ship and boat construction has prompted a continuing search by Naval activities for basic information on alternate species. The extensive tropical and sub-tropical forests offer the best prospects for finding such woods since they comprise the most extensive and diverse stands of timber in the world. It has been estimated that the tropics contain more than 3 billion, 400 million acres of productive forests consisting of thousands of species. Many of these species appear to possess desirable properties but adequate technical data are available for relatively few. From what is known about them, and from what information is being developed on this and similar programs at other laboratories there are indications that certain tropical species equal, or are superior, in many respects to the traditional Naval woods now in use.

The flow chart, Fig. 1, illustrates the organization of the Bureau of Ships foreign wood program and part played in it by the Naval Material Laboratory.

The program has been devised to progressively screen out unpromising species as technical information is developed on them and to continue research on those selected until, ultimately, the most qualified species are placed in service. The initial selection

is made from information supplied by importers of foreign timbers, or by local users in the countries to which the species is indigenous, or from references to the wood in technical or trade journals. Upon authorization by the Bureau of Ships a preliminary study is then undertaken. This consists of a more thorough search of the literature and limited laboratory testing of certain major physical and

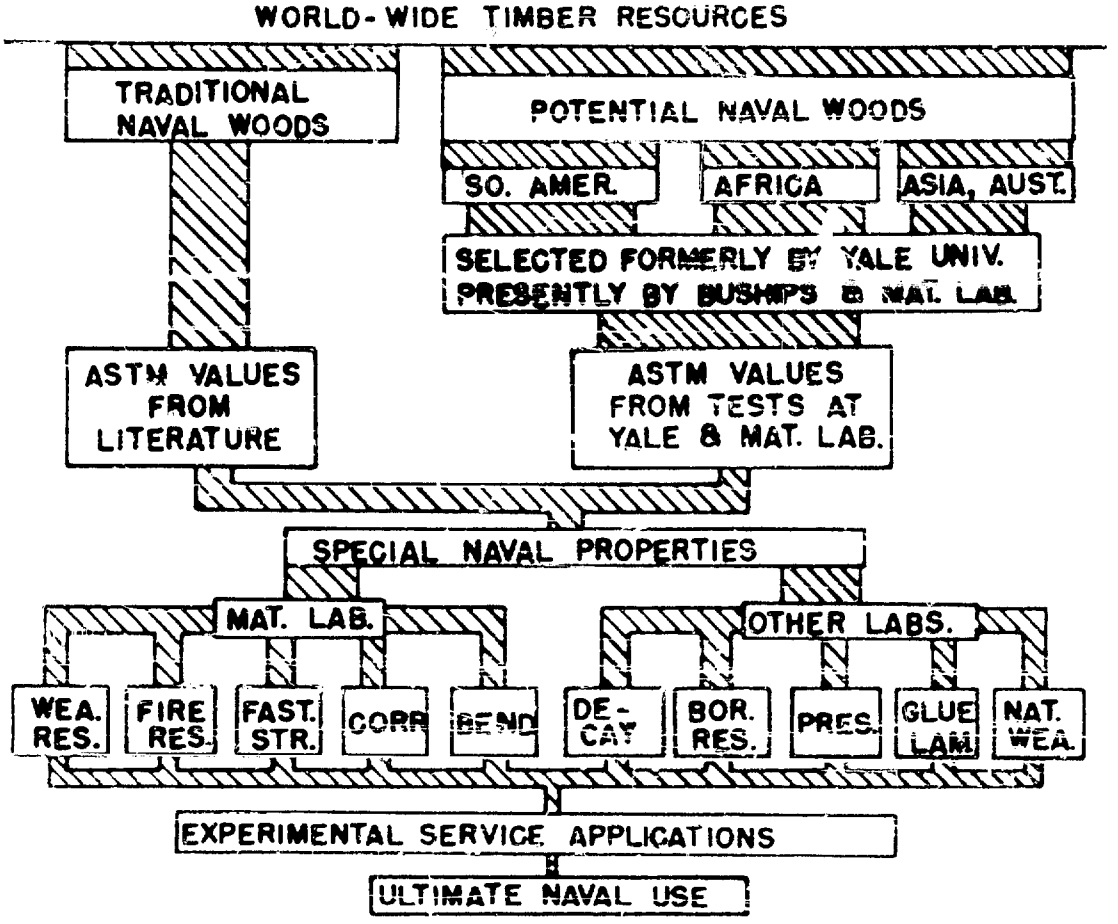

Fig. 1 Organization of BUSHIPS foreign wood program

mechanical properties to determine if further investigation is warranted. A favorable report initiates a comprehensive evaluation of the wood's physical and mechanical properties in the green and air-dry condition of moisture. These are ascertained by the established ASTM test procedures. The results are reviewed and compared against a background of similar information generally available from literature for the traditional shipbuilding woods. Following this phase, the more promising species are scrutinized for their behavior under

conditions pertinent to Naval use. These investigations are listed individually in the flow chart under "SPECIAL NAVAL PROPERTIES". Those conducted at the Naval Material Laboratory are: weathering and abrasion resistance, fire resistance, fastening strength, corrosivity of wood to metal and steam-bending to form. Those studies conducted at other laboratories are concerned with decay resistance, marine borer resistance, preservation, gluing and laminating, and natural weathering. Upon completion of this stage, or sometimes concurrent with it, experimental service applications may be authorized for the species in question. Finally, if the wood has shown high quality in all these respects, it is accepted for Naval use.

The species now being processed through the program and the geographical areas to which these woods are native are indicated in the world map, Fig. 2. The traditional shipbuilding woods are: teak, white oak, mahogany, Douglas fir, cypress, and Alaskan cedar. The

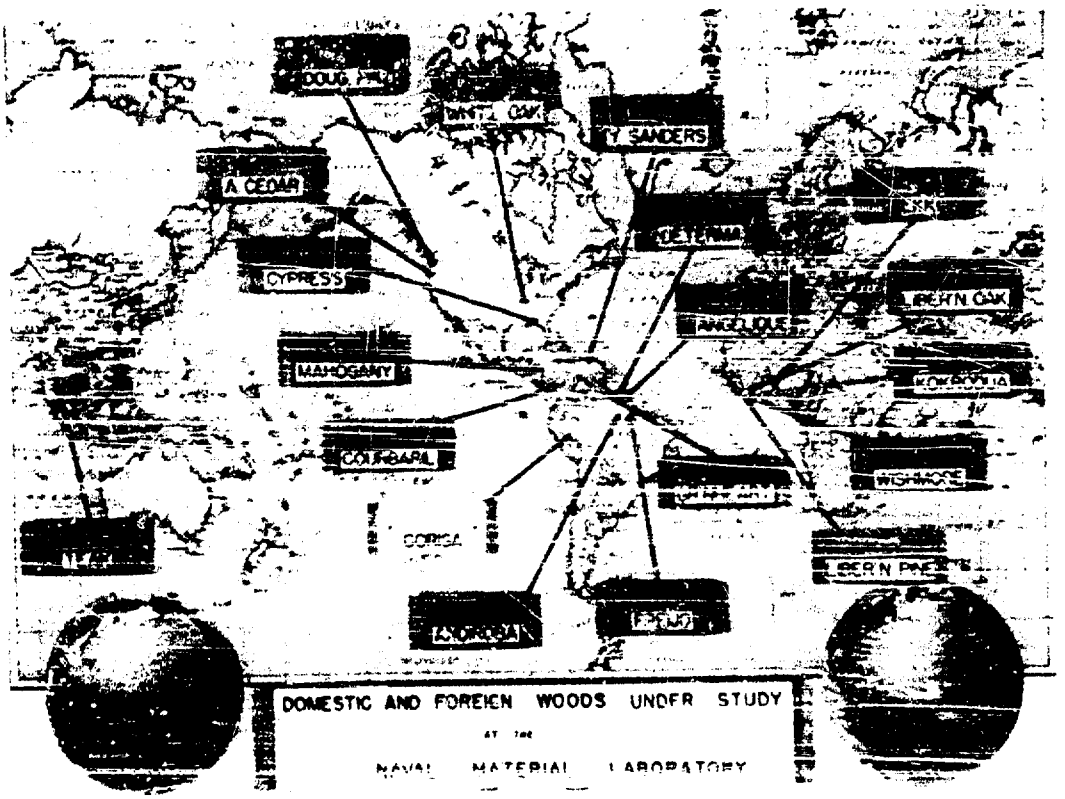

Fig. 2 Distribution of species currently in foreign wood program

South American species are: courbaril, angelique, andiroba, yellow sanders, freijo, determa, greenheart, and corisa. Those from Africa

are: ekki, kokrodua, Liberian pine, Liberian oak, and wishmore.

Most of the work on the physical and mechanical properties of these woods has been evaluated. Values for their mechanical properties are shown in Tables 1 and 2.

TABLE 1. STRENGTH PROPERTIES OF TRADITIONAL NAVAL SHIP BUILDING WOODS *

Common and Botanical Name	Source	Condition	Moisture Content %	Green & Oven-Dry Specific Gravity	Fiber Stress at Proportional Limit psi.	Modulus of Rupture psi.	Modulus of Elasticity 1000 psi	Work to Proportional Limit In-lb/In³	Work to Maximum Load In-lb/In³
White oak		Green	68	0.60	4,700	8,300	1,250	1.2[illegible]	11.6
Quercus sp.	Central U.S.	Air-dry	12	0.71	8,200	15,200	1,780	2.27	14.8
Teak		Green	52	0.58	[illegible],100	11,600	1,590	1.89	10.[illegible]
Tectona grandis	Burma, India	Air-dry	11	0.62	8,200	13,800	1,570	2.51	9.3
Mahogany	Central &	Green	51	0.42	5,100	8,400	1,140	1.14	7.3
Swietenia macrophylla	South America	Air-dry	13	0.46	7,700	10,300	1,[illegible]	2.52	7.5
Douglas fir	Northwest	Green	48	0.41	3,900	6,800	1,350	0.61	6.6
Pseudotsuga menziesii	U.S.	Air-dry	12	0.44	7,400	11,200	1,640	1.87	8.5
Baldcypress	Southern	Green	90	0.42	4,200	6,600	1,180	0.91	6.6
Taxodium distichum	U.S.	Air-dry	12	0.48	7,200	10,600	1,440	2.15	8.2
Alaskan cedar	Alaska & N.W.	Green	38	0.42	3,900	6,400	1,140	0.77	[illegible].2
Chamaecyparis nootkatensis	U.S.	Air-dry	12	0.44	7,100	11,100	1,420	2.04	10.4

Common Name	Condition	Compression Parallel to Grain: Fiber Stress at Proportional Limit psi.	Compression Parallel to Grain: Maximum Crushing Strength psi.	Compression Parallel to Grain: Modulus of Elasticity 1000 psi	Hardness End lb.	Hardness Side lb.	Compression Perpendicular to Grain** psi.	Tension Perpendicular to Grain psi.	Shear psi.	Cleavage lb/in. width	Toughness in-lb
White oak	Green	3,100	3,560	-	1,120	1,070	830	770	1,250	420	-
	Air-dry	4,800	7,440	-	1,520	1,360	1,320	[illegible]	2,000	450	225
Teak	Green	4,100	5,490	1,760	930	980	1,040	960	1,300	420	84
	Air-dry	5,200	7,520	1,590	[illegible]	1,150	1,190	980	1,360	340	-
Mahogany	Green	2,700	3,[illegible]	1,040	1,160	1,060	1,390	750	1,500	280	84
	Air-dry	4,200	5,680	1,200	1,030	[illegible]	1,250	620	1,510	280	-
Douglas fir	Green	2,600	3,900	-	520	450	420	300	840	190	170
	Air-dry	5,800	6,720	-	710	600	920	340	1,130	190	120
Baldcypress	Green	3,1[illegible]	3,580	-	[illegible]	390	500	300	810	180	-
	Air-dry	4,[illegible]	6,360	-	[illegible]	[illegible]	900	270	1,000	170	-
Alaskan cedar	Green	[illegible]	3,050	-	[illegible]	[illegible]	530	330	[illegible]	170	-
	Air-dry	[illegible]	6,310	-	[illegible]	580	770	[illegible]	1,130	190	120

* Data from literature ** Fiber stress at proportional limit

The bar graphs, Figs. 3, 4, 5 and 6, illustrate a typical evaluation of the present and potential alternate species used as structural members, planking, and decking for boats and ships and marine timbers for heavy construction, respectively. For the purpose of these illustrations only four properties have been included.

Preliminary to investigating the foreign woods for those special Naval properties for which the Naval Material Laboratory is responsible, it was necessary first to develop new testing techniques for these properties since there were not standards similar to the ASTM procedures for the mechanical properties of wood. With these techniques, reference values were obtained for the present navy woods. These values are discussed for four of the five special Naval

TABLE 2. STRENGTH PROPERTIES OF TYPICAL WOODS POTENTIALLY SUITABLE FOR NAVAL USE

Common and Botanical Name	Source	Condition	Moisture Content %	Green & Oven-Dry Specific Gravity	Static Bending: Fiber Stress at Proportional Limit psi.	Static Bending: Modulus of Rupture psi.	Static Bending: Modulus of Elasticity 1000 psi.	Static Bending: Work to Proportional Limit in-lb/cu.in.	Static Bending: Work to ultimate load in-lb/cu.in.
Courbaril (1)	Panama, P. Rico	Green	60.8	0.71	7,900	12,900	1,840	1.82	11.4
Hymenaea courbaril	Honduras	Air-dry	12.6	0.71	11,900	19,400	2,160	3.72	17.6
Anacolosa (1)		Green	78.7	0.60	7,700	11,400	1,840	1.57	12.0
Diecrynia guianensis	Surinam	Air-dry	11.8	0.69	11,600	17,400	2,190	3.32	15.7
Yellow sanders (1)		Green	65.1	0.59	6,300	10,100	1,460	1.69	8.8
Ruprechtia coriacea	Puerto Rico	Air-dry	10.7	0.66	7,700	13,000	1,650	2.74	8.7
Freije (1)		Green	63.4	0.52	7,500	10,500	1,830	1.58	11.2
Cordia Goeldiana	Brazil	Air-dry	10.7	0.59	10,600	14,700	2,090	3.00	15.9
Andiroba (1)	Brazil	Green	65.0	0.54	6,600	10,300	1,690	1.48	9.8
Carapa guianensis	Surinam	Air-dry	13.0	0.60	10,200	15,500	2,000	3.74	14.0
Waterma (1)	Br. Guiana	Green	83.2	0.52	6,400	7,800	1,460	1.18	6.8
Ocotea rubra	Surinam	Air-dry	12.8	0.58	7,600	10,500	1,820	2.00	8.4
Ekki (2)		Green	41.5	0.83	9,150	16,900	2,170	2.48	17.3
Lophira procera	W. Africa	Air-dry	17.3	0.89	13,900	22,900	2,730	3.96	31.9
Kokrodua (2)		Green	66.4	0.41	6,400	12,500	1,510	1.66	12.7
Afrormosia elata	Ghana	Air-dry	12.0	0.41	10,000	14,600	1,650	1.78	12.5
Liberian pine (2)		Green	51.7	0.56	8,100	12,900	2,250	1.67	13.0
Pseudocarpidiophora sp.	Liberia	Air-dry	13.1	0.65	11,300	18,600	2,580	2.75	21.3
Liberian oak (2)		Green	47.6	0.66	7,800	15,200	2,340	1.53	14.0
Piptadeniastrum sp.	Liberia	Air-dry	13.2	0.76	12,100	20,600	2,750	2.95	19.6
Wismore (2)		Green	71.4	0.54	6,100	12,000	1,910	1.11	10.9
Terretia utilis	Liberia	Air-dry	17.7	0.60	8,200	15,600	2,120	1.79	16.0
Greenheart (3)	Br. Guiana	Green	42.2	0.88	12,900	19,500	2,980	3.41	13.3
Ocotea rodiaei	Surinam	Air-dry	13.0	1.06	16,200	28,000	3,550	-	22.0

Common Name	Condition	Compression Parallel to Grain: Fiber Stress at Proportional Limit psi.	Compression Parallel to Grain: Maximum Crushing Strength psi.	Compression Parallel to Grain: Modulus of Elasticity 1000 psi.	Hardness: End lb.	Hardness: Side lb.	Compression Perpendicular to Grain psi.	Tension Perpendicular to Grain psi.	Shear psi.	Cleavage lb/in. width	Toughness in.-lb.
Courbaril	Green	4,330	5,870	1,560	1,780	1,970	1,640	1,830	1,770	540	231
	Air-dry	6,570	9,930	2,[illegible]	2,520	2,350	1,880	360	2,470	470	-
Anacolosa	Green	4,870	5,600	2,180	1,100	1,100	1,000	700	1,340	340	151
	Air-dry	[illegible]	[illegible]	[illegible]	[illegible]	[illegible]	[illegible]	[illegible]	[illegible]	360	-
Yellow Sanders	Green	3,800	5,100	1,[illegible]	1,350	1,230	1,070	800	1,340	430	123
	Air-dry	5,200	7,400	1,770	1,830	1,720	1,280	460	1,[illegible]	290	-
Freije	Green	4,200	4,900	1,[illegible]	[illegible]	1,020	520	610	1,090	270	195
	Air-dry	5,800	7,200	2,110	1,300	1,190	720	400	1,410	250	-
Andiroba	Green	4,000	4,800	1,[illegible]	960	880	730	560	1,220	340	112
	Air-dry	6,100	8,100	2,[illegible]	1,300	1,130	830	440	1,540	240	-
Waterma	Green	3,000	3,800	1,[illegible]	450	520	550	490	860	240	75
	Air-dry	4,[illegible]	5,[illegible]	1,[illegible]	590	660	660	640	940	220	-
Ekki	Green	5,300	7,800	2,[illegible]	2,360	2,150	1,290	840	1,690	510	200
	Air-dry	8,500	10,500	2,730	4,310	3,810	2,470	980	2,650	610	-
Kokrodua	Green	4,[illegible]	6,200	1,760	1,490	1,150	970	840	1,470	490	199
	Air-dry	5,[illegible]	8,[illegible]	1,930	1,710	1,390	1,540	580	1,[illegible]	360	186
Liberian pine	Green	4,[illegible]	5,800	2,[illegible]	960	910	680	640	1,900	410	-
	Air-dry	6,[illegible]	9,[illegible]	2,760	1,170	1,190	1,110	710	1,810	590	191
Liberian oak	Green	5,[illegible]	6,800	2,[illegible]	1,370	1,280	830	700	1,630	440	-
	Air-dry	7,[illegible]	10,[illegible]	2,[illegible]	1,[illegible]	1,[illegible]	1,400	980	1,650	980	175
Wismore	Green	3,[illegible]	5,[illegible]	1,760	970	920	700	710	1,230	450	179
	Air-dry	6,200	8,[illegible]	2,260	1,030	1,[illegible]	950	700	1,[illegible]	410	140
Greenheart	Green	7,800	10,300	3,[illegible]	2,710	2,230	2,020	1,070	1,[illegible]	980	-
	Air-dry	10,[illegible]	14,000	4,[illegible]	2,150	2,[illegible]	2,090	1,080	2,330	-	-

(1) Data from Yale University; (2) Data from Naval Material Laboratory; (3) Data from literature

* Fiber stress at proportional limit

properties, the first of which is weathering and abrasion resistance.

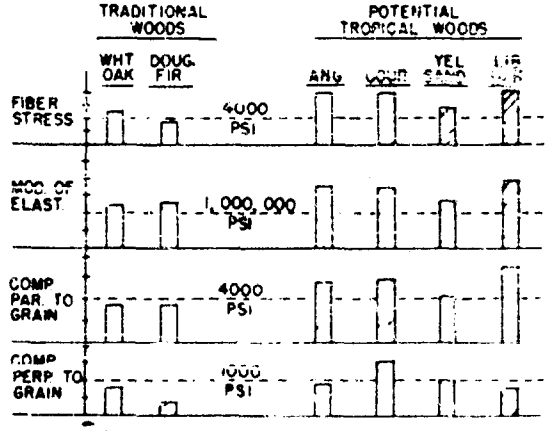

Fig. 3 Four mechanical properties of traditional shipbuilding woods compared with those tropical species potentially suitable as structural woods.

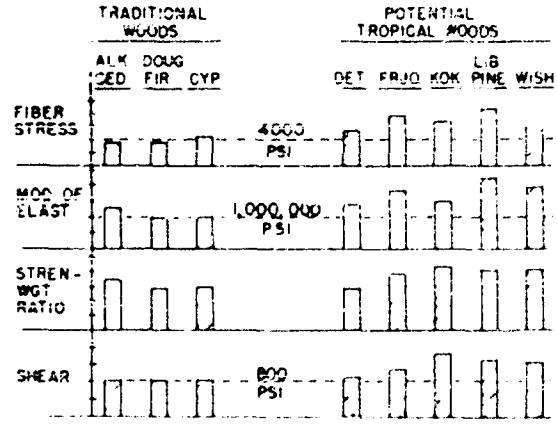

Fig. 4 Four mechanical properties of traditional shipbuilding woods compared with those tropical species potentially suitable as planking woods.

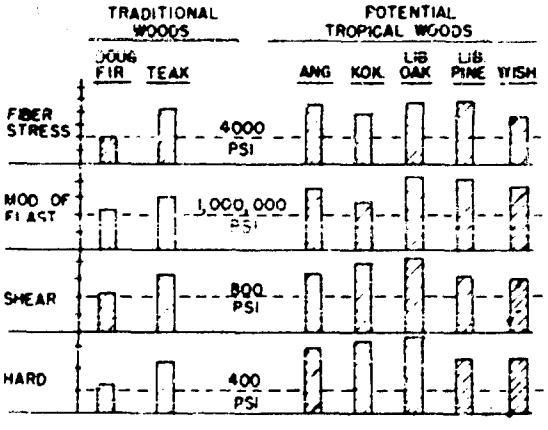

Fig. 5 Four mechanical properties of traditional shipbuilding woods compared with those tropical species potentially suitable as decking woods.

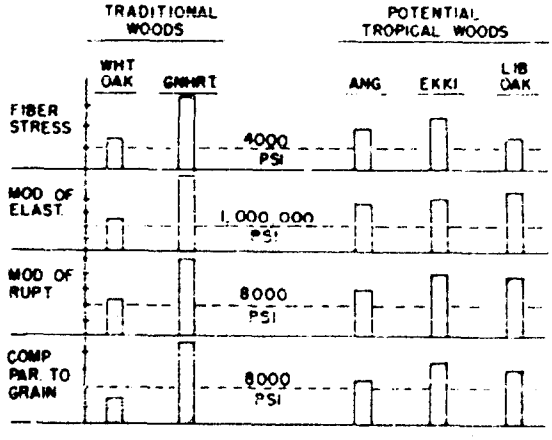

Fig. 6 Four mechanical properties of traditional shipbuilding woods compared with those tropical species potentially suitable as marine timbers for heavy construction.

WEATHERING AND ABRASION RESISTANCE

It has been demonstrated that the abrasion characteristics of a wood under heavy traffic are altered when, in addition, the wood is exposed to the deteriorating effects of outdoor weathering. These conditions are continually present in wood used as the flight decks of carriers or the weather decks of other vessels. This investigation attempted to quantitatively estimate the deterioration due to weathering and to determine the rate at which the weathered surface was being abraded. Teak and Douglas fir were selected as the reference species since they are the predominant decking woods. The abrasion phase has yet to be completed. But when it is finished these procedures will be employed in similar investigations of the tropical woods potentially suitable for deckings.

Essentially, the weathering study consisted of treating the surface of unweathered and laboratory weathered teak and Douglas fir with a radioactive isotope solution and determining the activity rate of each as then sections were sliced from the surface with a microtome until the background activity was reached. The instrumentation, shown in Figure 7, consisted of a microtome, Part A, for sequential sectioning of the test surface, a TGC geiger tube, Part B, mounted so

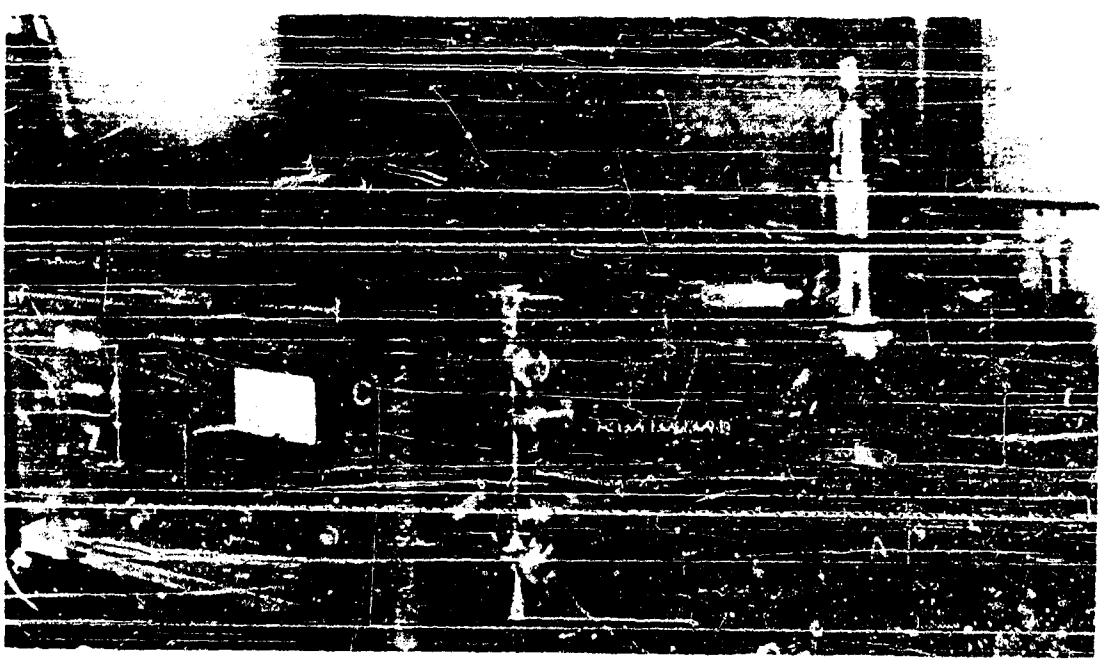

Fig. 7 Instrumentation used in conjunction with radio isotope tracer technique for determining weathering characteristics of wood.

as to enable it to be swung over the test surface when the activity count was read and away when the test surface was being sectioned, and a scaling unit, Part C, for recording the activity. The basic steps in the procedure were as follows: The four sides of the test block were coated with a paraffin wax and the surface to be evaluated was sealed with a proprietary silicon compound to prevent absorption of the isotope solution beneath the surface. The use of silicon compound did not occlude the cavities in the surface nor alter its contour. Radioactive phosphoric acid, with a little aerosol added as a wetting agent, was flowed onto the surface in excess and the treated block centrifuged to remove the excess. Centrifuging was continued until a constant activity count was established. The prepared block was carefully oriented in the microtome and an initial count taken. A 30 micron section was removed by slicing with the microtome knife. Alternately thereafter, counting and slicing were continued to background.

The following results were obtained: Figure 8 shows the results for teak and Figure 9, those for Douglas fir. The shaded

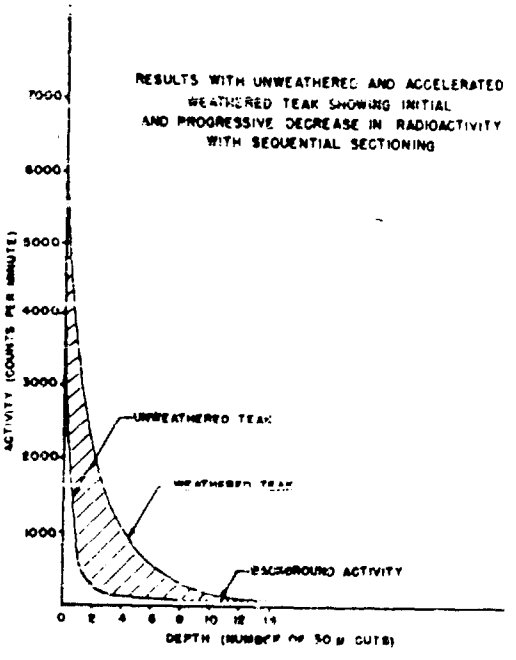

Fig. 8 Results for the accelerated weathering of teak.

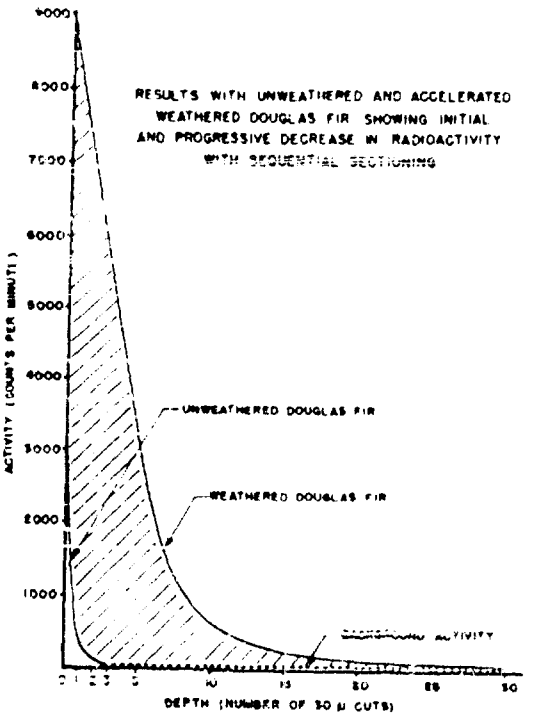

Fig. 9 Results for the accelerated weathering of Douglas fir.

areas, which represent the volume of weathered wood removed, indicate that teak weathers approximately three times better than Douglas fir and shipboard experience testifies to the superiority of teak.

Verification of the sensitivity of the radioisotope tracer technique in measuring the weathering effects was demonstrated in a series of associated experiments. The first experiment showed that the major deterioration produced by natural weather aging of wood could be reproduced by exposure in the Laboratory's accelerated light and weather aging apparatus. The results are illustrated in Figures 10 and 11. The first shows the change in teak before and after aging;

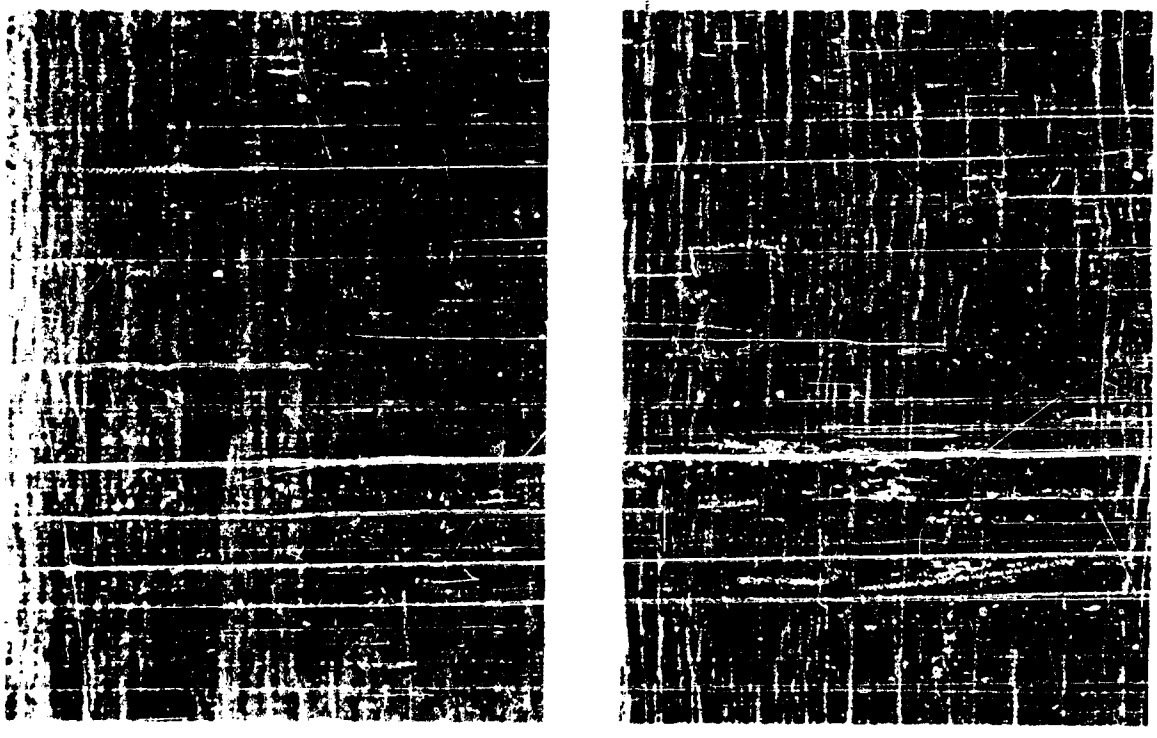

Fig. 10 Surface of teak before and after accelerated weathering.

the proliferation of surface checks and erosion of the softer parenchymatomous tissues are evident. The second reveals similar changes in Douglas fir with the accompanying effects of "raised grain" common in the natural weathering of softwoods. The second experiment indicated that the amount of surface deterioration induced by accelerated weathering could be integrated by the radioisotope tracer technique into a quantitative measure of this deterioration. To test this, sets of wood blocks, sawn from material which had been

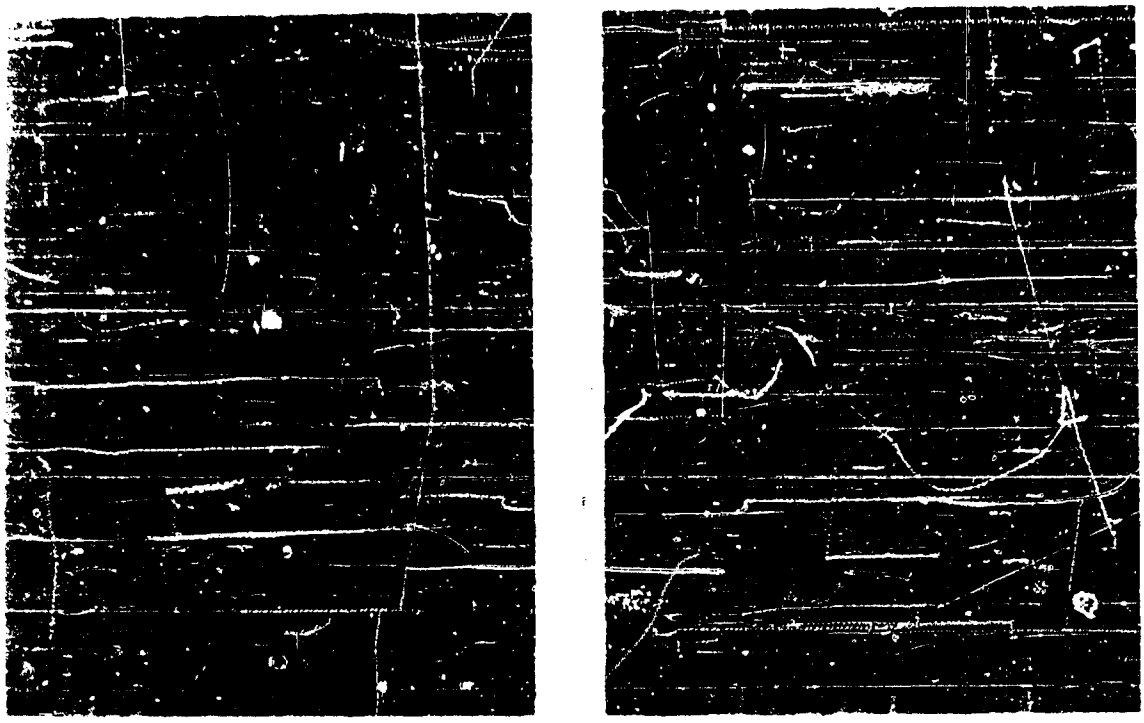

Fig. 11 Surface of Douglas fir before and after accelerated weathering.

previously planed smooth, were individually scored with 1, 2, 4, 8 and 16 grooves in a milling machine to a uniform depth of 1/32 inch. Initial activity counts were made on each block of each set; the average initial count of each set of blocks were plotted against the number of grooves. The results showed a linear increase in activity with an increase in the number of grooves. The third experiment demonstrated that the depth of surface deterioration could be determined by probing with the tracer solution. To confirm this, blocks similarly prepared to those above, were sequentially sectioned in the microtome and the number of sections required to be removed to reach background activity, was recorded. Each section averaged 30 microns in thickness. The average total number of sections removed multiplied by 30 microns equalled 0.0937 inch which is within 8 per cent of 1/32 inch. Moreover, it is of interest to note that the number of sections required to reach background for unweathered teak and Douglas fir, when multiplied by 30 microns, coincided well with the diameters of their largest wood cells which would show as troughs in the surface of wood planed smooth.

FASTENING STRENGTH

It became evident early in the investigation of fastening

strength that the standards developed for industrial use with the low to moderately dense U.S.-grown woods, using steel screws, were not directly applicable to the high density tropical woods for which naval construction requires the insertion of softer metal screws such as silicon bronze and brass. As the screw is driven deeper into the wood, driving resistance increases (Figures 12, 13 and 14) and, if sufficiently high, may result in torsional failure of the fastener.

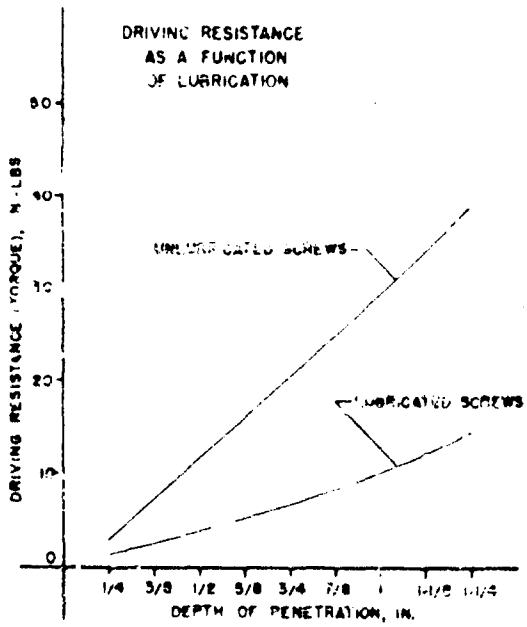

Fig. 12 Reduction in driving resistance due to lubrication of the screw before insertion.

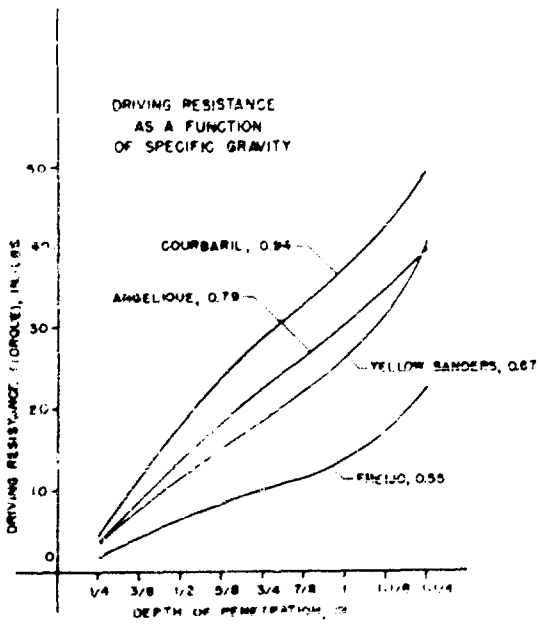

Fig. 13 Reduction in driving resistance due to a decrease in the specific gravity of the wood.

Driving resistance may be considerably reduced by the use of a lubricant (Figure 12). It is less with the lower density woods (Figure 13) and also decreases with an increase in the size of the lead hole (Figure 14).

But the over-riding factor is the lead hole size - if it is too small either the screw may fail in driving or the wood may split; if too large, holding power is lost. Consequently there is an optimum size for the lead hole. These were empirically determined for each foreign wood before the fastening strength value for the wood was investigated. The results for fastening strength show that, as a group, the tropical woods exceed the traditional woods in screw-holding power. This observation was further explored in a study of the relationship between specific gravity and fastening strength with values abstracted from the literature. The results

of this study are shown in Figure 15. The Wood Handbook equation represents predicted values for holding power derived from experimental data on domestic woods, the bulk of which lie in a specific

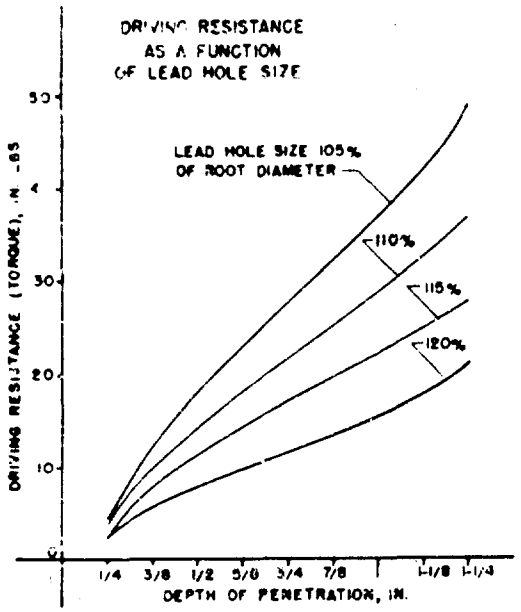

Fig. 14 Reduction in driving resistance screw due to an increase in the lead hole size.

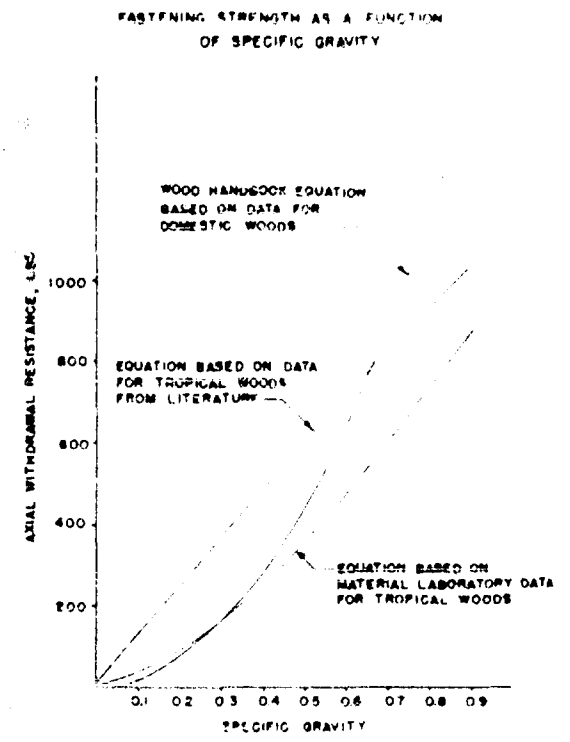

Fig. 15 Relationship between fastening strength of wood and its specific gravity.

gravity range between 0.40 and 0.70. The Material Laboratory equation is lower than that computed from the data for tropical woods taken from the literature since in the latter case holding power values were obtained with ferrous screws of short length, the combination of which permitted the use of smaller lead holes.

CORROSIVITY OF WOOD TO METAL

Wood and metal in intimate contact in a marine environment undergo a deterioration which involves electrochemical reactions that induce metallic corrosion and degeneration of wood fibers in the immediate vicinity of the metal. When it occurs in wooden vessels, it is commonly referred to as "nail sickness" since it is most frequently found in association with metal fasteners. In

advanced cases leakage around the fastener may [illegible]. The joint may become slack resulting in a structural weakness which may become aggravated by the working stresses of the vessel to a point where the vessel is no longer seaworthy.

Exposed to conditions which favor corrosion in a marine environment, all woods are subject to electrochemical attack. Woods differ, however, in their ability to resist such attack and in their inherent corrosiveness to various metals. In this investigation a technique was developed for determining the relative corrosivity of various woods to different classes of metal screws. Test specimens were prepared from each kind of wood with five classes of screws; each specimen consisted of a wood block, 1 x 1 x 2 inches, and an embedded screw countersunk and capped with a wood plug. Three sets of specimens were prepared; one set was placed in an accelerated corrosion test cabinet and subjected to continuous salt fog humidity at a temperature of 95°F. A second set was immersed in salt water at room temperature. This set and the salt fog humidity set were composed of specimens containing screws lubricated with a beeswax compound before insertion. The third set was also immersed in salt water but consisted of specimens with unlubricated screws. Lubrication of screws to ease insertion is a common shipyard practice and, therefore, was included in the test procedure. The screws were carefully cleaned and weighed before insertion. Periodically, eight specimens for each wood block-screw combination were removed from the test conditions. The blocks were then split open, and the screws extracted, chemically cleaned, and reweighed. The per cent loss in weight of metal was interpreted as a measure of the corrosivity of the wood.

The reference values obtained with the traditional shipbuilding woods are shown in Figures 16, 17 and 18. Figure 16 shows the relative corrosivity of five naval woods after various intervals of exposure to a high salt fog humidity at a temperature of 95°F. Each curve is the composite value of five different classes of screws. Figure 17 shows the same data that previously seen but here the relative difference in corrosion of the screws is indicated by averaging the values for the five kinds of wood. It is of interest to note the position of the silicon bronze screws with respect to brass and chromeplated brass. Figure 18 indicates the relative difference in corrosion effects induced by the three test conditions described above. The tendency of the screw lubricant to retrap corrosion is evident from the results for the salt water immersion test condition.

STEAM-BENDING

A common method for bending wood to form is to first

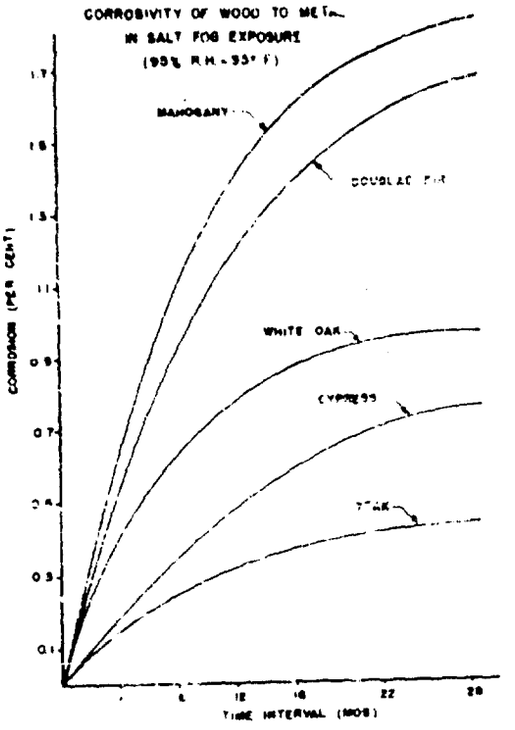

Fig. 16 Corrosivity of wood to metal under salt fog exposure (95% R.H. - 95°F).

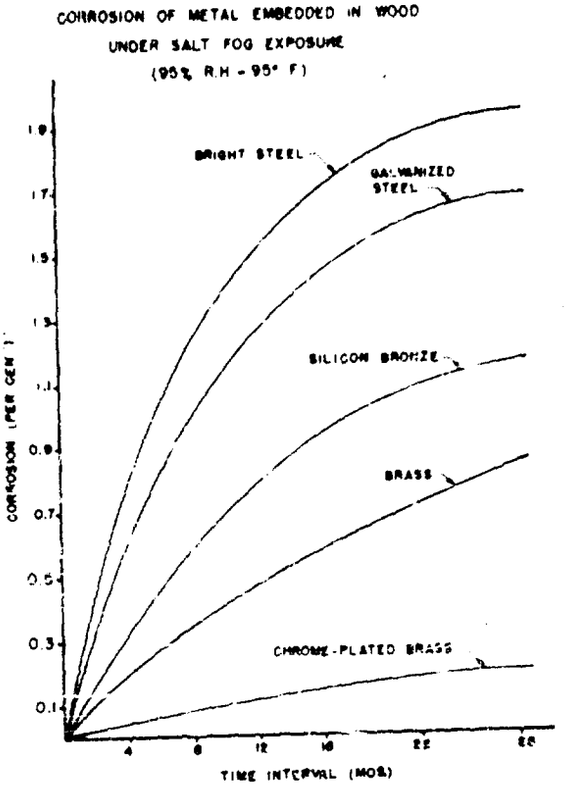

Fig. 17 Corrosion rates of metal screws embedded in wood under salt exposure (95% R.H. - 95°F).

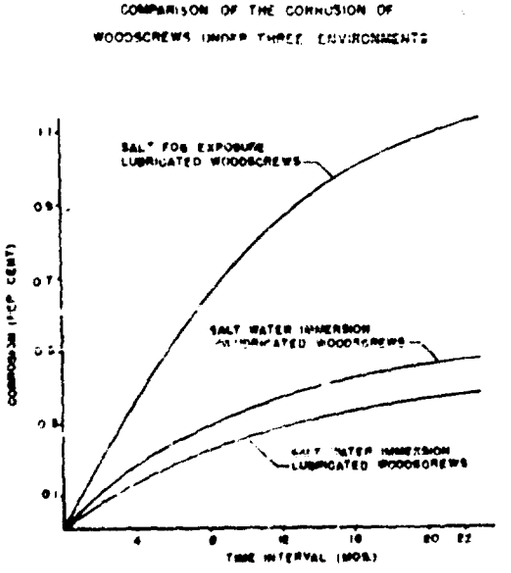

Fig. 18 Comparison of the corrosion rates of wood screws embedded in wood under three conditions of test.

plasticize the wood by steaming and then bend it in a machine to the desired shape. Several basic steps are followed in performing this operation. They are: (1) selection of suitable bending stock; (2) seasoning of the wood to a moisture content about 25 per cent; (3) sawing and planing the bending blank from the stock; (4) softening the bending blank by steaming; (5) bending the blank by machine into a bent member; and (6) fixing and drying the bent member.

Bending stock, which is predominantly obtained from white oak, is required to be straight grained, reasonably free of defects, and at a moisture content in excess of 20 per cent. After selection the stock is machined by sawing and planing to approximately the desired dimensions into bending blanks. The blanks are then softened by steaming at atmospheric pressure scheduled at one hour of steaming for each inch of thickness. After steaming the plasticized blank is placed in a bending machine and bent to form. End pressure is used to prevent excessive elongation of the convex side of the bend and to induce small uniformly distributed compression failures to form on the concave side. Following this operation the bent member is kept in restraint and dried to an appropriate moisture content, ready for use. The laboratory in its studies followed the above basic steps in preparation of test specimens of white oak, 1 x 1 3/4 x 28 1/2 inches in dimension. Figures 19 and 20 show a bent specimen at the start and completion of the bending operation. The code letters refer to the following parts:

Code Letter	Part
A-A'	Hydraulic rams
B-B'	End plates
C	Minor straps (with shackles for securing turnbuckle)
D	Wood test specimen
E	Bending form
F-F'	Reversed levers
G	Major strap (welded at ends to reversed levers)
H	Clamping screw
I	Elongation-indicator assembly
J-J'	Flexible high pressure hydrualic hose
K-K'	Hydraulic ram brackets (bolted to reversed levers)
L	High pressure copper tubing (connected to hydraulic pump, not shown)
M-M'	Flexible wire rope (pulled by winch connected to electric motor not shown)

Code Letter	Part
N	Double pulley assembly
O	Turnbuckle (for securing minor strap during drying
P	Stay lath - (a second stay lath is secured to underside of the bent specimen immediately after it is removed from the form to prevent twisting during drying.

Fig. 19 Wood bending machine showing specimen at start of bending operation.

The bent specimen is subsequently kept in restraint as shown in Figure 21 during the fixing and drying stage.

After drying, the bent specimens were evaluated for their residual strength by testing them in static bending and comparing the results for modulus of elasticity, fiber stress at the proportional limit and modulus of rupture with similar values obtained from static bending tests on matched straight specimens. Figure 22 show the start and finish of a static bending test on a bent specimen. Results for white oak indicate that this wood retains 45 per cent of its original stiffness, 72 per cent of its resistance to

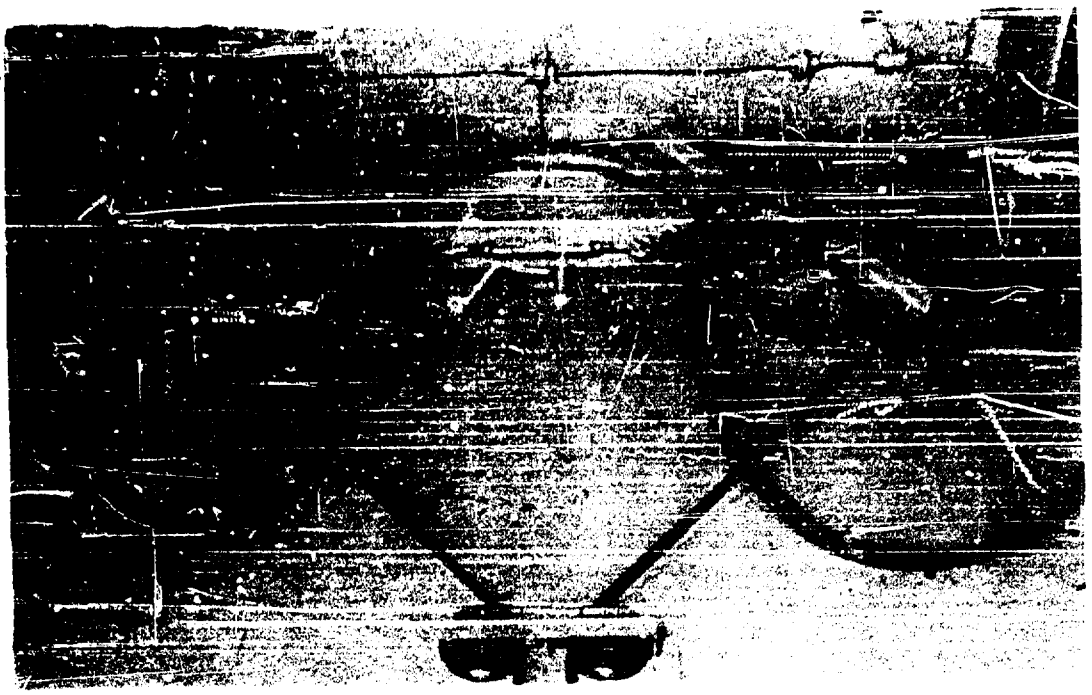

Fig. 20 Wood bending machine showing specimen at completion of bending operation.

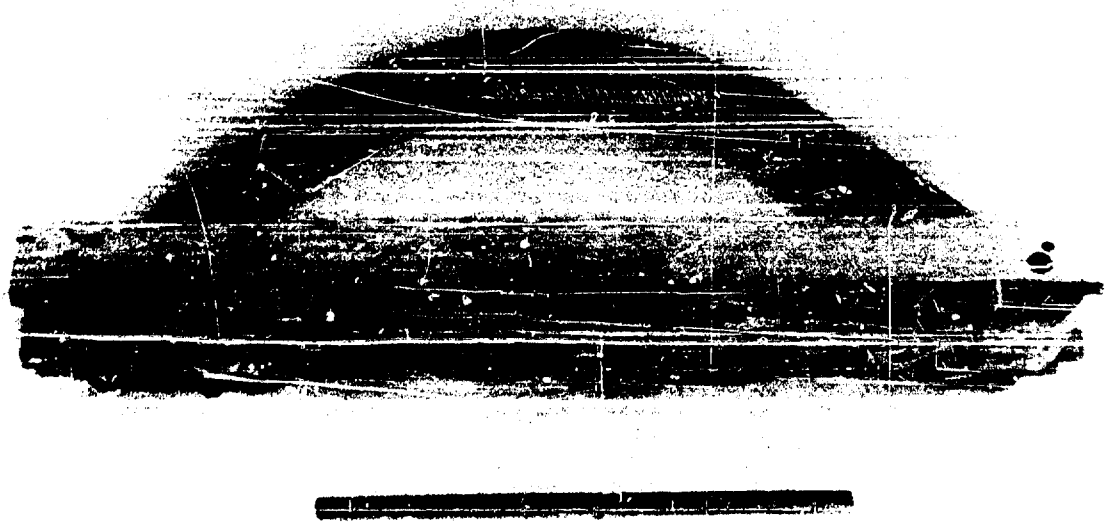

Fig. 21 Bending specimen showing system of restraint during fixing and drying phase.

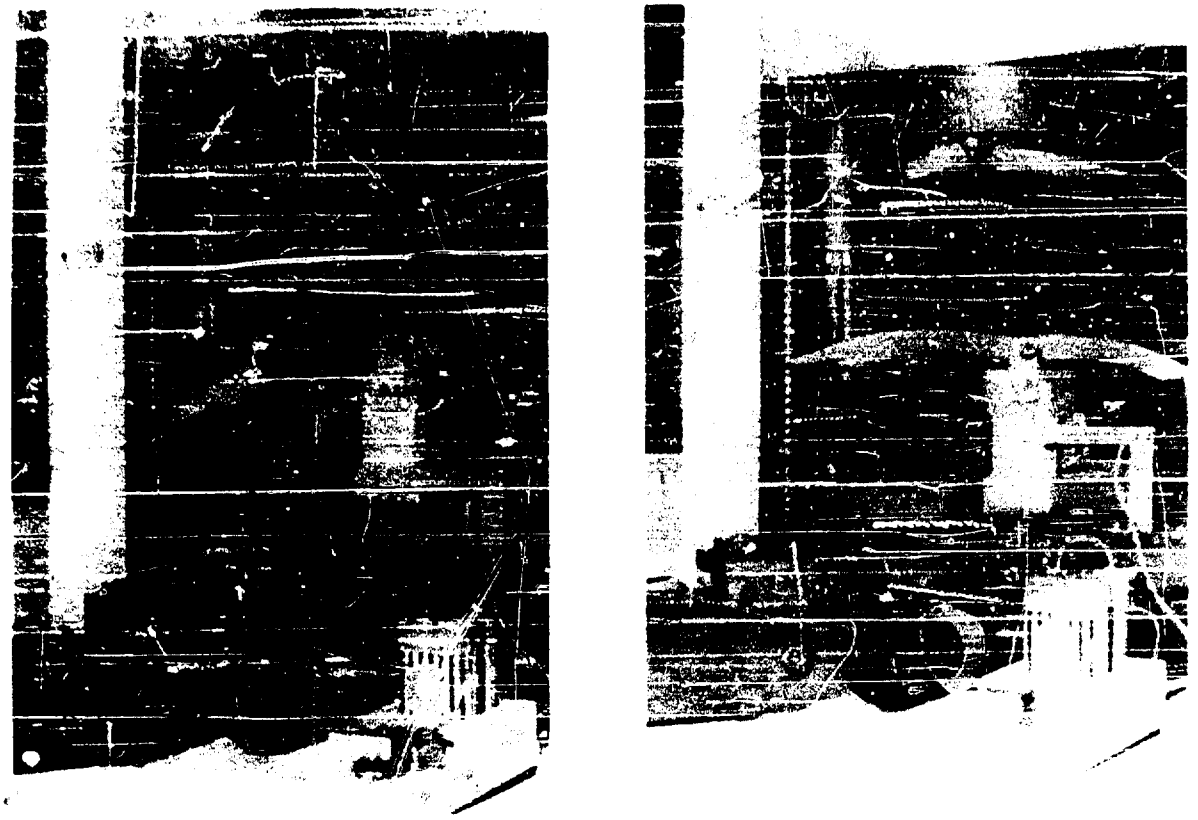

Fig. 22 Bending specimen at start and near completion of static bending test.

deformation and 74 per cent of its ultimate strength after bending. These values are considered as the references against which will be compared those similarly obtained on foreign woods.

TRIAL APPLICATIONS

Concurrent with these investigations trial applications of several of the foreign woods are in progress. An experimental installation of ekki and angelique has been made in the retractable fender system of the New York Naval Shipyard. Ekki is also in use, experimentally, as the bumper timbers in the bottoms of acid-pickling tanks in the shipyard while the Pattern Shop has found corisa to be a favorable alternate for mahogany for certain types of patterns.

ADDITIONAL BENEFITS TO THE NAVY

The ultimate objective of the foreign wood program was defined in the flow chart, Figure 1 and its realization is being

demonstrated in the trial applications just mentioned. But as in any research endeavor the solution of one problem generally uncovers others, new and unexpected. Or frequently, a laboratory technique, developed for one study may be applied, in its essentials, to another. For example, the radioisotope tracer technique developed in the weathering study has the potentialities of being used in preservation studies for tracing the absorption and penetration of wood preservatives. During the fastening strength investigation it was demonstrated that indiscriminate use of a commercially available countersink and wood drill to bore lead holes could result in a loss in holding power as much as 25 per cent in certain woods. This has generated interest in the small tool section of the Bureau of Ships. The need for exceptionally large lead holes to insert the nonferrous screws in high density tropical hardwoods to avoid failure of the screw has been brought to the attention of the wood screw industry by the Metallurgical Process Section of the Bureau for the purpose of developing higher strength screws. The reduction in driving resistance and in the rate of corrosion through the use of the beeswax compound demonstrated in the fastening strength and corrosivity investigations, respectively, point to the possibility of developing a polymerizing compound which in its liquid phase could be inserted into the lead hole to act as a screw lubricant, and in its polymerized state, encapsulate the fastener in an anti-corrosion coating while at the same time adding to the strength of the wood fibers deformed by the driven screw. The unanticipated behavior of the silicon bronze screws compared with that for brass and chromeplated brass screws in the corrosivity investigation warrants further examination. The difficulties experienced in bending certain tropical woods in the steam-bending investigations currently underway indicate a need for improving the methods of plasticizing the wood and for maintaining close control during the bending operation.

As the foreign wood program advances, undoubtedly other problems will also arise to demand solution, but, we trust, the results of all these efforts will accrue to the benefit of the Navy in those areas where the special properties of wood make it desirable for use.

RELIABILITY OF NAVY AIRCREW SAFETY AND SURVIVAL EQUIPMENT MECHANICAL SYSTEMS - MATERIAL SELECTION AND MANUFACTURING PROCESSES

Captain Roland A. Bosee, MSC, USN, James V. Correale, Jr., BS in ME and Dino A. Mancinelli, BS in ME, Air Crew Equipment Laboratory, Naval Air Material Center, Philadelphia 12, Pa.

The expanded flight envelope of current and future first line naval aircraft has demanded correspondingly expanded performance spectrum of the aircrew safety and survival equipment mechanical systems. Tolerances on performance is critical and it has been necessary to conduct a concurrent program of miniaturization and redesign. In order to satisfy these requirements and trends, designers have had to utilize the latest developments in material engineering and introduce the "unique" in basic designs.

This paper will deal exclusively with the recent development and production difficulties encountered with aviators' oxygen breathing regulators and the control system essential for the operation of the full pressure or space suit system.

BREATHING REGULATORS

New concepts in breathing regulator designs have made possible a reduction in the envelope of the regulator to the extent shown in figures 1 and 2 and a reduction of weight from 2.75 pounds to 0.5 pounds. The many possible advantages apparent from this major change led to an expedited program of prototype design evaluation, qualification tests, and preproduction tests.

Design prototypes of these equipment articles as shown in figure 2 were developed. After the normal developmental evaluation difficulties and redefinition and realignment of performance characteristics, qualification items were produced. At this point reliability and material selection difficulties were encountered.

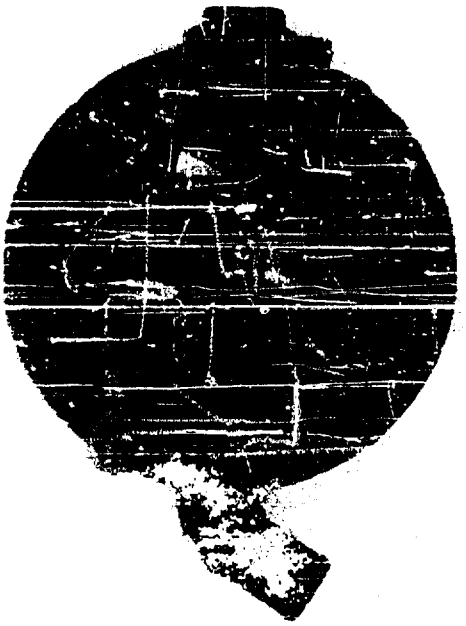

Figure 1 - Console mounted demand type oxygen breathing regulator

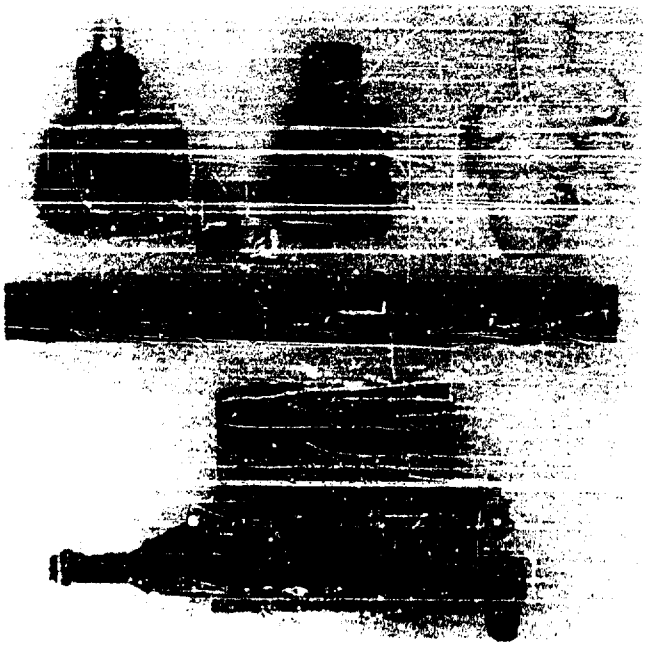

Figure 2 - Miniaturized demand type oxygen breathing regulator

On the first model oxygen regulator, the qualification item was approved after several minor performance problems were solved. Upon receipt of a procurement contract, the contractor submitted preproduction samples. Because of urgent delivery requirements and because prototype and qualification samples had been recently completely tested, lengthy endurance evaluations were not conducted and only spot tests were performed. As a result of this limited investigation the preproduction samples were approved. However, after limited operational use, leaks developed through the demand valve of the breathing regulator. A visual inspection revealed cuts in the valve seat, figure 3. A complete investigation including lengthy endurance tests revealed that the failure was due to the valve seat materials which originally were only marginally inadequate, these being improperly cured and adversely affected by a combination of the detail design deficiencies of the demand valve stem, motion of the demand valve stem, and inadequate mounting of the valve seat material. Figure 4 shows the geometry of motion of the demand valve. One of the demand valve design deficiencies was attributed to the sharp edge of the valve which bears against the valve seat, thus causing the seat to be cut. This seemingly simple "Monday morning quarterback" type of improvement was a result of the painful "process of elimination" type of evaluation procedure. As indicated the difficulty once determined was corrected by the simple process of increasing the radius of the demand valve stem.

The results of tests conducted on preproduction samples submitted for "follow on" procurement contracts revealed that the "pressure breathing" characteristics of the regulators were not reproducible. This difficulty was encountered after the regulators were permitted to remain static four to six days. The performance of the regulators when evaluated immediately after delivery was within specification requirements but after remaining static changes in performance characteristics were observed throughout the temperature range with a non-return to calibration when retested at standard conditions. Continued adjustment of calibration failed to stabilize the performance of the regulator in most instances. Further investigation revealed that the lack of performance reliability was due to the instability of the pressure breathing aneroid which was caused by a build-up of processing and material changes. The aneroid material was changed by a sub-contractor, to facilitate his increased production. The aging and curing procedure of aneroids and the aneroid seal material was changed by the prime contractor, also to facilitate increased production requirements. These changes were made without Navy approval and without tests to determine their effect on aneroid stability. Currently the contractor is endeavoring to correct this problem.

Figure 3 - Demand valve seat on miniature demand type oxygen breathing regulator showing cuts

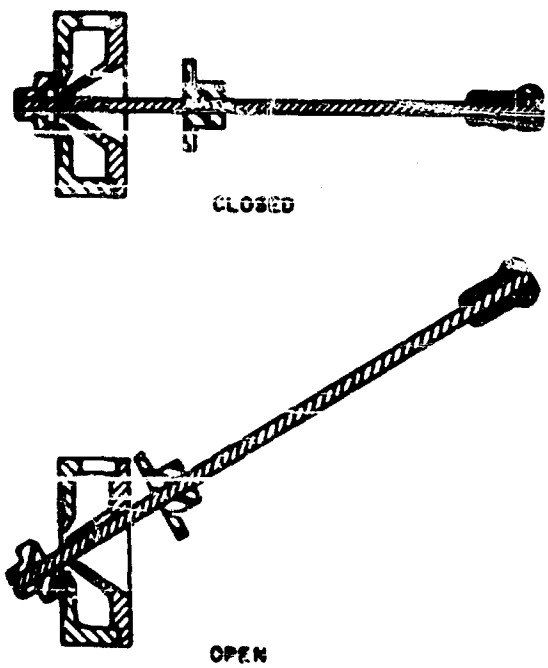

Figure 4 - Motion of demand valve of miniature demand type oxygen breathing regulator

On another contractor's qualification model, diaphragm and pilot valve instability were encountered during evaluation under maximum and minimum temperature specifications. Calibration shift and complete change in pressure output were encountered at -70°F and +160°F. However, original pressure/performance was restored when recalibrated at standard temperature conditions - thus indicating that the basic design was sound but that the behavior of the material of the silicone diaphragm and the metal aneroid varied excessively under the thermal stress. A change of the material of each component resulted in acceptable performance. Subsequent preproduction samples manufactured accordingly were approved.

On a third contractor's model, qualification samples were approved but with a reservation relative to the method of mounting and installing the inlet port, figure 5. The method used dictated the use of a clamp to retain the oxygen supply hose. A change in the method of attachment was made and preproduction models submitted. In this change, a gasket was used and retained by a screw down retaining method, figure 6. After several days a cold flow of the gasket material caused dimensional changes and thereby permitted leakage of oxygen. Additional tightening of the fitting to prevent leakage caused the gasket to fail, figure 7. A change in the design of the fitting whereby the gasket was retained within a slotted surface remedied this difficulty. In additional tests to ascertain conformance with the specification requirements, aneroid instability was also determined to exist in this model regulator. Investigations revealed that a change in the procedure for aging and curing of aneroids established by the production department which fabricated the preproduction sample differed from the procedures established by the engineering department, fabricators of the approved qualification sample.

The prototype design of the fourth regulator model, one which has been refined and designed to permit diluter demand type breathing (allows air to be mixed with the breathing oxygen to conserve the oxygen supply) is currently being evaluated. At this writing problems concerning application and performance of aneroid and diaphragm materials are being encountered.

From the foregoing examples it can be understood that equipment reliability depends greatly on the establishment of typical production techniques for the fabrication and assembly of qualification samples so that a minimum of changes are necessary for preproduction and subsequent production items.

SUIT CONTROLLERS

Figure 5 - Inlet port gasket installation of miniature demand type oxygen breathing regulator

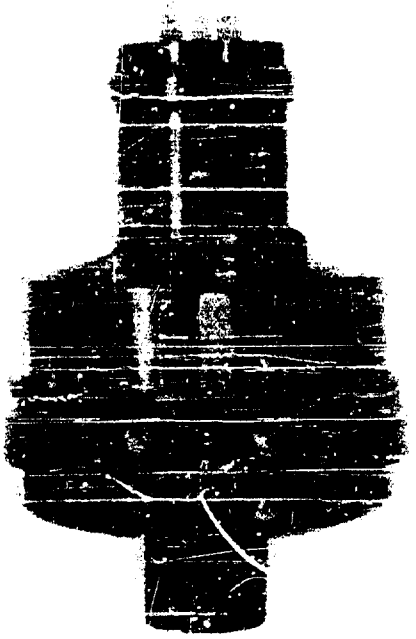

Figure 6 - Inlet port gasket installation of miniature demand type oxygen breathing regulator showing gasket "squeeze out"

Figure 7 - Inlet port gasket of miniature demand type oxygen breathing regulator showing damage

Fleet operational acceptance of the full pressure suit system is contingent on many factors. Since the suit system is flown more than 99 percent of the time in the normal condition and less than one percent of the time in the emergency condition, comfort in the normal condition is of prime importance to assure operational suitability. One primary factor in comfort is related to the amount of pressure build up in the suit system by the ventilating air required for thermal comfort. The garment is air impermeable and therefore stops normal perspiration loss which leads to heat imbalance. This pressure is for the most part caused by the resistance of the suit controller to the flow of air. The controller is located down stream to the suit. This reflected pressure is called "residual back pressure". A definitely unacceptable residual back pressure is above 1/2 inch of mercury. A desirable back pressure is below 1/4 inch of mercury. Available controllers incorporated slightly above 1/2 inch and pilot acceptance was poor. Therefore a redesign of some specific features of the controller was required.

Figure 8 illustrates three pressure suit controllers. The original controller has a flow restriction and high back pressure that precludes fleet acceptability of the suit system. The other two controllers have increased flow capability which enhances acceptability of the suit system. The first controller performs adequately under all environmental conditions and possesses stabilized performance. The second and third controllers performed satisfactorily only in the prototype design.

Qualification samples of the second controller would not hold calibration and the difficulty at this writing appears to be in the design and material selection of the aneroid assembly that controls the pressure output. The design was an extrapolation of the previously satisfactory design to an extent that so called "feather edge" performance was apparent in the design theory. However, all the shifts in performance could not be logically attributed to design extrapolation. This portion of the difficulty was clearly an unpredicted dimensional change of the aneroid caused by improper curing and/or incorrect material selection that produced poor behavior under temperature extremes and could not be adjudicated by calibration. The difficulty was identical in some aspects to the aneroid difficulty encountered in the breathing regulator. As a result of the two factors apparent unwarranted design extrapolation and apparently erroneous material selection, both a change in basic design and the selection of a more suitable material are necessary.

The qualification test sample of the third controller showed no inconsistency in performance up to 50,000 feet altitude throughout

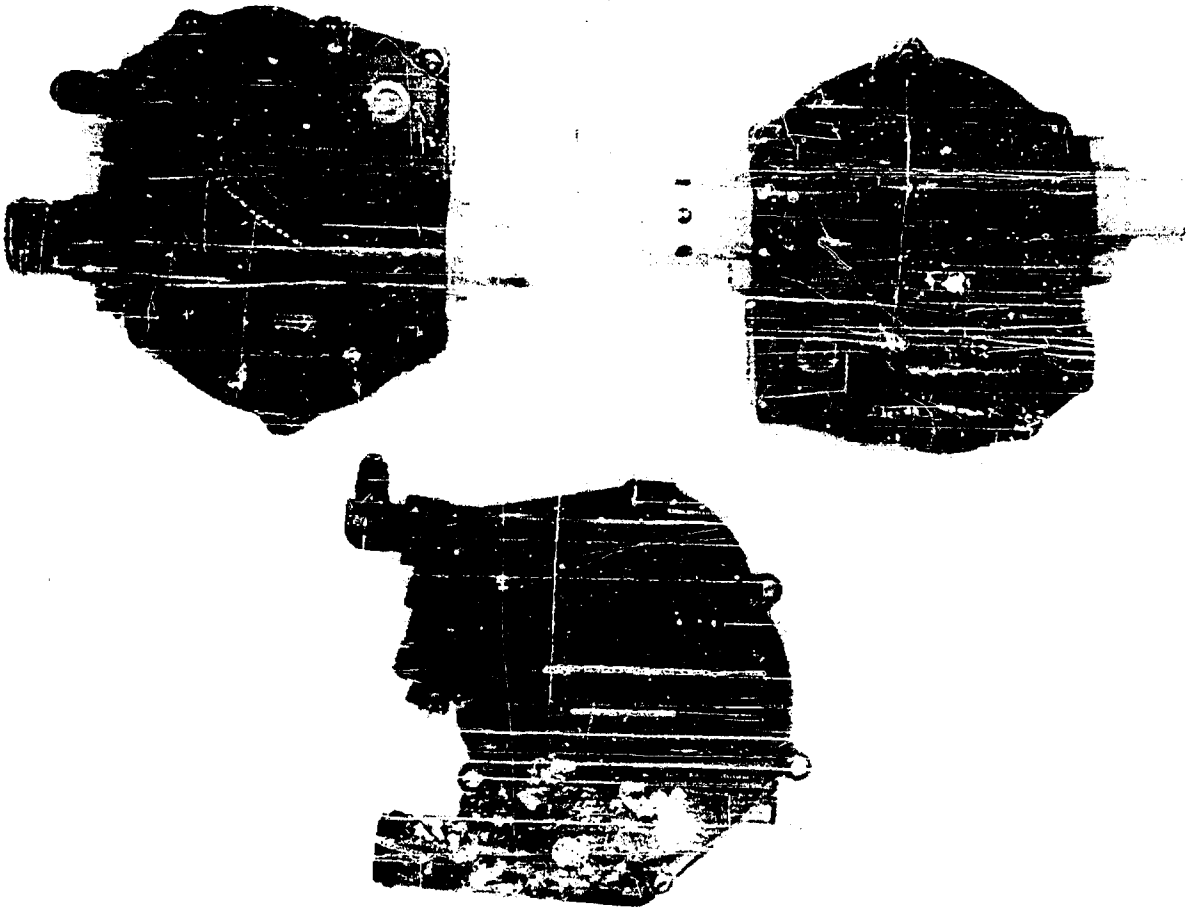

Figure 8 - Three full pressure suit pressure controllers

the environmental conditions of evaluation. This consistent performance did not persist in the altitude range above 50,000 feet. Above this pressure altitude, a shift in pressure schedule occurred that in effect produced higher pressure output. This resulted in undesirable and unacceptable residual back pressure in the suit system and caused restrictions and limitations in mobility. The fault was traced to the design shape of the diaphragm which at a specific pressure did not function smoothly but jumped to a new position. Design changes in diaphragm shape eventually remedied this condition.

The foregoing again illustrates an apparent difficulty in the transition between the prototype design, the qualification sample and the production item from the aspects of design details, material selection and quality of workmanship and the various combinations thereof. Great difficulty exists in establishing manufacturing processes which yield consistently acceptable and reliable equipment with a low reject quota. Some experience reveals that prototype design samples and qualification samples are produced by a certain segment of an organization that have not adequate technical liaison with the production segment. It appears that techniques and special knowledge are lost in this transition and that in some instances extremely critical features are not properly "flagged" and therefore do not receive the attention that is essential for the production of consistently reliable equipment. In addition other evidence reveals that the materials are substituted in the change from research and development to production due to more desirable production handling. This results in the loss of consistent and precise performance that is essential to aircrew equipment mechanical systems and not infrequently may mean the difference of survival or death.

DETERIORATION

Allen L. Alexander
U. S. Naval Research Laboratory
Washington 25, D. C.

Introduction

History descibing methods to combat degrading influences in nature on material is as old as written records. Indeed, there is considerable evidence to indicate that organic protective films in the form of natural gum solutions have been employed even longer. However, it's equally certain that these earliest formulators could hardly foresee the application of such films to the protection of equipment from the heat of a nuclear blast, for example. Present design criteria require that components and material, whether used alone or in complex weapons systems, be highly resistant to attack from all influences of the environments in which they must function. Preferably this required stability may be assured by a judicious selection of inherently resistant materials. Often, however, materials possessing the preferred properties do not exist and compromises must be made which often serve to allay considerably the deteriorating process where it cannot be stopped entirely. The situation within the Navy is aggravated particularly by the corroding influence of sea water and the salt-laden atmospheres in which the Navy operates.

Degrading assaults may be in the form of corrosive attack on metal components, or thermal destruction resulting from the absorption characteristics of a painted surface exposed to excessive heat. Organic polymers may degrade rapidly through exposure to energy frequencies producing depolymerization and secondary chemical reactions. And deterioration resulting from biological attack by bacteria, fungi, insects and marine organisms has been the subject of careful study for perhaps longer than any phase except possibly that produced by corrosion. Only recently the degradation of aviation

fuels by microbiological growths has been suspected for the loss of at least one aircraft. The drop in efficiency of transmission of sonar signals through accoustically transparent surfaces increases almost exponentially with the thickness of the layer of macro marine organisms attached to the surface. An improperly designed pier, erected at the cost of millions of dollars, under the exigencies of war time collapsed into the sea after only five years from attack by Limnoria and Teredo on its supporting piles. Another wartime incident is reported in which a detachment of marines was virtually isolated from its company through failure of its communication equipment which became inoperative from the destruction of insulation media by the action of cellulose-destroying fungi. Quite recently creosoted telegraph poles at a Pacific island base were observed to be rotting, not at the base but rather at the top, from attack by a strain of fungus subsequently demonstrated in our laboratory to be not only resistant to creosote but able to utilize it as a nutrient source.

Among the Navy's earliest problems was the continuing effort to maintain ships' hulls free from the attachment of encrustating organisms which retard speed and increase fuel consumption. Recently smoother hulls have assumed additional significance as they affect the noise level of submarines rigged for silent operation. An extension of this problem was manifest when 12 flying boats were anchored in tropical waters during maneuvers following which 11 could not get off the water until their hulls had been scraped to remove fouling.

Unfortunately some early efforts toward the solution of some of these problems were somewhat misguided. For example, at one stage copper sheathing was attached to iron hulls to combat fouling with rather disastrous results. Not only did the copper itself foul readily on becoming the cathode in a galvanic couple, but the corrosion rate of the steel hull plates was accelerated as they assumed the role of anodes in the circuit.

From this brief review of several types of deterioration it should be of interest to look at some specific situations where attack can be severe and to examine some measures which tend to eliminate the problem.

Among the papers which follow several are devoted to radiation effects, and one to damage resulting from thermal radiation. In each instance degradation may occur. Little attempt will be made here to discuss this type of deterioration although one reference to irradiation will be made. Subsequent papers also describe progress that is being made in corrosion control. Since damage from corrosion

may occur under varied circumstances and is among the most severe and costly types of deterioration, mention will be made of some of our studies designed to understand and thus control or at best retard the corrosion process.

Corrosion

No introduction is required to familiarize this audience with the effects of metallic corrosion. As mentioned earlier, however, the consequences of corrosion are of special concern to the Navy as its ships and aircraft are required to operate under, on and above the seas. No doubt the most effective means of eliminating corrosion is the specification of materials which do not corrode. Obviously, however, such materials are not economically available in quantities sufficient to meet even a small fraction of the fleet's requirements. Therefore considerable effort is being made to assure the selection of the most compatible components for use in corrosive environments and to devise continually improved means of protection for those metals subject to attack. This includes the proper application of inhibitive techniques which can be just as critical as their proper selection.

To illustrate this point attention is invited to Figure 1, a photograph of the outer hull of a submarine just below the water line. This hull was presumed to have been protected adequately since it had received some time earlier the standard bottom paint system currently specified for the protection of ships' hulls from corrosion and fouling. However, on checking the ship's log it was revealed that this normally adequate paint system had been applied during the month of February in a Northeastern yard during a snow storm at an ambient temperature of 21° F. As may be seen, all of the cold plastic antifouling paint along with most of the primary anticorrosive coats had long since disappeared - under the conditions of application any other result would have been surprising indeed. Of further interest is the quite obvious pit measuring 11/32 in. in depth which was traced to stray currents, arising from improperly insulated welding equipment that had been brought aboard, which found an easy return path through the hull and sea water to ground.

In spite of derelictions like these, organic coatings <u>properly applied</u> remain among the more formidable weapons against corrosion. The continuing development of film-forming polymers of new and distinct properties enhance their effectiveness and range of adaptability. Recent examples include the epoxies, polyurethanes, and vinyls. When applied alone or in combination with older materials, new properties are obtained. The epoxies, used in combination

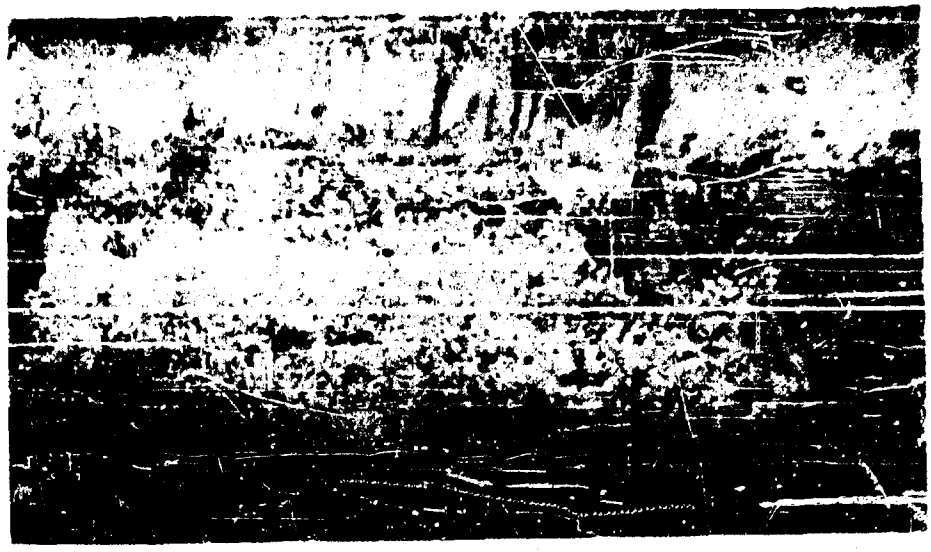

Figure 1 - Outer hull of submarine below water line

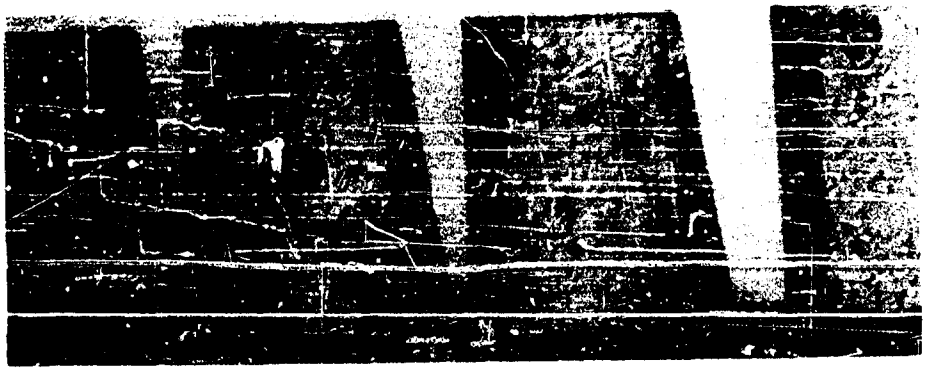

Figure 2 - Top side paint system exposed to salt spray for six months

Figure 3 - Top side paint system with one coat wash primer exposed to salt spray six months

with coal tar enamels as well as the vinyls, have made possible new applications of cathodic protection heretofore unavailable. Perhaps the single most significant development in this area in the past decade has been the wide scale adoption of the so-called wash primer (1) developed by industry under Bureau of Ships cognizance. This pretreatment for metal, consisting of a basic zinc yellow pigment dispersed in a solution of polyvinylbutyral and reduced with a mixture of phosphoric acid and alcohols, opened the new field to vinyls for metal protection and vastly improved many existing systems. To illustrate, Figure 2 is a photograph of four panels finished with a standard top side paint system for ships following exposure to four concentrations of salt spray for six months. Figure 3 shows the same system exposed to identical conditions for an equal period of time except that the metal received a 2-mil coat of wash primer prior to the application of the specification system.

The use of a coating which probably results in the formation of some phosphate crystals at the interface recalls the excellent results achieved through proprietary processes involving chemical bath treatments so widely used on automobiles and major household appliances. Burbank (2) in a study of phosphate crystal formation on ferrous surfaces makes the novel suggestion that inhibitive phosphate coatings, such as applied normally from hot chemical baths, might be applied successfully to major surfaces, a ship's hull for example, by means of a gel medium containing the required components. Zinc phosphate coatings were deposited from a hot solution and similarly from a gel medium onto steel surfaces. In the latter case the coating consisted of small adherent crystals that covered the surface uniformly. A photomicrograph of panels prepared in each fashion is shown in Figure 4. The similarity of the coating is apparent from these photomicrographs. Further, X-ray diffraction patterns suggest that both coatings are oriented, although along different crystal planes. Future work along these lines could result in revolutionary metal-pretreatment methods.

Beginning about 1953 both the Maritime Commission and the Navy adopted cathodic protection for retarding corrosion in their reserve fleets and this has proven to be a major factor in ships' preservation. Of course the general principles of this technique were quite well known but systems had to be tailored specifically to the ships involved. Resulting largely from work at the Naval Research Laboratory it has been demonstrated repeatedly that a current supply of 3 milliamperes per square foot of surface properly distributed is sufficient to protect adequately the hull of a ship in average need of repainting as compared with 10 milliamperes per square foot for bare steel. A newly painted hull will require as

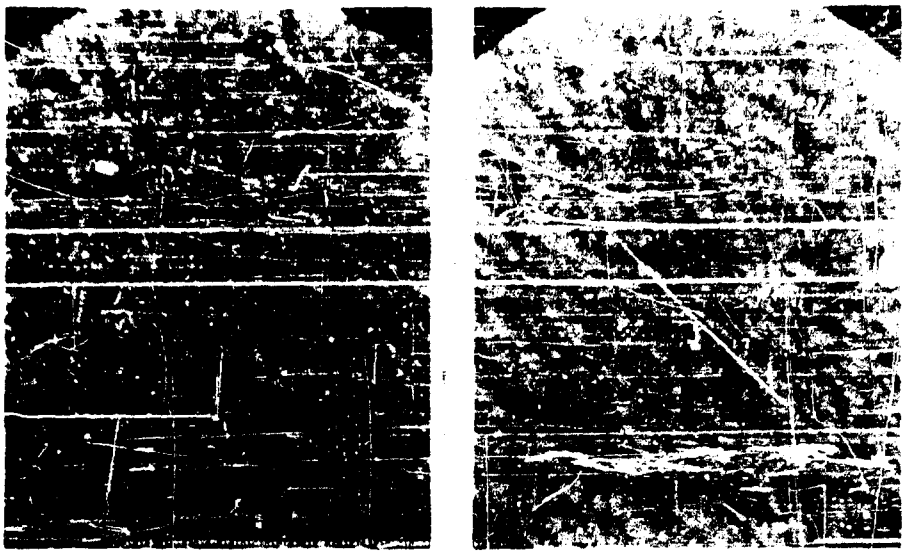

(a) (b)

Figure 4 - Zinc phosphate coatings on steel. (a) Panel phosphated in hot bath, (b) panel phosphated in Gel medium

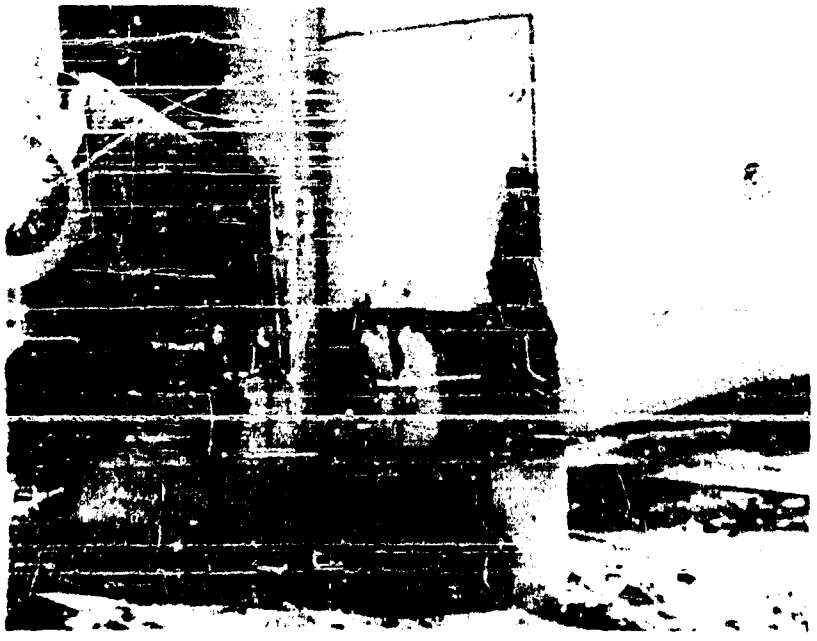

Figure 5 - Installation of zinc anode

little as 0.1 milliamperes per square foot. Care must be exercised to assure an even current distribution which has been most satisfactorily applied from carbon anodes appropriately spaced around the ships.

Related work (3) at NRL has described the advantages of high purity zinc for use as sacrificial anodes in protecting anodic areas of active ships. Such applications are normally made in proximity to propeller struts to combat the cathodic role of bronze propellers. A typical installation is shown in Figure 5.

During recent years we have made studies of the corrosion rates of metals in the tropics, and compared these in some instances with rates for the same metals and alloys in temperate latitudes. The results obtained to date with several pure metals and a number of structural steels should be of interest. Reference should be made to the original publications (4, 5, 6) for details of methods employed. In the data presented here corrosion rates are reported as average reduction in thickness or as average penetration in mils calculated from weight loss, as a function of time exposed. In Figure 6 the corrosion rate for a structural steel in the tropical marine atmosphere of Panama is compared with the corrosion rate of a similar alloy exposed at Kure Beach, N. C. As might be expected in the warmer humid climate of the tropics corrosion proceeds more rapidly. Figure 7 presents similar data for the same steels exposed at a site inland from the sea in the tropics and in the typically industrial atmosphere of Kearny, N. J. It is evident here that the warm, humid atmosphere of the tropics may be even more corrosive than an average industrial atmosphere in a more temperate climate.

The effect of mill scale on the corrosion rate of steels has received considerable attention. The data of Figure 8 offered some opportunity to observe mill scale effects on the corrosion of low-alloy steel in the tropics. For the shorter term it appears to make little difference. After 8 years, however, corrosion on panels from which mill scale was not removed proceeds somewhat further than on pickled surfaces. For continuous immersion in sea water, however, pickling helps; a particularly good example is shown in Figure 9 where pitting to perforation has occurred on a low-carbon unalloyed steel after 8 years in the sea whereas the pickled companion is comparatively intact.

It was something of a surprise to note that a low-carbon steel continuously immersed in sea water at Kure Beach, N. C. corroded at approximately the same rate as a similar sample at Ft. Amador, C. Z., Figure 10. Certainly the compositions of the environments were almost identical but the slightly higher average

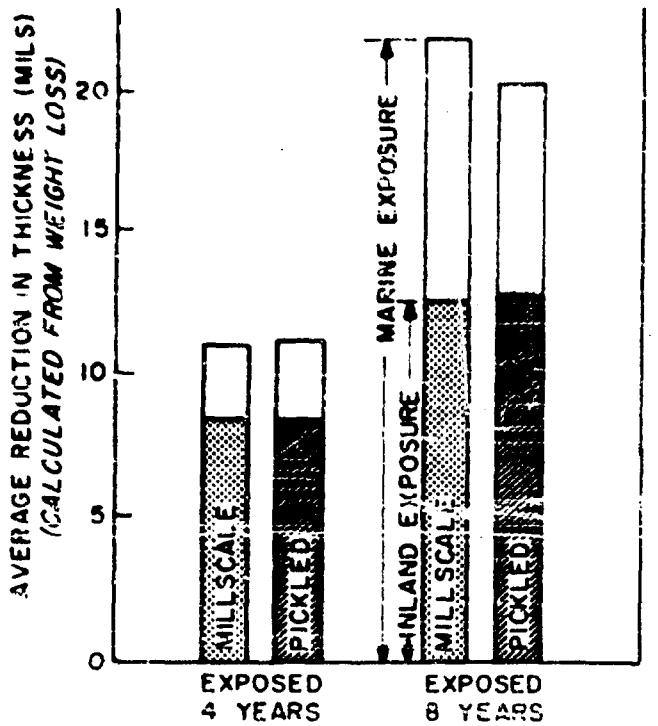

Figure 8. Comparison of Millscale and Pickled Surfaces Exposed to Atmosphere

(a) Millscale (b) Pickled

Figure 9. Appearence of Millscale and Pickled Surfaces after Eight Years Immersion in Sea Water

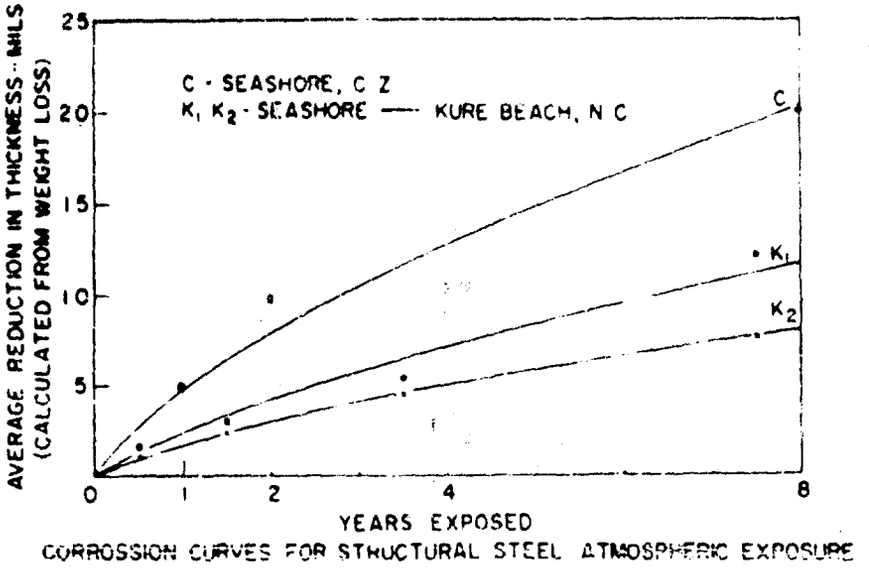

Figure 6. Relative Seashore Corrosion Rates

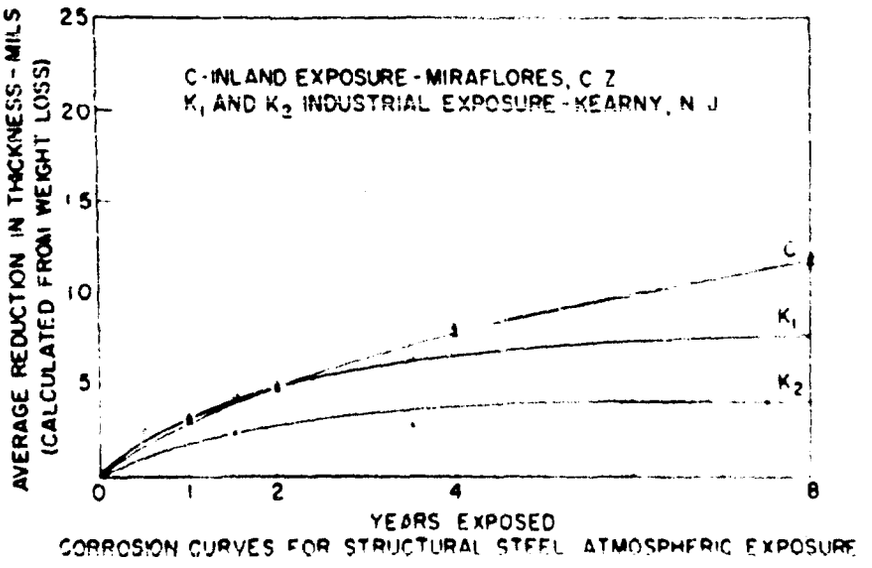

Figure 7. Relative Atmosphere Corrosion Rates

temperatures of the tropics did not induce the accelerated rate anticipated.

During the past two decades marked advances have been made in metallurgy in the production in commercial quantity of new alloys and metals which provide longer life in corrosive environments. Progress in supplementary techniques such as organic coatings also has advanced and may be expected to continue to improve. However, it is our belief that the more spectacular improvements next to appear will be provided by metallurgists in the alloys themselves although the coatings industry can be expected to continue its productive efforts.

Irradiation Effects

Succeeding papers will deal with specific problems related to radiation. It is believed, however, that one project presently in progress in our laboratory will be of some interest here. Among the sources of degradation of paint films the ultraviolet portion of the spectrum long has been recognized as rather severe. As a matter of fact most accelerated weathering machines designed for a rapid evaluation of organic coatings use a light source rich in ultraviolet. Work has been reported previously (7, 8) on the degradation of drying oil films by irradiation with ultraviolet light under ambient conditions and in the absence of air. The course of changes in film structure was followed by infrared spectrometry and the same technique was used for analysis of the gaseous products evolved. With the prospect that properly pigmented organic coatings would find some utility in controlling thermal radiation and emissivity from satellites and space vehicles, the current study was undertaken with a view of establishing the stability of film-forming polymers toward the short (unfiltered by air) ultraviolet. To date a number of such polymers have been irradiated in air and structural changes in films as detected by infrared spectroscopy have been followed. Similar films were then irradiated in a vacuum by an ultraviolet source at wavelengths ranging from 1150 A (LiF filter) into the visible. An example of the data derived from such measurements is shown in Figure 11. The resin studied was a phenyl silicone selected because it was used as the vehicle for a white coating used to paint the third stage of Vanguard I. In the presence of oxygen distinct absorbance changes were noted for bands characteristic of OH, CO_2, C=O and aromatics. In vacuum, or in the absence of oxygen no marked changes in absorbance at any of these bands were detected. Toward the end of the irradiation period in vacuum a small amount of oxygen was bled into the system following which small changes in absorbance were again observed in line with those shown in Figure 11.

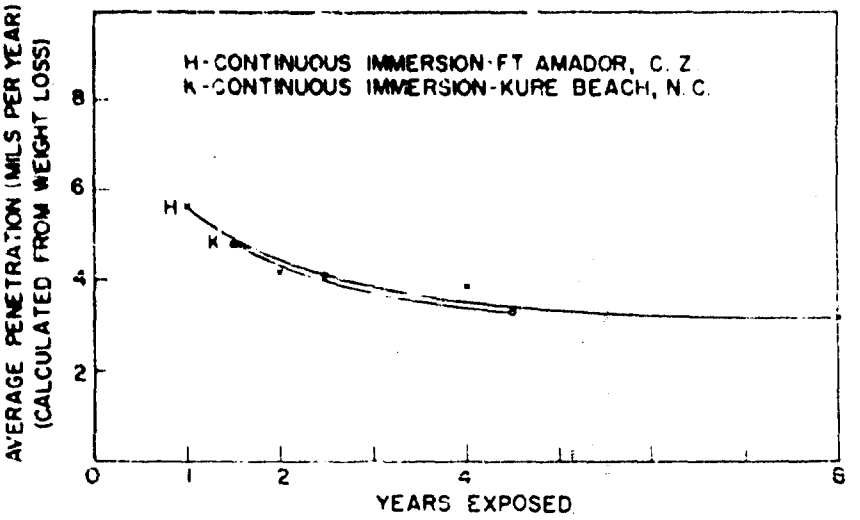

Figure 10. Comparison of Corrosion Rates at Kure Beach, N. C. and the Canal Zone

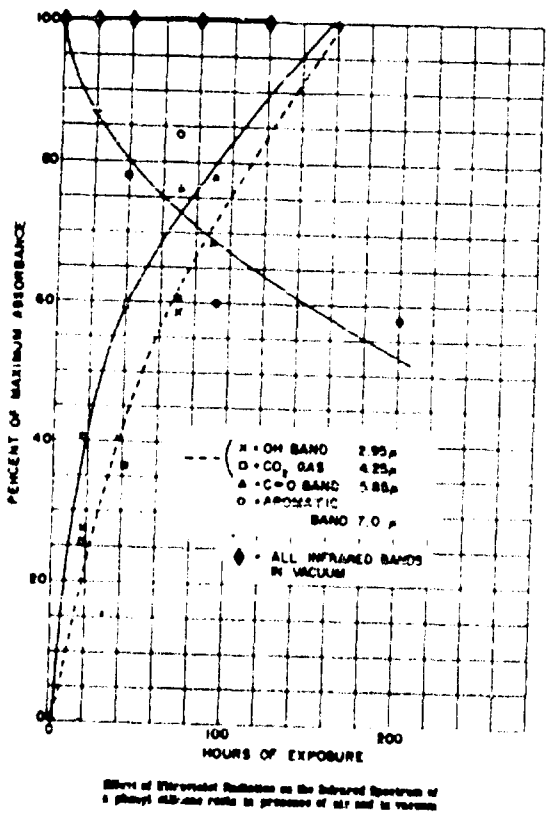

Figure 11

This work has not yet proceeded to a point to permit far-reaching conclusions but it is suggested that the rate of degradation induced by the short ultraviolet above the atmosphere, in the absence of oxygen, may not be so severe as expected.

Biofouling

As in the case of corrosion the deteriorating effects of both micro- and macroorganisms are mentioned in earliest recorded history and we are still working vigorously on the problem. The antiquity of the subject is illustrated certainly by reference to the latter part of the 13th chapter of Leviticus in the Old Testament where the scribe treats the matter of the "leprosy of garments," the criteria for determining whether a garment be clean or not, and the techniques for disposing of unclean garments. This "leprosy" which plagued the garments of the early Hebrews probably was no different in kind from that currently referred to as mildew, rot or fungus infection. Along with a change of nomenclature we also have achieved a better understanding of the nature of the problem but we have not yet succeeded in eliminating it.

Fungi Control - The interest of the Naval Research Laboratory was first directed to the effects of fungi as a result of repeated failure of electronic communication equipment, allegedly as the result of fungal action. As our studies developed this assumption was partially justified. Today specifications for the design and construction of all naval communication equipment are quite specific, first in the designation of materials and components inherently resistant to moisture and fungal attack and where this is not possible auxiliary measures are required to alleviate or reduce these effects as far as possible. To illustrate the type of thing which does happen, your attention is invited to Figure 12 which is a photograph of a 500 watt "portable" transmitter as it appeared after a period of storage, not in a tropical depot as is frequently required with such equipment, but rather in nearby Mechanicsburg, Pennsylvania. The equipment was covered over its top and sides by a waterproof package but was open at the bottom. In such an arrangement fungal spores had easy access to the equipment surfaces and the stagnant moist air within the enclosure provided stimulating conditions for growth and propagation. In this instance the mere presence of such growth constituted a severe hazard although no prior damage may have been imparted to the equipment in supporting fungus growth. The apparently parallel rings at the top of the figure are in fact sections of a coil under quite high potential of several thousand volts when activated. At such time as this equipment might be energized the conductivity of the fungal filaments to ground is

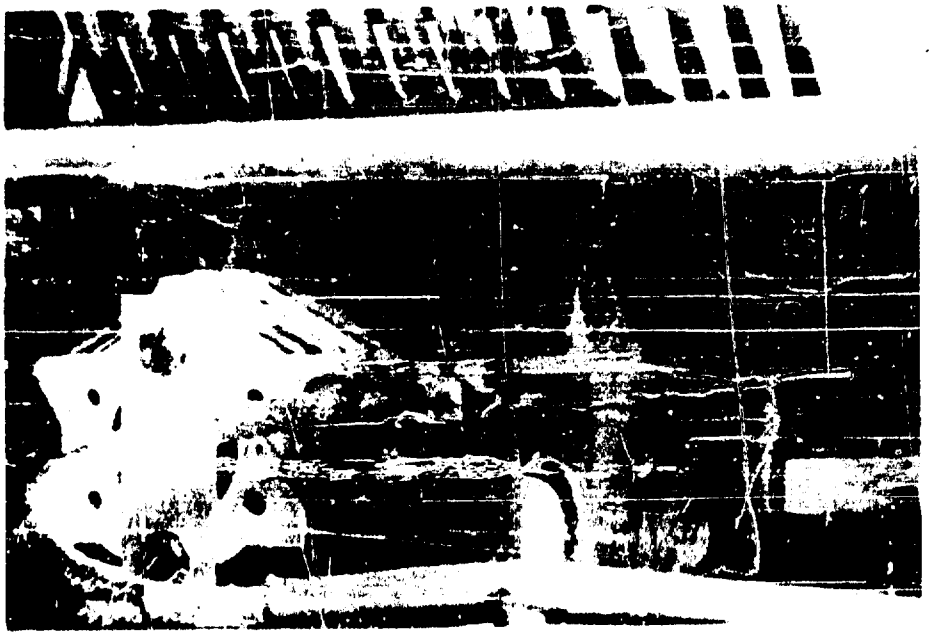

Figure 12. Fungus Infested Transmitter

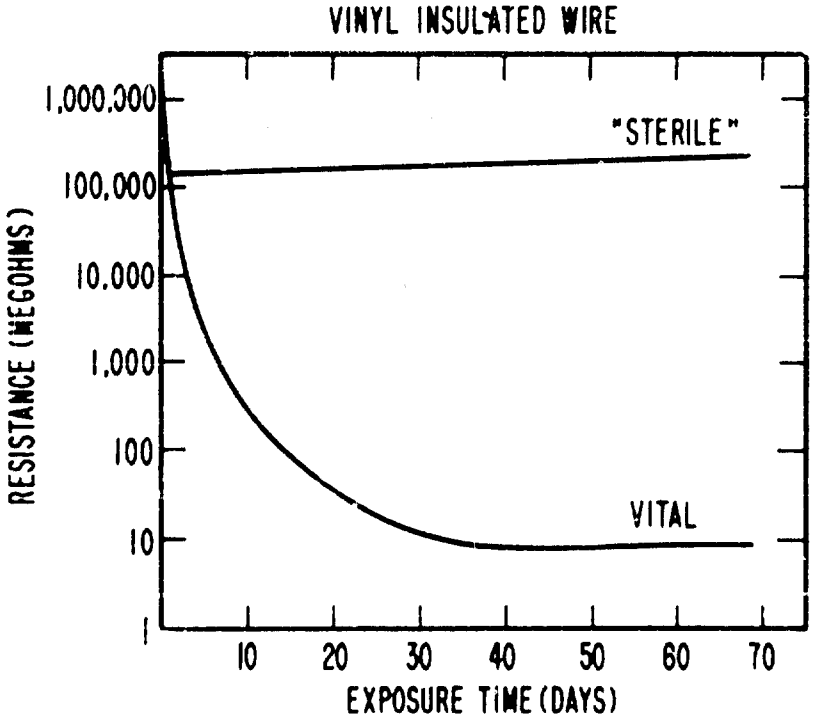

Figure 13. Resistance Change with Fungal Growth

quite sufficient to cause immediate shorting and thereby completely immobilizing the equipment. A notable gain in this area resulted simply from the design of a packing case which excludes moisture and fungal spores.

In an early approach to the problem as typified by the transmitter the practice was followed of grinding recognized fungicides into clear varnishes and lacquers and spraying or, where permissible, dipping entire assemblies with them. It was noted, however, that many potent fungicides as revealed by the usual bioassay techniques (petri dish experiments) were of little or no value after incorporation into organic matrices. Thus we were prompted to look more closely into the nature of fungicidal compounds themselves with special emphasis on functional substituent groups. The scope of this paper does not permit any detailed description of techniques and methods by which a considerable number of compounds were studied rather exhaustively for their fungicidal characteristics. These have been described in other publications (9, 10, 11, 12, 13). Some generalization should be of interest, however. For example, aliphatic hydrocarbons, with one or two exceptions, are notably inefficient as fungicides. Only a few of the higher alcohols possess fungicidal merit while, as might be predicted, phenolic compounds are among the more promising and there is evidence to suggest that the phenolic hydroxyl group is the most effective of the substituents studied in imparting toxicity toward fungi in a relatively simple organic molecule. An interesting point was raised, however, by the observation that carboxy phenols and their esters and amines generally are nontoxic. The phenols present an excellent example of the inadvisability of loading a molecule with an excessive number of substituents, toxic or not. For example, 2-hydroxy-5-nitrobenzyl thiocyanate, in spite of containing three very active groups, is itself without activity. Nearly all of the nontoxic phenols fall into this category of oversubstitution. An explanation may be in the fact that each group is involved in a separate, relatively individual biological mechanism. Steric hindrance is many times an important factor. An excellent example of this may be seen in the comparison of the molecular models of the fungicidal o-phenyl phenol with the considerably less active o-cyclohexanol. In the first case the hydroxyl group is perched in a free, conspicuous position, whereas in o-cyclohexyl phenol it is nestled neatly among adjacent substituents.

From numerous experiments additional facts have emerged, interesting examples of which will be mentioned. In the following tables the inhibition of specific compounds is listed in terms of growth rate of uninhibited controls, i.e., an inhibition of 25% indicates that the growth rate of the test fungus is only 75% of that

of an uninhibited control at equal concentrations of toxic. Table 1 lists a number of aromatic compounds along with the degree to which they inhibit growth.

Table 1

Inhibition of Aromatic Compounds

Benzene	25%
Toluene	14
M-xylene	4
Mesitylene	11
Tetramethylbenzene	57
Pentamethylbenzene	78
Hexamethylbenzene	44
Cyclohexane	-44

It is interesting to note that in this instance inhibition generally increases with the substitution of methyl groups (xylenes excepted) until complete replacement of hydrogen is reached whereupon molecular activity is somewhat reduced. On the other hand some side chain additives such as that on p-cymene, which is saturated, show decided stimulating properties.

The nitro compounds, particularly where some chlorine substitution also has been included, provide some interesting data. The inhibition qualities of a number of aliphatic nitro compounds are shown in Table 2.

Table 2

Inhibition of Aliphatic Nitro Compounds

Nitromethane	0%
Nitroethane	-20
1-Nitropropane	-16
2-Nitropropane	-33
1-Chloro-1-nitropropane	-2
2-Chloro-2-nitropropane	53
1.1-Dichloro-1-nitropropane	50
Nitrocyclohexane	0

In each instance where substitution of one group or another has been made the compound tends to stimulate fungal growth rather than suppress it. On the other hand, inhibitive qualities are usually stimulated by introducing both a nitro group and a chlorine group into the same molecules. Similar studies revealed that the presence of bromine alone in the absence of a nitro group imparted considerable inhibition, and in some instances the greater the degree of

substitution the more pronounced the inhibition.

Returning again to the ring compounds, substitution by both chlorine and the nitro group are required for optimum fungal growth inhibition. This is illustrated by the data of Table 3.

Table 3

Inhibition of Aromatic Nitro Compounds

Nitrobenzene	75%
m-Nitrotoluene	100
2-Nitrocymene	67
1-Nitronaphthalene	90
m-Dinitrobenzene	100
2,4-Dinitrotoluene	100
1,3,5-Trinitrobenzene	100
1-Chloro-2-nitrobenzene	100
1-Chloro-4-nitrobenzene	100
1-Chloro-2,4-dinitrobenzene	100

For example chlorobenzene (not shown) is almost nontoxic and nitrobenzene is only partially effective; both substituents introduced into the same ring provide complete protection. In additional experiments it was demonstrated that chlorine introduced directly into the ring was much more active than when attached to a side chain where its effect was neutral.

Before concluding the discussion of fungi as they might affect electronic components we would like to cite one experiment of significant interest because it represents an ingenious separation of two almost inseparable phenomena - moisture and fungus. Samples of a vinyl insulated wire were cleansed and one set contaminated with "sterile" or dead fungus spores as a control. The second set was inoculated with perfectly normal live spores of the same species and both sets incubated under optimum conditions for stimulating growth. Periodically the resistance of the insulation was measured with the results shown in Figure 13. In the case of the sterile insulation no breakdown in resistance was noted even under conditions of high humidity. With the growth and multiplication of the healthy spores a situation quickly developed which could cause direct shorting and resulting damage even though the insulating medium itself was not necessarily degraded.

Quite recently the role which fungi, and bacteria for that matter, can and do assume in another area has been demonstrated rather forcibly. Instances have been reported where biological

growths have contributed directly to the degradation of aviation fuel. This deterioration has been manifested by an accumulation of the organisms themselves and mycelia or debris associated with them. When further complicated by corrosion product the result can be the clogging of filters at critical moments in flight. Figure 14 shows a collection of such debris and organisms sustained at the water-fuel interface of a sample removed from the tanks of an aircraft carrier. Subsequently a culture was made of these organisms, the result of which is shown in Figure 15. The darker areas are fungus whereas the light spots are bacteria. The fungus, a photomicrograph of which is shown in Figure 16, was subsequently identified tentatively as belonging to the Hormodendron genera and is capable of utilizing either the fuel or the bacteria inevitably associated with it as its source of carbon. The solution to this problem is rather complex. The inclusion of chemical additives which could be expected to eliminate most biological activity is not always compatible with fuel ingredients. Presently recommended practices require immaculate care and good housekeeping at all stages of fuel transfer.

Before leaving our work on fungi and their control we would like to add that our hopes were that work of the type described would lead to the suggestion of a structure for an ideal fungicide. However, as is too often the case in studying the habits, attitudes and behavior of naturally occurring organisms, these behaviors cannot be too well predicted and perhaps in some cases these "beasts" of nature are thoroughly capable of changing their normal habits to combat with some success changing situations confronting them. It is impossible to go very far beyond the generalizations already cited with reference to specific classes of compounds. In the formulation of specific inhibitive coatings reliance must be placed on field performance of such materials without specific reference to the toxic's behavior under carefully controlled <u>in vitro</u> conditions. Examples of popular additives for inducing toxicity to organic films are pentachlorophenol and phenylmercuric salicylate, both of which respond convincingly to petri dish tests but which require excessive loadings in organic films for comparable protection. Better results to be expected in the field may be obtained from salicylanilide and para-toluene-sulfonamide which require more feasible loadings as well as being more economical. In concluding this phase of this discussion, it should be pointed out that suitable precaution must be observed in handling and applying products containing the organomercurials and their use should be avoided in proximity with sensitive selenium rectifiers in many electronic assemblies.

<u>Macro Organisms</u> - The problems of protecting wood piling and hulls from destruction by shipworms and maintaining ships' hulls

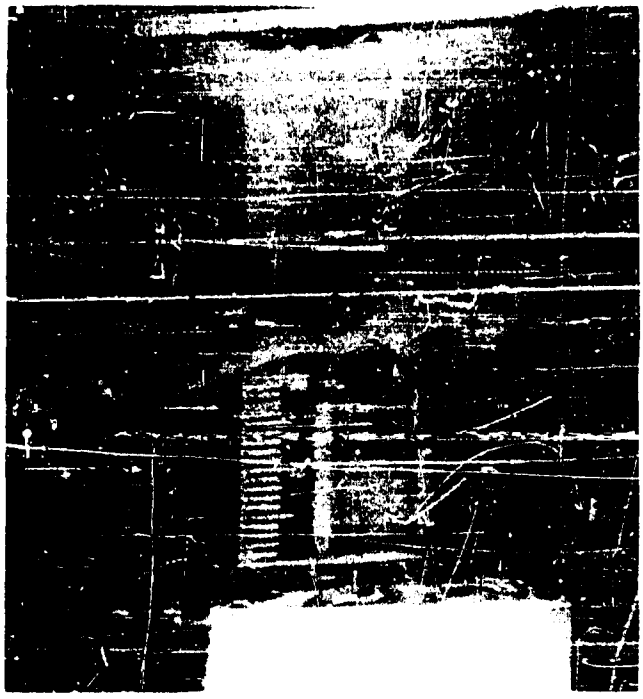

Figure 14. Fungal Debris at Fuel-Water Interface

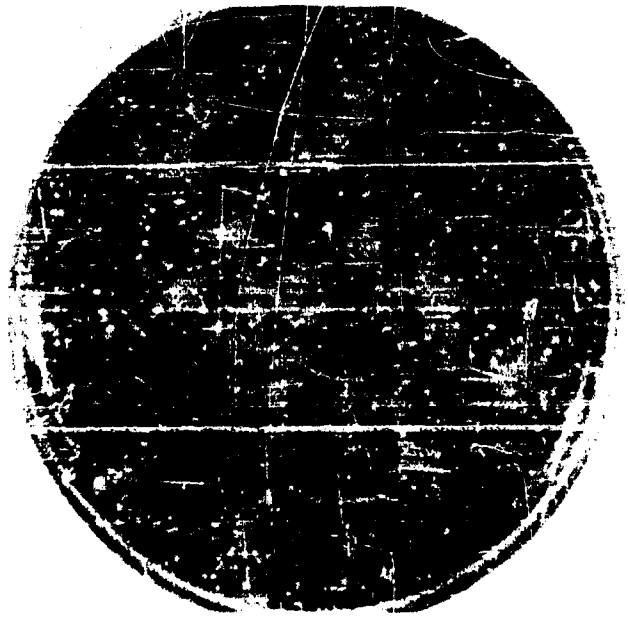

Figure 15. Culture of Organisms Removed from Fuel Tank

free of encrustating fouling attachment is as old as the history of sea power and improved methods are still being sought to meet them. To illustrate the severity of fouling attachment to unprotected surfaces attention is invited to Figure 17, which is a photograph of a PBM wing pontoon anchored in Biscayne Bay at Miami for 12 weeks. The left side was protected with a thin film antifouling paint designed for flying boat hulls and the right side had received a coating of nontoxic enamel. This subject has been reviewed so often that the discussion here will be limited to a brief resume of present practices. During World War II investigators at the Woods Hole Oceanographic Institution (14) clearly demonstrated that any painted surface immersed in the sea would remain free of fouling attachment for such time as the paint could provide copper metal available at the surface for solution in the sea at a minimum rate of 10 micrograms per square decimeter of surface per 24 hours. This provided a highly useful tool which has been widely adapted to the development of presently specified ship bottom paints. The result has been the formulation of a variety of several paint types with specific properties related to particular application requirements. Thin film paints based on chlorinated rubber are available for application to accoustical surfaces of underwater sound gear. Plastics paints (both hot and cold at time of application) are available in thick films for major ships which are capable of giving protection for up to three years. Hard films, usually based on vinyl resins, are applied to racing hulls and so on. Opportunity for further improvements in this field would appear to derive from advances in the physical properties of the paints or perhaps in the evolution of an effective organic toxicant to replace the inevitable copper or mercury. Some progress has been made in the use of supersonics and radiation as a means of fouling control but attendant requirements are somewhat incompatible with the operation of ships of the fleet.

Before concluding any discussion on deterioration some reference must be made to the destructive effects of the shipworm. Perhaps the most troublesome organisms with which we must deal in this area are the Teredo and Limnoria. The piling shown in Figure 18 illustrates the damaging onslaughts of which Limnoria are capable. These piles are as neatly severed as if by beavers constructing a dam. Limnoria do not inhabit wood but attack it from its surface. On the other hand Teredo seek wood as a place of abode and systematically destroy wooden structures while seeking a home. This is shown quite clearly in the cutaway piling in Figure 19. Between them these two organisms comprise a formidable foe. Historically the most effective means of protecting wood from such deterioration has been relatively heavy impregnations with creosote or blends of creosote with coal tar. In the past decade a number of alternate treatments have been proposed and indeed a few have been adopted for the

Figure 16. Photograph of Fungus in Fuel

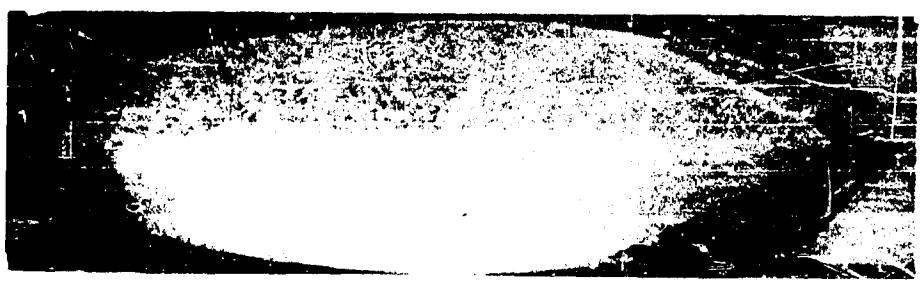

Figure 17. PBM Wing Pontoon after Exposure to Fouling Attack for Three Months

Figure 18. Piling Destroyed by Limnoria

impregnation of wood to be used in terrestrial installations. Examples are pentachlorophenol and several varieties of copper compounds. No such treatments, however, have proved entirely effective in marine service.

In reviewing the history of the development of current creosote specifications it appears that most modifications have resulted from factors other than a redefinition of some chemical or toxicological property which would describe a more effective preservative. Work has been in progress at NRL during the past six years, the objective of which has been the characterization of creosote with a view of correlating specific properties, preferably chemical, with its efficacy as a preservative.

The approach has been to separate creosote into fractions which subsequently are amenable to study by ultraviolet and infrared spectroscopy. Simultaneously these fractions were evaluated for their protective qualities by exposing panels impregnated with them to a marine environment heavily infested with Teredo and Limnoria. There is little evidence that some well defined fraction of creosote is substantially richer in preservative qualities than the whole. Valuable data have been produced, however, to suggest that some fractions contribute to the staying power of the preservative whereas others contribute more forcibly to its toxicity. Obviously the most effective poison is of little or no value if it is leached rapidly and thus exhausted. Reference is made to published papers (15-20) for details of this work.

I would like to cite one technique that has proven of value in attacking this problem. It has been difficult in the past to determine by experiment, short of a full term exposure of a representative batch sample, the efficiency of a creosote sample. This is related closely to the fact that creosote steadily leaches from the wood until finally a point is reached beyond which its preservative qualities are lost. In order to simulate this behavior, some leaching experiments were conducted in which sapwood panels were impregnated with measured retention quantities and then leached under artificial but accelerated conditions. Figure 20 describes the rate at which whole creosote is leached from wood under several sets of conditions. Following a number of experiments the conclusion was reached that flowing water at 80° C provided an accelerated condition that more closely approximated studies on samples leached naturally in the sea. For example it may be seen from Figure 20 that following an initial interval the amount of creosote removed from wood by flowing water at 80° C after any given number of hours is approximately equivalent to the amount removed in as many days at

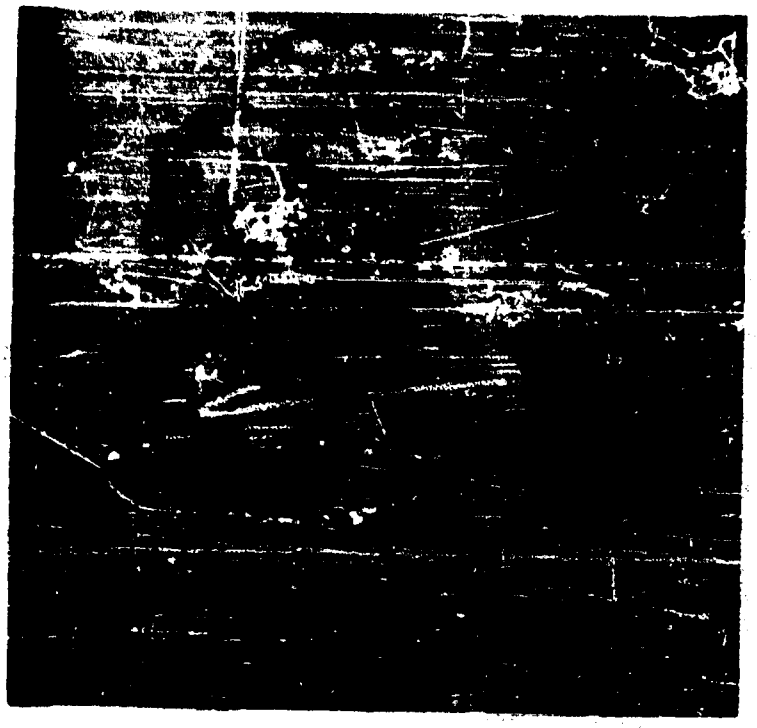

Figure 19. Piling Attacked by Teredo

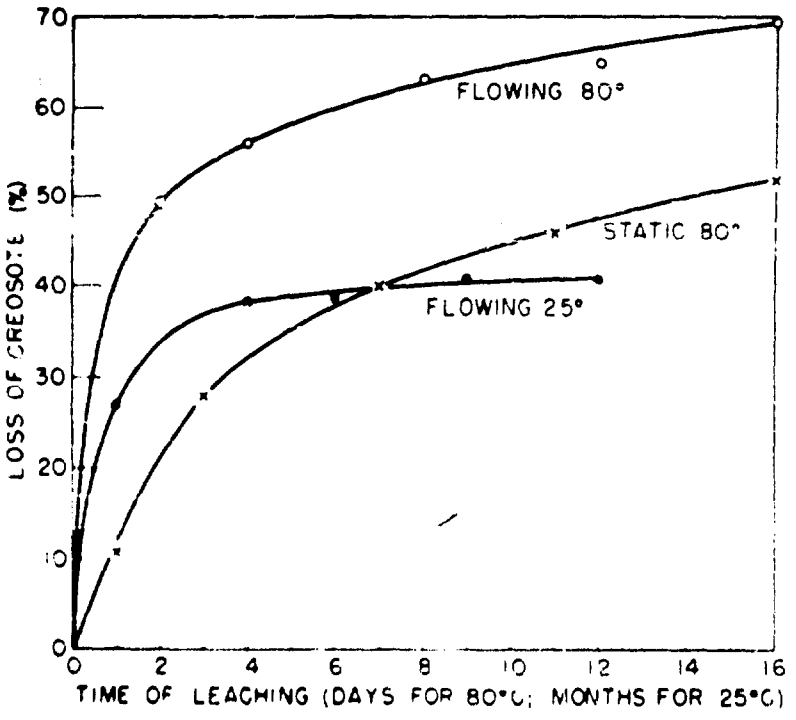

Figure 20. Leaching of Creosote from Wood

25° C in stagnant water.

This technique was used to study the rate at which individual fractions of creosote might be removed from wood. The data from one such experiment are shown in Figure 21. As might be expected, the heavier the fraction the stronger its staying power.

With the major chemical constituents known it was thought to be of interest to observe the rate at which these individual compounds might be leached from wood. The result is shown in Figure 22. Following this result a "synthetic" creosote was prepared from pure chemicals which on exposure was quite comparable to a creosote control when unleached before placing on test. However, a sample leached for 16 days prior to exposure failed early when compared to a leached creosote control. Thus the synthetic lacked the staying power of the natural product. Current experiments to improve this property are in progress in which resins are being added to simulate the inevitable residue present in creosote.

In conclusion I would like to show you that not only wood but some metals as well are attacked by marine organisms looking for an abode. Figure 23 is a photograph of a 1/4" magnesium panel immediately on its removal from 7-1/2 years' immersion in the sea at Ft. Amador, C. Z. The perforations in this panel were made by the organism Lithophaga which in this case may be seen in the burrows. Figure 24 is a duplicate panel that has been cleaned and in which the perforations are quite evident.

It has been the purpose of this paper to point out some of the many factors in nature that are continuously at work to degrade the materials of human productivity. Also we have tried to point to a few instances where successful efforts are being made to eliminate or at least reduce the impact of these forces.

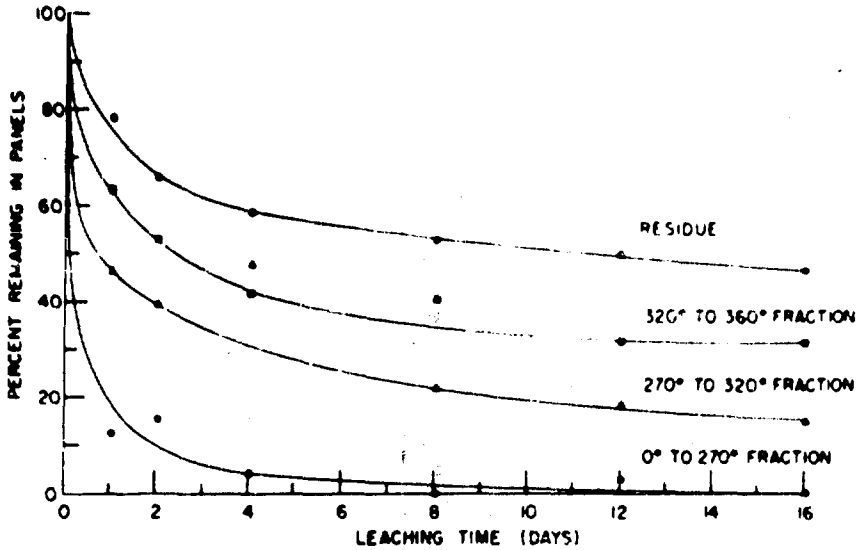

Figure 21. Leaching of Creosote Fractions from Wood

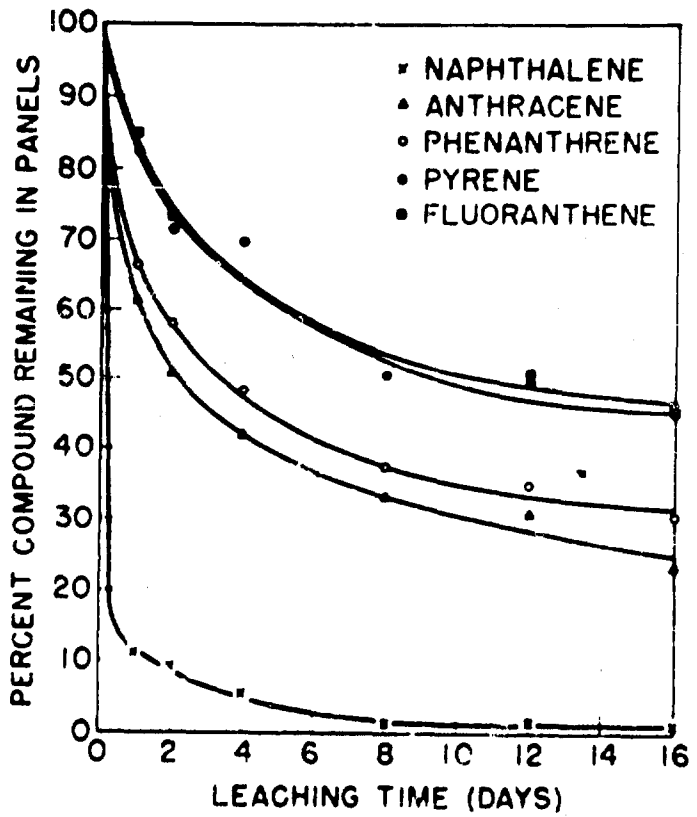

Figure 22. Leaching of Constituents of Creosote from Wood

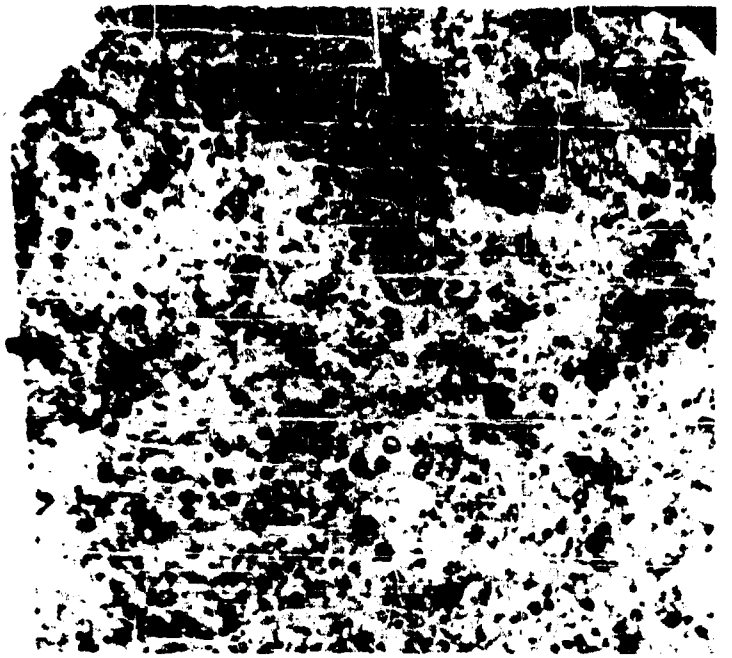

Figure 23. Lithophaga "Infested" Magnesium

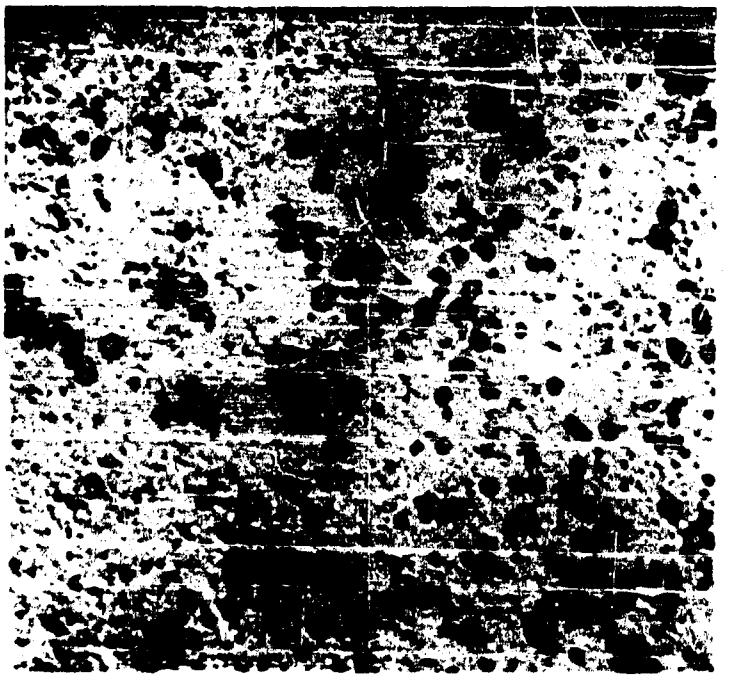

Figure 24. Magnesium Panel Showing Lithophaga Damage

REFERENCES

1. Whiting, L. R. and Wangner, P. E. U. S. Patent 2,525,107 (1950)

2. Burbank, Jeanne B. Naval Research Laboratory Reports Nos. C3481 dated June 1, 1949, and C3510 dated July 28, 1949

3. May, T. P., Gordon, Geo. S., and Schuldiner, S. "Cathodic Protection - A Symposium." The Electrochemical Society and The National Ass'n of Corrosion Engineers, 1949. Also NRL Report No. C3277 dated April 13, 1948

4. Forgeson, B. W., Southwell, C. R., Alexander, A. L., Munat, H. W. and Thompson, L. J. Corrosion 14, February 1948, 73t.

5. Southwell, C. R., Forgeson, B. W., and Alexander, A. L. Corrosion 14, September 1958, 437t.

6. Forgeson, B. W., Southwell, C. R., and Alexander, A. L. NRL Report No. 5153 dated August 8, 1958

7. Crecelius, S. B., Kagarise, R. E., and Alexander, A. L. Ind. Eng'g Chem. 47 1643 (1955)

8. Crecelius, S. B., Kagarise, R. E., Ferguson, E. E. and Alexander, A. L. Ind. Eng'g Chem. (in press)

9. Leonard, J. M. and Larson, Helen L. NRL Report No. 4228 dated Oct. 1953

10. Williams, K. C. and Lempke, C. T. NRL Report No. 3935 dated February 6, 1952

11. Leonard, J. M. and Blackford, V. L. NRL Report No. C3413 dated March 15, 1949

12. Leonard, J. M. and Weaver, W. E. NRL Report No. C3403 dated March 14, 1949

13. Leonard, J. M. and Bultman, J. D. NRL Report No. 4563 dated July 15, 1955

14. Ketchum, B. H., Ferry, J. D., and Burns, A. E. Jr., Ind. Eng'g Chem. 37 456-60 (1945)

15. Sweeney, T. R. and Walter, C. R. Jr. NRL Report No. 3940 dated February 6, 1952

16. Sweeney, T. R., Bultman, J. D. and Alexander, A. L. NRL Reports Nos. 4409 dated September 13, 1954 and 4411 dated September 10, 1954

17. Sweeney, T. R., Price, T. R., and Alexander, A. L. NRL Report No. 4672 dated December 15, 1955

18. Sweeney, T. R., Price, T. R. and Saunders, R. A. NRL Report No. 4822 dated August 30, 1956

19. Sweeney, T. R., Price, T. R., Saunders, R. A., Miller, S. M. and Smith, F. G. Walton, Corrosion 14 295t., 1958

20. Sweeney, T. R., Price, T. R. and Miller, S. M. Corrosion 14 348t., 1958

RESPONSE OF AIRCRAFT SKIN MATERIALS TO RADIATION FROM HIGH-TEMPERATURE SOURCES

J. Bracciaventi - T. I. Monahan
Material Laboratory
New York Naval Shipyard
Brooklyn 1, New York

INTRODUCTION

Since 1950 the Naval Material Laboratory under the sponsorship of the Armed Forces Special Weapons Project has been engaged in a study of the effects of the thermal radiation of nuclear detonations on materials. The study has included not only participation in the several AEC-DOD field tests at the Nevada and Eniwetok Proving Grounds, but also extensive experimental investigations in the laboratory. For this program, a number of high-intensity sources of thermal radiation have been developed, either at the Laboratory or under the Laboratory's technical cognizance. These sources simulate the heat output of a nuclear detonation. In addition to prosecuting several problems of a research nature, the Laboratory has studied the thermal damage phenomenology of materials of interest to the several Military and Civil Defense agencies.

The Naval Material Laboratory has collaborated with the Strategic Air Command, the Wright Development Center, the Bureau of Aeronautics and the Naval Air Material Center in studies to determine the thermal radiation characteristics of the various components of an aircraft, so as to estimate the capabilities and limitations involved in dropping a nuclear weapon from an aircraft without damaging the plane or its escort craft. Experience has shown that aircraft in the line of sight of a nuclear detonation can be severly damaged and rendered non-operational by the intense thermal radiation of the burst. As the yield of a nuclear weapon increases and approaches that of a thermonuclear weapon, protection against thermal radiation becomes more important than protection against either blast or ionizing radiation. In these cases the distance of closest safe approach

to the burst will be limited more by the optical and thermal properties of the aircraft skin than by its structural strength.

The critical areas on an aircraft are those which "see" the fireball of an explosion, and on which the fireball radiation is incident and, therefore, at least partially absorbed. Consequently, the paint system covering an aircraft is critical. Flaming, charring and blistering of the paint, due to the direct absorpiton of radiant energy, are hazards involving possible destruction of the aircraft; in addition, stresses generated in the aircraft by the unequal distribution of temperatures in the structure arising from the heating of the skin may cause buckling and, therefore, destruction. The thinner or less massive the aircraft skin and the greater the absorptance of the surface, the greater will be the thermal hazard. Particularly susceptible are the thin control surfaces that "see" the burst. The thicknesses of aircraft skin are dictated by design requirements and are not readily amenable to change. The surface condition of the skin, as it affects the absorptance or color, lends itself more easily to modification at the needs of the service.

The Naval Material Laboratory has collaborated with the Bureau of Aeronautics and the Air Force in a program to develop a satisfactory coating. The Laboratory has been concerned with the physics of the problem. The chemistry of the paint systems has been a direct concern of the other agencies, their laboratories and contractors.

DAMAGE CRITERIA

A principal consideration in evaluating a painted surface is its reflectance, which determines the amount of energy which is absorbed by the paint layer. Assuming that the paints of two aircraft have reflectances of 20 and 80 percent, respectively, the radiant energy absorbed by these surfaces would vary in the ratio of 4 to 1.

The studies at the Naval Material Laboratory, have included measurements of the spectral reflectance of several paint systems. While the absorptance of the paints in the ultraviolet is appreciable, the percentage of the bomb spectrum in the ultraviolet is relatively small, less than 10 percent. Consequently, reflectance measurements were not made in the ultraviolet, but were confined to the visible and infrared regions.

A second criterion to be employed in considering an aircraft skin coating is its "critical radiant exposure", that is, the thermal energy corresponding to specific damage to the paint. Charring and

blistering of the paint surface are such points, which define the limitations of a given paint system, and which can be recognized readily upon examination.

The third criterion to be employed in considering an aircraft paint system is its temperature characteristic. A paint system may suffer little damage in itself but may cause the temperature of the aircraft's skin to rise to a dangerous level, generating stresses in the aircraft which lead to buckling and destruction.

THERMAL RADIATION SOURCE

In evaluating the damage to several panels of materials exposed during Operation CROSSROADS, several laboratory methods of duplicating thermal damage were tried at the Naval Material Laboratory, leading to the development of the carbon-arc source of intense thermal radiation, in which the radiation emitted by the arc is imaged by appropriate optics.

The source employed in these studies consists of a standard Navy 36-inch carbon-arc searchlight. The arc utilizes 16 mm diameter positive carbons and 11 mm diameter negative carbons, and normally operates at 78 volts and 155 amps. An optical diagram of the thermal source is shown in Figure 1. In operation, a crater in the positive carbon is filled by a glowing gas ball which emits the radiation. This gas ball is at the focus of a paraboloidal mirror with 36-inch diameter which collimates the radiation. A second, similar 36-inch paraboloidal mirror mounted coaxially with the first several feet away, refocuses the radiation at the focal point of the mirror and forms an image of the glowing gas ball. Exposures of materials are generally made in the focal region. With optics in good condition, the spot has an irradiance which averages 90 cal/cm^2 sec over an area 5 mm in diameter, and which falls to an average of 70 cal/cm^2 sec over a region 9 mm in diameter. This irradiance is more than sufficient for most exposures since it represents the peak irradiance at less than one mile from a 20 kt burst. Screens are inserted in the collimated beam to reduce the irradiance to the desired level.

Control of exposure time is exercised by a solenoid-operated knife-blade shutter placed just forward of the focal plane as shown in Figure 2. The shutter system is actuated by an electronic timing circuit and the "open" time is registered on an electric clock. This shutter operation produces an essentially square wave pulse whose total radiant exposure is given by the product of the irradiance and time.

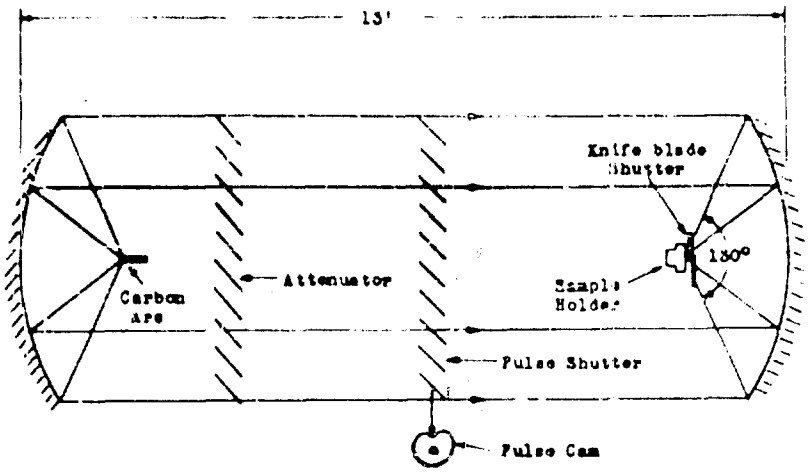

Figure 1 - NML 36-inch paraboloidal-mirror arc-image source of thermal radiation

Figure 2 - Knife-blade shutter at focus of thermal radiation source

Exposures are monitored by exposing a copper-button calorimeter with an appropriate aperture, which for the aircraft skin specimens is a 9 mm round aperture in a polished aluminum plate.

At distances of operational interest, the spectral (wavelength) distribution of the incident thermal radiation, integrated with respect to time, resembles very closely the spectral distribution of sunlight. For each, slightly less than one-half of the radiation occurs in the visible region of the spectrum, approximately one-half occurs in the infrared region, and a very small fraction (rarely greater than 10 percent) lies in the ultraviolet region of the spectrum. The color temperatures of the sun and of an air burst are both about 6000°K. The color temperature of the carbon arc is approximately 5800°K, and there is substantially more infrared energy in its spectrum than in that of the sun or nuclear detonation.

The results of numerous field tests have shown that the ball of fire in a nuclear detonation does not behave as a perfect radiator. This is due to a number of factors. The surface temperature during the first radiation pulse is modified by the disturbed air immediately around the fireball and, at later time, the temperature is not that of the surface but the result of radiation some distance within the fireball. The radius of the fireball during the second thermal pulse is very difficult to determine because the surface of the luminous fireball becomes very diffuse. Since the radii and surface temperatures will depend on the energy yield of the explosion, a different curve will be obtained for every value of yield. However, it is possible to generalize the results by means of scaling laws, so that a curve applicable to the second pulse for all energy yields can be obtained from a single set of calculations. Actually, the power P, is measured directly as a function time, t, for each explosion. However, instead of plotting P versus t, a curve is drawn of the scaled power, i.e., P/P max versus the scaled time, t/t max, where P max is the maximum value of the thermal power, corresponding to the temperature maximum in the second pulse, and t max is the time at which this maximum is attained. The resulting curve, shown in Figure 3, is of general applicability, irrespective of the yield of the explosion. Also shown in Figure 3 is the irradiance-time characteristic of the laboratory source, which results from the modulation of the radiation by a cam-operated venetian blind shutter placed in the collimated beam. The properly cut cam is driven by a variable speed motor and pulses are produced corresponding to weapon yields in the range from 50 kilotons to many megatons. The pulsing shutter and drive mechanism are shown in Figure 4. The timing of the pulse is again controlled by the knife-blade shutter and timer system which is synchronized with the cam. The knife blade shutter is set to open as the venetian

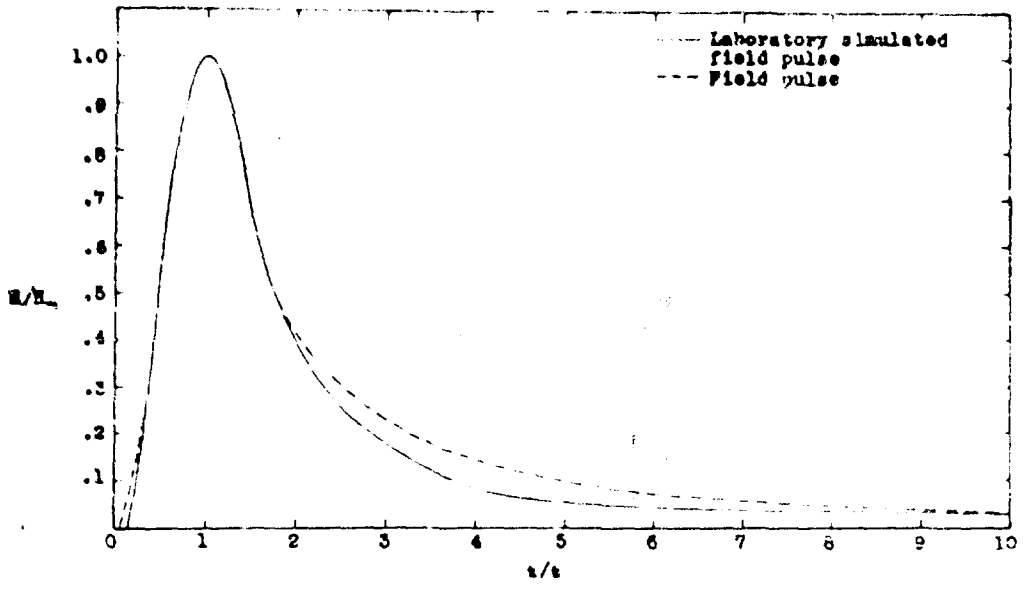

Figure 3 - Laboratory replication of generalized field pulse

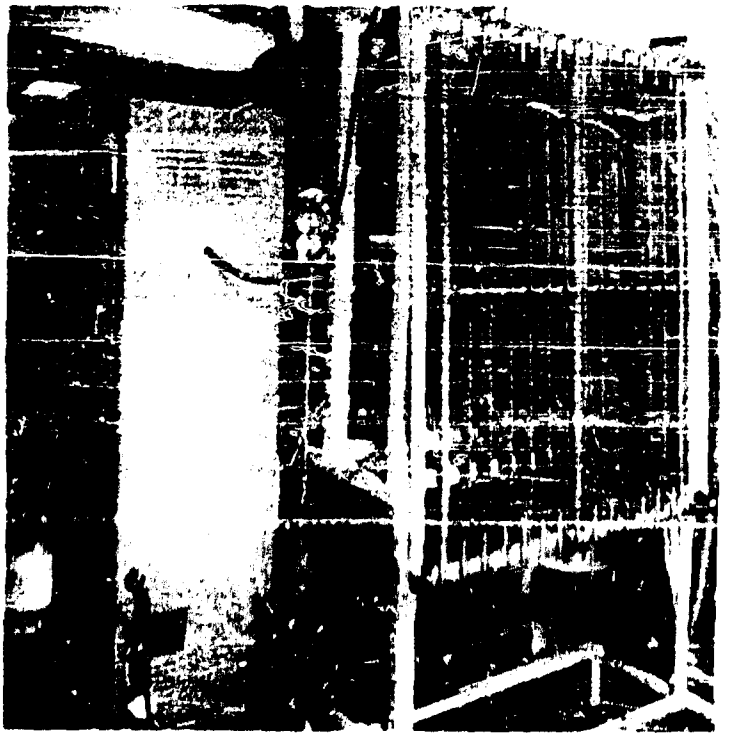

Figure 4 - Shutter and drive mechanism of thermal radiation source

blind starts to open and to close at a time equal to approximately 10 times the time to maximum irradiance.

Table 1

Critical Radiant Exposures of Various Coatings (2 mil) on 0.032 Aluminum

Coating Color	Absorptance	Critical Radiant Exposure (cal/cm^2)	
		50 kt	1 Mt
White	0.27	43	61
Gray	0.68	22	32
Blue	0.93	12	17

SPECTRAL REFLECTANCE DATA

The spectral reflectance measurements were made in the spectral region from 4000 to 27,000 Angstroms. In general, the data in the visible and near infrared regions (4000-10,000 Angstroms) were obtained, using a General Electric Recording Spectrophotometer (1); a Perkin-Elmer Infrared Spectrometer (2) was the basic instrument employed for the measurements beyond 10,000 Angstroms. The measurements using the Perkin-Elmer instrument were extended to those wave lengths covered by the General Electric Spectrophotometer to enable proper correlation of the two sets of data, an important consideration because of the different methods employed to irradiate the sample and collect the reflected energy.

Reflectance measurements with the General Electric Spectrophotometer were taken in a straightforward manner. Special auxiliary equipment (3), designed and constructed at the Naval Material Laboratory, was employed for the reflectance measurements in the infrared. This attachment is essentially a hemispherical integrator mounted at the exit window of the Perkin-Elmer monochromator.

The reflectance data for three paint colors used in Naval aircraft are given in Figure 5. From these data one concludes that the gull gray and sea blue coatings are 2.5 and 3.5 times as absorbing as the ensign white coating.

CRITICAL RADIANT EXPOSURE

To determine the critical radiant exposure which could cause the paint to blister, specimens, 9 mm in diameter, were stamped out of painted sheets of aluminum. The size of the specimen is dictated by the size of the irradiated spot. The specimens were mounted in

the focal plane of the condensing mirror between three knife-edge pins, as shown in Figure 6. Since these measurements were made prior to the development of the nuclear pulse simulator, constant-irradiance pulses were applied to the three paint systems which are typical of those employed in Naval aircraft. For given pulse lengths the irradiance was varied and the threshold thermal flux to cause blistering of the paint was determined, using an "up-and-down" statistical method. From the data obtained and from empirical relationships developed in a similar investigation the critical radiant exposures were determined for laboratory pulses simulating nuclear weapon yields of 50 and 1,000 kt. The data are given in Table 1. The superiority of the white paint is demonstrated. Also, it may be noted that the critical radiant exposure of a given paint system is inversely proportional to its absorptance.

SPECIFIC TEMPERATURE RISE

The Naval Material Laboratory has developed a convenient method to measure reliably the transient temperature rise of a specimen which results from exposure to intense thermal radiation for durations as short as 0.3 second. A thermocouple technique is employed, with the thermocouple's output read on a recording potentiometer. Contact with the rear surface of the specimen is achieved without affecting the physical characteristics of the paint-on-metal surface.

A constantan and an iron wire are held against the back of the specimen by spring pressure, and the other ends of the wires are connected to the potentiometer. The circuit through the thermocouple is completed by the specimen itself. This provides a rapid method of screening samples without the necessity for welding, soldering or peening thermocouples into the specimen.

For comparative purposes, samples with different coatings were exposed to constant-irradiance pulses of equal duration and intensity level, and from the observed temperatures, the specific temperature rise (the temperature rise per unit radiant exposure) was computed. As mentioned above, the specific temperature rise is a measure of the relative protecting power of a coating.

The dependence of the specific temperature rise on the absorptance of the irradiated painted specimen is shown in Figure 7. In this phase of the study heat losses in the system were disregarded. It is to be noted that any strict relationship breaks down due to failure to account for heat losses in the system, and to degradation of the coating and attendant changes in absorptance. These data clearly indicate the drastic effect which dark colors have in causing

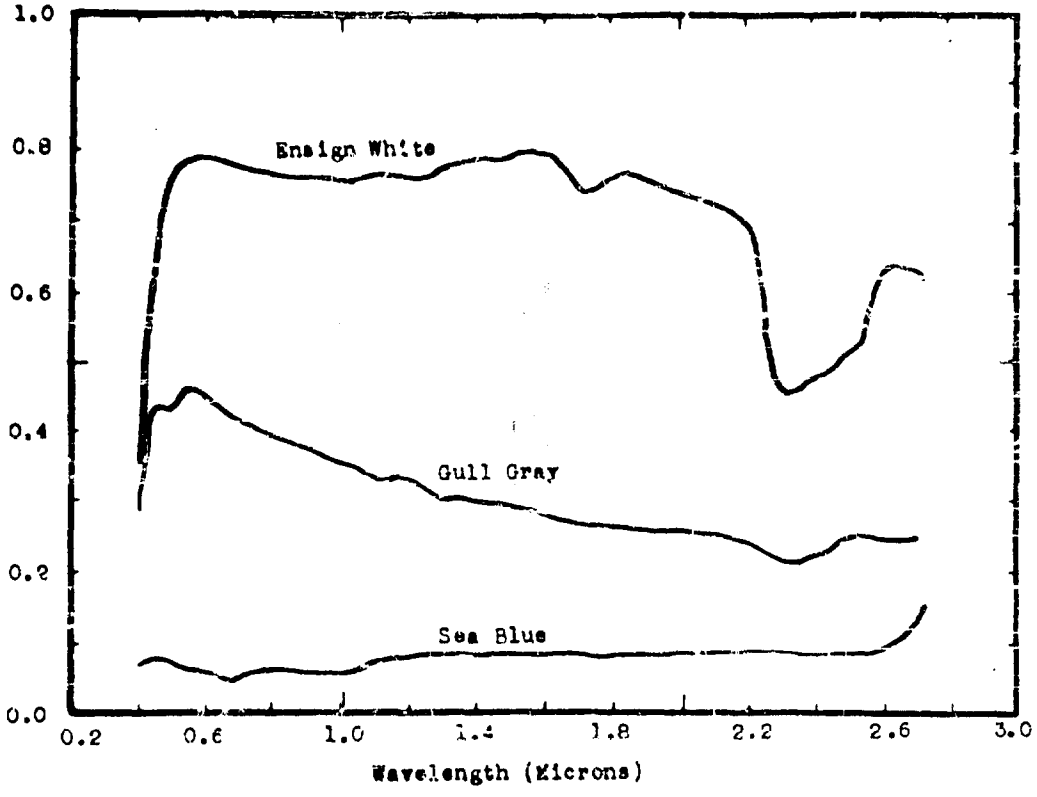

Figure 5 - Spectral reflectance of naval aircraft paints

Figure 6 - Method of mounting samples for exposure to intense thermal radiation

extreme temperatures and, thereby, possible damage to an aircraft. For the lightest color, the temperature rise is higher for the 0.3 second pulse than for the 1.5 second pulse, indicating that not only is the total flux important but also the rate at which it is applied.

The effect of thickness of the metal substrate on the temperature rise of the system is shown in Figure 8. As expected, the temperature rise of the substrate is inversely proportional to its thickness. If the data given in Figures 7 and 8 are compared one may note that gray paint on 0.080 inch thick substrate gives a temperature rise roughly equivalent to that on a white-painted 0.032 inch thick alloy. Decreasing the absorptance by approximately one-half provides the same degree of protection as increasing the mass of the metal by 150 percent.

Another variable which has been investigated is paint film thickness. Some results for one paint are given in Figure 9. It is to be noted that a 100-percent increase in film thickness gives a 32 percent decrease in temperature rise. This added protection, of course, is at the cost of additional weight.

It has been shown that varying the relative concentrations of the pigment solids in a paint can affect the temperature rise of the substrate by as much as 25 percent. Similarly, increasing the pigment-vehicle concentration can also affect the temperature rise of the substrate by as much as 15 percent. In actual usage, however, control of these variables does not always yield a desirable paint; such qualities as adhesion and resistance to hydrocarbons are lost.

The temperature rise data presented thus far have been derived from constant-irradiance exposures and are not corrected for losses due to re-radiation and conduction. Such data have merit for comparing the relative value of various paint systems as temperature-rise inhibitors, but do not yield a ready estimate of expected temperature rises in the skin of aircraft exposed to actual nuclear detonations. Use of the pulsing shutter developed by the Naval Material Laboratory together with a simple correction for heat losses provides a more realistic estimate of the temperature rise and degree of damage that can be expected from a given pulse. The data for one paint system in both the clean and soiled condition and in two color modifications of the system are presented in Figure 10. For the two colors, small amounts of blackening were added to the original white paint to approximate different degrees of soiling. The soiled specimens were exposed to an industrial atmosphere for a period of approximately six months, during which time they received an uneven, oily, sooty coat of soil. These specimens were exposed to the laboratory

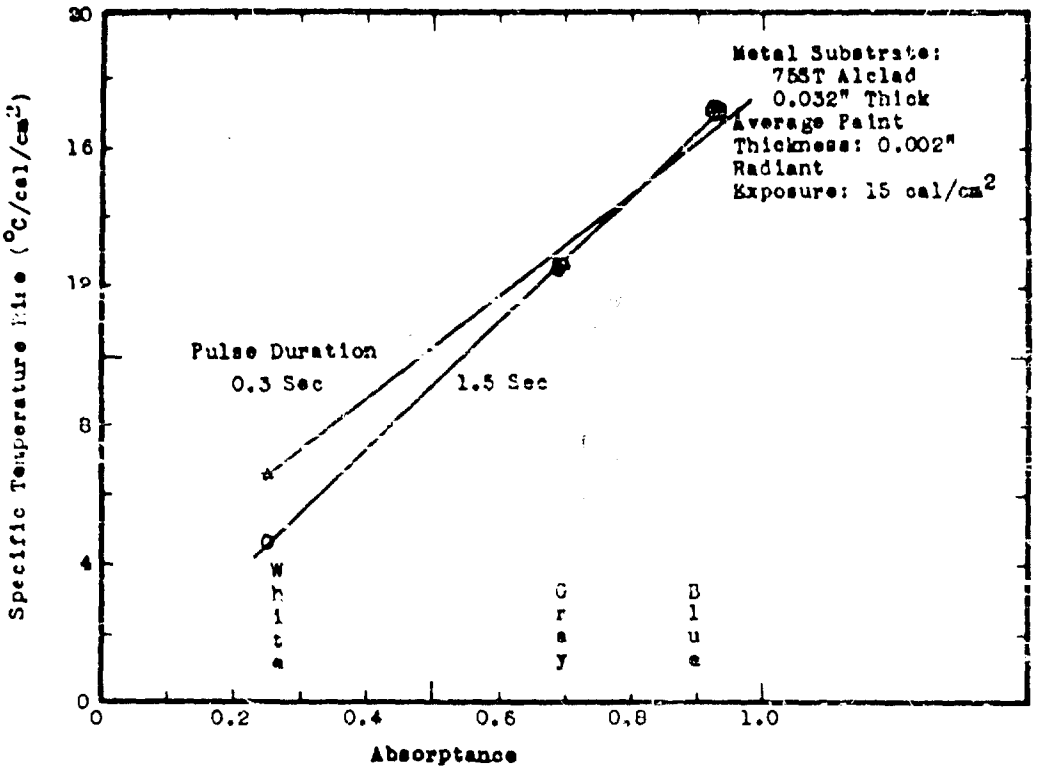

Figure 7 - Temperature rise of coated aircraft skin as a function of absorptance

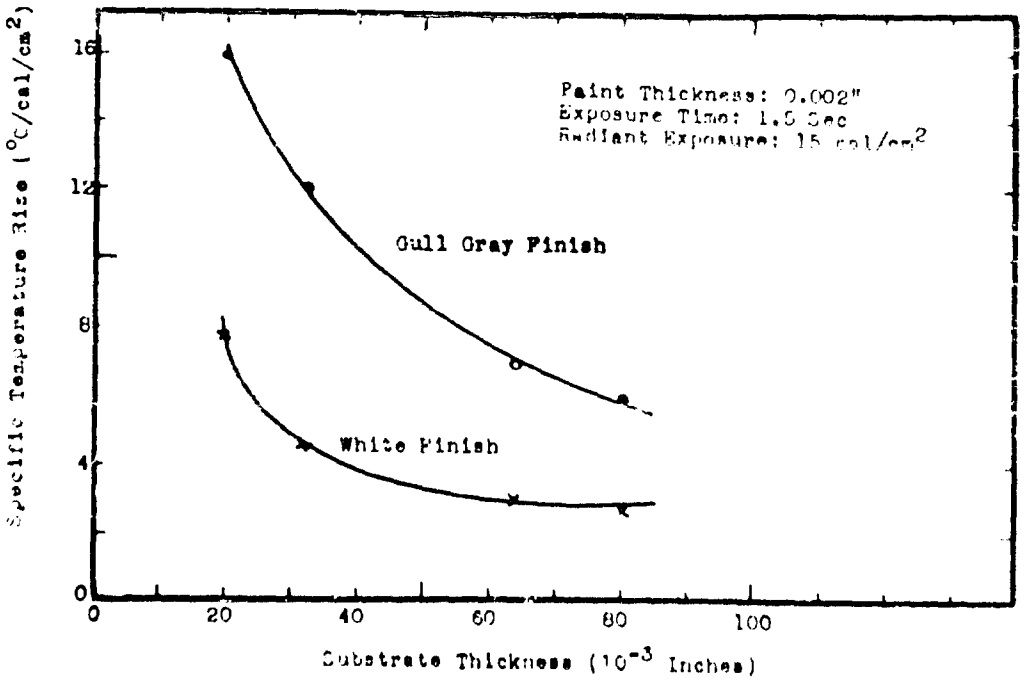

Figure 8 - Temperature rise of coated aircraft skin as a function of substrate thickness

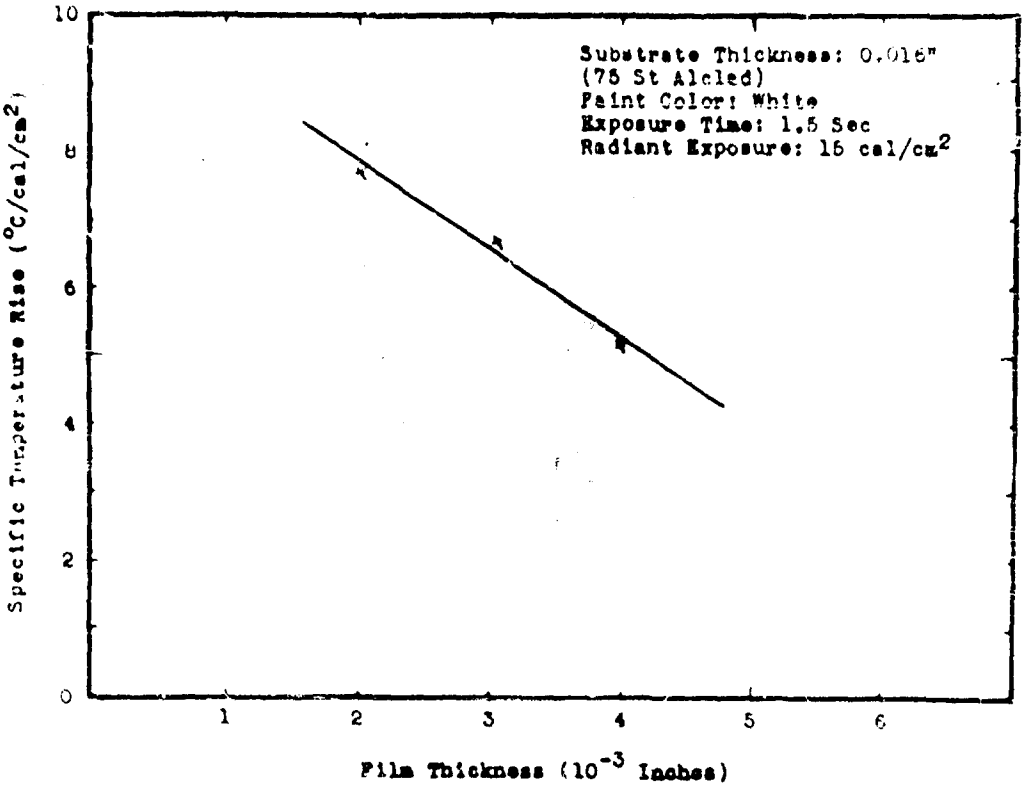

Figure 9 - Temperature rise of coated aircraft skin as a function of film thickness

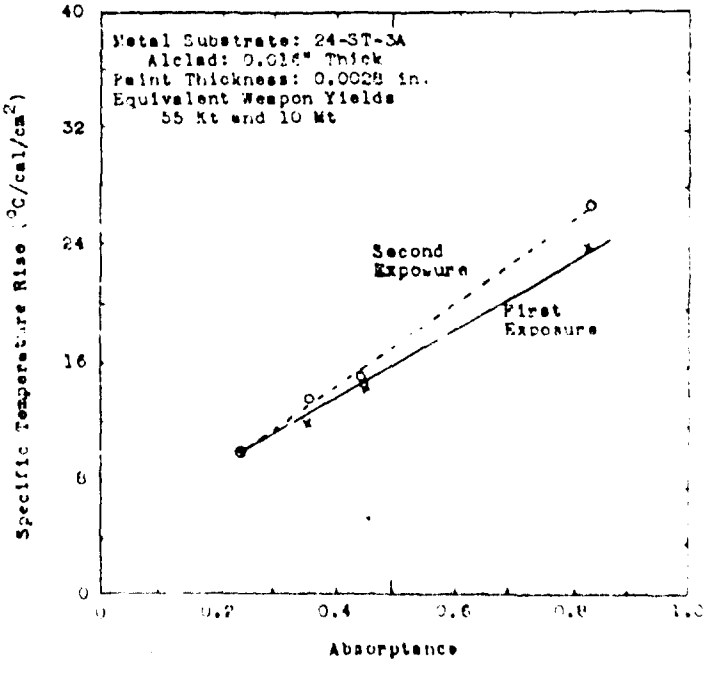

Figure 10 - Temperature rise of painted aircraft skin when irradiated by nuclear weapon pulses

simulated-field pulses for equivalent weapon yields of approximately 55 kt and 10 Mt. All specimens were then irradiated by a second pulse equivalent to a 55 kt detonation. Temperature corrections were made by exposing unpainted, blackened specimens of the same type through a large range of radiant exposures for each pulse of interest. Loss-less temperatures for such exposures on these specimens were calculated; loss rate curves for each pulse were determined as a function of the measured temperatures. The corrections indicated by the curves for each case were applied to the painted specimens. The temperature rises of the paint systems, particularly for the more highly reflecting paints, are proportional to their absorptances. It is to be noted that the curve for the second exposure shows a linear relationship between temperature rise and absorptance, with a higher slope than that which the data for the first exposures indicate. It is believed that the higher absorbing paints suffer greater degradation during exposure, which then cause a higher temperature rise rate during the second exposure. Blistering and emission of volatile products by a paint film cause a loss of desirable film properties, and a decrease in thermal resistance on re-exposure.

CONCLUSIONS

The results of these studies at the Naval Material Laboratory have led to the adoption of a white aircraft coating by the Navy and Air Force. In addition to providing the basic data for determing the thermal envelopes of aircraft, the studies have indicated the directions for improving these coatings. In collaboration with the Naval Air Material Center the Laboratory is continuing its efforts to develop a superior coating. Such a system must have initially, and maintain in service, a low radiant absorptance. The coating must be able to withstand repeated exposures to thermal radiation, yet have a reasonable thickness.

REFERENCES

1. Michaelson, J. L., Construction of the General Electric Recording Spectrophotometer, J. Opt. Soc. Am., 28, 365 (1938)

2. Barnes, R. B., McDonald, R. S., Williams, V. Z., and Kinnaird, R. F., Small Prism Infrared Spectrometry, J. App. Phys., 16, 77 (1945)

3. Derksen, W. L., Monahan, T. I., and Lawes, A. J., A Recording Reflectometer for Measuring Diffuse Reflectance in the Visible and Infrared Regions, J. Opt. Soc. Am. 47, (1957)

CHOICE OF RUBBERS FOR GASKETS IN NUCLEAR RADIATION FIELDS

Ross E. Morris
Rubber Laboratory, Mare Island Naval Shipyard
Vallejo, California

In order to design equipment for operation in a nuclear radiation field, it is important to know the effects of the radiation on the materials to be used in the structure. The working life of a material under these conditions depends on the length of time that its properties which are critical to the operation remain at adequate levels. The chemical changes which occur in a material during irradiation are of consequence only in so far as they affect its physical properties, or affect the physical properties of adjacent materials.

Rubber items are often necessary parts of mechanical devices, particularly for sealing fluids at joints and at sliding contacts of hydraulic systems. The unique properties of a rubber vulcanizate which make it outstanding for this purpose are its softness and its recovery stress against the restraining surfaces. Its softness enables it to conform to minor irregularities on the restraining surfaces, and its recovery stress prevents the passage of fluid. These are the critical properties which must be retained by gaskets and seals used in nuclear radiation fields.

Softness or its inverse, hardness, is an easy property to measure and is being employed by this laboratory as a criterion in the development of vulcanizates for gaskets and seals to be subjected to nuclear radiation. The objective is to find a vulcanizate which undergoes the least change in softness after extensive exposure to nuclear radiation. The ability of a vulcanizate to retain its recovery stress while under compression is a more difficult property to measure, and therefore is not being used as a criterion at this

stage of the development work. Instead, the compression set of the vulcanizate after irradiation is being used. Compression set is a measure of the inability of a compressed rubber specimen to recover its original height when released. This property is generally regarded as being directly related to stress relaxation (1).

Considerable information on the deterioration of rubber vulcanizates by nuclear radiation has already been obtained. This information has been ably summarized by the Radiation Effects Information Center (2). The only previous data concerning the effect of radiation on compression set were published by Bopp and Sisman (3). They compressed specimens of various types of rubbers to 75% of their original height and exposed them to neutron and gamma radiation in a water-cooled channel of a graphite reactor. They found that natural, styrene-butadiene and acrylonitrile-butadiene rubber vulcanizates exhibited the least compression set after irradiation. The silicone, Thiokol and butyl rubber vulcanizates reached 100% set and the latter was depolymerized to a tarry fluid. A neoprene vulcanizate attained a high compression set even though not irradiated. This latter behavior was not discussed by Bopp and Sisman. It was perhaps due to the tendency of neoprene to crystallize when compressed at moderate temperatures.

The investigation described here differed from that of Bopp and Sisman in the following regards: more types of rubbers were tested; the rubbers were compounded in such a manner that the vulcanizates met definite requirements for initial softness and resistance to compression set engendered by heat; and only gamma rays were used for irradiating the compressed specimens.

With regard to the use of gamma radiation in lieu of the more complex radiation emitted from nuclear reactors, Bopp and Sisman (3) and Charlesby (4) believe that similar changes are produced in polymers by different types of nuclear radiation when the effects of the radiations are compared on the basis of equal energy absorption. Gamma radiation is usually more convenient to employ for testing purposes than other nuclear radiations (alpha, beta, slow neutrons or fast neutrons) because it has greater penetration and it does not induce radioactivity in the samples. Good penetration is desirable in order that many rubber specimens in a metallic container can be subjected throughout to an even dosage.

The variables studied in the present investigation were: type of rubber, type of curing agent, presence and type of antioxidant, presence and type of high resonant energy ingredient, and dosage of gamma radiation.

RUBBERS AND COMPOUNDING INGREDIENTS USED IN TESTS

Twenty-three rubbers were selected for preparation of test specimens. These included representatives of all types of commercial rubbers except butyl and Thiokol, which were not included in this survey in view of the findings of Bopp and Sisman. Table 1 lists the rubbers tested and their chemical compositions as defined by the respective manufacturers. Although a silicone rubber, Silastic 7-170, had poor resistance to radiation according to Bopp and Sisman, silicone rubbers which differed chemically from Silastic 7-170 were included in the present investigation.

Sulfur was used for curing all of the vulcanizates of the several styrene-butadiene rubbers and acrylonitrile-butadiene rubbers which were tested except one of each, which was cured with dicumyl peroxide. Other rubbers were cured with the usual ingredients.

Loughborough and coworkers at the B. F. Goodrich Company(5) found that the presence of certain antioxidants in rubber vulcanizates increased their resistance to deterioration of tensile properties by gamma radiation. They coined the term "antirad" for these materials. Many antioxidants were tested in this investigation to find antirads for protecting vulcanizates against compression set caused by gamma radiation. The amount of antioxidant compounded into the various rubbers was generally 5 parts per 100 parts by weight of rubber. Antioxidants were not compounded into rubbers to be cured by dicumyl peroxide or other peroxides since they interfered with the peroxide cure.

The presence of benzene rings in polymers is known to bring about improved resistance to nuclear radiation (2, 3), possibly due to their high resonance energy (6). It therefore seemed worthwhile to find out whether the presence in the vulcanizates of low-molecular-weight chemicals containing benzene rings or condensed aromatic structures would be beneficial. The antioxidants mentioned above were materials of this type, but they also contained amine or phenolic groups which are reactive with free radicals. It was desired to evaluate other aromatic compounds for use as antirads. Accordingly, a number of plasticizers containing benzene rings, for example, butyl benzyl phthalate, were compounded into different rubber stocks in the amount of 10 parts per 100 parts of rubber. In addition, other chemicals with higher melting points and containing benzene rings or condensed aromatic structures, for example, phenanthrene, were compounded into different rubber stocks in the amount of 5 parts per 100 parts of rubber, in most cases.

TABLE 1. RUBBERS USED FOR PREPARING TEST SPECIMENS
(Sheet 1 of 2 sheets)

Name	Type
Natural rubber	Isoprene polymer
Synpol 1000	Styrene/butadiene copolymer (about 23% combined styrene)
Naugapol 1023	Styrene/butadiene copolymer (about 13% combined styrene)
Synpol 1500	Styrene/butadiene copolymer (about 23% combined styrene) low-temperature polymerized
Naugapol 1506	Styrene/butadiene copolymer (about 12% combined styrene) low-temperature polymerized
Hycar 2001	Styrene/butadiene copolymer (higher combined styrene than Synpol 1500)
Hycar 1001	Acrylonitrile/butadiene copolymer (about 40% combined acrylonitrile)
Hycar 1002	Acrylonitrile/butadiene copolymer (about 33% combined acrylonitrile)
Hycar 1014	Acrylonitrile/butadiene copolymer (about 20% combined acrylonitrile)
Hycar 1041	Acrylonitrile/butadiene copolymer (about 40% combined acrylonitrile) low-temperature polymerized
Hycar 1042	Acrylonitrile/butadiene copolymer (about 33% combined acrylonitrile) low-temperature polymerized
Hycar 1043	Acrylonitrile/butadiene copolymer (about 29% combined acrylonitrile) low-temperature polymerized
Hycar 1071	Acrylonitrile/butadiene copolymer (Hycar 1041 modified to contain carboxyl groups)
Hycar 1072	Acrylonitrile/butadiene copolymer (Hycar 1042 modified to contain carboxyl groups)

TABLE 1. RUBBERS USED FOR PREPARING TEST SPECIMENS
(Sheet 2 of 2 sheets)

Name	Type
Philprene VP-25	2-Methyl-5-vinyl pyridine/butadiene copolymer (about 25% pyridine derivative)
Neoprene WRT	Chloroprene polymer
Viton A-HV	Vinylidene fluoride/hexafluoropropylene copolymer
Genthane S	Polyurethane (iodine no. = 1)
Adiprene C	Polyurethane (iodine no. = 26)
Hycar 4021	Acrylic acid ester/halogen-containing-derivative polymer
Silicone W96	Methyl vinyl siloxane polymer
Silicone 2048	Compounded methyl phenyl siloxane polymer (higher than normal phenyl content)
Silicone LS-53	Compounded fluorine-containing siloxane polymer

The recipes for all of the vulcanizates, except those of Philprene VP-25, Viton A-HV and the silicone rubbers, contained Philblack A as a reinforcing filler. Philblack A is a carbon black classified as a fast extruding furnace black. The Philprene VP-25 vulcanizate contained no carbon black since adequate properties were obtained without its use. The Viton A-HV vulcanizate contained Thermax, which is classified as a medium thermal black. The Silicone W96 vulcanizate contained HiSil X303, a very fine silica. The mineral fillers in the Silastic S-2048 and Silastic LS-53 vulcanizates were not identified by the manufacturer of these stocks.

In the case of each stock compounded by this laboratory, the content of reinforcing filler was adjusted to yield a vulcanizate having a 15-second Shore A hardness of 70±5. The hardness of Silastic S-2048 was 60 and that of Silastic LS-53 was 57. All of the vulcanizates including the two Silastics had compression sets of 40% or less after 70 hours at 212°F when tested by ASTM D395-55, Method B. Thus, most of these vulcanizates had the hardness and resistance to hot compression set of a typical O-ring seal.

METHOD OF TESTING

The vulcanizates were exposed to gamma radiation in the form of compressed cylindrical specimens. The specimens originally 0.75 inch in diameter and 0.50 inch thick, were compressed during exposure to a thickness of 0.35 inch (30% compression). Three replicate specimens of each vulcanizate were subjected to each of the conditions to be described later.

The specimens were held in special containers during exposure to gamma radiation. One of these devices is shown in Figure 1. It consisted of a stack of eight square plates made from 61S aluminum, held together by five aluminum tie rods (aluminum is essentially transparent to gamma radiation). Rubber specimens were clamped between each pair of plates in the stack. The top plate was plane on both faces. The other plates were plane on their bottom face, but were milled out on their top face to provide a flat bearing surface for the specimens as well as shoulders for limiting the compression of the specimens. The aluminum surfaces in contact with the specimens had a roughness not greater than 63 microinches.

The arrangement of the specimens on each plate of the containers is shown in Figure 2. Each container held 42 specimens distributed between seven levels. The locations of the three

Figure 1 - Assembled aluminum container for exposing compressed rubber specimens to gamma radiation

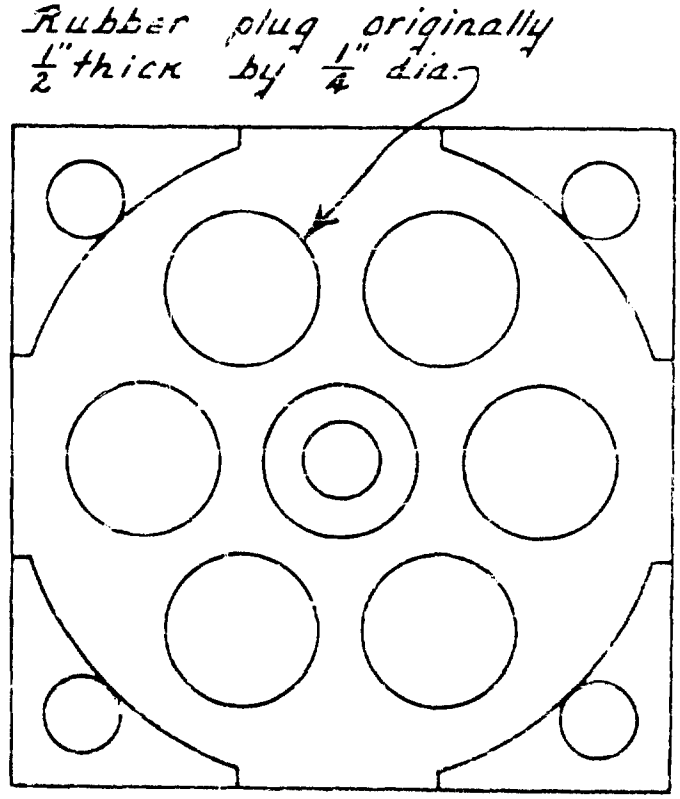

Figure 2 - Arrangement of specimens on each milled plate of container

replicate specimens of each vulcanizate, which were being subjected to the same test conditions, were randomized between two containers and the seven levels of each container. The purpose of the random arrangement was to reduce the error in the averaged test results in the event that intensity of gamma radiation was non-uniform.

The loaded containers were sent to the Atomic Energy Division of the Phillips Petroleum Company at Idaho Falls, Idaho. Containers holding three specimens of each vulcanizate which was sent for irradiation were retained at the laboratory in a room maintained at 73.5±2°F. These specimens served as air-exposed controls.

The exposure to gamma radiation was carried out in the water columns shown in Figures 3 and 4. The canal in which the water columns stood had a water depth of 15 1/2 feet down to the fuel element grid plate. The water columns were closed at the bottom, but had a demineralized water line injecting clean water into the lower part of the columns which overflowed at the top and thus purged the columns continuously. The water temperature was about 75°F. The containers were raised to the upper end of the water columns when it was desired to remove them from the field of radiation but keep them in the water. This was done when replicate specimens were being exposed to different dosages of gamma radiation, and it was desired to leave all of them in water for the same period.

Containers holding three specimens of each vulcanizate were immersed in the water but kept out of the radiation field. These specimens served as water-exposed controls.

When the containers were returned from Idaho Falls, all specimens, including the air-exposed and water-exposed controls, were released at the same time. The specimens were let stand for 24 hours at 73.5±2°F and then measured for thickness.

An indentation reading was obtained on each specimen including the controls by means of a Mast Indentometer, Model 650-2. Since most of the specimens were somewhat cupped, they were supported on a 1/4-inch diameter flat pedestal centered under the indentor while taking the reading. The critical features of this test were 0.125-inch diameter hemispherical indentor, 1000-gram weight resting on the indentor for exactly one-minute reading, and the indentation expressed in hundredths of a millimeter. The higher the reading on the Mast Indentometer, the softer was the stock. The Mast Indentometer measured hardness (inversely) more precisely than did the Shore durometer.

Figure 3 - MTR fuel elements positioned around various water columns in canal

Figure 4 - Aluminum containers being held above the positions they occupied in the water columns

Since some of the specimens showed poor recovery from compression even though they had not been exposed to radiation, all of the specimens were placed in an oven for 4 hours at 212°F, cooled on a wooden surface for 30 minutes, then again measured for height. This treatment was for the purpose of overcoming the effect of high internal viscosity and thereby hastening any recovery in height which would eventually occur.

The compression set values, before and after the oven treatment, were calculated using the following equation:

$$\text{Percent compression set} = \frac{T_o - T_r}{T_o - T_c} \times 100$$

Where T_o = specimen thickness before compression
T_c = specimen thickness when compressed
T_r = specimen thickness after recovery

RESULTS OF TESTS

In the first phase of this investigation, compressed specimens were exposed to gamma-ray dosages of 10^7, 10^8 and 10^9 roentgens. The results of these tests showed that all of the vulcanizates had less than 95% compression set after exposure to 10^7 roentgens, that most of them had not reached 95% set after exposure to 10^8 roentgens, but that all of them had attained 95-100% set after exposure to 10^9 roentgens. Figure 5 shows the difference in thickness of specimens of the same vulcanizate after receiving various amounts of radiation. Since 10^8 roentgens was the highest dosage of those tried at which there was a graded behavior of the vulcanizates, most of the testing was done with this dosage.

The water-exposed and air-exposed controls, with two exceptions, exhibited negligible compression set after release and oven treatment. This was the case even though some of the specimens had been compressed for periods as long as 29 days. The exceptions were the Silicone W96 and Silastic S-2048 specimens. The water-exposed and air-exposed controls of these rubbers had about 30% set.

Table 2 shows the results of exposures to 10^8 roentgens. All of the basic vulcanizates are listed in this table, also those which contained Neozone D, an antioxidant (candidate antirad), and those which contained the most effective antirad or combination of antirads found to date. The compression set values given in this

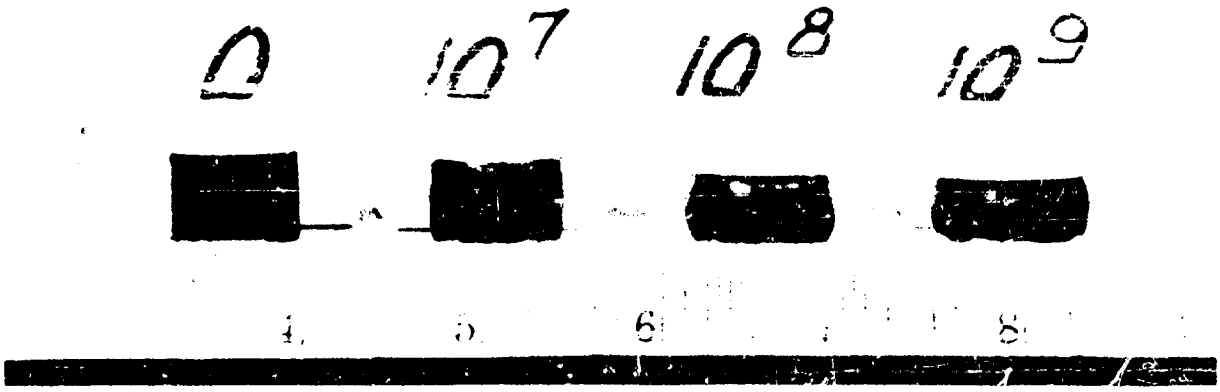

Figure 5 - Appearance of specimens of same vulcanizate after different dosages (roentgens) of radiation. They had been compressed 30% during exposure.

TABLE 2. COMPRESSION SET AND SOFTNESS OF VULCANIZATES AFTER EXPOSURE TO 10^8 ROENTGENS
(Sheet 1 of 5 sheets)

Rubber	Curing System	Antioxidant	High Resonant Energy Ingredient	Comp. Set %	Softness Indent. mm
Natural	Thionex (1)-sulfur			80	39
Natural	Thionex-sulfur	Neozone D (2)		73	50
Synpol 1000	Thionex-sulfur			83	31
Synpol 1000	Thionex-sulfur	Neozone D		71	48
Naugapol 1023	Thionex-sulfur			86	36
Naugapol 1023	Thionex-sulfur	Neozone D		79	50
Synpol 1500	Thionex-sulfur			75	43
Synpol 1500	Thionex-sulfur	Neozone D		64	59
Synpol 1500	Thionex-sulfur	Santoflex GP (3)		55	64
Synpol 1500	Thionex-sulfur	Thermoflex A (4)		59	60
Synpol 1500	Thionex-sulfur	Thermoflex A	dibenzyl phthalate	49	64
Synpol 1500	Thionex-sulfur		acridine	54	68

TABLE 2. COMPRESSION SET AND SOFTNESS OF VULCANIZATES AFTER EXPOSURE TO 10^8 ROENTGENS
(Sheet 2 of 5 sheets)

Rubber	Curing System	Antioxidant	High Resonant Energy Ingredient	Comp. Set %	Softness Indent. mm
Sympol 1500	DiCup 40C (5)			59	48
Naugapol 1504	Thionex-sulfur			85	28
Naugapol 1504	Thionex-sulfur	Neozone D		71	45
Hycar 2001	Thionex-sulfur			81	40
Hycar 2001	Thionex-sulfur	Neozone D		73	52
Hycar 1001	Thionex-sulfur			83	28
Hycar 1001	Thionex-sulfur	Neozone D		77	40
Hycar 1002	Thionex-sulfur			84	27
Hycar 1002	Thionex-sulfur	Neozone D		78	38
Hycar 1014	Thionex-sulfur			90	25
Hycar 1014	Thionex-sulfur	Neozone D		85	42
Hycar 1041	Thionex-sulfur			88	26

TABLE 2. COMPRESSION SET AND SOFTNESS OF VULCANIZATES AFTER EXPOSURE TO 10^8 ROENTGENS
(Sheet 3 of 5 sheets)

Rubber	Curing System	Antioxidant	High Resonant Energy Ingredient	Comp. Set %	Softness Indent. mm
Hycar 1041	Thionex-sulfur	Neozone D		82	41
Hycar 1041	Thionex-sulfur	Neozone D	Santicizer 160 (6)	66	58
Hycar 1041	Thionex-sulfur	Age Rite Hipar (7)		69	52
Hycar 1041	DiCup 40C			91	31
Hycar 1042	Thionex-sulfur			83	27
Hycar 1042	Thionex-sulfur	Neozone D		74	41
Hycar 1043	Thionex-sulfur			85	32
Hycar 1043	Thionex-sulfur	Neozone D		74	51
Hycar 1071	Thionex-sulfur			79	22
Hycar 1071	Thionex-sulfur	Neozone D		71	43
Hycar 1072	Thionex-sulfur			79	21
Hycar 1072	Thionex-sulfur	Neozone D		67	40

TABLE 2. COMPRESSION SET AND SOFTNESS OF VULCANIZATES AFTER EXPOSURE TO 10^8 ROENTGENS
(Sheet 4 of 5 sheets)

Rubber	Curing System	Antioxidant	High Resonant Energy Ingredient	Comp. Set %	Softness Indent. mm
Hycar 1072	Thionex-sulfur	Wingstay 100 (8)		58	46
Philprene VP-25	Ethyl Tuads (9)-Sulfasan R (10) p-xylene hexachloride			77	12
Neoprene WRT	Thiate B (11)			87	18
Neoprene WRT	Thiate B	Neozone A (12)		74	38
Viton A-HV	HMDA Carbamate (13) Zinc oxide-Dyphos (14)			100	23
Genthane S	DiCup 40C			81	103
Adiprene C	DiCup 40C			59*	54
Adiprene C	DiCup 40C		Sarcicizer 160	56*	67
Hycar 4021	Triethylene tetramine			90	48
Silicone W96	Ditertiary butyl peroxide			98	22

TABLE 2. COMPRESSION SET AND SOFTNESS OF VULCANIZATES AFTER EXPOSURE TO 10^8 ROENTGENS
(Sheet 5 of 5 sheets)

Rubber	Curing System	Antioxidant	High Resonant Energy Ingredient	Comp. Set %	Softness Indent. mm
Silastic S2048	Not known			97	30
Silastic LS-53	Not known			103	49

* Some of the specimens were crushed during the period of compression. This indicated that the ultimate elongation of the vulcanizate was marginal.

(1) Tetramethyl thiuram monosulfide
(2) N-phenyl-beta-naphthylamine
(3) N-cyclohexyl-N'-phenyl-p-phenylenediamine
(4) 50% N-phenyl-beta-naphthylamine
25% 4,4'-dimethoxydiphenylamine
25% N,N'-diphenyl-para-phenylenediamine
(5) 40% dicumyl peroxide, 60% inert filler
(6) Butyl benzyl phthalate
(7) 50% p-isopropoxy diphenylamine
50% diphenyl-p-phenylenediamine
(8) Composition not disclosed by manufacturer
(9) Tetraethyl thiuram disulfide
(10) 4,4'-dithio dimorpholine
(11) "Trialkyl" thiourea
(12) N-phenyl-alpha-naphthylamine
(13) Hexamethylene diamine carbamate
(14) Dibasic lead phosphite

table were those calculated from thickness measurements made after the oven treatment.

One of the two rubbers which were found to have the best inherent resistance to gamma radiation was Adiprene C, a polyurethane. Its compression set was low (56% with Santicizer 160 plasticizer) and its indentation was high (67) after a dosage of 10^8 roentgens. Some of the specimens of this vulcanizate, however, were found to be crushed when released from the containers after being compressed for 22 days. The crushing occurred whether the specimens had been irradiated or not. This behavior indicated that the Adiprene C vulcanizate was too brittle for use in a gasket or seal.

The rubber which equalled Adiprene C in resistance to gamma radiation was Synpol 1500, a styrene-butadiene copolymer. The specimens of this rubber were not crushed by compression. The Synpol 1500 stock cured by dicumyl peroxide had better resistance to radiation than the sulfur-cured stock, although the resistance of the latter was enhanced by compounding with an antioxidant and a plasticizer which contained benzene rings. For example, Synpol 1500 cured with sulfur and containing Thermoflex A antioxidant and dibenzyl phthalate had the lowest compression set (49%) after a dosage of 10^8 roentgens of any vulcanizate tested in this program. It also had a high indentation (64). Acridine, a high resonant energy material, also proved to be an efficient antirad for Synpol 1500. It was as beneficial as the best antioxidant, Santoflex GP.

Properly compounded Synpol 1500 (or its equivalent) is therefore the best rubber found to date for use in gaskets and seals where resistance to gamma radiation is required. This rubber, however, is not resistant to petroleum oils or gasoline. Where gaskets and seals with resistance to petroleum oils as well as to gamma radiation are required, Hycar 1072, an acrylonitrile-butadiene copolymer modified to contain carboxyl groups, is the best rubber to use. Its compression set was quite low (58%) and its indentation was reasonably high (46) after a dosage of 10^8 roentgens, providing that the stock contained a suitable antioxidant such as Wingstay 100. If gaskets or seals are to be used in contact with aromatic gasoline, they should be made from Hycar 1071. This rubber is similar to Hycar 1072 except that it contains more acrylonitrile. It is slightly inferior to Hycar 1072 in resistance to radiation.

The vulcanizates included in this investigation which possessed the ultimate in heat resistance were a fluoro rubber, a fluorinated silicone rubber and two silicone rubbers. These four rubbers had less than 95% set after 10^7 roentgens, but had reached

95 to 100% set after 10^8 roentgens. However, the fluorine-containing rubbers, Viton A-HV and Silastic LS-53, were decomposed by the radiation with liberation of a corrosive chemical, probably hydrofluoric acid. The aluminum plates which pressed against specimens of these vulcanizates during irradiation were corroded on and near the area of contact. The condition of the surface of a plate which pressed against a Viton A-HV specimen is shown in Figure 6. The product of corrosion was an aluminum fluoride. In view of this finding, it is concluded that rubbers containing fluorine should not be used in a radiation field, and that a gasket or seal required to operate at temperatures above 300°F in a radiation field should be made from a silicone rubber not containing fluorine.

The findings of this investigation have certain theoretical implications. The permanent compression set of fully vulcanized rubber is believed to be caused by one or two chemical reactions; (1) breaking of primary valence bonds in stressed polymer chains, or in cross links between the chains, with consequent flow of the residues to positions of lower stress, and (2) formation of new cross links between stressed polymer chains, or chain residues, which tend to hold them in their new positions. Both of these molecular phenomena also affect the mechanical stiffness of the rubber; the first tends to soften it and the second tends to harden it. The hardnesses of all of the vulcanizates included in this investigation, except Genthane S, a polyurethane, were consistently increased by exposure to radiation. Thus it appears that the compression sets of these rubbers were largely due to the formation of new cross links. Genthane S apparently experienced considerable breakage of primary valence bonds in the earlier stages of irradiation.

SUMMARY

To summarize the results of this investigation, it has been shown that none of the rubbers tested would yield gaskets or seals capable of performing satisfactorily after being irradiated with 10^9 roentgens of gamma rays. For lower dosages of radiation, best results would be obtained by using properly compounded styrene-butadiene rubber, or acrylonitrile-butadiene rubber containing carboxyl groups if oil and gasoline resistance is required. Silicone rubber is the best where the gasket or seal must also resist high temperatures.

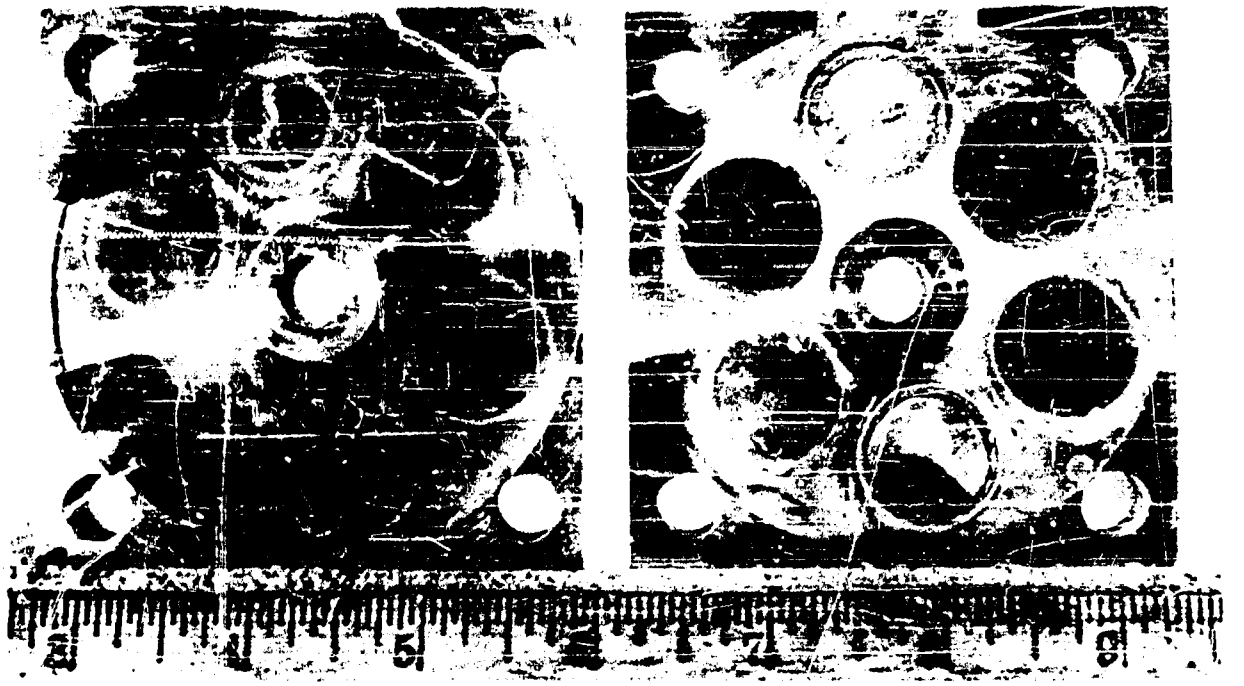

Figure 6 - Aluminum plates showing corrosion caused by philprene VP-25 specimen (top circular area on left plate) and viton A-HV specimen (top circular area on right plate) during irradiation

ACKNOWLEDGEMENT

The author wishes to express his appreciate to Messrs. R. R. James and F. Caggegi of this laboratory for their help in the experimental work, and to Messrs. F. L. McMillan and D. L. Funke of the Phillips Petroleum Co., Atomic Energy Division, for their assistance in designing the compression device and for carrying out the irradiation of the specimens.

REFERENCES

(1) "Effect of Some Accelerators on the Physical Properties of Nitrile Rubber Vulcanizates", by R. E. Morris, R. R. James and I. P. Seegmen; Rubber World, January, 1949.
(2) "The Effect of Nuclear Radiation on Elastomeric and Plastic Materials", by N. J. Broadway et al; May 31, 1958, The Radiation Effects Information Center, Battelle Memorial Institute.
(3) "Radiation Stability of Elastomers", by C. D. Bopp and C. Sisman; Nucleonics, vol. 13, page 28, July 1955; Rubber Chemistry and Technology, vol. 29, page 1233, 1956.
(4) "Cross-Linking of Polythene by Pile Radiation", by A. Charlesby; Proceedings of the Royal Society (London), vol. 215A, Page 187, 1952.
(5) "A Study of the Effects of Nuclear Radiations on Elastomeric Compounds and Compounding Materials", by D. L. Loughborough, A. E. Juve, J. R. Beatty and J. W. Born, B. F. Goodrich Co.; Wright Air Development Center Report 55-58, December 1954.
(6) "The Theory of Resonance and Its Applications to Organic Chemistry", by G. W. Wheland; John Wiley and Sons, Inc., New York, 1944.

NUCLEAR RADIATION EFFECTS IN MAGNETIC CORE MATERIALS AND PERMANENT MAGNETS

D. I. Gordon, R. S. Sery and R. E. Lundsten
U. S. Naval Ordnance Laboratory
White Oak, Silver Spring, Maryland

In view of the increasing severity of environmental requirements for materials needed in electronic equipment for nuclear-powered weapons and space vehicles, the U. S. Naval Ordnance Laboratory, White Oak (Magnetic Materials Division) has been conducting studies of the effects of some of these environmental factors on magnetic materials. High temperature effects and pressure effects in magnetic materials were reported in recent publications (1, 2).

Nuclear radiation effects are also included in this environmental effects program. The Naval Ordnance Laboratory results on soft (i.e. high permeability - low coercive force) magnetic materials have been reported (3-7). Detailed results of radiation effects on hard (i.e. "permanent" or high coercive force) magnetic materials will be presented in NAVORD Report 6276 (8). It is the purpose of this paper to present the highlights of both of these irradiation studies and to summarize the status of research in this area.

The Advisory Group on Electronic Parts (AGEP) has published an environmental requirements guide which represents the needs of the three military departments (9). The neutron radiation conditions, summarized in Table I, are shown in three groups, Groups VII, IX, and X, the flux level increasing with group number. The Naval Ordnance Laboratory magnetic materials discussed here were irradiated in the Brookhaven National Laboratory (BNL) Reactor

TABLE I. NUCLEAR RADIATION TEST ENVIRONMENTS*

	AGEP Environ. Group VII	NOL Test Environ. (ENL Reactor)	AGEP Environ. Group IX	AGEP Environ. Group X
Application	Nuclear propelled aircraft and Ballistic missiles		Nuclear powered weapons	Nuclear powered weapons
Fast** flux-nv (Neutrons/cm^2 sec.)	10^9	10^{11}	10^{11}	10^{13}
Time of radiation exposure	3×10^6 sec. 1,000 hours	10^6 sec. 325 hours	3×10^6 sec. 1,000 hours	3×10^6 sec. 1,000 hours
Integrated fast flux-nvt (neutrons/cm^2)	3×10^{15}	10^{17}	3×10^{17}	3×10^{19}

* Adapted from 'Environmental Requirements Guide for Electronic Parts" AGEP, Office of Assistant Secretary of Defense, Research and Engineering, October 1957.

**"Fast" generally refers to the energy range from 0.02 Kev to 10 Mev. However, as defined by the Air Force and the AGEP, it refers to the reactor energy spectrum as modified by a boron or boral shield. This is approximately equivalent to cadmium shielding (Cd cutoff cross-section is $\sim$0.5 ev). In this report, "fast" and "epicadmium" ($E > 0.5$ ev) are used as synonyms.

at an epicadmium flux (nv) of $\sim 10^{11}$ neutrons/cm^2 sec. for one reactor operating period ($\sim$2 weeks). The corresponding integrated epicadmium flux (nvt) was $\sim 10^{17}$ neutrons/cm^2. Details of the test conditions are given in Table II. Comparing this radiation condition with the AGEP test levels shown in Table I, one sees that the Naval Ordnance Laboratory test level exceeds that of Environmental Group VII (for nuclear powered aircraft and ballistic missiles) by two orders of magnitude and corresponds very closely to the Group IX level (for other nuclear powered weapons). The Group X level ($\sim 10^{19}$ nvt) is being considered for future tests.

Physical Picture

Coercive force and initial permeability are among the several structure sensitive properties of magnetic materials. They may change in value by large amounts as a result of small changes in metallurgical treatment and impurity of the material. By contrast, properties which are not normally structure sensitive are density and saturation magnetization. Although the physics of structure sensitive properties is not well understood, coercive force is generally thought of as a measure of the resistance to domain wall motion due to imperfections and non-uniformity in the bulk material*. These in turn are attributed to inhomogeneous internal strains, non-magnetic inclusions, crystallite dimensions, etc. Since nuclear irradiation is known to introduce imperfections and inhomogeneities in the lattice through the production of vacancies and interstitials, or other mechanisms, one might anticipate that those materials with the lowest coercive force (i.e. with the minimum number of imperfections) would be affected most by the radiation created imperfections. Similarly, one might expect the high coercive force materials (which already have large numbers of imperfections and non-uniformities) to be unaffected.

---

* In the case of materials composed of very small grains or fine powders, coercive force depends upon magnetocrystalline anisotropy, shape anisotropy, strain, and particle size.

TABLE II. BROOKHAVEN NATIONAL LABORATORY REACTOR TEST CONDITIONS OF THE NOL MAGNETIC MATERIALS IRRADIATIONS

NOL Experiment Number	I	II	III
Date	July 1956	August 1957	Oct. 1958
Kind of Magnetic Material	SOFT	SOFT	PERMANENT
No. of Samples Irradiated	7	10	26
Ambient Temperature in Hole (°C)	55-65	not measured	87
Sample Temperature (°C)	not measured	74-80	90
Neutron flux (nv) - Total	1.8×10^{12}	2.1×10^{12}	5.6×10^{12}
- Epicadmium	0.7×10^{11}	2×10^{11}	2.7×10^{11}
->2.8 Mev	not measured	not measured	1.1×10^{10}
Integrated neutron flux (nvt) - Total	2.7×10^{18}	2.1×10^{18}	5.9×10^{18}
- Epicadmium	1×10^{17}	2×10^{17}	2.8×10^{17}
->2.8 Mev	not measured	not measured	1.2×10^{16}
Irradiation Time (hours)	393	302	292
Gamma flux (photons/cm^2sec.)	$10^{11} - 10^{12}$	$10^{11} - 10^{12}$	$10^{11} - 10^{12}$
Gamma energy (Mev)	1 - 2	1 - 2	1 - 2
Post-irradiation activity (Curies)	~ 2	< 1	~ 12

Since ordering is related both to magnetic hardness and magnetic softness through the degree and manner of producing imperfections, and since neutron irradiation has been shown to affect ordering, one might expect those magnetic materials whose properties are correlated with degree of order to be radiation sensitive.

General Results

In general agreement with the physical picture sketched above, magnetic materials with pre-irradiation coercive forces less than ~ 0.5 oersted showed appreciable changes in properties, while those materials with pre-irradiation coercive forces greater than ~ 0.5 oersted showed no appreciable changes. In other words, only the softest magnetic materials changed. The harder core materials and the permanent magnet materials showed no appreciable changes. However, the soft magnetic materials that did change are of considerable technological importance and their changes were generally drastic degradations. Table III shows the changes in dc properties of the soft magnetic materials, while their changes in 60 cps properties are shown in Table IV. For the permanent magnets, the results are shown in Table V. Essentially, all of the permanent magnet changes are within the limits of experimental error.

Radiation Sensitivity of Structure Sensitive Properties

Also in agreement with the physical picture, the results show that saturation induction, a structure insensitive property, did not change for any of the materials irradiated. This is illustrated in Figure 1, which shows magnetic saturation as a function of integrated neutron flux. The small initial decrease which appears in some of the curves is explainable in terms of temperature effects. The sensitivity to radiation of structure sensitive properties is shown very effectively in Figures 2, 3 and 4, which are semi-log plots of coercive force, initial permeability, and maximum permeability respectively, as functions of integrated neutron flux. (The data shown were obtained from in-pile measurements). These curves show (as do Tables III and IV) that the highest permeability, lowest coercive force materials (Supermalloy, 4-79 Mo-Permalloy, Mumetal, oriented 50 nickel-iron, and 48 nickel-

TABLE III. D-C MAGNETIC PROPERTIES (SOFT MAGNETIC MATERIALS)
PERCENTAGE CHANGE AS RESULT OF IRRADIATION WITH ~2 x 10^{18} N/CM^2 (TOTAL)

Materials	$\frac{\Delta \mu_{20}}{\mu_{20}}$	$\frac{\Delta \mu_{max}}{\mu_{max}}$	$\frac{\Delta H_c}{H_c}$	$\frac{\Delta B_r}{B_r}$	$\frac{\Delta B_m}{B_m}$	$\frac{\Delta (B_r/B_m)}{B_r/B_m}$
SUPERMALLOY	-93	-93	815	-38	-3	-36
4-79 MO PERMALLOY	-89	-79	403	-44	1	-44
MUMETAL	-65	-38	158	-26	-3	-23
48 NICKEL-IRON	-70	-10	99	-26	-2	-26
50 NICKEL-IRON (ORIENTED)	-31	15	-28	-24	-4	-21
3.5 SILICON-IRON	8	-1	6	1	0	1
3 SILICON-IRON (ORIENTED)	18	1	-2	-3	-1	-1
3-1 SILICON-ALUMINUM-IRON	1	1	-2	-2	1	-1
16 ALUMINUM-IRON (ORDERED)	34	15	-8	8	-5	13
16 ALUMINUM-IRON (DISORDERED)	-4	-4	-2	--	--	--
2 V PERMENDUR	3	2	-2	-1	-1	0

μ_{20} - permeability at induction of 20 gausses

μ_{max} - maximum permeability

H_c - coercive force

B_r - residual induction or remanence

B_m - induction at field intensity of 30 oersteds

B_r/B_m - loop rectangularity or squareness ratio

TABLE IV. 60 CPS MAGNETIC PROPERTIES
(SOFT MAGNETIC MATERIALS) PERCENTAGE CHANGE
AS RESULT OF IRRADIATION WITH $\sim 2 \times 10^{18}$ N/CM^2 (TOTAL)

Material	$\frac{\Delta H_c'}{H_c'}$	$\frac{\Delta B_r'}{B_r'}$
SUPERMALLOY	1,000	-46
4-79 MO-PERMALLOY	110	-51
MUMETAL	35	-16
48 NICKEL-IRON	70	-33
50 NICKEL-IRON (ORIENTED)	44	-20
3.5 SILICON-IRON	9	2
3 SILICON-IRON (ORIENTED)	0	0
3-1 SILICON-ALUMINUM-IRON	0	0
16 ALUMINUM-IRON (ORDERED)	8	-2
16 ALUMINUM-IRON (DISORDERED)	0	0
2 V PERMENDUR	5	-6

H_c' - 60 Cps coercive force

B_r' - 60 Cps residual induction

TABLE V. PERCENTAGE CHANGE IN MAGNETIC PROPERTIES OF PERMANENT MAGNETS AS A RESULT OF IRRADIATION WITH 6×10^{18} N/CM^2 (TOTAL)

Material	$\Delta B_r/B_r$		$\Delta H_c/H_c$		$\Delta (BH)_{max}/(BH)_{max}$		$\Delta B_{omc}/B_{omc}$	
	Sample	Control	Sample	Control	Sample	Control	Sample	Control
3-1/2 CHROMIUM STEEL	-2	+4	-7	+10	-15	+27	-1	.5
36 COBALT STEEL	<-1		-5		-12		-2	-1
ALNICO II A	+3	-1	+2	-3	+2	-6	-15	-.5
ALNICO V C	-1	+1	+4	-1	+4	-1	-1	-.5
ALNICO XII	< 1	+1	+5	+9	-2	+8	-1	<.5
CUNICO I	+1	-1	-5	+2	+3	+2	-1.5	<.5
CUNIFE I	-4	-15	+2	+11	-7	<-1	-3.5	-5.5
SILMANAL	+4	+3	+8	+18	+11	+16	-1.5	+.5
FINE IRON A	<-1	--	+2	--	+1	--	-2.5	.5
FINE IRON B	-2		+7		+14		-7	--
PLATINUM COBALT	+8	-2	+3	+7	+4	+18	-1.5	-1
BARIUM FERRITE (UNORIENTED)	-2	+3	+3	+1	+5	+7	-2	<.5
BARIUM FERRITE (ORIENTED)	< 1	< 1	<+1	+9	< 1	-3	-4	-1
EXPERIMENTAL ERROR	±3	±3	±10	±10	±15	±15	±2	±1

B_r - residual induction

H_c - coercive force

B_{omc} - open magnetic circuit induction

$(BH)_{max}$ - maximum energy product

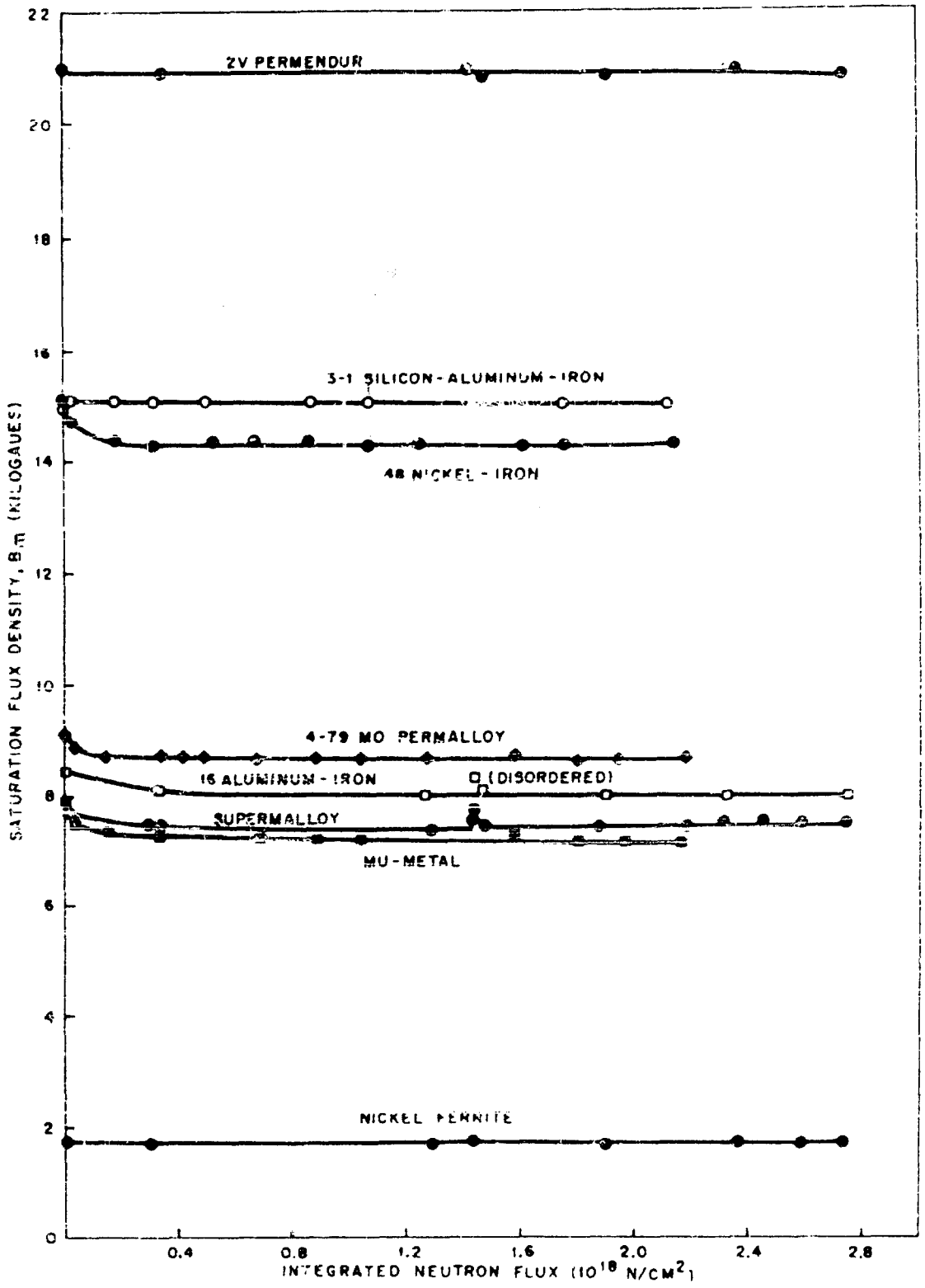

Figure 1 - Magnetic "saturation" (induction at a field strength of 30 oersteds) as a function of integrated neutron flux

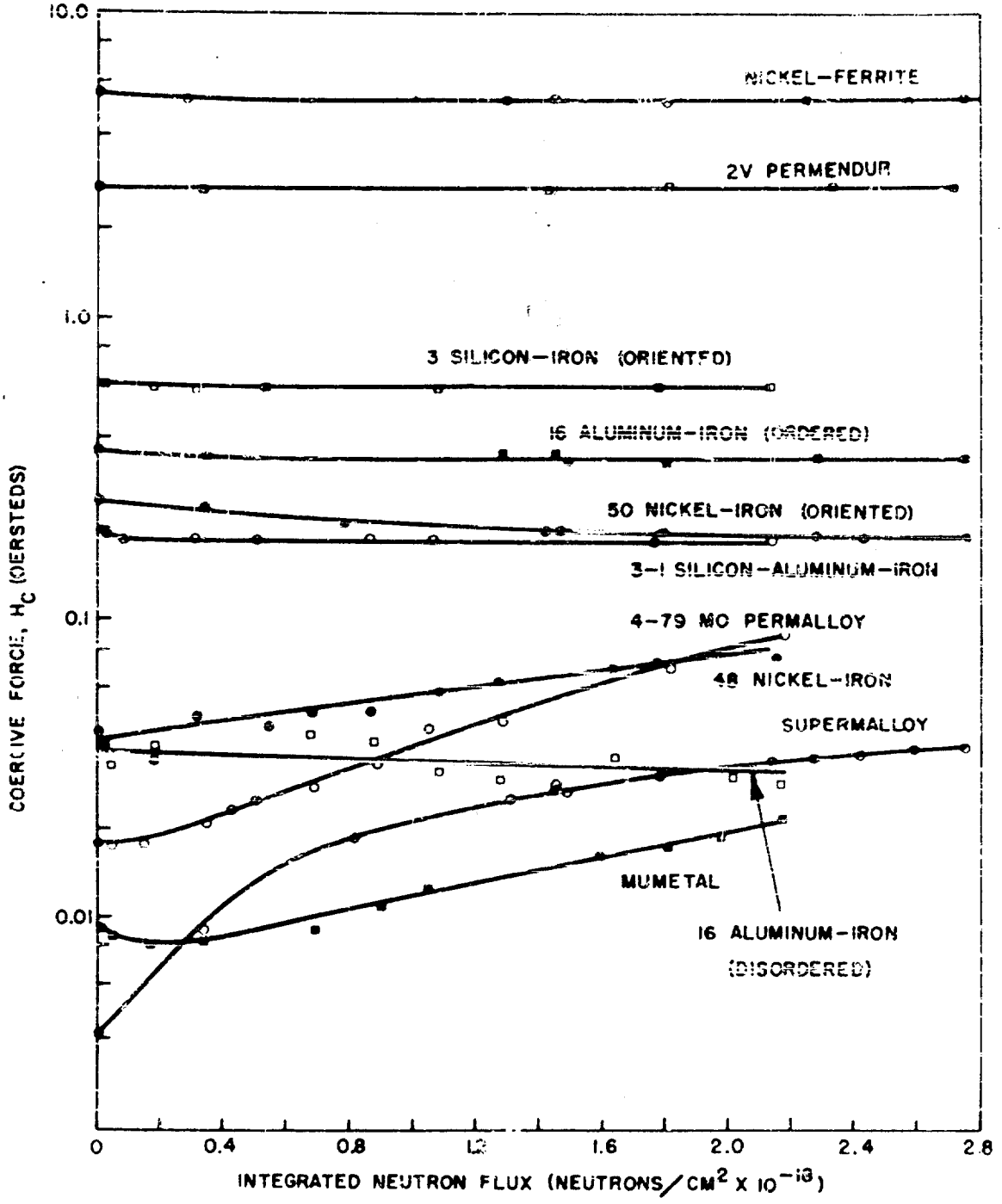

Figure 2 - Coercive force as a function of integrated neutron flux

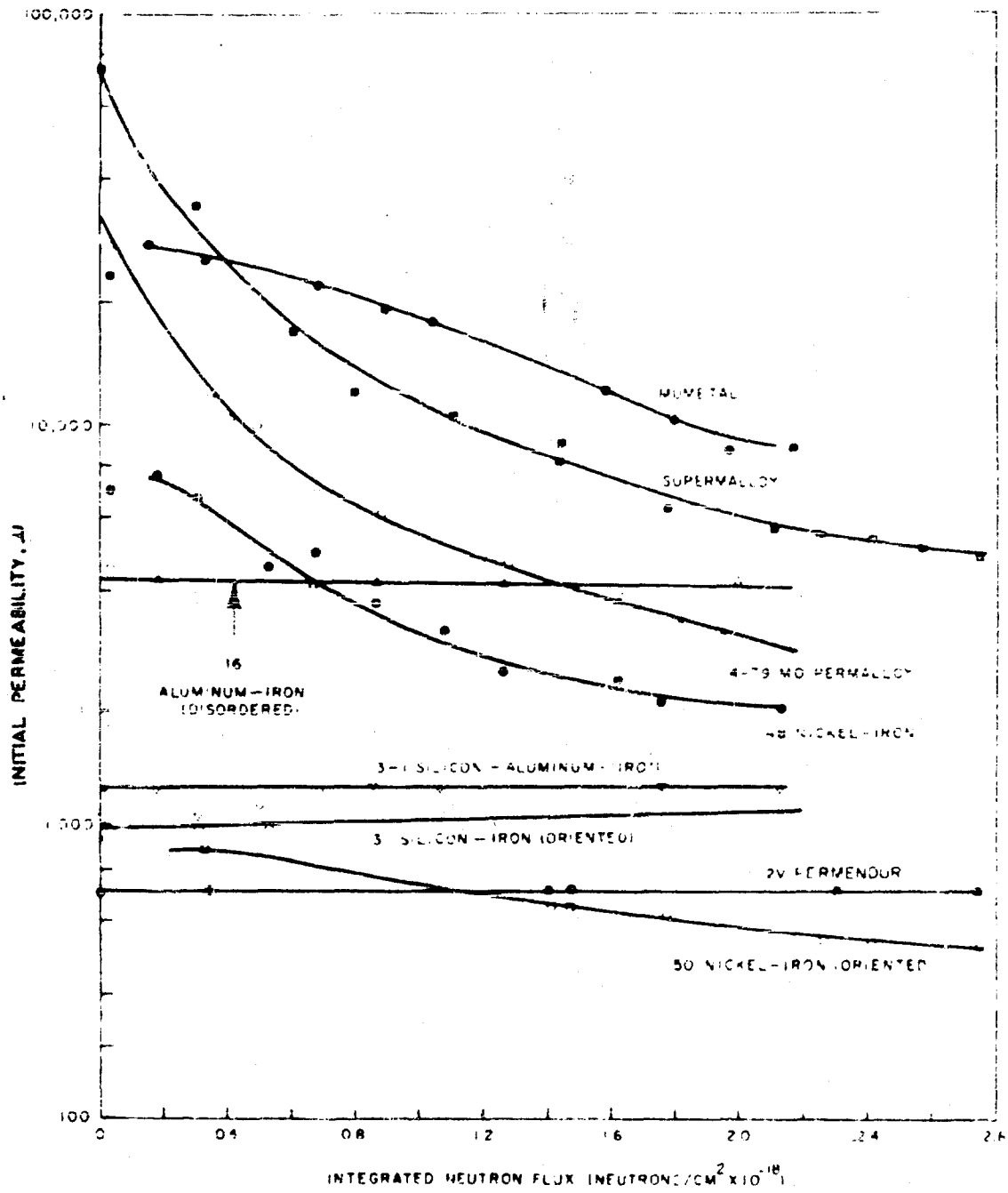

Figure 3 - Initial permeability as a function of integrated neutron flux

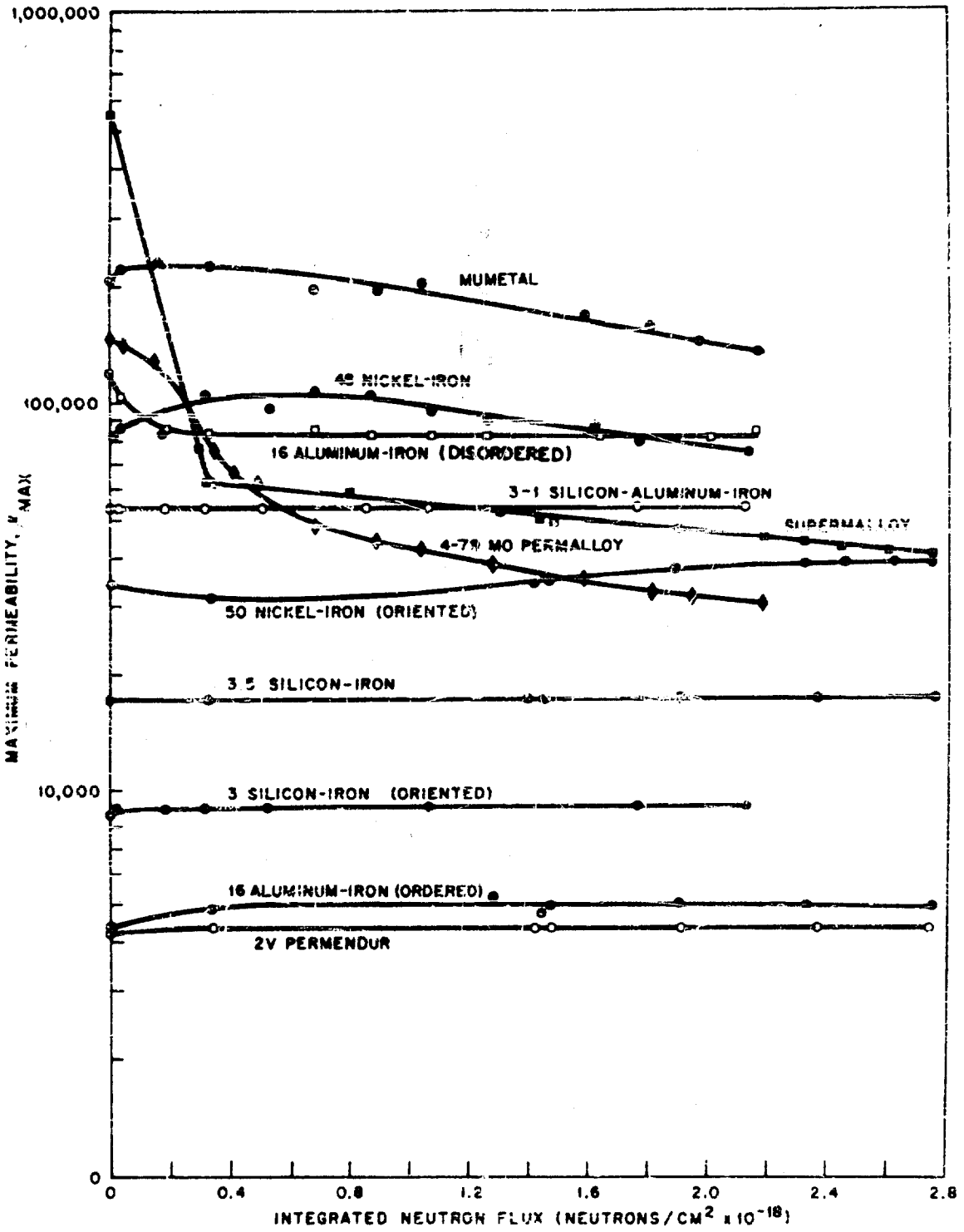

Figure 4 - Maximum permeability as a function of integrated neutron flux

iron, were degraded the most*. For example, permeabilities of Supermalloy decreased 93% with a corresponding 800% increase in coercive force. The higher coercive force materials (ordered 16 aluminum-iron, silicon-iron, silicon-aluminum-iron, and Permendur) showed little or no change.

Fast Neutron Integrated Flux Meter

Further inspection of Figures 2, 3 and 4 shows progressive changes of structure sensitive properties with increasing nvt. In fact, the experimental curves of initial permeability (μ_o) vs. nvt are hyperbolic, as evidenced by the linear relationship of $1/\mu_o$ vs. nvt shown in Figure 5. This behavior indicates the possibility of dynamic metering of integrated fast neutron flux by in-pile measurement of one of the radiation sensitive magnetic properties. Present experience indicates that such a meter would be insensitive to gamma and thermal neutron radiation. This could be a useful tool for in-pile metering of fast neutrons used in radiation effects studies of engineering materials.

Effect of Reannealing after Irradiation

Measurements of the magnetic properties of the laminated and tape wound toroidal cores as late as one year after irradiation indicate that the radiation damage is permanent. However, reheat treatment of irradiated cores can restore the original pre-irradiation properties. This was demonstrated in the case of a 4-79 Mo-Permalloy (1/8 mil tape wound) core originally heat treated to produce a good switching field vs. time characteristic for computer memory application. As shown in Figure 6, neutron irradiation destroyed this good switching characteristic. However, by giving this irradiated core the same heat treatment it had received before irradiation, the original switching characteristic and d-c magnetic properties were restored, as shown in Figure 6. This experiment indicates that transmutation effects (i.e. changes in chemical composition) were either not present or were

---

*Disordered 16 aluminum-iron (Alfenol) is a notable exception to this group. Although its pre-irradiation coercive force was less than 0.5 oersted, it suffered only negligible radiation damage.

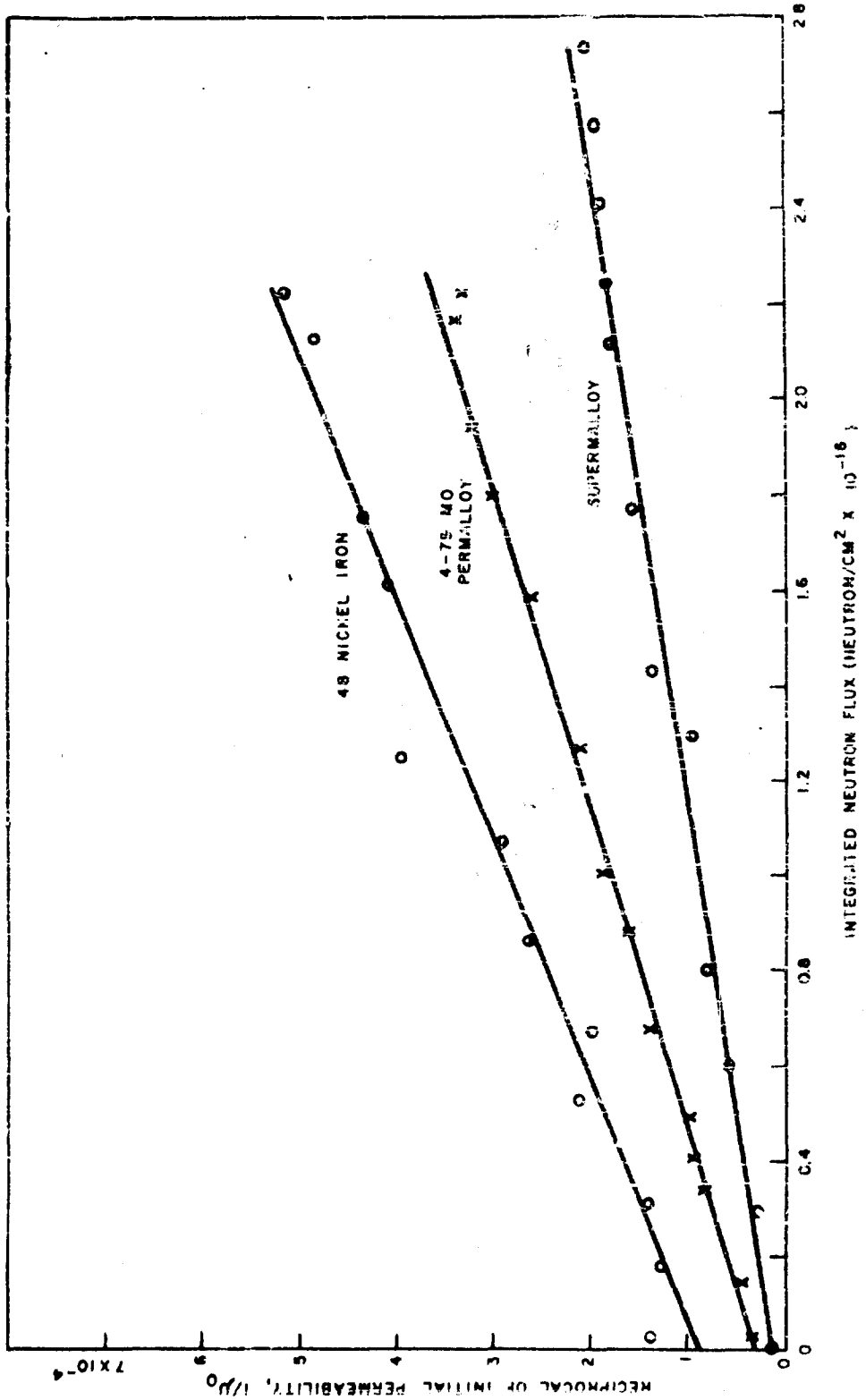

Figure 5 - Reciprocal of initial permeability as a function of integrated neutron flux

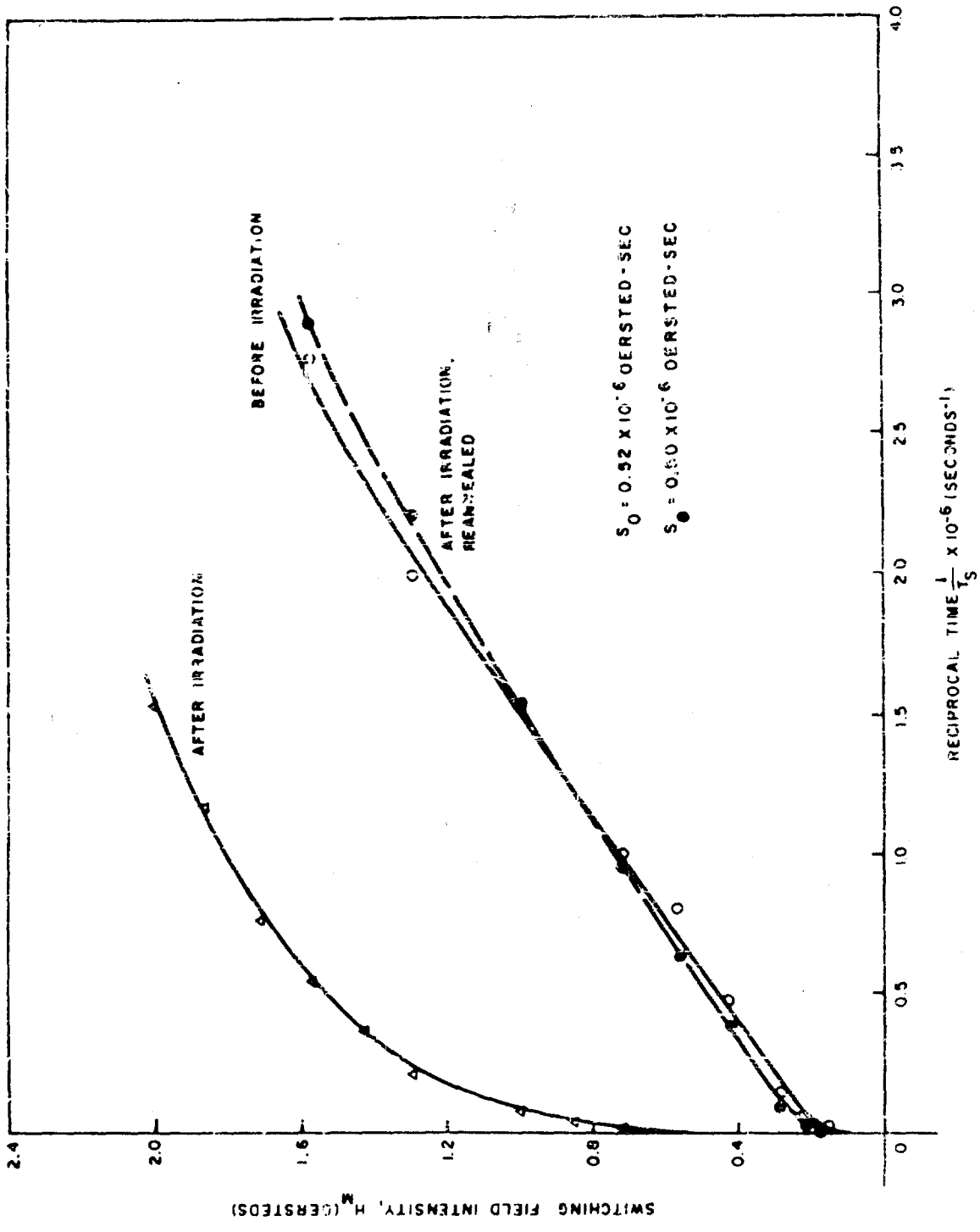

Figure 6 - Effect of reheat treatment of irradiated 4-79 Mo-Permalloy: switching curves for 1/8-Mil tape wound bobbin core

insignificant. For had there been a composition change, reannealing could not have restored the original magnetic properties. The experiment indicates, rather, that magnetic hardness (i.e. higher coercive force and lower initial permeability) was increased through the production of additional inhomogeneities in the form of vacancies and interstitials, or more complex defects, and that this added hardness could be removed by proper annealing.

"Softest" Core Materials

Examples of the drastic changes which occurred in the properties of the magnetically softest materials are shown in Figures 7 - 12, which illustrate the effects of irradiation on induction curves and hysteresis loops of Supermalloy, 4-79 Mo-Permalloy, and oriented 50 nickel-iron (Orthonol). In addition to severe lowering of permeability, increases in coercive force, and drops in remanance, distortions of hysteresis loop shape also resulted from the neutron irradiation. Figures 8, 10 and 11 show this "kink" effect clearly. These distortions or kinks may be associated with changes in degree of order as previously suggested by the authors (3-7) and by Schindler, Salkovitz, et al (10). The distortions may also be due to non-uniform radiation damage in the sample caused by self shielding, i.e., by the possibility that the interior of the sample may receive significantly less radiation than the outer portion. This would in effect produce a composite core with consequent distortions in loop shape (6, 7).

"Harder" Magnetic Core Materials

Magnetic core (soft) materials with higher coercive forces (>0.5 oersted), which showed little or no change in properties are illustrated in Figures 13 - 16. Here one sees examples of the insensitivity to irradiation of materials in this category, which includes 3.5% silicon-iron, oriented 3% silicon-iron, 3-1% silicon-aluminum-iron, ordered 16 aluminum-iron, and 2V Permendur. Because of its high cobalt content (49%), the Permendur core became highly radioactive. However, its magnetic properties were not affected.

Powder and Ferrite Cores

As shown in Table VI, nickel ferrite, 2-81 Mo-Permalloy dust, and Sendust flake exhibited significant increases in high

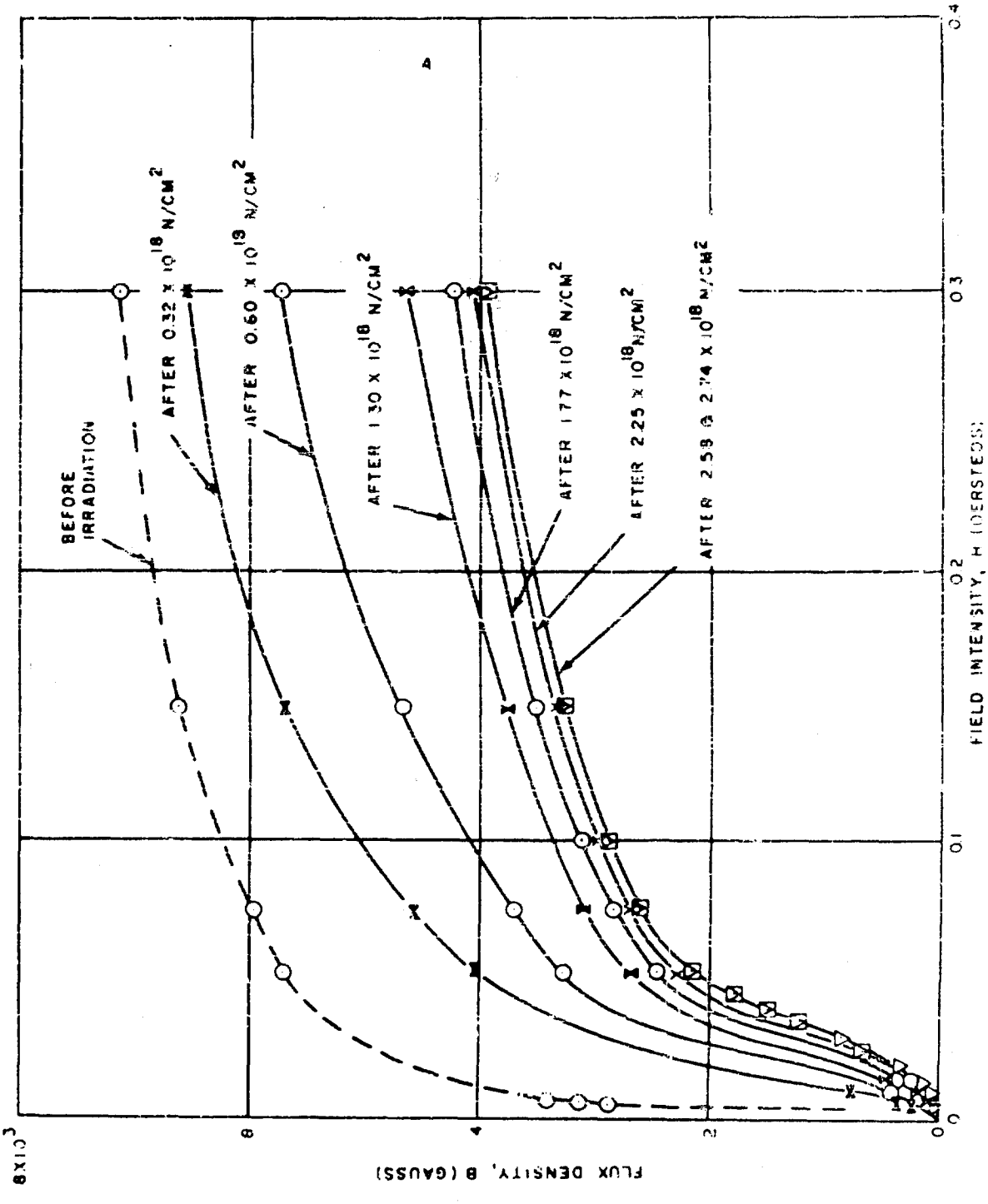

Figure 7 - Supermalloy: effect of irradiation on normal induction curve

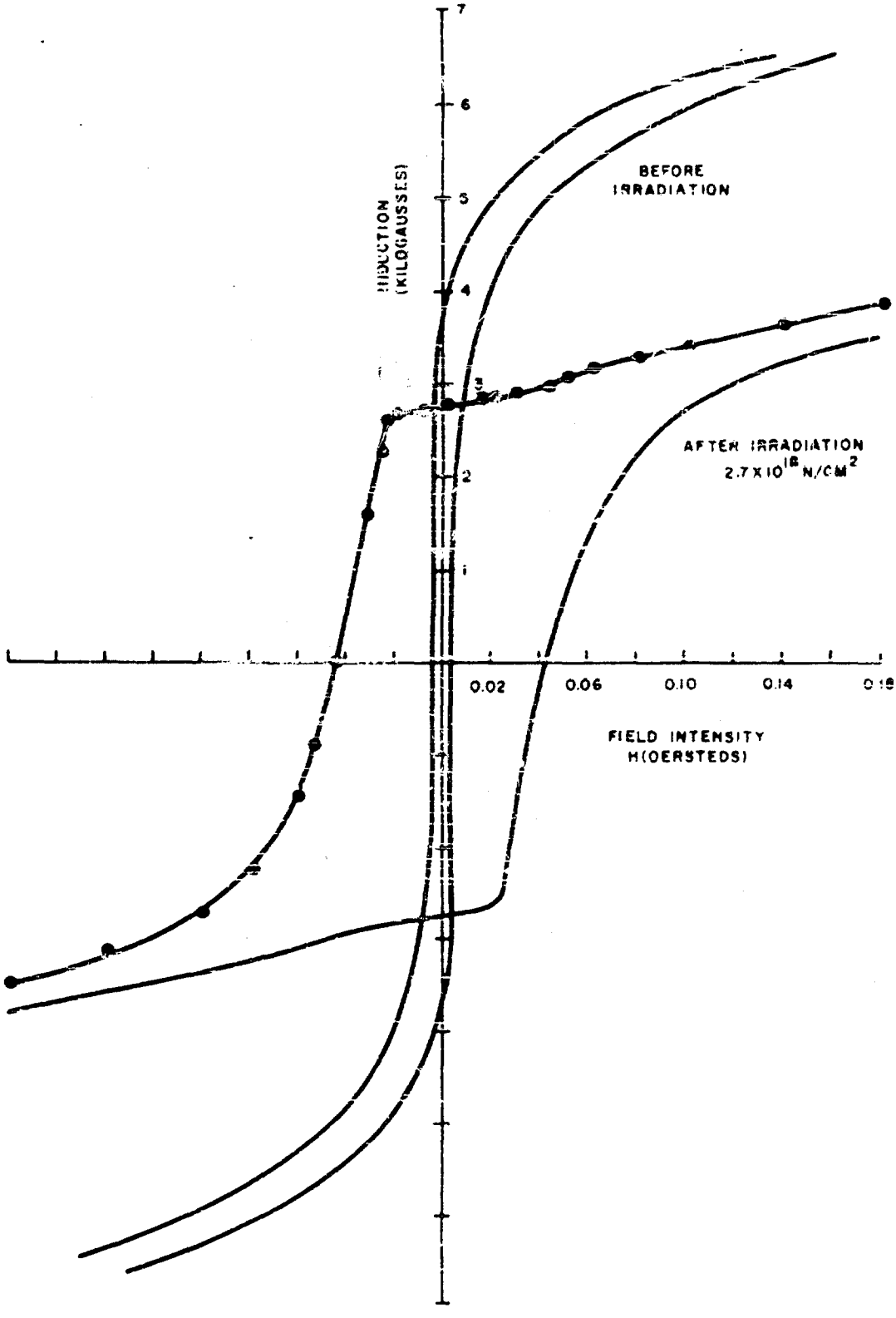

Figure 8 - Supermalloy: effect of irradiation on hysteresis loop

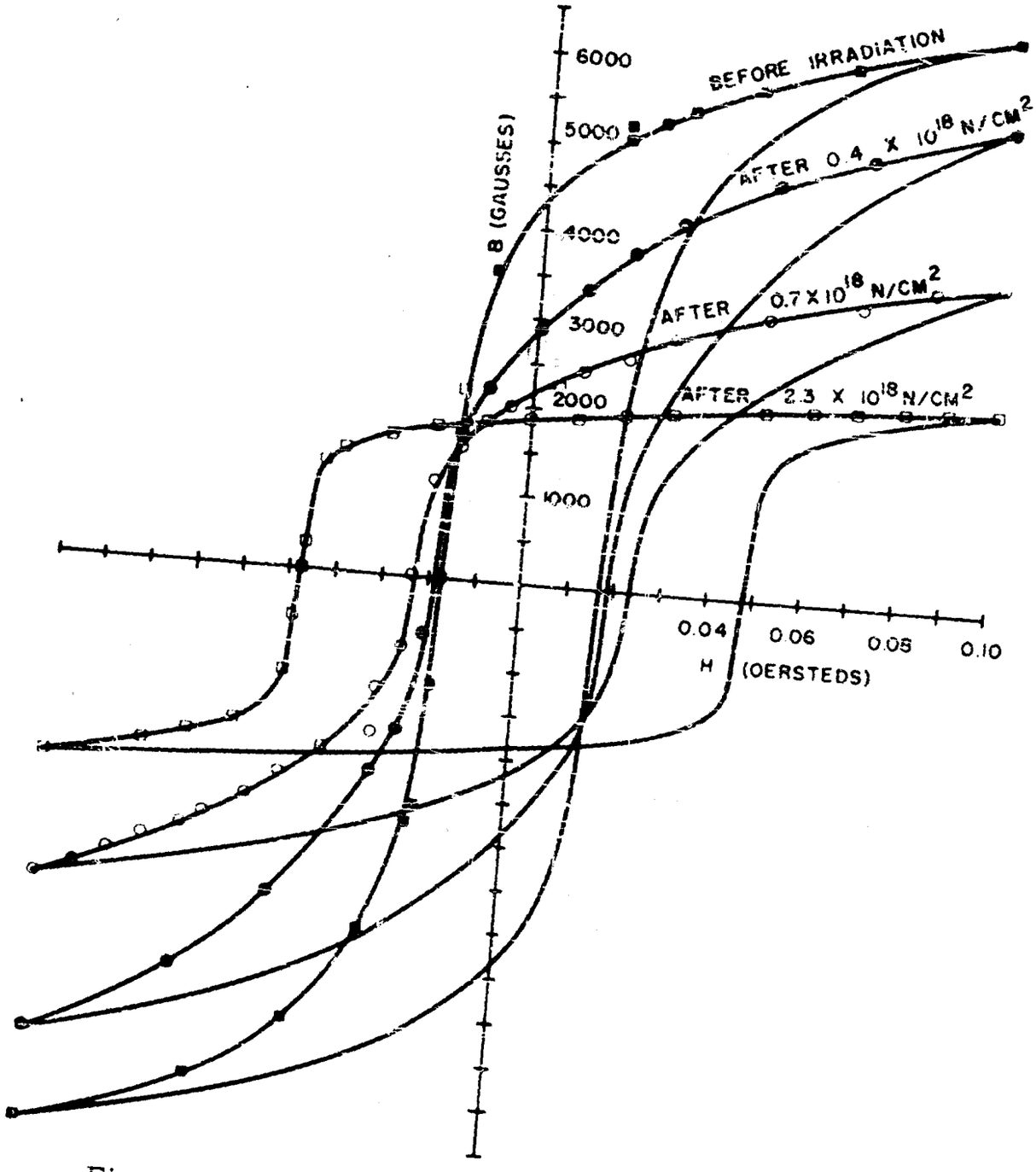

Figure 9 - 4-79 Mo-Permalloy: effect of irradiation on hysteresis loop

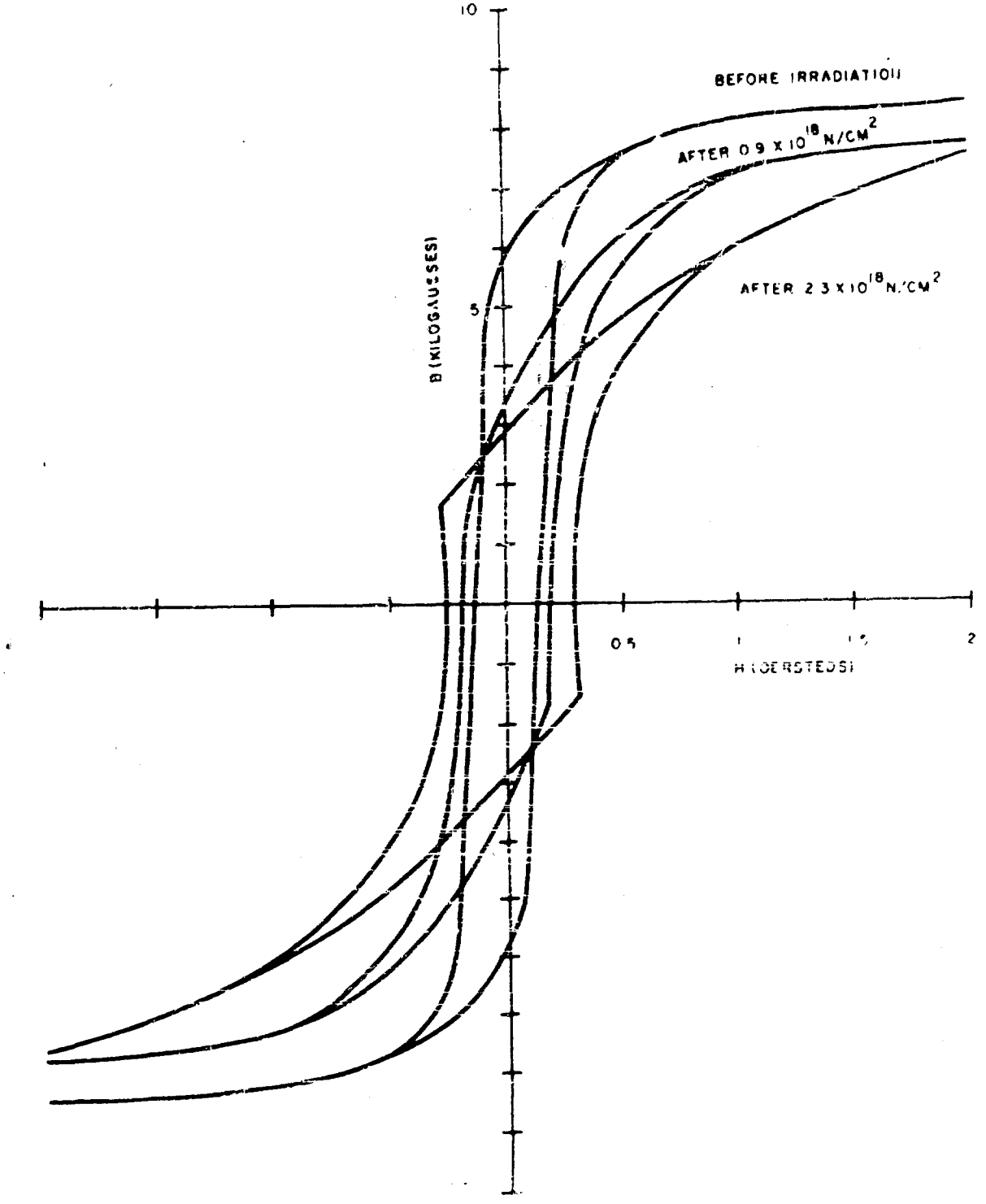

Figure 10 - 4-79 Mo-Permalloy: effect of irradiation on 60 cps loop

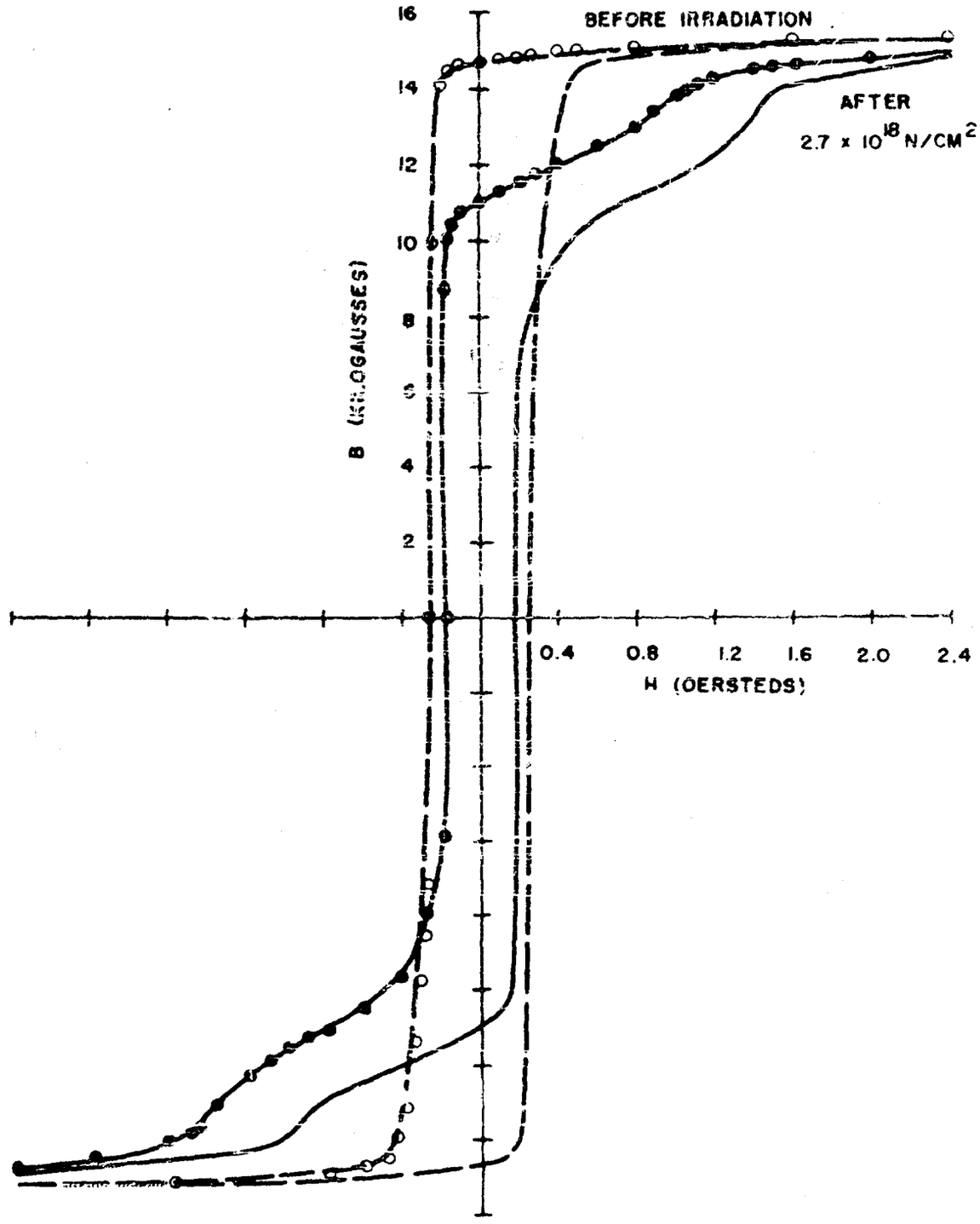

Figure 11 - 50 nickel-iron (oriental): effect of irradiation on hysteresis loop

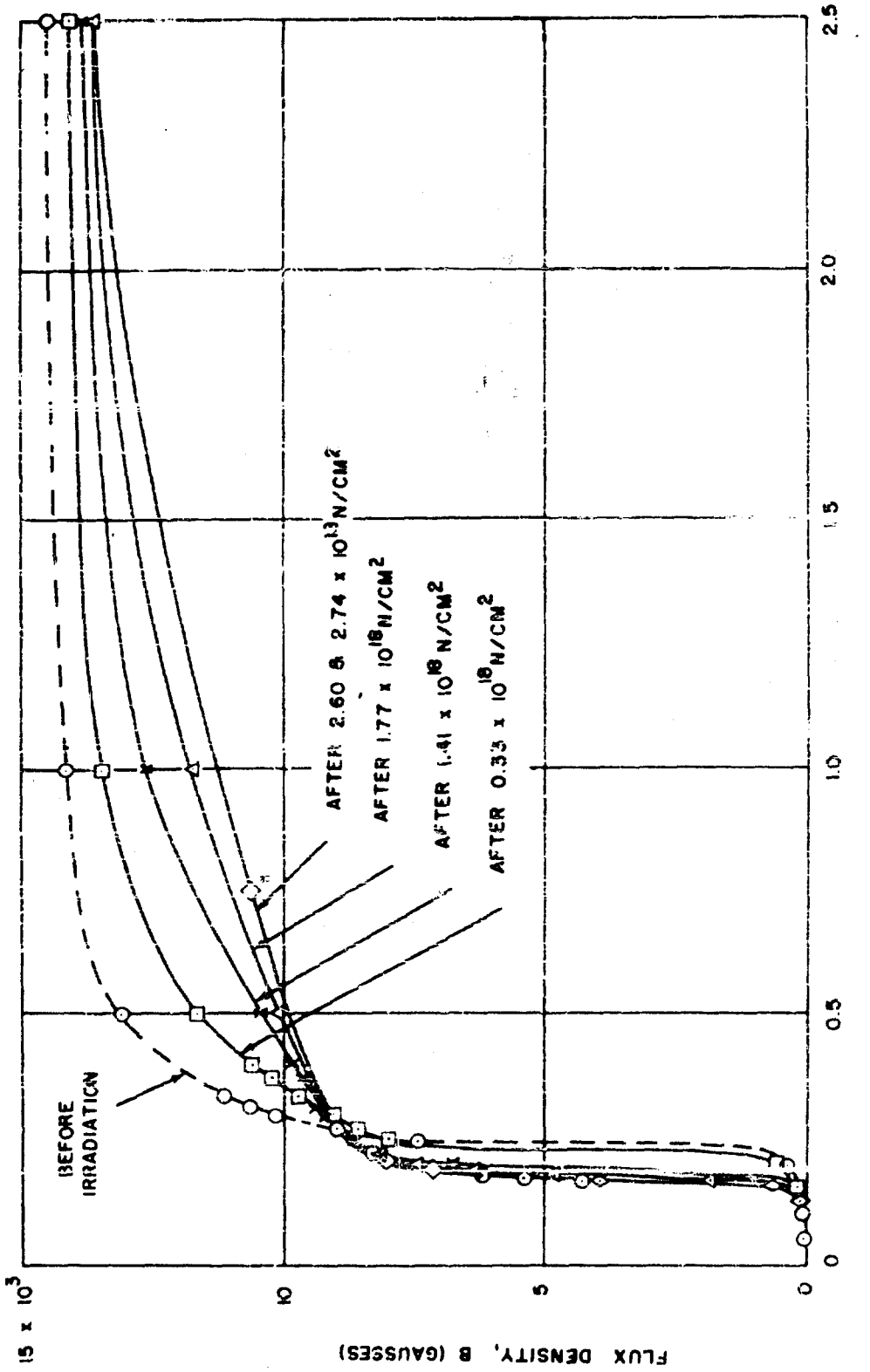

Figure 12 - 50 nickel-iron oriented: effect of irradiation on normal induction curve

frequency losses. However, (within experimental error) Carbonyl iron dust cores showed none. The high frequency loss separation measurements which showed overall loss increases showed no changes in permeability or in hysteresis for any of the materials. This was confirmed by d-c and power frequency measurements which also indicated no changes in permeability or hysteresis, or other low frequency properties.

The nickel-ferrite core and the 2-81 Mo-Permalloy were retested 10 months after irradiation. In contrast to the laminated and tape wound cores, the results here show some degree of recovery with time toward the original pre-irradiation properties. Recovery of properties of ferrites with time was also observed by Sakiotis et al (11) in microwave measurements. Salkovitz, Schindler, et al are conducting an extensive study of radiation effects in ferrites (12).

Permanent Magnets

As shown in Table V, permanent magnets exposed to the same nuclear environment as were the soft materials, showed no appreciable changes beyond the limits of experimental error. Demagnetization curves of the thirteen representative materials studied are shown in Figure 17. This group covers most of today's technologically important permanent magnets. Coercive forces range from 60 to 2,200 oersteds. In this experiment, complete demagnetization curves were measured before and after irradiation on one set of samples. Open magnetic circuit induction values (before and after irradiation) were measured on a second set of samples. In addition, both open circuit induction values and demagnetization curves were obtained on unirradiated control samples which were held in a furnace for twelve days at the reactor hole temperature of 90°C.

Pre- and post-irradiation demagnetization curves of the Alnicos are shown in Figure 18. As Table V indicates, results for the other permanent magnets were similar. In a more limited experiment, using open circuit magnets only, Fennel, et al, also obtained a negative result for effects of irradiation on the magnetic properties of similar magnets, such as "Alni" (13% Al, 25% Ni, 4% Cu, 0.06% C) and of 6% tungsten steel (13).

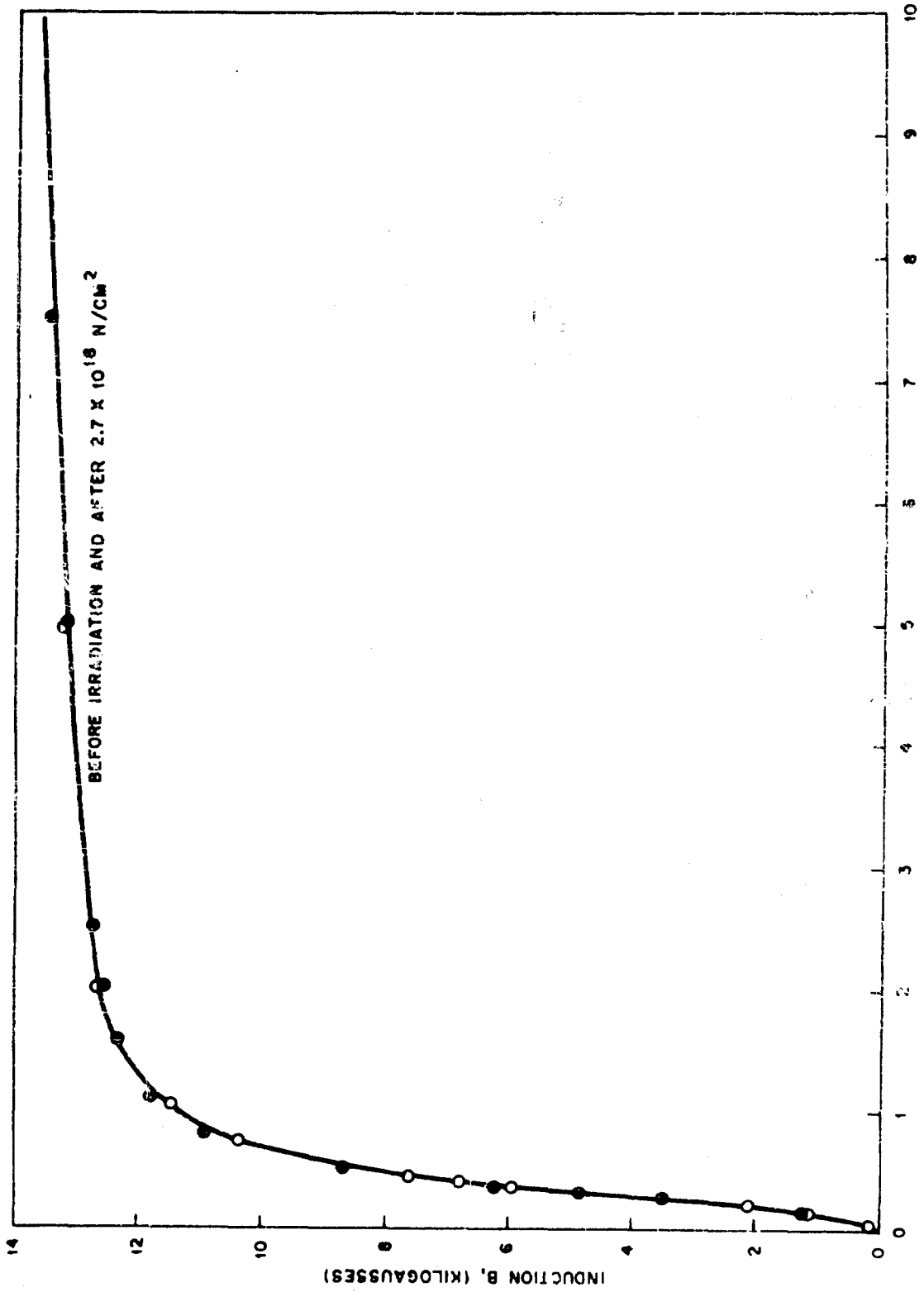

Figure 13 - 3.5 silicon iron: effect of irradiation on normal induction curve

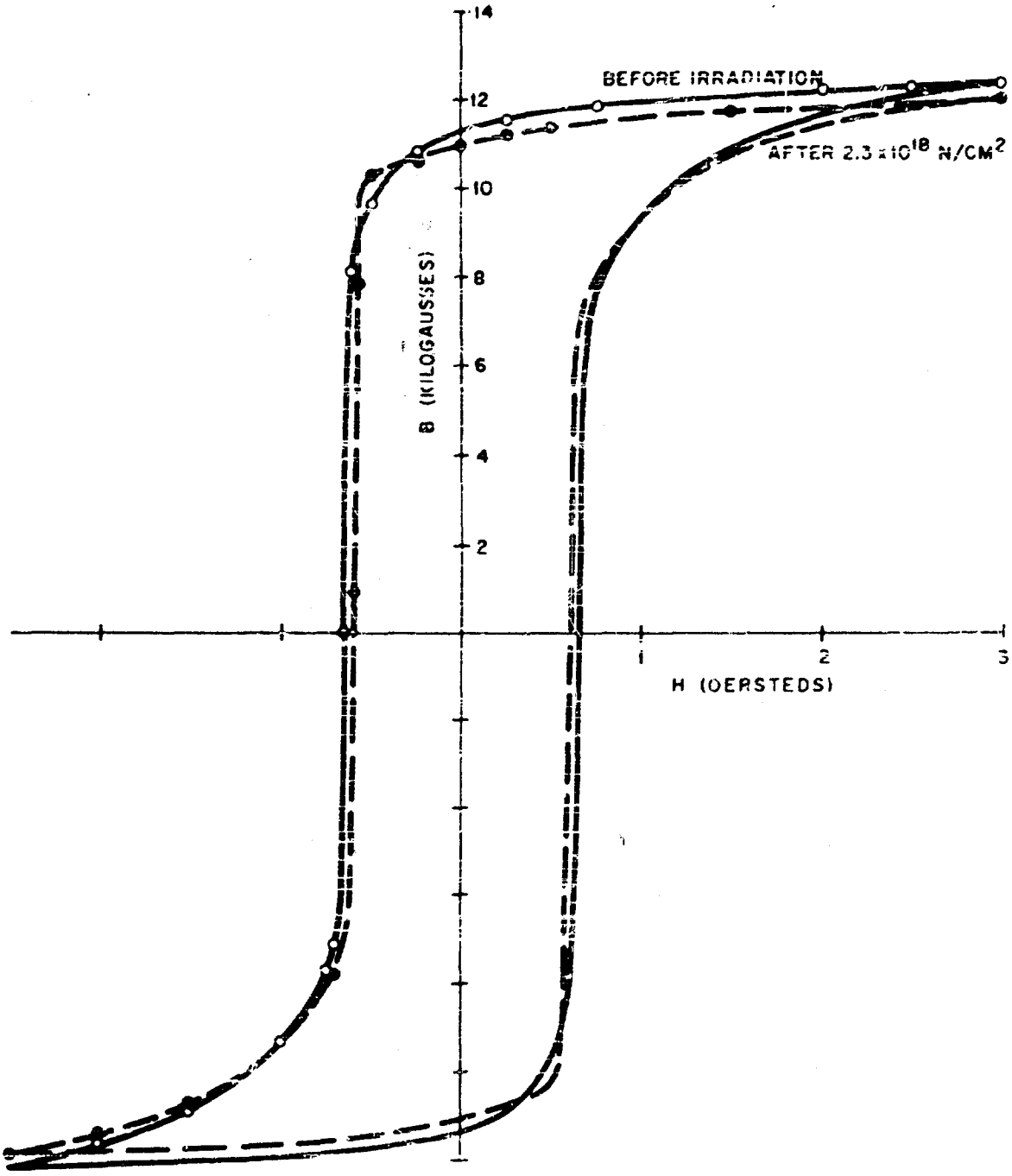

Figure 14 - 3-silicon-iron (oriented): effect of irradiation on hysteresis loop

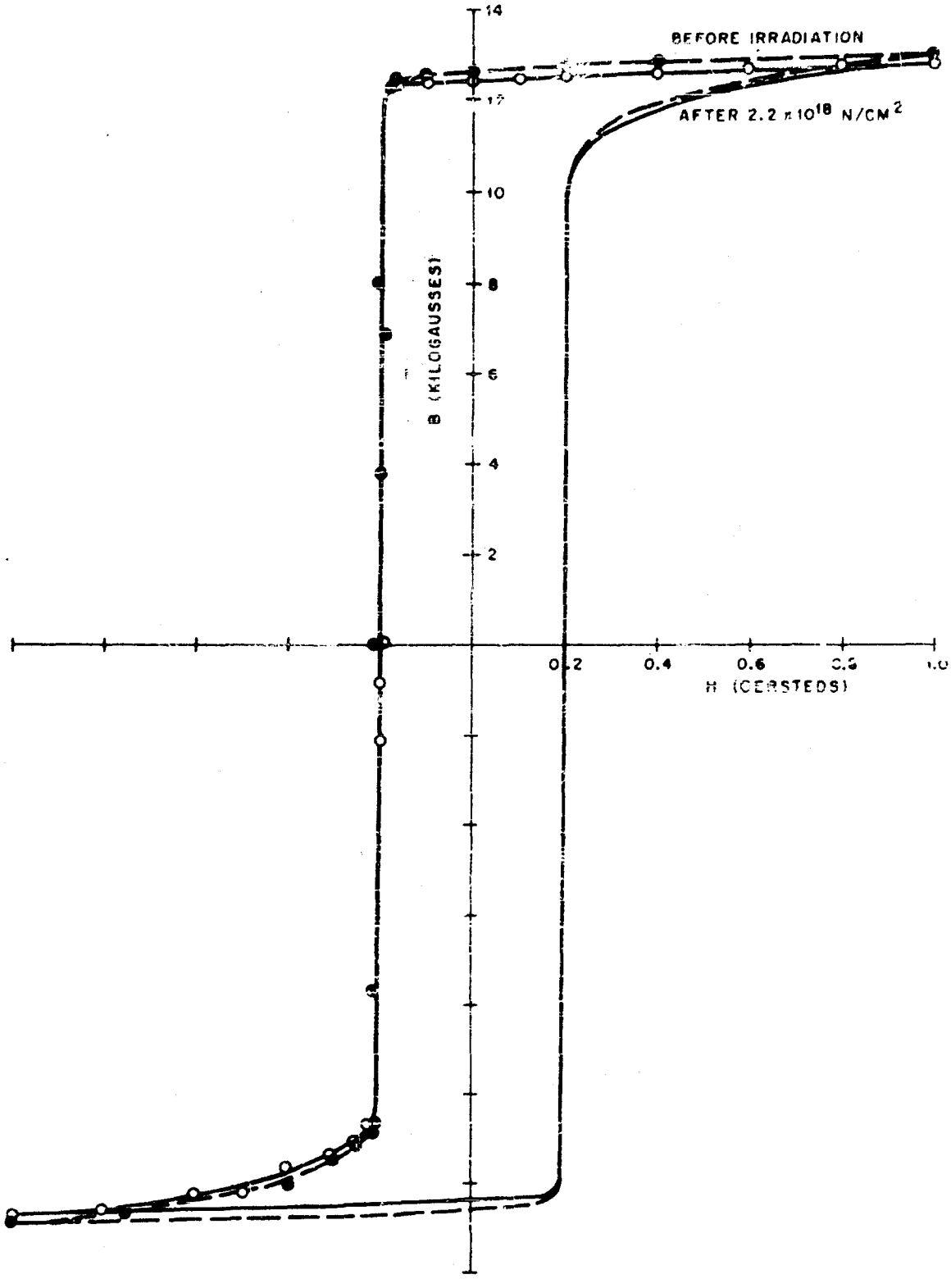

Figure 15 - 3-1 silicon-aluminum-iron: effect of irradiation on hysteresis loop

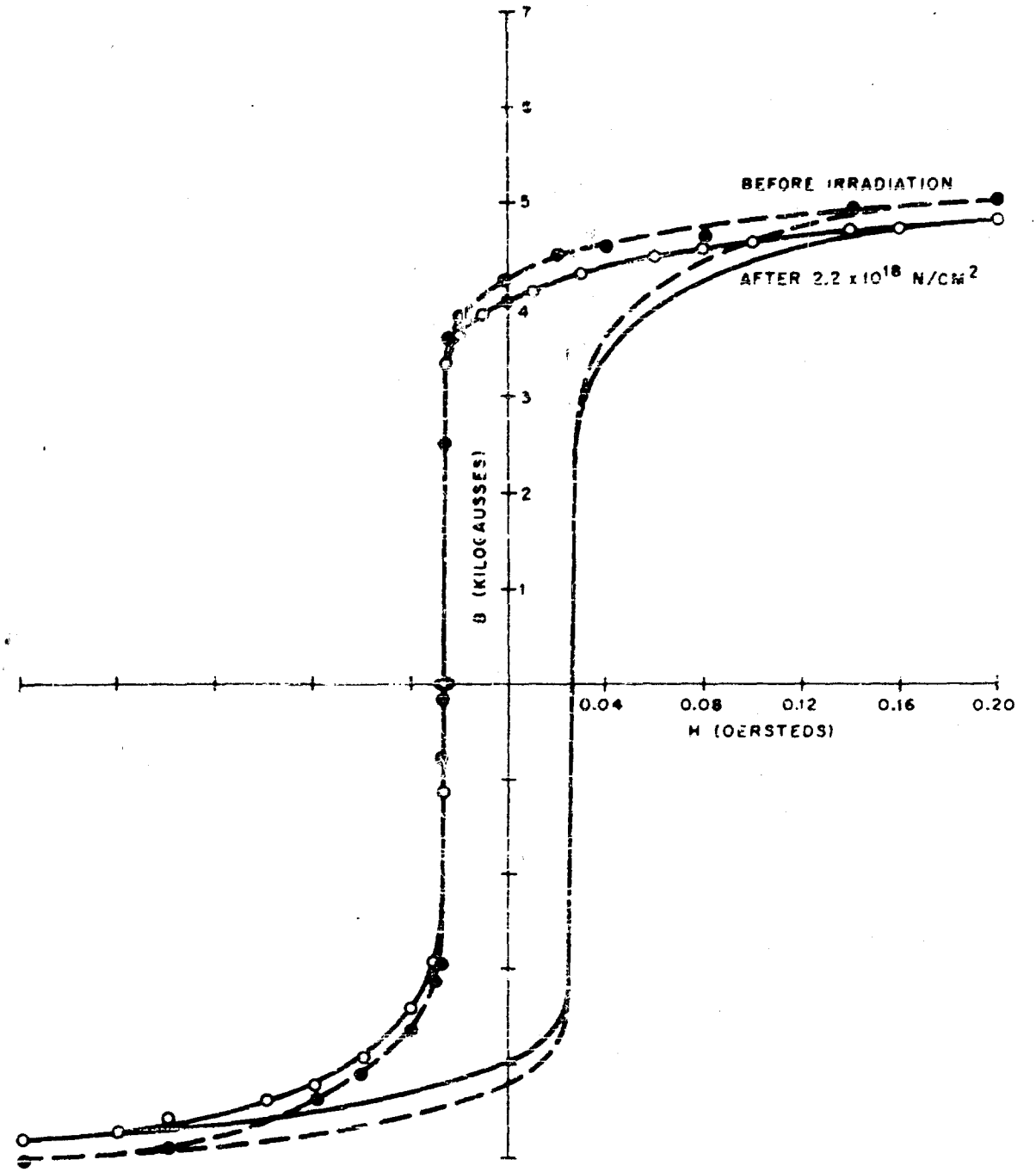

Figure 16 - 16 aluminum iron (disordered): effect of irradiation on hysteresis loop

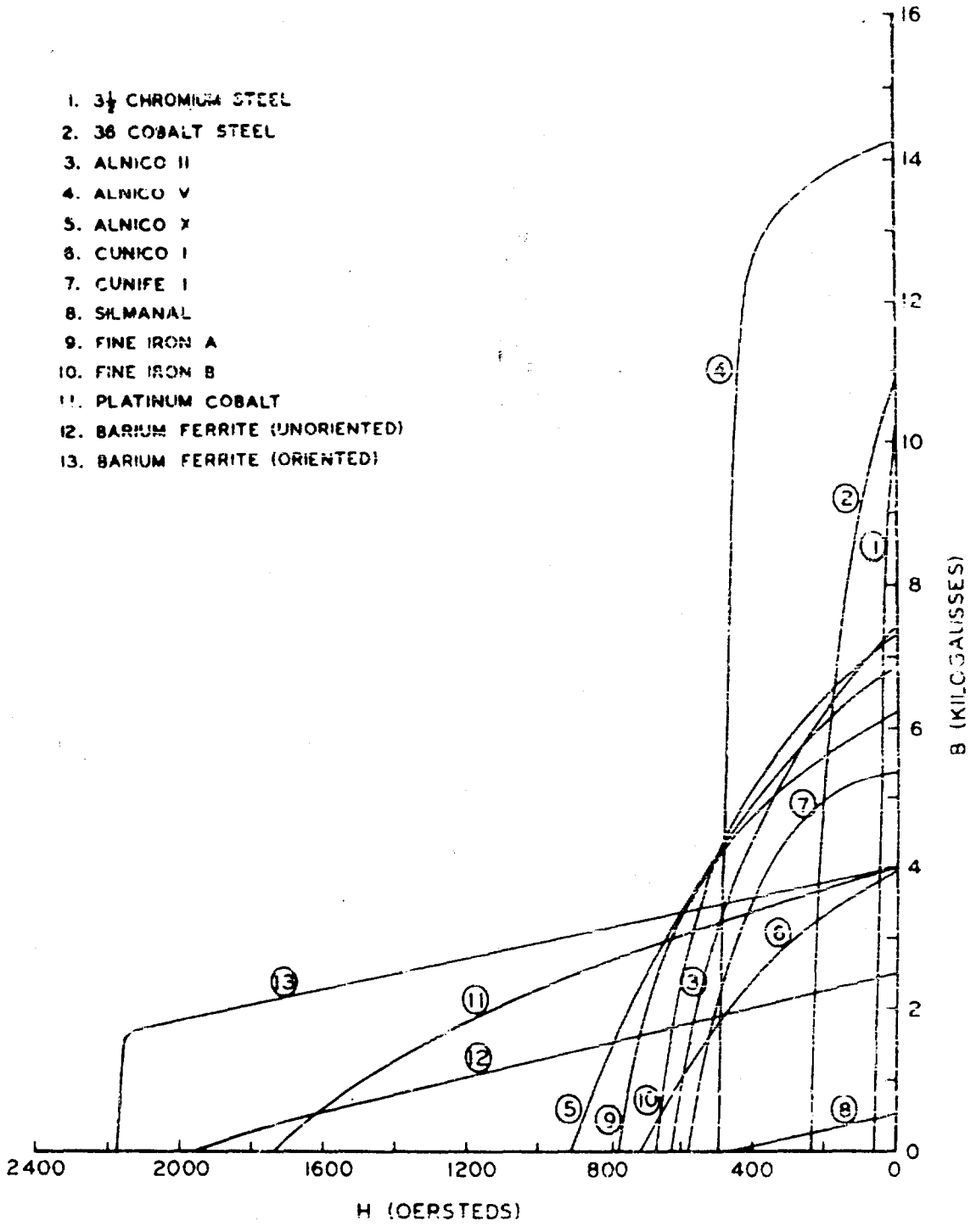

Figure 17 - Demagnetization curves of the permanent magnet materials irradiated

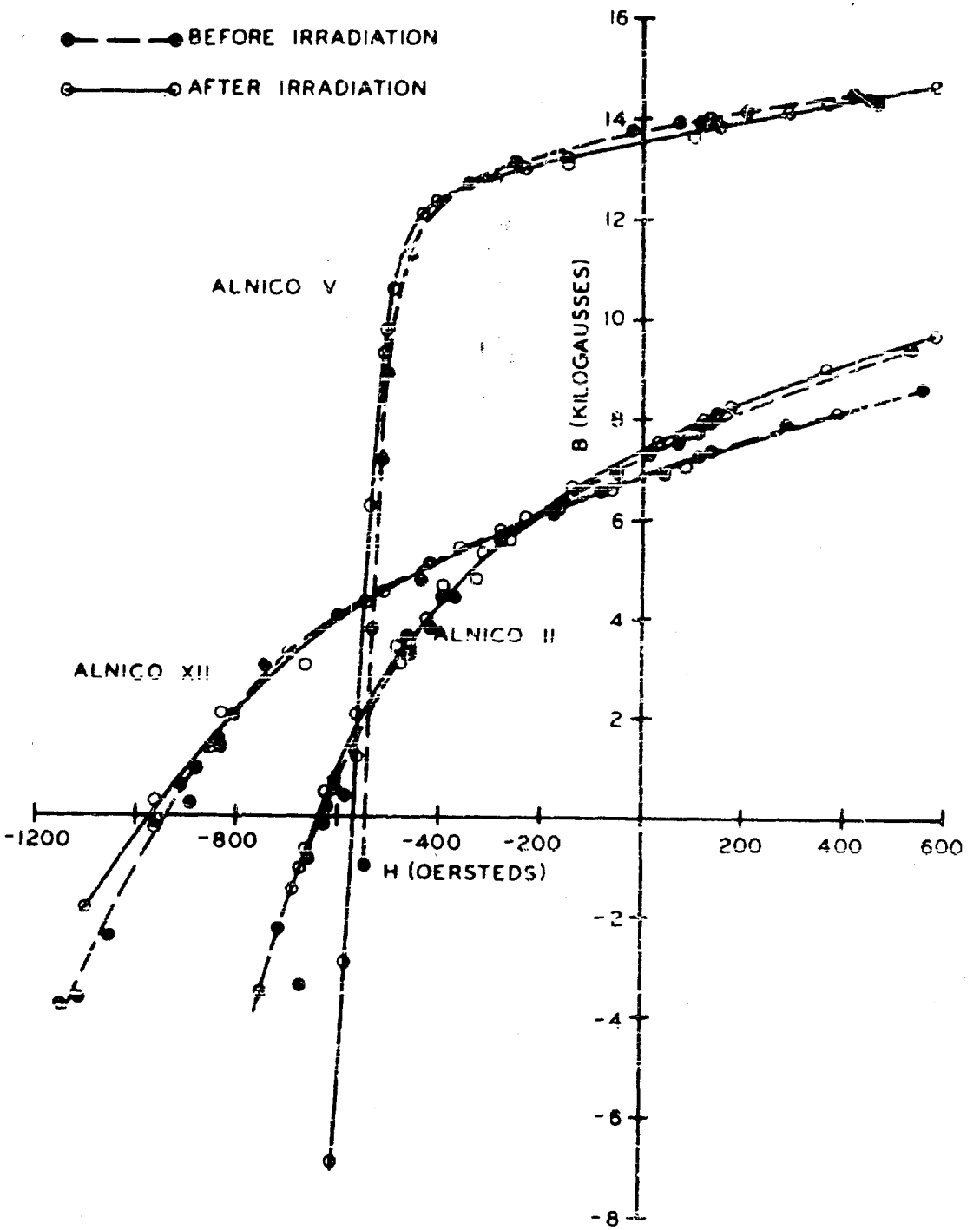

Figure 18 - Alnico: effect of irradiation on demagnetization curves

TABLE VI. EFFECTS OF IRRADIATION
WITH ~2 × 10^{18} N/CM^2 (TOTAL)
ON POWDER AND FERRITE CORES

Material		μ	a	e	c	$\frac{R}{\mu Lf}$
NICKEL FERRITE	Before	14	450	-	-	9,000
	After	14	400			13,000 (50Kc, 1g)*
2-81 MO-PERMALLOY	Before	123	1.5	20	10	500
	After	122	1	40	10	1,000 (25Kc,20g)
CARBONYL IRON (PLASTIC BINDER)	Before	9	-	2	-	3,500
	After	9		2.5		2,500 (500Kc,1.7g)
CARBONYL IRON (GLASS BINDER)	Before	9	-	2.5	-	3,000
	After	9		1.5		3,500 (500Kc,1.4g)
SENDUST FLAKE (FLAKENOL)	Before	175	10	5	180	500
	After	195	11	30	20	1,100 (25Kc,20g)

$$\frac{2\pi}{\mu Q} = \frac{R}{\mu Lf} = aB + ef + c$$

where $\frac{R}{\mu Lf}$ = core loss factor (Legg)

a = hysteresis loss coefficient

e = eddy current loss coefficient

c = residual loss coefficient

* g = gauss (or gausses)

In-pile Measurements on Core Materials

The soft (magnetic core) material samples were all toroidal in shape. Most of these were fabricated of punched ring laminations, some were tape wound, and others were rings of pressed metallic powder, flake, or ferrite. The toroids were mounted on core holders as shown in Figure 19 with each core's primary and secondary test windings connected internally to octal receptacles built into the ends of the holders. Using this arrangement, it was possible to make in-pile measurements of magnetic properties by plugging appropriate cables into the core holder receptables and connecting the other ends of the cables to the remotely located magnetic measurement instrumentation. Most of the data shown in the curves for the soft magnetic materials were obtained by this kind of in-pile measurement.

Permanent Magnet Test Samples

Unlike the soft materials, whose low coercive force permits their evaluation in relatively low magnetic fields (usually not more than 30 oersteds), permanent magnets require high field intensities (up to 15,000 oersteds) for magnetization and proper evaluation. Therefore, the toroidal form is generally not suitable for permanent magnet test samples. Instead, short rods or bars which may be placed between the pole pieces of high-field producing electromagnets are used. In this experiment, cylinders with diameters ranging from approximately 0.1" to 0.5" and lengths ranging from 0.2" to 3" were used. For the closed circuit (i.e., demagnetization curve) tests, a length to diameter ratio of approximately one was used. For the open magnetic circuit induction tests, the length to diameter ratio chosen for any particular sample depended upon the demagnetization curve of that sample. An attempt was made to operate in the neighborhood of the maximum energy product (i.e., optimum operating point) wherever possible.

Because of the high field requirement in testing permanent magnets and because of pile-hole space limitations, in-pile measurements were not made on the permanent magnets. The data presented above are the result of pre-irradiation and post-irradiation measurements, on irradiated samples and unirradiated controls, both in open magnetic circuit condition and in closed

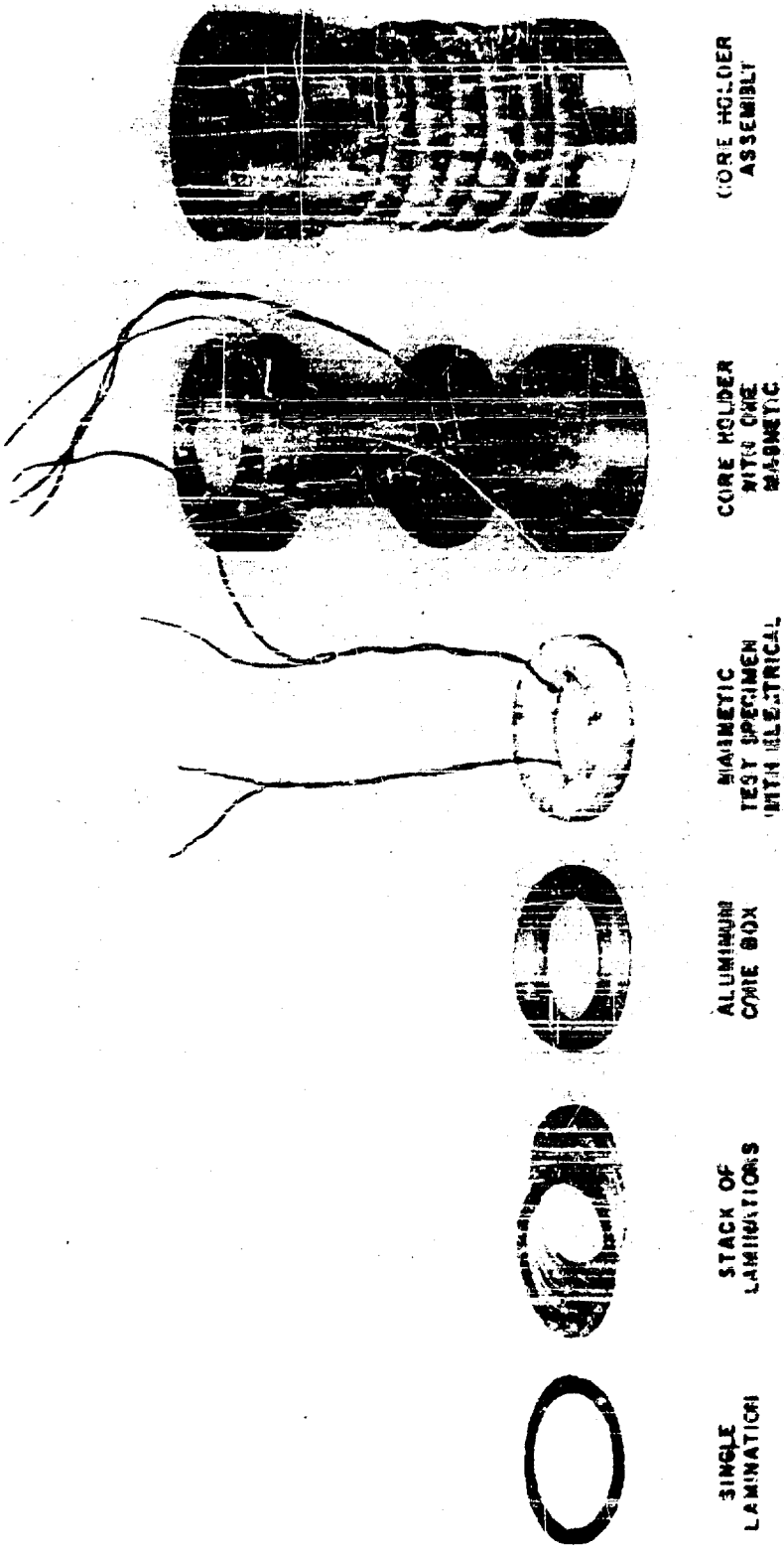

Figure 19 - Toroidal magnetic cores and radiation test holder (components and assembly)

magnetic circuit operation.

For the irradiation, the samples were placed in four specially designed aluminum trays, shown in Figure 20. The two smaller trays contain the demagnetization curve samples. Here proximity of adjacent magnets was not important, since these were remagnetized in post-irradiation tests. For the open circuit samples, however, it was important to make the space between adjacent magnets large enough to prevent mutual magnetic interaction. Hence, these were placed on the larger trays. After assembly, the four trays were placed in the rectangular aluminum box shown in Figures 20 and 21. This box is a standard Brookhaven pile hole container.

BNL Reactor Test Conditions

The temperature and radiation conditions of the soft and hard magnetic materials irradiations are given in Table II. It is the epicadmium neutron flux which is of concern in military applications. In order to eliminate temperature as a variable in these experiments, measurements on unirradiated controls held at reactor temperatures were also made.

Radioactivity and Post-irradiation Testing

Because of induced radioactivity (primarily in the cobalt, but also in iron, nickel and some of the other elements) post-irradiation testing presented some special handling problems. In the case of the soft materials, the pre-wired core assembly (which had become radioactive) shown in Figure 19, was transferred from its shipping container to a specially designed lead shielded test container, whose covers contained cables and octal plugs which mated with the receptacles in the core holder. It was then possible to make the magnetic measurements without the use of a hot cell.

For the permanent magnets, however, such a procedure was not possible. Here, each magnet tested, whether for a complete demagnetization curve or for an open circuit induction test, had to be handled individually. This necessitated the use of a hot-cell facility with master-slave hand and power manipulators. A schematic floor plan of the arrangement used for testing radioactive permanent magnets is shown in Figure 22. The U. S. Naval Research

Figure 20 - Permanent magnet samples in radiation test holders (tray covers, spacer frame, and container are also shown)

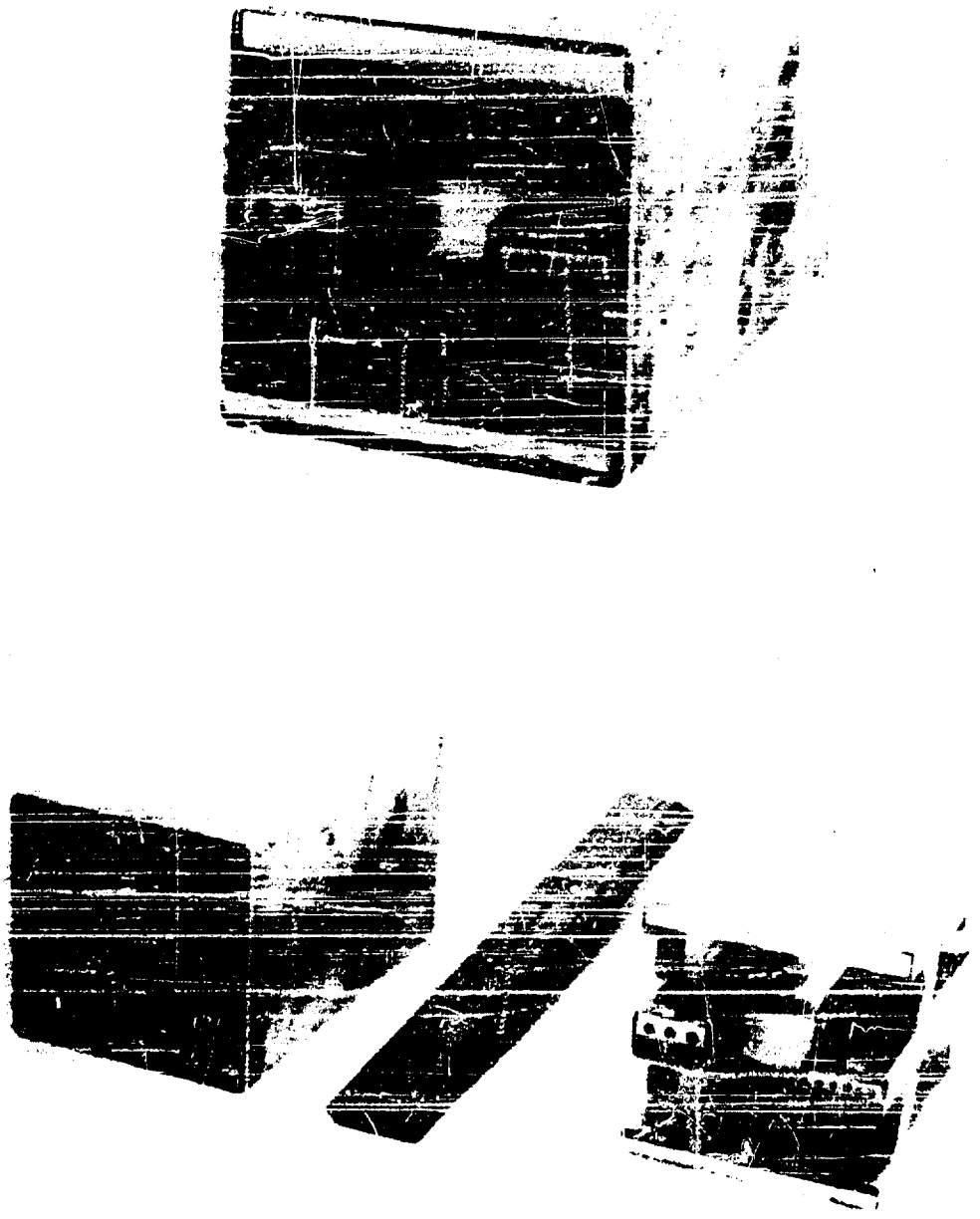

Figure 21 - Permanent magnet radiation test assembly

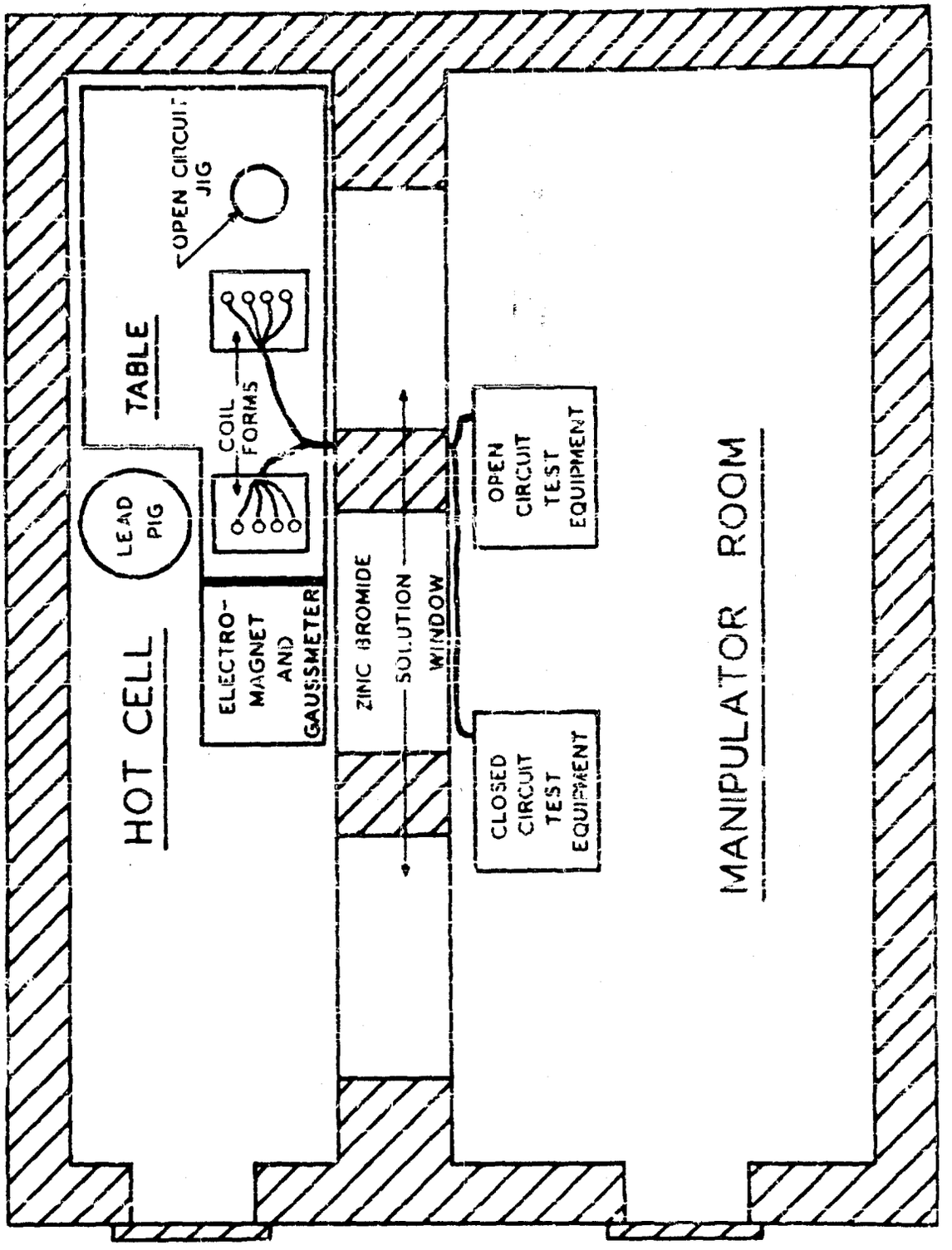

Figure 22 - Post-irradiation testing arrangement for magnetic testing of radioactive permanent magnets

Laboratory Reactor Hot Cell Facility was used for these tests.

Summary

A comprehensive survey of the effects of reactor irradiation (10^{17} epithermal neutrons/cm^2) on technologically important magnetic materials (soft and hard) has been made. It was found that except for radioactivity, all permanent magnetic materials and those soft materials with coercive force greater than 0.5 oersted (such as silicon-irons, aluminum-irons, and Permendur) showed no appreciable changes in this environment. However, the softer core materials, i.e., with coercive force less than 0.5 oersted (such as Supermalloy, 4-79 Mo-Permalloy and other nickel-irons) were drastically degraded, some properties changing as much as ten times. As a matter of fact, Table VII adapted from Sisman and Wilson (14), shows that of all the physical properties of metals and alloys, the structure sensitive magnetic properties of the nickel-iron alloys (containing large amounts of nickel) are the most sensitive to fast neutron irradiation. (They approach the sensitivity of silicon diodes, which show loss of rectification at 10^{16} nvt.) This sensitivity may find application in fast neutron dosimetry problems.

This means that most magnetic materials will perform adequately in presently required nuclear environments, although future applications (and some present ones) will require testing at higher radiation levels. For the nickel-irons, however, significant damage occurs at 3×10^{16} epithermal nvt.

TABLE VII. RADIATION SENSITIVITY OF ENGINEERING MATERIALS

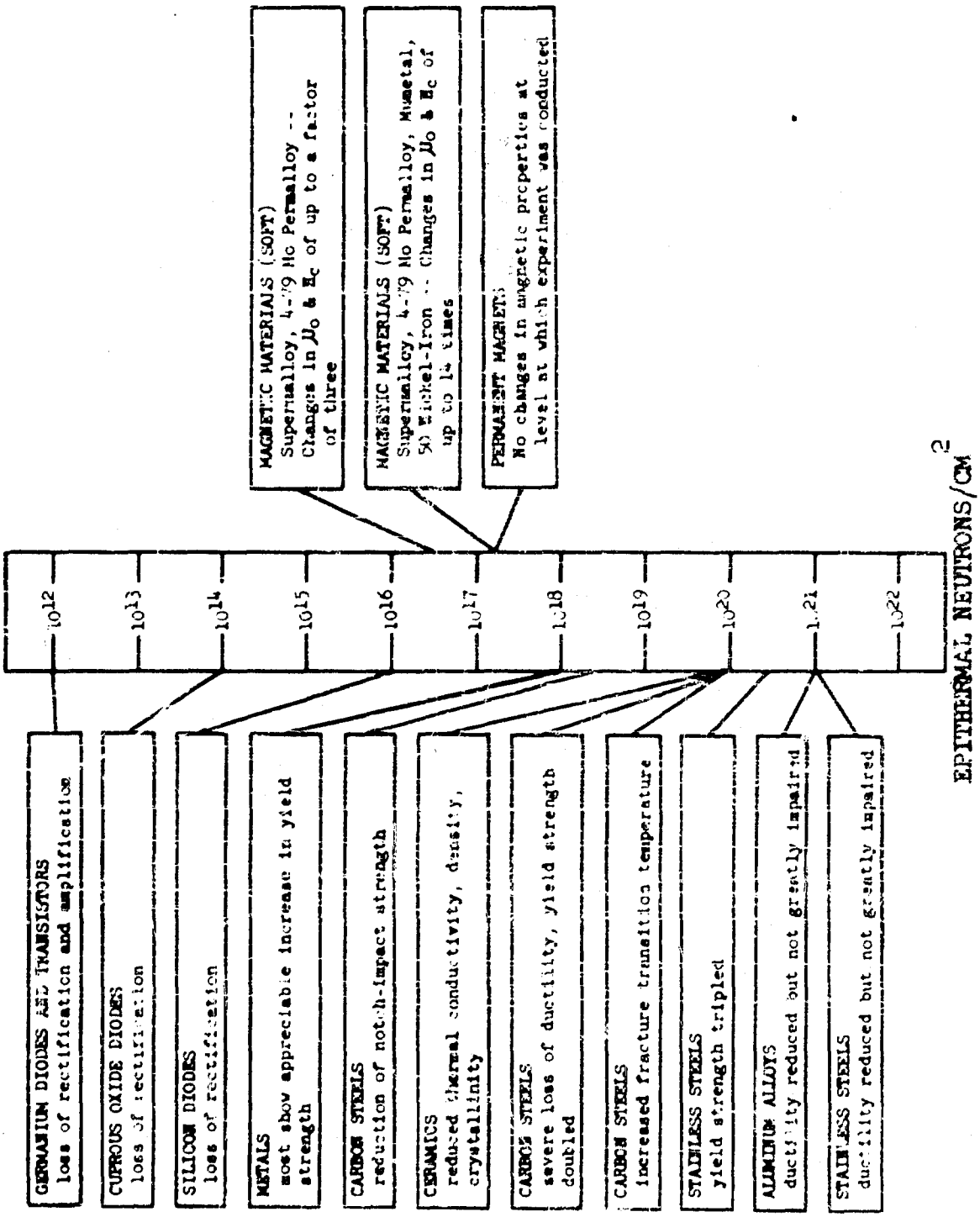

References

1. M. Pasnak and R. H. Lundsten
   (a) NAVORD Report 6132 (U. S. Naval Ordnance Laboratory, White Oak, Silver Spring, Maryland, 10 July 1958)

   (b) Paper presented at Fourth Conference on Magnetism and Magnetic Materials, Philadelphia, Nov. 1958. To be published in J. Appl. Phys. (April 1959)

2. C. Q. Adams and C. M. Davis, Jr.
   (a) NAVORD Report 4285 (U. S. Naval Ordnance Laboratory, White Oak, Silver Spring, Maryland, 20 February 1958)

   (b) J. Appl. Phys. 29, 372 (1958)

3. Sery, Fischell, and Gordon, Conference on Magnetism and Magnetic Materials, Boston, October 1956 (American Institute of Electrical Engineers, February 1957)

4. Gordon, Sery, and Fischell, Nucleonics 16, No. 6, 73 (1958)

5. R. S. Sery and D. I. Gordon, Bull. Am. Phys. Soc. Ser. II, 3, 11 (1958)

6. D. I. Gordon and R. S. Sery, Paper presented at International Conference on Solid State Physics in Electronics and Telecommunications, Brussels, June 1958. To be published by Academic Press, Inc. 1959

7. R. S. Sery and D. I. Gordon, NAVORD Report 6127 (U. S. Naval Ordnance Laboratory, White Oak, Silver Spring, Maryland, 3 June 1958)

8. Sery, Gordon and Lundsten
(a) Paper submitted for presentation at American Physical Society Meeting, Cambridge, March-April 1959

(b) NAVORD Report 6276 (U. S. Naval Ordnance Laboratory, White Oak, Silver Spring, Maryland. To be published)

9. Advisory Group on Electronic Parts (AGEP), Office of Assistant Secretary of Defense (Research and Engineering), Environmental Requirements Guide for Electronic Parts (PB-131423, Office of Technical Services, Dept. of Commerce, Washington, Oct. 1957)

10. Schindler, Salkovitz, Ansell, Paper presented at Fourth Conference on Magnetism and Magnetic Materials, Philadelphia, Nov. 1958. To be published in J. Appl. Physics (April 1959)

11. N. G. Sakiotis et al, Paper presented at International Conference on Solid State Physics in Electronics and Telecommunications, Brussels, June 1958. To be published by Academic Press, Inc. 1959

12. Salkovitz, Schindler, and Ansell, Bull. Am. Phys. Soc. Ser. II, 3, 117 (1958)

13. Fennell, Hancock, Barnes, AERE M/TN 48 (Atomic Energy Research Establishment, Harwell, Berkshire, England, April 1958)

14. O. Sisman and J. C. Wilson, Nucleonics 14, No. 9, 58 (1956)

CORROSION MECHANISMS IN THE REACTION OF STEEL WITH WATER AND OXYGENATED SOLUTIONS AT ROOM TEMPERATURE AND 316°C

M. C. Bloom and Mary Boehm Strauss
U. S. Naval Research Laboratory
Washington 25, D. C.

At the ONR symposium held in Washington two years ago a summary of results obtained in a basic study of corrosion mechanisms of mild steel under conditions pertinent to boiler operation was given[1]. This paper is a report of further progress in these mechanism studies. Some highlights of the report given at the 1957 Symposium are illustrated in the first two figures. These figures illustrate (1) the protective film of magnetite (Fe_3O_4) which forms on mild steel subjected to treatment with water at 316°C (600°F) in the absence of oxygen and (2) the pits surrounded by red patches of hematite (α-Fe_2O_3) which develop when this steel is exposed to oxygenated water at room temperature and then subjected to further exposure to oxygenated water at 316°C (600°F), a temperature approached in modern Naval boiler plant operations.

This development of pits seems to be associated with the development of the corrosion product γ-FeOOH at room temperature and its subsequent conversion to α-Fe_2O_3 upon heating to 316°C.

Continued studies of corrosion-mechanisms in capsule systems have led to a further clarification of the corrosion reactions, which is the subject of this report. The method of fabrication of the capsules employed was described in the previous report[1]. A typical capsule is shown in Figure 3. For examination of the reaction products formed in oxygenated systems, mild steel capsules of this kind filled with air-saturated water or hydrogen peroxide solutions were used. In the presence of ferrous or ferric ions generated by the corrosion process, hydrogen peroxide decomposes readily to form oxygen and water and these solutions thus provide a simple means for

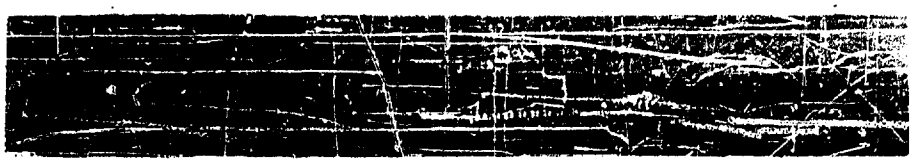

Figure 1a - Mild steel pipe after 131 days' treatment at 316°C with high purity water

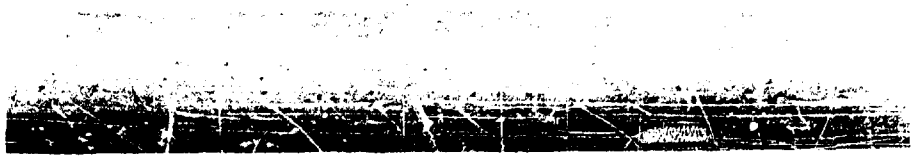

Figure 1b - After 21 days treatment at 316°C with high purity water pressurized with oxygen at room temperature prior to heating

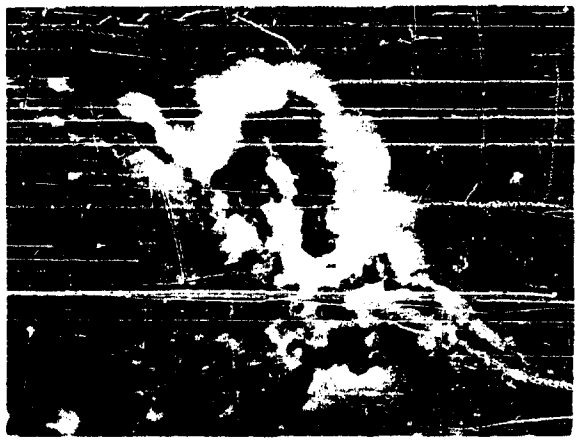

Figure 2 - Cross section through one of red islands in lower half of Fig. 1. 1150 X

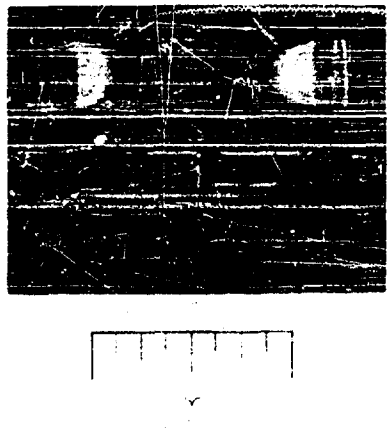

Figure 3 - Capsule

introducing oxygen into the sealed capsules. The specimens were exposed at room temperature (25°C) and 316°C for selected lengths of time. The capsules were then opened and the pH measured. In some cases, samples of the liquid were evaporated to dryness and analyzed spectroscopically. Any suspended solids were tested with a magnet to determine the possible presence of ferromagnetic corrosion products, and then all of the suspended solids were collected on filters, dried, and analyzed by X-ray diffraction, aided in some cases by chemical analysis. After removal of the fluid from the capsules the walls were examined microscopically to determine the extent and character of the attack and were subjected to X-ray and electron diffraction analysis to determine the nature of the corrosion product films.

The data obtained from the examination of the corrosion products formed at room temperature in capsules initially filled with distilled water are shown in Figure 4. Attention is directed to the following facts:-

The water was initially air-saturated and the small variation in pH at the outset is probably due to variations in the carbon dioxide content of the laboratory atmosphere. It may be noted that after six hours the pH has risen to 9.4. This is approximately the pH of a saturated solution of $Fe(OH)_2$. Subsequently the pH rises to 9.9 where it is found one year later. This further rise in pH was shown to be due to the presence of manganese in the steel and the formation of $Mn(OH)_2$ which in saturated solution produces this high pH. Next it may be noted that the initial product of reaction is γ-FeOOH. This phase shows up both as islands on otherwise unattacked metal and as suspended material in solution. Finally, it may be noted that within 24 hours, the spinel phase (Fe_3O_4) has made its appearance. The fact that the pH of the solution has reached the saturation pH of $Fe(OH)_2$ at the time the spinel phase appears suggests that the spinel phase is formed by the decomposition of $Fe(OH)_2$ which is known to take place under analogous conditions (2,3,4).

Figure 5 summarizes data at several oxygen concentrations. It may be observed that when oxygen is absent, the pH rises rapidly to 9.3, the saturation value for $Fe(OH)_2$ and a little less rapidly to 9.9-10, the saturation value for $Mn(OH)_2$. In the presence of sufficient oxygen, however, this rise in pH is arrested in the region of 8.5 undoubtedly due to the removal of $Fe(OH)_2$ and $Mn(OH)_2$ by oxidation. It may further be noted that in the absence of oxygen, the spinel phase (Fe_3O_4) is the solid corrosion product but that in the presence of oxygen γ-FeOOH is the initial corrosion product and

Corrosion Products Formed by the Action of Water* in Mild Steel Capsules at 25°C

Solution pH before reaction**	Time metal was exposed to solution	Solution pH after reaction**	Appearance of solution	Appearance of metal	Corrosion products on metal
5.9	1 hr.	8.5	Yellow tinge	Speckled with brownish yellow islands	γ-FeOOH
5.8	6 hr.	9.4	Clear, Colorless	Same as above	γ-FeOOH and possibly spinel
6.0	24 hr.	9.5	Clear, Colorless	Same as above	γ-FeOOH and spinel
6.0	1 wk.	9.6	Clear, Colorless	Same as above	γ-FeOOH and spinel
6.0	12 wk.	9.6	Clear, Colorless	Thin gray brown film	Spinel and some γ-FeOOH
6.0	52 wk.	9.6	Few particles of spinel	Continuous black film	Spinel

*The water was initially air saturated.
**Each value represents the mean of 6 capsules.

Figure 4

Summary of Corrosion Products Formed by the Action of Water* and H_2O_2 Solutions in Mild Steel Capsules at 25°C

Time of Exposure	H_2O		0.2% H_2O_2		4% H_2O_2	
	pH	Product	pH	Product	pH	Product
1 hour	8.5	γ-FeOOH	7.1	γ-FeOOH	7.1	γ-FeOOH
24 hours	9.5	γ-FeOOH and Spinel	6.6	Spinel and some γ-FeOOH	7.3	γ-FeOOH
1 week	9.8	γ-FeOOH and Spinel	7.4	Spinel	8.2	α-FeOOH
4 weeks	--	--	8.6	Spinel	8.6	α-FeOOH
1 year	9.9	Spinel	10.0	Spinel	8.5	α-FeOOH

*The water was initially air saturated.

Figure 5

α -FeOOH is the secondary corrosion product when sufficient oxygen is present and the pH rises above 8.

When capsules exposed to room temperature treatment in this way were subsequently heated to 316°C the following observations were made:-

The pH dropped back to the vicinity of 7 within 24 hours, any γ -FeOOH or α -FeOOH present being converted to α -Fe_2O_3 which was subsequently reduced to magnetite when the oxygen in the capsule had been used up.

It would appear that the presence of γ -FeOOH, a non-adherent corrosion product which appears when oxygen is present at room temperature, is to be avoided. Not only has its genesis been accompanied by incipient pit formation, but also the α -Fe_2O_3 to which it is converted and the Fe_3O_4 to which it will be reduced by subsequent operations at elevated temperature will be a loose material which may be transported in the flowing stream and deposited at some point in the system where it may interfere with heat transfer, or act as a mechanical plug.

A further deleterious effect of γ -FeOOH was discovered in the course of some transformation studies. In these studies a commercial supply of γ -FeOOH was introduced into capsules in a slurry with water and heated to 316°C. Some of the capsules burst as indicated in Figure 6 and all showed stress corrosion cracking of the type illustrated in Figure 7. Investigation showed that this cracking was due to the presence of a small quantity of chloride ion with the γ -FeOOH and emphasized the deleterious effects which the γ -FeOOH can produce when precipitated in the presence of chloride. It was found that less than 100 parts per million (ppm) of chloride reacting with γ -FeOOH can cause this type of stress corrosion cracking, which is apparently associated with the formation of $FeCl_3$.

Experiments in these static systems indicate that the boiler water treatment chemicals may have more effect upon the avoidance of the formation of γ -FeOOH and pits during shut-down periods when air may be present than upon the general corrosion rate at boiler operating temperatures.

Figure 8 shows the appearance of capsule walls opened up after 24 hours of contact at room temperature with a solution within the specifications for Naval boilers operating at 1200 psi and 950°F superheat. The air was initially air-saturated. It may be noted that the addition of NaOH localized the pitting somewhat, that the

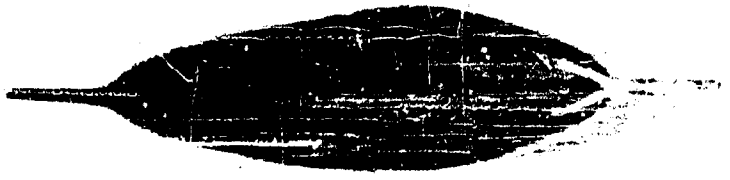

Figure 6 - Burst capsule heated at 316°C with γ-FeOOH containing chloride

Figure 7 - Stress-corrosion cracking of mild steel capsule heated at 316°C with γ-FeOOH containing chloride

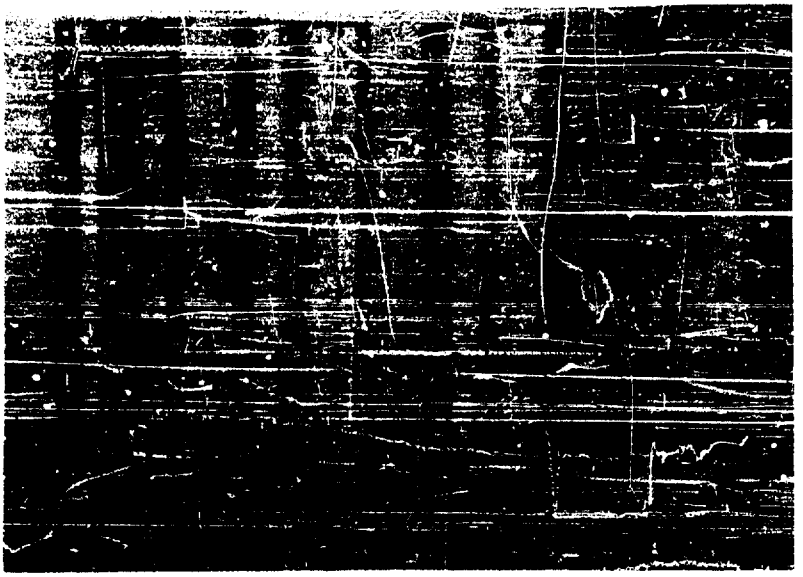

Figure 8 - Appearance of mild steel treated at room temperature for one day with Navy boiler water treatment additives as follows: A - pure water, B - NaOH solution (pH 10.6), C - NaOH solution with 25 ppm phosphate as Na_2HPO_4 (pH 10.6), D - NaOH solution with 25 ppm chloride as NaCl (pH 10.5)

phosphate addition nearly eliminated it, but that if 350 ppm of chloride was allowed to enter even in the presence of both caustic and phosphate, the attack became much worse. Additional experiments have only served to confirm this indication. That the attack can be eliminated even in the presence of air when sufficient phosphate is present has been clearly demonstrated, but the quantity of phosphate necessary may be very large if much chloride is present. A ratio of phosphate to chloride greater than 10 to 1 may be required.

To summarize the most important practical conclusions: It appears that boiler water additions within present specifications may have more effect upon the reactions taking place in the presence of air at room temperature than upon the rate of corrosion at boiler operating temperatures.

The presence of substantial amounts of chloride in boiler water systems may be very deleterious, and present boiler water treatment specifications are not adequate to control its possible ravages under shut-down conditions with access of air.

REFERENCES

(1) A Decade of Basic and Applied Science in the Navy, ONR Symposium, March 19 and 20, 1957, pp. 572-579.

(2) Corey, R. C., and Finnegan, T. J., Am. Soc. Testing Materials Proc. 39:1242 (1939).

(3) Evans, U. R., and Wanklyn, J. N., Nature 162:27 (1948).

(4) Shipko, F. J., and Douglas, D. L., "Thermal Stability of Ferrous Hydroxide Precipitates", Knolls Atomic Power Lab. KAPL-1377, November 1, 1955.

ACKNOWLEDGMENTS

The authors are indebted to W. A. Fraser and G. N. Newport for assistance throughout the course of this work; to C. O. Timmons for the preparation and treatment of many of the specimens; to Evelyn Cisney and W. G. Sadler for X-ray diffraction patterns; to D. H. Price for the metallography, to the Analytical Branch for chemical analyses, to A. J. Pollard for aid in the exploration of phosphate-chloride ratios and to Jeanne B. Burbank for assistance with the electron diffraction studies.

RECENT CONTRIBUTIONS OF CHEMISTRY IN THE PREVENTION AND CONTROL OF CORROSION IN THE NAVY

W. L. Miller
Material Laboratory
New York Naval Shipyard
Brooklyn 1, New York

Corrosion control in the Navy is at times accomplished by mechanical means such as improved design or substitution of materials, but in general it is necessary to use chemical methods or products to stop the widespread corrosive destruction. A comprehensive coverage of this subject would require an excessively long presentation. Consequently, this paper is limited to high spots of comparatively recent Naval usages, particularly where the New York Naval Material Laboratory has participated.

In any review of chemical control of corrosion, the development of new coatings must take a prominent place. Recent developments in epoxy resin coatings are being used for cargo ballast tanks of tanker ships and aviation fuel tanks of carrier vessels. Epoxy polyamide types in particular are showing promise in applications under difficult conditions. The Laboratory is currently exploring such coatings with painting being done on water-wet surfaces. The Laboratory has also investigated the use of conversion coatings in which the basis metal is oxidized, either chemically or electrochemically, to produce an adherent film. Aluminum radar waveguides have demonstrated the value of such coatings following extensive exposure at Kure Beach, North Carolina. Consequently a new specification will be drawn to require suitable conversion coatings on the waveguides.

The value of corrosion inhibitors has been recognized by the Navy, especially in aircraft fuels. Some formerly used inhibitors have shown undesirable side effects, such as emulsification tendencies. The Material Laboratory has conducted a study of the extent of emulsification of jet fuel by corrosion inhibitors. Fortunately,

inhibitors that do not cause serious emulsification are available and are specified. Another study by the Laboratory was made of the use of chloride as an inhibiting additive to hot sulfuric acid pickling baths. As a result of this study, 1.5 percent of sodium chloride is now specified as an additive to sulfuric acid baths for pickling Special Treatment Steel. This is in addition to the commonly used organic pickling inhibitors. Various other developments in inhibitors have been made throughout the Navy. High pressure boilers are now inhibited by careful control of pH and phosphate ion. Nitrite inhibitors are used in wet sand blasting. New inhibitors have been developed for lubricating and preservative oils and greases. Vapor phase inhibitors are being used in packaging and octadecyl amine is being used as a volatile film-forming inhibitor for steam lines, including those throughout the New York Naval Shipyard.

Among other chemical controls for corrosion, the use of ion exchange resins is important for obtaining high purity water necessary for battery make-up and cooling water in submarines and for pressurized water nuclear powered systems. The Navy has consequently maintained a study of composition and uses of newly developed resins for water purification.

Among developments by Material Laboratory chemists is an acid descaling process suitable for removing heavy rust scale from large tanks. This originated as an independent idea of the inventors and a patent application has been filed by the Navy in their names. While not an anticorrosive measure in itself it is an economical process for use in connection with pretreatments for painting or other corrosion control methods. So far the method has been used on tanker ships with two Navy MSTS oilers and at least six commercial ships using it during 1958. Using one-half percent by volume of sulfuric acid the method is capable of descaling the cargo tanks of tanker ships at a cost of less than two cents per square foot of descaled surface for acid with an approximately equal cost for labor. The descaled surfaces may then be given a brush sandblasting with a savings of about 30 cents per square foot over heavy descaling and blasting as prepaint treatment. Note: Two slides are shown to illustrate a heavily rusted tank bulkhead of the USS MARIAS before and after descaling.

Metallic corrosion in aqueous environment is an electrochemical process and one of the most effective means of stopping it is by applying electrochemical counter measures, in other words, cathodic protection. Cathodic protection is now widely used by the Navy in large and small applications using either impressed current systems, sacrificial anodes, or mixed systems. An impressed current system is used in the protection of underground cables and piping

Figure 1 - No. 1 starboard tank, section of forward bulkhead-before descaling

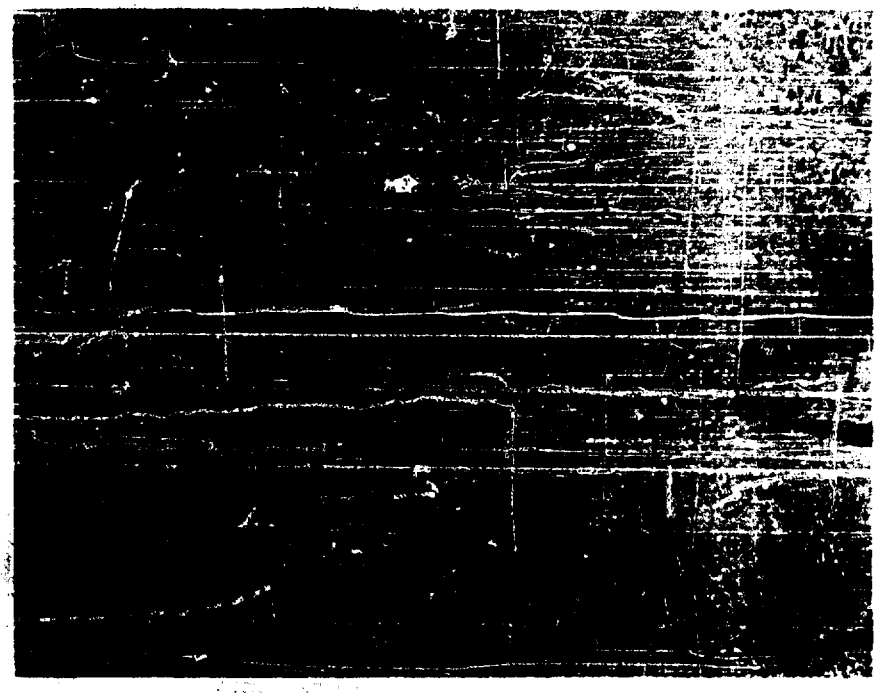

Figure 2 - No. 1 starboard tank, section of forward bulkhead-after descaling

throughout the New York Naval Shipyard. This system uses twenty rectifiers, with each one having a vertical ground bed 100 feet deep containing a string of graphite anodes. During operation for the past two years, only one blowout of underground power cables has occurred. Prior to this period, the average time between cable blowouts was approximately twenty-four days.

The Material Laboratory started its cathodic protection studies with the development of Specification MIL-A-18279 covering impregnated graphite rod anodes for protection of Reserve Fleet ships. Anodes used previously in ground beds by the Maritime Administration were modified by incorporating more flexible cables, chlorine and oxygen resistant collars and an improved cable anchor within the anode. With normal use at sea water sites these anodes have an estimated life of at least five years. With a moderate expenditure for current, 22 anodes suspended over the sides of an aircraft carrier for example, can prevent corrosion of the underwater hull. Fouling by marine organisms is not prevented, and maintenance painting is still required, but time intervals between drydockings have already been doubled with very large savings to the Navy.

In the ONR 1957 Symposium the writer gave detailed information on the relative performance of graphite versus silicon-iron anodes at various current densities and in waters of various resistivities. Subsequent to this, additional Laboratory tests supplemented by service tests have since resolved the selection of anodes into the following for reserve ship hulls:

a. Either graphite or silicon-iron in low-resistivity (sea) water at current densities up to 10 asf,

b. Graphite for sea water use at current densities above 10 asf,

c. Silicon-iron for all current densities in high-resistivity (fresh or somewhat brackish) water.

In March of 1958 an experimental system was installed on the USS LEXINGTON in an attempt to prevent cavitation erosion of the propellers by electrolytic generation of hydrogen gas on the propeller blades. The system was designed jointly by the Bureau of Ships, the New York Naval Shipyard, and a contractor, and was installed by the Puget Sound Naval Shipyard. The Material Laboratory coordinated the work and analyzed operational reports of the system as recorded and forwarded by ship personnel. After two months of operation there was a noticeable increase in electrical resistance. By August the resistance showed a large increase to the point where protection was

probably impaired. This increase in resistance could have resulted from failed anodes, line fuses or certain other causes. Unfortunately, the ship was operating in a remote area and laboratory inspection was infeasible. The system was secured and eleven of sixteen anodes were removed from the ship's hull. These have subsequently been inspected at the Material Laboratory and five of these were found to be incapable of operation. Inspection of the ship's stern area by the repair facility showed loss of some coatings on struts and rudders but with no pitting or corrosion evident. Some light roughening of propeller blades was reported. Pending further work on electrolytic prevention of cavitation erosion the results appear inconclusive.

In connection with cathodic protection the Laboratory has noted unusual dielectric shielding properties in a coal tar modified epoxy resin coating which can be applied by brush or spray. A steel panel coated with this material was made the cathode in a synthetic sea water electrolyte. At 115 volts D.C. a small hole was formed in the coating and arcing began. The potential was regulated to 35 volts and electrolysis was continued for several weeks. As the hole in the coating enlarged, the current automatically increased and the potential dropped slowly to about 22 volts. It then remained constant for more than one month with no further change, nor was there any further increase in the size of the opening. This can now be recognized as an effective means of determining the limiting potential in testing electrolytically resistant coatings and the Laboratory anticipates use of this method in determining the effectiveness of such coatings. It is assumed that the limiting potential for any one coating is a balance point between adhesion and the pressure of hydrogen produced under the edge of the coating. A coating must have exceptional adhesion to withstand 22 volts continuously in an electrolytic circuit. It may be added at this time that as a result of this test, future use is anticipated for modified epoxy resin coatings on ship hulls as dielectric shielding for impressed current cathodic protection systems. This will include use on the newer submarines.

As part of its cathodic protection program, the Material Laboratory explores various metals and combinations of metals for anodes. As a result of one Laboratory study, experimental applications are now being made of platinum-clad tantalum anodes. Platinum-clad titanium may also be used, but is limited to a 10-volt potential. The tantalum base anodes may be subjected to much higher potentials without deterioration of the tantalum in the event of damage to the thin platinum coating. Such anodes should be ideal for mounting on active ship hulls. A good possibility for low-cost impressed current anodes lies in antimony-silver-lead alloys. Laboratory tests indicate very good performance for these alloys at current densities up to 15 asf except in 1000-ohm centimeter (brackish) water. If improved

alloy composition or other means can solve the problem of the high resistivity deterioration it may become feasible to protect a ship with a single lead cable mounted along each side of the underwater hull.

Although the Laboratory is concerned mostly with impressed-current cathodic protection systems, it also does work on sacrificial systems. During the past year a novel system was installed on an MSTS oiler ship with Laboratory assistance. This system consists of magnesium anodes, all mounted in the bottoms of cargo-ballast tanks and having the tank bottoms and bottom structures painted with a solvent-resistant dielectric coating. The coating serves a triple purpose as an electrolytic reflector to direct current uniformly to all uncoated tank areas, to protect the tank bottoms from corrosion caused by small amounts of water in empty tanks, and to insure against sparking hazards in the event of an anode falling while the tank has explosive vapors. The novel features of this system are covered in a patent application.

Numerous references could be made to new chemical techniques for identifying types of corrosion and measuring corrosion rates, but proper description of this work would need a sizeable paper in itself.

DETERIORATION OF PLASTICIZED POLYMERIC MATERIALS; APPLICATION OF RADIOCHEMICAL TECHNIQUES

J. L. Kalinsky and L. H. Handler
Material Laboratory
New York Naval Shipyard
Brooklyn 1, New York

The present study of the degradation of plasticized polymeric materials has been subdivided into two categories: (a) degradation of polymeric insulation and sheathing components of communication cable, caused by migration of plasticizers, and (b) degradation of rubber materials, designed for low temperature service, caused by solvent leaching of the plasticizers. In both cases, plasticizer dislocation occurs by diffusion, in other words, the mechanism of degradation in each is similar. The extent of degradation is a function of the amount of plasticizer diffusion and such effect would be reflected in the change of chemical, physical and electrical properties.

Plasticizers play an essential role in the formulation of several of the synthetic polymeric insulation, sheathing, and sealant components of electrical communication cable. The recent emphasis on reduced diameter cable has accentuated the service problems associated with the loss of properties due to plasticizer migration. Excessive migration of plasticizer from vinyl sheaths may cause stiffening of the plastic, softening and deterioration of other components which absorb the plasticizer with consequent deleterious effects on the dielectric strength and power factor of conductor insulation. Therefore, the study of the rate extent, and prevention of plasticizer migration is of considerable interest and importance.

A diffusion mechanism also plays a strong role in the leaching of plasticizers from rubber stocks designed for low temperature use. The problem of designing elastomeric materials for use under low temperature service conditions has confronted the rubber industry and the Department of Defense for a considerable time. Resistance to solvents such as hydraulic fluids, fuels, oil, and water,

with continued serviceability under extreme shipboard conditions, is therefore of concern to the Navy. The solvent extraction resistances of some specially formulated rubber stocks were studied.

Various commonly used test methods for studying plasticizer migration require measurement of dimensional changes (such as volume swell tests), burial of specimen in activated charcoal or silica gel,(1) lacquer crazing, weight loss by vacuum (2) or rub-off.(3) These methods are time consuming, and in addition the test conditions are unreal, often requiring extreme extrapolation of test data to simulate actual service conditions. The most direct and valid approach to this problem is to provide a rapid, sensitive, and quantitative method for the determination of plasticizer ingress or egress under conditions simulating as closely as possible those actually encountered in shipboard service. Such a method is available through the use of radioisotope tracers, which provide extreme sensitivity, reliability and precision.

With the use of a sliding microtome and radioactively labeled plasticizers, rapid and reliable determinations can be made regarding the rate and extent of neat or compounded plasticizer migration into various insulating and protective materials such as polyvinyl chloride, silicone rubbers, and polyethylene.

Three radioactively labeled plasticizers were used. Two were monomeric, phosphorous-32 tagged tricresyl phosphate (TCP) and carbon-14 tagged di-octyl (2-ethyl hexyl) phthalate (DOP), and the third was a polymeric plasticizer of a proprietary nature. These radioactive plasticizers, were synthesized at the Material Laboratory. Two series of experiments were run, one where a thin film of neat or uncompounded radioactive plasticizer is placed between two polymeric discs of identical composition, and the second, where a plastic compounded with the radioactive plasticizer is placed between two unplasticized polymer discs. The specimens are maintained in intimate contact as a sandwich. The time and temperature used are controlled to avoid complete penetration of the polymer by the plasticizer, so that the boundary conditions are in accordance with the limitations set up by the derivation of Fick's Second Law. The center part of each disc is cored out with a leather punch to eliminate edge effects, and the cored center is serially sectioned on the microtome at 40 microns thickness. The companion disc for each set is kept in a chilled condition before slicing to retard additional diffusion. For calibration purposes, the sectioned portions are weighed on a semi-micro balance.

Figure 1a represents a plot of the specific activity of TCP diffusing into Dow Corning Silastic Rubber 172 after one-half hour at

room temperature. By plotting the specific activity of plasticizer as a function of penetration for both top and bottom discs, a typical bell shaped symmetrical curve is obtained. However, if the log of the specific activity is plotted against the square of the penetration (Figure 1b) a straight line is obtained for each disc, the closeness of the curves obtained depending on the reproducibility of the results obtained for duplicate discs.

The self diffusion of neat TCP into TCP-plasticized polyvinyl chloride is illustrated in Figure 2. The specific activity of TCP, normalized to 1000 c/m/mg, at 24°, 50°, and 75°C, respectively, is plotted against the square of the penetration. The equation shown is derived from Fick's Second Law (4) and relates the concentration as a function of the diffusion coefficient, time, and surface area of the disc. The diffusion coefficient is calculated knowing the slope of the line and time of exposure, and is expressed in terms of cm^2/sec. As expected, the higher the temperature, the greater the penetration. The dependence of the diffusion coefficient, D, on the absolute temperature is illustrated in Figure 3. D rises exponentially with temperature, obeying the Arrhenius Equation shown.(5) Therefore, knowing the energy of plasticization and the activation constant, it should be possible to predict the diffusion characteristics of plasticized polymers at different temperatures, provided there is no phase transition.

The effect of plasticizer concentration of the plasticized vinyl on the self diffusion coefficient is illustrated in the semi-log plot of Figure 4, where it is seen that the diffusion coefficient increases with increasing concentration. This indicates that the diffusion coefficient is not truly concentration-independent as assumed in the derivation of Fick's equation. It also indicates that at lower plasticizer contents, there should be less diffusion or exudation.

A comparison of D values for different polymer systems, particularly heterogenous systems, is of limited value and might not show up true differences in migration rate. Therefore another term called the "K" value has been used to measure more realistically the rate and extent of migration.(6) The "K" value is expressed as a function of the amount of plasticizer migrated per unit surface area of polymer per square root of time.

Figure 5 shows results of experiments performed with the proprietary polymeric plasticizer. Due to the expected spread in molecular weights in the synthesis of this polymeric material, more than one component is present. Therefore the diffusion curves obtained differed from those obtained for monomeric plasticizers.

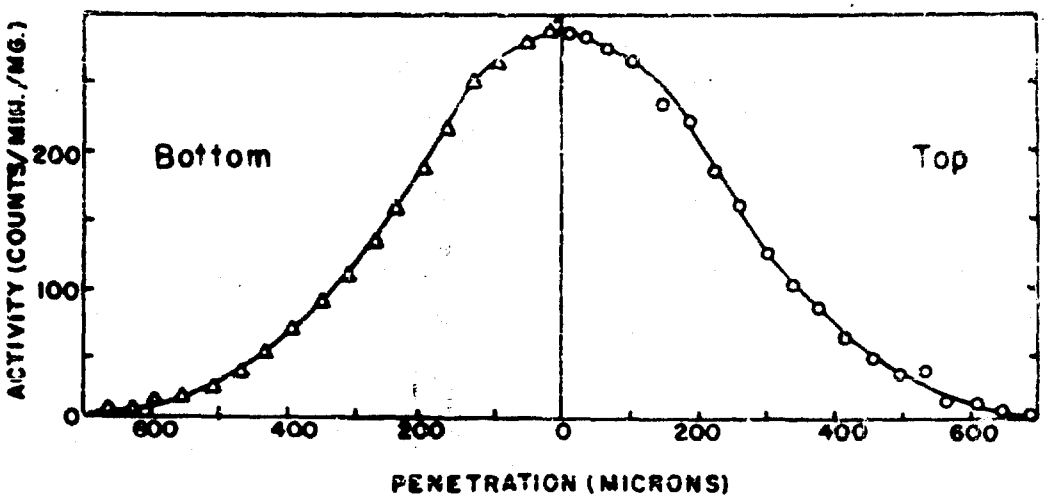

a. Plasticizer Distribution As A Function Of Penetration

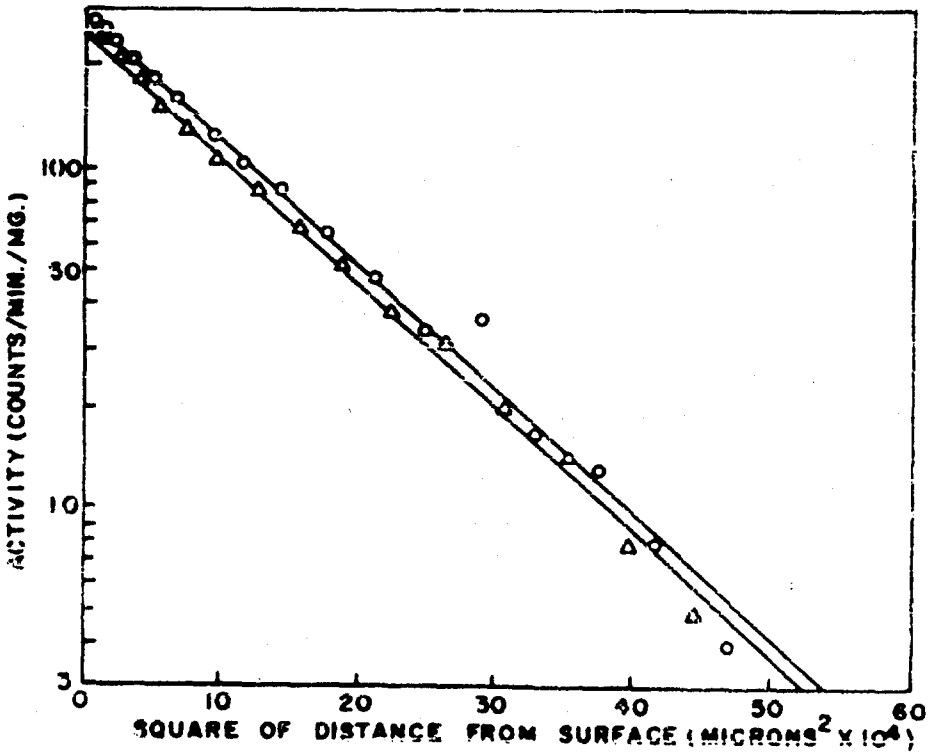

b. Plasticizer Distribution As A Function Of Penetration^2

Figure 1 - Diffusion of TCP in chemically cured silastic 172 at 29°C

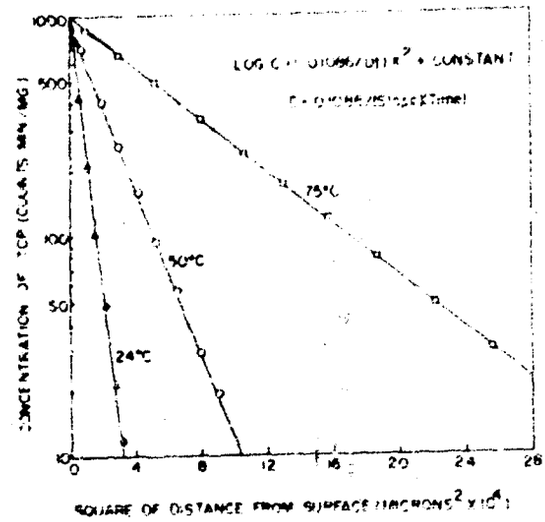

Figure 2

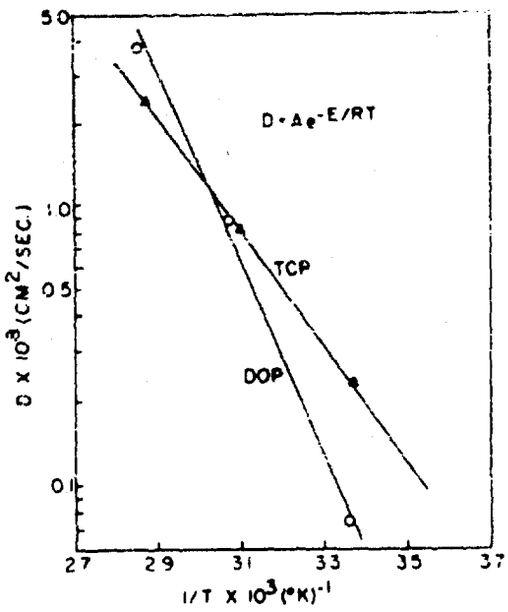

Figure 3

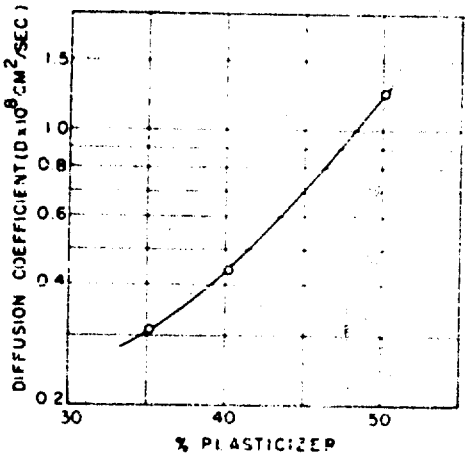

Figure 4

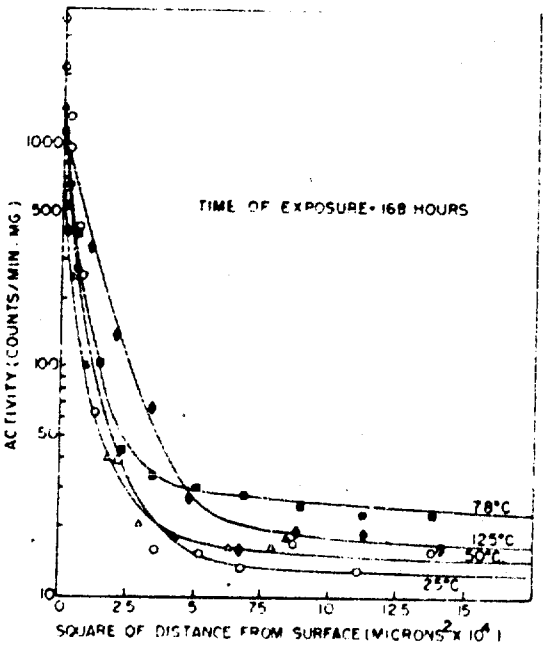

Figure 5

Shown here is the diffusion of polymeric plasticizer into Silastic 181 at 25°, 50°, 75° and 125°C. The lower molecular weight component diffused rapidly, giving a horizontal straight line, which indicates that this component has reached an equilibrium concentration in the rubber. The high molecular weight component diffuses much more slowly, giving a steep vertical line. Temperature had very little effect on the diffusion of polymeric plasticizer, and the amounts diffused were in all cases very much lower than for monomeric plasticizers. Exposure times of at least 166 hours were used, as opposed to one-half hour for monomeric plasticizers.

Table 1 is a summary of results obtained for the diffusion of uncompounded monomeric and polymeric plasticizers into dielectric cable materials, showing the differences in migration rates for a silicone rubber and polyethylene by diffusion coefficients and "K" values. It was found that both TCP and DOP migrated to the same extent in the silicone rubber, a standard dimethylpolysiloxane stock cured with benzoyl peroxide. However diffusion of polymeric plasticizer was much slower, an exposure time of 168 hours at 125°C yielding a very low "K" value. Experiments involving polymeric plasticizer were performed at temperatures ranging from 25°C to 125°C, but the effect of temperature on the diffusion characteristics of the plasticizer was almost negligible. The temperature shown here represents the highest encountered in actual cable testing, and under service conditions. Polyethylene was much more resistant to plasticizer diffusion, "K" values being considerably lower. Polyethylene was found to be more resistant to plasticizer migration over extended periods of time at 50°C for both TCP and DOP. The "K" value for polymeric plasticizer diffusing into polyethylene is so low as to be almost meaningless.

Table 2 shows the effect of polymer composition on the diffusion of DOP in insulation and sheathing materials. The effect of cure can be seen in the "K" values obtained for different types of silicone rubbers. Chemically cured Silastic 2010, a vinyl modified polysiloxane stock cured with dichlorobenzoyl peroxide, had a higher "K" value, in other words, was less resistant to migration than conventional stocks as represented by Silastics 181 and 172, which are straight dimethylpolysiloxane stocks cured with benzoyl peroxide. Curing of Silastic 181 by gamma irradiation improved its resistance to migration by 28%. A dose of 1.3×10^7 rep was used. A fluorine modified silicone was found to have greater migration resistance than all the other silicones tested, but was less resistant than both polyethylene and polyvinyl chloride.

Table 1

Diffusion of Uncompounded Monomeric and Polymeric Plasticizers into Polymeric Cable Materials

Plasticizer	Dielectric	Time (Hrs.)	Temp. (°C.)	D ($cm^2/sec.$)	"K" ($ug/cm^2/hr^{\frac{1}{2}}$)
TCP	Silastic *	0.5	26	0.25×10^{-6}	225
	Polyethylene	24	50	0.47×10^{-8}	53
DOP	Silastic *	0.5	28	0.25×10^{-6}	268
	Polyethylene	24	52	0.19×10^{-8}	13
Polymeric	Silastic ‡	168	125	3.91×10^{-11} (Major)	2.1 (Major)
				---	1.1 (Minor)
	Polyethylene	1200	78	---	0.2 (Minor)

Table 2

Effect of Polymeric Composition on the Diffusion of DOP in Insulation and Sheathing Materials

Polymer	Time (Hrs.)	Temp. (°C)	D ($cm^2/sec.$)	"K" ($ug/cm^2/hr^{\frac{1}{2}}$)
Silastic 181 *	0.5	28	0.25×10^{-6}	268
Irradiated Silastic 181 ‡	0.75	28	0.24×10^{-6}	192
Silastic 2010 +	0.5	27	0.20×10^{-6}	318
Silastic 172 *	0.5	29	0.16×10^{-6}	211
Fluorinated Silastic LS-53	20	25	0.91×10^{-8}	115
Polyethylene	24	52	0.19×10^{-8}	13
Polyvinyl Chloride (40% DOP)	24	25	0.07×10^{-8}	36

* Dimethylpolysiloxane; benzoyl peroxide cure.

\+ Less than 1% vinyl monomer added; dichlorobenzoyl peroxide cure.

‡ Cured by gamma irradiation, 1.3×10^{7} rep.

The results of experiments involving compounded DOP diffusing from a polyvinyl chloride organosol into a silicone rubber are shown in Figure 6. As expected, diffusion was greater at 50°C than at 25°C, equilibrium being attained after 2 days of exposure, as compared to 5 days at 25°C. A comparison of the diffusion of uncompounded and compounded monomeric and polymeric plasticizers into chemically cured Silastic 181 is shown in Table 3. It can be seen that the diffusion of uncompounded DOP is much more rapid over a very short period of time than compounded DOP over a longer exposure time. Uncompounded polymeric plasticizer diffused very slowly compared to DOP. The diffusion of "minor" component of polymeric plasticizer was the same for both compounded and uncompounded material for the same temperature and exposure time, and "major" component diffusion was not much higher. Compounded polymeric plasticizer diffusing into silicone rubber reached on equilibrium concentration of "minor" component in less than 200 hours which did not increase on additional exposure up to 840 hours. This was equivalent to 0.12 percent of total plasticizer, as compared to 3.12 percent diffusion of total plasticizer for compounded DOP at 50°C after 13 hours. The differences between monomeric and polymeric plasticizer diffusion are apparent, and demonstrate the superior qualities of polymeric plasticizer in this respect.

Table 3

Comparison of the Diffusion of Neat and Compounded Plasticizers into Chemically Cured Silastic 181

Plasticizer	Time (Hrs.)	Temp. (°C.)	D ($cm^2/sec.$)	ugm Diffused	"K" ($ugm/cm^2/hr^{\frac{1}{2}}$)
DOP - Uncompounded	0.5	28	0.25×10^{-6}	253	268
DOP - Compounded	24	25	1.31×10^{-13}	279	43
Polymeric Plasticizer - Uncompounded	168	50	1.82×10^{-11} (Major)	50	2.9 (Major)
			---	17	1.0 (Minor)
Polymeric Plasticizer - Compounded	168	50		19.0	
	504	50		18.6	
	840	50		18.6	

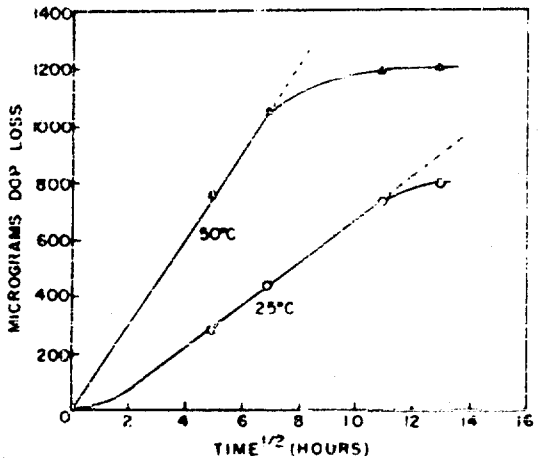
1400
1200
1000
800
600
400
200
0
MICROGRAMS DOP LOSS
50°C
25°C
2
4
6
8
10
12
14
16
TIME^1/2 (HOURS)

Figure 6

Radioisotope techniques have thus provided a rapid and reliable method for measuring the migrational tendencies of plasticizers in polymeric cable components. These techniques make possible the prediction of plasticizer behavior at different temperatures with a minimum of assumptions, and under test conditions more realistic than previously used. This information is necessary in the study of compatibility of materials and in-service degradation of cable components. In summary of this first phase of work, it has been demonstrated that:

a. The migration resistance of conventional silicone stocks is of the same order of magnitude for both TCP and DOP.

b. Conventional silicone stocks are quite vulnerable to monomeric plasticizer migration, although polymethylsiloxane rubbers are less vulnerable to plasticizer sorption than vinyl modified silicone rubbers.

c. Cure by irradiation instead of by chemical means somewhat improves the migration resistance of conventional dimethylpolysiloxane silicone rubber.

d. Fluorine modified silicone rubber is more resistant to monomeric plasticizer diffusion than conventional stocks.

e. Migration resistance of polyethylene at 50°C or less, is better than plasticized polyvinyl chloride, which in turn is superior to silicone rubber.

f. Quantitative data has been presented to show the low migrational tendencies of polymeric plasticizer at temperatures higher than those encountered in actual service.

In the second phase of studies concerning diffusion regulated processes, tracer techniques were utilized to study the effect of different plasticizers, activated carbon black, polymer, and type of cure-that is, chemical versus nuclear irradiation, on the leaching of plasticized rubber stocks by water and various solvents, respectively. Rubbers are plasticized so that under low temperature conditions a maximum amount of flexibility is retained. Monomeric plasticizers such as tributyl carbitol formal (TP-90B), TCP, trioctyl phosphate (TOF), and di-octyl adipate (DOA), are commonly used for this purpose. Leaching of plasticizer tends to reduce the flexibility, hence the serviceability of rubbers, and plays havoc with gaskets and other parts used in critical applications. By the use of

radioisotope tracer techniques, additional information regarding the retention characteristics of plasticizers in polymers can be obtained.

It has long been established in carbon-black studies that different types of carbon-black have different reinforcement qualities in rubber stocks. The degree of reinforcement of a rubber stock by a specific carbon black is dependent on the agglomerate structure of the pelletized black used, the sorptive capacity which depends on the particle diameter and surface area of the carbon black, and the mode and number of carbon black-rubber attachments. It is to be expected that a carbon black with a larger surface area should have a larger sorptive capacity, and thus have higher plasticizer retention. For this reason the effect of an activated carbon black-Nuchar, was studied.

The production of cross-links in rubber when subjected to high energy radiation has been previously shown by many workers.(7,8,9) It was shown that crosslinking predominates upon gamma irradiation if active sites are present, such as are found in straight chain polymer structures. Thus, natural rubber, and synthetics such as the Hycars, would be cross-linked. It has also been previously shown that the cross link density increases with, and is directly proportional to the radiation dose.(7) This results in increased solvent retention properties, and would be expected to affect the plasticizer retention properties favorably.

Tests were set up in the laboratory to simulate as realistically as possible actual conditions of solvent extraction, so that the rate, extent, and mechanism of plasticizer extraction by various solvents could be determined. Neoprene-GN, Hycar-OR, and GR-S stocks were used in the accelerated extraction tests. It was found that the accelerated depletion of plasticizers by water extraction proceeds by mechanisms which involve the surface resistance of the rubber and the diffusion coefficient of the plasticizer; the net result being dependent on the sample thickness.

Three plasticizers, two of which were labeled with phosphorus-32, TCP and tri-octyl phosphate, and one carbon-14 labeled plasticizer, di-octyl adipate, were studied in low temperature formulations of Hycar-OR rubber stocks. Figure 7 shows comparative extraction rates of plasticizers from Hycar-OR rubber, 1.6 mils thick, by water at 60°C. It can be seen that both TOF and DOA were superior to TCP, DOA showing the highest extraction resistance of the three plasticizers studied.

The effect of vulcanization time on extractability of TCP from Neoprene-GN stocks by water and gasoline was also studied.

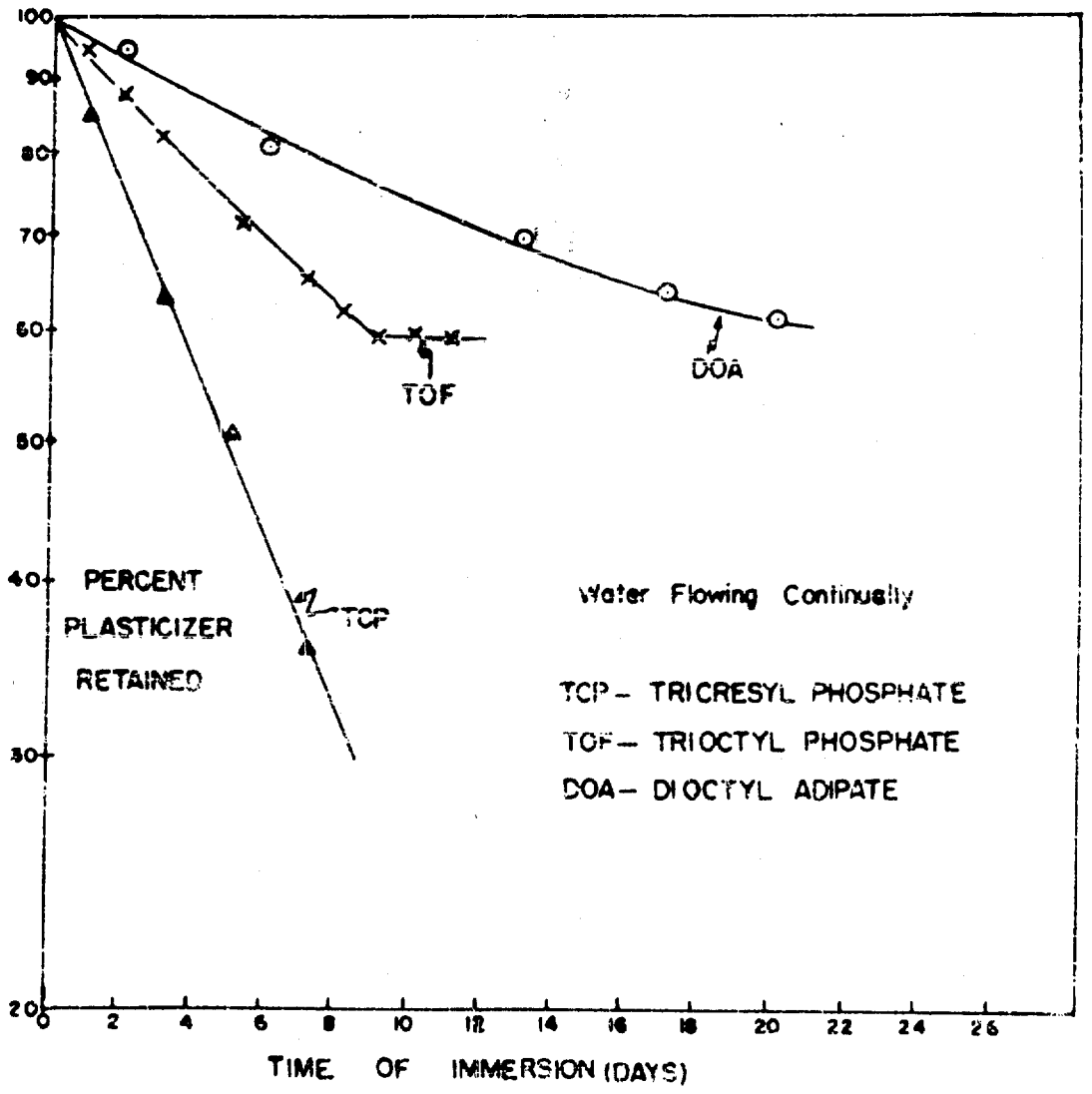

Figure 7 - The comparative extraction rates of plasticizers from plasticized hycar rubber, 1.6 mils thick, by water at 60°C

Longer curing time was found to be correlated with greater resistance to solvent extraction. It was also found that a straight line relationship is obtained on plotting percent plasticizer retained versus the square root of time, indicating that extraction proceeds via a diffusion process. Similar results were obtained for the substitution of Nuchar activated carbon black for the conventional furnace and thermal blacks, and it was found that such a substitution markedly reduces the rate of extraction of TCP from plasticized elastomers by water at 60°C, and gasoline at room temperature. Although the desired physical properties of the vulcanizates were adversely affected initially by the use of activated carbon, the greater retention of plasticizer would tend to enhance the physicals in low temperature service. Gasoline extraction was used in these experiments as an index of the resistance of rubber stocks to the general class of petroleum type liquids.

Figure 8 shows the effect of gamma irradiation on the extractability of TCP from Hycar-OR stocks by gasoline. It is seen that irradiation of Hycar stocks at 25 megarep improves their resistance to plasticizer leaching as compared to a Hycar stock cured by chemical means. At 63 megarep, this solvent resistance is further improved but with some reduction in physical properties. The same order of extractabilities is found for water extraction. The effect of plasticizer composition on extractability was also studied; using TP-90B, a more volatile liquid given in the Bureau of Ships Rubber Formulary as a plasticizer for low temperature rubber stocks. It was found that a stock formulated with 15 parts of TP-90B and 15 parts of TCP had a higher extraction rate than a stock formulated with 30 parts of TCP alone. This is shown as a dotted line in this figure.

A summary of the effects of polymer, carbon black, and gamma irradiation on extractability of TCP by water is given in Figure 9 as a bargraph. The same effects were found in gasoline extraction. Neoprene chemically vulcanized stocks are seen to offer the greatest resistance to extraction compared to Hycar and GR-S. The use of Nuchar activated carbon in place of conventional furnace and thermal blacks, greatly improves the resistance of all stocks to plasticizer extraction by gasoline, resulting in a four-fold increase in plasticizer retention. Total substitution of Nuchar does, however, adversely affect initial physical properties. High energy nuclear irradiation enhances the retention of plasticizer in Hycar stock subjected to leaching, a dose of 25-60 megarep being required to effect a cure with efficient plasticizer retention properties. The results given here for the extraction resistance of various low temperature rubber stocks may be utilized as a guide in the selection of polymer, curing time, type of curing, etc.

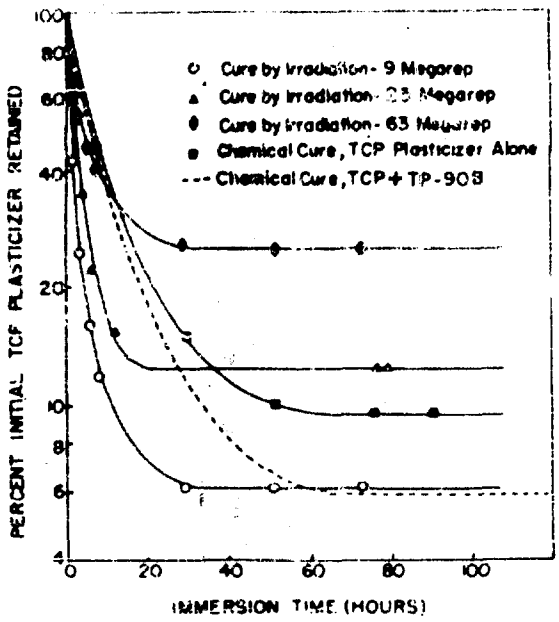

Figure 8

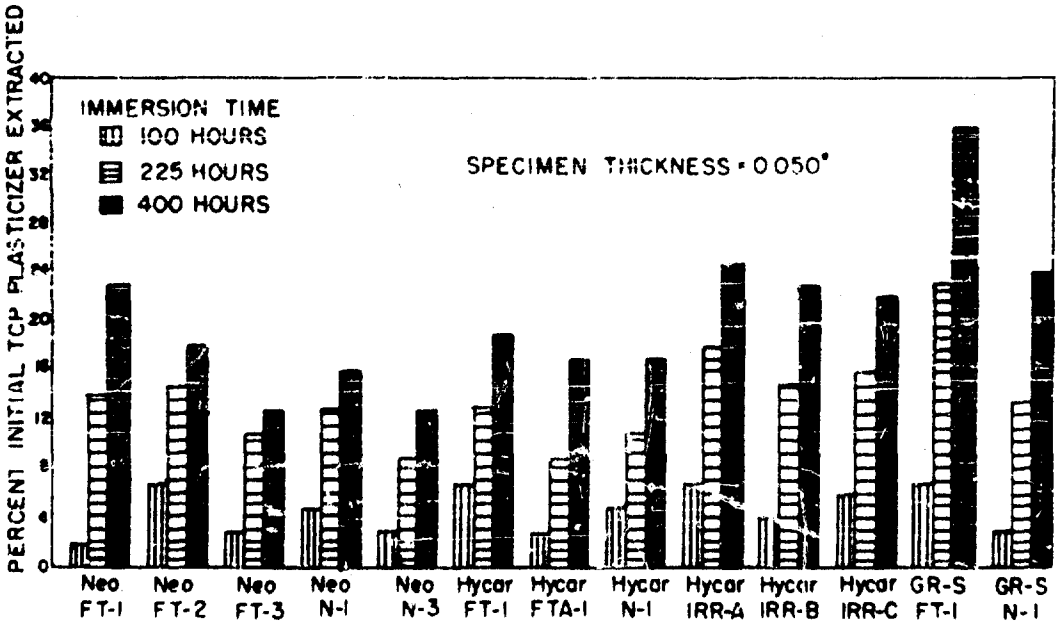

Figure 9 - Summary of effects of polymer, carbon black and gamma irradiation on extractability of TCP by water (60°C)

Radioisotope techniques have provided a rapid and reliable method for measuring the migrational tendencies of plasticizers in polymeric cable components and low temperature rubbers. These techniques make possible the prediction of plasticizer behavior under different conditions with a minimum of assumptions, and under test conditions more realistic than previously used, which is necessary in the study of compatibility of materials and in-service degradation of plasticized materials.

The authors wish to acknowledge the efforts and guidance of Mr. V. Saitta and the late Mr. T. Werkenthin of the Bureau of Ships, and Mr. A. R. Allison of the Naval Material Laboratory, in fostering the application of radioisotope tracer techniques in Naval material problems.

BIBLIOGRAPHY

1. Geenty, J. R., India Rubber World, pp 646-649, Aug. 1952.

2. Quackenbos, Jr., H. M., Ind. Eng. Chem. 46, No. 6, pp. 1335-1344 (1954).

3. Reed, M. C., Klemm, H. F., and Schulz, E. F., Ind. Eng. Chem. 46, No. 6, pp. 1344-1349 (1954).

4. Johnson, W. A., Trans. Am. Mining Met. Engrs., Inst. Met. Div. 143, p. 107 (1941)

5. Liebhafsky, H. A., Marshall, A. L., and Verhoek, F. H., Ind. Eng. Chem. 34, No. 6, pp. 704-8 (1942).

6. Reed, M. C., Klemm, H. F., and Schulz, E. F., Ind. Eng. Chem. 46, No. 6, pp. 1344-9 (1954).

7. Charlesby, A., "The Cross Linking of Rubber by Pile Radiation," Atomics, Jan. 1954.

8. Gehman, S. D., and Auerbech, I., "Gamma-Ray Vulcanization of Rubber," Int. Journal of Radiation and Isotopes, Jul-Aug. 1956.

9. Jackson, W. W., and Hale, D., "Vulcanization of Rubber with High Intensity Gamma Radiation," Rubber Age 77, pp. 865-71 (Sept. 1955).

ENVIRONMENTAL DETERIORATION OF RIGID PLASTICS

N. Fried
S. E. Yunstein
Naval Material Laboratory
New York Naval Shipyard
Brooklyn, New York

The rational application of a material of construction in the design of a specific end item depends upon a knowledge of the conditions which may be encountered in service and the characteristics of the material under such conditions. Thus, interest may be centered on the behavior of a reinforced plastic laminate exposed to a temperature of 1,000°C for 10 seconds or, at the other extreme, information may be required on the characteristics of a boat hull material after immersion in sea water for a number of years. Obviously, the variations in service conditions may be practically limitless.

The most fruitful approach to such problems would be the development of detailed, comprehensive knowledge of the physicochemical characteristics of materials, sufficient to enable the prediction of response to specific conditions. In the absence of such information, the investigator must resort to studies of the behavior of the materials in actual service or under laboratory conditions. In some instances "accelerated" tests may be applied but results of such evaluations must be interpreted judiciously, with particular attention to correlation with behavior under actual service conditions. The technical literature abounds with reports of such simulated service investigations and, undoubtedly, this type of work will continue until such time as more fundamental information is developed. This report discusses a number of programs of this nature, which have been, or are being, conducted at the Naval Material Laboratory, to determine the effects on plastic materials

of specific environmental conditions of interest in Naval applications, including extended exposure to elevated temperature and high humidity ambients, immersion in sea water and other media, and outdoor weather aging.

EFFECTS OF ELEVATED TEMPERATURE

Elevated temperature studies have been limited to temperature levels at which plastic insulating materials might conceivably be required to operate. Investigations have been conducted on both laminated and molded thermosetting plastic materials after exposure to elevated temperatures up to 250°C for periods of time up to 768 hr. (32 days). In this work, mechanical and electrical properties were determined, at intervals, both at the conditioning temperature and at room temperature, on specimens which had been heated and then cooled.

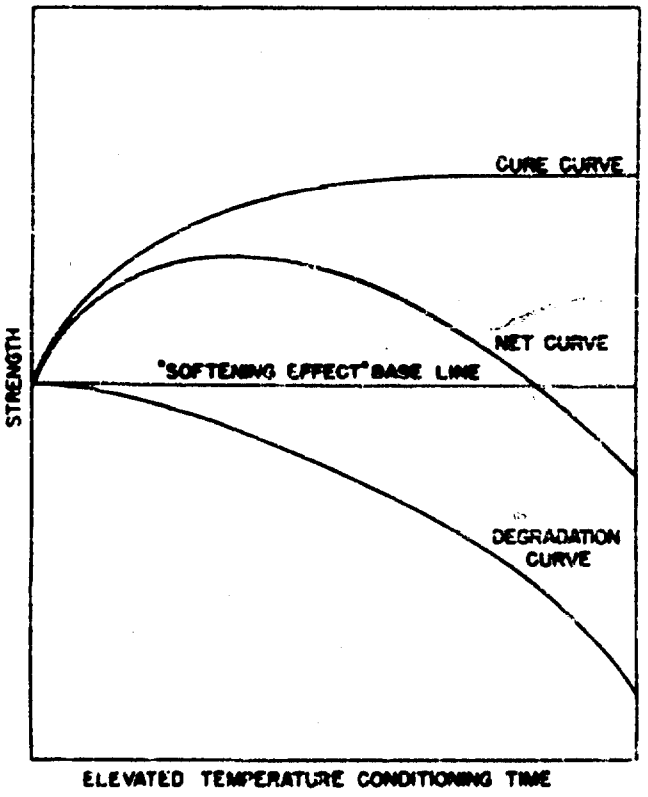

Figure 1 - Hypothetical strength vs time curve for thermosetting laminates

It has been found (1) that, when tested at elevated temperatures, thermosetting materials, in general, demonstrate a marked decrease in strength and stiffness after a relatively short time of exposure, the extent of the decrease being temperature dependent. Under certain conditions, depending on the material, this may be followed by increasing strength as heating continues. Finally, particularly at the higher temperatures, strength may fall off again as chemical degradation becomes the controlling factor. Stiffness characteristics parallel this behavior. It is hypothesized that the observed pattern may be due to three main effects which are superimposed on one another. An initial "softening", which is a physical effect analogous to a decrease in viscosity, and which results in decreased strength and stiffness, occurs after a short

heating period. Additional cure, which is a time dependent chemical reaction, may occur in the resin upon further heating. It would be expected that this would be rapid at first, levelling off with time as reactive sites are consumed, and that the overall effect would be an increase in strength and stiffness. Finally, bond scission and decomposition of resin and filler may occur, which would tend to degrade and weaken the material. The net result would be a curve of the form shown in Fig. 1.

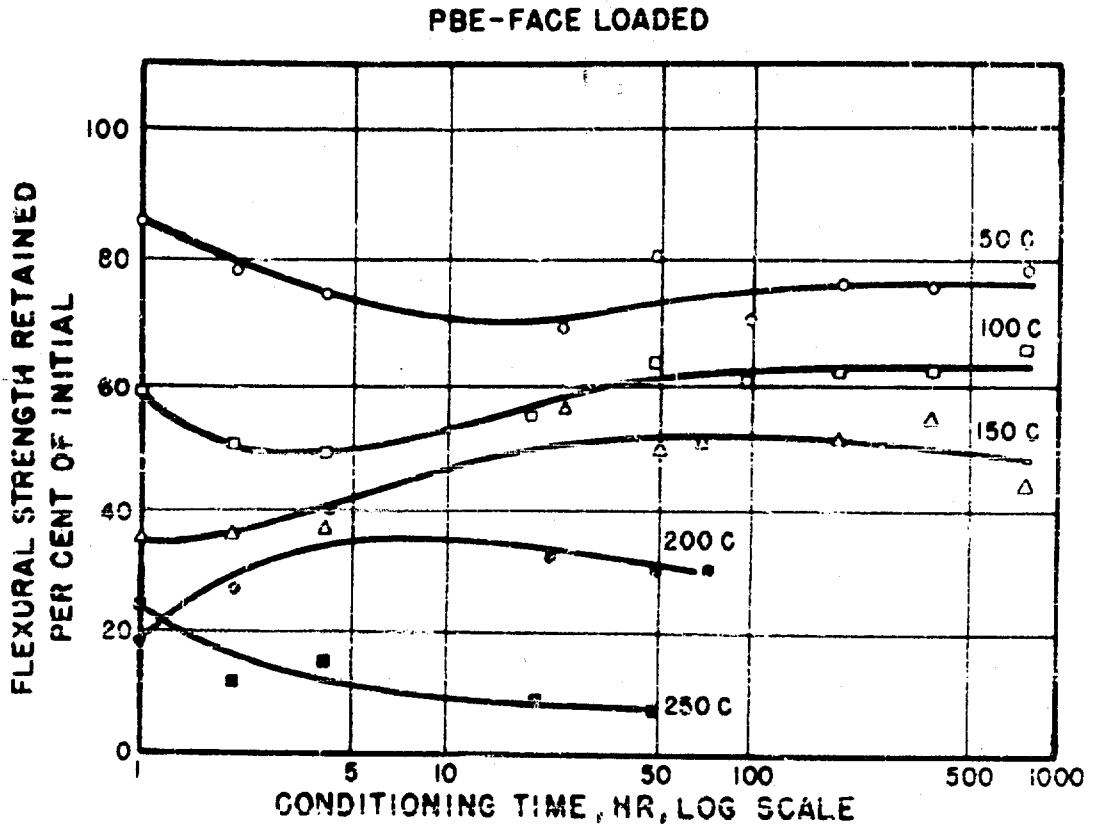

Figure 2 - Elevated temperature flexural strength vs time of exposure: Paper base phenolic laminate

A typical set of data, for a paper base phenolic laminate, is shown in Fig. 2, in which per cent of initial (room temperature) flexural strength retained is plotted against time of exposure at various temperatures. At 50°C the predominant factor is the "softening" effect, so that strength drops and levels off, although there is some slight evidence of recovery on prolonged heating. At 100°C, the softening is more marked but recovery, due to further cure is, quite evident. This is again noted at 150°C but, at this temperature prolonged heating begins to cause degradation. Degradation effects

are again noted at 200°C and these effects are so marked at 250°C as to mask any effects due to additional cure.

Analogous effects to those described above have been noted in studies of the electrical characteristics of thermosetting plastics at elevated temperatures (2); this work is discussed in another paper in this symposium.

As a result of these studies, the Bureau of Ships has established an elevated temperature strength retention requirement for heat resistant materials, which has been incorporated in a number of specifications (3, 4). It has been determined that, in general, conventional phenolic laminates (i.e., Navy Types PBE and FBG) may be employed at temperatures in the range of 100-150°C and glass-melamine (Navy Type GMG) materials in the range 150-200°C. Silicone materials generally show low strength characteristics after short time exposures but are inherently stable chemically at temperatures up to 250°C. Recently developed materials include phenolics with excellent heat resistance and glass-epoxy materials (Navy Type GEB), used for printed circuits, which may be operated as Class B insulation at temperatures up to 130°C.

WATER AND FUEL IMMERSION

The effects of moisture on plastic materials have been studied in a number of separate investigations, commencing with an evaluation of the characteristics of conventional high pressure thermosetting laminates after extended exposure to several different "wet" ambients. Electrical characteristics were determined under conditions of high humidity and after immersion in distilled water, and in synthetic sea water, at 25°C and 50°C, for periods up to 1,000 hr. Mechanical properties were studied after prolonged immersion in synthetic sea water and distilled water at 25°C and 50°C for periods up to 4,500 hr. In both instances the ability of the materials to "recover" by drying was also investigated. The laminates included in these investigations were paper and fabric base phenolics (Navy Types PBE and FBG), and glass base melamine and silicone (Navy Types GMG and GSG). Results are typified in Figs. 3 and 4 and listed, in part, in Tables 1 and 2. It was found (5) that there was no essential difference in effects on mechanical properties between immersion in sea water as against distilled water, nor did raising the temperature of the water to 50°C produce any substantial differences in effects. On the other hand, in studies of electrical characteristics, the effects of sea water, as might be expected, were much more severe than those caused by distilled water. Further, increasing the temperature of the immersion medium to 50°C also

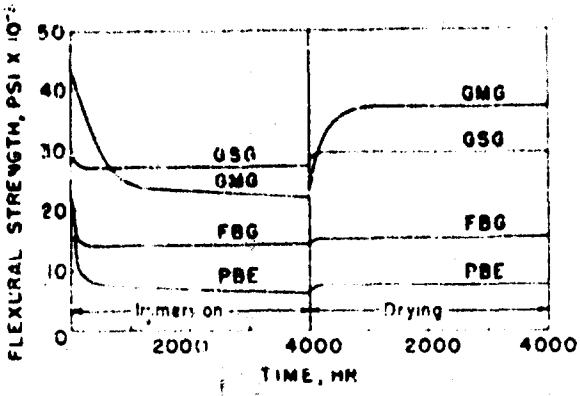

Figure 3 - Flexural strength (face loaded) vs time of immersion in sea water at 50°C and after subsequent drying

constituted a more severe condition, so that the most deleterious medium, with respect to electrical properties was synthetic sea water at 50°C. Of the four materials evaluated, the glass-silicone laminate was most resistant to degradation by humidity or water immersion, both mechanically and electrically. Further, this material showed excellent recovery of mechanical strength upon drying following immersion; however, recovery of electrical characteristics upon drying was limited. The phenolic laminates were most sensitive to water, suffering severe degradation in both mechanical and electrical properties on immersion.

The emergence of the low pressure laminates, such as the glass reinforced polyesters, as materials of construction for boat hulls and in similar applications, necessitated the development of information on the effects of extended sea water immersion on such materials. An investigation along these lines, which will extend over a five year period, is currently being conducted by the Naval Material Laboratory. Samples of polyester laminates, fabricated with five different typical reinforcement layups, are being immersed

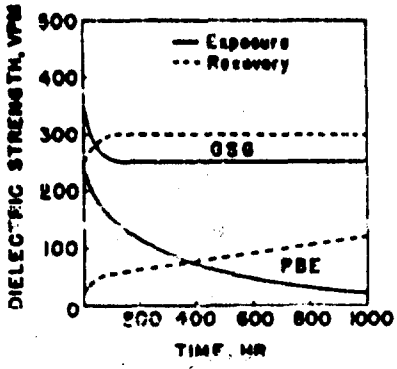

Figure 4 - Dielectric strength vs conditioning time at 96 percent RH, 50°C; recovery at 25°C, 50 percent RH. Glass - silicone and paper base phenolic laminates.

in sea water at the W. F. Clapp Laboratories exposure site at Wrightsville Beach, N. C. A group of samples is removed from the immersion site annually and shipped, under water, to the Material Laboratory for evaluation. Tests are conducted on samples in the wet condition and after drying. Four year immersion data are shown in Table 3 (6). In interpreting immersion data, due consideration should be given to resin content, since experience has shown that for a given reinforcement, laminates with too low a resin content are susceptible to degradation by water. Results to date indicate that the laminate with the fine weave-improved finish glass cloth reinforcement (Style 181) is most resistant to deterioration by

TABLE 1

Strength Retention of Plastic Laminates After Immersion and on Recovery[a]

Laminate (Navy Type)	A. Per cent of initial flexural strength retained			
	Face Loaded		Edge Loaded	
	Immersion	Recovery	Immersion	Recovery
PBE	30	40	65	85
FBG	70	75	75	75
GMG	50	80	50	80
GSG	85	100	85	90

Laminate (Navy Type)	B. Per cent of initial compressive strength ret'd			
	Face Loaded		Edge Loaded	
	Immersion	Recovery	Immersion	Recovery
PBE	45	80	40	75
FBG	80	90	70	85
GMG	80	80	50	70

[a]Immersion - Average per cent of initial strength retained after immersion for 4500 hr.
Recovery - Average per cent of initial strength retained after extended drying for 4500 hr. preceded by 4500 hr. of immersion in distilled water at 25°C.

TABLE 2

Dielectric Properties of Plastic Laminates After Immersion and on Recovery[a]

Laminate (Navy Type)	Per cent of initial dielectric strength retained[b]	
	Immersion	Recovery
PBE	15	85
FBG	8	79
GMG	11	93
GSG	43	61

[a]Immersion - Immersion in water at 25°C - 1000 hr.
Recovery - Drying 1000 hr. following immersion.
[b]Dielectric strength parallel to forming pressure, volts/mil (S/S).

TABLE 3

Immersion of Polyester - Glass Laminates

Property	Condition[b]	Laminate[a] 181 Cloth	1,000 Cloth	Mat	Woven Roving
Flexural Strength, psi x 10^{-3}	A	45.1	35.0	29.2	28.8
	1 yr S.W.	50.4	34.9	23.6	22.9
	2 yr S.W.	49.3	32.7	21.5	24.4
	3 yr S.W.	52.4	31.9	22.6	23.0
	4 yr S.W.	45.1	28.1	20.5	22.1
	4 yr S.W. & Dry	49.3	32.0	20.0	26.3
Compressive Strength, psi x 10^{-3}	A	37.4	26.9	27.3	20.8
	1 yr S.W.	33.9	21.2	18.8	12.3
	2 yr S.W.	35.2	19.4	18.1	12.4
	3 yr S.W.	29.7	17.2	17.0	11.0
	4 yr S.W.	26.0	17.0	17.7	11.9
Resin Content, % by wt	A	58.1	44.7	72.6	50.5

[a] 181 - Garan glass cloth.
1,000 - Volan glass cloth.
1 1/2 oz - Garan glass mat, high solubility binder.
Garan finished woven roving, 5 x 4, 24 oz.

[b] A - Reference condition.
S.W. - Sea water immersion
S.W. & Dry - Sea water immersion plus 4 week drying.

water immersion; the coarse woven roving reinforcement produces a laminate which is most water sensitive. While flexural properties of the laminates are adversely affected by immersion, edge compressive properties are degraded to a greater extent. Significantly, it has been found that specimens cut from internal areas of an immersed sample are no less adversely affected than are specimens taken from the edge of a sample, indicating that water does not enter exclusively at the edges of a laminate but diffuses through all surfaces.

The projected application of reinforced plastics in the fabrication of fuel tanks necessitated a study of the effects of the more common fuels on such materials. Investigation has shown that polyester and epoxy laminates which are properly fabricated

and cured are essentially unaffected by immersion in diesel fuel or jet fuels such as JP-5.

As an adjunct to the above, it was also necessary to determine whether the reinforced plastic materials had any deleterious effects on stored fuels. Such an investigation has been conducted at USNEES, Annapolis on a number of sample laminates submitted by the Naval Material Laboratory. This group of materials included glass reinforced polyester and epoxy laminates fabricated with several different resin systems, under different curing conditions, by a number of different techniques. Materials were evaluated by immersing sample strips in aviation gasoline, JP-4 jet engine fuel, marine diesel fuel, and Navy Special fuel for 6 months at 110°F, and noting permeability (as measured by gain in weight) and tendency to increase gum content of aviation gasoline. Results indicated (7) that glass reinforced polyester and epoxy laminates can be produced which are impermeable to fuels and which do not significantly increase the gum content of aviation gasoline. On the other hand, the data indicated that not all polyester resins are inert, i.e. certain resin systems have a tendency to increase gum content of aviation fuels. Furthermore, undercured polyester resins may also be expected to have a similar effect. In the case of epoxy-resins, different amine hardeners may not be equally inert and there is some evidence to indicate that excessive hardener concentration may have deleterious effects.

OUTDOOR WEATHER AGING

The most common, and perhaps the most important, of the conditions which may affect the serviceability of plastics is outdoor exposure. Weathering investigations to determine such effects are most extensive, not only for plastics, but for materials of construction in general. Some years ago the Naval Material Laboratory undertook a program to study the effects of outdoor weather aging on a number of thermoplastic and thermosetting transparent materials and several representative plastic laminates. In order to obtain a representation of the different climatological conditions to which such materials might be exposed, five exposure sites were selected, as follows: Panama, C. Z. (tropical), New York (temperate), New Mexico (dry, desert), Fort Churchill, Can. (sub-arctic), and Pt. Barrow, Alaska (arctic).

The original program ran for three years, during which period samples were removed from exposure sites at intervals and shipped to the Naval Material Laboratory for evaluation of mechanical, electrical, and optical properties. Results are summarized,

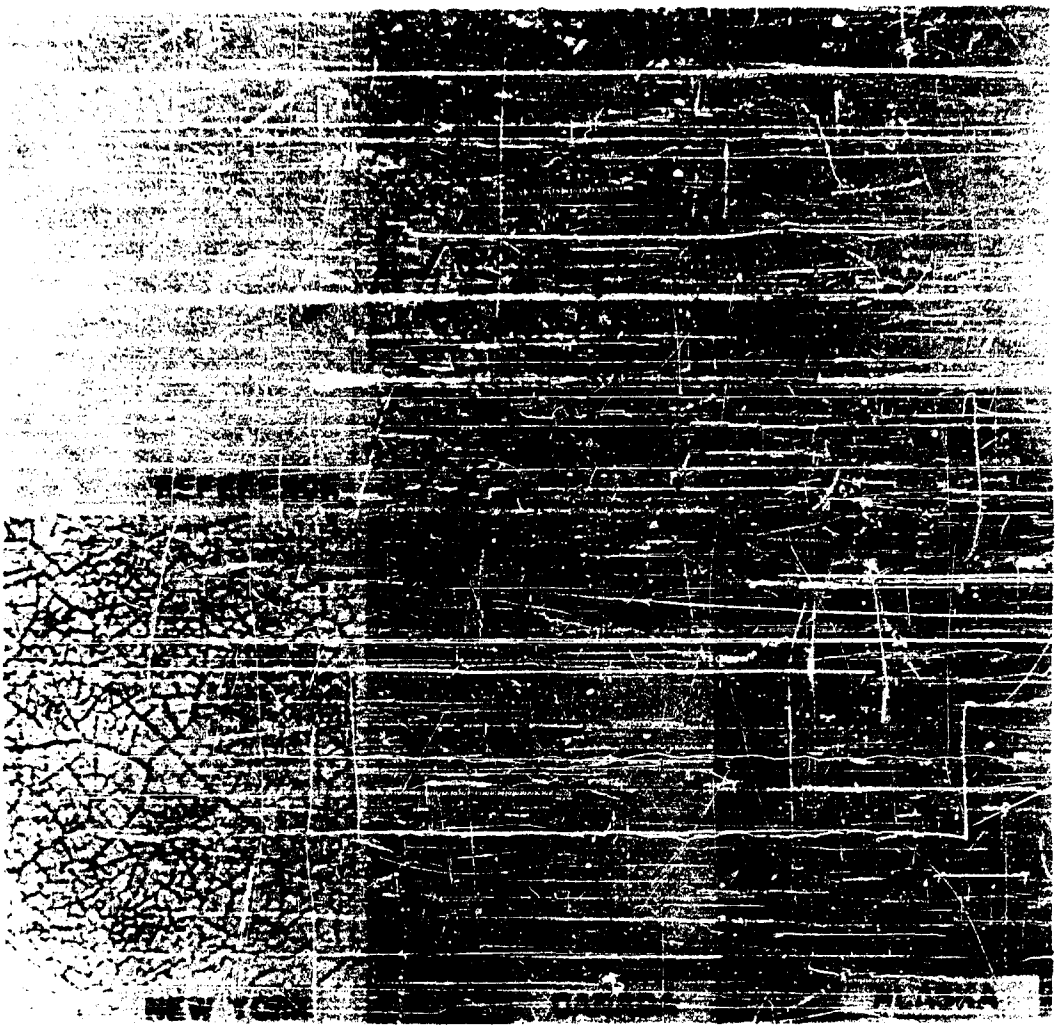

Figure 5 - Cast phenolic exposed at various sites for 3 years

qualitatively, in Table 4. In essence, it was found (8) that, of the transparent materials tested, methyl methacrylate and cast allyl were relatively unaffected; the laminated materials were mechanically stable but showed some surface erosion and degradation in electrical properties. These materials most sensitive to light, such as the vinyl copolymer, were seriously degraded at New Mexico, which climate otherwise proved relatively mild. It is interesting to note, also, that the Canada and Alaska sites were most deleterious to electrical characteristics of laminated insulating materials. On

Figure 6 - Cast phenolic exposed at New York for periods up to 2 years

TABLE 4

Summary of Effects of Three Year Weather Aging on Plastic Materials

Material	Mechanical	Electrical	Optical
Methyl Methacrylate	Negligible effects all sites	Slight effects	Slight yellowing at Pan. and N.M.
Cellulose Acetate	Severe degradation at N.Y.; lesser degradation at Pan.	Slight effects	Parallel mechanical effects
Cast Allyl	Slight effects all sites	Slight effects	Slight yellowing Pan. and N.M.; Haze 7% at N.Y.
Vinyl	Moderate degradation, at Pan. and N.M.	Slight effects	Severe darkening at Pan. and N.M.; marked darkening other sites
Cast Phenolic	Degradation at all sites, most severe at N.Y. and Pan.	Degraded at N.Y. and Pan.; slightly improved at N.M.	Severe degradation N.Y. and Pan. marked yellowing at all sites
Polyester-Glass Laminate	Slight degradation all sites	General moderate degradation, most severe at Can. and Alaska	---
GMG	Slight effects	Degradation at Can. and Alaska	---
PBE	Slight effects	Degradation at Can. and Alaska	---
FBG	Slight effects	Degradation at Can. and Alaska	---
GSG	Slight effects	Degradation at Can. and Alaska	---

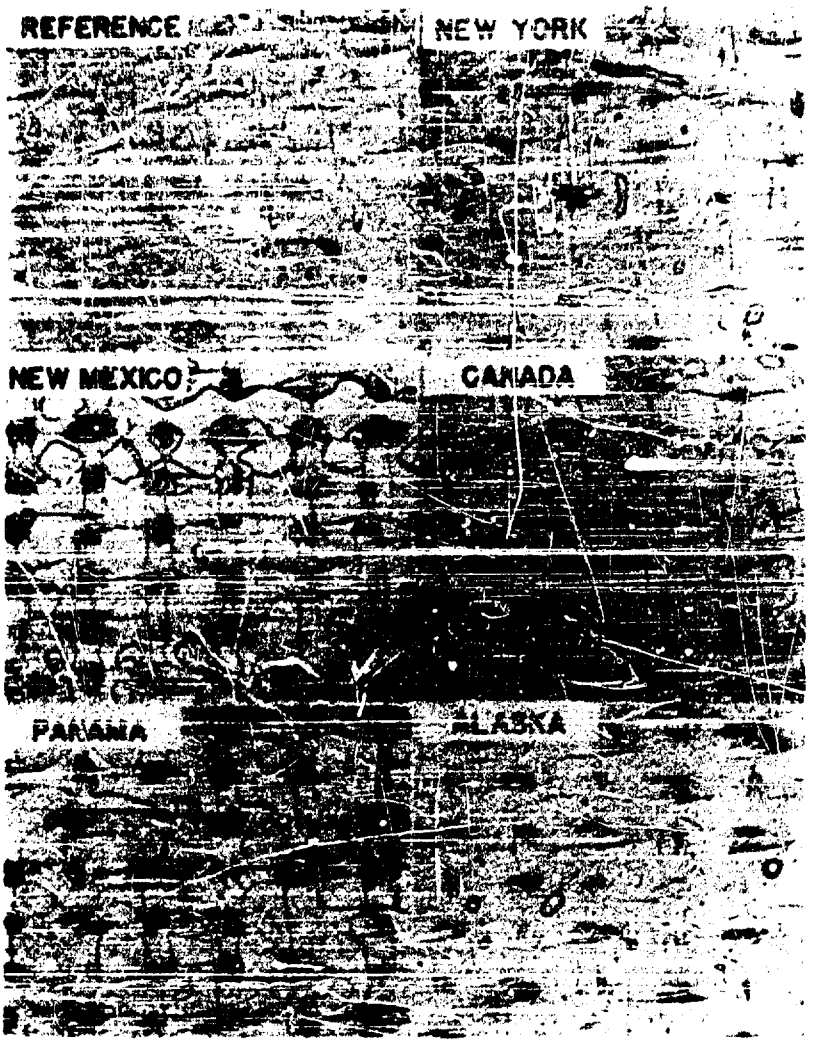

Figure 7 - Melamine-glass laminate exposed at various sites for 2 years

an overall basis, the New York climatological conditions were quite severe, reflecting the combined effects of a seaboard location and an industrial atmosphere.

Upon completion of the 3 year program it was decided to extend the duration of the test period to ten years at one site, New York, using serviceable material which had been exposed in the original program. Six year data indicate that methyl methacrylate and cast allyl continue to be relatively unaffected while the

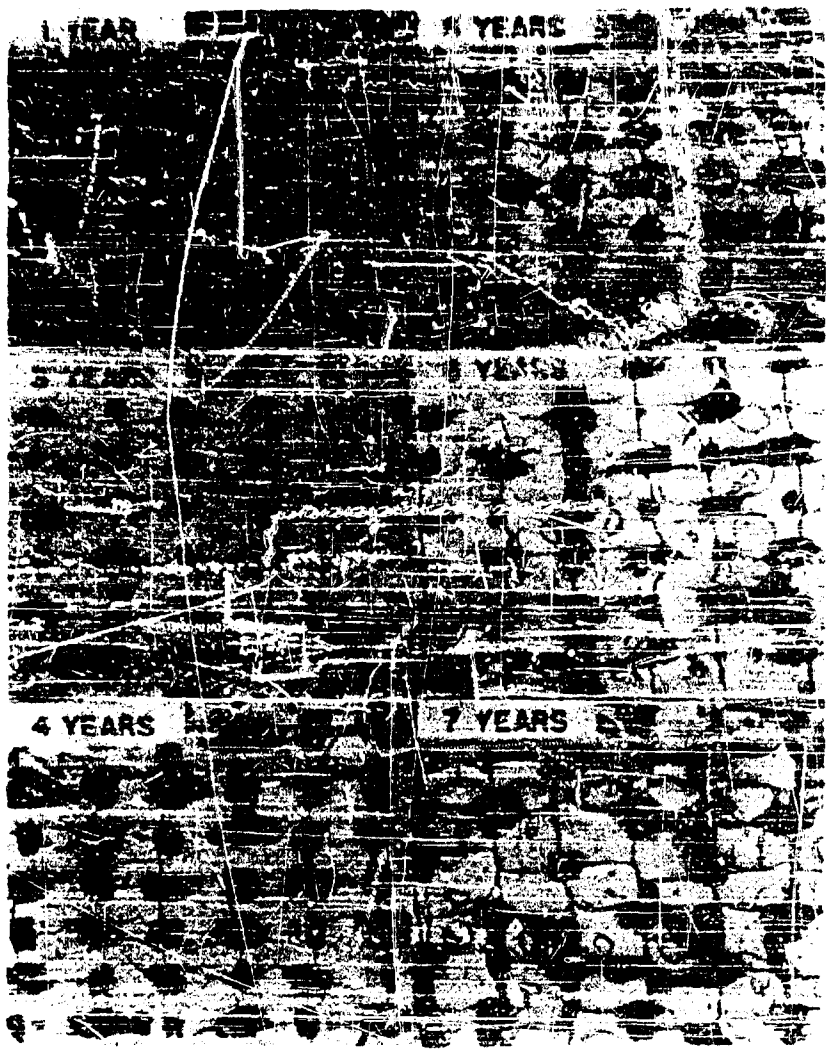

Figure 8 - Melamine-glass laminate exposed at New York for periods up to 7 years

sensitive cellulose acetate, vinyl, and cast phenolic materials have degraded further; all of the laminated materials show further erosion of surface resin. Surface effects are shown in the photomicrographs, Figs. 5 through 8.

NEW PROGRAMS

At present, the Naval Material Laboratory is scheduling a new weathering investigation, with emphasis on reinforced plastics including both polyester and epoxy laminates fabricated with various

glass reinforcements, and incorporating a study of the effects of a number of fabricational variables. Also included in this program will be such newly developed materials as Lexan and Delrin.

In addition to the above projected program, there is in the planning stage at the Laboratory a program for studying the erosive effects on glass reinforced plastics of water flowing over the laminate surfaces at velocities up to 100 ft/sec. For this investigation a simulative test is being devised and an attempt will be made to develop an accelerated procedure.

Considering the investigations described above, and similar work performed by many other laboratories, it is still difficult to arrive at any broad generalizations with regard to environmental effects on plastic materials. The development of information on the behavior of a material under one set of conditions will not, in general, enable the prediction of behavior under other conditions, particularly if the conditions are widely different or a new environmental factor is added. It may therefore be predicted that, as new plastics are developed and as presently available materials are extended to new applications, investigations of the type described above will continue to be required, at least until such time as the fundamental physical chemistry of materials has been completely defined.

REFERENCES

(1) M. Fried, R. R. Winans and L. E. Sieffert; Proceedings, Am. Soc. Testing Matls; V 50, 1383 (1950)

(2) R. R. Winans and W. Hand; Am. Soc. Testing Matls Special Technical Publication No. 161, 1954

(3) Specification MIL-M-14E, as Amended 20 September 1957

(4) Specification MIL-P-18177B, 31 March 1958

(5) R. R. Winans, M. Fried, and W. Hand; Elec. Manuf., July 1955, p 106

(6) P. M. Goldfarb; MATLAB NAVSHIPYDNYK Project 4860-J-4, Progress Report 5, 18 September 1958

(7) R. L. Walsh; USNEES R & D Report 070357B, 15 March 1957

(8) S. E. Yustein, R. R. Winans, and H. J. Stark; Am. Soc. Testing Matls Bull. No. 196, 29 (1954)

A Discussion of Some of the Problems of Thermoelectric Efficiency and Coefficient of Performance

William H. Lucke
U. S. Naval Research Laboratory
Washington 25, D. C.

INTRODUCTION

Any discussion of the analysis of thermoelectric devices necessarily involves the use of the terms which describe quantitatively the phenomena or properties of interest. Accordingly, we introduce our discussion by defining the pertinent terms and presenting the symbols we shall use to represent them.

$\mathcal{E}$ Seebeck Voltage. - The open circuit voltage of a thermocouple supporting a temperature difference.

$\alpha = \frac{d\mathcal{E}}{dT}$ Thermoelectric Power. - The derivative of the Seebeck voltage with respect to absolute temperature. Since two materials are necessary to form a thermocouple α necessarily depends on both. However, it is possible to determine the α for a single material by making measurements of its Thomson coefficient and using the first Kelvin relation. Such an α is called "absolute." The determination of absolute α's for various metals has been carried out by Borelius (1) and others.

π Peltier Coefficient. - The product of π and the electric current through junction of two dissimilar materials gives the rate at which Peltier heat is absorbed or evolved at the junction.

τ The Thomson Coefficient. - The product of τ, the current I, and the temperature gradient dT/ dX gives the rate at which Thomson heat is absorbed or evolved in a length dX of a thermocouple element. We shall in this paper also make use of the magnitude of the Thomson coefficient, writing the sign explicitly. For this purpose, it is convenient to use the symbol $\mathcal{T}$ where $\mathcal{T} = |\tau|$

z The Figure of Merit. - An approximate calculation of generator efficiency leads directly to z. We suppose that the generator consisting of the two elements a and b, is working into a matched load, hence the power out is

$$P_0 = i^2 R_L = \frac{\mathcal{E}^2}{4R}$$

where R is the resistance of the couple and is the sum of R_a and R_b, the electrical resistances of the elements.

Now $\mathcal{E}$ may be equated to $\bar{\alpha}(T_h - T_c)$ where $\bar{\alpha}$ is an average or effective α such that

$$\bar{\alpha}(T_h - T_c) = \int_{T_c}^{T_h} \alpha \, dT \qquad (1)$$

where T_h is the absolute temperature of the hot junction, and T_c that of the cold. Hence, we may write

$$P_0 = \frac{\bar{\alpha}^2 (T_h - T_c)^2}{4R}$$

The power into the couple is applied as heat flow. This heat flow is composed of the sum of several terms of which the heat converted to electricity is one, but the larges term by far is that of the conducted heat. Ignoring the others, the power in is

$$\dot{Q}_{in} = K(T_h - T_c)$$

where $K = K_a + K_b$, the sum of the thermal conductances of the elements.

Thus, the efficiency, η, is

$$\eta = \frac{\bar{\alpha}^2 (T_h - T_c)^2}{4RK\,(T_h - T_c)}$$

$$= \frac{T_h - T_c}{T_h} \times \frac{T_h}{4} \times \frac{\bar{\sigma}^2}{RK} \qquad (2)$$

It is easily shown that the optimum geometric proportioning of the two legs leads to (2)

$$RK = \left[\sqrt{P_a k_a} + \sqrt{P_b k_b}\right]^2$$

where ρ and k stand for the electrical resistivity and thermal conductivity respectively. Moreover, in this case

$$\frac{R_a}{R_b} = \frac{K_a}{K_b} = \sqrt{\frac{\rho_a k_a}{\rho_b k_b}}$$

Thus, the figure of merit z is defined for a couple as

$$z = \frac{\bar{\alpha}^2}{\left[\sqrt{\rho_a k_a} + \sqrt{\rho_b k_b}\right]^2}$$

There is no easy way of breaking this down into a z for each element. However, if one makes use of the fact that the highest thermoelectric powers are achieved by a combination of N and P-type semiconductors, in which case the absolute α's are added, z becomes

$$a = \frac{(\alpha_a + \alpha_b)^2}{\left[\sqrt{\rho_a k_a} + \sqrt{\rho_b k_b}\right]^2}$$

Clearly, if the α's of each material are each made as large as possible, and the products of ρk as small as possible, z will be as large as possible. Hence, it is commonly accepted practice to speak of the z of a material and to write it $z_a = \frac{\alpha_a^2}{\rho_a k_a}$

We have written equation (2) so that a Carnot efficiency term is explicit. From the point of view that it is profitable to compare the efficiency of any thermal engine with that of a Carnot engine, this is justified. However, the implication that the maximum theoretical efficiency of a thermocouple is Carnot is not in general justifiable as we shall see presently.

THOMSON HEAT

Of the terms so far discussed, there is the greatest confusion concerning the Thomson heat. Text book definitions of it are generally vague and confused, and give little aid to the designer of a generator or refrigerator. There is even confusion concerning the proper sign to be used in relating it to the derivative of the thermoelectric power, i.e., the first Kelvin relation

$$\frac{\tau}{T} = -\frac{d\lambda}{dT}$$

One of the primary objectives of this paper is to clarify this situation by showing how the magnitude of Thomson heat may easily be calculated, and what its role is in the calculation of efficiency.

Thomson Heat For P-Type Materials

Instead of writing the Seebeck voltage of a circuit in the usual way as the sum of the Peltier and Thomson voltages, i.e.,

$$\mathcal{E} = \pi(T_h) - \pi(T_c) + \int_{T_c}^{T_h} \tau \, dT$$

we begin with the fact of the definition of λ as the temperature derivative of $\mathcal{E}$, hence

$$\mathcal{E} = \int \lambda \, dT + \text{const.}$$

For convenience, we shall assume that we are dealing with a thermocouple composed of a P-type semiconductor as one element and an ideal reference substance having no thermoelectric activity as the other. (Strictly, this reference substance would have to be a metal in a superconducting state. However, copper approximates

to our ideal quite well at ordinary temperatures, having a thermoelectric power of a few microvolts per degree (1), whereas our P-type material may have an α of a few hundred microvolts per degree.) Suppose that an experimental plot of the thermoelectric power of this couple (which is really a plot of the absolute thermoelectric power of the P-type material) is as shown in Figure 1 by the segment x - y.

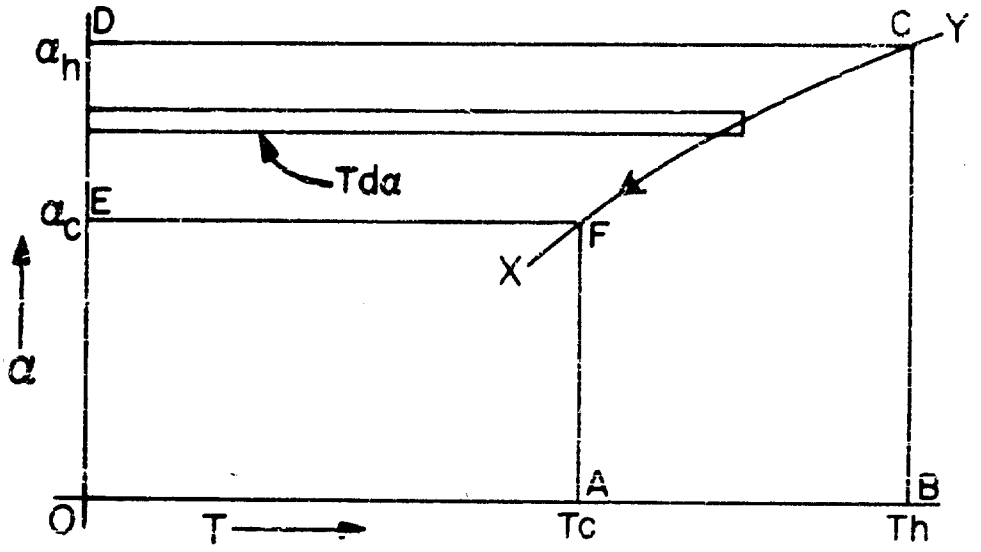

Figure 1. The α Characteristic of Type I Material.

Therefore, we have

$$\mathcal{E} = \int_{T_c}^{T_h} \alpha_P \, dT$$

Integrating by parts we get $\mathcal{E} = \left[\alpha_P T\right]_{T_c}^{T_h} - \int_{\alpha_c}^{\alpha_h} T \, d\alpha_P$

$$\mathcal{E} = \alpha_{Ph} T_h - \alpha_{Pc} T_c - \int_{\alpha_c}^{\alpha_h} T d\alpha_P$$

We see that the first term is the area $\overline{OBCDO}$. This area represents the Peltier voltage at the hot junction since, by the second Kelvin relation, $\pi = \alpha T$. $\alpha_{Pc} T_c$ is the area $\overline{OAFEO}$, and represents the Peltier voltage at the cold junction. Finally, examining the integral term we see that $Td\alpha P$ is the element of area of the area $\overline{EFCDE}$ and that the integral itself gives the total area. That this integral represents the Thomson voltage can be seen by transforming it to integration with respect to T.

$$\int_{\alpha_{Pc}}^{\alpha_{Ph}} T d\alpha_P = \int_{T_c}^{T_h} T \frac{d\alpha_P}{dT} dT = \int_{T_c}^{T_h} -\tau \, dT$$

The last equality holds by virtue of the first Kelvin relation. Therefore, we may write

$$\mathcal{E} = \alpha_h T_h - \alpha_c T_c - \int_{T_c}^{T_h} T \frac{d\alpha}{dT} dT$$

and the magnitude of each of the terms is clearly seen by referring to Figure 1.

It will be seen from this that Joffe's use of an average or effective α such that

$$\mathcal{E} = \bar{\alpha}(T_h - T_c) = \overline{ABCFA}$$

is justifiable and quite useful, but that his policy of ignoring the Thomson voltage is not. Since the area representing the Thomson term extends back to the absolute zero of temperature, it does not take a large difference between the α_h and α_c to produce a voltage quite comparable to the net voltage.

It is seen from the figure that the Peltier voltage at the hot junction, $\overline{OBCDO}$, is equal to the voltage generated, $\overline{ABCFA}$, plus the Peltier voltage of the cold junction $\overline{OAFEO}$ plus the Thomson voltage $\overline{EFCDE}$.

Now if we multiply the equation for $\mathcal{E}$ by I we have

$$\mathcal{E}I = I\,\alpha_{Ph}T_h - I\,\alpha_{Pc}T_c - I\int_{T_c}^{T_h} T\,\frac{d\alpha}{dT}\,dT$$

The term on the left is power generated, and the terms on the right represent rates of absorption or rejection of heat. This can be done graphically by multiplying all the ordinates of Figure 1 by I. Thus

$$I \times \overline{OBCDO} = I \times \overline{ABCFA} + I \times \overline{OAFEO} + I \times \overline{EFCDE}$$

$$I \times \alpha_{Ph}T_h = I \times \mathcal{E} + I \times \alpha_{Pc}T_c + I \times \int_{T_c}^{T_h} T\,\frac{d\alpha}{dT}\,dT$$

Clearly, since $I\alpha_{Pc}T_c$ represents the Peltier heat rejected at the cold junction, the Thomson heat term, having the same sign, also represents heat rejected. We see, moreover, that this Thomson heat was originally absorbed at the hot junction as Peltier heat.

Now the direction of conventional current in a thermoelectric generator such as we have assumed is down the temperature gradient in the P-element (the direction from C to F in Figure 1). In other words, for P-type material with $d\alpha/dT > 0$ and current flow down the gradient Thomson heat is rejected. We shall designate this as a type I element.

In Figure 2 we represent an experimental plot of a thermocouple similar to the first, except that the slope is negative. We designate this a type II element. (See next page.)

Here again, the areas represent voltages and the product of areas by current, power, or heat flow.

$$I\,\mathcal{E} = I \times \overline{ABCDA}$$

$$I\,\alpha_h T_h = I \times \overline{OBCFO}$$

$$I\,\alpha_c T_c = I \times \overline{OADEO}$$

$$\text{Thomson heat} = I\int_{T_c}^{T_h} \mathcal{T}_P\,dT = I \times \overline{FCDEF}$$

and

$$\mathcal{E} = \alpha_h T_h - \alpha_c T_c + \int_{T_c}^{T_h} T \left| \frac{d\alpha}{dT} \right| dT.$$

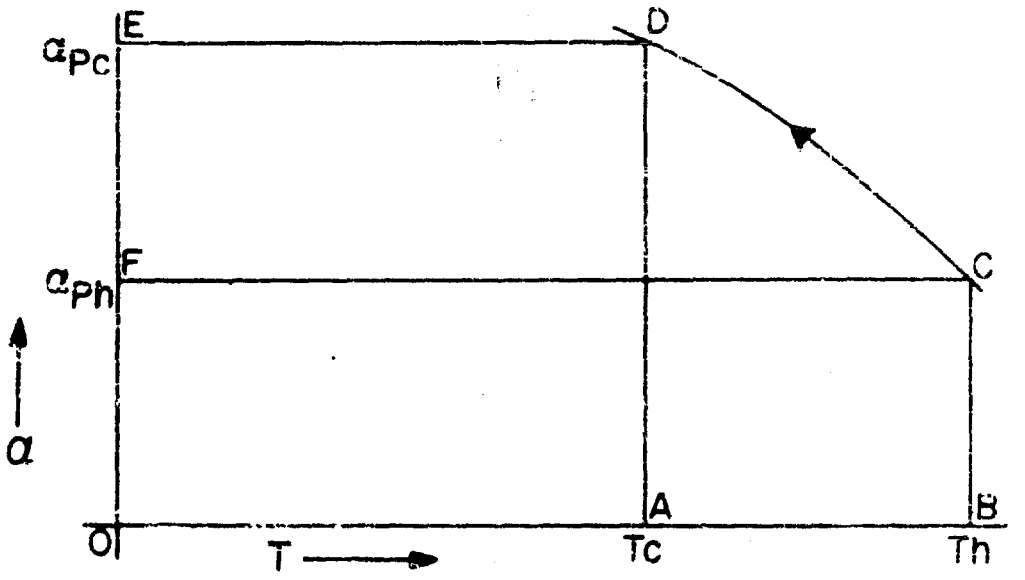

Figure 2. The α Characteristic of a Type II Material.

The total rate of heat absorption is given by the area I x $\overline{OBCDEO}$ (the sum of the Thomson and hot junction Peltier heats). Subtraction of the cold junction Peltier heat I x $\overline{OADEO}$, leaves the area I x $\overline{ABCDA}$, which is just the electrical power generated. Thus, Thomson heat is absorbed when current flows down the gradient in a P-type element, with $d\alpha/dT < 0$.

As Thomson originally envisaged it, this heat was absorbed through the lateral surfaces of the element. However, in present

generator practice these surfaces are thermally insulated and the question arises as to the source of this Thomson heat. An approximate solution, correct to within about 2%, of the heat conduction equation of an element, shows that half of the Thomson heat flows directly from the hot junction and that the other half is abstracted from the ordinary conducted heat. (This will be discussed in greater detail further on.)

Thomson Heat for N-Type Materials

N-type elements may be analyzed in the same way as the P-types. The figure for type III materials may be obtained by a reflection of Figure 1 in the T axis since the absolute thermoelectric power of N-type materials is negative. Such a reflection changes the sign of the slope (i.e., $d\alpha/dt < 0$). However, in an N-element used in a generator, current flow is up the temperature gradient from F' to C', thus the negative slope combines with the reversal of current to give rejection of Thomson heat. The same argument holds for type IV materials, i.e., reflection of a type II characteristic gives a positive slope, but again the current flow is reversed so that absorption of Thomson heat occurs.

The case of both P and N-type materials in which a maximum or minimum of α occurs between the temperatures T_h and T_c can also be handled by the present analysis, but we shall not discuss it here.

It is worth pointing out that the present analysis is quite practical. It requires only an experimental plot of the absolute thermoelectric power of an element which can easily be obtained by using copper as the reference since values of the absolute thermoelectric power of copper have been published. (1). The areas representing generated voltage, hot and cold junction Peltier heats and Thomson heat can then be found graphically.

Combination of P and N-Type Materials

We suppose now that we have a thermoelectric generator composed of a type I P-element and a type IV N-element. The characteristic is shown in Figure 3. (See next page.) Clearly, the total voltage generated is the sum of the individual voltages

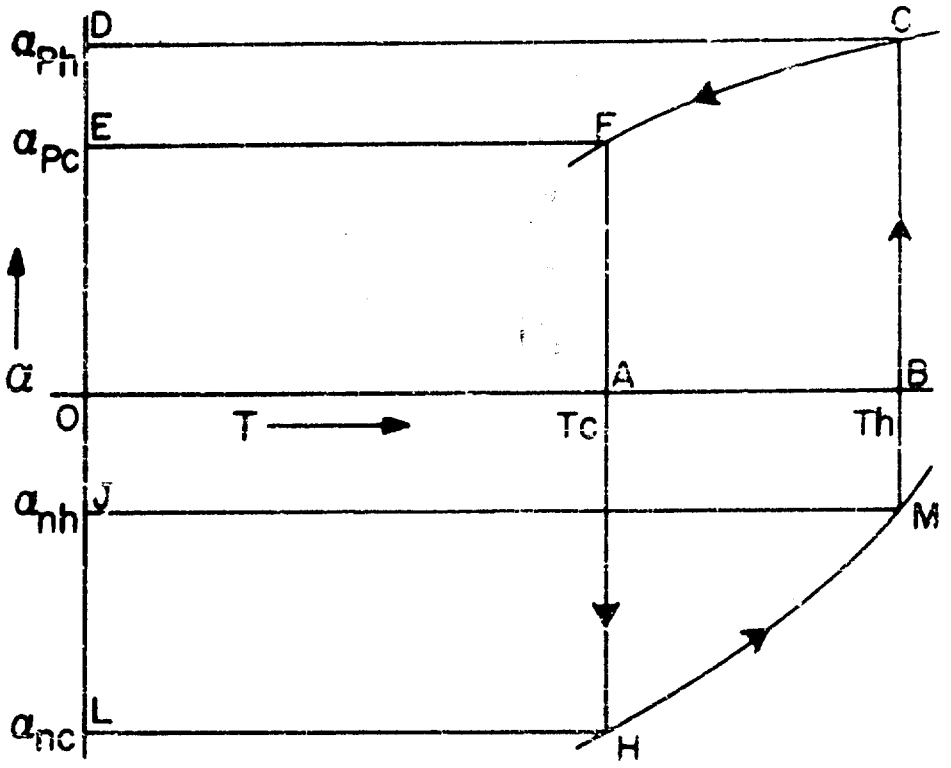

Figure 3. The Characteristics of a Generator Composed of Type I and IV Elements. (Arrows indicate conventional current flow.)

or the area $\overline{HMCFH}$. The total Peltier heat absorbed at the hot junction is given by the product of the current and the area $\overline{JMCDJ}$. The Peltier heat rejected at the cold junction is the current times the area $\overline{LHFEL}$. The net Thomson voltage is a positive term being the difference between the areas $\overline{LHMJL}$ AND $\overline{EFCDE}$, i.e., Thomson heat is rejected by the P-element and absorbed by the N-element. The absorbed Thomson heat is greater than the rejected Thomson heat in this hypothetical case.

Thus, the total heat absorbed is

$$I \times \overline{JMCDJ} + I \times \overline{LHMJL} = I \alpha_h T_h + I \times \int_{T_c}^{T_h} \tilde{\tau}_m \, dT \quad (3)$$

The total heat rejected is

$$I \times \overline{LHFEL} + I \times \overline{EFCDE} = I \times \alpha_c T_c + I \times \int_{T_c}^{T_h} \mathcal{F} P dT \quad (4)$$

EFFICIENCY

We are now in a position to write the expression for the reversible or theoretical efficiency for the case of Figure 3. Using the expression

$$\text{Efficiency} = \eta = \frac{Q_{in} - Q_{out}}{Q_{in}}$$

and substituting from equations (3) and (4) above

$$\eta = \frac{I\left(\alpha_h T_h + \int_{T_c}^{T_h} \mathcal{F}_n dT\right) - I\left(\alpha_c T_c + \int_{T_c}^{T_h} \mathcal{F} P dT\right)}{I\left(\alpha_h T_h + \int_{T_c}^{T_h} \mathcal{F} n dT\right)}$$

$$= \frac{\alpha_h T_h - \alpha_c T_c + \int_{T_c}^{T_h} \mathcal{F} n dT - \int_{T_c}^{T_h} \mathcal{F} P dT}{\alpha_h T_h + \int_{T_c}^{T_h} \mathcal{F} n dT}$$

It is seen at once that this is not Carnot efficiency. Carnot efficiency will be achieved only when $\mathcal{F}_n = \mathcal{F}_P = 0$ (in which case, $\alpha_h = \alpha_c = \alpha$). That is

$$\eta_c = \frac{\alpha T_h - \alpha T_c}{\alpha T_h} = \frac{T_h - T_c}{T_h} .$$

This leads at once to the important conclusion that to achieve the highest efficiencies materials must be sought having negligible

Thomson coefficients in the operating range.

Conversevly, higher efficiencies may be obtained by limiting the operating range of temperature to that part of the $\mathcal{S}$ characteristic having the smallest Thomson coefficient. In such a case, increasing the temperature difference, $T_h - T_c$, may, by including a region of high $\mathcal{T}$, lead to a lower efficiency than is obtainable with a smaller value of $T_h - T_c$.

As a corollary it may be shown that setting the operating range equally above and below a maximum (or minimum) in the characteristic so that $\mathcal{S}_h = \mathcal{S}_c$ but the $\mathcal{T}$'s are not zero still does not give Carnot efficiency. Practically, however, this will usually confine us to a region of small $\mathcal{T}$ so that the best efficiencies may be realized.

Refrigeration

The same hypothetical thermocouple whose characteristic is diagramed in Figure 3 may be used as a refrigerator. In this case, the current is reversed, i.e., flow is clockwise.

Since the currents are reversed, heat absorption and rejection are reversed. The Peltier heat absorbed at the cold junction $\mathcal{S}_c T_c$ is now given by the product of I and the area $\overline{LHFEL}$. The Peltier heat rejected at the hot junction, $\mathcal{S}_h T_h$, is I times the area $\overline{JMCDJ}$. Thomson heat,

$$I\int_{T_c}^{T_h} \mathcal{T}_P dT,$$

is absorbed by the P-element in the amount I times $\overline{EFCDE}$ and the Thomson heat,

$$I\int_{T_c}^{T_h} \mathcal{T}_n dT,$$

rejected by the N-element is I times the area $\overline{LHMJL}$. The voltage against which the current source works is given by the area $\overline{HMCFH}$.

Here again the question is raised: What happens to the Thomson heat absorbed or rejected in a laterally insulated element? The answer is the same as before. To a good approximation, half the Thomson heat absorbed (in the P-element) is taken from the cold

junction and half the heat rejected (from the N-element) goes to the cold junction.

The reversible or theoretical coefficient of performance (COP) is

$$COP = \frac{\overline{LHFEL} + \overline{EFCDE}}{\overline{HMCFH}}$$

or in terms of Thomson and Peltier heats,

$$COP = \frac{\alpha_c T_c + \int_{T_c}^{T_c} \mathcal{T}_P dT}{\alpha_h T_h + \int_{T_c}^{T_h} \mathcal{T}_n dT - \alpha_c T_c - \int_{T_c}^{T_h} \mathcal{T}_P dT}$$

Here again, if $\mathcal{T}_P = \mathcal{T}_n = 0$ (so that $\alpha_h = \alpha_c = \alpha$)

$$\omega = \frac{\alpha T_c}{\alpha T_h - \alpha T_c} = \frac{T_c}{T_h - T_c}$$

and a Carnot coefficient of performance is achieved for this special case. In this connection, it is interesting to note that if a couple were constructed of type II and IV materials so that both the P-element and the N-element reject Thomson heat and α_h is very much smaller than α_c, a theoretical coefficient of performance greater than Carnot can be demonstrated. (See Figure 4 on next page.)

That is, $COP = \frac{\overline{FCDEF}}{\overline{CHDGC}}$

The COP for a Carnot refrigerator would be given by the ratio

$$\frac{\overline{FCDEF}}{\overline{CABDC}}$$

which is clearly smaller. However, we realize that since Thomson heat is rejected at temperatures less than T_h we are effectively

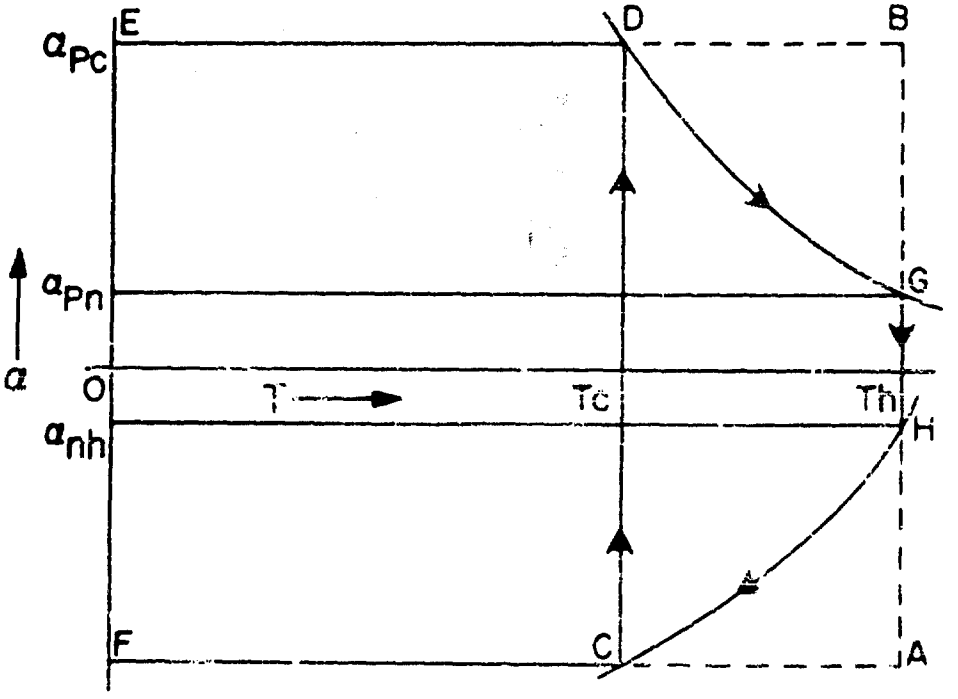

Figure 4. Refrigerator Using Type II and IV Materials. (Dotted lines indicate the Carnot cycle which would have the same refrigerating capacity.)

cooling by a lesser amount than the Carnot which rejects all its heat at T_h. Hence, the larger apparent COP is not surprising.

Heat Pump

The analysis of the heat pump proceeds quite similarly to that of the refrigerator, hence we shall not undertake to discuss it here.

Thomson Heat and Practical Efficiency

The calculation of practical efficiencies involves the

inclusion of the irreversible processes of heat conduction and Joulean heating. The calculation of heat conduction involves a knowledge of the thermal gradient. Unfortunately, our boundary conditions are known only in terms of the operating temperatures T_h and T_c, hence we must solve the heat conduction equation to get the temperature T as a function of the spatial coordinates and then differentiate to get the gradient. In this calculation we visualize the thermocouple element as cylindrical, taking the axis of the cylinder as the x-axis, and assuming that current flow and temperature distribution are independent of the y and z axes. In the most general case, the thermal conductivity, k, the Thomson coefficient $\mathcal{T}$ and the electrical resistivity, ρ, are all functions of the absolute temperature T and the heat conduction equation is

$$\frac{d}{dx}\left[k(T)\frac{dT}{dx}\right] \pm J\,\mathcal{T}(T)\frac{dT}{dx} + J^2\rho(T) = 0$$

Clearly this is a job for a computer. However, for many materials some or all these parameters are practically independent of temperature, and for many more their variation with temperature is not large. Hence, while a solution of the heat equation, treating the parameters as constants is only approximate, it gives some insight into the problem.

Treating k, $\mathcal{T}$ and ρ as constants we have

$$k\frac{d^2T}{dx^2} \pm \left(\frac{I}{A}\right)\mathcal{T}\frac{dT}{dx} + \left(\frac{I}{A}\right)^2\rho = 0$$

where I/A is the current density assumed constant over the cross-section A. The plus sign in front of the Thomson heat term is used when Thomson heat is evolved, and the minus when it is absorbed.

The solution is

$$T = T_c \mp rx \pm \left[\frac{rL \pm (T_h - T_c)}{1 - e^{\mp\beta L}}\right](1 - e^{\mp\beta x})$$

where $r = \frac{I\rho}{A\mathcal{T}}$, $\beta = \frac{I\mathcal{T}}{Ak}$, and L = length of element.

Making use of an appropriate series expansion, we find the heat flow into the hot end of the element to be

$$\dot{Q}_h = \frac{kA}{L}(T_h - T_c) \mp \frac{1}{2} I \mathcal{F}(T_h - T_c) - \frac{1}{2} I^2 \frac{\rho L}{A} + C \quad (5)$$

and the heat flow out of the cold end is

$$\dot{Q}_0 = \frac{KA}{L}(T_h - T_c) \pm \frac{1}{2} I \mathcal{F}(T_h - T_c) + \frac{1}{2} I^2 \frac{\rho L}{A} + C, \quad (6)$$

where the correction term is

$$C = \left[\frac{1}{2} I \mathcal{F}(T_h - T_c) - \frac{1}{2} I^2 \frac{\rho L}{A}\right] \left\{\frac{1}{6} \frac{I \mathcal{F}(T_h - T_c)}{\frac{kA}{L}(T_h - T_c)} - \right.$$

$$\left. - \frac{1}{360} \times \left[\frac{I \mathcal{F}(T_h - T_c)}{\frac{kA}{L}(T_h - T_c)}\right]^3 \right\}$$

It will be noted that the terms in the first bracket are identical with the last two terms in equations (5) and (6). The two terms in the braces represent the first two terms in an alternating series expansion, in which the variable is the ratio of the Thomson heat to the conducted heat. In any practical case, this ratio is probably no greater than 1 to 10. Hence, the correction term represents less than 2% of the terms immediately preceding it and we shall neglect it.

For the purpose of exposition we write the equation for heat flow into the hot end of a type I element used in a generator (i.e., Thomson heat evolved).

$$\dot{Q}_h = \frac{kA}{L}(T_h - T_c) - \frac{1}{2} I \mathcal{F}(T_h - T_c) - \frac{1}{2} I^2 \frac{\rho L}{A}$$

The first term is seen to be simply the heat conducted because of the temperature difference $T_h - T_c$. The coefficient kA/L is just the thermal conductance K. The third term is clearly half the total Joulean heat evolved since $\rho L/A$ is just the resistance R. The minus sign indicates that the heat flow into the hot end is diminished by half the total Joulean heat generated, in other words half the Joulean heat flows "back" to the hot end.

The second term is half the total Thomson heat generated and since it is evolved, has the same sign as the Joulean term. Here again, half the Thomson heat flows back to the hot end, diminishing the demand on the hot source. However, the original source of this Thomson heat is, as we have already seen, the Peltier heat absorbed by the hot junction. Hence, the evolution of Thomson heat costs, in terms of the heat taken from the hot source, half of the total Thomson heat.

The heat flow out of the cold end of the type I element is

$$\dot{Q}_c = K(T_h - T_c) + \frac{1}{2} I \mathcal{T}(T_h - T_c) + \frac{1}{2} I^2 R$$

Here we see that the net Thomson heat absorbed from the hot source is simply rejected to the cold reservoir as is half the Joule heat.

Thomson Heat and Practical COP

The heat flow into the hot end of a type II element acting as a generator (i.e., Thomson heat absorbed)is

$$\dot{Q}_h = K(T_h - T_c) + \frac{1}{2} I \mathcal{T}(T_h - T_c) - \frac{1}{2} I^2 R$$

In this case, half of the Thomson heat is taken from the hot source (which is the same as the net result for the previous case) by what may be considered an apparent increase in the thermal conductivity. Since the heat flow out of the cold end for the present case is

$$\dot{Q}_c = K(T_h - T_c) - \frac{1}{2} I \mathcal{T}(T_h - T_c) + \frac{1}{2} I^2 R$$

we see that the heat flow out of the cold end is diminished by half the total Thomson heat. We may think of this in terms of half the Thomson heat being abstracted from the conducted heat. In any event, the total Thomson heat is the source of part of the Peltier heat rejected at the cold junction (See Figure 2). Thus, the net effect for this case is the same as that of the previous one: The heat taken from the hot source is increased by half the Thomson heat, and this is just the net amount of Thomson heat which appears

at the cold junction.

Taking the case of a type I element (Figure 1, with current reversed) used as a refrigerator, we note that since the direction of current flow is reversed Thomson heat is now absorbed. The heat flowing to the refrigerated junction is

$$\dot{Q}_c = K(T_h - T_c) - \frac{1}{2} I \mathcal{T} (T_h - T_c) + \frac{1}{2} I^2 R$$

and the heat flowing from the hot junction (toward the cold) is

$$\dot{Q}_h = K(T_h - T_c) + \frac{1}{2} I \mathcal{T} (T_h - T_c) - \frac{1}{2} I^2 R$$

In this case, the Thomson heat aids us in that it diminishes the flow of heat to the refrigerated junction. Of the total Thomson heat, half is abstracted from the conducted heat and half from the hot junction. Since the total Thomson heat is rejected at the hot junction as part of the Peltier heat and only half of this flows back through the element the net effect is to abstract half the Thomson heat from the refrigerated junction (though strictly we only diminish the inevitable flow of conducted heat to the junction by this amount) and reject it to the hot reservoir.

Turning now to a type II element used to refrigerate (Figure 2 with current reversed), Thomson heat is evolved. The heat flow into the refrigerated junction is

$$\dot{Q}_c = K(T_h - T_c) + \frac{1}{2} I \mathcal{T} (T_h - T_c) + \frac{1}{2} I^2 R$$

and the heat flow from the hot junction toward the cold is

$$\dot{Q}_h = K(T_h - T_c) - \frac{1}{2} I \mathcal{T} (T_h - T_c) - \frac{1}{2} I^2 R$$

Here most of the Thomson heat is abstracted from the refrigerated junction in the form of Peltier heat (the rest being furnished by the current source), but by the equation for Q_c half is allowed to flow back with the conducted heat. From the Q_h equation, we see that the conducted heat flow from the hot reservoir is diminished by half the Thomson heat. Hence, the net effect is again to remove about half the Thomson heat from the refrigerated junction and pass it to the hot reservoir.

The above discussion of Thomson heat has been carried out on the basis of type I and II elements only for the sake of simplicity. A little thought will show that the same arguments hold for types III and IV. Thus, to the extent that our solution of the thermal conduction equation is correct, there is little choice to be made between the types for use as either refrigerator or generator insofar as the absorption or rejection of Thomson heat is concerned.

THE CALCULATION OF PRACTICAL EFFICIENCY

The calculation of the practical efficiency of the generator whose characteristic is shown in Figure 3 is straightforward, though highly algebraic.

The heat flow from the hot junction for the P-element is

$$\dot{Q}_{h(P)} = K_P (T_h - T_c) - \frac{1}{2} I \mathcal{F}_P (T_h - T_c) - \frac{1}{2} I^2 R_P$$

For the N-element it is

$$\dot{Q}_{h(N)} = K_N (T_h - T_c) + \frac{1}{2} I \mathcal{F}_N (T_h - T_c) - \frac{1}{2} I^2 R_N$$

The total heat abstracted from the hot source is obtained by summing these flows and adding the Peltier heat. Thus

$$Q_{in} = I \alpha_h T_h + K_P (T_h - T_c) - \frac{1}{2} I \mathcal{F}_P (T_h - T_c) - \frac{1}{2} I^2 R_P$$

$$+ K_N (T_h - T_c) + \frac{1}{2} I \mathcal{F}_N (T_h - T_c) - \frac{1}{2} I^2 R_N$$

$$= I \alpha_h T_h + K (T_h - T_c) + \frac{1}{2} \mathcal{F} I (T_h - T_c) - \frac{1}{2} I^2 R$$

where $\alpha_h = \alpha_{Ph} + \alpha_{nh}$; $K = K_P + K_N$; $\mathcal{F} = \mathcal{F}_n - \mathcal{F}_P$; $R = R_P + R_n$. The net Thomson coefficient may be plus or minus or zero.

The power out may be found by finding the heat flow out of the cold junction, adding the cold junction Peltier heat and subtracting the result from the heat flow in. This approach, however, produces an algebraic expression which simply reduces to the one found by the usual electrical approach, i.e.,

$$P_0 = \mathcal{E}^2 \frac{R_L}{(R + R_L)^2}$$

It is simplest to express $\mathcal{E}$ as

$$\mathcal{E} = \bar{\alpha} (T_h - T_c).$$

Thus, the efficiency is

$$\frac{\bar{\alpha}^2 (T_h - T_c)^2 \times \frac{R_L}{(R+R_L)^2}}{I \alpha_h T_h + K(T_h - T_c) + \frac{1}{2} \mathcal{T} I (T_h - T_c) - \frac{1}{2} I^2 R} \qquad (7)$$

Using $I = \dfrac{\bar{\alpha} (T_h - T_c)}{R + R_L}$

and proceeding as Joffe does to find the value of the ratio of R_L to R giving the greatest efficiency we find

$$\left(\frac{R_L}{R}\right)_{\text{opt.}} = \sqrt{1 + \frac{z}{2} \left[T_h \left(\frac{2\alpha_h}{\bar{\alpha}} - 1 \right) + T_c + \mathcal{T} \right]}$$

If $\alpha_h = \alpha_c = \alpha$ (in which case $\mathcal{T} = 0$), this reduces to Joffe's expression. In the practical case if ρ and k are known, the other necessary parameters may be determined graphically and the optimum value of the load is then readily determined. Substitution of this value into equation (7) gives the optimum efficiency.

It should be evident from this example that using equations (5) and (6), the calculation of generator efficiencies is straightforward and simple. If Thomson heat is evolved, the sign of the second term in the equation is negative (the same as the Joulean term); if Thomson heat is absorbed, it is positive (the opposite of the Joulean term which is always negative since Joule heat is always evolved). Summing the heat flows of the two elements and adding the Peltier heat gives the total heat abstracted from the hot source.

THE CALCULATION OF PRACTICAL COP

Suppose now that the couple whose characteristic is diagramed in Figure 3 is to be used as a refrigerator. Since the current is reversed, Thomson heat will be absorbed in the P-element and evolved in the N-element. Hence

$$\dot{Q}_{c(P)} = K_P (T_h - T_c) - \tfrac{1}{2} \mathcal{T}_P I (T_h - T_c) + \tfrac{1}{2} I^2 R_P$$

$$\dot{Q}_{c(N)} = K_N (T_h - T_c) + \tfrac{1}{2} \mathcal{T}_n I (T_h - T_c) + \tfrac{1}{2} I^2 R$$

and the total heat flow to the cold junction is

$$\dot{Q}_f = K (T_h - T_c) + \tfrac{1}{2} I \mathcal{T} (T_h - T_c) + \tfrac{1}{2} I^2 R$$

where $\mathcal{T} = \mathcal{T}_n - \mathcal{T}_P$

Hence, the heat abstracted from the cold reservoir is the Peltier heat minus the flow to the cold junction or

$$Q_R = I \partial_c T_c - K (T_h - T_c) - \tfrac{1}{2} I \mathcal{T} (T_h - T_c) - \tfrac{1}{2} I^2 R \quad (8)$$

In this case, the Thomson heat is seen to subtract from the refrigerated heat. However, if $\mathcal{T}_P$ were greater than $\mathcal{T}_n$ or if a couple composed of types I and III elements were used the Thomson heat term would be positive, i.e., aiding the refrigerated heat. In such a case, it can be shown that the maximum temperature difference available under conditions of zero refrigerator load is

$$(\Delta T)_{max} = \frac{\tfrac{1}{2} Z T_c^2}{1 - \tfrac{1}{2} Z T_c^2 (\frac{\mathcal{T}}{\partial_c})}$$

If $\mathcal{T}$ is zero, this is seen to reduce to Joffe's expression for maximum temperature difference. For $\mathcal{T}$ comparable to ∂_c the present expression indicates a larger maximum temperature difference than that indicated by Joffe.

The basis on which equation (8) for the refrigerator heat is derived is clearly quite similar to those already outlined for the generator. As usual the electrical power required can be written

$$\mathcal{E} I + I^2 R$$

or

$$I \bar{\alpha} (T_h - T_c) + I^2 R.$$

Hence, the COP is given by

$$\text{COP} = \frac{I \alpha_c T_c - K (T_h - T_c) - \frac{1}{2} I \mathcal{T} (T_h - T_c) - \frac{1}{2} I^2 R}{I \bar{\alpha} (T_h - T_c) + I^2 R}$$

Calculations for optimum current and best COP proceed in a straightforward, if somewhat laborious manner.

Heat Pump

Using the thermocouple of Figure 3 as a heat pump. We note that here, as in the refrigerator, the P-element absorbs Thomson heat and the N-element rejects it. Therefore, we have for the heat flow from the hot junction

$$Q_{hP} = K_P (T_h - T_c) - \frac{1}{2} I \mathcal{T}_P (T_h - T_c) + \frac{1}{2} I^2 R$$

$$Q_{hN} = K_N (T_h - T_c) + \frac{1}{2} I \mathcal{T}_n (T_h - T_c) + \frac{1}{2} I^2 R$$

Hence, the heat rejected to the hot reservoir is the Peltier heat minus the flow away

$$\dot{Q}_e = \alpha_h T_h - K (T_h - T_c) - \frac{1}{2} I \mathcal{T} (T_h - T_c) - \frac{1}{2} I^2 R.$$

The electrical power required is the same as that for the refrigerator and we have

$$\text{COP} = \frac{I \alpha_h T_h - K (T_h - T_c) - \frac{1}{2} I \mathcal{T} (T_h - T_c) - \frac{1}{2} I^2 R}{I \bar{\alpha} (T_h - T_c) + I^2 R}$$

Here again we may improve the COP by making $\mathcal{T}_P$ greater than $\mathcal{T}_N$ or by choosing types I and III elements to make $\mathcal{T}$ large and the Thomson term positive. This consideration may, however, be overbalanced by the importance of making $\alpha_h T_h$ as large as possible.

GENERAL REMARKS AND SUMMARY

It is hoped that the foregoing discussion makes clear the qualitative aspects of the phenomena of Thomson and Peltier heating. It is also hoped that the method of graphical analysis of thermoelectric characteristics has been made clear. This method should prove to be a valuable tool in design.

The calculation of practical efficiencies demands the solution of the heat conduction equation including terms for both Thomson and Joulean heats. The fact that a rigorous solution of the general equation demands that the coefficients be expressed as functions of the temperature means that the solution presented here has a distinctly limited accuracy. However, the present solution, including as it does the Thomson heat, represents a step beyond Joffe's work. Calculations of generator efficiency, where large temperature differences are used, will probably be considerably in error. The present solution may, however, be entirely adequate for use in calculating refrigerator coefficients of performance since here the temperature differences are relatively small. Work is being planned to verify this prediction.

The third point which it is hoped is clarified is that the reversible thermoelectric cycle is not a Carnot cycle. This misapprehension may have been fostered by Joffe's work in which he sets the Thomson coefficient equal to zero, thereby allowing the Seebeck voltage to be written simply as

$$\mathcal{E} = \alpha(T_h - T_c).$$

A further simplification results from the fact that the Peltier heats may be written as αT_h and αT_c which permits the collection of either of these terms with the terms expressing the Seebeck voltage.

It has been my experience that where Joffe's simplification is not followed, calculations are expedited if an average value of α (i.e., $\bar{\alpha}$) is used in the expression for the voltage. Hence, it is suggested that where the figure of merit Z arises in the course of a computation based on a fixed temperature difference that it be understood to denote

$$Z = \frac{\bar{\alpha}^2}{\rho k}$$

where $\bar{\alpha}$ is the quantity defined in equation (1).

REFERENCES

1. Der Metallische Zustand Der Materie by G. Borelius, p. 398, Handbuch Der Metallphysik, Band I, Teil II, Akademische Verlagsgesellschaft, Leipzig, 1934.

2. Maria Telkes, J. Appl. Phys., 18, 1116 (1947).

THERMAL PROPERTIES OF CADMIUM ANTIMONIDE

G. G. Kretschmar, R. F. Potter
U. S. Naval Ordnance Laboratory
Corona, California

The determination of the thermal conductivity and the Seebeck coefficient of a thermoelectric material is of importance for the evaluation of the "figure of merit" of the material with possibilities for refrigeration or electrical generation. For an efficient refrigerator, for example, one needs a material having a high Seebeck coefficient and a low heat conductivity and low electrical resistivity over the temperature range of interest.

Heat conductivity measurements were made on samples of CdSb, which holds some promise as a thermoelectric material. The measurements were made by means of a modified form of the Fitch conductivity apparatus[1] familiar to many college physics students. The Fitch method offers a means of determining conductivity in a rapid manner with relatively small sample size. It can also be adapted to measurements over a considerable range of temperature. In conventional thermal conductivity measurements, the sample is placed between a measured source of heat and a sink and the heat required to maintain a steady temperature gradient is determined. In the Fitch experiment the problem of measuring heat conductivity is greatly simplified because the sink or receiver is allowed to vary in temperature; only the source remains constant and the rate of change of temperature of the receiver block is measured. With a knowledge of the block mass and the gram heat capacity, the rate of heat flow into the block can be determined. Fitch equated this to the heat flow through the sample, obtaining the heat conductivity in terms of the slope of a linear plot of the temperature readings.

The heat through a sample of cross section A and length L with temperature difference $T_o - T_B$ and thermal conductivity K is given by:

$$\left(\frac{\Delta Q}{\Delta t}\right)_S = KA\,\frac{(T_o - T_B)}{L} \qquad (1)$$

The rate of gain of the Block B with gram heat capacity C_B, mass M_B and a rate of temperature change of $\frac{\Delta T_B}{\Delta t}$

$$\left(\frac{\Delta Q}{\Delta t}\right)_B = C_B M_B \frac{\Delta T_B}{\Delta t} \qquad (2)$$

Equating (1) and (2) and integrating, we get

$$\ln\frac{(T_o - T_B)}{(T_o - T_B)_o} = \frac{KA}{C_B M_B L}(t - t_o)$$

For any two successive values of t this becomes

$$\ln\frac{(T_o - T_B)_1}{(T_o - T_B)_2} = \frac{KA}{C_B M_B L}(t_2 - t_1)$$

From which $K = \frac{C_B M_B L}{A}\left[\ln\frac{(T_o - T_B)_1}{(T_o - T_B)_2}\right]/(t_2 - t_1)$ (3)

It is to be noted that the tacit assumption is made that the heat capacity of the receiver is very much greater than that of the sample; in other words, the energy retained by the sample is negligible. This condition is easily realized in practice by making the receiver large and of a material of high specific heat, and the sample proportionately very small. The error introduced by this assumption is of the order $(C_s M_s)/_2 C_B M_B$ where the subscript S refers to the sample.

Experimental

The apparatus as constructed for our experiment is shown in Fig. 1. The sample is at L. It should be from about 2 to 10 mm in length. The copper heat receiver is K and it is supported only by the sample, so that conduction losses are only those due to the slight contacts of the thermocouple ceramic tubing. The receiver K is completely surrounded by the copper radiation shield J. The heat receiver has a nickel wire sensing element E wound around it,

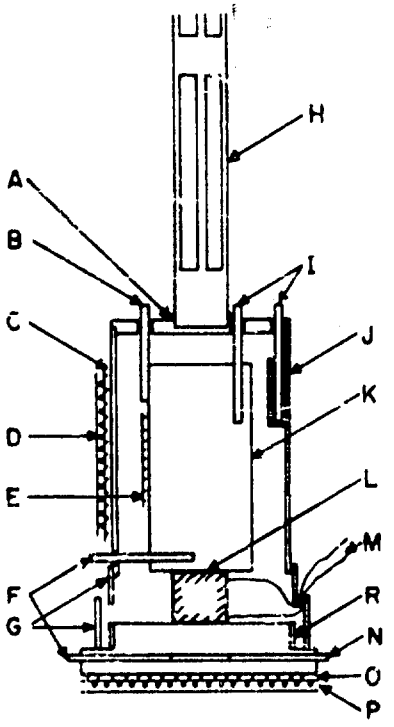

Figure 1 - Cross section of assembled apparatus

and this is one arm of a Wheatstone bridge of which the opposite arm is C, the control element of the copper heat shield. By means of an electronic control circuit, the temperature of the heat shield is made to follow the temperature of the receiver to a difference of less than 0.1°C. Thus, for a large range of temperature the radiation losses from the receiver can be taken as negligible. The temperature equality of the receiver and the heat shield is monitored by the 4 mil cooper constantan thermocouple I.

The copper base R is attached to the shield by three very thin stainless steel supports (not shown). It has a sensing winding O and a heater P, which can hold the base to a very constant predetermined temperature by means of a separate sensitive electronic control. The base temperature is monitored by means of the thermocouple N and it can usually be held constant to less than 0.01°C for periods longer than 10 minutes. The wires attached to the sample M are probes for measuring the thermal EMF developed by the sample material at different gradients across the sample.

The whole apparatus is put inside of a large pyrex glass tube and pumped out to a vacuum of about 10^{-5}mm so that gaseous convection losses are eliminated. The pyrex tube also permits immersion in liquid nitrogen or dry ice, or in a heating furnace, so that the experiment can be made over an extended temperature range.

The differential thermocouple F measures the changing temperature difference between the base and the heat receiver. Its output is fed into a Liston-Folb DC amplifier and thence into a Brown recorder. The photograph Fig. 2 shows the thermal conductivity apparatus attached to a vacuum system and around it can be seen the two Leeds and Northrup potentiometer indicators, a large Dewar for cold immersion and a temperature controller for use with furnace immersion. In the rack are the DC amplifier, the Brown recorder and the two temperature controllers. Since the thermal conductivity of CdSb is quite low, about that of glass or hard wood, it is necessary to make a good thermal contact between the sample and the copper base and also between the sample and the heat receiver. The best technique to date seems to be to make the surfaces flat and then press them together with a small amount of Dow Corning high vacuum grease between.

Experimental Results

Measurements were made on an n-type sample of CdSb over the range 160°K to 476°K. The results are presented in Fig. 3 for the thermal conductivity and in Fig. 4 for the Seebeck coefficient. Similar data for the p-type sample are presented in Fig. 5 and Fig. 6. Low temperature runs for sample 34 P showed considerable scatter and are considered unreliable because of uncertain thermal contact with the base and receiver.

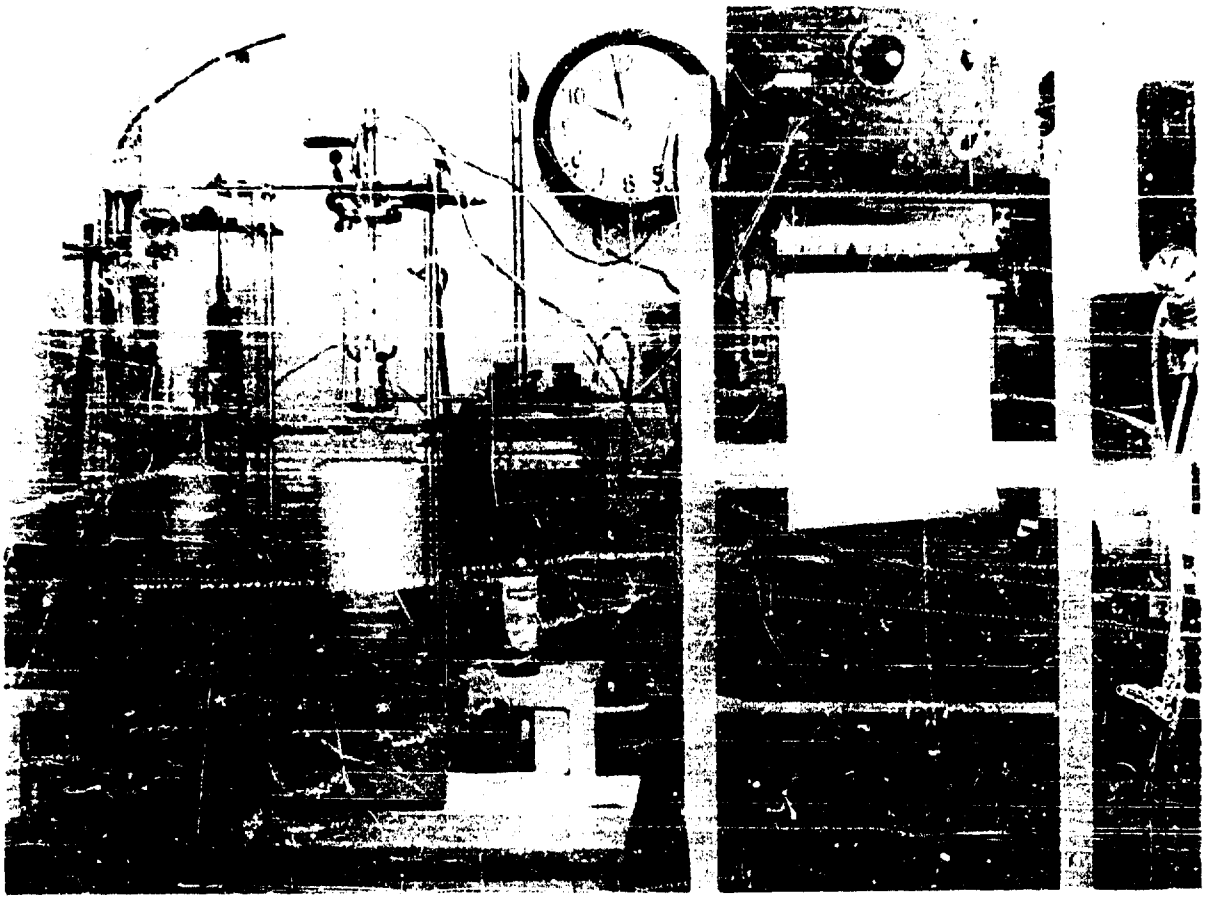

Figure 2 - Conductivity apparatus and accessory measuring equipment

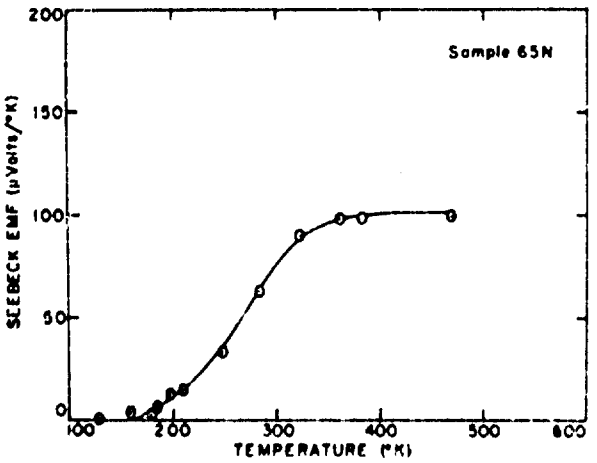

Figure 3 - Seebeck EMF as a function of temperature

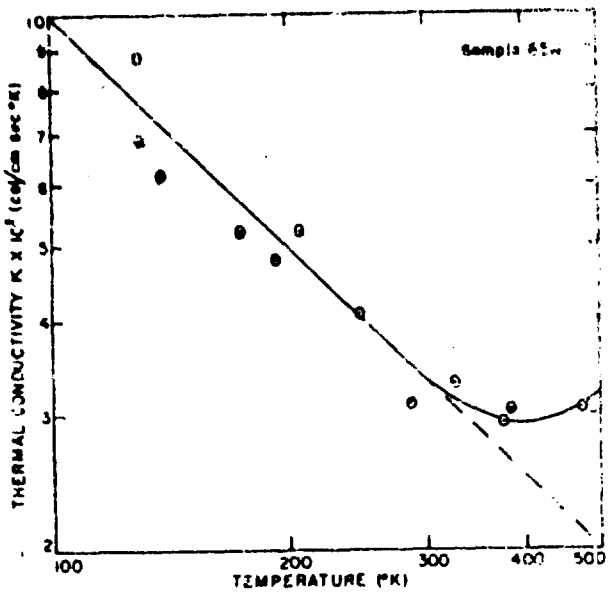

Figure 4 - Thermal conductivity as a function of temperature

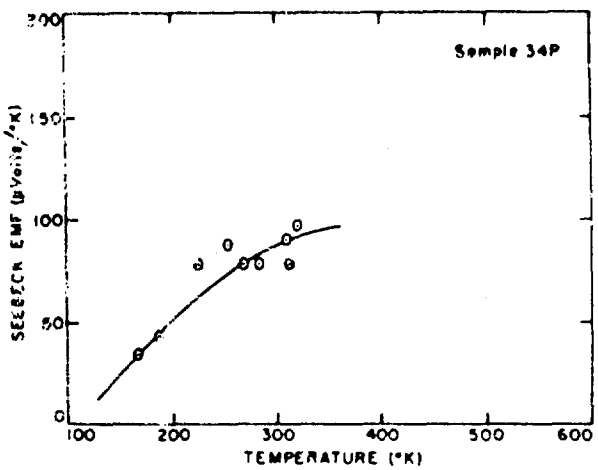

Figure 5 - Seebeck EMF as a function of temperature

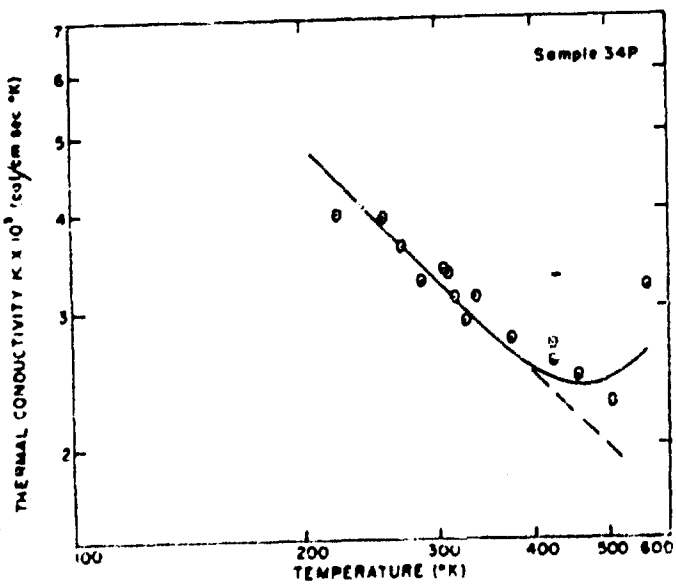

Figure 6 - Thermal conductivity as a function of temperature

Discussion

a. Thermal Conductivity

It is apparent from Figs. 4 and 6 that the thermal conductivity of the two samples is very similar over the range of 100°K to 500°K. Each sample exhibits a behavior $K \propto T^{-1}$ up to a temperature of between 300 and 400°K at which point a deviation from this law occurs. The conductivity is assumed to consist of two terms; one due to a phonon contribution K_p, the other attributed to a spurious thermal conductance caused by radiation (K_R), e.g. $K = K_p + K_R$.

b. Phonon Thermal Conductivity

The thermal conductivity of insulating crystals has shown a T^{-1} dependance at temperatures corresponding to or larger than, their respective Debye characteristic temperature [2]. It is also generally accepted that this behavior is characteristic of phonon interaction with the lattice. Dugdale and MacDonald [3] have given an approximate expression for the product KT by considering a mean free path l_p for phonons (by which momentum is transported) and having that l_p limited by the anharmonic nature of the lattice.

$$T = V_c^{1/3} C_v V / \alpha \gamma \qquad (4)$$

where V_c - volume of unit cell

C_v - Specific heat/vol

V - sound velocity

α - coefficient of linear expansion

γ - Gruneisen's constant

By considering a suggestion by Pierls [4] that thermal resistance effects are contributed by Umklapp processes (such processes correspond to phonons undergoing Bragg reflections in a periodic lattice) Klemens [5] and Subfried and Schloemann [6] obtain an expression for KT. The latter obtained the following estimate

$$KT = 3.0 \left(\frac{1}{\gamma}\right)^2 \left(\frac{k}{h}\right)^3 \frac{}{m} (V_c)^{1/3} \theta^3 \qquad (5)$$

Although there are many approximations in (5), it is of interest to compare it with the experimental value obtained from CdSb; $KT \simeq 4$ watts/cm as determined from Figs. 3 and 5. When this value is equated with (2) using $\gamma = 2$, $\bar{m} = 9.0 \times 10^{-23}$ grms and $(V_c)^{1/3} = 7.4 \times 10^{-8}$ cm one obtains a value for θ of 85°K. A reasonable guess for the Debye temperature for CdSb would place it between 100° and 200° K. Thus within the guess for θ and γ values

the experimental data is in reasonable agreement with (5).

c. Gray Body Radiation Effects

It is estimated that at 500°K a correction of approximately $\kappa \approx 10^{-4}$ (cal/cm sec deg) must be made to the thermal conductivity measured with the apparatus of Fig. 1. This is caused by the exposure of the receiver K to the heat source R. The correction term is given by $\kappa_r \simeq 4\sigma\varepsilon T^3 L A_K/A_L$, where σ = Stephan-Boltzman constant and ε = emissivity of copper. The ratio $A_K/A_L \simeq 3$ $L \simeq 1$ cm and $\varepsilon \simeq 0.2$ are used for the estimate.

Figs. 4 and 6 show such an effect at temperatures above 400°K. The apparatus is being modified by extending the radiation shielding in order to reduce the ratio A_K/A_L and minimize κ_r.

d. Electronics Contribution to Thermal Contribution.

The estimate for the radiation conductance does not appear large enough to account for all the extra conductance observed. Ambipolar diffusion of electrons and holes has been suggested as a possible source of thermal conductance in semiconductors [7].

For an intrinsic semiconductor with equal hole and electron mobilities this electronic thermal conductivity κ_e can be approximated by

$$\kappa_e \simeq \left(\frac{E_g}{e}\right)^2 \frac{\sigma}{4} \frac{1}{T} \qquad (6)$$

The approximation is valid when electron scattering terms of the order 2 to 6 can be neglected compared to Eg (kT.)

Eg - energy gap (0.4 ev. for CdSb)

e - electron change

σ - electrical conductivity (50 (ohm cm) $^{-1}$ for CdSb)

T - absolute temperature

The values for κ_e determined from eq 6 are of the right magnitude to fit the observations if the radiation effects are no larger than estimated in paragraph c. It is intended to check this with the new apparatus.

e. Seebeck e.m.f.

The thermoelectric potentials were observed against copper electrodes. As can be seen from Figs. 3 and 5, the emf values drop off at the lower temperatures which is normal behavior for similar materials. Future studies will determine how the Seebeck emf values behave as function of impurity content and crystalline nature.

Summary

The thermal conductivity of the semiconductor CdSb has been measured from 100°K to 500°K using a modified Fitch's apparatus. The principal mode of conductance up to 400°K is that contributed by the lattice. At higher temperatures, the conductivity deviates from the T^{-1} law characteristic of phonon conductance. A modification of the apparatus should minimize spurious effects due to radiation, allowing a determination whether an electronic thermal conductance is present at higher temperatures.

The Seebeck emf was seen to fall off at lower temperatures. Future experiments with improved crystals and various doping agents may indicate how the Seebeck emf can be raised or suitably modified in a suitable temperature range.

The authors wish to thank D. H. Johnson who took most of the measurements reported here.

References

1. F. L. Fitch, Am. Jour. of Physics, 3, 135 (1935)

2. P. G. Klemens, Solid State Physics, Vol.7, Academic Press, Inc., New York (1958)

3. J. S. Dugdale and D. K. C. MacDonald, Phys. Rev. 98, 1751 (1955)

4. R. E. Peierls, Quantum Theory of Solids, Clarendon Press, Oxford (1955)

5. P. G. Klemens, Proc Roy Soc A 208, 108 (1951)

6. P. G. Klemens, Solid State Physics, Vol.7, Academic Press, Inc., New York p. 46 (1958)

7. P. J. Price, Phil. Mag. 46, 1252 (1955)

SOME ASPECTS OF THE LUMINESCENCE OF GLASS AND ITS APPLICATIONS

Robert J. Ginther and James H. Schulman
U. S. Naval Research Laboratory
Washington, D. C.

Introduction

While a large number of luminescent glass compositions are known there has been no large application of luminescent glass in devices which require a high luminescent light output. There is a general impression that the luminescence of glass phosphors is less efficient than that of crystalline materials and that this difference in efficiency is accentuated when the phosphors are excited by high energy radiation such as high velocity electrons(1). A lower efficiency for glasses than for crystals seems reasonable since glasses, lacking long range order, might not be expected to transfer energy from absorbing to emitting sites as efficiently as do crystals. This should be true not only for electrons but for any process in which energy is absorbed in ions of the glass structure other than emitting centers. It should be true for x-rays, for gamma rays and even for ultraviolet light absorbed in other than a discrete absorption band of the activator. However, when light is absorbed in the characteristic absorption band of the activator there seems to be no fundamental reason for a lower efficiency in glass phosphors than in crystals.

Since the efficiency of glass phosphors with high energy excitation is very likely restricted by the limited transfer of energy one might expect to improve the efficiency of glasses by preparing samples of either high activator concentration or of high concen-

trations of ions which can transfer energy to the activator by resonance processes. With increasing concentration of either of these species an increasing portion of the incident energy will be absorbed by either the activator ions or at sites favorable to the transfer of energy to the activator. A requirement of such an improvement would be that the high concentrations employed do not quench the luminescence process.

The current program of the investigation of luminescence in glass has as its primary practical goal the development of an inorganic glass scintillation phosphor. In the course of this program the performance of some of the glasses prepared were examined with cathode-ray excitation, and as a result of this examination a program of preparation of cathodoluminescent glass has recently been started.

Glass scintillators have the obvious advantage that they could presumably be fashioned in almost any desired shape or thickness and at a cost much lower than that of clear single crystals. A glass phosphor could even conceivably be made an integral part of the electronic detector such as the window of a photomultiplier tube. Glass cathode ray screens would have the advantages afforded by their transparency. These include improved resolution, and contrast as demonstrated for transparent cathodoluminescent films by Studer and Cusano[2] and by Feldman and O'Hara[3].

Only a few glass scintillators have been reported previously. Kovacevic and Kostic have employed a uranium glass for the detection of neutrons,[4] but its efficiency is believed to be very low. The Corning Glass Co. has prepared a gamma-ray sensitive cerium-activated 96.0% silica glass, similar in type to the high silica glass known as "Vycor". Corning has also prepared several experimental cerium-activated glasses of undisclosed composition, which detect gamma rays.

Experimental Procedure

The evaluation of scintillating glasses consisted of comparison of their pulse heights with that of a Harshaw crystal of thallium activated sodium iodide. Pulses excited by a gamma ray source were detected with RCA photomultiplier tubes 6655 or

6903 in an Atomic Instruments Company model 223 scintillation head, and observed on a Tektronix type 545 oscilloscope equipped with a 53/54K plug-in unit.

The evaluation of the response of the glasses to neutron excitation was made by Drs. Lowell Bollinger and Frank Thomas of the Argonne National Laboratory.

Performance with cathode ray excitation consisted of measurement of the screen brightness as a function of applied voltage at constant beam currents, and the determination of emission spectra and decay rate. Samples were excited in either a demountable cathode-ray tube or in sealed tubes prepared by the N.R.L., Electron Tube Engineering Section. Both the demountable and sealed tubes employed R.C.A. type 5AB electron guns. Screen brightnesses were measured with a Spectra Brightness Spot Meter (Photo Research Corp. 1/2° Ultrasensitive Model). Emission spectra were determined with a calibrated spectroradiometer. Decay times were obtained by exciting the phosphors with a square wave cathode ray pulse of 100-microsecond duration and observing the decay of the luminescence with a photomultiplier tube and oscilloscope.

Cerium activated high silica glass was prepared by the Corning Glass Co. presumably by impregnating porous 96% silica glass with a cerium solution and then heating the impregnated samples to a high temperature to produce a luminescent glass[5]. In our laboratory, luminescent high silica glass was prepared by impregnating Corning No. 7930 porous glass with solution of Ce, Eu, Sm, Tl, Mn, Sn, V, Cu, U, and Yb and heating subsequently to 1200°C. It was found that samples prepared with No. 7930 glass as received would not produce efficient phosphors since the porous glass was contaminated with both organic matter and inorganic impurities. Boiling the No. 7930 glass with concentrated nitric and sulfuric acids, followed by extended washing with water in a Soxhlet extractor rendered the porous glass suitable for the preparation of luminescent high silica glass.

Meltable type glasses were prepared by melting together the component oxides, carbonates, or oxalates and either casting the melts into a steel mold or allowing them to cool in the crucible

in which they were prepared. Simple borate glasses could be melted at temperatures as low as 1000°C, but samples containing high concentrations of Al_2O_3 or SiO_2 required a melting temperature of about 1400°C. Silicate glasses containing no boron were melted at 1500°C. Samples containing cerium require melting in a reducing atmosphere. This was conveniently provided by placing the platinum crucible containing the raw materials in an alumina crucible of about the same size, and suspending the latter crucible on a bed of carbon inside a large covered alumina crucible. The reducing atmosphere was also used for samples containing Eu and Mn.

The raw materials employed in glass preparation were generally of reagent grade or were specially purified in our laboratory. Reagent grade sodium carbonate, borax, and boric acid were used. Magnesium carbonate was of a grade employed in the preparation of luminescent magnesium tungstate. Linde A. alumina was used as the source of aluminum. Lithium carbonate and cerous oxalate were prepared in our own laboratory as random selection of commercially available lots gave erratic results. Potter's sand was used in early silicate glasses, but it was found that substitution of silica prepared from ethyl silicate gave improved scintillation efficiency.

Results

A. Development and evaluation of glass scintillators.

Of the various glass samples submitted to our laboratory for evaluation by commercial manufacturers only the Corning cerium-activated high silica glass and some cerium activated meltable glasses also prepared by the Corning Glass Co. exhibited scintillation pulses. The pulse height of these materials were 7.0 and 3.5% of that of thallium activated sodium iodide respectively. The samples prepared in our laboratory included borate, silicate, borosilicate and phosphate glasses activated with most of the ions generally known to produce luminescence in crystal phosphors. Of these, promising scintillation pulses were observed only with cerium activated samples.

The first materials prepared were alkali borate and borosilicate glasses. Development of these materials is best illus-

trated with reference to Table I.

Table I

Sample	Composition	Pulse Height as percent of NaI(Tl)
1	$1.0Na_2O$ $0.03 Ce_2O_3$ $4.0 B_2O_3$	1.5
2	$1.0 Na_2O$ $0.03 Ce_2O_3$ $4.0(B_2O_3+SiO_2)$	1.5
3	$1.0 Na_2O$ $0.10 Ce_2O_3$ $4.0(B_2O_3+SiO_2)$	1.8
4	$1.0Al_2O_3$ $1.0 Na_2O$ $0.03 Ce_2O_3$ $4.0(B_2O_3+SiO_2)$	3.0
5	$1.0Al_2O_3$ $1.0 Na_2O$ $0.10 Ce_2O_3$ $4.0(B_2O_3+SiO_2)$	5.0
6	$1.3Al_2O_3$ $1.0 Na_2O$ $0.10 Ce_2O_3$ $1.0 B_2O_3$ $1.5 SiO_2$	7.0

The first scintillating samples were sodium borate glasses. The most efficient of these proved to have a Na_2O-B_2O_3 ratio of 1-4. The optimum cerium content proved to be the maximum amount which could be incorporated, 0.03 mole. Substitution of silica for boric oxide did not change the efficiency at least up to a ratio of $1.0 B_2O_3$ - $3.0 SiO_2$. With higher silica content smaller pulses were obtained. In samples containing at least 1.0 mole of SiO_2 the cerium solubility was increased to at least 0.10 mole with a slight improvement of efficiency. Alumina was found to improve the efficiency further as shown by samples 4 and 5. Variation of the mole ratio of all of the constituents has produced the optimum formula represented by sample 6. Its pulse height of 7.0% is equal to that of the Corning cerium-activated high silica glass. Further variation of the composition of this material has not led to improvement. It has been found that substitution of either potassium or lithium for sodium produced slightly poorer pulses, whereas the incorporation of alkaline earths produced more serious quenching. Calcium and strontium incorporation reduced the pulse height greatly, and barium produced complete quenching when these ions were substituted for half the alkali. When phosphorus was used to replace silica or boron, similar

quenching occurred. Ions which would be reduced to metal or to highly colored products by the reducing atmosphere could not be employed, even though among these are a number of ions which would be of great interest both because of their glass forming and gamma ray absorption properties.

Cerium activated high silica glass has been prepared in our laboratory with a pulse height 6.0% of that of NaI(Tl), but the 7.0% efficiency of the Corning product was not obtained. Our most efficient samples were obtained only by prolonged purification of the Corning No. 7930 porous glass raw material and it appears likely that the discrepancy between the efficiency of the Corning product and our own is due to variation in the purity of the porous glass employed.

Among the crystalline compounds which have been activated with cerium to produce cathode ray excited phosphors, the most efficient appear to be the compounds $MgO \cdot CaO \cdot 2SiO_2$; $2CaO \cdot MgO \cdot 2SiO_2$[6] and $2CaO \cdot Al_2O_3 \cdot SiO_2$[7]. The first of these was chosen as a model to explore as a scintillating glass since glasses of rather similar composition have been reported by Larsen[8] and since the other two compounds would very likely require melting temperatures in excess of 1500°C, the upper limit of our present furnaces. The development of glasses based originally on magnesium calcium silicate is outlined in Table II.

Table II

No.	Composition						Pulse Height as % of NaI (Tl)
	MgO	CaO	SiO_2	Ce_2O_3	Li_2O	Al_2O_3	
1	.326	.234	.44				0
2	.301	.209	.44	.025			1.5
3	.276	.184	.44	.025	.025		3.5
4	.226	.134	.44	.025	.05	.025	6.5
5	.26		.50	.005	.065	.05	14.0

Glass number 1 is a formula of Larsen. Activation of this glass with cerium produces a weak pulse as shown by sample No. 2. It has been observed that the substitution of cerium for a divalent

ion in some crystalline compounds is facilitated by the simultaneous incorporation of an equal concentration of a monovalent ion(9). The total positive ion charge is thereby unchanged from that of the substituted divalent ions. This was the basis of the original addition of lithium to this glass even though there has not been any demonstration that this type of "charge compensation" is useful in glass formulation. The lithium addition is shown by sample 3 to improve the pulse height to 3.5%. The incorporation of aluminum followed from its beneficial effect in borate and boro-silicate samples and the first aluminum-containing glass of this series exhibited a pulse height of 6.5%. The most efficient glass produced to date is the final composition of Table II. It was obtained by empirical variation of the component oxides and employment of the purest raw materials available. It was found that the concentrations employed were not extremely critical. Silica may be varied from 0.45-0.55 mole without appreciable changes in pulse height. The same pulse is obtained within a cerium concentration limit of 0.01-0.03 mole, and the Li/Mg ratio can be doubled without affecting the pulse height. Further increase of lithium reduces the pulse. The aluminum concentration is not critical with regard to pulse height but at least 0.08 mole Al_2O_3 must be present to produce clear glass. The presence of calcium in the original formula was found to be detrimental as was the incorporation of other alkaline earths. Substitution of boric oxide for silica produced much smaller pulses.

At the request of Dr. Lowell Bollinger samples of boron and lithium containing glasses were submitted to the Argonne National Laboratory in order to test their performance as neutron scintillators. The behavior of selected samples, representing the four types of glasses prepared, to both neutron and gamma excitation at Argonne is shown in Table III. From this table it is apparent that all four types are neutron sensitive as well as gamma sensitive. Sample 2 is the best for time of flight experiments because of its high boron content although its neutron pulse is the lowest of the four and its neutron to gamma pulse ratio the poorest, this ratio is superior to that of presently employed boron loaded liquids(10). Although sample 3 has a better neutron pulse and neutron to gamma ratio, its lower boron content is believed to render it less useful for time of flight experiments. The 96.0% silica glass is of such low boron content that its use as a neutron scintillator is not likely. The largest neutron excited pulses as well as the most favorable

neutron to gamma ratios have been obtained with lithium-containing glasses of the type represented by sample 4. The relatively low lithium content as well as the lower neutron cross section of lithium compared to that of boron render this glass of less interest for time of flight work than the borate glasses. The lithium content has been increased to 2.5 times the concentration of sample 4 , but this increase is not considered a significant quantity when compared to the boron concentrations obtainable in borate glasses. Increased lithium lowers the gamma excited pulse height and improves the neutron to gamma ratio. Other parameters such as the resolution of the gamma pulse have been found to be dependent on glass composition, so that choice of an optimum composition of the lithium containing glasses will depend upon their intended use.

Table III

Sample	Composition	Relative height with neutrons	Pulse with neutrons / Pulse with 2.3 Mev
1	Ce-activated 96% silica	120	.218
2	$1.0Na_2O, 1.3Al_2O_3, 3.0B_2O_3, 0.10Ce_2O_3$	39	.064
3	$1.0Na_2O, 1.3Al_2O_3, 1.0B_2O_3, 1.5SiO_2, 0.10Ce_2O_3$	56	.085
4	$0.25MgO, 0.065Li_2O, 0.05Al_2O_3, 0.50SiO_2, 951$ $0.01Ce_2O_3$		.277

B. Evaluation of Glass Cathode Ray Screens

One of the routine tests applied to the glass samples prepared in the scintillator development program was the observation of their luminescence under excitation with a low pressure gas discharge intended to simulate their performance under cathode rays. Of the samples tested the most promising appeared to be the high silica glasses activated with cerium, copper, and manganese. Accordingly, an investigation of the properties of these materials as cathode ray screens was undertaken. Included in the test was a uranium glass, Corning No. 3750, whose cathodoluminescence had been observed to be outstanding among commercially available transmission glasses.

The emission spectra of the glasses chosen are shown in Fig. 1.

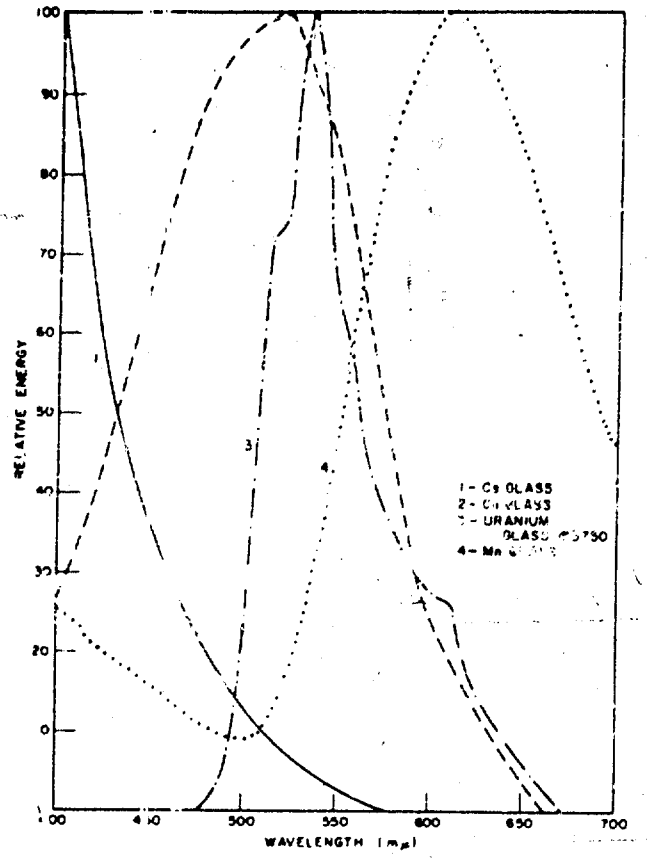

Figure 1 - Spectral distribution of luminescence of cathodoluminescent glasses

The uranium glass has the green emission typical of uranium activated phosphors. Copper activation produced a blue-green luminescence. The manganese activated glass has its main emission peak near 6200A, but in addition to the familiar orange-yellow manganese emission the emission spectrum reveals a blue component believed to be identical to the emission of unactivated high silica glass. The cerium activated glass has only a portion of its emission in the visible region. Fig. 2 shows a curve of its

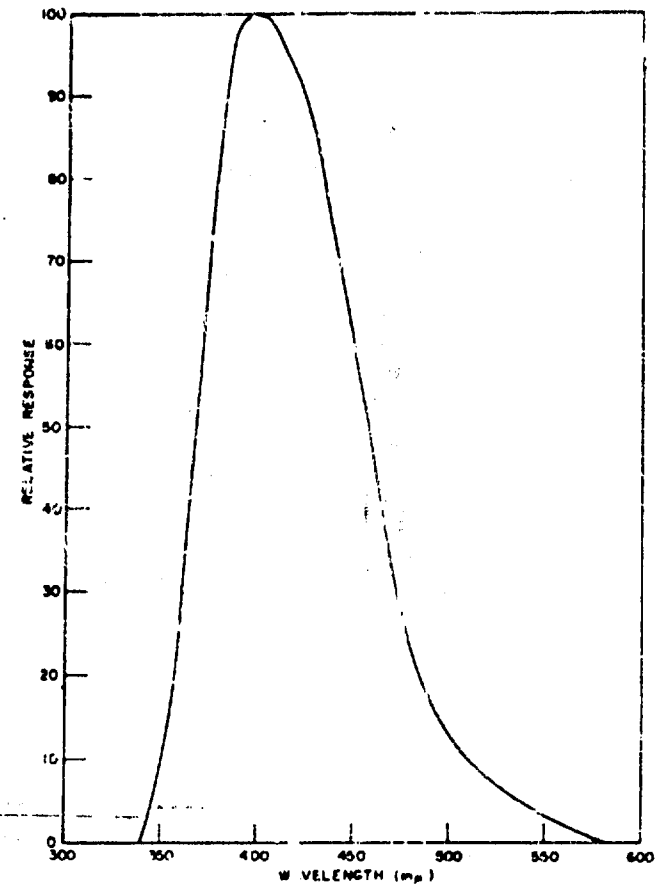

Figure 2 - Uncorrected phototube response curve of cerium activated glass

uncorrected emission spectrum observed through a Bausch & Lombe grating monochromator with a 1P28 photomultiplier tube.

Fig. 3 shows the brightness of the cerium, manganese, and uranium glasses as a function of accelerating voltage at a current density of 5.0 ua/cm^2. Test conditions did not permit a similar measurement of the copper activated samples.

Figs. 4 and 5 show the afterglow of the glass samples excited by a square wave pulse of 100 microsecond duration. Fig. 4 indicates that the decay time of the manganese glass is in the millisecond range. Various samples have been found to have decay times between 2.0x10^{-3} and 4.0x10^{-3} sec. There is in addition to

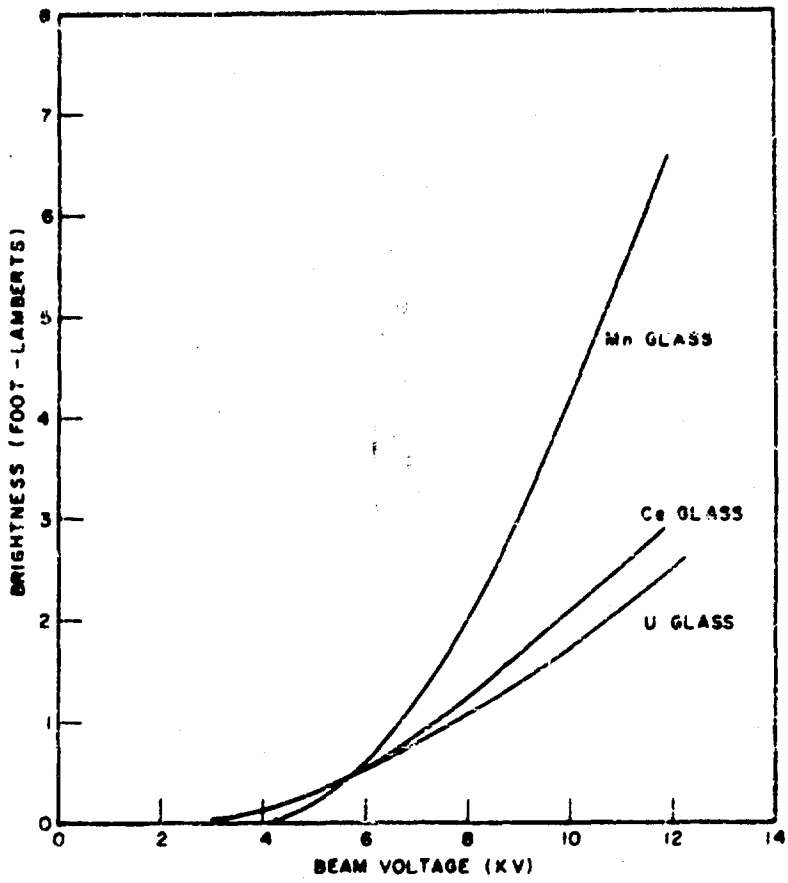

Figure 3 - Brightness of glass screens as a function of electron beam voltage; beam current approximately 5 microamperes per sq cm

the initial exponential decay a long afterglow associated with the manganese emission. Our equipment did not permit accurate determination of emission intensity at levels lower than 10 percent of the initial value. The decay curves of the cerium, uranium and copper activated glasses are shown in Fig. 5. The copper activated material apparently decays exponentially with two different time constants. For the initial portion of the curve the decay time is about 2×10^{-5} sec. The uranium glass decays exponentially with a decay time of about 10^{-4} sec. The cerium glass has the shortest afterglow; its decay time is not more than about 4 microseconds.

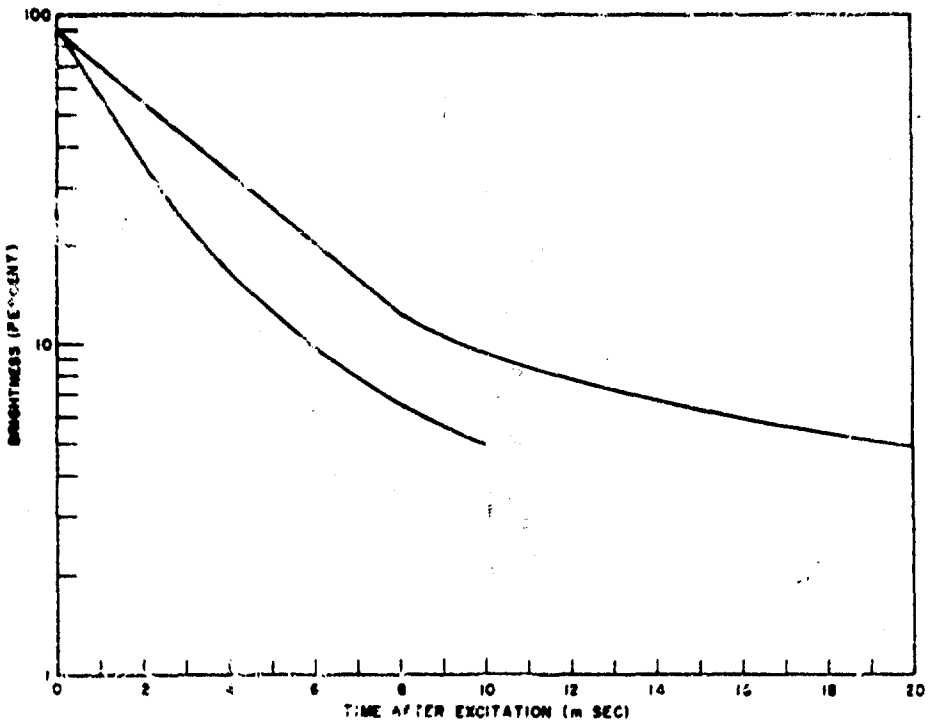

Figure 4 - Decay rates of manganese activated glasses after 100 microsecond pulse of cathode ray excitation

Discussion

The results obtained in the preparation of glass scintillators have been encouraging. Gamma detectors with an efficiency fourteen percent of thallium activated sodium iodide as well as glasses sensitive to neutrons have been prepared. To date little attention has been given to an investigation of the mechanism of scintillation in glass, and progressive improvement of the glass samples was obtained by the general procedures employed in phosphor development. These have included choice of glass matrices having good solubility for the activator, and the use of materials and processing techniques which do not introduce impurities into the samples. A number of interesting questions related to the scintillation behavior of these glasses deserve attention. The role of ions such as barium and phosphorus which quench the scintillation process but do not seriously affect photoluminescence behavior is unknown. Similarily, the beneficial effect upon the scintillation behavior of borate and phosphate glasses produced by incorporation

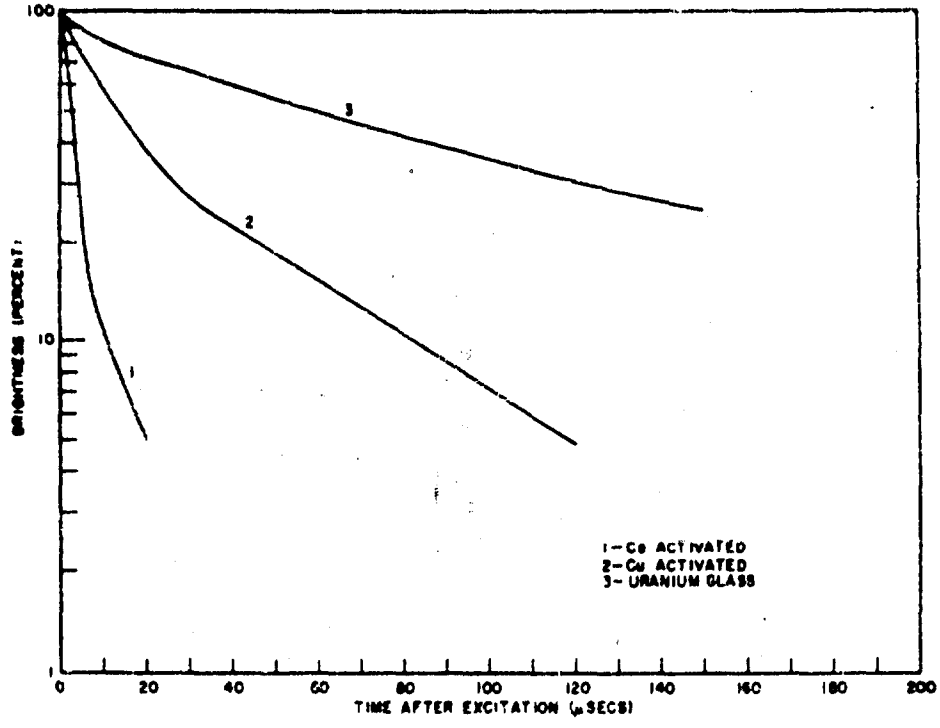

Figure 5 - Decay rates of cerium, copper, and uranium glasses after 100 microsecond pulse of cathode ray excitation

of aluminum is unaccompanied by any change in photoluminescence efficiency. It seems reasonable to assume that the role of these ions is to improve or quench energy transfer processes in the glass, but no proof can yet be offered. Measurements of absolute conversion efficiency as well as optical studies of the glasses may help to elucidate these mechanisms.

The field of scintillation glass development has by no means been completely explored, but some of the present findings if continuously confirmed would appear to limit the search for new scintillating compositions. Among these findings are the fact that to date only cerium activation has been useful despite the fact that photoluminescent glasses activated by a large number of ions are known. At present best performance has been obtained in only borate, and silicate glasses containing only alkalis, magnesium or aluminum. Introduction of any other ion has never improved the pulse height, and most often produced quenching. The inability to

employ heavy elements which would be reduced to metals by the reducing atmosphere required by cerium is a further restriction. On the other hand, the possible combinations of the ions which have been found useful with cerium have by no means been exhausted. It is entirely possible that gradual further improvement of the present glasses can be obtained by variation of the presently permitted components. The use of activators other than cerium is not precluded by the present results, however, for it is entirely possible that glasses so far prepared with these activators contain quenchers for these activators which do not quench cerium scintillation.

The screen brightnesses obtained with cathodoluminescent excitation of the glasses prepared in this prgram are low compared to those obtainable with conventional settled screens of polycrystalline phosphors. Since the luminescence of glass phosphors along with that of transparent crystalline films is subject to total internal reflection, glass screens cannot be expected to approach the brightness of polycrystalline layers and should more properly be compared to transparent phosphor films of approximately the same emission spectra. By comparison with the results of Feldman with transparent screens it appears that the uranium glass has a brightness of only 4.0% of a clear Zn_2SiO_4:Mn screen, the manganese glass 33.0% of a ZnS:Mn screen, and the cerium glass 30.0% of a $CaWO_4$ screen. Comparison of screen brightness does not give a comparison of energy efficiency since the samples compared do not have identical emission spectra. When allowance is made for the relative luminosity of the spectra compared it appears that the energy efficiency of the manganese glass is 38-40% of the ZnS:Mn film and the cerium glass is 60% as efficient as the $CaWO_4$ film.

It is unlikely that glass screens can be prepared whose brightnesses would approach those of polycrystalline screens, but for applications in which contrast or definition are more important than brightness it would appear that further research on cathodoluminescent screens is in order. We have recently undertaken a program of cathodoluminescent glass development whose primary purpose is to obtain meltable glasses whose persistence characteristics would enable their employment in military field devices. To date greatest attention has been devoted to silicate and borosilicate glasses activated by manganese. Efficiencies produced to date are

superior to that of the manganese activated high silica glass reported, but no glass of useful persistence is yet available.

References

(1) H. W. Leverenz, Luminescence of Solids, p322, Wiley and Sons, New York 1950

(2) F. J. Studer and D. A. Cusano, J. Opt. Soc. Am. 45, 493(1955)

(3) C. Feldman and M. O'Hara, J. Opt. Soc. Am. 47, 300 (1957)

(4) Kovacevic and Kostic, Bulletin of The Institute of Nuclear Sciences "Boris Kidrick" 79, 49(1950); Nucleonics 13, No. 8, 62 (1955)

(5) M. E. Nordberg and H. E. Rumenapp, U.S. Patent 2,303,756 Dec. 1, 1954

(6) A. L. Smith, Trans. Electrochem. Soc. 96, 287(1949)

(7) A. Bril and H. Klasens, Philips Res. Rept. 7, 421 (1952)

(8) E. S. Larsen, Am. J. Sci., 28, 263(1909)

(9) H. C. Froelich and J. M. Margolis, J. Electrochem. Soc. 98, 400 (1951)

(10) L. M. Bollinger and G. E. Thomas, R. S. I. 28, 489 (1957)

AUTHOR INDEX

Note: Pages 387 - 764 appear in Volume 4.

NOTIFICATION OF MISSING PAGES

INSTRUCTIONS: This form is inserted into ASTIA cataloged documents to denote missing pages.

DOCUMENT	CLASSIFICATION (CHECK ONE)		
	Unclassified	Confidential	Secret
AD	✓		
ATI			

The pages, figures, charts, photographs, etc., missing from this document are:

BLANK

DO NOT REMOVE